

Report  
**P-17-24**  
March 2019



# Project SFR-extension

**Single-hole injection tests in boreholes  
KFR27 and KFR105**

**Johan Harrström**  
**Oskar Sjöberg**  
**Ellen Walger**

SVENSK KÄRNBRÄNSLEHANTERING AB

SWEDISH NUCLEAR FUEL  
AND WASTE MANAGEMENT CO

Box 3091, SE-169 03 Solna  
Phone +46 8 459 84 00  
skb.se

SVENSK KÄRNBRÄNSLEHANTERING



ISSN 1651-4416

**SKB P-17-24**

ID 1592335

March 2019

## **Project SFR-extension**

### **Single-hole injection tests in boreholes KFR27 and KFR105**

Johan Harrström, Oskar Sjöberg, Ellen Walger  
Geosigma AB

**Keywords:** AP SFR-15-002, SFR, Forsmark, Hydrogeology, Hydraulic tests, Injection tests, Single-hole tests, Hydraulic parameters, Transmissivity, Flow logging.

This report concerns a study which was conducted for Svensk Kärnbränslehantering AB (SKB). The conclusions and viewpoints presented in the report are those of the authors. SKB may draw modified conclusions, based on additional literature sources and/or expert opinions.

Data in SKB's database can be changed for different reasons. Minor changes in SKB's database will not necessarily result in a revised report. Data revisions may also be presented as supplements, available at [www.skb.se](http://www.skb.se).

A pdf version of this document can be downloaded from [www.skb.se](http://www.skb.se).

© 2019 Svensk Kärnbränslehantering AB



## Abstract

SKB has performed supplementary hydraulic investigations in two core-drilled boreholes, KFR27 and KFR105, as a part of the preparations for a construction of an extension of the final repository of short-lived operational radioactive waste, SFR, in Forsmark. Borehole KFR27 is almost vertical and drilled from the ground surface to an elevation of about –500 m. Borehole KFR105 is drilled with a downward plunge of 10° to a depth of about 306 m starting from an elevation of about –105 m inside the existing SFR tunnel.

This report presents the results of injection tests performed in boreholes KFR27 and KFR105 using the pipe string system PSS2 together with the Water Injection Controller (WIC, HWIC). The test section transmissivity data determined from the injection tests, determined with transient methods, were compared with the transmissivity results of the Posiva Flow Log (PFL) measurements previously performed in the same borehole sections. The PFL-measurements were made under stationary flow after about two days of pumping hence evaluated with a stationary method based on specific capacity. The injection tests had an injection time of about 15–20 minutes.

One particular issue of interest in this comparison was to see if the difference in test time between the PFL measurements and the injection tests affected the interpreted transmissivities. The longer test time with PFL might drain fractures near the borehole (hydraulic choke) that still leads water during the shorter injection test. Sections of interest were injection tests with interpreted no-Flow boundaries (NFB) and these were compared with PFL-measurements and their final flow. No stronger connection between interpreted NFB and a flow below measurement limit during PFL could be seen. The results from both test types showed similar results especially in KFR27 whilst in KFR105 there was some small differences. However no significant difference in results could be seen connected to the timescale of the tests.

For almost 80 % of the injection tests in both KFR27 and KFR105, some period of pseudo-radial flow could be identified making a relatively straight-forward transient evaluation of the injection tests possible. The highest transmissivity in KFR105 was  $1.7 \times 10^{-6} \text{ m}^2/\text{s}$  and in KFR27  $3.2 \times 10^{-4} \text{ m}^2/\text{s}$ , this value from section 189.4–194.4 m was much higher than the other sections in KFR27 and the second largest had a transmissivity of  $4.1 \times 10^{-6} \text{ m}^2/\text{s}$ .

## Sammanfattning

SKB har utfört kompletterande injektionstest i två kärnborrade hål, KFR27 och KFR105. Dessa test ingår i förberedelserna för utbyggnaden av slutförvaret för kortlivat radioaktivt avfall, SFR, i Forsmark. KFR27 är borrat nästan vertikalt från ytan ner till ett djup av 500 m medan KFR105 är borrat nästan horisontellt (10 grader nedåt) på ett djup av 105 meter ned i SFR-tunneln och hålet är cirka 306 m långt.

Denna rapport redovisar resultaten från injektionstester utförda med hjälp av PSS2 (pipe string system) och WIC (water injection controller) i KFR27 och KFR105. Resultaten för varje 5-meterssektion utvärderades transient och transmissiviteten jämfördes sedan med resultat från tidigare utförda mätningar med Posiva Flow Log (PFL) i samma sektioner. PFL-testen utfördes under stationära flödesförhållanden efter en flödesperiod på cirka två dygn och utvärderades med stationära metoder baserat på specifik kapacitet.

En intressant aspekt som undersöktes var om det blev någon skillnad i mätvärden för dessa två mätmetoder, främst beroende på de olika testtiderna. Vissa sprickor i borrhålets närhet kan ha blivit helt dränerade under PFL men varit vattenförande under de kortare injektionstesterna. De sektioner som indikerade en ”No-Flow Boundary” under injektionstesterna jämfördes med slutflodet från PFL-mätningen i samma sektioner. Dock kunde inget starkare samband mellan NFB och ett flöde under nedre mätgräns under PFL-loggningen hittas. Resultaten från PFL- och PSS-mätningar visade på liknande resultat främst i KFR27 men även i KFR105. Inget större skillnad kunde hittas mellan resultat och testtider för de olika testtyperna.

I närmare 80 % av testerna i både KFR27 och KFR105 kunde en viss period med pseudo-radiellt flöde identifieras vilket underlättade en standardmässig transient utvärdering. Den högsta transmissiviteten i KFR105 tolkades till  $1.7 \times 10^{-6} \text{ m}^2/\text{s}$  och i KFR27 var det högsta värdet  $3.2 \times 10^{-4} \text{ m}^2/\text{s}$ . Detta värde för sektion 189.4–194.4 m var betydligt högre än de andra i KFR27, där den näst högsta transmissiviteten var  $4.1 \times 10^{-6} \text{ m}^2/\text{s}$ .

# Contents

<b>1</b>	<b>Introduction</b>	7
<b>2</b>	<b>Objectives</b>	9
<b>3</b>	<b>Scope</b>	11
3.1	Borehole data	11
3.2	Performed tests	12
3.2.1	KFR27	12
3.2.2	KFR105	14
3.3	Equipment checks	15
<b>4</b>	<b>Description of equipment</b>	17
4.1	Overview	17
4.1.1	Measurement container	17
4.1.2	Down-hole equipment	18
4.2	Measurement sensors	19
4.3	Data acquisition system	19
<b>5</b>	<b>Execution</b>	21
5.1	Preparation	21
5.1.1	Calibration	21
5.1.2	Cleaning of equipment	21
5.2	Test performance	21
5.2.1	Test principle	21
5.2.2	Test procedure	21
5.3	Data handling	22
5.4	Analysis and interpretation	22
5.4.1	General	22
5.4.2	Measurement limit of flow rate and specific flow rate	22
5.4.3	Qualitative analysis	23
5.4.4	Quantitative analysis	24
5.5	Nonconformities	26
<b>6</b>	<b>Results</b>	27
6.1	Nomenclature and symbols	27
6.2	Routine evaluation of the single-hole injection tests	27
6.2.1	General test data	27
6.2.2	Length corrections	27
6.2.3	General results	27
6.2.4	Flow regimes	35
<b>7</b>	<b>Comparison between injection tests and PFL-tests</b>	39
7.1	KFR27	39
7.2	KFR105	41
<b>References</b>		47
<b>Appendix 1</b>	General test data	49
<b>Appendix 2</b>	Test diagrams – Injection tests in KFR27	55
<b>Appendix 3</b>	Test diagrams – Injection tests in KFR105	177
<b>Appendix 4</b>	Test diagrams – Injection tests – long tests in KFR105	247
<b>Appendix 5</b>	Test diagrams – Injection tests – Fixed installations in KFR105	249



# 1 Introduction

Injection tests were carried out in boreholes KFR27 and KFR105 at Forsmark, Sweden. The tests in KFR27 were conducted during December 2015 and January 2106 and in KFR105 May and June 2016.

The location of the boreholes are shown in Figure 1-1. KFR27 is an almost vertical borehole about 500 m deep and drilled from the surface. The first 12 m has a casing and the entire borehole has a diameter of 76 mm. KFR105 is drilled in the SFR-tunnel at a depth of about 105 m below sea level at an angle of 10° (downwards) from the horizontal plane. It has a short casing of 3 m and the entire borehole has a diameter of 76 mm. For more technical information see Figure 3-1.



**Figure 1-1.** The investigated boreholes, KFR27 and KFR105, in Forsmark in relation to existing SFR (yellow) and planned extension (grey) seen from an angle (a) and straight from above (b). Borehole KFR105 is situated in the SFR-tunnel at about 106 m depth and KFR27 is drilled from the surface.

This document reports the results obtained from the injection tests in boreholes KFR27 and KFR105. The activity is performed within the research program for the extension of the final repository for short-lived operational radioactive waste, SFR, in Forsmark. The work was carried out in compliance with the SKB internal controlling documents presented in Table 1-1. Data and results were delivered to the SKB site characterization database, Sicada, where they are traceable by the Activity Plan number.

**Table 1-1. SKB internal controlling documents for performance of the activity.**

Activity Plans	Number	Version
Injektions- och interferenstester i KFR27, KFR103, KFR105	AP SFR-15-002	1.0
Method documents	Number	Version
Mätsystembeskrivning (MSB) – Allmän del. Pipe String System (PSS3)	SKB MD 345.100	1.0
Mätsystembeskrivning för: Kalibrering, PSS3	SKB MD 345.122	1.0
Mätsystembeskrivning för: Skötsel, service, serviceprotokoll, PSS3	SKB MD 345.124	1.0
Metodbeskrivning för hydrauliska injektionstester	SKB MD 323.001	1.0
Instruktion för analys av injektions- och enhålpumptester	SKB MD 320.004	1.0
Instruktion för rengöring av borrhålsutrustning och viss markbaserad utrustning	SKB MD 600.004	1.0

Original data from the reported activity are stored in the primary database Sicada, where they are traceable by the Activity Plan number (AP SFR-15-002). Only data in SKB's databases are accepted for further interpretation and modelling. The data presented in this report are regarded as copies of the original data. Data in the databases may be revised, if needed. Such revisions will not necessarily result in a revision of the P-report, although the normal procedure is that major data revisions entail a revision of the P-report.

## **2      Objectives**

The main aim of the double-packer injection tests in borehole KFR27 and KFR105 was to characterize the hydraulic properties of the rock adjacent to the borehole on a 5 m test scale, i.e. length of a packer-test interval. The positions of all test section were chosen to correspond with the test sections of previously performed PFL logging in the boreholes (Väisäsvaara 2009, Pekkanen et al. 2008). The primary parameter to be determined was hydraulic transmissivity which then has been compared to the calculated transmissivity from previous PFL-measurements.

Other hydraulic parameters of interest were flow regimes and outer hydraulic boundaries. These parameters were analysed using transient evaluation on the double-packer-test responses during the flow- and recovery periods. The results were compared with the corresponding stationary calculated transmissivities from tests performed with PFL to see if any sections showed different results due to the different approaches and test times of each method.



### 3 Scope

#### 3.1 Borehole data

Technical data of the tested boreholes are shown in Table 3-1 and in Appendix 3. The reference point of the borehole is defined as the centre of top of casing (ToC), given as “Elevation” in the table below. The Swedish National coordinate system (RT90) is used for the horizontal coordinates together with RHB70 for the elevation. “Northing” and “Easting” refer to the coordinates of the ToC.

**Table 3-1. Pertinent technical data of borehole KFR105 and KFR27 (printout from SKB database, Sicada).**

<b>KFR105</b>					
<b>Borehole length (m):</b>	306.81				
<b>Drilling Period (s):</b>	<b>From Date</b> 2009-04-21	<b>To Date</b> 2009-06-02	<b>Secup (m)</b> 0.00	<b>Seclow (m)</b> 306.81	<b>Drilling Type</b> Core drilling
<b>Starting point coordinate:</b>	<b>Length (m)</b> 0.00 3.00	<b>Northing (m)</b> 6701789.85 6701786.87	<b>Easting (m)</b> 1633072.96 1633073.25	<b>Elevation</b> –106.82 –107.36	<b>Coord System</b> RT90-RHB70 RT90-RHB70
<b>Angles:</b>	<b>Length (m)</b> 0.00	<b>Bearing</b> 174.48	<b>Inclination ( – = down)</b> –10.12		<b>Coord System</b> RT90-RHB70
<b>Borehole diameter:</b>	<b>Secup (m)</b> 0.00 2.77	<b>Seclow (m)</b> 2.77 306.81	<b>Hole Diam (m)</b> 0.1160 0.0757		
<b>Core diameter:</b>	<b>Secup (m)</b> 0.00 2.77	<b>Seclow (m)</b> 2.77 306.81	<b>Hole Diam (m)</b> 0.1015 0.0502		
<b>Casing diameter:</b>	<b>Secup(m)</b> –0.33	<b>Seclow(m)</b> 2.64	<b>Case In(m)</b> 0.0800	<b>Case Out(m)</b> 0.1000	
<b>KFR27</b>					
<b>Borehole length (m):</b>	501.64				
<b>Drilling Period (s):</b>	<b>From Date</b> 1981-08-06 2008-06-02 2008-10-02	<b>To Date</b> 1981-09-10 2008-06-10 2008-10-22	<b>Secup (m)</b> 0.00 0.00 148.51	<b>Seclow (m)</b> 146.50 148.51 501.64	<b>Drilling Type</b> Core drilling Core drilling Core drilling
<b>Starting point coordinate:</b>	<b>Length (m)</b> 0.00 3.00	<b>Northing (m)</b> 6701714.42 6701714.37	<b>Easting (m)</b> 1633175.52 1633175.39	<b>Elevation</b> 2.87 –0.13	<b>Coord System</b> RT90-RHB70 RT90-RHB70
<b>Angles:</b>	<b>Length (m)</b> 0.00	<b>Bearing</b> 248.20	<b>Inclination ( – = down)</b> –87.42		<b>Coord System</b> RT90-RHB70
<b>Borehole diameter:</b>	<b>Secup (m)</b> 11.91 146.92 148.51 154.44 163.40 164.94 176.97 177.56 177.56 188.03 188.94 189.94 190.94 197.94	<b>Seclow (m)</b> 146.92 148.51 501.64 163.40 164.94 176.97 177.56 188.03 188.94 190.94 197.94 212.49	<b>Hole Diam (m)</b> 0.0765 0.0758 0.0758 0.0315 0.0502 0.0315 0.0502 0.0315 0.0502 0.0315 0.0502 0.0315 0.0840		
<b>Core diameter:</b>	<b>Secup (m)</b> 146.92 148.51 154.44 163.40 164.94 176.97 177.56 177.56 188.03 188.94 189.94 190.94 197.94	<b>Seclow (m)</b> 148.51 154.44 163.40 164.94 176.97 177.56 188.03 188.94 190.94 197.94 212.49	<b>Hole Diam (m)</b> 0.0502 0.0502 0.0315 0.0502 0.0315 0.0502 0.0315 0.0502 0.0315 0.0502 0.0315 0.0502 0.0315		
<b>Casing diameter:</b>	<b>Secup (m)</b> 0.00 430.90	<b>Seclow (m)</b> 11.91 432.90	<b>Case In (m)</b> 0.0770 0.0800	<b>Case Out (m)</b> 0.0840 0.0840	

## 3.2 Performed tests

The positions of the packers of the 5 m long injection test intervals were, as far as possible, the same as the positions of the rubber discs of the difference flow logging (Pekkanen et al. 2008, Väisäsvaara 2009, Hurmerinta and Väisäsvaara 2009). It was not possible to get exactly the same section limits as in the PFL tests but the differences were less than 0.1 m everywhere.

Part of the test procedure and the equipment are described in the measurement system description for PSS (SKB MD 345.100) and in the corresponding method descriptions for hydraulic injection tests (SKB MD 323.001, Table 1-1).

The test times varied a bit between KFR27 and KFR105 and they are listed in Table 3-2 and Table 3-3. Borehole KFR105 is situated down in the SFR-tunnel which is a controlled area. The restrictions for working times and passage down in that area made some test sequences very long in KFR105 since they, in order to save time, continued over night or through other periods where work could not be performed at the site.

### 3.2.1 KFR27

The injection tests in borehole KFR27 are listed in Table 3-2. The injection tests were carried out with the Pipe String System (PSS2) and Water Injection Controlling unit (WIC). The WIC was used to perform and log the injection tests and the PSS2 was used to control the down-hole equipment and the surrounding system (see Chapter 4 for technical details).

Some of the test sections were repeated for different reasons. For example, test section 189.4–194.4 m in KFR27 was measured twice because the time required during the first attempt for achieving a constant head in the test section was judged to be too long, this was due to an unexpected low transmissivity in the section measured. For the evaluation, data from the last test in each section were used.

**Table 3-2. Single-hole injection tests performed in borehole KFR27. Normal test time 20 min but shorter when flow is below lower or over upper measurement limit.**

Borehole	Test section		Section length	Test start date, time	Test stop date, time	Test time
Bh ID	secup	seclow	metres	YYYYMMDD hh:mm	YYYYMMDD hh:mm	min
KFR27	14.85	19.85	5.0	2015-12-18 15:59:07	2015-12-18 16:09:03	10
KFR27	19.85	24.85	5.0	2015-12-21 08:46:58	2015-12-21 09:07:06	20
KFR27	24.85	29.85	5.0	2015-12-21 10:19:33	2015-12-21 10:39:44	20
KFR27	29.85	34.85	5.0	2015-12-21 12:40:10	2015-12-21 13:00:18	20
KFR27	34.85	39.85	5.0	2015-12-21 13:47:18	2015-12-21 13:50:16	3
KFR27	39.85	44.85	5.0	2015-12-21 14:40:42	2015-12-21 15:01:00	20
KFR27	44.85	49.85	5.0	2015-12-21 16:06:52	2015-12-21 16:27:10	20
KFR27	49.85	54.85	5.0	2016-01-07 14:14:28	2016-01-07 14:34:45	20
KFR27	54.85	59.85	5.0	2016-01-07 15:27:16	2016-01-07 15:47:35	20
KFR27	59.85	64.85	5.0	2016-01-07 16:39:54	2016-01-07 17:00:48	21
KFR27	64.85	69.85	5.0	2016-01-08 09:41:04	2016-01-08 10:04:53	24
KFR27	69.85	74.85	5.0	2016-01-08 10:50:13	2016-01-08 11:01:38	11
KFR27	74.85	79.85	5.0	2016-01-08 13:26:13	2016-01-08 13:46:29	20
KFR27	79.85	84.85	5.0	2016-01-08 14:55:05	2016-01-08 15:15:26	20
KFR27	84.85	89.85	5.0	2016-01-08 16:08:22	2016-01-08 16:28:30	20
KFR27	89.85	94.85	5.0	2016-01-11 09:07:05	2016-01-11 09:27:06	20
KFR27	94.85	99.85	5.0	2016-01-11 10:26:30	2016-01-11 10:47:04	21
KFR27	99.85	104.85	5.0	2016-01-11 12:43:49	2016-01-11 13:03:54	20
KFR27	104.85	109.85	5.0	2016-01-11 13:54:48	2016-01-11 14:15:04	20
KFR27	109.85	114.85	5.0	2016-01-11 15:09:13	2016-01-11 15:30:04	21
KFR27	114.85	119.85	5.0	2016-01-11 16:16:02	2016-01-11 16:36:03	20
KFR27	119.85	124.85	5.0	2016-11-13 10:09:43	2016-11-13 10:29:52	20
KFR27	124.85	129.85	5.0	2016-11-13 11:22:50	2016-11-13 11:25:46	3
KFR27	129.85	134.85	5.0	2016-11-13 13:30:20	2016-11-13 13:33:25	3
KFR27	134.85	139.85	5.0	2016-11-13 14:27:53	2016-11-13 14:30:14	2
KFR27	139.4	144.4	5.0	2016-11-13 15:25:42	2016-11-13 15:46:19	21
KFR27	144.4	149.4	5.0	2016-01-15 12:13:07	2016-01-15 12:33:19	20
KFR27	149.4	154.4	5.0	2016-01-15 13:24:34	2016-01-15 13:44:48	20
KFR27	154.4	159.4	5.0	2016-01-15 14:50:06	2016-01-15 15:10:26	20
KFR27	159.4	164.4	5.0	2016-01-18 08:23:54	2016-01-18 08:37:35	14
KFR27	164.4	169.4	5.0	2016-01-18 09:26:44	2016-01-18 09:46:46	20

Borehole	Test section		Section length	Test start date, time	Test stop date, time	Test time
Bh ID	secup	seclow	metres	YYYYMMDD hh:mm	YYYYMMDD hh:mm	min
KFR27	169.4	174.4	5.0	2016-01-18 10:27:21	2016-01-18 10:47:21	20
KFR27	174.4	179.4	5.0	2016-01-18 12:32:58	2016-01-18 12:52:58	20
KFR27	179.4	184.4	5.0	2016-01-18 13:38:27	2016-01-18 13:58:27	20
KFR27	184.4	189.4	5.0	2016-01-18 14:44:50	2016-01-18 15:04:50	20
KFR27	189.4	194.4	5.0	2016-02-02 09:04:19	2016-02-02 09:30:10	26
KFR27	194.4	199.4	5.0	2016-01-19 09:23:04	2016-01-19 09:44:23	21
KFR27	199.4	204.4	5.0	2016-01-19 13:16:40	2016-01-19 13:38:01	21
KFR27	204.4	209.4	5.0	2016-01-19 14:49:19	2016-01-19 15:09:29	20
KFR27	209.4	214.4	5.0	2016-01-19 15:56:28	2016-01-19 16:16:44	20
KFR27	214.4	219.4	5.0	2016-01-20 08:18:54	2016-01-20 08:43:03	24
KFR27	219.4	224.4	5.0	2016-01-20 09:36:28	2016-01-20 09:56:37	20
KFR27	224.4	229.4	5.0	2016-01-20 10:43:26	2016-01-20 11:03:51	20
KFR27	229.4	234.4	5.0	2016-01-20 12:57:23	2016-01-20 13:18:19	21
KFR27	234.4	239.4	5.0	2016-01-20 14:05:01	2016-01-20 14:25:05	20
KFR27	239.4	244.4	5.0	2016-01-20 15:08:45	2016-01-20 15:18:56	10
KFR27	244.4	249.4	5.0	2016-01-20 16:08:59	2016-01-20 16:31:10	22
KFR27	249.4	254.4	5.0	2016-01-21 08:41:50	2016-01-21 09:02:00	20
KFR27	254.4	259.4	5.0	2016-01-21 09:56:02	2016-01-21 09:58:50	3
KFR27	259.4	264.4	5.0	2016-01-21 10:46:47	2016-01-21 11:07:42	21
KFR27	264.4	269.4	5.0	2016-01-21 13:06:20	2016-01-21 13:27:14	21
KFR27	269.4	274.4	5.0	2016-01-21 14:23:17	2016-01-21 14:43:26	20
KFR27	274.4	279.4	5.0	2016-01-21 15:25:40	2016-01-21 15:34:19	9
KFR27	279.4	284.4	5.0	2016-01-22 08:39:42	2016-01-22 09:00:07	20
KFR27	284.4	289.4	5.0	2016-01-22 09:45:06	2016-01-22 09:48:44	4
KFR27	289.4	294.4	5.0	2016-01-22 10:42:25	2016-01-22 11:02:56	21
KFR27	294.4	299.4	5.0	2016-01-22 12:44:12	2016-01-22 13:05:11	21
KFR27	299.4	304.4	5.0	2016-01-22 13:54:43	2016-01-22 14:15:13	20
KFR27	304.4	309.4	5.0	2016-01-22 14:59:32	2016-01-22 15:20:39	21
KFR27	309.4	314.4	5.0	2016-01-22 16:05:49	2016-01-22 16:25:56	20
KFR27	314.4	319.4	5.0	2016-01-25 08:35:35	2016-01-25 08:55:40	20
KFR27	319.4	324.4	5.0	2016-01-25 09:39:56	2016-01-25 10:00:19	20
KFR27	324.4	329.4	5.0	2016-01-25 10:48:44	2016-01-25 11:09:14	21
KFR27	329.4	334.4	5.0	2016-01-25 12:34:36	2016-01-25 12:54:54	20
KFR27	334.4	339.4	5.0	2016-01-25 13:37:07	2016-01-25 13:57:08	20
KFR27	339.4	344.4	5.0	2016-01-25 14:46:49	2016-01-25 15:06:51	20
KFR27	344.4	349.4	5.0	2016-01-25 15:54:49	2016-01-25 16:14:55	20
KFR27	349.4	354.4	5.0	2016-01-26 08:21:32	2016-01-26 08:41:45	20
KFR27	354.4	359.4	5.0	2016-01-26 09:40:09	2016-01-26 10:00:46	21
KFR27	359.4	364.4	5.0	2016-01-26 10:55:09	2016-01-26 11:15:21	20
KFR27	364.4	369.4	5.0	2016-01-26 12:46:01	2016-01-26 13:06:18	20
KFR27	369.4	374.4	5.0	2016-01-26 13:52:26	2016-01-26 14:13:28	21
KFR27	374.4	379.4	5.0	2016-01-26 14:56:35	2016-01-26 15:16:44	20
KFR27	379.4	384.4	5.0	2016-01-26 15:58:26	2016-01-26 16:00:26	2
KFR27	384.4	389.4	5.0	2016-01-27 08:07:33	2016-01-27 08:09:35	2
KFR27	389.4	394.4	5.0	2016-01-27 09:08:39	2016-01-27 09:32:08	23
KFR27	394.4	399.4	5.0	2016-01-27 10:19:35	2016-01-27 10:39:42	20
KFR27	399.4	404.4	5.0	2016-01-27 12:31:42	2016-01-27 12:56:01	24
KFR27	404.4	409.4	5.0	2016-01-27 13:38:25	2016-01-27 13:58:34	20
KFR27	409.4	414.4	5.0	2016-01-27 14:52:51	2016-01-27 15:13:37	21
KFR27	414.4	419.4	5.0	2016-01-27 16:01:06	2016-01-27 16:21:27	20
KFR27	419.4	424.4	5.0	2016-01-28 07:57:47	2016-01-28 08:16:49	19
KFR27	424.4	429.4	5.0	2016-01-28 09:14:28	2016-01-28 09:34:32	20
KFR27	429.4	434.4	5.0	2016-01-28 10:26:11	2016-01-28 10:46:13	20
KFR27	434.4	439.4	5.0	2016-01-28 12:34:37	2016-01-28 12:54:37	20
KFR27	439.4	444.4	5.0	2016-01-28 13:41:02	2016-01-28 14:01:04	20
KFR27	444.4	449.4	5.0	2016-01-28 14:57:34	2016-01-28 15:17:43	20
KFR27	449.4	454.4	5.0	2016-01-28 16:00:23	2016-01-28 16:02:13	2
KFR27	454.4	459.4	5.0	2016-01-29 08:37:04	2016-01-29 08:38:41	2
KFR27	459.4	464.4	5.0	2016-01-29 09:29:54	2016-01-29 09:51:11	21
KFR27	464.4	469.4	5.0	2016-01-29 10:38:29	2016-01-29 10:59:39	21
KFR27	469.4	474.4	5.0	2016-01-29 12:44:08	2016-01-29 12:45:41	2
KFR27	474.4	479.4	5.0	2016-01-29 13:30:47	2016-01-29 13:52:46	22
KFR27	479.4	484.4	5.0	2016-02-01 09:57:37	2016-02-01 09:59:30	2
KFR27	484.4	489.4	5.0	2016-01-29 16:17:59	2016-01-29 16:19:35	2
KFR27	489.4	494.4	5.0	2016-02-01 09:03:42	2016-02-01 09:05:50	2

### 3.2.2 KFR105

The injection tests performed in borehole KFR105 are listed in Table 3-3. The injection tests were carried out with the High Pressure Water Injection Controller (HWIC) system (see Chapter 4 for technical details). The test procedure and the equipment are described in the measurement system description for PSS (SKB MD 345.100) and in the corresponding method descriptions for hydraulic injection tests (SKB MD 323.001, Table 1-1). According to AP SFR-15-002 no recovery period was logged during the injection tests in KF105.

**Table 3-3. Single-hole injection tests performed in borehole KFR105, test time includes recovery.**

Borehole	Test section		Section length	Test start date, time	Test stop date, time	Test time <sup>3)</sup>
Bh ID	secup	seclow	metres	YYYYMMDD hh:mm	YYYYMMDD hh:mm	min*
KFR105	7.9	12.9	5.0	2016-05-17 12:21	2016-05-17 12:32	11
KFR105	12.9	17.9	5.0	2016-05-18 08:16	2016-05-18 08:26	11
KFR105	17.9	22.9	5.0	2016-05-18 09:38	2016-05-18 09:41	3
KFR105	22.9	27.9	5.0	2016-05-18 11:44	2016-05-18 12:26	41
KFR105	27.9	32.9	5.0	2016-05-18 13:52	2016-05-18 14:59	67
KFR105	32.9	37.9	5.0	2016-05-23 07:57	2016-05-23 08:39	42
KFR105	37.9	42.9	5.0	2016-05-23 09:39	2016-05-23 10:20	41
KFR105	42.9	47.9	5.0	2016-05-23 11:06	2016-05-23 12:29	83
KFR105	47.9	52.9	5.0	2016-05-23 13:18	2016-05-23 14:03	44
KFR105	52.9	57.9	5.0	2016-05-23 14:47	2016-05-23 15:27	40
KFR105	57.9	62.9	5.0	2016-05-24 08:47	2016-05-24 09:28	41
KFR105	62.9	67.9	5.0			
KFR105	67.9	72.9	5.0	2016-05-24 12:40	2016-05-24 13:02	22
KFR105	72.9	77.9	5.0	2016-05-24 13:48	2016-05-24 14:28	40
KFR105	77.9	82.9	5.0	2016-05-26 07:55	2016-05-26 08:36	41
KFR105	82.9	87.9	5.0	2016-05-26 09:31	2016-05-26 10:12	40
KFR105	87.9	92.9	5.0	2016-05-26 11:04	2016-05-26 11:31	26
KFR105	92.9	97.9	5.0	2016-05-26 13:09	2016-05-26 13:49	41
KFR105	97.9	102.9	5.0	2016-05-26 14:59	2016-05-26 15:22	23
KFR105	102.9	107.9	5.0	2016-05-27 08:59	2016-05-27 09:41	42
KFR105	107.9	112.9	5.0	2016-05-27 12:13	2016-05-27 12:59	46
KFR105	112.9	117.9	5.0	2016-05-27 13:43	2016-05-27 14:15	31
KFR105	117.9	122.9	5.0	2016-05-30 08:16	2016-05-30 08:19	3
KFR105	122.9	127.9	5.0	2016-05-30 11:33	2016-05-30 13:00	87
KFR105	127.9	132.9	5.0	2016-05-30 13:52	2016-05-30 14:32	41
KFR105	132.9	137.9	5.0	2016-05-31 08:35	2016-05-31 09:15	41
KFR105	137.9	142.9	5.0	2016-05-31 10:14	2016-05-31 10:57	44
KFR105	142.9	147.9	5.0	2016-05-31 12:14	2016-05-31 12:56	41
KFR105	147.9	152.9	5.0	2016-05-31 13:49	2016-05-31 14:30	41
KFR105	152.9	157.9	5.0	-	-	
KFR105	157.9	162.9	5.0	2016-06-01 09:07	2016-06-01 09:49	42
KFR105	162.9	167.9	5.0	2016-06-01 10:33	2016-06-01 11:14	41
KFR105	167.9	172.9	5.0	2016-06-01 12:23	2016-06-01 13:06	44
KFR105	172.9	177.9	5.0	2016-06-01 14:01	2016-06-01 14:41	41
KFR105	177.9	182.9	5.0	2016-06-02 07:50	2016-06-02 08:31	41
KFR105	182.9	187.9	5.0	2016-06-02 09:25	2016-06-02 10:18	53
KFR105	187.9	192.9	5.0	2016-06-02 11:03	2016-06-02 12:54	111
KFR105	192.9	197.9	5.0	2016-06-02 13:40	2016-06-02 13:54	14
KFR105	197.9	202.9	5.0	2016-06-02 14:41	2016-06-02 15:22	41
KFR105	202.9	207.9	5.0	2016-06-07 12:12	2016-06-07 12:53	41
KFR105	207.9	212.9	5.0	2016-06-07 14:13	2016-06-07 14:26	13
KFR105	212.9	217.9	5.0	2016-06-09 07:42	2016-06-09 08:23	41
KFR105	217.9	222.9	5.0	2016-06-09 09:16	2016-06-09 09:57	41
KFR105	222.9	227.9	5.0	2016-06-09 10:48	2016-06-09 10:50	2
KFR105	227.9	232.9	5.0	2016-06-09 12:43	2016-06-09 12:46	3
KFR105	232.9	237.9	5.0	2016-06-09 13:47	2016-06-09 13:49	2
KFR105	237.9	242.9	5.0	2016-06-09 14:43	2016-06-09 15:24	41
KFR105	242.9	247.9	5.0	2016-06-10 08:28	2016-06-10 09:08	41
KFR105	247.9	252.9	5.0	2016-06-10 09:54	2016-06-10 10:36	41
KFR105	252.9	257.9	5.0	2016-06-10 11:20	2016-06-10 12:44	84
KFR105	257.9	262.9	5.0	2016-06-10 13:59	2016-06-10 14:02	2

Borehole	Test section		Section length	Test start date, time	Test stop date, time	Test time <sup>3)</sup>
Bh ID	secup	seclow	metres	YYYYMMDD hh:mm	YYYYMMDD hh:mm	min*
KFR105	262.9	267.9	5.0	2016-06-13 07:52	2016-06-13 09:25	93
KFR105	267.9	272.9	5.0	2016-06-13 09:58	2016-06-13 10:39	40
KFR105	272.9	277.9	5.0	2016-06-13 11:28	2016-06-13 11:30	2
KFR105	277.9	282.9	5.0	2016-06-13 13:10	2016-06-13 13:52	42
KFR105	282.9	287.9	5.0	2016-06-13 14:37	2016-06-13 15:23	46
KFR105	287.9	292.9	5.0	2016-06-14 09:45	2016-06-14 09:49	4
KFR105	292.9	297.9	5.0	2016-06-14 10:33	2016-06-14 11:16	43
KFR105	297.9	302.9	5.0	2016-06-14 12:57	2016-06-14 13:39	41
KFR105 <sup>1)</sup>	152.9	157.9	5.0	2016-06-15 12:15	2016-06-15 15:16	181
KFR105 <sup>1)</sup>	32.9	37.9	5.0	2016-06-16 10:32	2016-06-16 14:33	241
KFR105 <sup>2)</sup>	265	303	42	2016-04-19 07:44	2016-04-19 08:45	31
KFR105 <sup>2)</sup>	170	264	94	2016-04-19 08:45	2016-04-19 09:45	30
KFR105 <sup>2)</sup>	138	169	31	2016-04-19 09:45	2016-04-19 10:35	30
KFR105 <sup>2)</sup>	120	137	17	2016-04-19 10:45	2016-04-19 11:45	30
KFR105 <sup>2)</sup>	4	119	115	2016-04-19 12:18	2016-04-19 13:20	31

<sup>1)</sup> Long test time, no recovery.

<sup>2)</sup> Tests in permanent installation in borehole.

<sup>3)</sup> Test time vary due to flow below measurement limit and other practical reasons.

### 3.3 Equipment checks

Functioning checks of sensors in WIC was made prior test start in KFR27. In order to check the function of the pressure sensors, the air pressure was recorded and found to be as expected. While lowering, the sensors showed good agreement with the total head of water (p/pg).

In KFR105, which is located in the SFR-tunnel, the HWIC-system was used including the newly developed pipe feeder. Simple functioning checks of down-hole sensors were done at every change of test section interval. Checks were also made continuously while lowering the pipe string along the borehole.



## 4 Description of equipment

### 4.1 Overview

#### 4.1.1 Measurement container

All of the equipment needed to perform the injection tests in KFR27 is located in a steel container (Figure 4-1) and the WIC is positioned beside the water tank within the PSS2. The container is divided into two compartments; a data-room and a workshop. The container is placed on pallets in order to obtain a suitable working level in relation to the borehole casing.

The hoisting rig is of a hydraulic chain-feed type. The jaws, holding the pipe string, are opened hydraulically and closed mechanically by springs. The rig is equipped with a load transmitter and the load limit may be adjusted. The maximum load is 22 kN.

The packers and the test valve are operated hydraulically by water filled pressure vessels. Expansion and release of packers, as well as opening and closing of the test valve, is done using magnetic valves manually controlled from the container.

The injection system consists of the WIC or HWIC-unit, a water tank, pipe system and a water tank. The HWIC unit is a modified WIC for handling the higher pressures prevailing in tunnels hence used for testing KFR105. Since HWIC has a more modern PLC-unit and controlling system both injection pressure and flow rate may be manually or automatically controlled in comparison to the WIC were only automatically controlled tests are possible.

Since regulations prohibited the use of PSS2 during tests down in the SFR tunnel, another set-up was used for the injection tests. The HWIC, a water tank, a pipe rig and a pressure vessel was located separately at the borehole in SFR. All downhole equipment was similar to the ones used in KFR27.

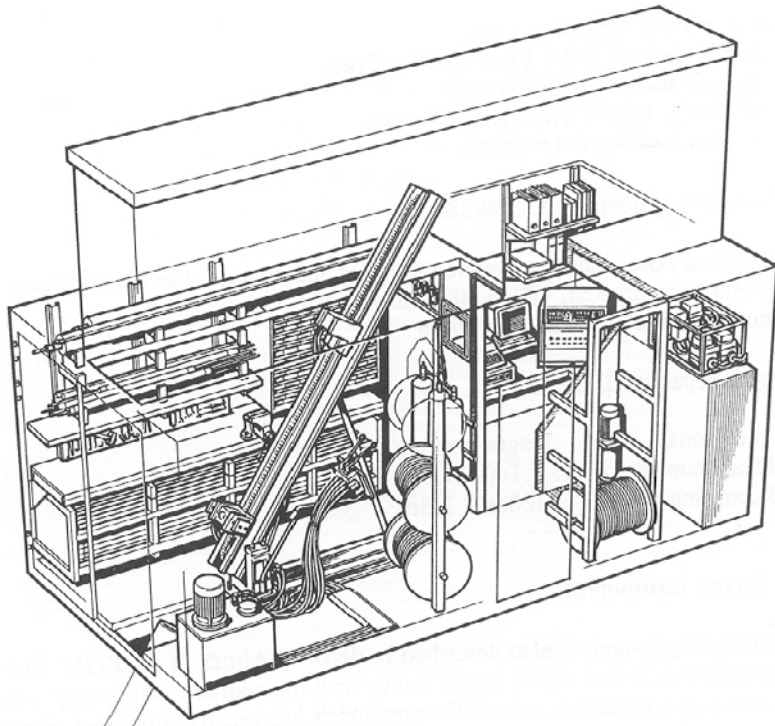


*Figure 4-1. Outline of the PSS2 container with equipment.*

#### 4.1.2 Down-hole equipment

A schematic drawing of the down-hole equipment is shown in Figure 4-2. The pipe string consists of aluminium pipes of 3 m length, connected by stainless steel taps sealed with double o-ring seals. Pressure is normally measured above ( $P_a$ ), within ( $P$ ) and below ( $P_b$ ) the test section, which is isolated by two packers, and the groundwater temperature in the test section is also measured. Since there was a lack of transducers, only pressure within the test section was measured during these tests. The hydraulic connection between the pipe string and the test section can be closed or opened by a test valve operated by the measurement system. At the lower end of the borehole equipment, a level indicator (calliper type) gives a signal as the reference depth marks along the borehole are passed. The length of the test section may be varied (normally 5, 20 or 100 metres).

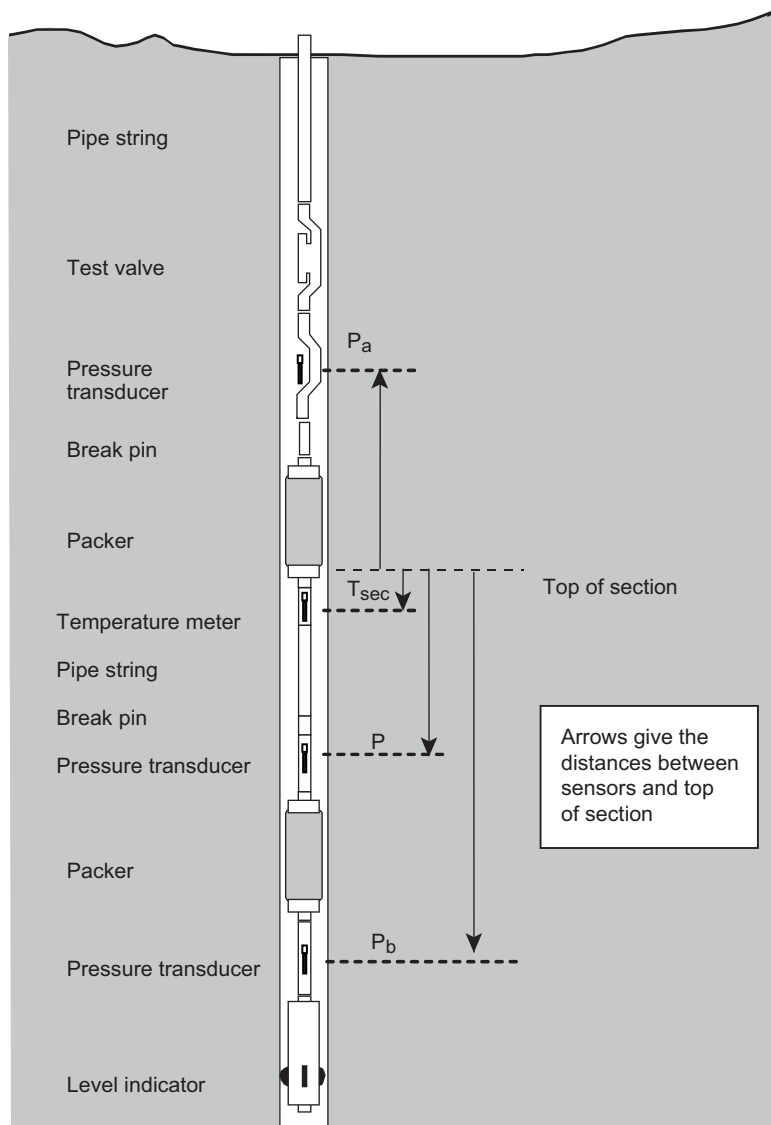


**Figure 4-2.** Schematic drawing of the down-hole equipment in the PSS system.  $T_{sec}$ ,  $P_a$  and  $P_b$  was not used in these tests.

## 4.2 Measurement sensors

Technical data for the measurement sensors in the PSS system together with corresponding data of the system are shown in Table 4-1. The sensors are components of the PSS system. The accuracy of the PSS system may also be affected by the I/O-unit, cf. Figure 4-3, and the calibration of the system.

The pressure sensor position is fixed relative to the top of the test section. In Table 4-2, the position of the sensor is given with top of test section as reference (Figure 4-2).

**Table 4-1. Technical data for sensors together with estimated data for the PSS system (based on current experience).**

Technical specification					
Parameter		Unit	Sensor	PSS	Comments
Absolute pressure	Output signal Meas. range Resolution Accuracy <sup>1)</sup>	mA MPa kPa % F.S	4–20 0–13.5 < 1.0 0.1		
Differential pressure, 200 kPa	Accuracy	kPa		< ±5	Estimated value
Temperature	Output signal Meas. range Resolution Accuracy	mA °C °C °C	4–20 0–32 < 0.01 ±0.1		
Flow Qbig (HWIC)	Output signal Meas. range Resolution Accuracy <sup>2)</sup>	mA m <sup>3</sup> /s m <sup>3</sup> /s % O.R	4–20 2·10 <sup>-6</sup> –1.5·10 <sup>-3</sup> 5·10 <sup>-9</sup> 0.2–20		The specific accuracy is depending on actual flow
Flow Qsmall (HWIC)	Output signal Meas. range Resolution Accuracy <sup>3)</sup>	mA m <sup>3</sup> /s m <sup>3</sup> /s % O.R	4–20 3·10 <sup>-8</sup> –3·10 <sup>-5</sup> 5·10 <sup>-9</sup> 0.5–30		The specific accuracy is depending on actual flow

<sup>1)</sup> 0.1 % of full scale. Includes hysteresis, linearity and repeatability.

<sup>2)</sup> Maximum error in % of actual reading (% o.r.). The higher numbers correspond to the lower flow.

<sup>3)</sup> Maximum error in % of actual reading (% o.r.). The higher numbers correspond to the lower flow.

**Table 4-2. Position of sensors in the borehole and displacement volume of equipment in the test section in borehole KFR27 and KFR105.**

Parameter	Length of test section (m)	
	5	
	(L)	(m)
Equipment displacement volume in test section <sup>1)</sup>	3.6	
Total volume of test section <sup>2)</sup>	22.56	
Position for sensor P, pressure in test section, (m above secup) <sup>3)</sup>	-4.10	

<sup>1)</sup> Displacement volume in test section due to pipe string, signal cable, sensors and packer ends (in litres).

<sup>2)</sup> Total volume of test section ( $V = \text{section length} \times \pi \times d^2/4$ ) (in litres).

<sup>3)</sup> Position of sensor relative top of test section. A negative value indicates a position below top of test section, (secup).

## 4.3 Data acquisition system

The data acquisition system used in these tests is a PLC in the WIC/HWIC unit seen in Figure 4-3. All data is stored on a SD-card in the PLC in a file with .txt-format (WIC) or .CSV (HWIC) and is easily transferred to a PC for backup. The data files can then be opened in an excel file for easy plotting or further processing. The WIC/HWIC unit also provide a plot function on the display making it possible to see all parameters graphically throughout the test. The PLC-unit is used for manual control of the pump, start and stop of test as well as field calibration of all transducers.



**Figure 4-3.** The HWIC (left) and WIC unit used in the injection tests in KFR105 and KFR27 respectively.

## 5 Execution

### 5.1 Preparation

#### 5.1.1 Calibration

All sensors included in WIC and HWIC systems are calibrated at the Geosigma engineering service station in Uppsala. Calibration is generally performed at least every year. Results from calibration, e.g. calibration constants, of sensors are kept at Geosigma (WIC) and SKB (HWIC). If a sensor is replaced at the test site, calibration constants are altered as well. If a new, un-calibrated, sensor is to be used, calibration may be performed afterwards and data re-calculated.

#### 5.1.2 Cleaning of equipment

Cleaning of the borehole equipment was performed according to the cleaning instruction SKB MD 600.004 (see Table 1-1), level 1.

### 5.2 Test performance

Generally, the tests were performed according to the Activity Plan AP SFR-15-002 specific for this project and the method document SKB MD 323.001. Exceptions to this are presented in Section 5.5.

#### 5.2.1 Test principle

The injection tests were carried out while maintaining a constant head of generally 200 kPa (ca. 20 m of freshwater) in the test section. Before start of the injection period in KFR27, approximately steady-state pressure conditions prevailed in the test section. In KFR105, which is located in the SFR tunnel below surface, the borehole had been open for a while hence the natural background pressure had to be calculated. After the injection period, the pressure recovery was measured in KFR105 but not in KFR27. By experience it is known that tests performed from the surface give sufficient data from the injection to be used for transient evaluation.

For injection tests in KFR27 and KFR105 the injection phase was interrupted if the injection flow was clearly below the measurement limit of 0.002 L/min.

#### 5.2.2 Test procedure

A test cycle of a standard injection test includes the following phases: 1) Transfer of down-hole equipment to the next section, 2) Packer inflation, 3) Pressure stabilisation, 4) Injection, 5) Pressure recovery (in KFR105) and 6) Packer deflation.

The estimated times for the various phases of the injection tests are presented in Table 5-1. In KFR27 no pressure recovery was made, Table 5-1. These times may however vary due to both practical reasons as well as borehole features. If a test, for instance, has a flow below measurement limit it is interrupted and in KFR105 no recovery is registered.

**Table 5-1. Packer inflation times, pressure stabilisation times and test times used for the injection tests in KFR27 and KFR105.**

Test section length (m)	Packer inflation time (min)	Time for pressure stabilisation (min)	Injection period (min)	Recovery period (min)	Total time/test (min) <sup>1)</sup>
KFR27	15	15	20	-	50
KFR105	15	15	20	20	70

<sup>1)</sup> Exclusive of trip times in the borehole.

## 5.3 Data handling

There are no documents or methods described in SKB's system for handling data from the equipment used for the injection tests in this project.

The WIC and HWIC files were, after been transferred to a PC, converted to an Excel® file using a macro. This file contains all data from the test including background data for the borehole, test position and performer of the test. The units presented for the logged data are kPa and L/min. The raw data files were delivered to the data base Sicada.

The macro used for converting files from WIC automatically names the file with borehole id, top of test section and part of test. In KFR27 a pre-test file with the extension 0 was made with the WIC to be able to collect data during packer expansion and pressure stabilization and another file with the extension 0.1 was made during the actual injection test (as for example KFR27K\_144.4\_0.xlsx and KFR27K\_149.4\_0.1.xlsx).

The data files from HWIC comes in a .CSV-format (i.e. SFRsecupM.CSV) that is possible to easily convert into Excel format without using a macro. Since the HWIC equipment enables logging of all test cycles only one file is generated for an entire test. The converted file is named KFR105 – secupm.xlsx (as for example KFR105 – 12m.xlsx).

The excel files from the tests are then analysed to derive background pressure ( $P_0$ ), time for test start ( $t_0$ ), time, flow and final pressure at test stop ( $t_i$ ,  $Q$  and  $P_i$ ), and pressure at stop of recovery ( $P_p$ ) to be used for the analysis with the AQTESOLV software (ver 4.5/Pro, Hydrosolve, Inc.).

Backup of data files were created on a regular basis by sending the files to the Geosigma server using internet. Raw data files from all the test has been sent to SKB and the files from KFR27 is named KFR27K\_(secup)\_0.txt or KFR27K\_(secup)\_0.1.txt were \_0 is the file were packer expansion is logged and \_0.1 is the file from the injection period. Files from tests in KFR105 are named SFR(secup)M.CSV.

## 5.4 Analysis and interpretation

### 5.4.1 General

The injection tests in KFR27 were performed as transient constant head tests without a recovery period to save time. The injection tests in KFR105 was however followed by a pressure recovery period. From the injection period, the (reciprocal) value of the flow rate ( $Q^{-1}$ ) was plotted in log-log and lin-log diagrams versus time together with the corresponding derivative ( $d(Q^{-1})/dt$ ). From the recovery period, the pressure was plotted versus Agarwal equivalent time (Aqtesolve 4.5) in lin-log and log-log diagrams, respectively, together with the corresponding derivative. The data processing of the measured data was done according to the description in Chapter 5.3.

For evaluation of the test data, no corrections of the measured flow rate and absolute pressure data (e.g. due to barometric pressure variations or tidal fluctuations) have been made. For short-time single-hole tests, such corrections are generally not needed, unless very small pressure changes are applied. No subtraction of the barometric pressure from the measured absolute pressure has been made, since the length of the test periods are short relative to the time scale for barometric pressure changes. In addition, relative pressure differences rather than the absolute pressure magnitudes are used in the evaluation.

### 5.4.2 Measurement limit of flow rate and specific flow rate

The estimated standard lower measurement limit of flow rate for injection tests with WIC and HWIC is set to 2 mL/min ( $3 \times 10^{-8} \text{ m}^3/\text{s}$ ). The lower measurement limit for transmissivity is defined in terms of the specific flow rate, i.e. flow rate divided by change in groundwater level (Q/s). The minimum specific flow rate corresponds to the estimated lower measurement limit of the flow rate together with the actual injection pressure during the test. The intention during this test campaign was to use a standard injection pressure of 200 kPa (20 m water column). Still, the injection pressure can be considerably different (see Section 6.2.3). An apparently low injection pressure is often the result of

a test section of low conductivity due to a pressure increase, caused by packer expansion, before the injection start. A highly conductive section may also result in a low injection pressure due to limited flow capacity of PSS.

Whenever the final flow rate ( $Q_p$ ) was not possible to define (eg., not clearly above the measurement noise before and after the injection period), the estimated lower measurement limit for specific flow rate was based on the estimated lower measurement limit for flow rate for the specific test and a standard injection pressure of 200 kPa. This is done in order to avoid excessively high, apparent estimates of the specific flow rate for these low conductivity sections, which would have resulted if the actual pressure difference at start of injection had been used as injection pressure.

The lower measurement limits for the flow rate correspond to different values of steady-state transmissivity,  $T_M$ , depending on the section lengths used in the factor  $C_M$  in Moye's formula, as described in the Instruction for analysis of injection and single-hole pumping tests (SKB MD 320.004). In this project the section length was 5 metres in all cases except for the tests conducted on the installed sections in KFR105.

The practical upper measurement limit of hydraulic transmissivity for the PSS system using WIC or HWIC is estimated at a flow rate of c 30 L/min ( $5 \times 10^{-4} \text{ m}^3/\text{s}$ ) and an injection pressure of c 1 m. Thus, the upper measurement limit for the specific flow rate is  $5 \times 10^{-4} \text{ m}^2/\text{s}$ . However, the practical upper measurement limit may vary, depending on e.g. depth of the test section (friction losses in the pipe string).

#### 5.4.3 Qualitative analysis

Initially, a qualitative evaluation of actual flow regimes, e.g. wellbore storage (WBS), pseudo-linear flow regime (PLF), pseudo-radial flow regime (PRF), pseudo-spherical flow regime (PSF) and pseudo-stationary flow regime (PSS), respectively, was performed. In addition, indications of outer boundary conditions during the tests were identified. The qualitative evaluation was mainly interpreted from the log-log plots of flow rate and pressure together with the corresponding derivatives.

In particular, time intervals with pseudo-radial flow, reflected by a constant derivative of zero slope in the test diagrams, were identified. Pseudo-linear flow may, at the beginning of the test, be reflected by a straight line of slope 0.5 or less in log-log diagrams, both for the measured variable (flow rate or pressure) and the derivative. A true spherical flow regime is reflected by a straight line with a slope of -0.5 for the derivative. However, other slopes may indicate transitions to pseudo-spherical (leaky) or pseudo-stationary flow. The latter flow regime corresponds to almost stationary conditions with a derivative approaching zero.

The interpreted flow regimes can also be described in terms of the distance from the borehole:

- **Inner zone:** Representing very early responses that may correspond to the fracture properties close to the borehole which may possibly be affected by turbulent head losses. These properties are generally reflected by the skin factor.
- **Middle zone:** Representing the first response from which it is considered possible to evaluate the hydraulic properties of the formation close to the borehole.
- **Outer zone:** Representing the response at late times of hydraulic structure(s) connected to the hydraulic feature for the middle zone. Sometimes it is possible to deduce the possible character of the actual feature or boundary and evaluate the hydraulic properties.

Due to the limited resolution of the flow meter and pressure sensor, the derivative may sometimes indicate a false horizontal line by the end of periods with pseudo-stationary flow. Apparent no-flow (NFB) and constant head boundaries (CHB), or equivalent boundary conditions of fractures, are reflected by an increase/decrease of the derivative, respectively.

#### 5.4.4 Quantitative analysis

##### **Injection tests**

A preliminary steady-state analysis of transmissivity according to Moye's formula (denoted TM) (Reference) was made for the injection period for all tests in conjunction with the qualitative analysis according to the following equations:

$$T_M = \frac{Q_p \cdot \rho_w \cdot g}{dp_p} \cdot C_M \quad (5-1)$$

$$C_M = \frac{1 + \ln\left(\frac{L_w}{2r_w}\right)}{2\pi} \quad (5-2)$$

$Q_p$  = flow rate by the end of the flow period ( $\text{m}^3/\text{s}$ )

$\rho_w$  = density of water ( $\text{kg}/\text{m}^3$ )

$g$  = acceleration of gravity ( $\text{m}/\text{s}^2$ )

$C_M$  = geometrical shape factor (-)

$dp_p$  = injection pressure  $p_p - p_i$  (Pa)

$r_w$  = borehole radius (m)

$L_w$  = section length (m)

From the results of the qualitative evaluation, appropriate interpretation models for the quantitative evaluation of the tests were selected. When possible, transient analysis was made on both the injection and recovery periods of the tests.

The transient analysis was performed using a special version of the test analysis software AQTESOLV, which enables both visual and automatic type curve matching. The quantitative transient evaluation is generally carried out as an iterative process of manual type curve matching and automatic matching. For the injection period, a model based on the Jacob and Lohman (1952) solution was applied for estimating the transmissivity and skin factor for an assumed value on the storativity when a certain period with pseudo-radial flow could be identified (first acting radial flow regime). The model is based on the effective wellbore radius concept to account for non-zero (negative) skin factors according to Hurst et al. (1969).

The storativity was calculated using an empirical regression relationship between storativity and transmissivity, see Equation 5-3 (Rhén et al. 1997).

$$S = 0.0007 \cdot T^{0.5} \quad (5-3)$$

$S$  = storativity (-)

$T$  = transmissivity ( $\text{m}^2/\text{s}$ )

Firstly, the transmissivity and skin factor were obtained by type curve matching on the data curve using a fixed storativity value of  $10^{-6}$ , according to the instruction SKB MD 320.004. From the transmissivity value obtained, the storativity was then calculated according to Equation 5-3 and the type curve matching was repeated. In most cases the change of storativity did not significantly alter the calculated transmissivity by the new type curve matching. Instead, the estimated skin factor, which is strongly correlated to the storativity using the effective borehole radius concept, was altered correspondingly.

For transient analysis of the recovery period, a model presented by Dougherty and Babu (1984) was used when a certain period with pseudo-radial flow could be identified. In this model, a variety of transient solutions for flow in fractured porous media are available, accounting for e.g. wellbore storage and skin effects, double porosity etc. The solution for wellbore storage and skin effects is analogous to the corresponding solution presented in Earlougher (1977) based on the effective wellbore radius concept to account for non-zero (negative) skin factors. However, for tests in isolated test sections, wellbore storage is represented by a radius of a fictive standpipe (denoted fictive casing radius,  $r(c)$ )

connected to the test section, cf. Equation 5-6. This concept is equivalent to calculating the wellbore storage coefficient C from the compressibility in an isolated test section according to Equation 5-5. The storativity was calculated using Equation 5-3 in the same way as described above for the transient analysis of the injection period. In addition, the wellbore storage coefficient was estimated, both from the simulated value on the fictive casing radius r(c).

For tests characterized by pseudo-spherical (leaky) flow or pseudo-stationary flow during the injection period, a model by Hantush (1959) for constant head tests was adopted for the evaluation. In this model, the skin factor is not separated but can be calculated from the simulated effective borehole radius according to Equation 5-4. This model also allows calculation of the wellbore storage coefficient according to Equation 5-6. In addition, the leakage coefficient K'/b' can be calculated from the simulated leakage factor r/B. The corresponding model for constant flow rate tests, Hantush and Jacob (1955), was applied for evaluation of the recovery period for tests showing pseudo-spherical- or pseudo-stationary flow during this period.

$$\zeta = \ln(r_w/r_{wf}) \quad (5-4)$$

$\zeta$  = skin factor

$r_w$  = borehole radius (m)

$r_{wf}$  = effective borehole radius

Some tests showed fracture responses (initial slope of 0.5 or less in a log-log plot). No transient interpretations were made at these fracture responses. But if needed a model presented in Ozkan and Raghavan (1991a, b) for a uniform-flux vertical fracture embedded in a porous medium model for an equivalent single fracture can be used for the transient analysis as a complement to standard models for pseudo-radial flow. With this model the hydraulic conductivity of the rock perpendicular ( $K_x$ ) and parallel ( $K_y$ ) to the fracture can be estimated. In this case, the ratio  $K_x/K_y$  was assumed to be 1.0 (one). Type curve matching provided values of  $K_x$  and  $L_f$  assuming a value on the specific storativity  $S_s$  based on Equation (5-3), where  $L_f$  is the theoretical fracture length. The test section length was then used to convert  $K_x$  and  $S_s$  to transmissivity  $T = K_x \cdot L$  and to storativity  $S = S_s \cdot L$ , respectively of the rock in analysis by fracture models. Such estimates of transmissivity from fracture models may be compared with corresponding values from models for pseudo-radial flow in the same test section.

The different transient estimates of transmissivity from the injection and recovery period, respectively, were then compared and examined. One of these was chosen as the best representative value of the transient transmissivity of the formation adjacent to the test section. This value is denoted  $T_T$ . In cases with more than one pseudo-radial flow regime during the injection or recovery period, the first one is in most cases assumed as the most representative for the hydraulic conditions in the rock close to the tested section.

Finally, a representative value of transmissivity of the test section,  $T_R$ , was chosen from  $T_T$  and  $T_M$ . The latter transmissivity is to be chosen whenever a transient evaluation of the test data is not possible or not being considered as reliable. If the flow rate by the end of an injection period ( $Q_p$ ) is too low to be defined, and thus neither  $T_T$  nor  $T_M$  can be estimated, the representative transmissivity for the test section is considered to be less than  $T_M$  based on the estimated lower measurement limit for Q/s (i.e.  $T_R < T_M = Q/s\text{-measl-L}\cdot C_M$ ).

Estimated values of the borehole storage coefficient, C, based on actual borehole geometrical data and assumed fluid properties are shown in Table 5-3 together with the estimated effective  $C_{eff}$  from laboratory experiments (Ludvigson et al. 2007). The net water volume in the test section,  $V_w$ , has in Table 5-3 been calculated by subtracting the volume of equipment in the test section (pipes and thin hoses) from the total volume of the test section. For an isolated test section, the wellbore storage coefficient, C, may be calculated as by Almén et al. (1986):

$$C = V_w \cdot c_w = L_w \cdot \pi \cdot r_w^2 \cdot c_w \quad (5-5)$$

$V_w$  = water volume in test section (m<sup>3</sup>)

$r_w$  = nominal borehole radius (m)

$L_w$  = section length (m)

$c_w$  = compressibility of water (Pa<sup>-1</sup>)

**Table 5-3. Calculated net values of C, based on the actual geometrical properties of the borehole and equipment configuration in the test section ( $C_{net}$ ) together with the effective wellbore storage coefficient ( $C_{eff}$ ) for injection tests from laboratory experiments. Equation 5-5.**

$r_w$ (m)	$L_w$ (m)	Volume of test section (m <sup>3</sup> )	Volume of equipment in section (m <sup>3</sup> )	$V_w$ (m <sup>3</sup> )	$C_{net}$ (m <sup>3</sup> /Pa)	$C_{eff}$ (m <sup>3</sup> /Pa)
0.038	5	0.023	0.004		0.019	8.6E-12

Furthermore, when using the model by Dougherty and Babu or Hantush, a fictive casing radius,  $r(c)$ , is obtained from the parameter estimation of the recovery period. This value can then be used for calculating C as by Almén et al. 1986:

$$C = \frac{\pi \cdot r(c)^2}{\rho \cdot g} \quad (5-6)$$

The radius of influence at a certain time may be estimated from Jacob's approximation of the Theis' well function, Cooper and Jacob (1946):

$$r_i = \sqrt{\frac{2.25 T t}{S}} \quad (5-7)$$

T = representative transmissivity from the test (m<sup>2</sup>/s)

S = storativity estimated from Equation 5-3

$r_i$  = radius of influence (m)

t = time after start of injection (s)

An  $r_i$ -index (-1, 0 or 1) is defined to characterize the hydraulic conditions by the end of the test. The  $r_i$ -index is defined as shown below.

- $r_i$ -index = 0: The transient response indicates that the size of the hydraulic feature tested is greater than the radius of influence based on the actual test time ( $t_2 = t_p$ ), i.e. the PRF is continuing at stop of the test. This fact is reflected by a flat derivative at this time.
- $r_i$ -index = 1: The transient response indicates that the hydraulic feature tested is connected to a hydraulic feature with lower transmissivity or an apparent barrier boundary (NFB). This fact is reflected by an increase of the derivative. The size of the hydraulic feature tested is estimated as the radius of influence based on  $t_2$ .
- $r_i$ -index = -1: The transient response indicates that the hydraulic feature tested is connected to a hydraulic feature with higher transmissivity or an apparent constant head boundary (CHB). This fact is reflected by a decrease of the derivative. The size of the hydraulic feature tested is estimated as the radius of influence based on  $t_2$ .

## 5.5 Nonconformities

The test programme in KFR27 and KFR105 was carried out according to the Activity Plan AP SFR-15-002 with the following exceptions:

- In order to use the same test section positions as with PFL, an overlapping section between 139.4 m and 139.85 m was measured in KFR27.
- In the 5 m section tests between 479.4–494.4 m in KFR27 the pressure was above the upper measurement limit of the pressure transducer in the borehole. Injection tests were performed with an internal pressure transducer in WIC at the surface.
- In the injection test in section 189.4–194.4 m in KFR27 the flow was above measurement limit. This could either be due to a very conductive fracture or due to leakage during the test.
- In KFR105 injection tests with longer injection time than usually and without recovery were performed in sections 32.9–37.9 m and 152.9–157.9 m.
- Data from the injection test in section 62.9–67.9 m in KFR105 is missing hence no plot or evaluation possible. The test was however stopped because flow dropped below measurement limit.
- Data from the injection test in section 152.9–157.9 m in KFR105 is missing hence no plot or evaluation possible. The test section was later rerun with a longer injection period (see above).

## 6 Results

### 6.1 Nomenclature and symbols

The nomenclature and symbols used for the results of the injection tests in KFR27 and KFR105 are in accordance with the Instruction for analysis of injection and single-hole pumping tests (SKB MD 320.004). Symbols used by the AQTESOLV software are explained in Appendix 2 and 3. Symbols used by the AQTESOLV software are explained in Appendix 2.

Original data from the reported activity are stored in the primary database Sicada. Data are traceable in Sicada by the Activity Plan number.

Nomenclature used:

$b$  = length of test section

$T_M$  = steady state transmissivity from Moye's equation

$T_F$  = transmissivity from transient evaluation of injection period, single-hole test

$T_S$  = transmissivity from transient evaluation of recovery period, single-hole test

$T_T$  = chosen transmissivity from transient evaluation of single-hole test

$T_R$  = transmissivity chosen as representative for the test section

$S$  = calculated storativity

$\xi$  = skin factor

$r_i$  = radius of influence from pumping

$r_{i,\text{index}}$  = hydraulic condition at the end of test

### 6.2 Routine evaluation of the single-hole injection tests

#### 6.2.1 General test data

General test data and selected pressure and flow data from all tests are listed in Appendix 2.

#### 6.2.2 Length corrections

The down-hole equipment is normally supplied with a level indicator located ca. 3 m below the lower packer in the test section, see Figure 4-2. The level indicator transmits a signal each time a reference mark in the borehole is passed. Reference marks were milled into the borehole wall at approximately every 50 m. This equipment was used in KFR27 but stopped working about halfway through the tests. No further adjustments after the measurements, e.g. by linear interpolation between reference marks were made.

At each detected mark, the length scale for the injection tests was adjusted according to the reported length to the reference mark. After the detection unit had failed the last noted adjustment of -0.21 m was used for all following test sections in KFR27.

#### 6.2.3 General results

For the injection tests, transient evaluation was conducted on the drawdown period and in KFR105 also on the recovery period (e.g. transmissivity  $T_f$  and  $T_s$ , respectively) according to the methods described in Section 5.4.4. The steady-state transmissivity ( $T_M$ ) was calculated by Moye's formula according to Equation 5-1. Injection tests with a final flow rate below the measurement limit,  $Q_p$ , or with a non-definable flow regime were only evaluated by the steady-state method. All other tests were evaluated with both transient and steady-state methods. The quantitative analysis was conducted using the AQTESOLV software.

For all test with a definable final flow rate a transient evaluation was possible and considered to give the most representative transmissivity value. In all of the tests with a final flow above measurement limit the result from the injection period was chosen as representative for the section. The only exception was one section in KFR105, 42.9–47.9 m, were the transient evaluation of the recovery period was chosen as representative. During the injection period a certain time interval with pseudo-radial flow was interpreted in about 60 % of the tests in KFR27 and 57 % in KFR105 be identified (80 % and 76 % of test with detectable flow respectively). The corresponding figure for the recovery period in KFR105 was 36 % of the tests which showed some period of PRF.

Consequently, standard methods for single-hole tests with wellbore storage and skin effects were commonly used for the routine evaluation of the tests.

If the final flow rate  $Q_p$  was below the actual test-specific measurement limit, the representative transmissivity value was assumed to be less than the estimated  $T_M$ , based on  $Q/s\text{-measl-L}$ . The estimated lower measurement limit for flow rate for the injection tests was c 2 mL/min. However, for approximately 25 % of the injection tests in KFR27 and KFR105, the final flow rate was below the standard lower measurement limit.

The lower standard measurement limit of steady-state transmissivity in 5 m sections based on a flow rate of 2 mL/min and an injection pressure of 20 m is indicated in Figure 6-1 and Figure 6-2. However, for some test sections, the actual injection pressure was different, as previously denoted in Section 5.4.2.

Since the section 189.4–194.4 m was deemed highly conductive and well above the flow capacity of the WIC-unit, the injection pressure was set to 30 kPa instead of 200 kPa to be able to get a stable injection pressure by the performance of the test.

Selected test diagrams from the injection tests in KFR27 are presented in Appendix 2 and from KFR105 in Appendix 3–5. For KFR 27, In general, one linear diagram showing the entire test sequence together with lin-log and log-log diagrams from the injection period are presented for the injection tests. For KFR105 the linear diagram is presented together with log-log diagrams from the injection- and recovery period respectively. The quantitative analysis was performed from such diagrams using the AQTESOLV software. From injection tests with a flow rate below the estimated lower measurement limit for the specific test, only the linear diagram is presented in the Appendix.

In Figure 6-1 and 6-2, comparisons of transmissivities of 5 m sections calculated from steady-state evaluation ( $T_M$ ) and transient evaluation ( $T_T$ ) are shown. The agreement between the two populations is good. In KFR27 the transmissivity values estimated from steady-state analysis are slightly higher than the transmissivity values estimated from the transient evaluation. This difference could be due to several reasons. For instance, a steady-state analysis of transmissivity according to Moye's formula (denoted  $T_M$ ) may result in a larger value than a transient analysis of transmissivity if the skin factor is negative and vice versa.

**Table 6-1. Summary of the routine evaluation of the single-hole injection tests in borehole KFR27.**

KFR27 Secup (m)	KFR27 Seclow (m)	Test start YYYY-MM-DD hh:mm:ss	b (m)	Flow regime <sup>1)</sup> injection	Final flow (m <sup>3</sup> /s)	T <sub>M</sub> (m <sup>2</sup> /s)	T <sub>T</sub> (m <sup>2</sup> /s)	T <sub>R</sub> <sup>2)</sup> (m <sup>2</sup> /s)	S (-)	x (-)	ri (m)	ri-index (-)
14.85	19.85	2015-12-18 15:59:07	5	-	< 3.33E-08	1.3E-09	1.3E-09	2.9E-07	-	8.4		
19.85	24.85	2015-12-21 08:46:58	5	PRF -> NFB	3.70E-06	1.5E-07	1.8E-07	1.8E-07	-2.21	40.4	1	
24.85	29.85	2015-12-21 10:19:33	5	PRF -> PSF	4.27E-05	1.7E-06	1.6E-06	1.6E-06	8.9E-07	-	70.4	0
29.85	34.85	2015-12-21 12:40:10	5	PRF ->	1.95E-06	7.8E-08	2.8E-08	2.8E-08	1.2E-07	-4.66	25.6	0
34.85	39.85	2015-12-21 13:47:18	5	-	< 3.33E-08	1.3E-09	1.3E-09	-	-	4.6		
39.85	44.85	2015-12-21 14:40:42	5	PRF ->	8.33E-06	3.3E-07	1.7E-07	1.7E-07	2.9E-07	-4.55	40.1	1
44.85	49.85	2015-12-21 16:06:52	5	PRF -> PSF	2.00E-07	8.0E-09	1.8E-09	1.8E-09	3.0E-08	-4.9	12.9	0
49.85	54.85	2016-01-07 14:14:28	5	PRF -> PSF	8.25E-05	3.3E-06	1.4E-06	1.4E-06	8.2E-07	-	67.8	0
54.85	59.85	2016-01-07 15:27:16	5	PRF ->PSF	3.85E-06	1.5E-07	5.9E-08	5.9E-08	1.7E-07	-	30.8	-1
59.85	64.85	2016-01-07 16:39:54	5	PRF ->PSF	1.27E-05	5.1E-07	4.8E-07	4.8E-07	4.9E-07	-	52.9	0
64.85	69.85	2016-01-08 09:41:04	5	PRF ->PSF	2.07E-05	8.2E-07	4.8E-07	4.8E-07	4.8E-07	-	56.3	0
69.85	74.85	2016-01-08 10:50:13	5	-	< 3.33E-08	1.3E-09	1.3E-09	-	-	9.0		
74.85	79.85	2016-01-08 13:26:13	5	PRF -> PSS?	8.33E-08	3.4E-09	2.1E-09	2.1E-09	3.2E-08	-3.28	13.3	-1
79.85	84.85	2016-01-08 14:55:05	5	PRF -> NFB	1.68E-06	6.8E-08	8.5E-08	8.5E-08	2.0E-07	-1.42	33.9	-1
84.85	89.85	2016-01-08 16:08:22	5	PRF	1.95E-05	7.9E-07	3.1E-07	3.1E-07	3.9E-07	-5.42	46.3	1
89.85	94.85	2016-01-11 09:07:05	5	PRF	7.85E-06	3.2E-07	1.5E-07	1.5E-07	2.7E-07	-4.67	38.9	0
94.85	99.85	2016-01-11 10:26:30	5	PRF	2.42E-05	9.9E-07	4.0E-07	4.0E-07	4.4E-07	-5.36	50.1	0
99.85	104.85	2016-01-11 12:43:49	5	PSF?	1.08E-06	4.3E-08	5.0E-09	5.0E-09	4.9E-08	-	16.5	0
104.85	109.85	2016-01-11 13:54:48	5	PLF?-> PRF	1.40E-06	5.6E-08	3.8E-08	3.8E-08	1.4E-07	-3.27	27.6	0
109.85	114.85	2016-01-11 15:09:13	5	PLF -> PSF?	3.17E-07	1.2E-08	1.8E-09	1.8E-09	2.9E-08	-5.76	13.0	0
114.85	119.85	2016-01-11 16:16:02	5	PRF->?	1.67E-07	6.6E-09	5.0E-09	50E-09	4.9E-08	-2.49	16.5	-1
119.85	124.85	2016-11-13 10:09:43	5	PRF->NFB	6.63E-07	2.7E-08	2.6E-08	2.6E-08	1.1E-07	-1.82	25.1	1
124.85	129.85	2016-11-13 11:22:50	5	-	< 3.33E-08	1.4E-09	1.3E-09	-	-	4.6		
129.85	134.85	2016-11-13 13:30:20	5	-	< 3.33E-08	1.4E-09	1.3E-09	-	-	4.7		
134.85	139.85	2016-11-13 14:27:53	5	-	< 3.33E-08	1.4E-09	1.3E-09	-	-	4.1		
139.4	144.4	2016-11-13 15:25:42	5	PLF? -> PSF	1.79E-06	7.4E-08	2.3E-08	2.3E-08	1.1E-07	-	24.6	0
144.4	149.4	2016-01-15 12:13:07	5	->PRF->?	1.57E-06	6.2E-08	5.5E-07	5.5E-07	5.2E-07	1.74	53.7	-1
149.4	154.4	2016-01-15 13:24:34	5	PRF	5.27E-06	2.1E-07	5.3E-07	5.3E-07	5.1E-07	5.83	53.3	0
154.4	159.4	2016-01-15 14:50:06	5	PSF	1.47E-06	5.9E-08	5.8E-08	5.8E-08	1.7E-07	-	30.7	-1
159.4	164.4	2016-01-18 08:23:54	5	-	< 3.33E-08	1.4E-09	3.2E-09	1.3E-09	4.0E-08	-	9.9	
164.4	169.4	2016-01-18 09:26:44	5	PLF-PRF	4.33E-07	1.7E-08	8.6E-09	8.6E-09	6.5E-08	-3.83	18.9	0
169.4	174.4	2016-01-18 10:27:21	5	PRF	4.00E-07	1.6E-08	6.4E-09	6.4E-09	5.6E-08	-4.4	17.5	0
174.4	179.4	2016-01-18 12:32:58	5	PSF->PSS?	1.08E-06	4.4E-08	5.0E-08	5.0E-08	1.6E-07	-	29.4	-1
179.4	184.4	2016-01-18 13:38:27	5	PSF	1.47E-06	6.0E-08	2.7E-08	2.7E-08	1.1E-07	-	25.1	0
184.4	189.4	2016-01-18 14:44:50	5	PRF	4.17E-07	1.7E-08	6.0E-09	6.0E-09	5.4E-08	-4.54	17.3	0
189.4	194.4	2016-02-02 09:04:19	5	NFB	1.88E-04	5.19E-05	3.3E-04	3.3E-04	1.3E-05	-0.09	299.8	1

KFR27 Secup (m)	KFR27 Seclow (m)	Test start YYYY-MM-DD hh:mm:ss	b (m)	Flow regime <sup>1)</sup> injection	Final flow (m <sup>3</sup> /s)	T <sub>M</sub> (m <sup>2</sup> /s)	T <sub>T</sub> (m <sup>2</sup> /s)	T <sub>R</sub> <sup>2)</sup> (m <sup>2</sup> /s)	S (-)	x (-)	ri (m)	ri-index (-)
194.4	199.4	2016-01-19 09:23:04	5	PSF ->PSS	3.17E-06	1.3E-07	3.3E-07	3.3E-07	4.0E-07	-	48.6	-1
199.4	204.4	2016-01-19 13:16:40	5	PSF	5.13E-06	2.1E-07	6.4E-07	6.4E-07	5.6E-07	-	57.4	-1
204.4	209.4	2016-01-19 14:49:19	5	PSF ->NFB?	4.73E-06	1.9E-07	6.9E-07	6.9E-07	5.8E-07	-	56.8	1
209.4	214.4	2016-01-19 15:56:28	5	PRF	5.67E-07	2.2E-08	2.6E-08	2.6E-08	1.1E-07	-1.14	25.2	0
214.4	219.4	2016-01-20 08:18:54	5	PRF-PSF?	2.17E-07	8.9E-09	2.4E-09	2.4E-09	3.5E-08	-4.87	15.2	-1
219.4	224.4	2016-01-20 09:36:28	5	PRF->NFB?	2.50E-07	1.0E-08	4.6E-09	4.6E-09	4.7E-08	-4.15	16.2	1
224.4	229.4	2016-01-20 10:43:26	5	PSF	1.17E-07	4.8E-09	2.4E-09	2.4E-09	3.4E-08	-	13.8	0
229.4	234.4	2016-01-20 12:57:23	5	PSF	1.65E-06	6.5E-08	2.5E-08	2.5E-08	1.1E-07	-	25.3	-1
234.4	239.4	2016-01-20 14:05:01	5	PRF -> PSF	6.67E-08	2.8E-09	4.3E-10	4.3E-10	1.5E-08	-	9.0	-1
239.4	244.4	2016-01-20 15:08:45	5	-	< 3.33E-08	1.3E-09		1.3E-09		-	8.5	
244.4	249.4	2016-01-20 16:08:59	5	-	< 3.33E-08	1.4E-09		1.3E-09		-	12.5	
249.4	254.4	2016-01-21 08:41:50	5	PRF?	1.50E-06	6.0E-08	8.2E-08	6.0E-08	2.0E-07	0.16	30.9	0
254.4	259.4	2016-01-21 09:56:02	5	-	< 3.33E-08	1.3E-09		1.3E-09		-	4.4	
259.4	264.4	2016-01-21 10:46:47	5	-	< 3.33E-08	1.3E-09		2.0E-09		-	13.4	
264.4	269.4	2016-01-21 13:06:20	5	PRF->NFB?	5.00E-08	2.1E-09	2.3E-09	2.1E-09	3.4E-08	-0.64	13.5	0
269.4	274.4	2016-01-21 14:23:17	5	PRF?	1.00E-07	4.1E-09	2.0E-09	4.1E-09	3.2E-08	-3.42	15.8	-1
274.4	279.4	2016-01-21 15:25:40	5	-	< 3.33E-08	1.4E-09		1.3E-09		-	7.8	
279.4	284.4	2016-01-22 08:39:42	5	-	< 3.33E-08	1.4E-09		1.3E-09		-	12.0	
284.4	289.4	2016-01-22 09:45:06	5	-	< 3.33E-08	1.4E-09		1.3E-09		-	5.1	
289.4	294.4	2016-01-22 10:42:25	5	PRF-NFB?	1.67E-07	7.0E-09	4.4E-09	4.4E-09	4.6E-08	-3.11	16.2	0
294.4	299.4	2016-01-22 12:44:12	5	PRF?	9.00E-07	3.6E-08	8.7E-09	8.8E-09	6.5E-08	-5.46	19.5	1
299.4	304.4	2016-01-22 13:54:43	5	PRF?	1.03E-05	4.1E-07	1.1E-07	1.1E-07	2.3E-07	-5.80	36.4	-1
304.4	309.4	2016-01-22 14:59:32	5	PRF->PSS?	1.78E-06	7.1E-08	7.8E-08	7.8E-08	2.0E-07	-1.84	33.7	0
309.4	314.4	2016-01-22 16:05:49	5	PRF->PSF	5.00E-08	2.1E-09	1.4E-09	1.4E-09	2.6E-08	-	12.0	-1
314.4	319.4	2016-01-25 08:35:35	5	PLF?->PRF	2.83E-07	1.1E-08	3.8E-09	3.8E-09	4.3E-08	-4.70	15.4	1
319.4	324.4	2016-01-25 09:39:56	5	PRF?	4.25E-06	1.7E-07	1.8E-07	1.8E-07	3.0E-07	-1.39	41.0	0
324.4	329.4	2016-01-25 10:48:44	5	->PRF?	8.90E-06	3.5E-07	4.4E-07	4.4E-07	4.7E-07	-0.65	51.3	-1
329.4	334.4	2016-01-25 12:34:36	5	PRF	1.75E-06	7.0E-08	6.4E-08	6.4E-08	1.8E-07	-2.04	31.4	0
334.4	339.4	2016-01-25 13:37:07	5	PRF->PSS?	4.72E-06	1.9E-07	1.4E-07	1.4E-07	2.7E-07	-2.95	38.3	-1
339.4	344.4	2016-01-25 14:46:49	5	PRF -> NFB?	3.57E-06	1.5E-07	4.3E-07	4.3E-07	4.6E-07	5.17	50.3	1
344.4	349.4	2016-01-25 15:54:49	5	PRF	2.03E-06	8.4E-08	1.1E-07	1.1E-07	2.3E-07	-0.38	35.9	0
349.4	354.4	2016-01-26 08:21:32	5	PRF -> NFB	8.33E-06	3.3E-07	3.6E-07	3.6E-07	4.2E-07	-3.34	48.5	1
354.4	359.4	2016-01-26 10:00:46	5	PRF	2.17E-07	8.9E-09	6.8E-09	6.8E-09	5.8E-08	-2.24	-	0
359.4	364.4	2016-01-26 10:55:09	5	PRF->PSF	1.53E-06	6.2E-08	2.7E-08	2.7E-08	1.2E-07	-	25.3	0
364.4	369.4	2016-01-26 12:46:01	5	PRF	1.20E-06	4.8E-08	2.9E-08	2.9E-08	1.2E-07	-3.57	25.9	0
369.4	374.4	2016-01-26 13:52:26	5	PRF	3.92E-06	1.6E-07	1.2E-07	1.2E-07	2.5E-07	-2.94	37.7	0
374.4	379.4	2016-01-26 14:56:35	5	PRF	3.38E-06	1.4E-07	1.0E-07	1.0E-07	2.3E-07	-3.06	35.4	0

KFR27 Secup (m)	KFR27 Seclow (m)	Test start YYYY-MM-DD hh:mm:ss	b (m)	Flow regime <sup>1)</sup> injection	Final flow (m <sup>3</sup> /s)	T <sub>M</sub> (m <sup>2</sup> /s)	T <sub>T</sub> (m <sup>2</sup> /s)	T <sub>R</sub> <sup>2)</sup> (m <sup>2</sup> /s)	S (-)	x (-)	ri (m)	ri-index (-)
379.4	384.4	2016-01-26 15:58:26	5	-	< 3.33E-08	1.4E-09	1.3E-09	-	-	3.8		
384.4	389.4	2016-01-27 08:07:33	5	-	< 3.33E-08	1.3E-09	1.3E-09	-	-	3.8		
389.4	394.4	2016-01-27 09:08:39	5	-	< 3.33E-08	1.4E-09	1.3E-09	-	-	12.9		
394.4	399.4	2016-01-27 10:19:35	5	PRF	5.00E-08	2.0E-09	1.5E-09	1.5E-09	2.7E-08	-1.78	12.3	0
399.4	404.4	2016-01-27 12:31:42	5	PSF	1.83E-07	7.5E-09	1.5E-09	1.5E-09	2.7E-08	-	13.5	0
404.4	409.4	2016-01-27 13:38:25	5	PRF	3.33E-08	1.4E-09	7.1E-10	7.1E-10	1.9E-08	-3.06	10.2	0
409.4	414.4	2016-01-27 14:52:51	5	PRF	8.00E-07	3.2E-08	2.3E-08	2.3E-08	1.1E-07	-2.90	24.6	1
414.4	419.4	2016-01-27 16:01:06	5	PRF -> PSS?	1.50E-06	6.0E-08	6.0E-08	6.0E-08	1.7E-07	-1.55	30.9	-1
419.4	424.4	2016-01-28 07:57:47	5	PRF -> NFB	2.10E-05	8.3E-07	8.7E-07	8.7E-07	6.5E-07	-2.57	58.6	1
424.4	429.4	2016-01-28 09:14:28	5	PRF -> PSS?	1.29E-04	5.2E-06	4.1E-06	4.1E-06	1.4E-06	-3.73	88.6	-1
429.4	434.4	2016-01-28 10:26:11	5	PSF	2.53E-05	1.0E-06	3.5E-07	3.5E-07	4.2E-07	-	47.9	0
434.4	439.4	2016-01-28 12:34:37	5	PRF -> NFB	3.27E-06	1.3E-07	3.6E-07	3.6E-07	4.2E-07	3.21	48.1	1
439.4	444.4	2016-01-28 13:41:02	5	PRF	2.50E-07	1.0E-08	8.7E-09	8.7E-09	6.5E-08	-1.65	19.0	1
444.4	449.4	2016-01-28 14:57:34	5	PRF	7.17E-07	2.9E-08	2.1E-08	2.1E-08	1.0E-07	-2.75	-	0
449.4	454.4	2016-01-28 16:00:23	5	-	< 3.33E-08	1.4E-09	1.3E-09	-	-	3.6		
454.4	459.4	2016-01-29 08:37:04	5	-	< 3.33E-08	1.3E-09	1.3E-09	-	-	3.4		
459.4	464.4	2016-01-29 09:29:54	5	PRF	6.67E-08	2.7E-09	5.3E-10	5.3E-10	1.6E-08	-4.83	9.7	0
464.4	469.4	2016-01-29 10:38:29	5	PLF -> PRF	6.67E-08	2.7E-09	5.2E-10	5.2E-10	1.6E-08	-	9.6	1
469.4	474.4	2016-01-29 12:44:08	5	-	< 3.33E-08	1.3E-09	1.3E-09	-	-	3.3		
474.4	479.4	2016-01-29 13:30:47	5	PRF->NFB->PSS?	4.87E-06	2.0E-07	2.7E-07	2.7E-07	3.6E-07	-0.52	46.7	-1
479.4	484.4	2016-02-01 09:57:37	5	-	< 3.33E-08	1.3E-09	1.3E-09	-	-	3.7		
484.4	489.4	2016-01-29 16:17:59	5	-	< 3.33E-08	1.3E-09	1.3E-09	1.3E-05	-	3.4		
489.4	494.4	2016-02-01 09:03:42	5	-	< 3.33E-08	1.3E-09	4.1E-06	1.3E-09	-	3.9		

<sup>1)</sup> The acronyms in the column "Flow regime" are as follows: wellbore storage (WBS), pseudo-linear flow (PLF), pseudo-radial flow (PRF), pseudo-spherical flow (PSF), pseudo-stationary flow (PSS) and apparent no-flow boundary (NFB). The flow regime definitions are further discussed in Section 5.4.3 above.

<sup>2)</sup> For the tests where Q<sub>p</sub> was not detected, T<sub>R</sub> was assumed to be less than T<sub>M</sub> based on the estimated Q/s-measL.

**Table 6-2. Summary of the routine evaluation of the single-hole injection tests in borehole KFR105.**

32

SKB P-17-24

KFR105 Secup (m)	KFR105 Seclow (m)	Test start YYYY-MM-DD hh:mm	b (m)	Flow regime <sup>1)</sup>	Final flow (m <sup>3</sup> /s)	T <sub>M</sub> (m <sup>2</sup> /s)	T <sub>f</sub> (m <sup>2</sup> /s)	T <sub>s</sub> (m <sup>2</sup> /s)	T <sub>T</sub> (m <sup>2</sup> /s)	T <sub>R</sub> <sup>2)</sup> (m <sup>2</sup> /s)	S (-)	x (-)	C (m <sup>3</sup> /Pa)	r <sub>i</sub> (m)	r <sub>i</sub> -index (-)	
				Injection	Recovery											
7.9	12.9	2016-05-17 12:21	5	-	-	< 3.33E-08	1.4E-09	-	-	1.4E-09	-	-	-	8.8		
12.9	17.9	2016-05-18 08:16	5	-	-	< 3.33E-08	1.4E-09	-	-	1.4E-09	-	-	-	8.7		
17.9	22.9	2016-05-18 09:38	5	-	-	< 3.33E-08	1.4E-09	-	-	1.4E-09	-	-	-	4.6		
22.9	27.9	2016-05-18 11:44	5	PRF->	PLF->PRF	1.88E-06	7.6E-08	2.2E-08	2.5E-08	2.2E-08	1.0E-07	-	1.6E-10	24.0	-1	
27.9	32.9	2016-05-18 13:52	5	PSF->?	PSF->PSS	4.45E-06	1.7E-07	2.1E-07	2.3E-07	2.1E-07	2.1E-07	3.2E-07	-	1.3E-10	42.2	-1
32.9	37.9	2016-05-23 07:57	5	PRF-> NFB?	PSF	1.94E-05	7.9E-07	1.3E-06	1.1E-06	1.3E-06	1.3E-06	7.9E-07	0.71	2.4E-10	66.6	1
37.9	42.9	2016-05-23 09:39	5	PLF->PRF	PLF->PRF	1.97E-05	8.0E-07	3.8E-07	4.3E-07	3.8E-07	3.8E-07	4.3E-07	-4.93	9.2E-15	44.5	0
42.9	47.9	2016-05-23 11:06	5	PSF->NFB	PSF	2.32E-06	9.3E-08	1.1E-08	1.9E-07	1.9E-07	1.9E-07	3.0E-07	-	8.6E-10	41.0	1
47.9	52.9	2016-05-23 13:18	5	PRF	PRF-> PSF	1.03E-07	4.1E-09	2.5E-09	3.3E-09	2.5E-09	2.5E-09	3.5E-08	-	4.1E-11	14.0	1
52.9	57.9	2016-05-23 14:47	5	PSF	PSF	2.80E-07	1.1E-08	5.2E-09	4.5E-10	5.2E-09	5.2E-09	5.0E-08	-	3.8E-11	16.7	1
57.9	62.9	2016-05-24 08:47	5	PSF	PSF	2.78E-07	1.1E-08	4.7E-09	4.7E-09	4.7E-09	4.7E-09	4.8E-08	-	7.2E-11	16.4	-1
62.9 <sup>3)</sup>	67.9	-	5	-	-	< 3.33E-08	1.4E-09	-	-	1.4E-09	-	-	-	0.0		
67.9	72.9	2016-05-24 12:40	5	-	-	< 3.33E-08	1.4E-09	-	-	1.4E-09	-	-	-	3.6		
72.9	77.9	2016-05-24 13:48	5	PRF	WBS?>PRF	2.06E-06	8.2E-08	2.2E-07	3.8E-07	2.2E-07	2.2E-07	3.3E-07	6.63	4.6E-11	42.5	0
77.9	82.9	2016-05-26 07:55	5	PRF	PRF?>PSS	3.42E-07	1.4E-08	2.7E-08	4.5E-08	2.7E-08	2.7E-08	1.1E-07	3.32	3.9E-11	25.4	0
82.9	87.9	2016-05-26 09:31	5	PSF	(PSF)?>PSS	3.92E-07	1.6E-08	1.0E-08	1.0E-08	1.0E-08	1.0E-08	7.1E-08	-	6.3E-11	19.9	-1
87.9	92.9	2016-05-26 11:04	5	-	-	< 3.33E-08	1.4E-09	-	-	1.4E-09	-	-	-	4.0		
92.9	97.9	2016-05-26 13:09	5	PRF	(PRF)->PSS	8.28E-08	3.3E-09	1.7E-09	2.2E-09	1.7E-09	1.7E-09	2.9E-08	-1.72	6.5E-11	12.6	0
97.9	102.9	2016-05-26 14:59	5	-	-	< 3.33E-08	1.4E-09	-	-	1.4E-09	-	-	-	4.3		
102.9	107.9	2016-05-27 08:59	5	PRF->PSS?		1.63E-06	6.8E-08	6.0E-08	-	6.0E-08	6.0E-08	1.7E-07	-1.98	0.00E+00	30.8	-1
107.9	112.9	2016-05-27 12:13	5	PRF	WBS->PRF	1.25E-06	4.9E-08	8.7E-08	1.4E-07	8.7E-08	8.7E-08	2.1E-07	2.25	8.7E-11	25.7	0
112.9	117.9	2016-05-27 13:43	5	-	-	< 3.33E-08	1.4E-09	-	-	1.4E-09	-	-	-	8.5		
117.9	122.9	2016-05-30 08:16	5	-	-	< 3.33E-08	1.4E-09	-	-	1.4E-09	-	-	-	4.4		
122.9	127.9	2016-05-30 11:33	5	PRF	PSF->PSS?	5.67E-06	2.3E-07	5.7E-07	-	5.7E-07	5.7E-07	5.3E-07	5.82	-	49.3	0
127.9	132.9	2016-05-30 13:52	5	PRF?	WBS->PSS	3.63E-07	1.4E-08	5.5E-08	-	5.5E-08	5.5E-08	1.6E-07	13.3	-	27.4	1
132.9	137.9	2016-05-31 08:35	5	PRF->(NFB)	PRF	3.34E-05	1.3E-06	1.7E-06	2.4E-06	1.7E-06	1.7E-06	9.2E-07	-1.04	5.9E-10	64.9	1
137.9	142.9	2016-05-31 10:14	5	PRF	PSF?->PSS	1.01E-06	3.9E-08	8.0E-08	7.3E-08	8.0E-08	8.0E-08	2.0E-07	3.94	2.8E-11	30.2	1
142.9	147.9	2016-05-31 12:14	5	PRF	PSF?->PSS	6.58E-07	2.5E-08	6.9E-08	4.7E-08	6.9E-08	6.9E-08	1.8E-07	7.13	3.2E-11	29.0	0
147.9	152.9	2016-05-31 13:49	5	PSF->	PSF	3.93E-06	1.5E-07	1.7E-07	1.6E-07	1.7E-07	1.7E-07	2.9E-07	-	1.0E-10	39.6	0
152.9 <sup>3)</sup>	157.9	-	5	-	-	-	-	-	-	-	-	-	-	-		
157.9	162.9	2016-06-01 09:07	5	(PRF)->PSF	-	9.60E-07	3.7E-08	2.5E-08	-	2.5E-08	2.5E-08	1.1E-07	-	-	24.7	-1
162.9	167.9	2016-06-01 10:33	5	?->PRF	-	6.68E-07	2.6E-08	2.8E-08	-	2.8E-08	2.8E-08	1.2E-07	-0.87	-	25.8	0
167.9	172.9	2016-06-01 12:23	5	PRF->NFB?	PRF	1.25E-05	5.1E-07	1.2E-06	2.7E-06	1.2E-06	1.2E-06	7.6E-07	4.27	1.2E-10	66.1	1
172.9	177.9	2016-06-01 14:01	5	PRF->(NFB)?	PRF	1.23E-05	4.9E-07	8.5E-07	2.7E-06	8.5E-07	8.5E-07	6.4E-07	1.18	1.6E-10	59.7	1
177.9	182.9	2016-06-02 07:50	5	PRF	PSF?->	3.55E-06	1.4E-07	3.2E-08	3.9E-07	3.2E-08	3.2E-08	1.3E-07	-	3.6E-10	26.6	0
182.9	187.9	2016-06-02 09:25	5	PRF->NFB	(PSF)?->PSS	8.13E-07	3.2E-08	3.8E-08	1.0E-07	3.8E-08	3.8E-08	1.4E-07	-0.78	4.6E-11	27.7	1

	KFR105 Secup (m)	KFR105 Seclow (m)	Test start YYYY-MM-DD hh:mm	b (m)	Flow regime <sup>1)</sup> Injection	Recovery	Final flow (m <sup>3</sup> /s)	T <sub>M</sub> (m <sup>2</sup> /s)	T <sub>f</sub> (m <sup>2</sup> /s)	T <sub>s</sub> (m <sup>2</sup> /s)	T <sub>T</sub> (m <sup>2</sup> /s)	T <sub>R</sub> <sup>2)</sup> (m <sup>2</sup> /s)	S (-)	x (-)	C (m <sup>3</sup> /Pa)	r <sub>i</sub> (m)	ri-index (-)
187.9	192.9	2016-06-02 11:03	5	PRF->NFB	?->PSS		9.95E-07	4.0E-08	1.0E-07	4.8E-09	1.0E-07	1.0E-07	2.2E-07	6.17	7.9E-11	35.3	1
192.9	197.9	2016-06-02 13:40	5	-	-	< 3.33E-08	1.4E-09	-	-	-	1.4E-09	-	-	-	-	9.8	
197.9	202.9	2016-06-02 14:41	5	PRF?	-		6.60E-08	2.7E-09	9.1E-10	-	9.1E-10	9.1E-10	2.1E-08	-3.74	-	11.0	0
202.9	207.9	2016-06-07 12:12	5	PRF	PRF->?		5.59E-07	2.0E-08	1.1E-08	1.2E-08	1.1E-08	1.1E-08	7.3E-08	-3.58	4.8E-11	18.3	0
207.9	212.9	2016-06-07 14:13	5	-	-	< 3.33E-08	1.4E-09	-	-	-	1.4E-09	-	-	-	-	9.8	
212.9	217.9	2016-06-09 07:42	5	PRF	WBS->PRF?		3.57E-07	1.4E-08	8.3E-09	2.4E-08	8.3E-09	8.3E-09	6.4E-08	-2.84	7.6E-11	17.1	0
217.9	222.9	2016-06-09 09:16	5	PLF->PSS?	WBS->PRF?		8.40E-08	3.3E-09	2.1E-10	1.0E-09	2.1E-10	2.1E-10	1.0E-08	-6.13	7.7E-12	7.6	-1
222.9	227.9	2016-06-09 10:48	5	-	-	< 3.33E-08	1.4E-09	-	-	-	1.4E-09	-	-	-	-	3.6	
227.9	232.9	2016-06-09 12:43	5	-	-	< 3.33E-08	1.4E-09	-	-	-	1.4E-09	-	-	-	-	4.5	
232.9	237.9	2016-06-09 13:47	5	-	-	< 3.33E-08	1.4E-09	-	-	-	1.4E-09	-	-	-	-	3.7	
237.9	242.9	2016-06-09 14:43	5	PSF	(PRF)->PSF		8.20E-08	3.2E-09	9.5E-09	2.4E-09	9.5E-09	9.5E-09	6.8E-08	-	8.5E-11	14.8	0
242.9	247.9	2016-06-10 08:28	5	PRF	->PRF?		1.01E-07	4.0E-09	5.4E-09	1.3E-08	5.4E-09	5.4E-09	5.1E-08	1.72	1.5E-11	16.8	0
247.9	252.9	2016-06-10 09:54	5	(PSS)->PRF	->PRF?		1.05E-07	4.2E-09	1.2E-09	1.4E-08	1.2E-09	1.2E-09	2.4E-08	-4.21	4.6E-11	11.7	0
252.9	257.9	2016-06-10 11:20	5	PRF-> PSS	WBS->		1.07E-07	4.2E-09	2.0E-09	7.1E-09	2.0E-09	2.0E-09	3.2E-08	-2.78	7.5E-11	10.8	-1
257.9	262.9	2016-06-10 13:59	5	-	-	< 3.33E-08	1.4E-09	-	-	-	1.4E-09	-	-	-	-	4.0	
262.9	267.9	2016-06-13 07:52	5	PRF	PSF->		1.50E-06	6.0E-08	8.3E-08	8.4E-08	8.3E-08	8.3E-08	2.0E-07	-	1.7E-11	30.4	0
267.9	272.9	2016-06-13 09:58	5	PRF1->PRF2	PSF-PSS?		8.18E-07	3.2E-08	7.4E-08	4.1E-07	7.4E-08	7.4E-08	1.9E-07	5.00	3.6E-11	13.2	0
272.9	277.9	2016-06-13 11:28	5	-	-	< 3.33E-08	1.4E-09	-	-	-	1.4E-09	-	-	-	-	3.7	
277.9	282.9	2016-06-13 13:10	5	PRF	PSF->?		9.54E-08	3.7E-09	1.7E-09	2.7E-09	1.7E-09	1.7E-09	2.9E-08	-2.48	5.0E-11	12.6	-1
282.9	287.9	2016-06-13 14:37	5	PRF->(NFB)	->PRF?		1.00E-07	4.0E-09	3.2E-09	1.0E-10	3.2E-09	3.2E-09	4.0E-08	-0.85	2.1E-12	11.3	1
287.9	292.9	2016-06-14 09:45	5	-	-	< 3.33E-08	9.6E-10	-	-	-	1.4E-09	-	-	-	-	4.9	
292.9	297.9	2016-06-14 10:33	5	PRF->(PSF)	->PRF		2.78E-07	1.1E-08	1.4E-08	2.6E-08	1.4E-08	1.4E-08	8.4E-08	-	1.7E-10	19.6	-1
297.9	302.9	2016-06-14 12:57	5	PRF->	PSF		2.52E-07	9.9E-09	9.7E-09	9.9E-09	9.7E-09	9.7E-09	6.9E-08	-0.66	2.8E-11	19.7	0
32.9	37.9	2016-06-16 10:32	5	PRF->NFB	-		1.63E-05	5.8E-07	1.2E-06	-	1.2E-06	1.2E-06	7.5E-07	0.27	-	49.1	1
152.9	157.9	2016-06-15 12:15	5	PRF1->PRF2	-		2.05E-06	7.2E-08	1.5E-07	-	1.5E-07	1.5E-07	2.7E-07	3.08	-	50.1	0
4	119	2016-04-19 12:18	115	PLF (WBS)->PRF	-		1.38E-08	9.9E-07	1.5E-07	-	1.5E-07	1.5E-07	2.7E-07	-6.4	-	48.9	0
120	137	2016-04-19 10:45	17	PRF	-		2.88E-05	2.0E-06	3.0E-06	2.3E-06	3.0E-06	3.0E-06	1.2E-06	1.57	-	100.4	0
138	169	2016-04-19 09:45	31	PRF1->PRF2	PRF->?		5.75E-06	3.6E-07	3.0E-07	2.6E-07	3.0E-07	3.0E-07	3.8E-07	-1.35	-	26.5	0
170	264	2016-04-19 08:45	94	PRF	-		2.02E-05	1.7E-06	1.6E-06	-	1.6E-06	1.6E-06	8.8E-07	-0.01	-	85.4	0
265	303	2016-04-19 07:44	42	>PSF?	-		2.02E-06	1.3E-07	1.4E-07	2.6E-08	1.4E-07	1.4E-07	2.6E-07	-	-	48.6	-1

<sup>1)</sup> The acronyms in the column "Flow regime" are as follows: wellbore storage (WBS), pseudo-linear flow (PLF), pseudo-radial flow (PRF), pseudo-spherical flow (PSF), pseudo-stationary flow (PSS) and apparent no-flow boundary (NFB). The flow regime definitions are further discussed in Section 5.4.3 above.

<sup>2)</sup> For the tests where Q<sub>p</sub> was not detected, T<sub>R</sub> was assumed to be less than T<sub>M</sub> based on the estimated Q/s-measl-L.

<sup>3)</sup> Data from test is missing.

Transmissivity values close to the lower measurement limit could also differ for steady-state and transient evaluation respectively. Values estimated from transient evaluation may, in some cases, be below the lower (standard) measurement limit of the steady-state evaluation. The evaluation of the high-transmissivity section in KFR27, 189.4–194.4 m is uncertain due to high initial flow rate which then was rapidly decreasing throughout the test, the pressure was also dropping a bit at the end.

In cases where apparent no-flow outer boundaries appear at the end of the injection period and transient evaluation is performed on the early part of the data curve, the steady-state transmissivity  $T_M$  may be low in comparison with the transient estimate. In some cases, two different radial flow regimes in the bedrock are observed during the early and late parts of the injection period, respectively. In such cases, the transient evaluation should be based on the early regime.

As discussed above, Skin effects (both positive and negative) may cause discrepancies between transient and steady-state evaluation. For example, a test resulting in a strong negative skin factor (fracture response) with an interpreted PLF from the transient evaluation of the injection period may result in a much higher (up to c. one order of magnitude) steady-state transmissivity.

Figure 6-1 and 6-2 show plots of estimated  $T_M$  against  $T_T$  and it seems that in KFR27  $T_M$  is lower than  $T_T$  while in KFR105 they show similar results. This fact may possibly be due to the orientation of the boreholes, KFR27 is drilled vertical while KFR105 is drilled horizontal, in relation to the dominating fracture orientation in the boreholes. Both boreholes are, according to the boremap mapping (Winell 2009, Winell et al. 2009), dominated by sub-horizontal fractures.

If a borehole is drilled sub-horizontal through this type of fractures the interpreted skin often is negative resulting in higher values on  $T_M$ . Whereas in a horizontal borehole as KFR105 the intersection with the fractures are more indirect or partial giving a more positive skin and a better fit between  $T_M$  and  $T_T$ . The plots also show that the estimated  $T$ -values in KFR27 is a bit higher which also might be an effect of the borehole orientation. Sub-horizontal fractures may be underestimated in KFR105 which may explain the lower transmissivity in this borehole.

The transmissivity values considered as the most representative,  $T_R$ , from the injection tests in KFR27, along the depth of the borehole are shown in Figure 6-3.

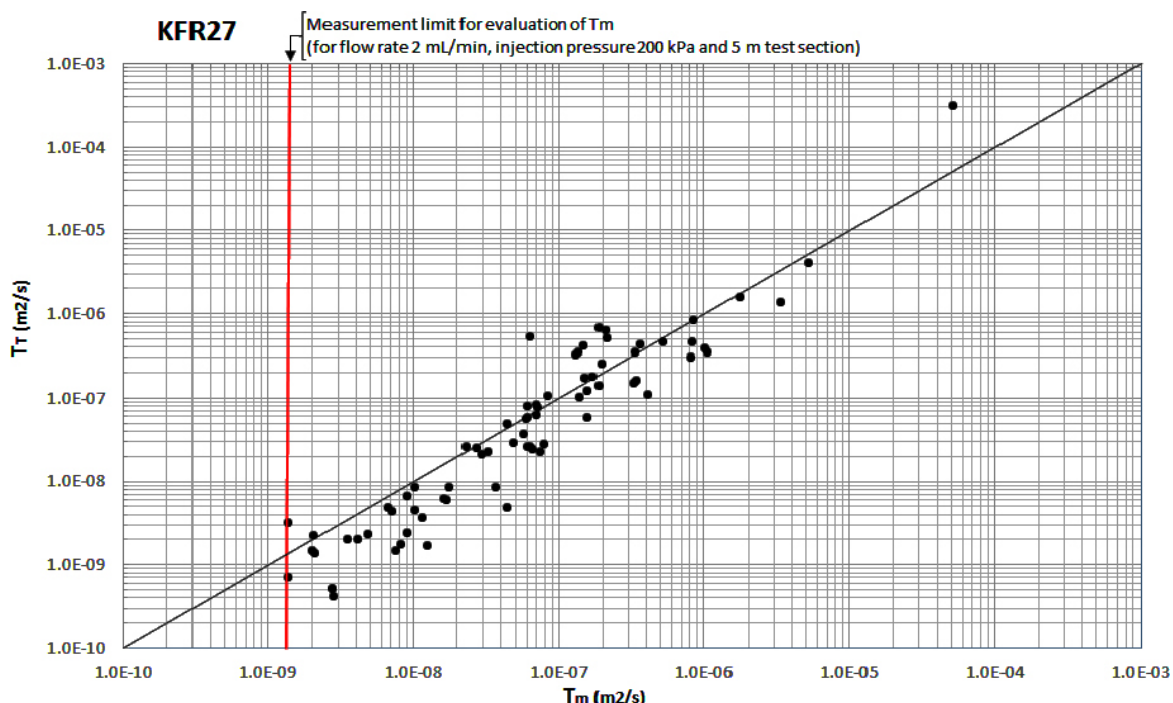


**Figure 6-1.** Estimated transmissivities in 5 m sections from steady-state ( $T_M$ ) and transient ( $T_T$ ) evaluation for the injection tests in KFR27, drilled vertically.

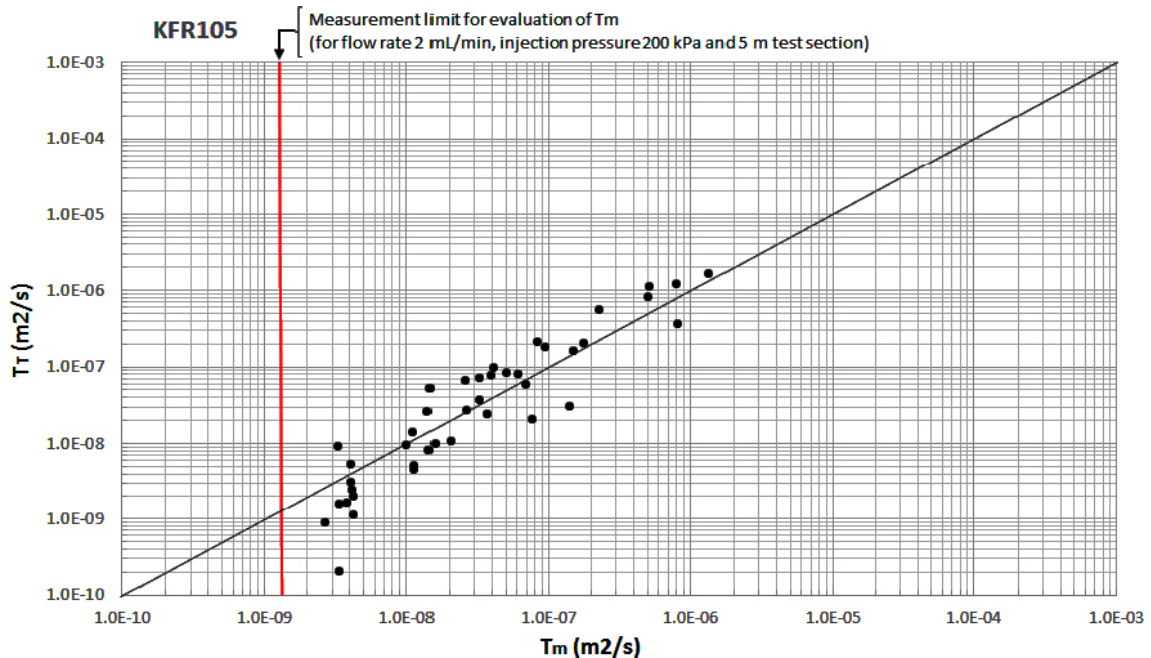


**Figure 6-2.** Estimated transmissivities in 5 m sections from steady-state ( $T_m$ ) and transient ( $T_t$ ) evaluation for the injection tests in the sub-horizontally drilled KFR105.

The transmissivity values considered as the most representative,  $T_r$ , from the injection tests in KFR105 in the tested sections of 5 m length as well as from tests in permanently installed sections, respectively, are shown in Figure 6-4. This figure demonstrates a fairly good agreement between results obtained from tests on different scales in KFR105. However, some tests in short (5 m) section lengths display a higher transmissivity than the corresponding longer section length. This discrepancy may be caused by hydraulic interference with adjacent sections. The total transmissivity of KFR105 is dominated by the intervals between 22.9–47.9 and 122.9–192.9 m. The most conductive sections, in both tests, were found at a depth of 122.9–137.9 m.

#### 6.2.4 Flow regimes

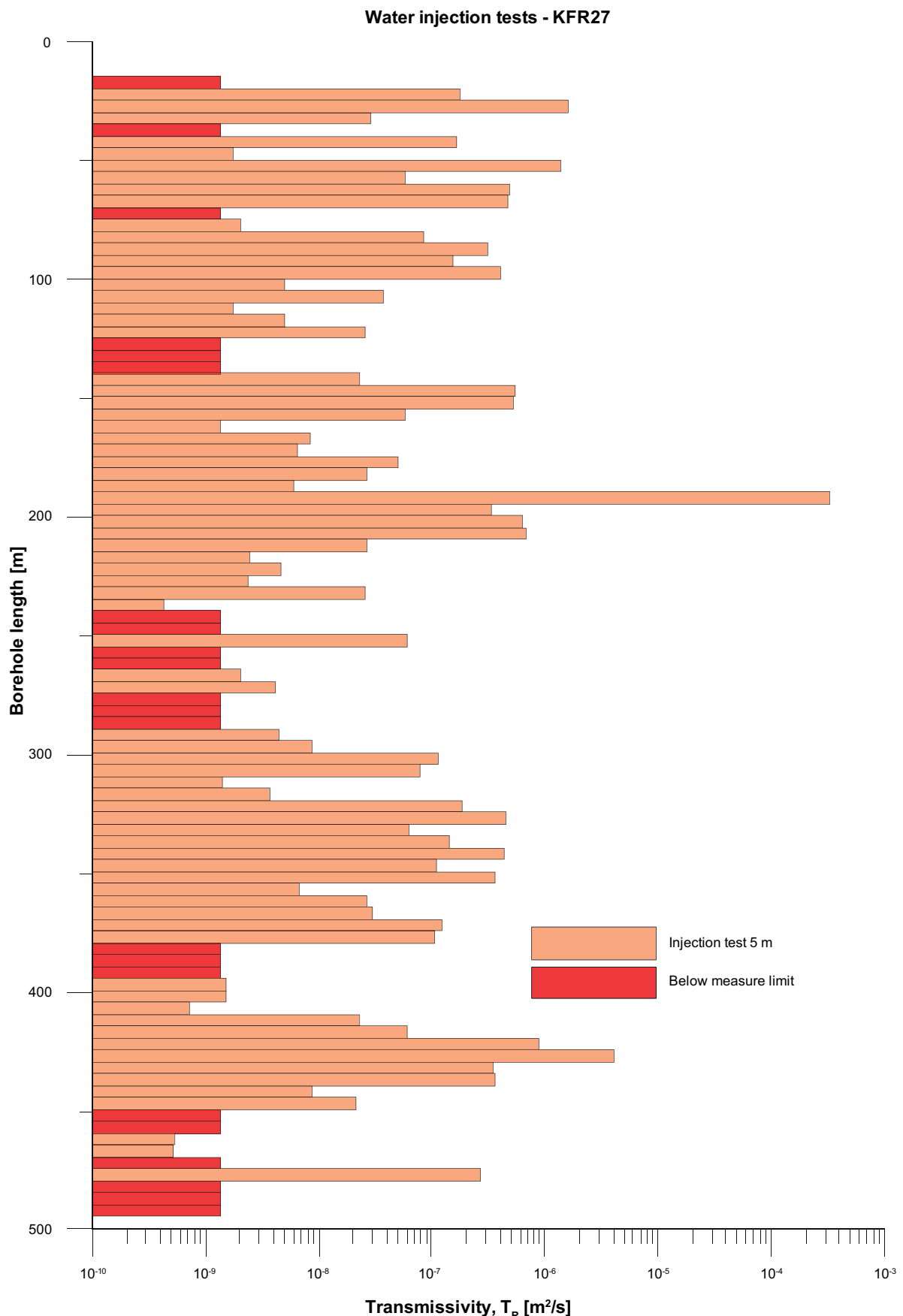
A summary of the frequency of identified flow regimes on different scales is presented in Table 6-3, which shows all identified flow regimes during the tests. For example, a pseudo-radial flow regime (PRF) transitioning to a pseudo-spherical flow regime (PSF) will contribute to one observation of PRF and one observation of PSF. The numbers within parenthesis denote the number of tests where the actual flow regime is the only one present.

It should be noted that the interpretation of flow regimes is only tentative and just based on visual inspection of the data curves. It should also be observed that the number of tests with a pseudo-linear flow regime during the beginning of the injection period may be underestimated due to the fact that a certain time is required for achieving a constant pressure, which fact may mask the initial flow regime.

**Table 6-3. Interpreted flow regimes during the injection tests in KFR27 and KFR105. The figures within the parentheses show the number of tests with only one interpreted flow regime.**

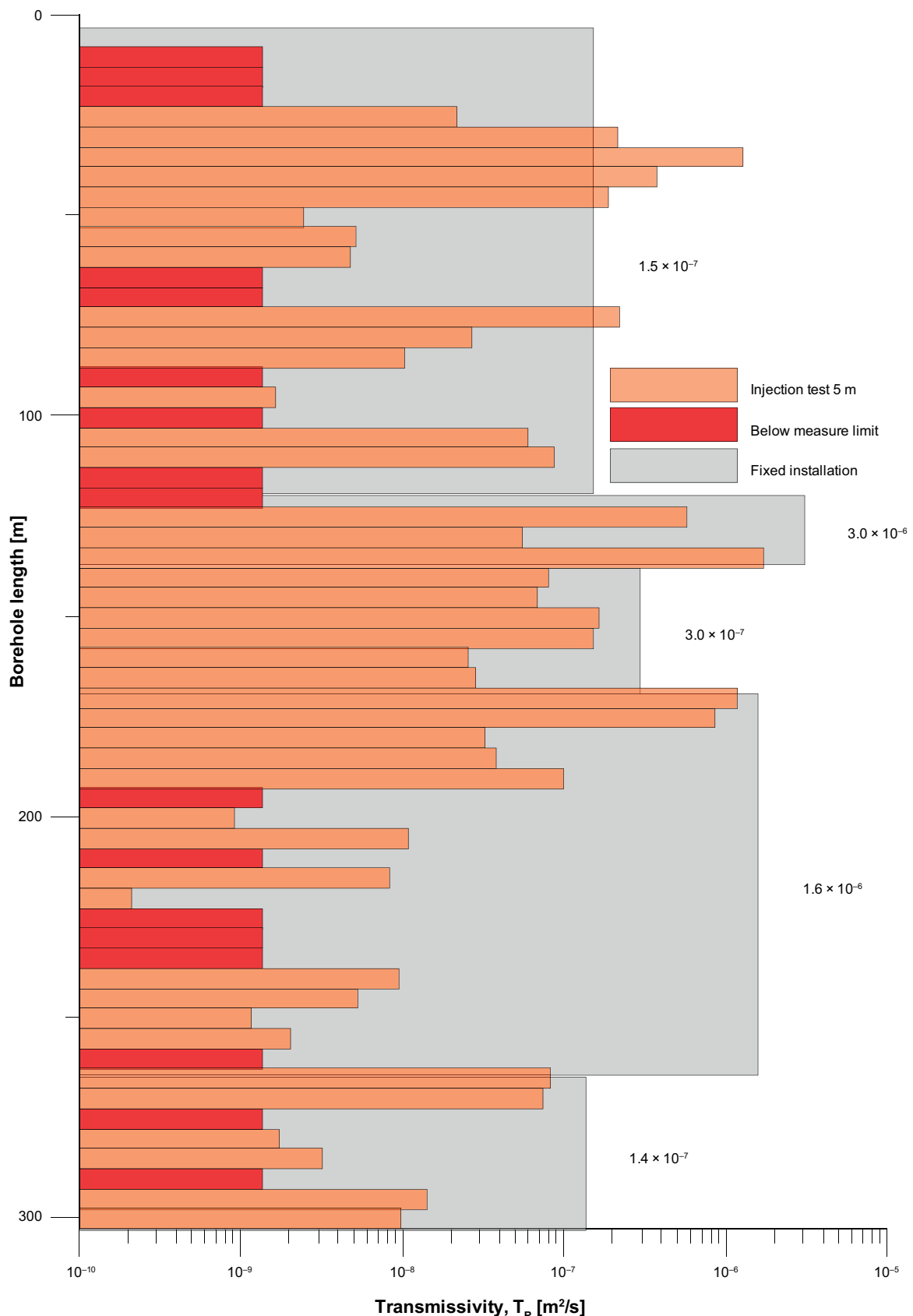
Bore-hole	Tests	Borehole interval (m)	Number of tests with definable $Q_p$	Injection period					Recovery period					
				PLF	PRF	PSF	PSS	NFB	WBS	PLF	PRF	PSF	PSS	NFB
KFR27	96	14.85–494.0	74	6(0)	59(28)	23(8)	8	14(2)	-	-	-	-	-	-
KFR105	65	7.9–302.9	50	3(0)	38(20)	11(6)	3(0)	8(0)	6(1)	2(0)	18(8)	18(9)	10(1)	0

Table 6-3 shows that in c 80 % of the tests with a definable final flow rate, a certain period of pseudo-radial flow during the injection period could be identified for KFR27 and KFR105. For the recovery period, the corresponding result is c 28 % for KFR105.



**Figure 6-3.** The transmissivity values considered the most representative values (TR) from the injection tests of sections of 5 m length in borehole KFR27. Test sections in which flow was below measurement limit are indicated with red.

### Water injection tests - KFR105



**Figure 6-4.** The transmissivity values considered the most representative values ( $TR$ ) from the injection tests of sections of 5 m length in borehole KFR105. Test sections in which flow was below measurement limit is indicated with red. The transmissivity values considering the most representative values ( $TR$ ) from transient evaluation from injection test in fixed installation are shown in grey. Test sections in which flow was below measurement limit are indicated with red.



## 7 Comparison between injection tests and PFL-tests

There are some major differences in the features of these boreholes and one of the major difference, according to Öhman et al. (2012), is that the almost vertical borehole KFR27, has a strong sampling bias against steep fractures (average inclination of  $-86^\circ$ ) and the sub-horizontal KFR105 has a consequently strong bias against horizontal/gently dipping fractures (average inclination of  $-10^\circ$ ). Most of the larger transmissivities are seen in the more shallow part of the rock in this area and most of the water is transported in horizontal fractures.

### 7.1 KFR27

Transmissivity-values from the transient evaluation of the injection tests in KFR27 versus transmissivity-values from the PFL-tests are plotted In Figure 7-1. Only tests in which the final flow rate was above the measurement limit were included in this plot. As seen in Figure 7-1, Transmissivity-values from the injection tests in KFR27 show a good agreement with the transmissivity-values from the PFL-tests. According to Öhman et al. (2012) the entire borehole KFR27 lies inside the modelled geometric bounds of a steeply dipping deformation zone called ZFMWNW0835. There are also two distinct so-called target intercepts, one below 320 m and one between  $-105$  and  $-117$  m. The deeper one has a strong hydraulic signature of the zone whilst the upper one doesn't.

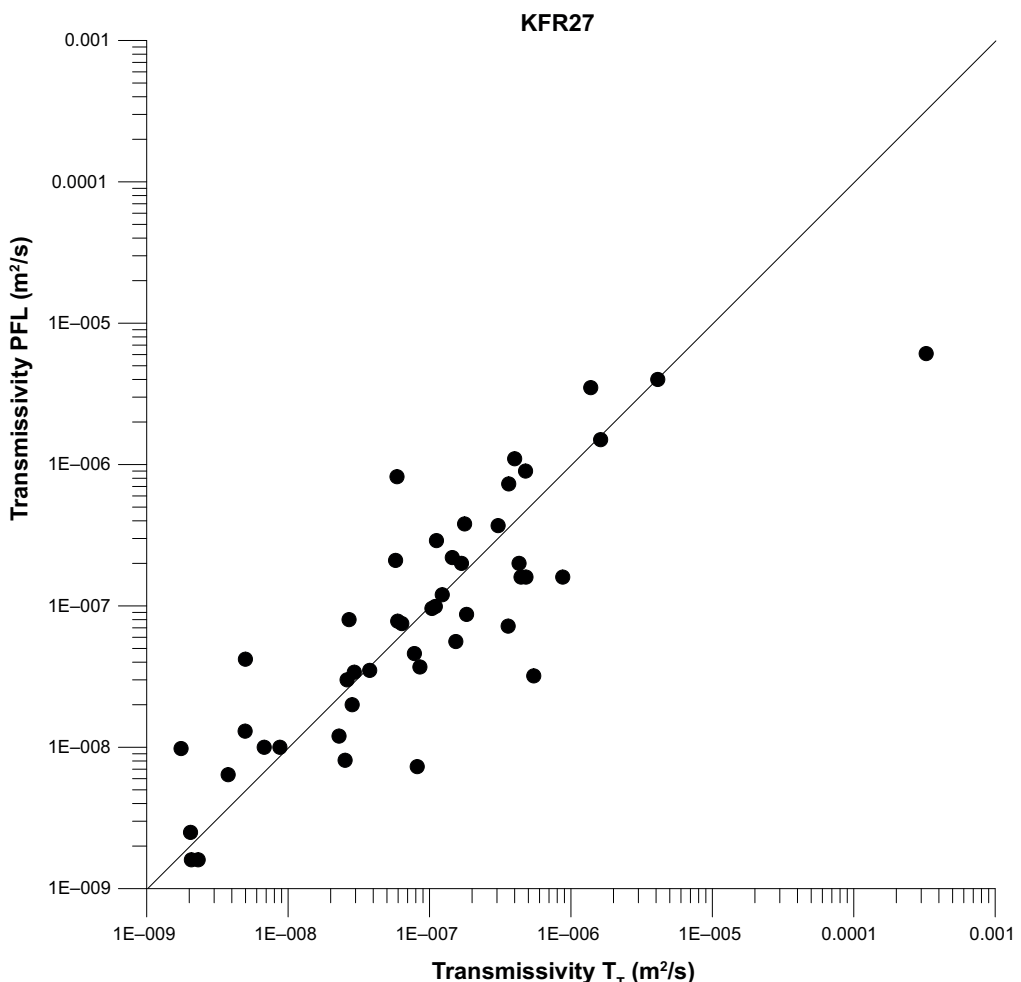


**Figure 7-1.** Transmissivity from transient evaluation for injections tests in KFR27 compared with transmissivity from PFL-tests. Only tests in which the final flow rate was above the measurement limit were included in this plot.

In Figure 7-2, the chosen representative transmissivity values from the injection tests in KFR27 and the transmissivity values from the PFL-tests are plotted in 5 m sections along the depth of the bore-hole. If the final flow rate  $Q_p$  was below the actual test-specific measurement limit, the representative transmissivity value was based on  $Q/s\text{-measl-L}$ . For the injection tests this value was  $1.35\text{E-}9 \text{ m}^2/\text{s}$  and for the PFL-tests  $1.70\text{E-}9 \text{ m}^2/\text{s}$ .

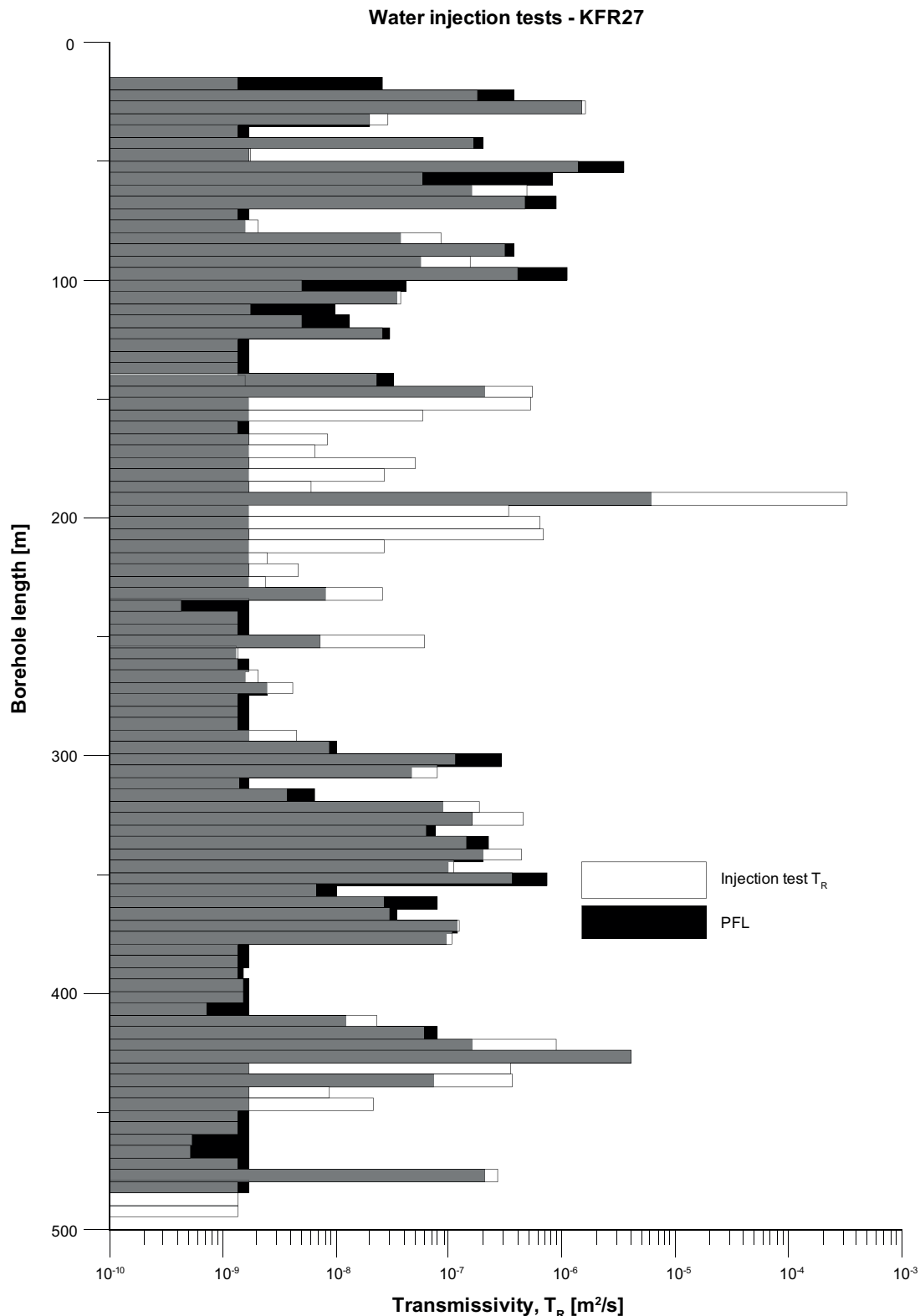


**Figure 7-2.** Representative transmissivity  $TR$  for injection tests in KFR27 compared with transmissivity from PFL-tests, in 5 m sections along the depth of the borehole. Areas in grey correspond to overlapping data values.

On 0–150 m depth, the injection tests and PFL-tests show a relative good agreement, with slightly larger transmissivity values from the PFL-tests. On 150–300 m depth, most of the PFL-tests were below measurement limit. In comparison, the injection tests in section 150–240 m show significantly larger transmissivities with mostly PSF flow regimes. In section 190–195 m both the injection tests and the PFL-tests indicate a highly conductive fracture although the transmissivity from the PFL-test is much smaller than the transient evaluation of the injection test which is considered uncertain. This test is conducted in a large horizontal zone in KFR27, which is one of few horizontal features in that borehole. Since the PFL-tests however showed high transmissivity in the corresponding section, a highly conductive fracture is more likely than a possible leakage between packers. On 300–500 m depth, the both tests show a good agreement, except in section 430–450 m in which the transmissivity values from the injection tests are larger than from the PFL-tests.

## 7.2 KFR105

In Figure 7-3, transmissivity-values from the transient evaluation of the injection tests in KFR105 are plotted versus transmissivity-values from the PFL-tests. Only tests in which the final flow rate was above the lower measurement limit were included in this plot. This plot shows that the results from the PFL-tests are, in general, lower than results from HWIC measurements in corresponding sections. In this case the reason might be that during the PFL-measurements the borehole was completely open and drained throughout the test. The hydraulic head used in the calculations could not be measured hence estimated from maximum possible drawdown in the borehole, which might not have been the case during the tests. The high outflow from the borehole might also result in lower transmissivities as an impact from skin effects and friction losses from turbulence. In KFR27 the head used for calculations of the transmissivity for PFL-measurements are more precise giving similar results for T-PFL and  $T_T$ .

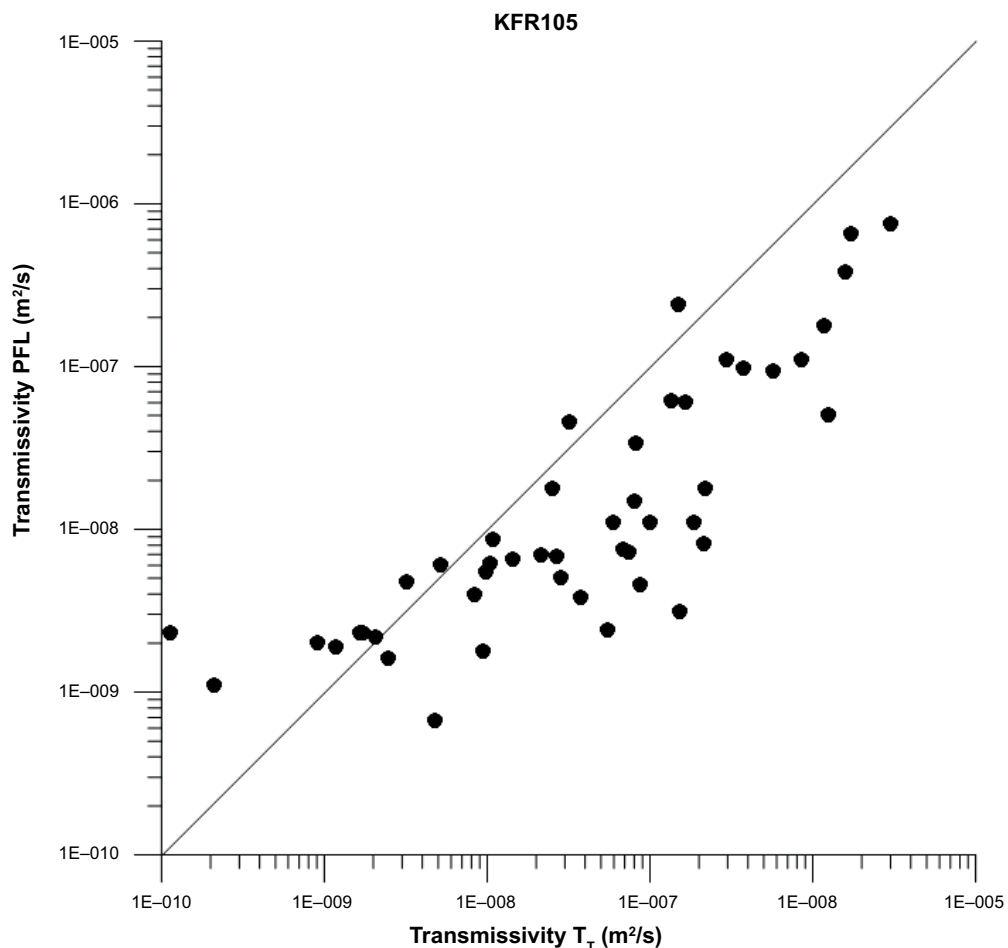


**Figure 7-3.** Transmissivity from transient evaluation for injections tests in KFR105 compared with transmissivity from PFL-tests. Only tests in which the final flow rate was above the lower measurement limit were included in this plot.

KFR105 covers the interval –105 to –157 m and since it is horizontally drilled it intersect more steep fractures than KFR27. This is further discussed in Öhman et al. (2012). In Figure 7-4, the chosen representative transmissivity values from the injection tests in KFR105 and the transmissivity values from the PFL-tests are plotted in 5 m sections along the depth of the borehole. Only injection tests on 5 m sections are included in this plot and in this plot as well it is seen that the transmissivity from the injection tests are larger than the transmissivity from the PFL-tests, with some exceptions. In this area most of the flow occurs in more or less horizontal fractures.

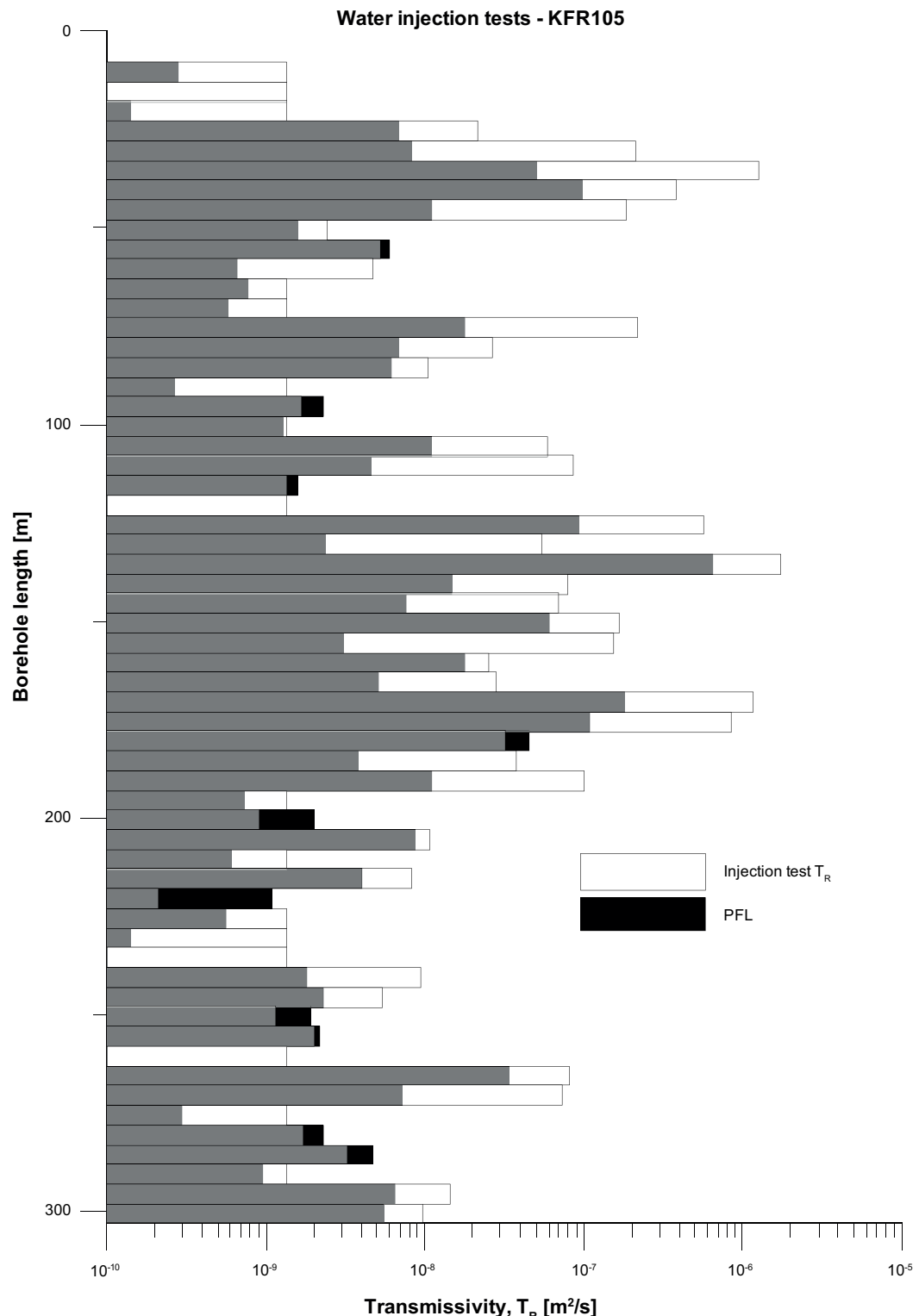


**Figure 7-4.** Representative transmissivity  $T_R$  for injection tests in KFR105 compared with transmissivity from PFL-tests, in 5 m sections along the depth of the borehole. Areas in grey correspond to overlapping data values.

In Table 7-1, estimated transmissivity values in 5 m test sections in KFR27 and KFR105 according to steady-state ( $T_M$ ), transmissivity from transient evaluation ( $T_T$ ), most representative evaluation ( $T_R$ ) and transmissivity from the PFL-tests are listed. When the transmissivity values were below the measurement limit ( $Q_p$  could not be defined), the most representative transmissivity value,  $T_R$ , was considered to be less than  $T_M$ , based on Q/s-measl-L, for the test section.

In Table 7-1 all sections with an interpreted No Flow Boundary (NFB) during the injection tests is marked in the most right column. The PFL logging is conducted after a much longer pumping period than the injection tests leading to drainage of fractures in a larger scale. An interpreted NFB flow regime might in some cases be a sign that fractures in the close vicinity of the borehole are about to be drained. In tests in KFR27 14 sections had an interpreted NFB but only two sections in KFR27 with flow below measurement limit during PFL indicated NFB during injection test in the same sections.

**Table 7-1. Estimated transmissivity values in the corresponding borehole intervals from the injection tests and the PFL-tests in KFR27 and KFR105.**

Bore-hole Id code	Secup inj. tests (m)	Seclow inj. tests (m)	$L_w$ (m)	$T_M$ inj. tests ( $m^2/s$ )	$T_T$ inj. tests ( $m^2/s$ )	$T_R$ inj. tests ( $m^2/s$ )	$T$ PFL-tests ( $m^2/s$ )	Interpreted NFB
KFR27	14.85	19.85	5	1.3E-09		1.3E-09	2.6E-08	
KFR27	19.85	24.85	5	1.5E-07	1.8E-07	1.8E-07	3.8E-07	X
KFR27	24.85	29.85	5	1.7E-06	1.6E-06	1.6E-06	1.5E-06	
KFR27	29.85	34.85	5	7.8E-08	2.8E-08	2.8E-08	2.0E-08	
KFR27	34.85	39.85	5	1.3E-09		1.3E-09	-	
KFR27	39.85	44.85	5	3.3E-07	1.7E-07	1.7E-07	2.0E-07	
KFR27	44.85	49.85	5	8.0E-09	1.8E-09	1.8E-09	-	
KFR27	49.85	54.85	5	3.3E-06	1.4E-06	1.4E-06	3.5E-06	
KFR27	54.85	59.85	5	1.5E-07	5.9E-08	5.9E-08	8.2E-07	
KFR27	59.85	64.85	5	5.1E-07	4.8E-07	4.8E-07	1.6E-07	
KFR27	64.85	69.85	5	8.2E-07	4.8E-07	4.8E-07	9.0E-07	
KFR27	69.85	74.85	5	1.3E-09		1.3E-09	-	
KFR27	74.85	79.85	5	3.4E-09	2.1E-09	2.1E-09	1.6E-09	
KFR27	79.85	84.85	5	6.8E-08	8.5E-08	8.5E-08	3.7E-08	X
KFR27	84.85	89.85	5	7.9E-07	3.1E-07	3.1E-07	3.7E-07	
KFR27	89.85	94.85	5	3.2E-07	1.5E-07	1.5E-07	5.6E-08	
KFR27	94.85	99.85	5	9.9E-07	4.0E-07	4.0E-07	1.1E-06	
KFR27	99.85	104.85	5	4.3E-08	5.0E-09	5.0E-09	4.2E-08	
KFR27	104.85	109.85	5	5.6E-08	3.8E-08	3.8E-08	3.5E-08	
KFR27	109.85	114.85	5	1.2E-08	1.8E-09	1.8E-09	9.8E-09	
KFR27	114.85	119.85	5	6.6E-09	5.0E-09	50E-09	1.3E-08	
KFR27	119.85	124.85	5	2.7E-08	2.6E-08	2.6E-08	3.0E-08	X
KFR27	124.85	129.85	5	1.4E-09		1.3E-09	-	
KFR27	129.85	134.85	5	1.4E-09		1.3E-09	-	
KFR27	134.85	139.85	5	1.4E-09		1.3E-09	-	
KFR27	139.4	144.4	5	7.4E-08	2.3E-08	2.3E-08	-	
KFR27	144.4	149.4	5	6.2E-08	5.5E-07	5.5E-07	3.2E-08	
KFR27	149.4	154.4	5	2.1E-07	5.3E-07	5.3E-07	-	
KFR27	154.4	159.4	5	5.9E-08	5.8E-08	5.8E-08	2.1E-07	
KFR27	159.4	164.4	5	1.4E-09	3.2E-09	1.3E-09	-	
KFR27	164.4	169.4	5	1.7E-08	8.6E-09	8.6E-09	-	
KFR27	169.4	174.4	5	1.6E-08	6.4E-09	6.4E-09	-	
KFR27	174.4	179.4	5	4.4E-08	5.0E-08	5.0E-08	-	
KFR27	179.4	184.4	5	6.0E-08	2.7E-08	2.7E-08	-	
KFR27	184.4	189.4	5	1.7E-08	6.0E-09	6.0E-09	-	
KFR27	189.4	194.4	5	5.19E-05	3.3E-04	3.3E-04	6.1E-06	X
KFR27	194.4	199.4	5	1.3E-07	3.3E-07	3.3E-07	-	
KFR27	199.4	204.4	5	2.1E-07	6.4E-07	6.4E-07	-	
KFR27	204.4	209.4	5	1.9E-07	6.9E-07	6.9E-07	-	

Bore-hole Id code	Secup inj. tests (m)	Seclow inj. tests (m)	L <sub>w</sub> (m)	T <sub>M</sub> inj. tests (m <sup>2</sup> / s)	T <sub>T</sub> inj. tests (m <sup>2</sup> /s)	T <sub>R</sub> inj. tests (m <sup>2</sup> /s)	T PFL-tests (m <sup>2</sup> /s)	Interpreted NFB
KFR27	209.4	214.4	5	2.2E-08	2.6E-08	2.6E-08	-	
KFR27	214.4	219.4	5	8.9E-09	2.4E-09	2.4E-09	-	
KFR27	219.4	224.4	5	1.0E-08	4.6E-09	4.6E-09	-	X
KFR27	224.4	229.4	5	4.8E-09	2.4E-09	2.4E-09	-	
KFR27	229.4	234.4	5	6.5E-08	2.5E-08	2.5E-08	8.1E-09	
KFR27	234.4	239.4	5	2.8E-09	4.3E-10	4.3E-10	-	
KFR27	239.4	244.4	5	1.3E-09		1.3E-09	-	
KFR27	244.4	249.4	5	1.4E-09		1.3E-09	-	
KFR27	249.4	254.4	5	6.0E-08	8.2E-08	6.0E-08	7.3E-09	
KFR27	254.4	259.4	5	1.3E-09		1.3E-09	1.3E-09	
KFR27	259.4	264.4	5	1.3E-09		2.0E-09	-	
KFR27	264.4	269.4	5	2.1E-09	2.3E-09	2.1E-09	1.6E-09	X
KFR27	269.4	274.4	5	4.1E-09	2.0E-09	4.1E-09	2.5E-09	
KFR27	274.4	279.4	5	1.4E-09		1.3E-09	-	
KFR27	279.4	284.4	5	1.4E-09		1.3E-09	-	
KFR27	284.4	289.4	5	1.4E-09		1.3E-09	-	
KFR27	289.4	294.4	5	7.0E-09	4.4E-09	4.4E-09	-	X
KFR27	294.4	299.4	5	3.6E-08	8.7E-09	8.8E-09	1.0E-08	
KFR27	299.4	304.4	5	4.1E-07	1.1E-07	1.1E-07	2.9E-07	
KFR27	304.4	309.4	5	7.1E-08	7.8E-08	7.8E-08	4.6E-08	
KFR27	309.4	314.4	5	2.1E-09	1.4E-09	1.4E-09	-	
KFR27	314.4	319.4	5	1.1E-08	3.8E-09	3.8E-09	6.4E-09	
KFR27	319.4	324.4	5	1.7E-07	1.8E-07	1.8E-07	8.7E-08	
KFR27	324.4	329.4	5	3.5E-07	4.4E-07	4.4E-07	1.6E-07	
KFR27	329.4	334.4	5	7.0E-08	6.4E-08	6.4E-08	7.5E-08	
KFR27	334.4	339.4	5	1.9E-07	1.4E-07	1.4E-07	2.2E-07	
KFR27	339.4	344.4	5	1.5E-07	4.3E-07	4.3E-07	2.0E-07	X
KFR27	344.4	349.4	5	8.4E-08	1.1E-07	1.1E-07	9.9E-08	
KFR27	349.4	354.4	5	3.3E-07	3.6E-07	3.6E-07	7.3E-07	X
KFR27	354.4	359.4	5	8.9E-09	6.8E-09	6.8E-09	1.0E-08	
KFR27	359.4	364.4	5	6.2E-08	2.7E-08	2.7E-08	8.0E-08	
KFR27	364.4	369.4	5	4.8E-08	2.9E-08	2.9E-08	3.4E-08	
KFR27	369.4	374.4	5	1.6E-07	1.2E-07	1.2E-07	1.2E-07	
KFR27	374.4	379.4	5	1.4E-07	1.0E-07	1.0E-07	9.6E-08	
KFR27	379.4	384.4	5	1.4E-09		1.3E-09	-	
KFR27	384.4	389.4	5	1.3E-09		1.3E-09	-	
KFR27	389.4	394.4	5	1.4E-09		1.3E-09	1.5E-09	
KFR27	394.4	399.4	5	2.0E-09	1.5E-09	1.5E-09	-	
KFR27	399.4	404.4	5	7.5E-09	1.5E-09	1.5E-09	-	
KFR27	404.4	409.4	5	1.4E-09	7.1E-10	7.1E-10	-	
KFR27	409.4	414.4	5	3.2E-08	2.3E-08	2.3E-08	1.2E-08	
KFR27	414.4	419.4	5	6.0E-08	6.0E-08	6.0E-08	7.8E-08	
KFR27	419.4	424.4	5	8.3E-07	8.7E-07	8.7E-07	1.6E-07	X
KFR27	424.4	429.4	5	5.2E-06	4.1E-06	4.1E-06	4.0E-06	
KFR27	429.4	434.4	5	1.0E-06	3.5E-07	3.5E-07	-	
KFR27	434.4	439.4	5	1.3E-07	3.6E-07	3.6E-07	7.2E-08	X
KFR27	439.4	444.4	5	1.0E-08	8.7E-09	8.7E-09	-	
KFR27	444.4	449.4	5	2.9E-08	2.1E-08	2.1E-08	-	
KFR27	449.4	454.4	5	1.4E-09		1.3E-09	-	
KFR27	454.4	459.4	5	1.3E-09		1.3E-09	-	
KFR27	459.4	464.4	5	2.7E-09	5.3E-10	5.3E-10	-	
KFR27	464.4	469.4	5	2.7E-09	5.2E-10	5.2E-10	-	
KFR27	469.4	474.4	5	1.3E-09		1.3E-09	-	
KFR27	474.4	479.4	5	2.0E-07	2.7E-07	2.7E-07	2.1E-07	X
KFR27	479.4	484.4	5	1.3E-09		1.3E-09	-	

Bore-hole Id code	Secup inj. tests (m)	Seclow inj. tests (m)	L <sub>w</sub> (m)	T <sub>M</sub> inj. tests (m <sup>2</sup> / s)	T <sub>T</sub> inj. tests (m <sup>2</sup> /s)	T <sub>R</sub> inj. tests (m <sup>2</sup> /s)	T PFL-tests (m <sup>2</sup> /s)	Interpreted NFB
KFR27	484.4	489.4	5	1.3E-09		1.3E-09	-	
KFR27	489.4	494.4	5	1.3E-09	4.1E-06	1.3E-09	-	
KFR105	7.9	12.9	5	1.4E-09	-	1.4E-09	2.8E-10	
KFR105	12.9	17.9	5	1.4E-09	-	1.4E-09	1.3E-010	
KFR105	17.9	22.9	5	1.4E-09	-	1.4E-09	1.4E-10	
KFR105	22.9	27.9	5	7.6E-08	2.2E-08	2.2E-08	6.9E-09	
KFR105	27.9	32.9	5	1.7E-07	2.1E-07	2.1E-07	8.2E-09	
KFR105	32.9	37.9	5	7.9E-07	1.3E-06	1.3E-06	5E-08	X
KFR105	37.9	42.9	5	8.0E-07	3.8E-07	3.8E-07	9.7E-08	
KFR105	42.9	47.9	5	9.3E-08	1.9E-07	1.9E-07	1.1E-08	X
KFR105	47.9	52.9	5	4.1E-09	2.5E-09	2.5E-09	1.6E-09	
KFR105	52.9	57.9	5	1.1E-08	5.2E-09	5.2E-09	6E-09	
KFR105	57.9	62.9	5	1.1E-08	4.7E-09	4.7E-09	6.7E-10	
KFR105	62.9	67.9	5	1.4E-09	-	1.4E-09	7.7E-10	
KFR105	67.9	72.9	5	1.4E-09	-	1.4E-09	5.8E-10	
KFR105	72.9	77.9	5	8.2E-08	2.2E-07	2.2E-07	1.8E-08	
KFR105	77.9	82.9	5	1.4E-08	2.7E-08	2.7E-08	6.8E-09	
KFR105	82.9	87.9	5	1.6E-08	1.0E-08	1.0E-08	6.2E-09	
KFR105	87.9	92.9	5	1.4E-09	-	1.4E-09	2.7E-10	
KFR105	92.9	97.9	5	3.3E-09	1.7E-09	1.7E-09	2.3E-09	
KFR105	97.9	102.9	5	1.4E-09	-	1.4E-09	1.3E-09	
KFR105	102.9	107.9	5	6.8E-08	6.0E-08	6.0E-08	1.1E-08	
KFR105	107.9	112.9	5	4.9E-08	8.7E-08	8.7E-08	4.6E-09	
KFR105	112.9	117.9	5	1.4E-09	-	1.4E-09	1.6E-09	
KFR105	117.9	122.9	5	1.4E-09	-	1.4E-09	7.7E-011	
KFR105	122.9	127.9	5	2.3E-07	5.7E-07	5.7E-07	9.4E-08	
KFR105	127.9	132.9	5	1.4E-08	5.5E-08	5.5E-08	2.4E-09	
KFR105	132.9	137.9	5	1.3E-06	1.7E-06	1.7E-06	6.5E-07	X
KFR105	137.9	142.9	5	3.9E-08	8.0E-08	8.0E-08	1.5E-08	
KFR105	142.9	147.9	5	2.5E-08	6.9E-08	6.9E-08	7.6E-09	
KFR105	147.9	152.9	5	1.5E-07	1.7E-07	1.7E-07	6.1E-08	
KFR105	152.9	157.9	5	-	-	-	3.1E-09	
KFR105	157.9	162.9	5	3.7E-08	2.5E-08	2.5E-08	1.8E-08	
KFR105	162.9	167.9	5	2.6E-08	2.8E-08	2.8E-08	5.1E-09	
KFR105	167.9	172.9	5	5.1E-07	1.2E-06	1.2E-06	1.8E-07	X
KFR105	172.9	177.9	5	4.9E-07	8.5E-07	8.5E-07	1.1E-07	X
KFR105	177.9	182.9	5	1.4E-07	3.2E-08	3.2E-08	4.6E-08	
KFR105	182.9	187.9	5	3.2E-08	3.8E-08	3.8E-08	3.8E-09	X
KFR105	187.9	192.9	5	4.0E-08	1.0E-07	1.0E-07	1.1E-08	X
KFR105	192.9	197.9	5	1.4E-09	-	1.4E-09	7.3E-10	
KFR105	197.9	202.9	5	2.7E-09	9.1E-10	9.1E-10	2E-09	
KFR105	202.9	207.9	5	2.0E-08	1.1E-08	1.1E-08	8.7E-09	
KFR105	207.9	212.9	5	1.4E-09	-	1.4E-09	6.1E-10	
KFR105	212.9	217.9	5	1.4E-08	8.3E-09	8.3E-09	4E-09	
KFR105	217.9	222.9	5	3.3E-09	2.1E-10	2.1E-10	1.1E-09	
KFR105	222.9	227.9	5	1.4E-09	-	1.4E-09	5.7E-10	
KFR105	227.9	232.9	5	1.4E-09	-	1.4E-09	1.4E-10	
KFR105	232.9	237.9	5	1.4E-09	-	1.4E-09	7.7E-011	
KFR105	237.9	242.9	5	3.2E-09	9.5E-09	9.5E-09	1.8E-09	
KFR105	242.9	247.9	5	4.0E-09	5.4E-09	5.4E-09	2.3E-09	
KFR105	247.9	252.9	5	4.2E-09	1.2E-09	1.2E-09	1.9E-09	
KFR105	252.9	257.9	5	4.2E-09	2.0E-09	2.0E-09	2.2E-09	
KFR105	257.9	262.9	5	1.4E-09	-	1.4E-09	7.7E-011	
KFR105	262.9	267.9	5	6.0E-08	8.3E-08	8.3E-08	3.4E-08	
KFR105	267.9	272.9	5	3.2E-08	7.4E-08	7.4E-08	7.3E-09	

Bore-hole Id code	Secup inj. tests (m)	Seclow inj. tests (m)	$L_w$ (m)	$T_M$ inj. tests ( $m^2/s$ )	$T_T$ inj. tests ( $m^2/s$ )	$T_R$ inj. tests ( $m^2/s$ )	$T$ PFL-tests ( $m^2/s$ )	Interpreted NFB
KFR105	272.9	277.9	5	1.4E-09	-	1.4E-09	3E-10	
KFR105	277.9	282.9	5	3.7E-09	1.7E-09	1.7E-09	2.3E-09	
KFR105	282.9	287.9	5	4.0E-09	3.2E-09	3.2E-09	4.8E-09	X
KFR105	287.9	292.9	5	9.6E-10	-	1.4E-09	9.5E-10	
KFR105	292.9	297.9	5	1.1E-08	1.4E-08	1.4E-08	6.6E-09	
KFR105	297.9	302.9	5	9.9E-09	9.7E-09	9.7E-09	5.5E-09	
KFR105 <sup>1)</sup>	152.9	157.9	5	7.2E-08	1.5E-07	1.5E-07	1.8E-08	
KFR105 <sup>1)</sup>	32.9	37.9	5	5.8E-07	1.2E-06	1.2E-06	5E-08	X
KFR105 <sup>2)</sup>	265	303	42	1.3E-07	1.4E-07	1.4E-07	-	
KFR105 <sup>2)</sup>	170	264	94	1.7E-06	1.6E-06	1.6E-06	-	
KFR105 <sup>2)</sup>	138	169	31	3.6E-07	3.0E-07	3.0E-07	-	
KFR105 <sup>2)</sup>	120	137	17	2.0E-06	3.0E-06	3.0E-06	-	
KFR105 <sup>2)</sup>	4	119	115	9.9E-07	1.5E-07	1.5E-07	-	

1) Test performed with long recovery interval.

2) Test performed on fixed installation in KFR105.

## References

SKB's (Svensk Kärnbränslehantering AB) publications can be found at [www\(skb.com/publications](http://www(skb.com/publications).

- Almén K-E, Andersson J-E, Carlsson L, Hansson K, Larsson N-Å, 1986.** Hydraulic testing in crystalline rock. A comparative study of single-hole test methods. SKB TR 86-27, Svensk Kärnbränslehantering AB.
- Cooper H H, Jacob C E, 1946.** A generalized graphical method for evaluating formation constants and summarizing well-field history. *Transactions, American Geophysical Union* 27, 526–534.
- Dougherty D E, Babu D K, 1984.** Flow to a partially penetrating well in a double-porosity reservoir. *Water Resources Research* 20, 1116–1122.
- Earlougher R C, 1977.** Advances in well test analysis. New York: Society of Petroleum Engineers of AIME.
- Hantush M S, 1959.** Nonsteady flow to flowing wells in leaky aquifer. *Journal of Geophysical Research* 64, 1043–1052.
- Hantush M S, Jacob C E, 1955.** Nonsteady radial flow in infinite leaky aquifers. *Transactions, American Geophysical Union* 36, 95–100.
- Hurmerinta E, Väisäsvaara J, 2009.** Site investigation SFR. Difference flow logging in boreholes KFR104 and KFR27 (extension). SKB P-09-20, Svensk Kärnbränslehantering AB.
- Hurst W, Clark J D, Brauer E B, 1969.** The skin effect in producing wells. *Journal of Petroleum Technology* 21, 1483–1489.
- Jacob C E, Lohman S W, 1952.** Nonsteady flow to a well of constant drawdown in an extensive aquifer. *Transactions, American Geophysical Union* 33, 559–569.
- Ludvigson J-E, Hansson K, Hjerne C, 2007.** Forsmark site investigation. Method evaluation of single-hole hydraulic injection tests at site investigations in Forsmark. SKB P-07-80, Svensk Kärnbränslehantering AB.
- Ozkan E, Raghavan R, 1991a.** New solutions for well-test analysis problems. Part 1, Analytical considerations. *SPE Formation Evaluation* 6, 359–368.
- Ozkan E, Raghavan R, 1991b.** New solutions for well-test analysisproblems; Part 2, Computational considerations and applications. *SPE Formation Evaluation* 6, 369–378.
- Pekkanen J, Pöllänen J, Väisäsvaara J, 2008.** Site investigation SFR. Difference flow logging in boreholes KFR101 and KFR27. SKB P-08-98, Svensk Kärnbränslehantering AB.
- Rhén I (ed), Gustafson G, Stanfors R, Wikberg P, 1997.** Äspö HRL – Geoscientific evaluation 1997/5. Models based on site characterization 1986–1995. SKB TR 97-06, Svensk Kärnbränslehantering AB.
- Väisäsvaara J, 2009.** Site investigation SFR. Difference flow logging in borehole KFR105. SKB P-09-09, Svensk Kärnbränslehantering AB.
- Winell S, 2009.** Site investigation SFR. Boremap mapping of core drilled borehole KFR105. SKB P-09-59, Svensk Kärnbränslehantering AB.
- Winell S, Döse C, Strähle A, Carlsten S, Selnert E, 2009.** Site investigation SFR. Boremap mapping of core drilled boreholes KFR104 and KFR27 (from 147.5 m). SKB P-09-39, Svensk Kärnbränslehantering AB.
- Öhman J, Bockgård N, Follin S, 2012.** Bedrock hydrogeology. Site investigation SFR. SKB R-11-03, Svensk Kärnbränslehantering AB.



## Appendix 1

### General test data

#### Summary of pressure and flow data for all tests in KFR27

Borehole:	KFR27	Testtype:	CHi (Constant Head injection)	Field crew:	J. Harrström, Sofia Hedberg, Johanna Ragnvald, Jonas Robertsson, Carolina Ackander	General comment:	
Test section setup (m)	Test section seelow (m)	Start of flow period YYYYMMDD hh:mm:ss	Stop of flow period YYYYMMDD hh:mm:ss	Total flow time t <sub>p</sub> (min)	Initial pressure p <sub>i</sub> (kPa)	Pressure at flow end p <sub>f</sub> (kPa)	
14.85	19.85	2015-12-18 15:59:07	2015-12-18 16:09:03	10	210	410	
19.85	24.85	2015-12-21 08:46:58	2015-12-21 09:07:06	20	269	470	
24.85	29.85	2015-12-21 10:19:33	2015-12-21 10:39:44	20	320	521	
29.85	34.85	2015-12-21 12:40:10	2015-12-21 13:00:18	20	369	571	
34.85	39.85	2015-12-21 13:47:18	2015-12-21 13:50:16	3	430	630	
39.85	44.85	2015-12-21 14:40:42	2015-12-21 15:01:00	20	458	661	
44.85	49.85	2015-12-21 16:06:52	2015-12-21 16:27:10	20	519	721	
49.85	54.85	2016-01-07 14:14:28	2016-01-07 14:34:45	20	560	761	
54.85	59.85	2016-01-07 15:27:16	2016-01-07 15:47:35	20	609	811	
59.85	64.85	2016-01-07 16:39:54	2016-01-07 17:00:48	21	659	859	
64.85	69.85	2016-01-08 09:41:04	2016-01-08 10:04:53	24	708	911	
69.85	74.85	2016-01-08 10:50:13	2016-01-08 11:01:38	11	763	969	
74.85	79.85	2016-01-08 13:26:13	2016-01-08 13:46:29	20	803	999	
79.85	84.85	2016-01-08 14:55:05	2016-01-08 15:15:26	20	852	1051	
84.85	89.85	2016-01-08 16:08:22	2016-01-08 16:28:30	20	902	1101	
89.85	94.85	2016-01-11 09:07:05	2016-01-11 09:27:06	20	954	1152	
94.85	99.85	2016-01-11 10:26:30	2016-01-11 10:47:04	21	1004	1201	
99.85	104.85	2016-01-11 12:43:49	2016-01-11 13:03:54	20	1058	1261	
104.85	109.85	2016-01-11 13:54:48	2016-01-11 14:15:04	20	1110	1311	
109.85	114.85	2016-01-11 15:09:13	2016-01-11 15:30:04	21	1145	1351	
114.85	119.85	2016-01-11 16:16:02	2016-01-11 16:36:03	20	1196	1399.4	
119.85	124.85	2016-11-13 10:09:43	2016-11-13 10:29:52	20	1250	1451	
124.85	129.85	2016-11-13 11:22:50	2016-11-13 11:25:46	3	1322	1519	
129.85	134.85	2016-11-13 13:30:20	2016-11-13 13:33:25	3	1360	1559.8	
134.85	139.85	2016-11-13 14:27:53	2016-11-13 14:30:14	2	1400	1598.7	
139.4	144.4	2016-11-13 15:25:42	2016-11-13 15:46:19	21	1434	1630.7	
144.4	149.4	2016-01-15 12:13:07	2016-01-15 12:33:19	20	1487	1691	
149.4	154.4	2016-01-15 13:24:34	2016-01-15 13:44:48	20	1538	1740	
154.4	159.4	2016-01-15 14:50:06	2016-01-15 15:10:26	20	1588	1790	

Borehole:	KFR27					
Testtype:	CHi (Constant Head injection)					
Field crew:	J. Harrström, Sofia Hedberg, Johanna Rагvальд, Jonas Robertsson, Carolina Åckander					
General comment:						
Test section setup (m)	Test section seelow (m)	Start of flow period YYYYMMDD hh:mm:ss	Stop of flow period YYYYMMDD hh:mm:ss	Total flow time t <sub>p</sub> (min)	Initial pressure p <sub>i</sub> (kPa)	Pressure at flow end p <sub>p</sub> (kPa)
159.4	164.4	2016-01-18 08:23:54	2016-01-18 08:37:35	14	1642	1840
164.4	169.4	2016-01-18 09:26:44	2016-01-18 09:46:46	20	1678	1880
169.4	174.4	2016-01-18 10:27:21	2016-01-18 10:47:21	20	1740	1941
174.4	179.4	2016-01-18 12:32:58	2016-01-18 12:52:58	20	1769	1970
179.4	184.4	2016-01-18 13:38:27	2016-01-18 13:58:27	20	1813	2010
184.4	189.4	2016-01-18 14:44:50	2016-01-18 15:04:50	20	1868	2070
189.4	194.4	2016-02-02 09:04:19	2016-02-02 09:30:10	26	1924	1954
194.4	199.4	2016-01-19 09:23:04	2016-01-19 09:44:23	21	1963	2161
199.4	204.4	2016-01-19 13:16:40	2016-01-19 13:38:01	21	2028	2230
204.4	209.4	2016-01-19 14:49:19	2016-01-19 15:09:29	20	2075	2281
209.4	214.4	2016-01-19 15:56:28	2016-01-19 16:16:44	20	2125	2329
214.4	219.4	2016-01-20 08:18:54	2016-01-20 08:43:03	24	2162	2359
219.4	224.4	2016-01-20 09:36:28	2016-01-20 09:56:37	20	2221	2421
224.4	229.4	2016-01-20 10:43:26	2016-01-20 11:03:51	20	2272	2469
229.4	234.4	2016-01-20 12:57:23	2016-01-20 13:18:19	21	2305	2510
234.4	239.4	2016-01-20 14:05:01	2016-01-20 14:25:05	20	2364	2558
239.4	244.4	2016-01-20 15:08:45	2016-01-20 15:18:56	10	2399	2599
244.4	249.4	2016-01-20 16:08:59	2016-01-20 16:31:10	22	2404	2601
249.4	254.4	2016-01-21 08:41:50	2016-01-21 09:02:00	20	2450	2651
254.4	259.4	2016-01-21 09:56:02	2016-01-21 09:58:50	3	2525	2731
259.4	264.4	2016-01-21 10:46:47	2016-01-21 11:07:42	21	2539	2741
264.4	269.4	2016-01-21 13:06:20	2016-01-21 13:27:14	21	2584	2781
269.4	274.4	2016-01-21 14:23:17	2016-01-21 14:43:26	20	2663	2861
274.4	279.4	2016-01-21 15:25:40	2016-01-21 15:34:19	9	2741	2939
279.4	284.4	2016-01-22 08:39:42	2016-01-22 09:00:07	20	2792	2989
284.4	289.4	2016-01-22 09:45:06	2016-01-22 09:48:44	4	2881	3080
289.4	294.4	2016-01-22 10:42:25	2016-01-22 11:02:56	21	2897	3089
294.4	299.4	2016-01-22 12:44:12	2016-01-22 13:05:11	21	2950	3151
299.4	304.4	2016-01-22 13:54:43	2016-01-22 14:15:13	20	2995	3201
304.4	309.4	2016-01-22 14:59:32	2016-01-22 15:20:39	21	3048	3251
309.4	314.4	2016-01-22 16:05:49	2016-01-22 16:25:56	20	3094	3289
314.4	319.4	2016-01-25 08:35:35	2016-01-25 08:55:40	20	3140	3340
319.4	324.4	2016-01-25 09:39:56	2016-01-25 10:00:19	20	3186	3391
324.4	329.4	2016-01-25 10:48:44	2016-01-25 11:09:14	21	3237	3441

Borehole:	KFR27					
Testtype:	CHi (Constant Head injection)					
Field crew:	J. Harrström, Sofia Hedberg, Johanna Ragnvald, Jonas Robertsson, Carolina Åckander					
General comment:						
Test section setup (m)						
Test section setup (m)	Test section section (m)	Start of flow period YYYYMMDD hh:mm:ss	Stop of flow period YYYYMMDD hh:mm:ss	Total flow time $t_p$ (min)	Initial pressure $p_i$ (kPa)	Pressure at flow end $p_f$ (kPa)
329.4	334.4	2016-01-25 12:34:36	2016-01-25 12:54:54	20	3286	3489
334.4	339.4	2016-01-25 13:37:07	2016-01-25 13:57:08	20	3335	3541
339.4	344.4	2016-01-25 14:46:49	2016-01-25 15:06:51	20	3384	3583
344.4	349.4	2016-01-25 15:54:49	2016-01-25 16:14:55	20	3434	3631
349.4	354.4	2016-01-26 08:21:32	2016-01-26 08:41:45	20	3485	3691
354.4	359.4	2016-01-26 10:00:46	2016-01-26 09:40:09	-21	3532	3730
359.4	364.4	2016-01-26 10:55:09	2016-01-26 11:15:21	20	3581	3780
364.4	369.4	2016-01-26 12:46:01	2016-01-26 13:06:18	20	3630	3831
369.4	374.4	2016-01-26 13:52:26	2016-01-26 14:13:28	21	3676	3880
374.4	379.4	2016-01-26 14:56:35	2016-01-26 15:16:44	20	3731	3930
379.4	384.4	2016-01-26 15:58:26	2016-01-26 16:00:26	2	3812	4010
384.4	389.4	2016-01-27 08:07:33	2016-01-27 08:09:35	2	3840	4040
389.4	394.4	2016-01-27 09:08:39	2016-01-27 09:32:08	23	3883	4080
394.4	399.4	2016-01-27 10:19:35	2016-01-27 10:39:42	20	3926	4130
399.4	404.4	2016-01-27 12:31:42	2016-01-27 12:56:01	24	3972	4170
404.4	409.4	2016-01-27 13:38:25	2016-01-27 13:58:34	20	4023	4220
409.4	414.4	2016-01-27 14:52:51	2016-01-27 15:13:37	21	4068	4270
414.4	419.4	2016-01-27 16:01:06	2016-01-27 16:21:27	20	4117	4320
419.4	424.4	2016-01-28 07:57:47	2016-01-28 08:16:49	19	4167	4371
424.4	429.4	2016-01-28 09:14:28	2016-01-28 09:34:32	20	4216	4419
429.4	434.4	2016-01-28 10:26:11	2016-01-28 10:46:13	20	4273	4470
434.4	439.4	2016-01-28 12:34:37	2016-01-28 12:54:37	20	4323	4521
439.4	444.4	2016-01-28 13:41:02	2016-01-28 14:01:04	20	4371	4570
444.4	449.4	2016-01-28 14:57:34	2016-01-28 15:17:43	20	4421	4621
449.4	454.4	2016-01-28 16:00:23	2016-01-28 16:02:13	2	4494	4690
454.4	459.4	2016-01-29 08:37:04	2016-01-29 08:38:41	2	4511	4720
459.4	464.4	2016-01-29 09:29:54	2016-01-29 09:51:11	21	4571	4770
464.4	469.4	2016-01-29 10:38:29	2016-01-29 10:59:39	21	4619	4819
469.4	474.4	2016-01-29 12:44:08	2016-01-29 12:45:41	2	4676	4880
474.4	479.4	2016-01-29 13:30:47	2016-01-29 13:52:46	22	4709	4911
479.4	484.4	2016-02-01 09:57:37	2016-02-01 09:59:30	2		
484.4	489.4	2016-01-29 16:17:59	2016-01-29 16:19:35	2		
489.4	494.4	2016-02-01 09:03:42	2016-02-01 09:05:50	2		

## Summary of pressure and flow data for all tests in KFR105

Borehole:	KFR105								
Testtype:	CHir (Constant Head injection recovery)								
Field crew:	Sofia Hedberg, Johanna Ragnvald, Jonas Robertsson, Carolina Ackander								
<b>General comment:</b>									
Test section sectop (m)	Test section sectlow (m)	Start of flow period YYYYMMDD hh:mm:ss	Stop of flow period YYYYMMDD hh:mm:ss	Total stop time t <sub>p</sub> hh:mm:ss	Total flow time t <sub>f</sub> (min)	Total recovery time t <sub>r</sub> (min)	Initial pressure p <sub>i</sub> (kPa)	Pressure at flow end p <sub>e</sub> (kPa)	Final pressure p <sub>f</sub> (kPa)
7.9	12.9	2016-05-17 12:21	2016-05-17 12:32	-	11	321	1249	228	1255
12.9	17.9	2016-05-18 08:16	2016-05-18 08:26	-	11	158	1258	200	1293
17.9	22.9	2016-05-18 09:38	2016-05-18 09:41	-	3	20	1475	208	1328
22.9	27.9	2016-05-18 11:44	2016-05-18 12:05	2016-05-18 12:26	20	47	200	199	1333
27.9	32.9	2016-05-18 13:52	2016-05-18 14:12	2016-05-18 14:59	20	21	199	1322	1335
32.9	37.9	2016-05-23 07:57	2016-05-23 08:18	2016-05-23 08:39	20	63	202	1326	1335
37.9	42.9	2016-05-23 09:39	2016-05-23 09:59	2016-05-23 10:20	21	24	203	1326	1335
42.9	47.9	2016-05-23 11:06	2016-05-23 11:26	2016-05-23 12:29	20	20	203	1339	1345
47.9	52.9	2016-05-23 13:18	2016-05-23 13:38	2016-05-23 14:03	20	20	203	1339	1345
52.9	57.9	2016-05-23 14:47	2016-05-23 15:07	2016-05-23 15:27	20	20	202	1337	1342
57.9	62.9	2016-05-24 08:47	2016-05-24 09:07	2016-05-24 09:28	20	186	1335	1338	1348
62.9	67.9	2016-05-24 12:40	2016-05-24 12:41	2016-05-24 13:02	2	20	198	1340	1340
67.9	72.9	2016-05-24 13:48	2016-05-24 14:08	2016-05-24 14:28	20	20	203	1337	1339
72.9	77.9	2016-05-26 07:55	2016-05-26 08:16	2016-05-26 08:36	20	20	203	1339	1339
77.9	82.9	2016-05-26 09:31	2016-05-26 09:51	2016-05-26 10:12	20	20	203	1339	1339
82.9	87.9	2016-05-26 11:04	2016-05-26 11:06	2016-05-26 11:31	2	24	201	1370	1383
87.9	92.9	2016-05-26 13:09	2016-05-26 13:29	2016-05-26 13:49	20	20	203	1338	1338
92.9	97.9	2016-05-26 14:59	2016-05-26 15:02	2016-05-26 15:22	3	20	204	1339	1335
97.9	102.9	2016-05-27 08:59	2016-05-27 09:19	2016-05-27 09:41	20	22	195	1338	1343
102.9	107.9	2016-05-27 12:13	2016-05-27 12:34	2016-05-27 12:59	20	26	205	1344	1344
107.9	112.9	2016-05-27 13:43	2016-05-27 13:54	2016-05-27 14:15	10	21	207	1343	1343
112.9	117.9	2016-05-30 08:16	2016-05-30 08:19	-	3	204	1348	1331	1342
117.9	122.9	2016-05-30 11:33	2016-05-30 11:54	2016-05-30 13:00	21	66	203	1334	1339
122.9	127.9	2016-05-30 13:52	2016-05-30 14:12	2016-05-30 14:32	20	20	203	1349	1356
127.9	132.9	2016-05-31 08:35	2016-05-31 08:55	2016-05-31 09:15	20	20	210	1350	1350
132.9	137.9	2016-05-31 10:14	2016-05-31 10:34	2016-05-31 10:57	20	23	210	1350	1350
137.9	142.9	2016-05-31 12:14	2016-05-31 12:35	2016-05-31 12:56	20	21	210	1345	1345
142.9	147.9	2016-05-31 13:49	2016-05-31 14:09	2016-05-31 14:30	20	21	216	1349	1349
147.9	152.9	2016-06-01 09:07	2016-06-01 09:27	2016-06-01 09:49	20	23	212	1345	1345
152.9	157.9	2016-06-01 10:33	2016-06-01 10:53	2016-06-01 11:14	20	21	210	1346	1346
157.9	162.9	2016-06-01 12:23	2016-06-01 12:43	2016-06-01 13:06	21	23	201	1345	1346
162.9	167.9	2016-06-01 14:01	2016-06-01 14:41	2016-06-01 14:41	20	21	201	1345	1348
167.9	172.9	2016-06-02 07:50	2016-06-02 08:11	2016-06-02 08:31	21	21	206	1349	1349

Borehole:	KFR105								
Testtype:	CHir (Constant Head injection recovery)								
Field crew:	Sofia Hedberg, Johanna Ragnvald, Jonas Robertsson, Carolina Åckander								
General comment:									
Test section setup (m)	Test section seelow (m)	Start of flow period YYYYMMDD hh:mm:ss	Stop of flow period YYYYMMDD hh:mm:ss	Test stop YYYYMMDD hh:mm:ss	Total flow time $t_p$ (min)	Total recovery time $t_r$ (min)	Initial pressure $p_i$ (kPa)	Pressure at flow end $p_e$ (kPa)	Final pressure $p_f$ (kPa)
General comment:									
182.9	187.9	2016-06-02 09:25	2016-06-02 09:46	2016-06-02 10:18	20	32	205	1338	1140
187.9	192.9	2016-06-02 11:03	2016-06-02 11:24	2016-06-02 12:54	20	90	201	1338	1142
192.9	197.9	2016-06-02 13:40	2016-06-02 13:54	2016-06-02 13:54	13	0	204	1316	1321
197.9	202.9	2016-06-02 14:41	2016-06-02 15:02	2016-06-02 15:22	21	20	201	1321	1177
202.9	207.9	2016-06-07 12:12	2016-06-07 12:32	2016-06-07 12:53	21	21	225	1335	1133
207.9	212.9	2016-06-07 14:13	2016-06-07 14:26	-	13	21	215	1335	1155
212.9	217.9	2016-06-09 07:42	2016-06-09 08:02	2016-06-09 08:23	21	21	203	1342	1201
217.9	222.9	2016-06-09 09:16	2016-06-09 09:37	2016-06-09 09:57	21	20	205	1329	
222.9	227.9	2016-06-09 10:48	2016-06-09 10:50	-	2	2	206	1363	
227.9	232.9	2016-06-09 12:43	2016-06-09 12:46	-	3	3	207	1347	
232.9	237.9	2016-06-09 13:47	2016-06-09 13:49	-	2	2	202	1406	
237.9	242.9	2016-06-09 14:43	2016-06-09 15:04	2016-06-09 15:24	21	20	205	1345	1142
242.9	247.9	2016-06-10 08:28	2016-06-10 08:48	2016-06-10 09:08	20	20	204	1345	1126
247.9	252.9	2016-06-10 09:54	2016-06-10 10:16	2016-06-10 10:36	21	20	204	1346	1144
252.9	257.9	2016-06-10 11:20	2016-06-10 11:41	2016-06-10 12:44	21	63	206	1348	1142
257.9	262.9	2016-06-10 13:59	2016-06-10 14:02	-	2	217	1359		
262.9	267.9	2016-06-13 07:52	2016-06-13 08:13	2016-06-13 09:25	21	72	204	1346	1082
267.9	272.9	2016-06-13 09:58	2016-06-13 10:17	2016-06-13 10:39	19	21	205	1349	1144
272.9	277.9	2016-06-13 11:28	2016-06-13 11:30	-	2	205	1349		
277.9	282.9	2016-06-13 13:10	2016-06-13 13:30	2016-06-13 13:52	20	22	206	1349	1153
282.9	287.9	2016-06-13 14:37	2016-06-13 15:02	2016-06-13 15:23	25	20	201	1349	1148
287.9	292.9	2016-06-14 09:45	2016-06-14 09:49	2016-06-14 09:49	3	0	339	1346	241
292.9	297.9	2016-06-14 10:33	2016-06-14 10:55	2016-06-14 11:16	22	21	205	1348	1148
297.9	302.9	2016-06-14 12:57	2016-06-14 13:18	2016-06-14 13:39	20	21	205	1349	1148
(1)		152.9	157.9	2016-06-15 12:15	2016-06-15 15:16	-	181	231	1346
32.9		32.9	37.9	2016-06-16 10:32	2016-06-16 14:33	-	241	227	1337
(2)		265	303	2016-04-19 07:44	2016-04-19 08:15	2016-04-19 08:45	31	30	177
170		264	2016-04-19 08:45	2016-04-19 09:15	2016-04-19 09:45	30	30	154	1473
138		169	2016-04-19 09:45	2016-04-19 10:15	2016-04-19 10:35	30	20	173	1498
120		137	2016-04-19 10:45	2016-04-19 11:15	2016-04-19 11:45	30	30	142	1466
4		119	2016-04-19 12:18	2016-04-19 12:49	2016-04-19 13:20	31	31	182	1412

(1) Long injection tests  
(2) Fixed installation



## Appendix 2

### Test diagrams – Injection tests in KFR27

In the following pages the selected test diagrams are presented for all test sections. A linear diagram of pressure and flow rate is presented for each test. For most tests are lin-log and log-log diagrams presented, from injection period. From the tests with a flow rate below the estimated lower measurement limit for the specific test, only the linear diagram is presented. Additionally, for a few tests, a type curve fit is displayed in the diagrams despite the fact that the estimated parameters from the fit are judged as non-representative. For these tests, the type curve fit is presented, as an example, to illustrate that an assumption of a certain flow regime is not justified for the test. Instead, some other flow regime is likely to dominate.

Nomenclature for Aqtesolv:

T = transmissivity ( $\text{m}^2/\text{s}$ )

S = storativity (-)

$K_z/K_r$  = ratio of hydraulic conductivities in the vertical and radial direction (set to 1)

$S_w$  = skin factor

$r(w)$  = borehole radius (m)

$r(c)$  = effective casing radius (m)

C = well loss constant (set to 0)

r/B = leakage factor (-)

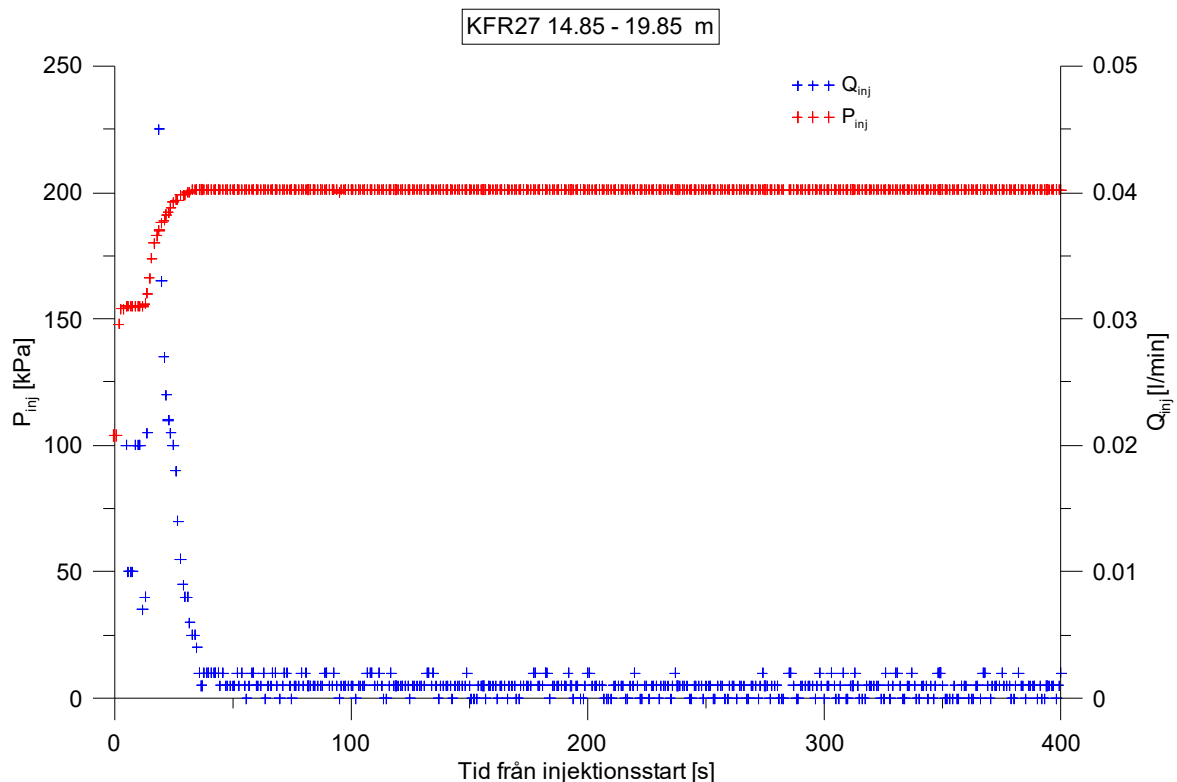


**Figure A2-1.** Linear plot of flow rate ( $Q$ ) and pressure ( $P$ ) versus time from the injection test in section 14.85-19.85 m in borehole KFR27.

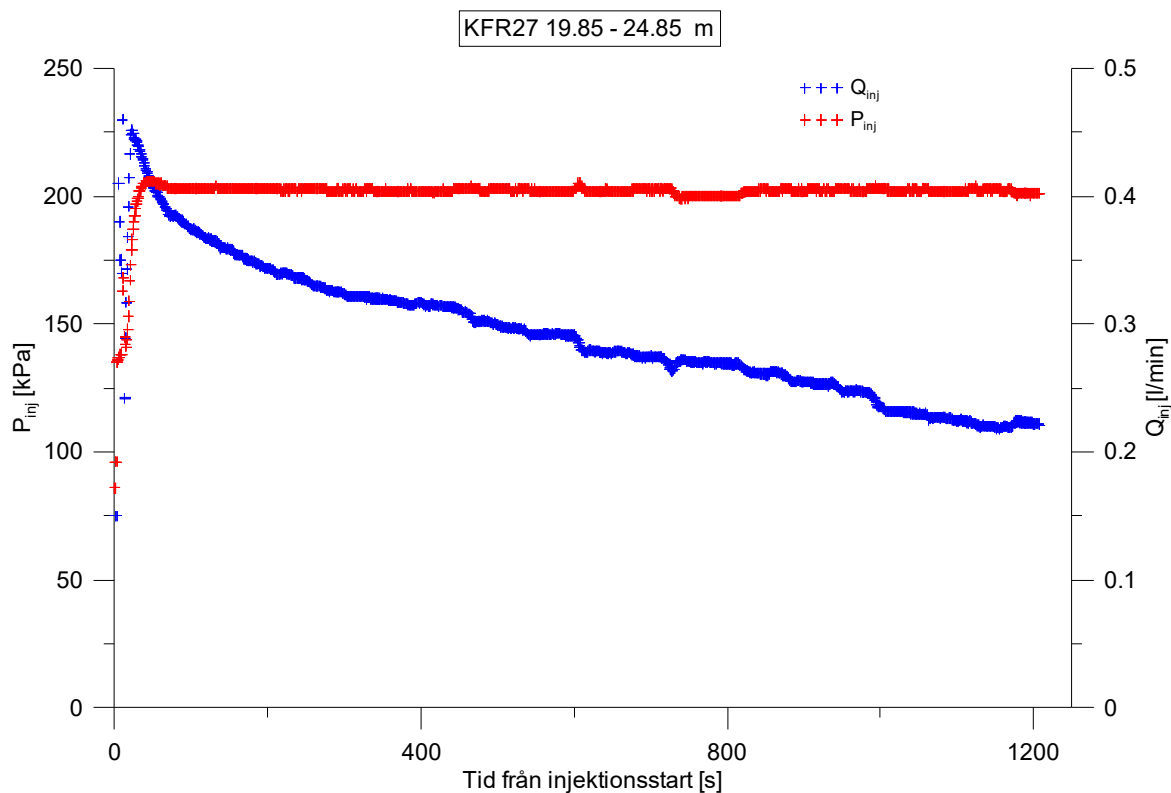


**Figure A2-2.** Linear plot of flow rate ( $Q$ ) and pressure ( $P$ ) versus time from the injection test in section 19.85-24.85 m in borehole KFR27.

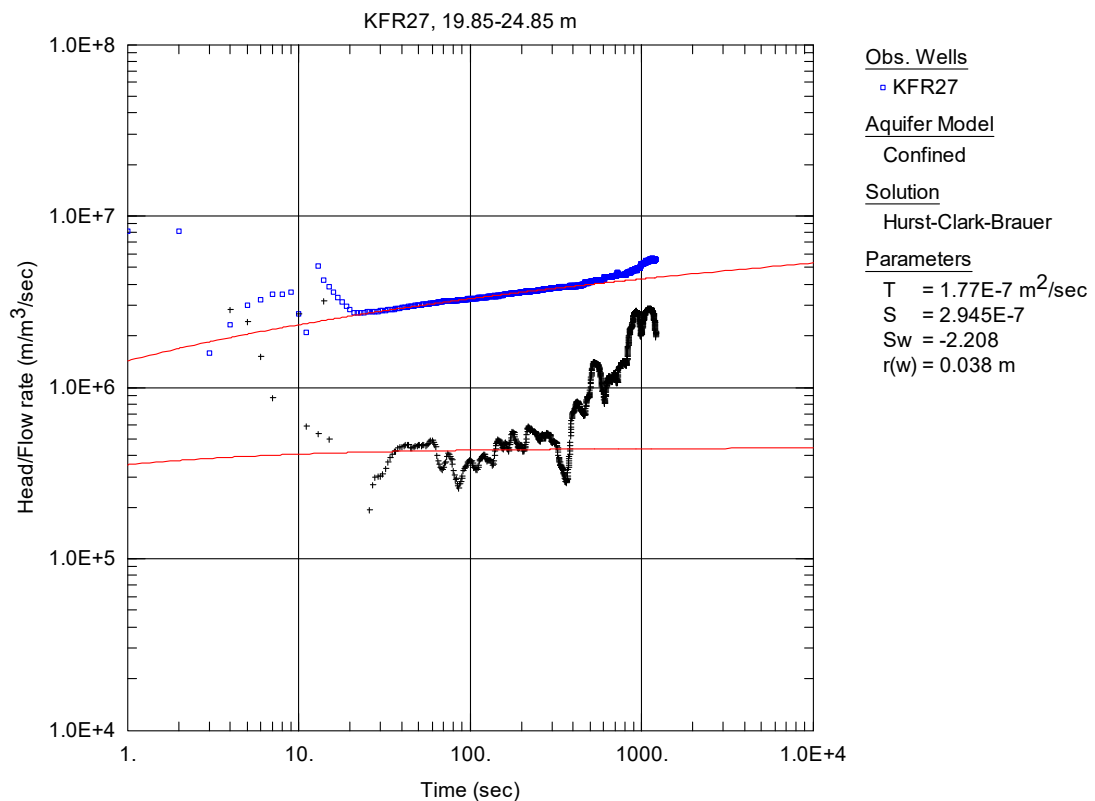


**Figure A2-3.** Log-log plot of head/flow rate ( $\square$ ) and derivative ( $+$ ) versus time, from the injection test in section 19.85-24.85 m in KFR27.

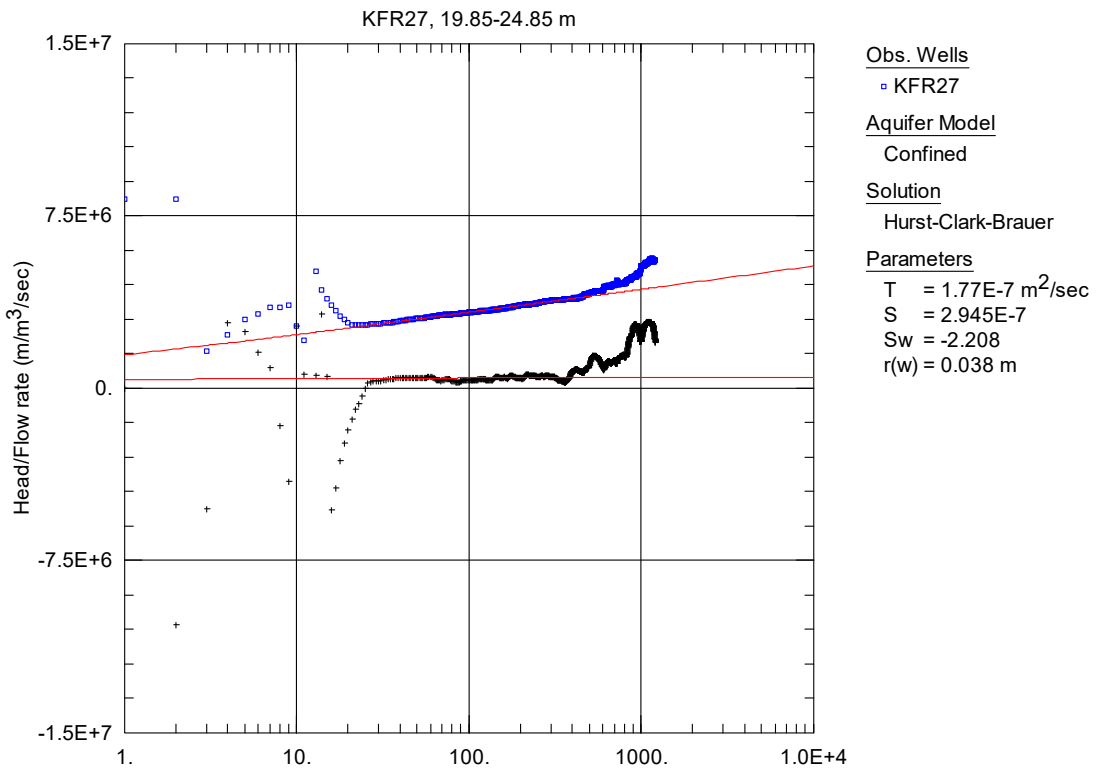


**Figure A2-4.** Lin-log plot of head/flow rate (□) and derivative (+) versus time, from the injection test in section 19.85-24.85 m in KFR27.

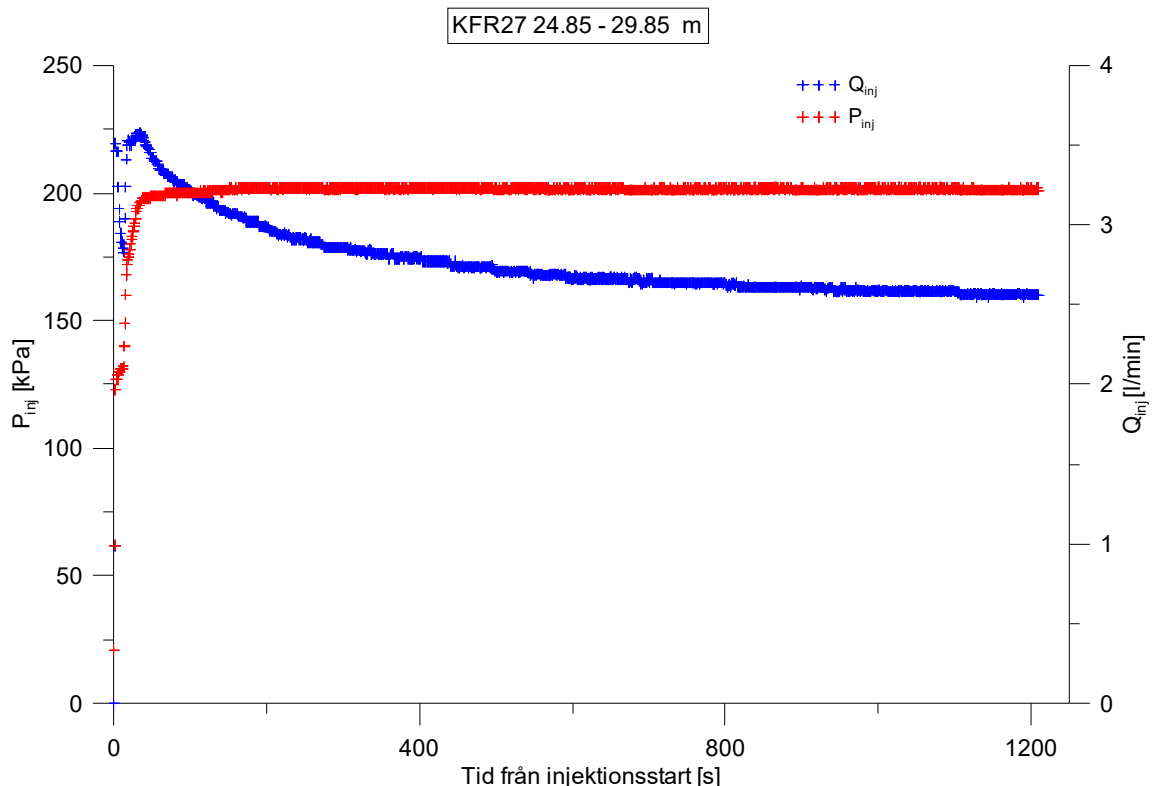


**Figure A2-5.** Linear plot of flow rate ( $Q$ ) and pressure ( $P$ ) versus time from the injection test in section 24.85-29.85 m in borehole KFR27.

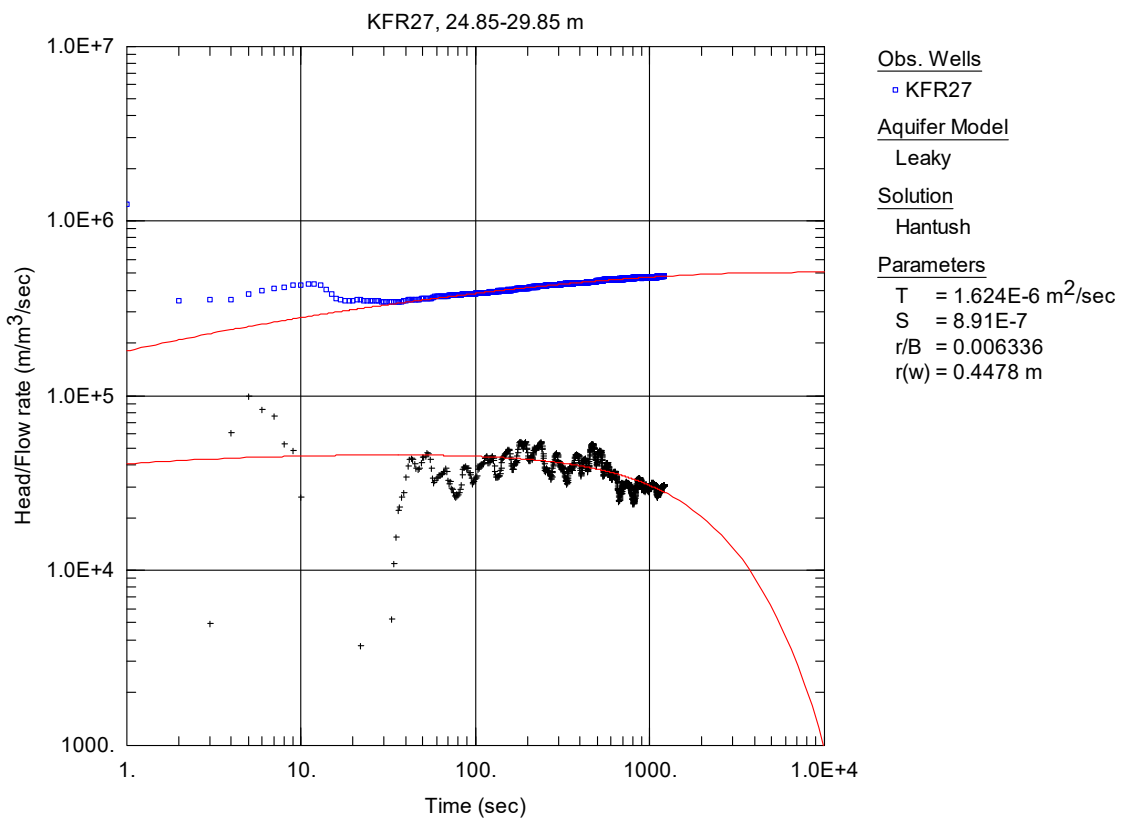


**Figure A2-6.** Log-log plot of head/flow rate (□) and derivative (+) versus time, from the injection test in section 24.85-29.85 m in borehole KFR27.

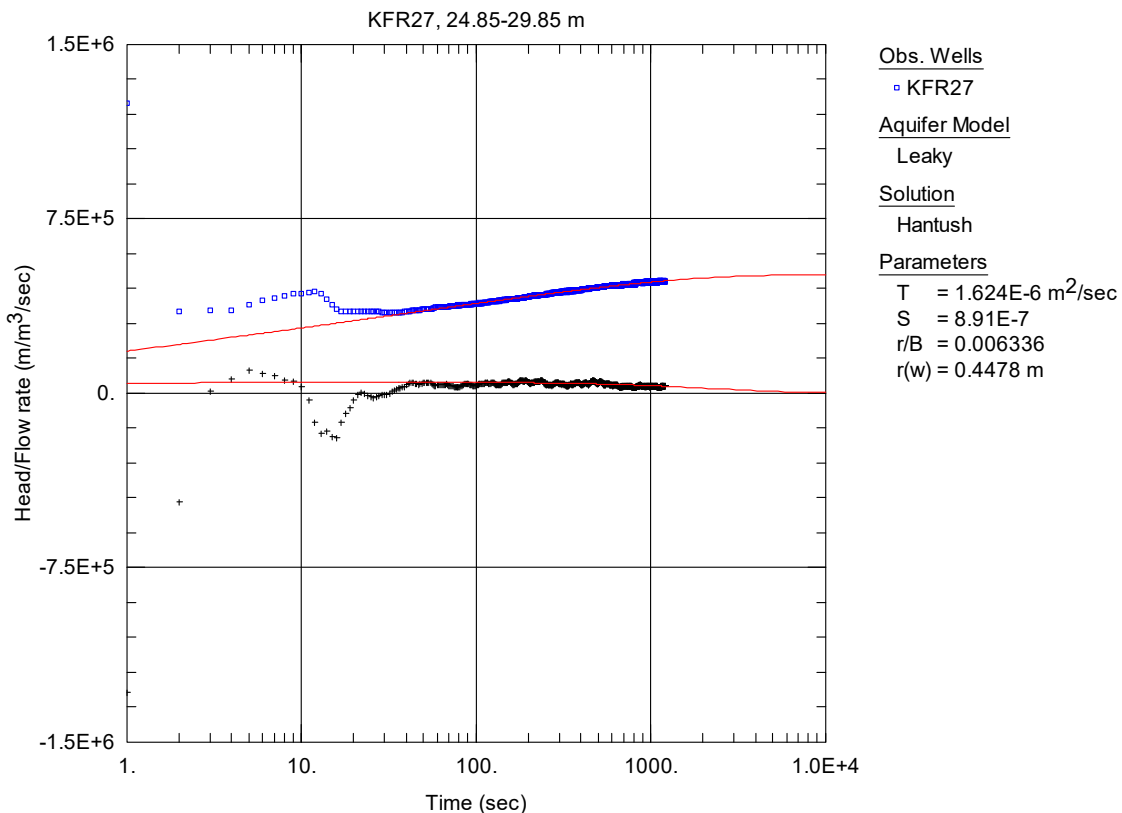


**Figure A2-7.** Lin-log plot of head/flow rate (□) and derivative (+) versus time, from the injection test in section 24.85-29.85 m in borehole KFR27.

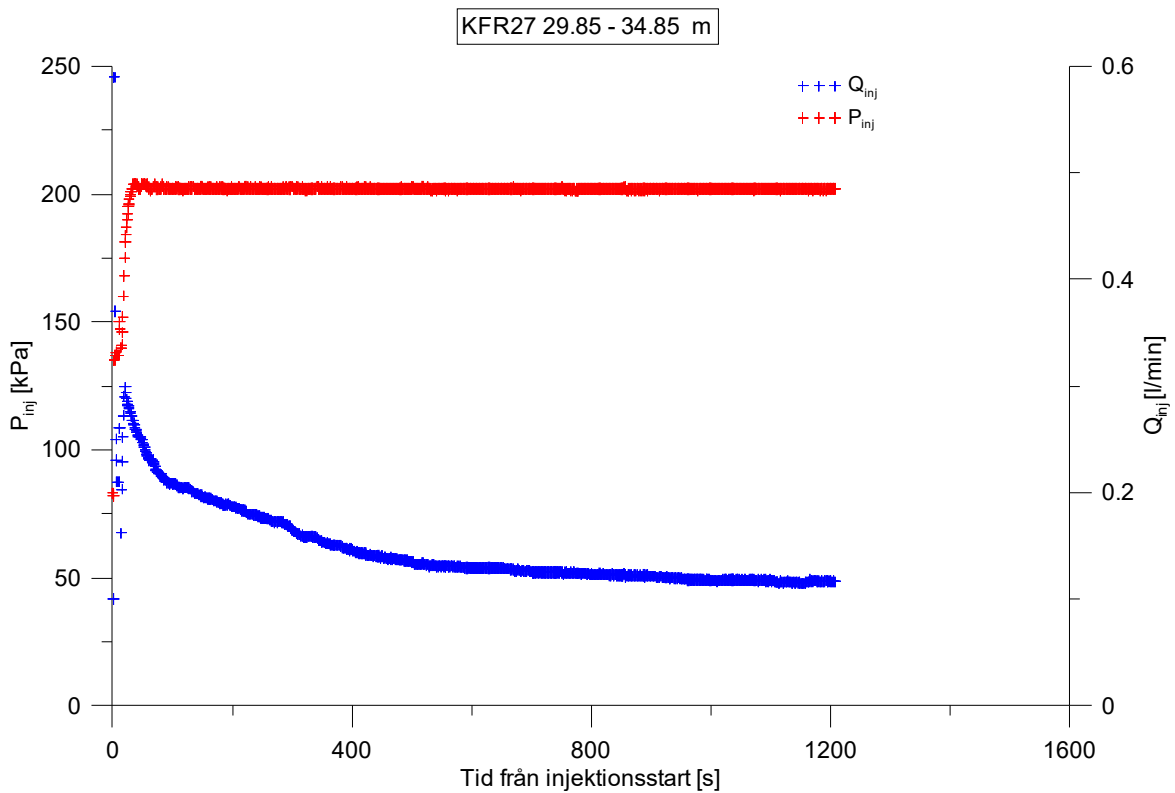


**Figure A2-8.** Linear plot of flow rate ( $Q$ ) and pressure ( $P$ ) versus time from the injection test in section 29.85-34.85 m in borehole KFR27.

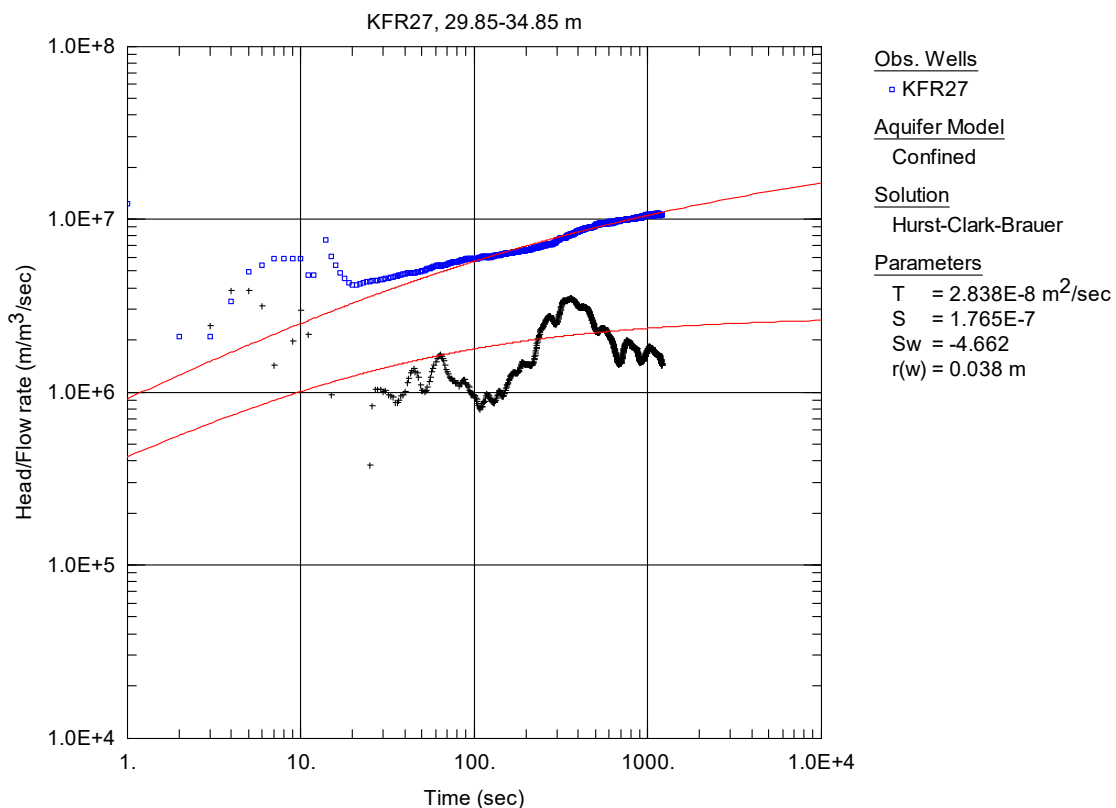


**Figure A2-9.** Log-log plot of head/flow rate (□) and derivative (+) versus time, from the injection test in section 29.85-34.85 m in borehole KFR27

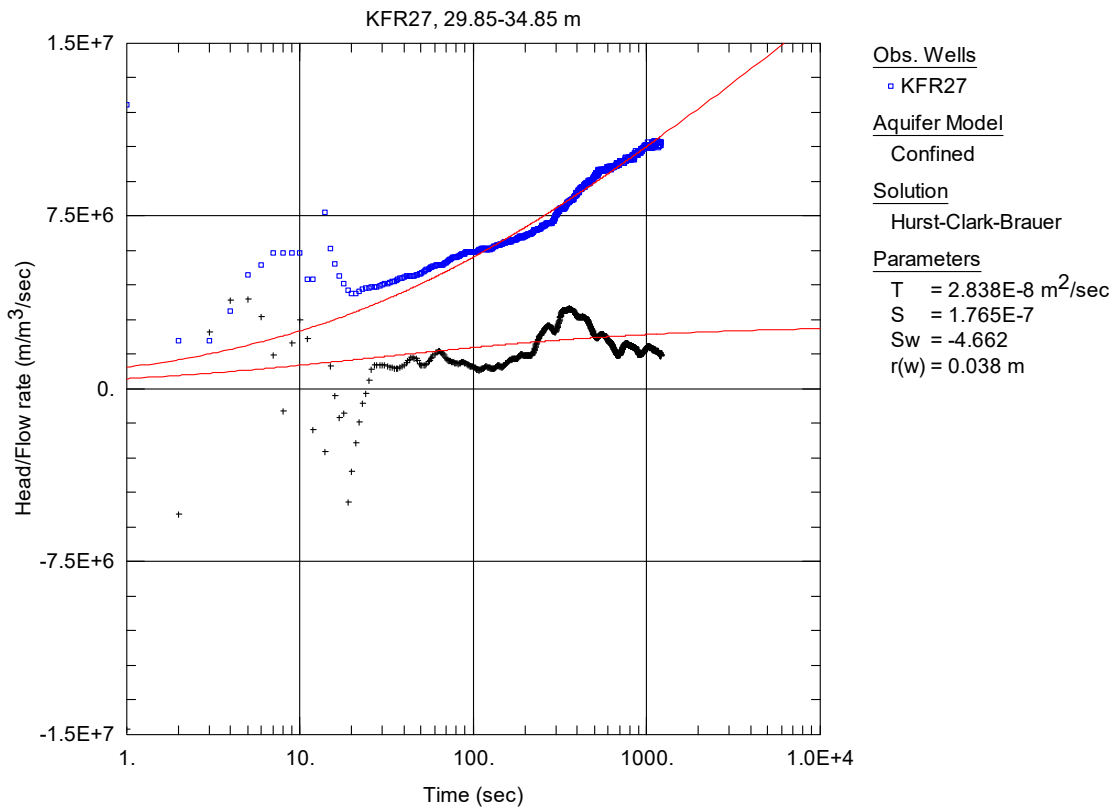


**Figure A2-10.** Lin-log plot of head/flow rate (□) and derivative (+) versus time, from the injection test in section 29.85-34.85 m in borehole KFR27.

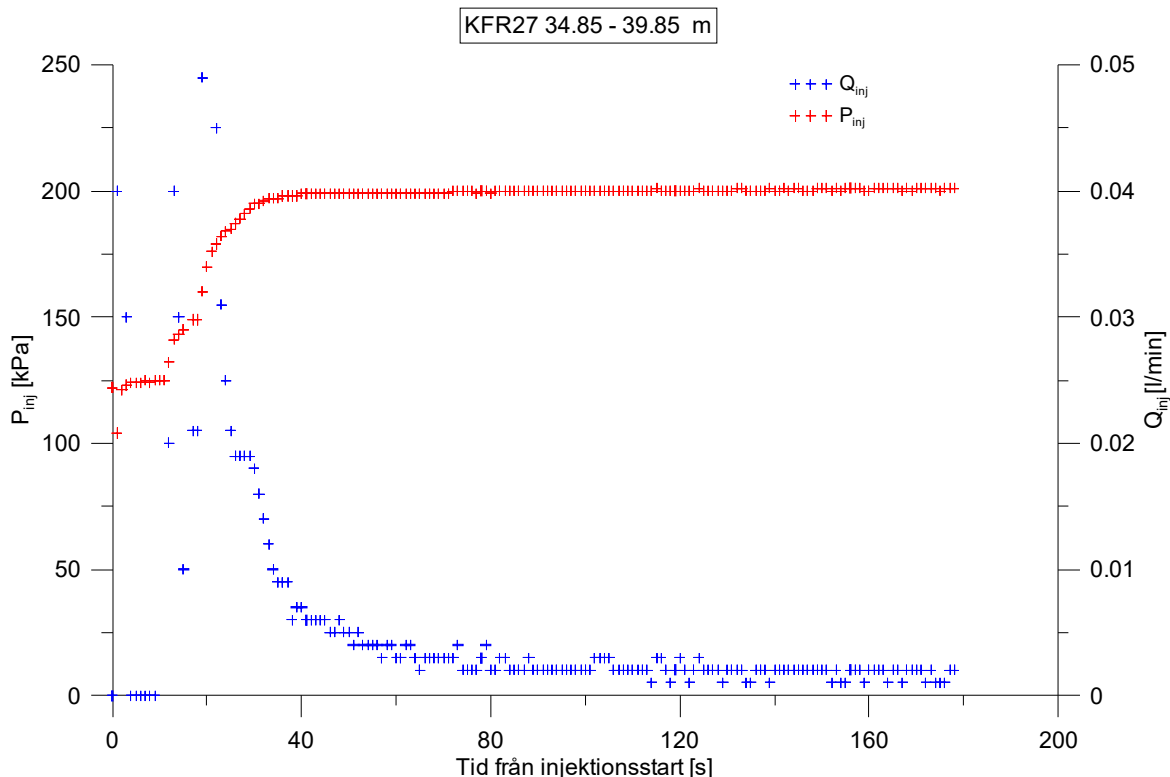


**Figure A2-11.** Linear plot of flow rate (Q) and pressure (P) versus time from the injection test in section 34.85-39.85 m in borehole KFR27.

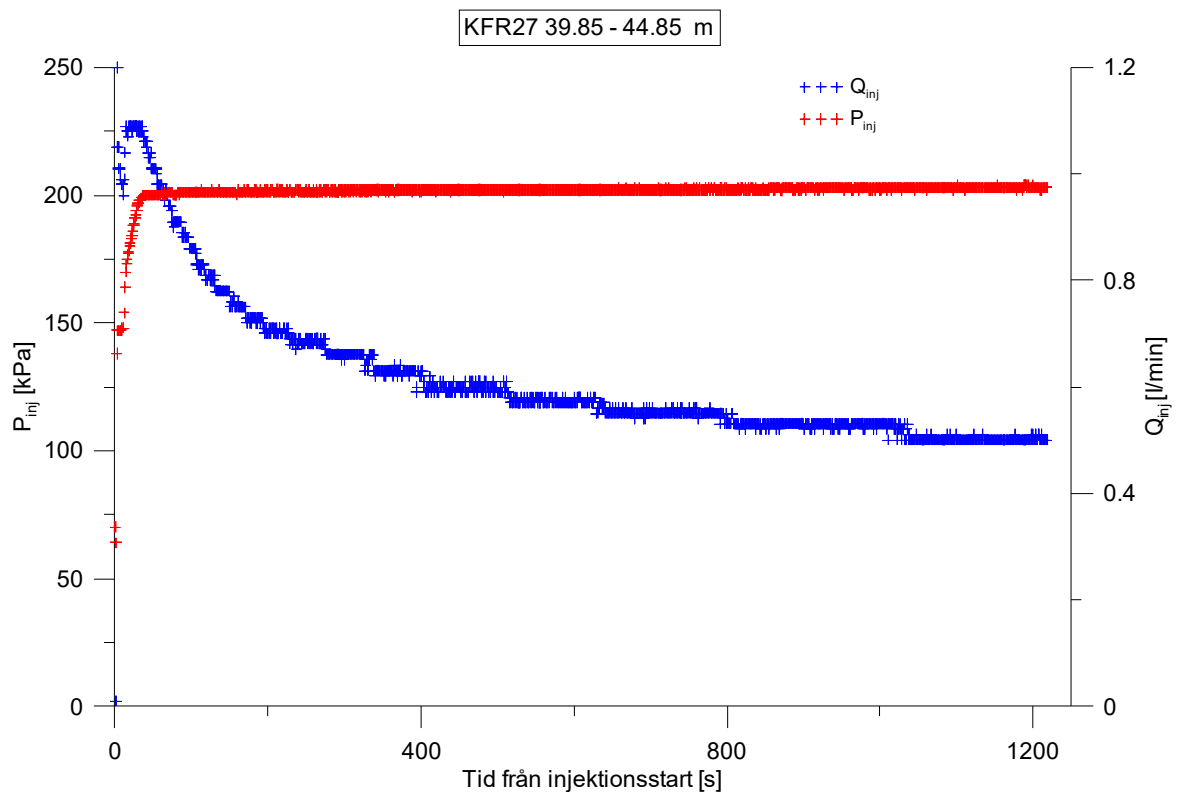


**Figure A2-12.** Linear plot of flow rate ( $Q$ ) and pressure ( $P$ ) versus time from the injection test in section 39.85-44.85 m in borehole KFR27.

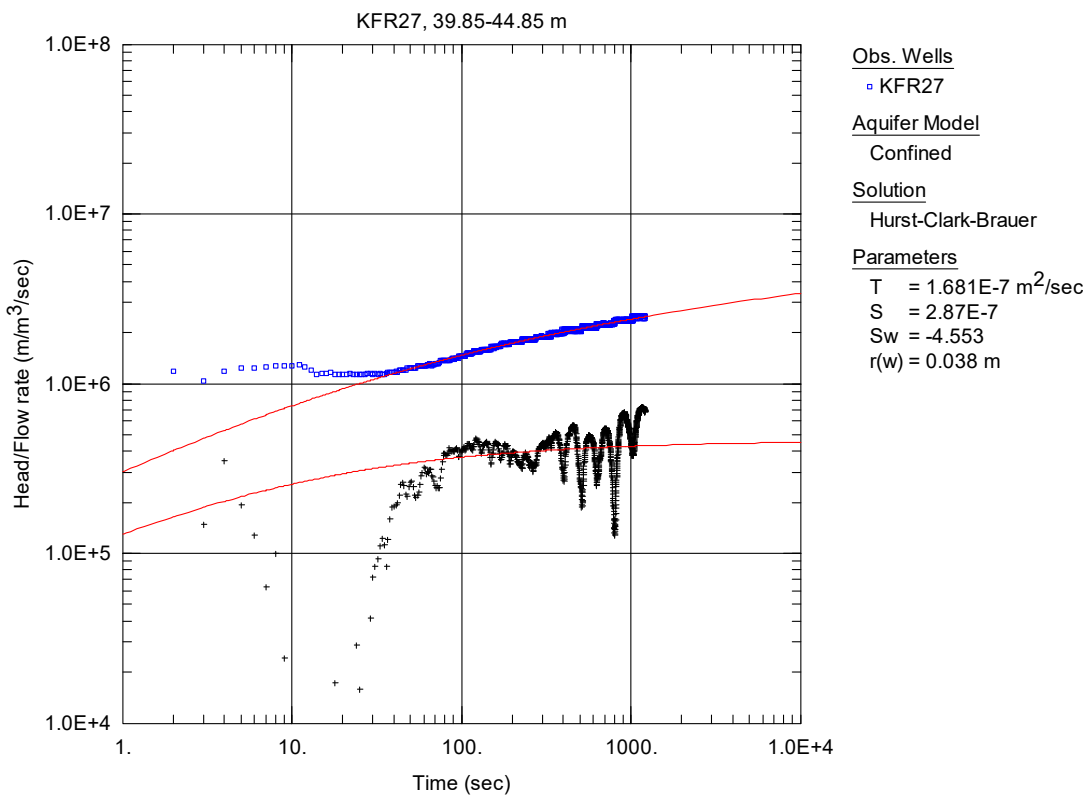


**Figure A2-13.** Log-log plot of head/flow rate ( $\square$ ) and derivative ( $+$ ) versus time, from the injection test in section 39.85-44.85 m in borehole KFR27.

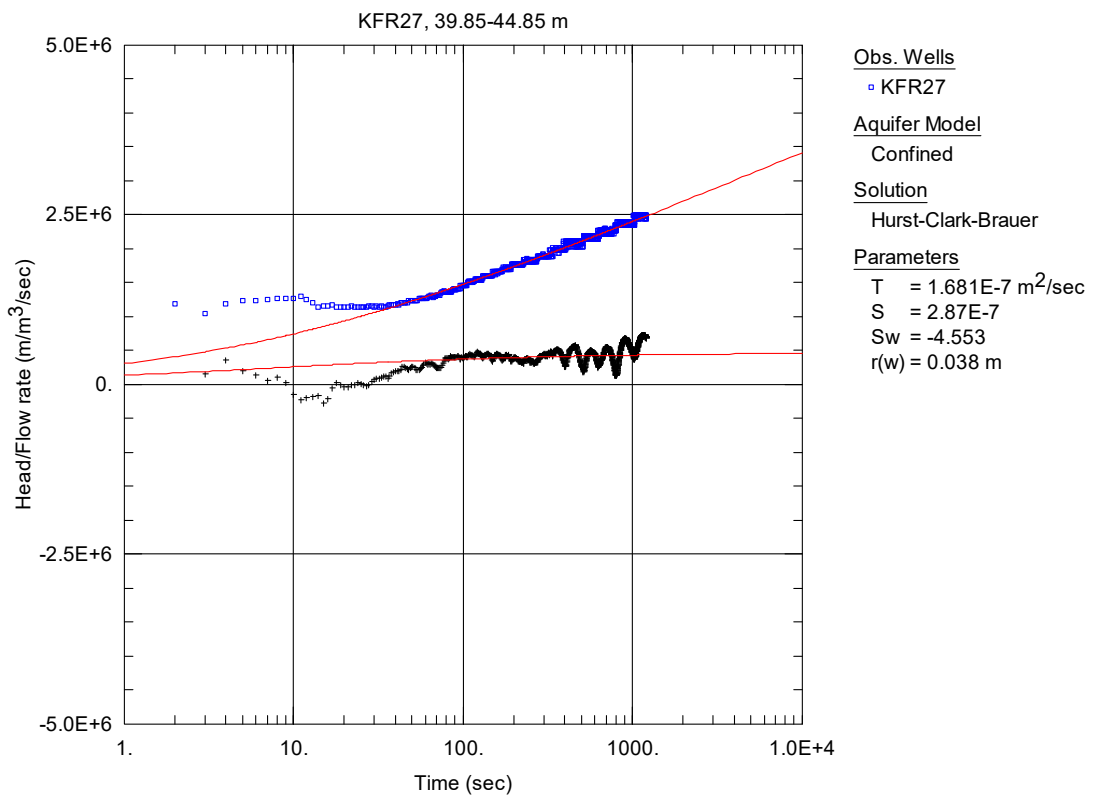


**Figure A2-14.** Lin-log plot of head/flow rate (□) and derivative (+) versus time, from the injection test in section 39.85-44.85 m in borehole KFR27.

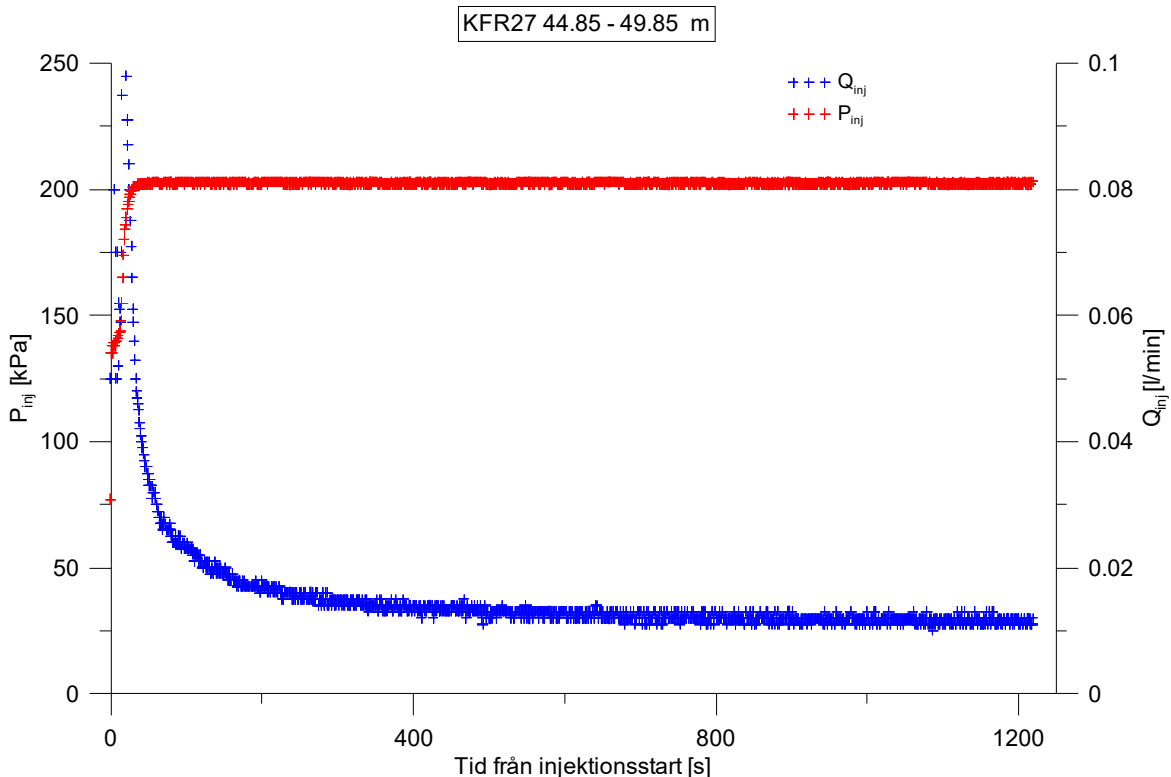


**Figure A2-15.** Linear plot of flow rate ( $Q$ ) and pressure ( $P$ ) versus time from the injection test in section 44.85-49.85 m in borehole KFR27.

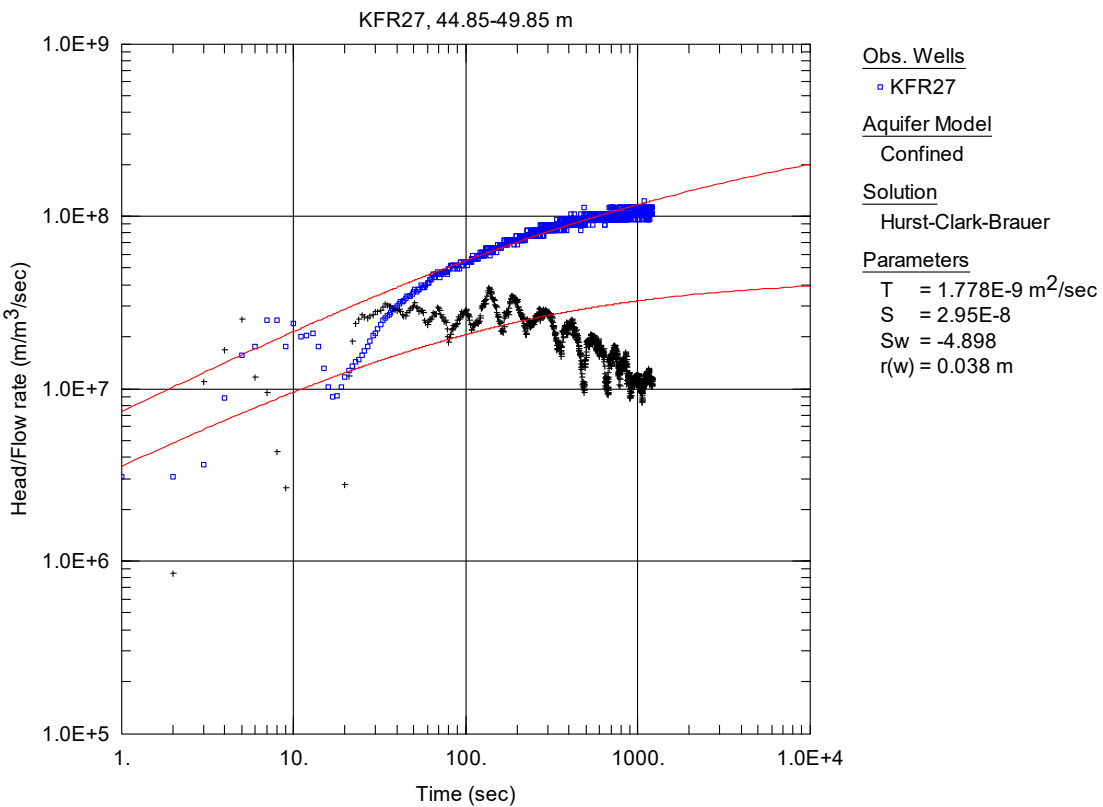


**Figure A2-16.** Log-log plot of head/flow rate (□) and derivative (+) versus time, from the injection test in section 44.85-49.85 m in borehole KFR27.

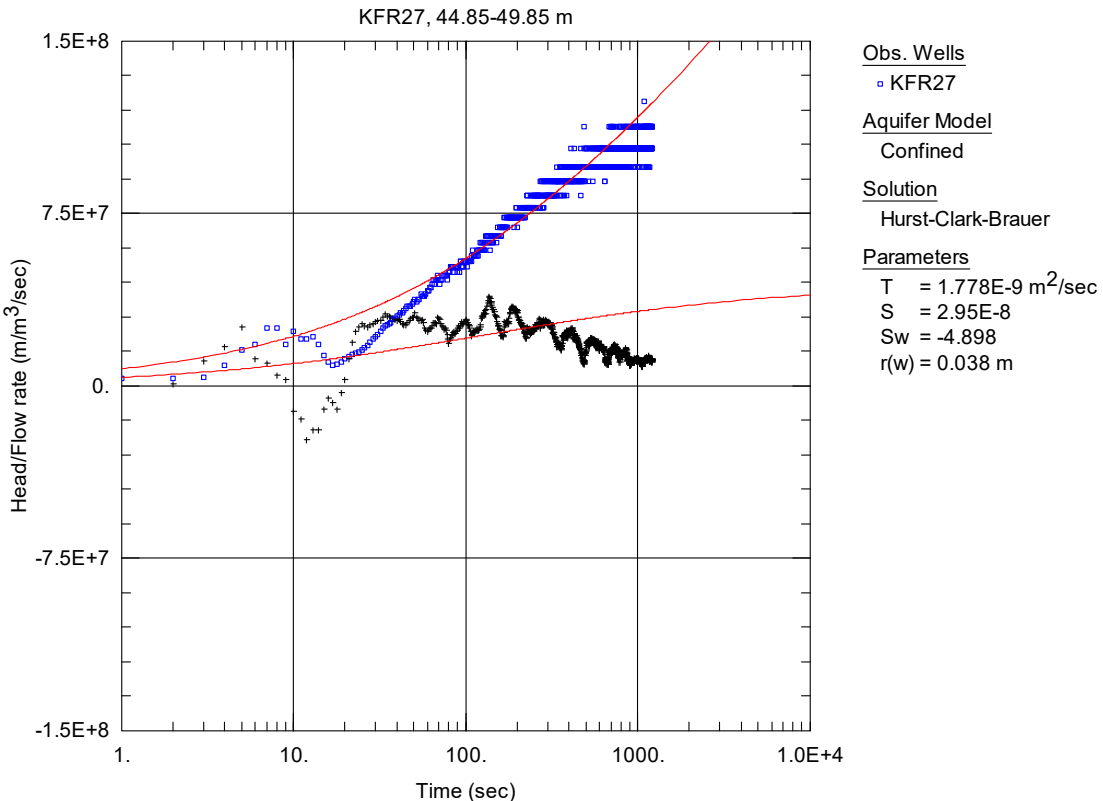


**Figure A2-17.** Lin-log plot of head/flow rate (□) and derivative (+) versus time, from the injection test in section 44.85-49.85 m in borehole KFR27.

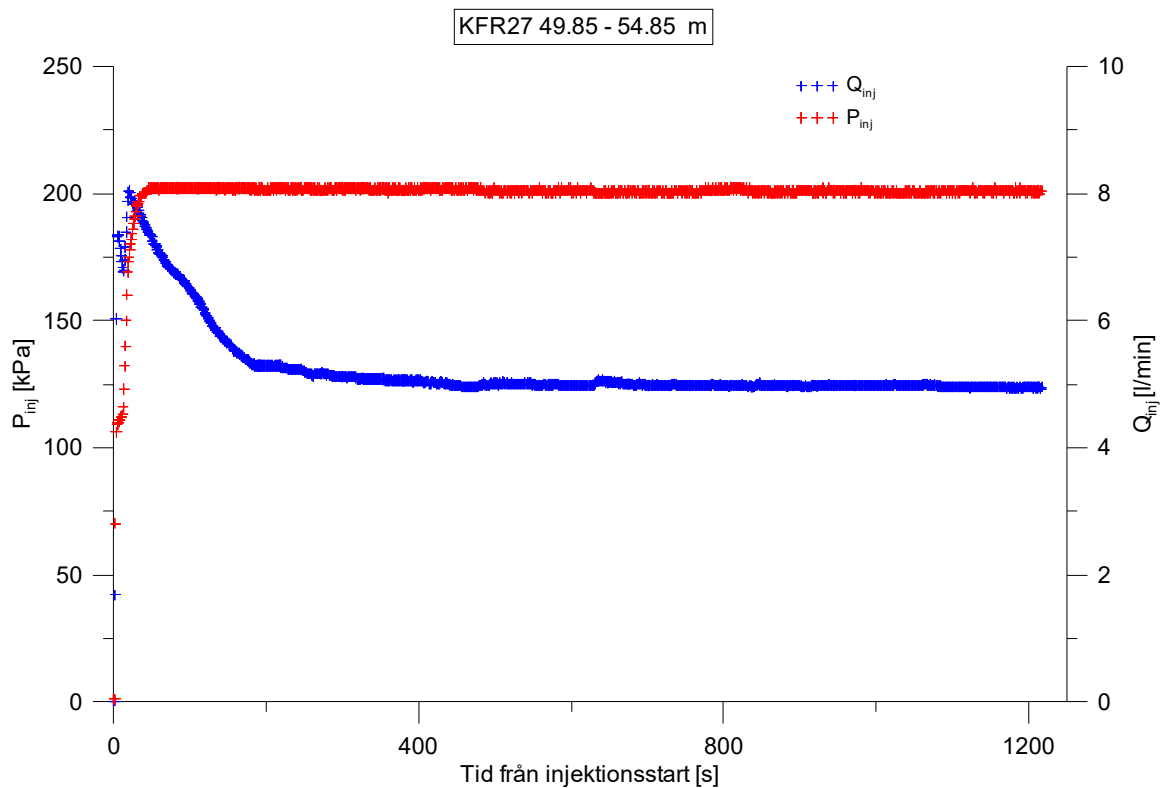


**Figure A2-18.** Linear plot of flow rate ( $Q$ ) and pressure ( $P$ ) versus time from the injection test in section 49.85-54.85 m in borehole KFR27.

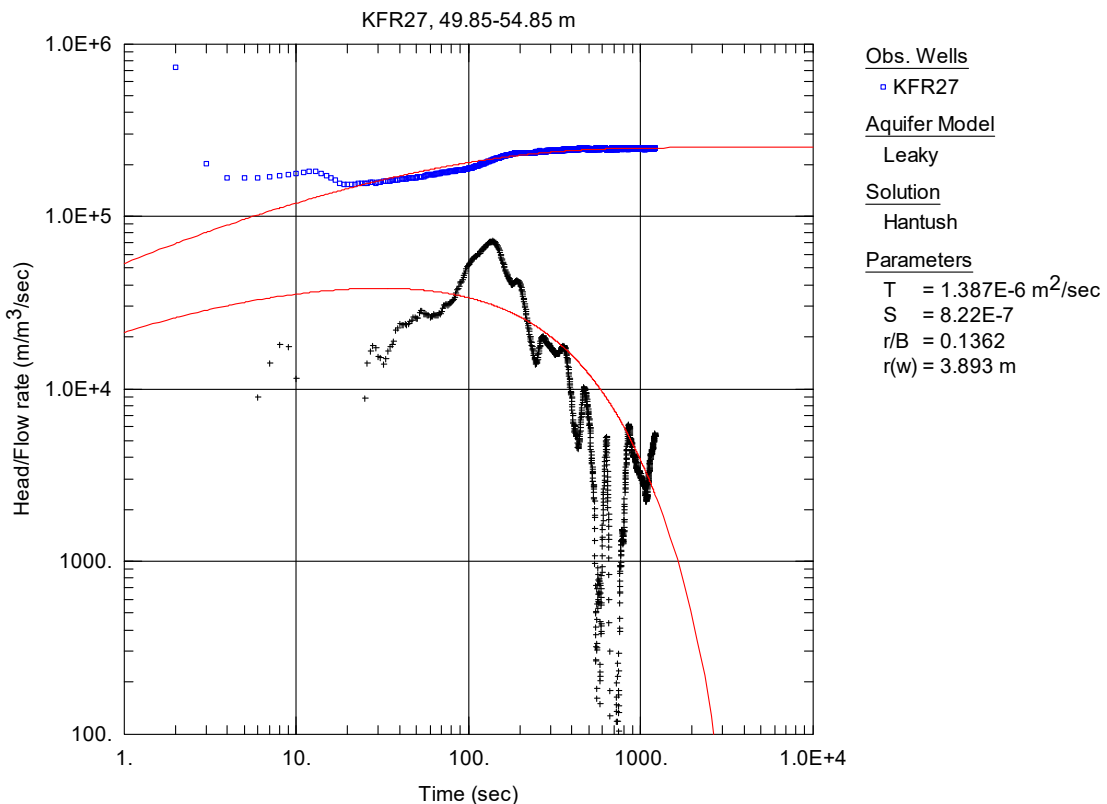


**Figure A2-19.** Log-log plot of head/flow rate (□) and derivative (+) versus time, from the injection test in section 49.85-54.85 m in borehole KFR27.

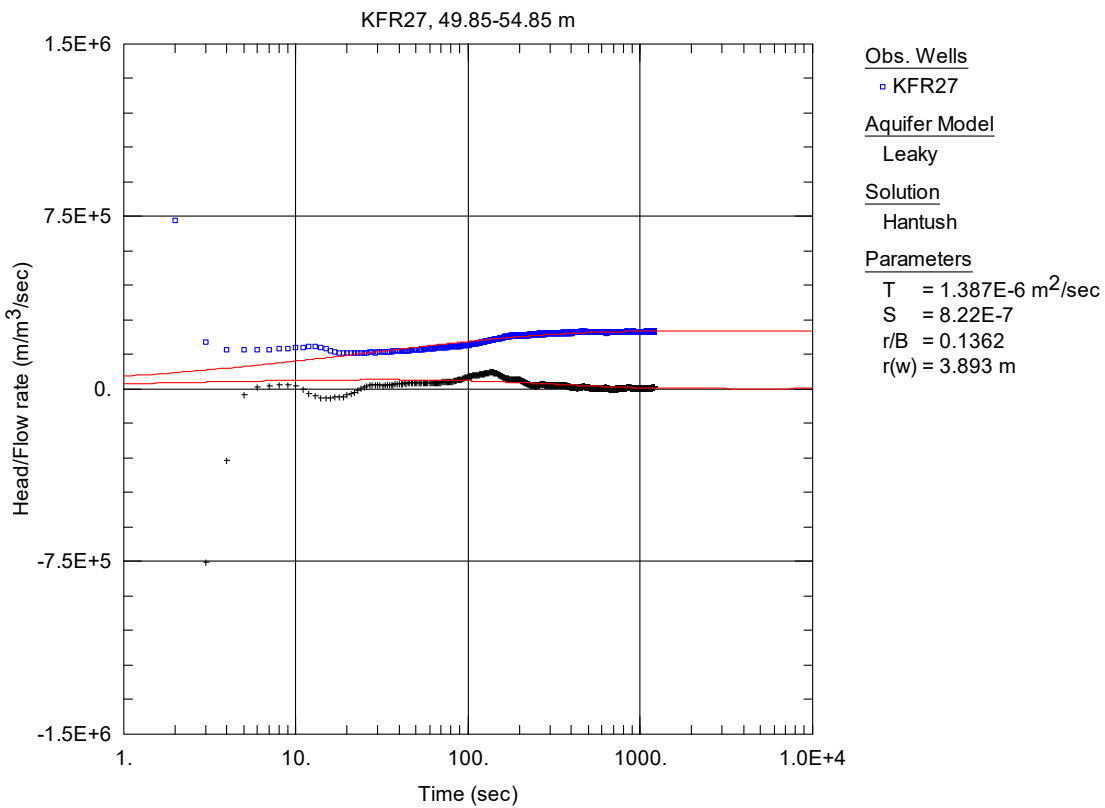


**Figure A2-20.** Lin-log plot of head/flow rate ( $\square$ ) and derivative (+) versus time, from the injection test in section 49.85-54.85 m in borehole KFR27.

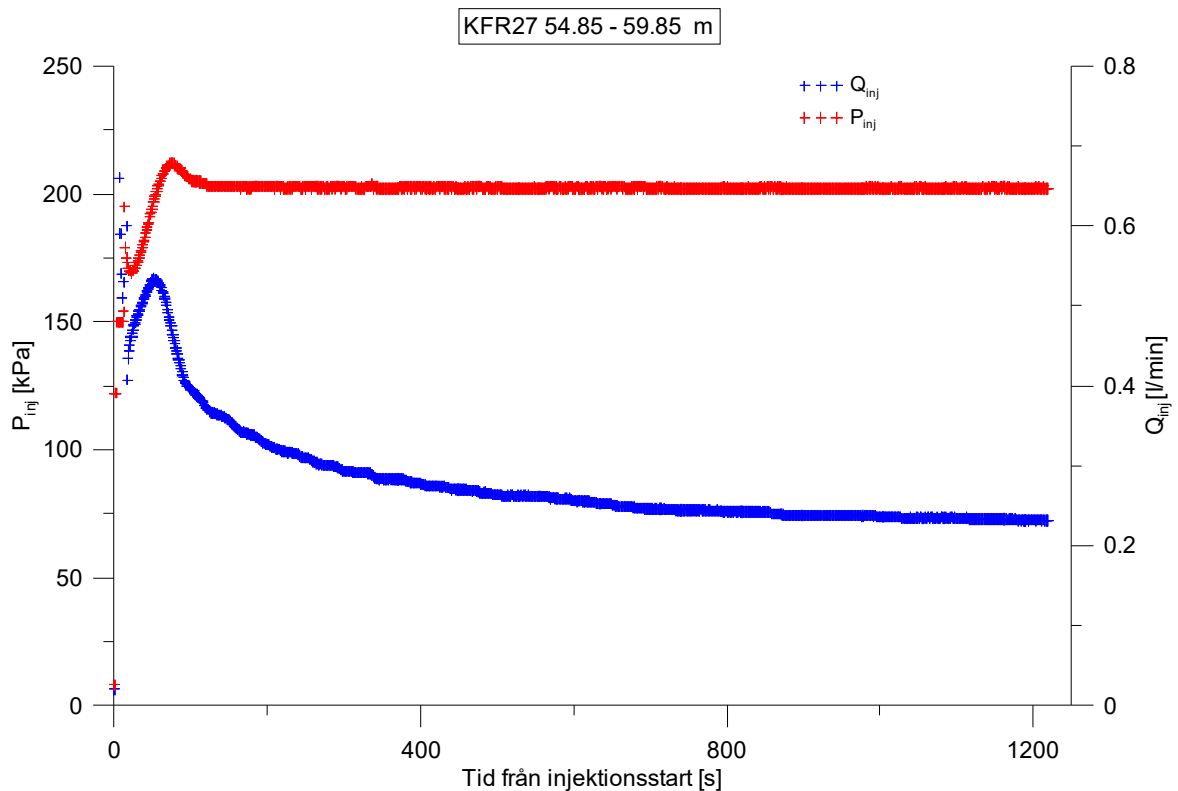


**Figure A2-21.** Linear plot of flow rate ( $Q$ ) and pressure ( $P$ ) versus time from the injection test in section 54.85-59.85 m in borehole KFR27.

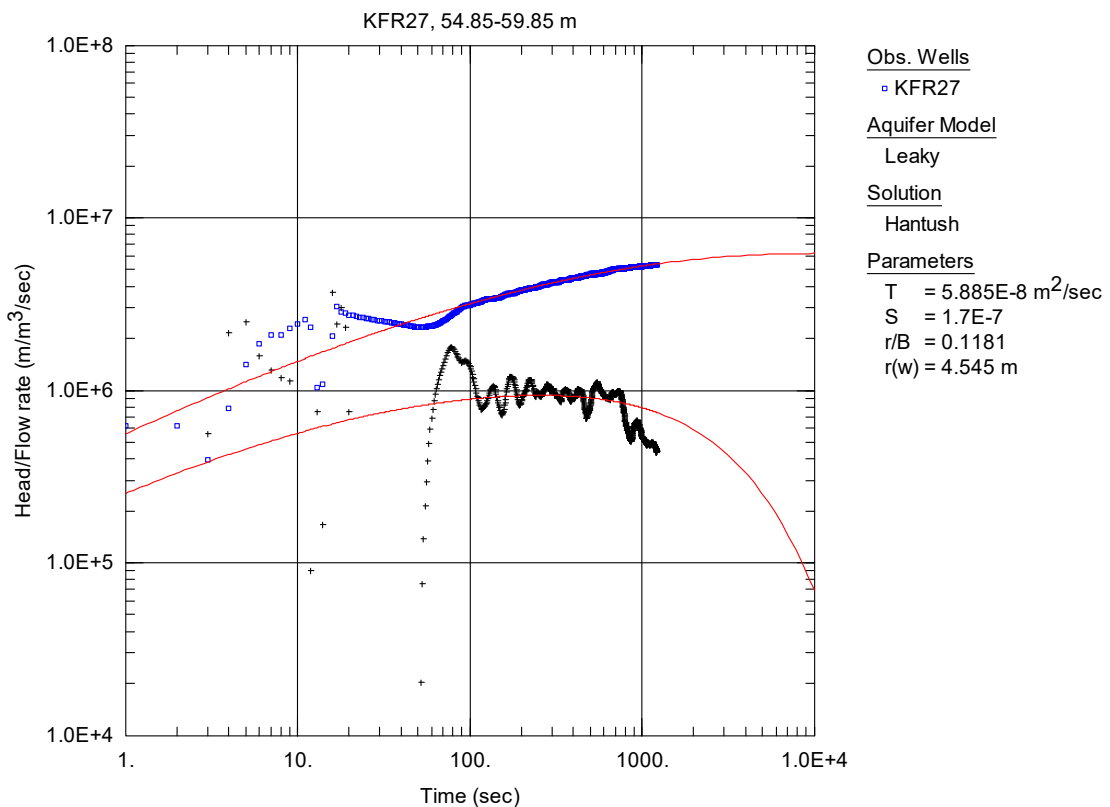


**Figure A2-22.** Log-log plot of head/flow rate (□) and derivative (+) versus time, from the injection test in section 54.85-59.85 m in borehole KFR27.

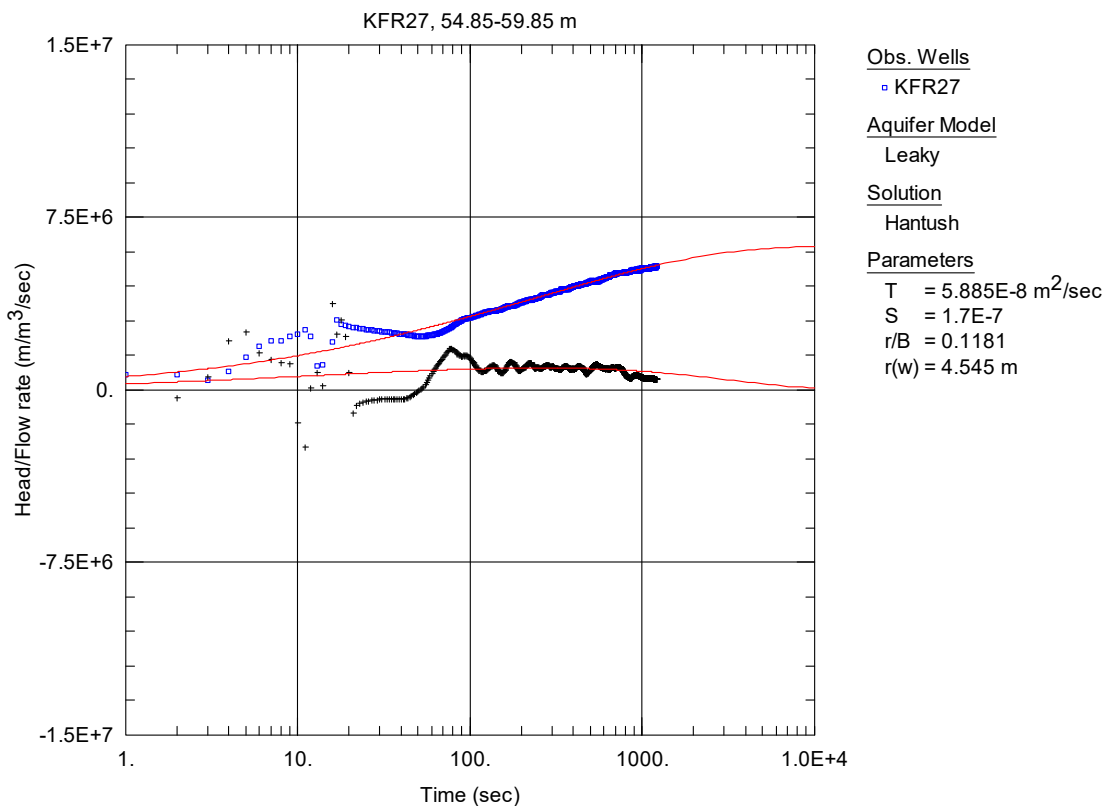


**Figure A2-23.** Lin-log plot of head/flow rate (□) and derivative (+) versus time, from the injection test in section 54.85-59.85 m in borehole KFR27.

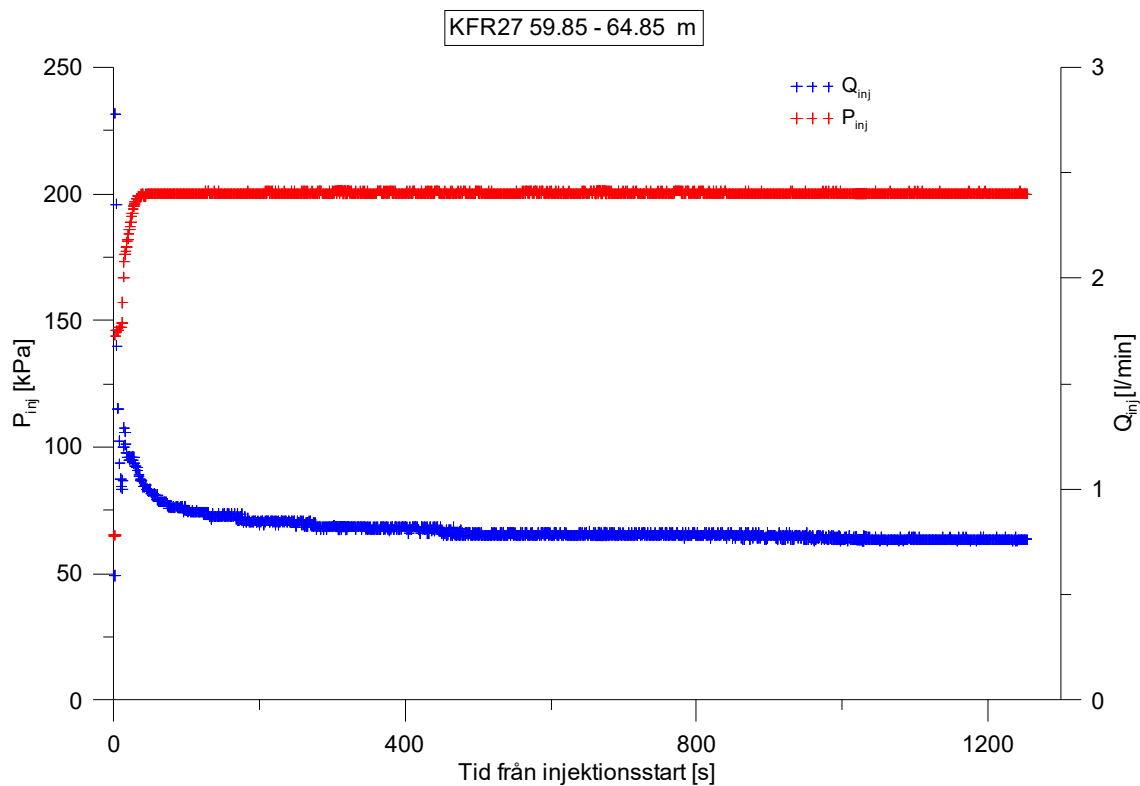


**Figure A2-24.** Linear plot of flow rate ( $Q$ ) and pressure ( $P$ ) versus time from the injection test in section 59.85-64.85 m in borehole KFR27.

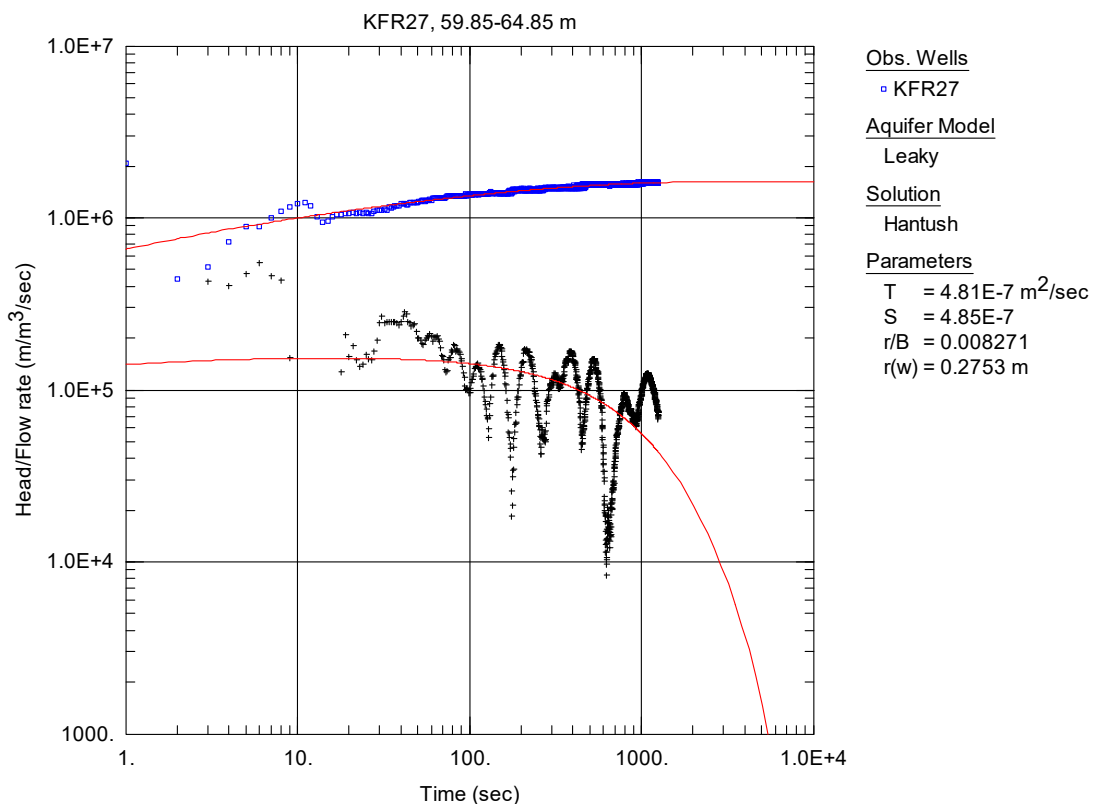


**Figure A2-25.** Log-log plot of head/flow rate ( $\square$ ) and derivative ( $+$ ) versus time, from the injection test in section 59.85-64.85 m in borehole KFR27.

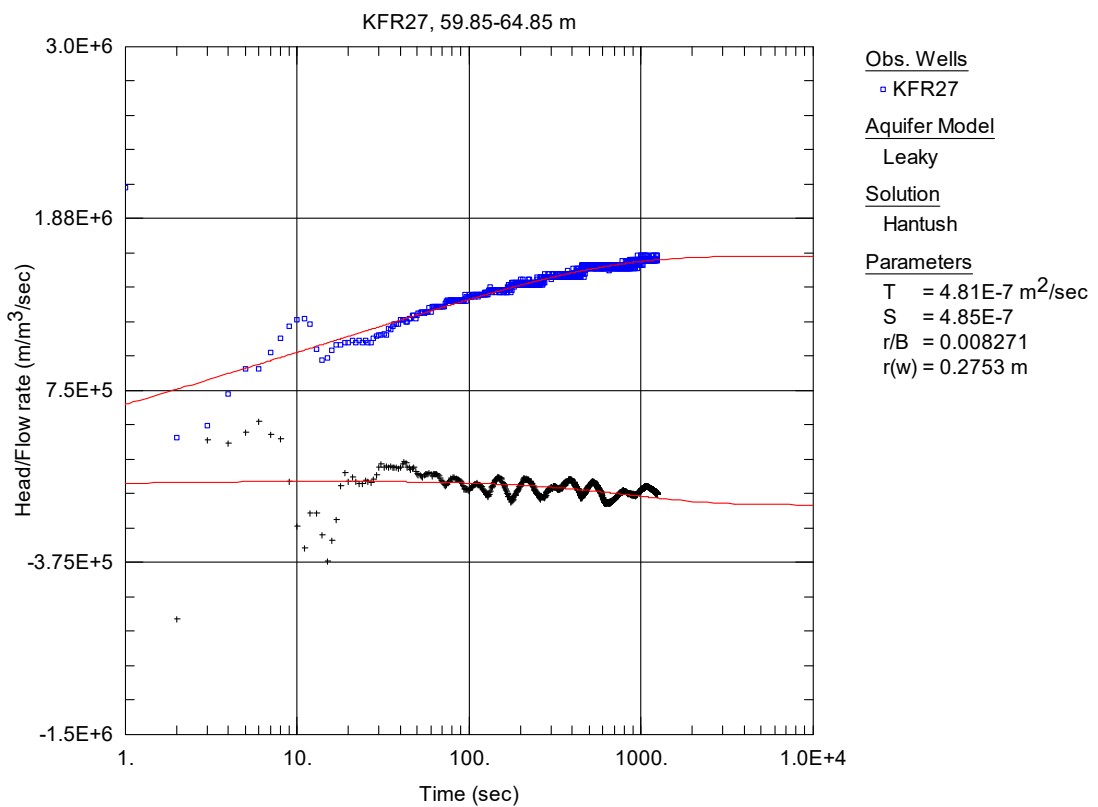


**Figure A2-26.** Lin-log plot of head/flow rate (□) and derivative (+) versus time, from the injection test in section 59.85-64.85 m in borehole KFR27.

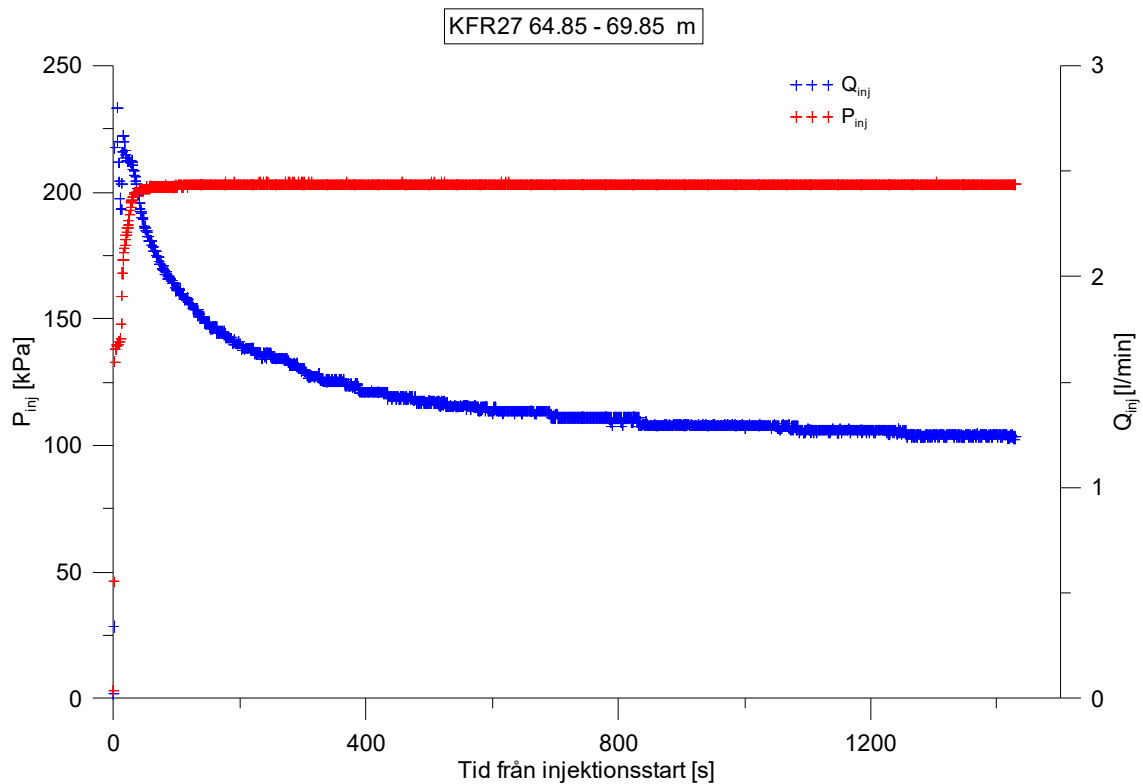


**Figure A2-27.** Linear plot of flow rate ( $Q$ ) and pressure ( $P$ ) versus time from the injection test in section 64.85-69.85 m in borehole KFR27.

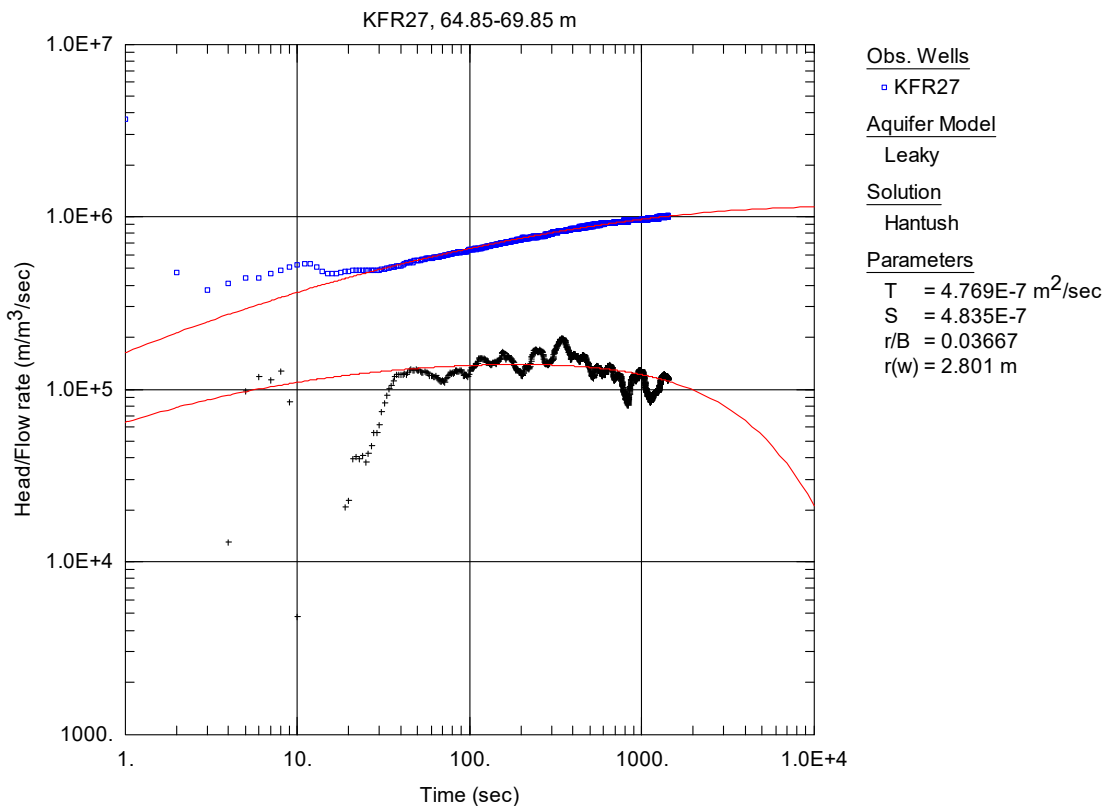


**Figure A2-28.** Log-log plot of head/flow rate (□) and derivative (+) versus time, from the injection test in section 64.85-69.85 m in borehole KFR27.

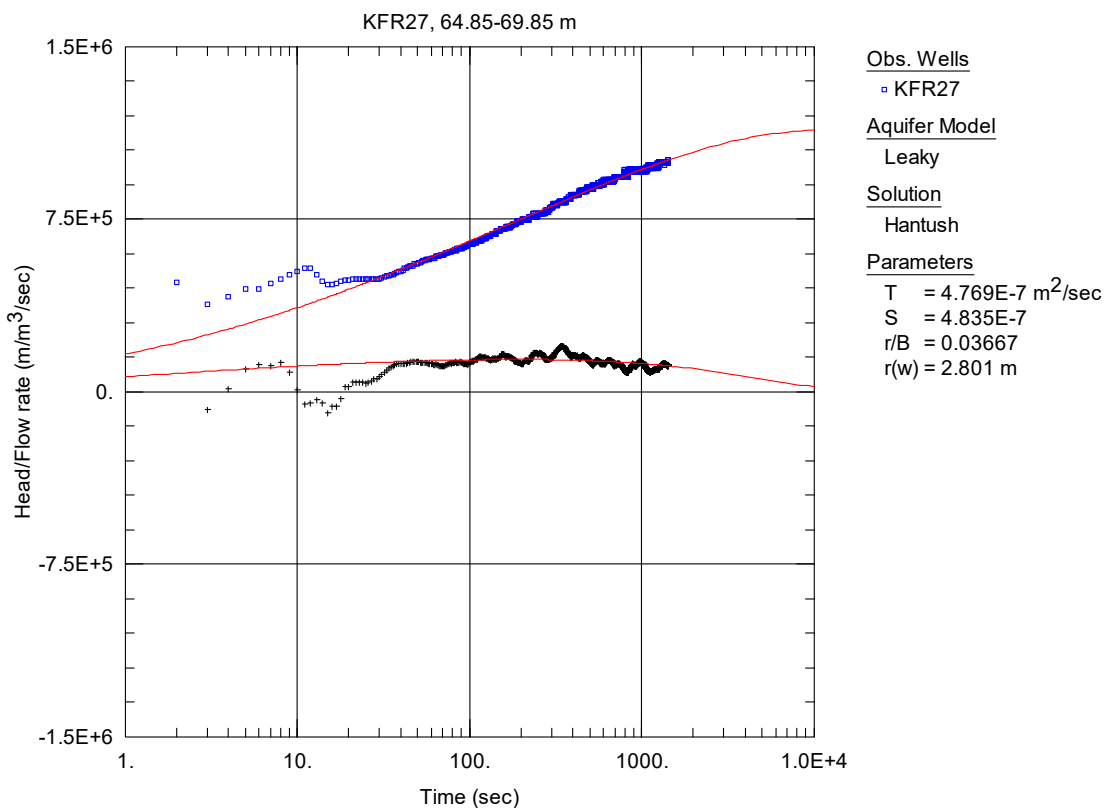


**Figure A2-29.** Lin-log plot of head/flow rate (□) and derivative (+) versus time, from the injection test in section 64.85-69.85 m in borehole KFR27.

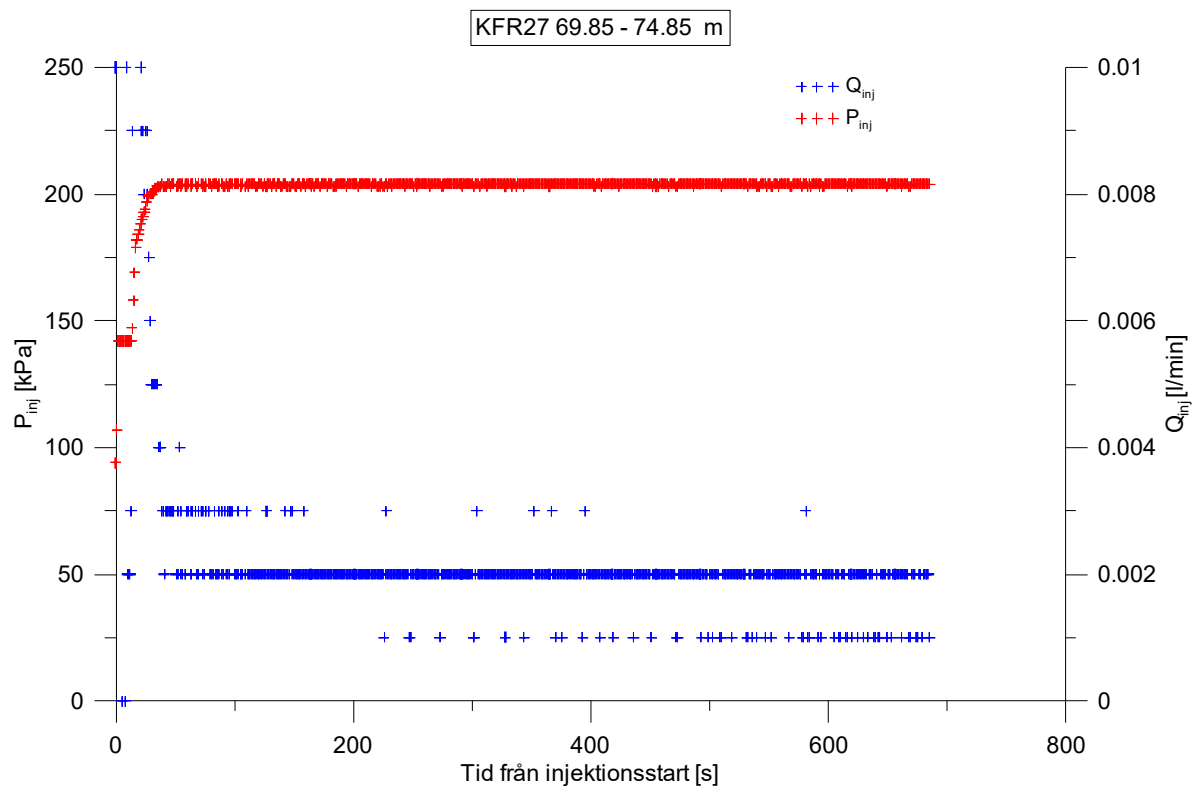


**Figure A2-30.** Linear plot of flow rate ( $Q$ ) and pressure ( $P$ ) versus time from the injection test in section 69.85-74.85 m in borehole KFR27.

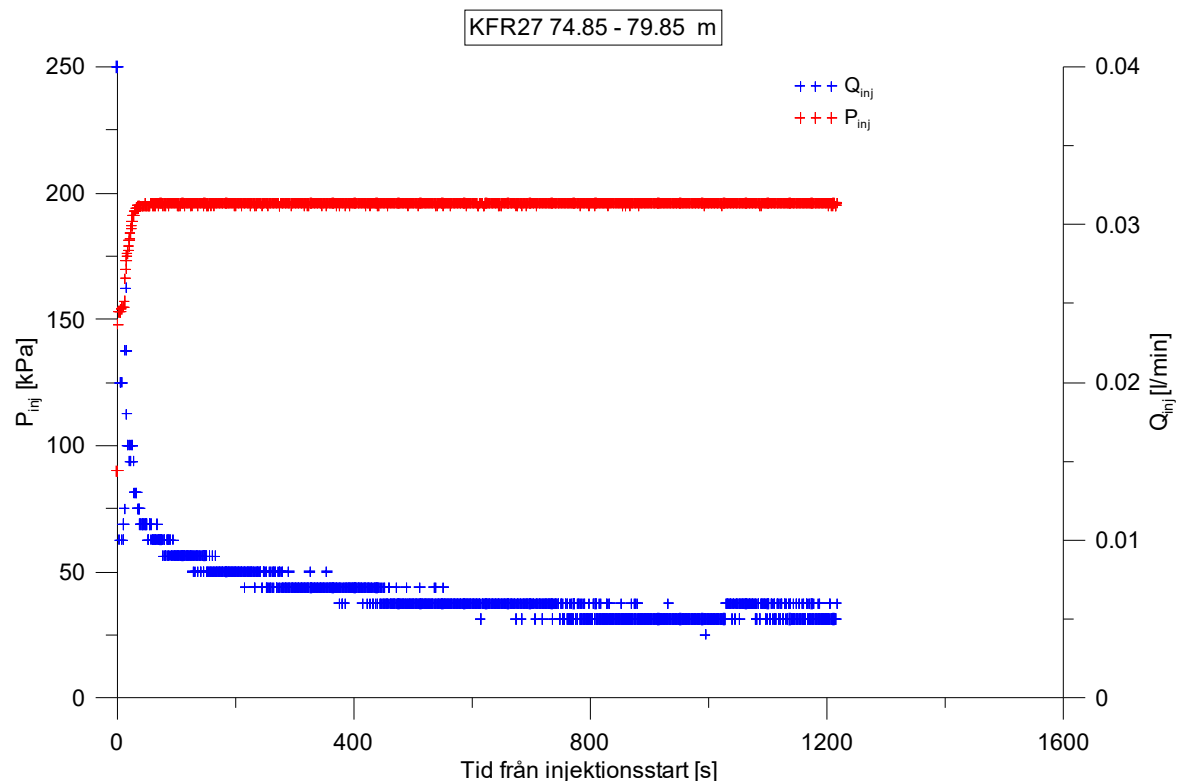


**Figure A2-31.** Linear plot of flow rate ( $Q$ ) and pressure ( $P$ ) versus time from the injection test in section 74.85-79.85 m in borehole KFR27.

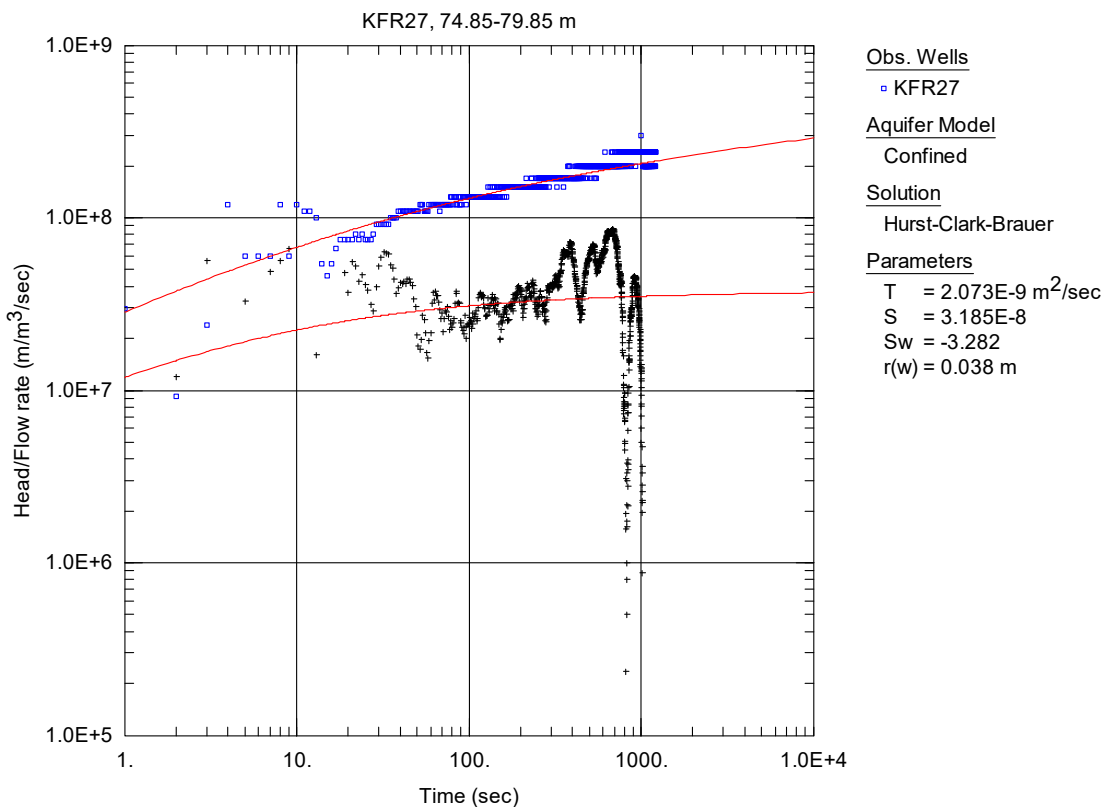


**Figure A2-32.** Log-log plot of head/flow rate (□) and derivative (+) versus time, from the injection test in section 74.85-79.85 m in borehole KFR27.

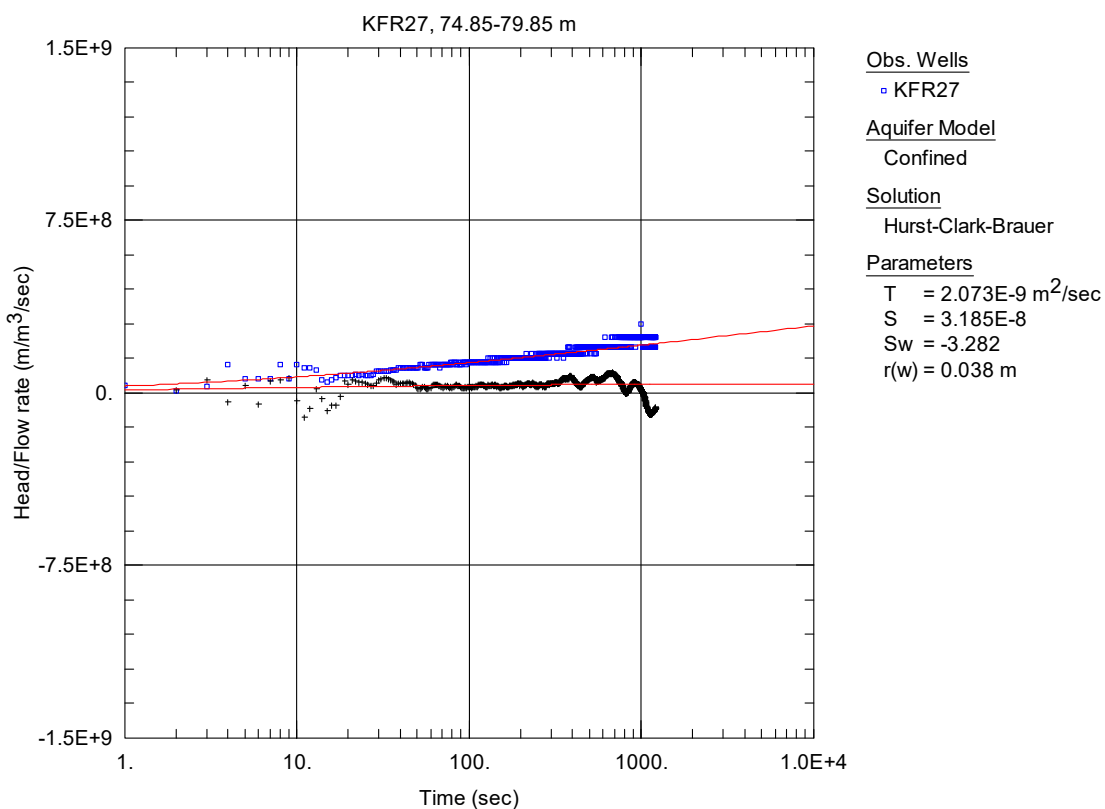


**Figure A2-33.** Lin-log plot of head/flow rate (□) and derivative (+) versus time, from the injection test in section 74.85-79.85 m in borehole KFR27.

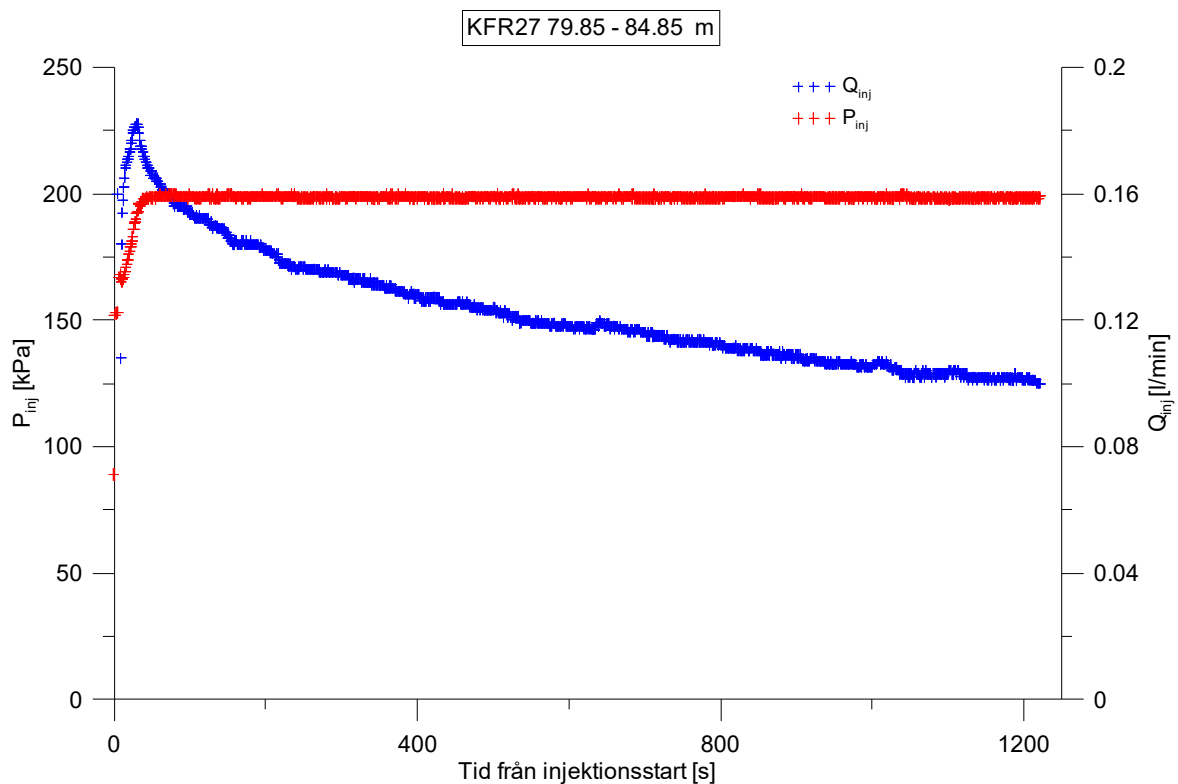


**Figure A2-34.** Linear plot of flow rate ( $Q$ ) and pressure ( $P$ ) versus time from the injection test in section 79.85-84.85 m in borehole KFR27.

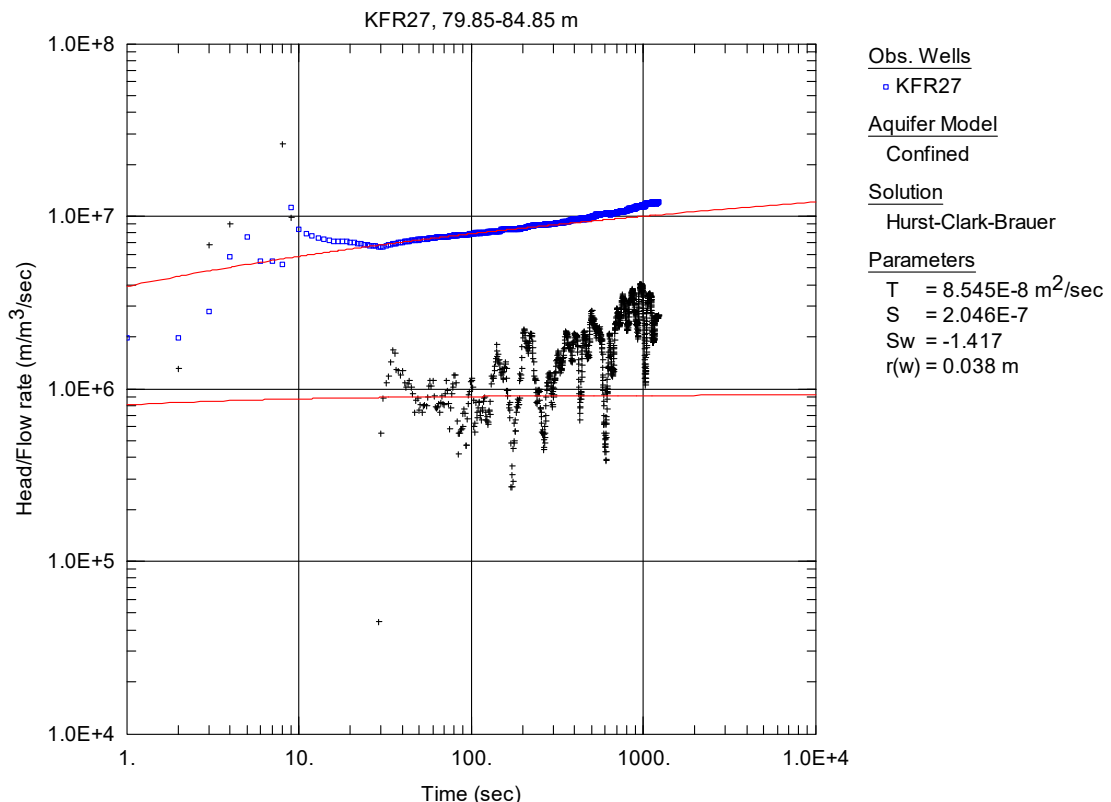


**Figure A2-35.** Log-log plot of head/flow rate ( $\square$ ) and derivative ( $+$ ) versus time, from the injection test in section 79.85-84.85 m in borehole KFR27.

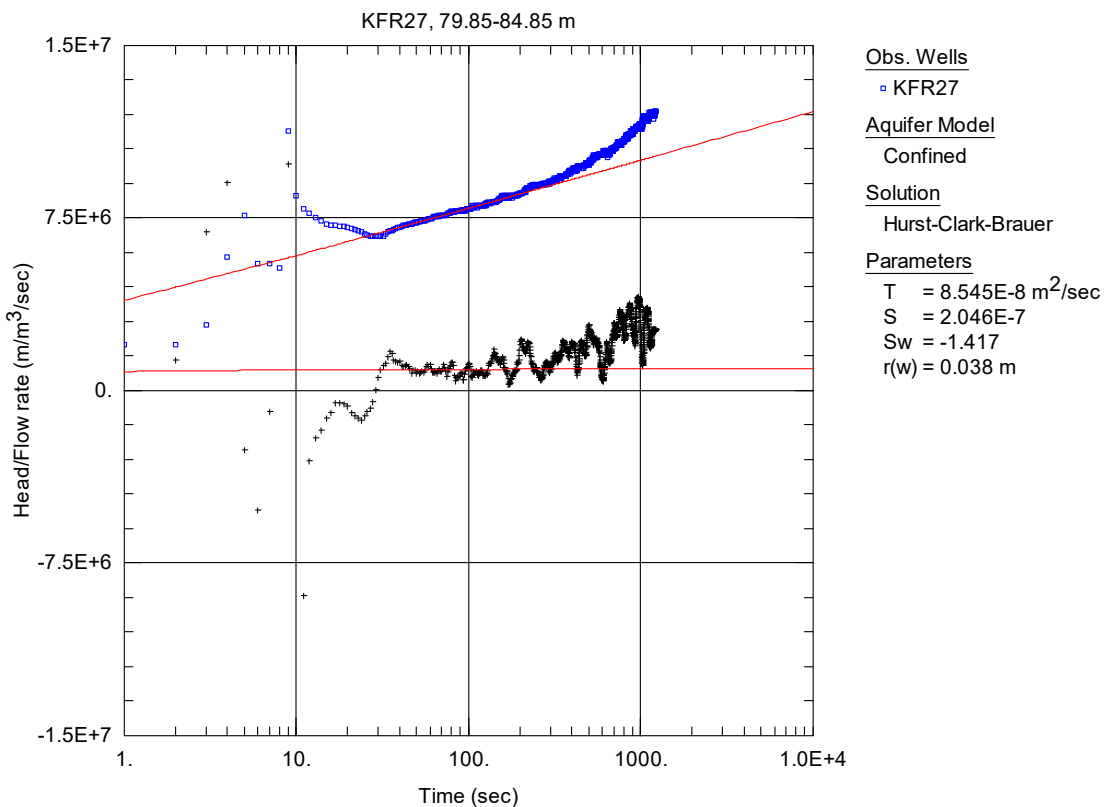


**Figure A2-36.** Lin-log plot of head/flow rate (□) and derivative (+) versus time, from the injection test in section 79.85-84.85 m in borehole KFR27.

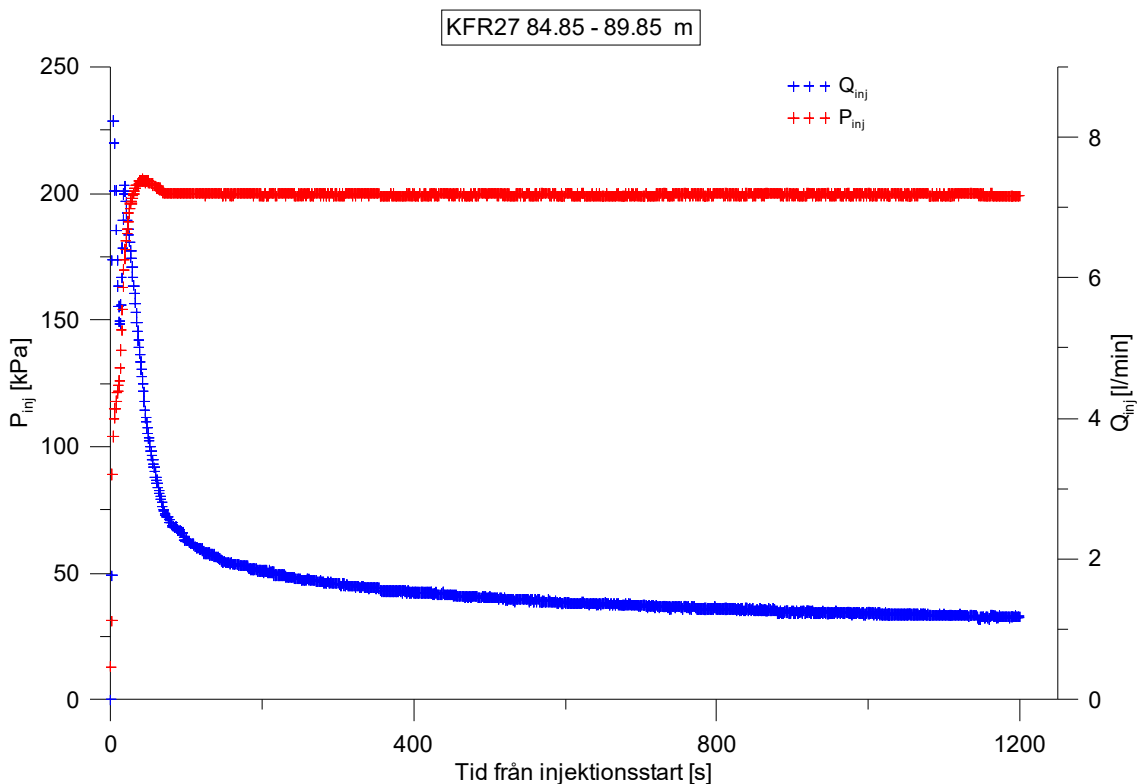


**Figure A2-37.** Linear plot of flow rate ( $Q$ ) and pressure ( $P$ ) versus time from the injection test in section 84.85-89.85 m in borehole KFR27.

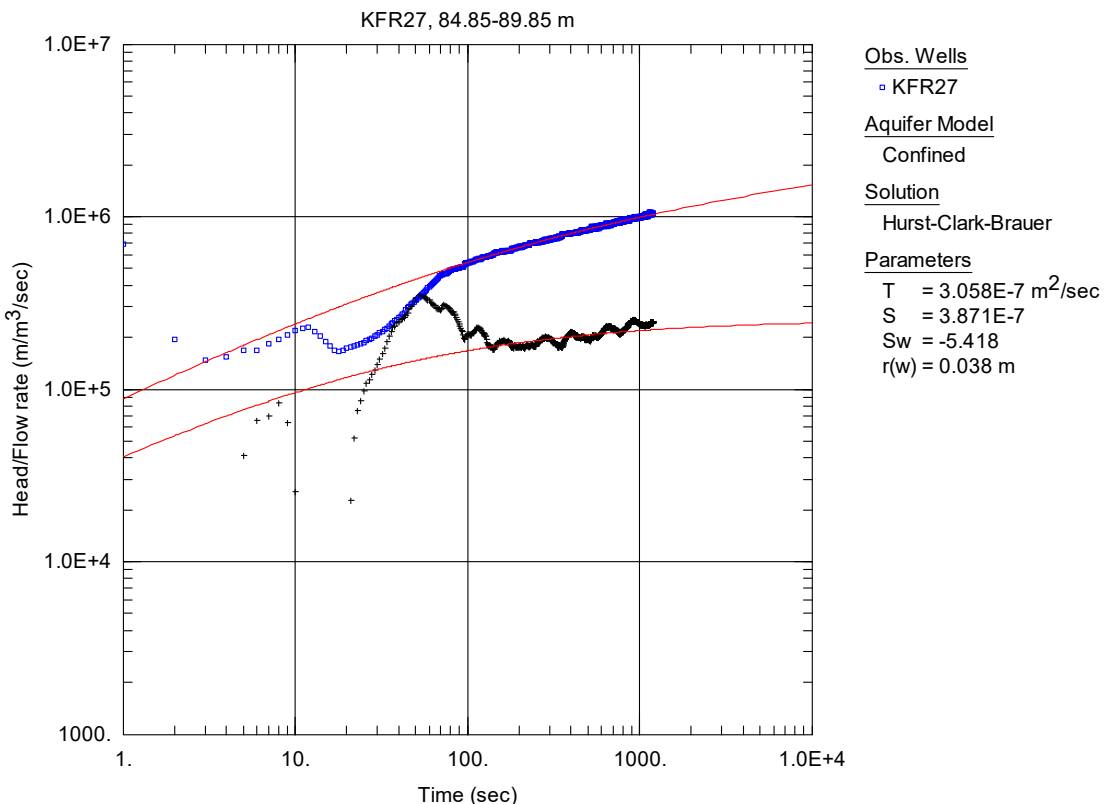


**Figure A2-38.** Log-log plot of head/flow rate (□) and derivative (+) versus time, from the injection test in section 84.85-89.85 m in borehole KFR27.

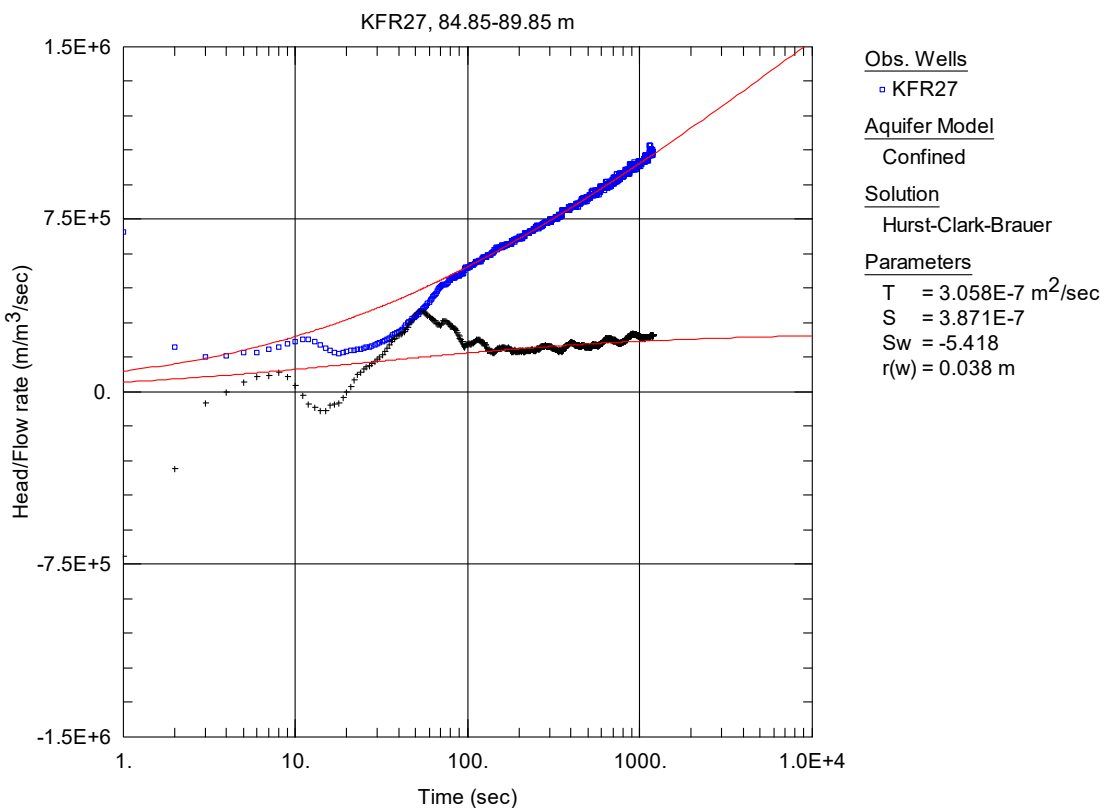


**Figure A2-39.** Lin-log plot of head/flow rate (□) and derivative (+) versus time, from the injection test in section 84.85-89.85 m in borehole KFR27.

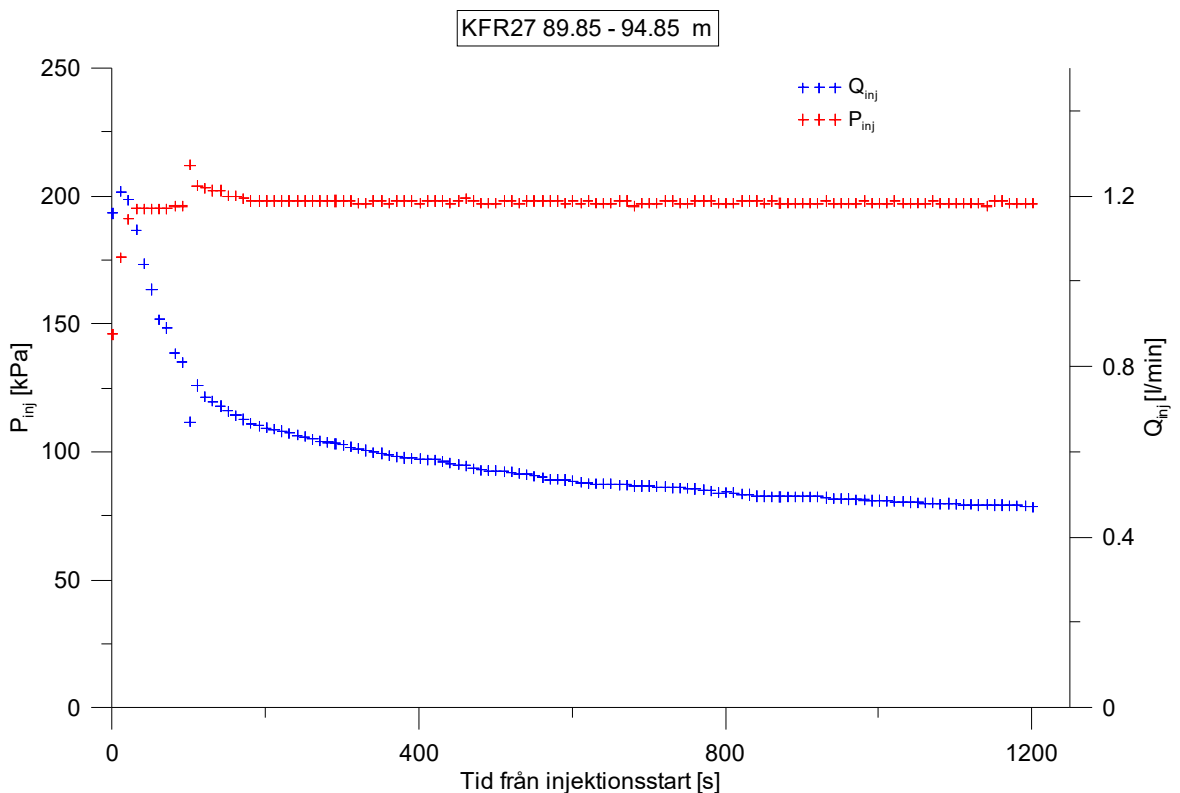


**Figure A2-40.** Linear plot of flow rate ( $Q$ ) and pressure ( $P$ ) versus time from the injection test in section 89.85-94.85 m in borehole KFR27.

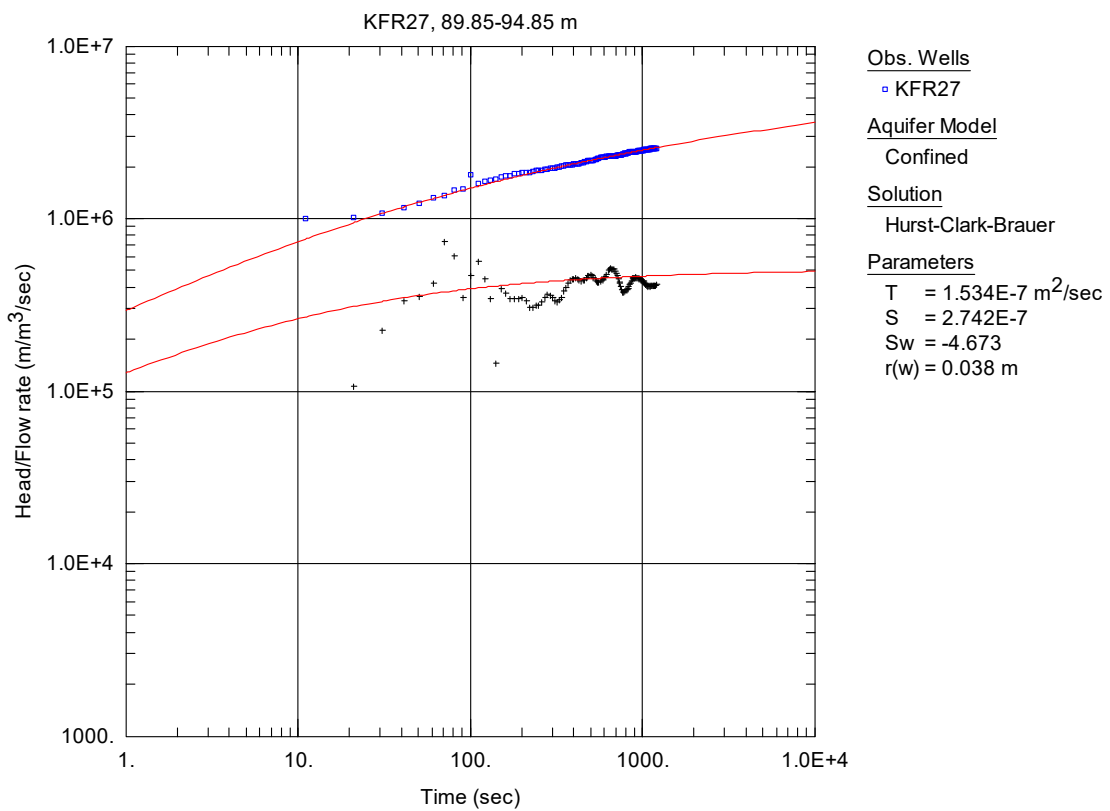


**Figure A2-41.** Log-log plot of head/flow rate (□) and derivative (+) versus time, from the injection test in section 89.85-94.85 m in borehole KFR27.

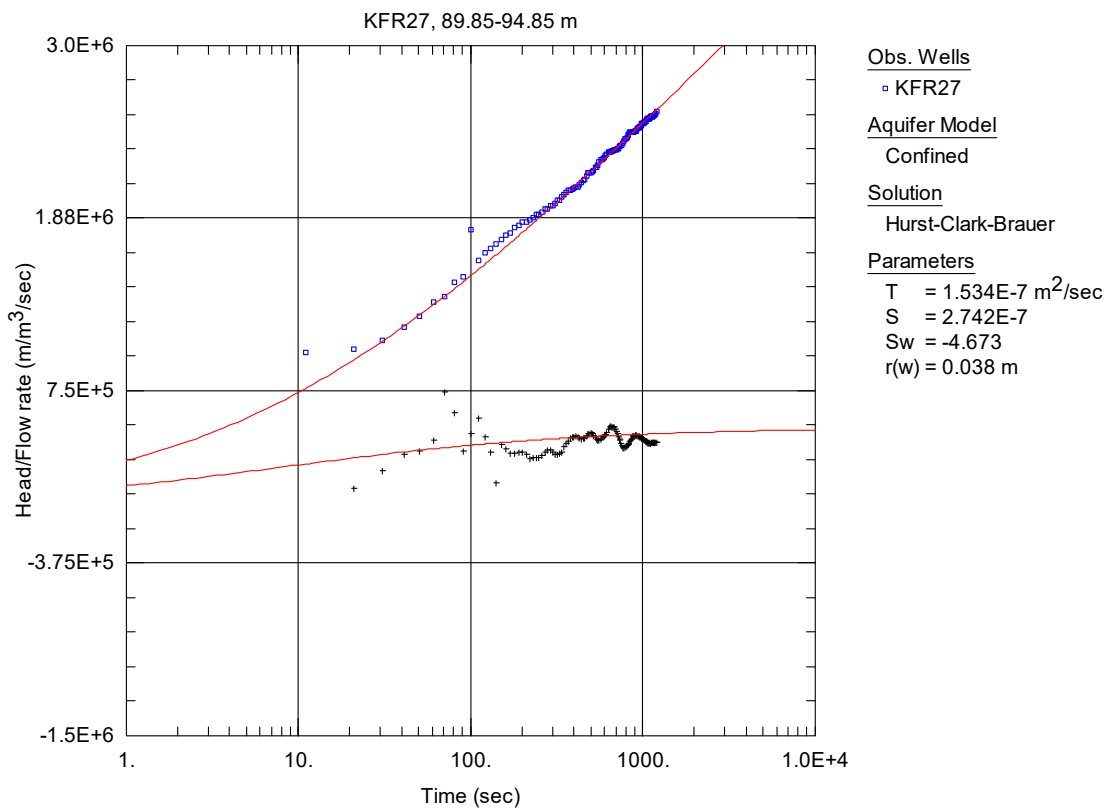


**Figure A2-42.** Lin-log plot of head/flow rate (□) and derivative (+) versus time, from the injection test in section 89.85-94.85 m in borehole KFR27.

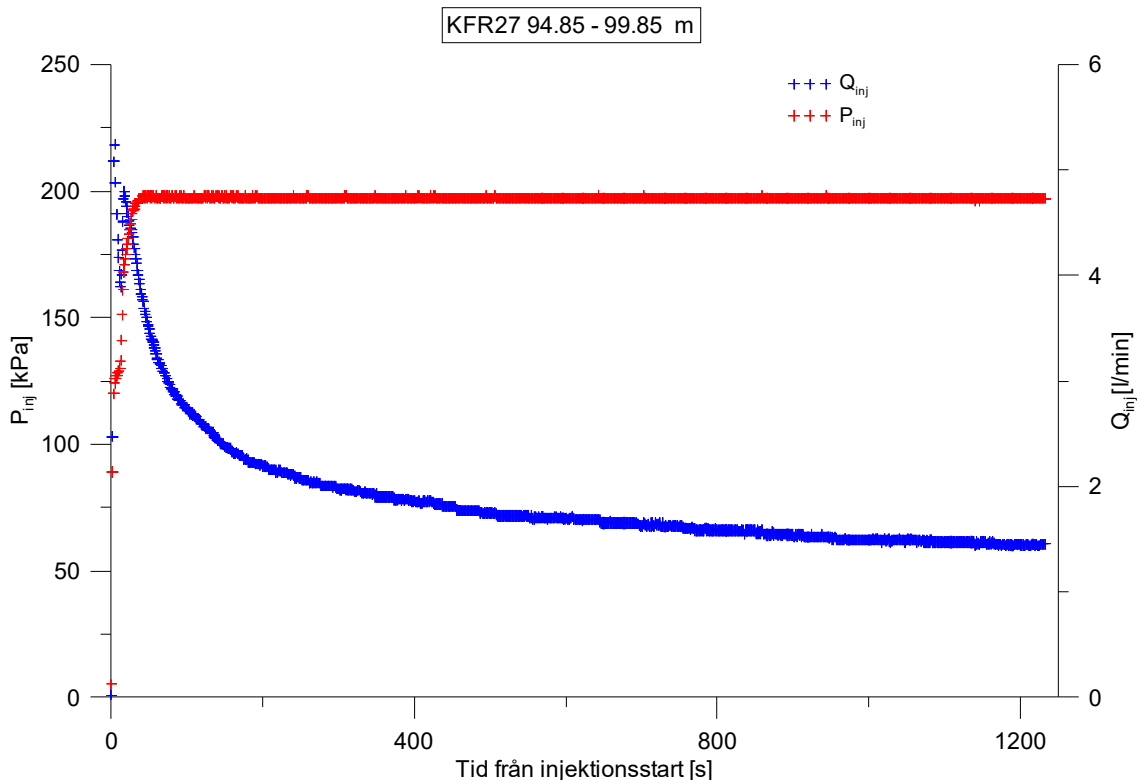


**Figure A2-43.** Linear plot of flow rate ( $Q$ ) and pressure ( $P$ ) versus time from the injection test in section 94.85-99.85 m in borehole KFR27.

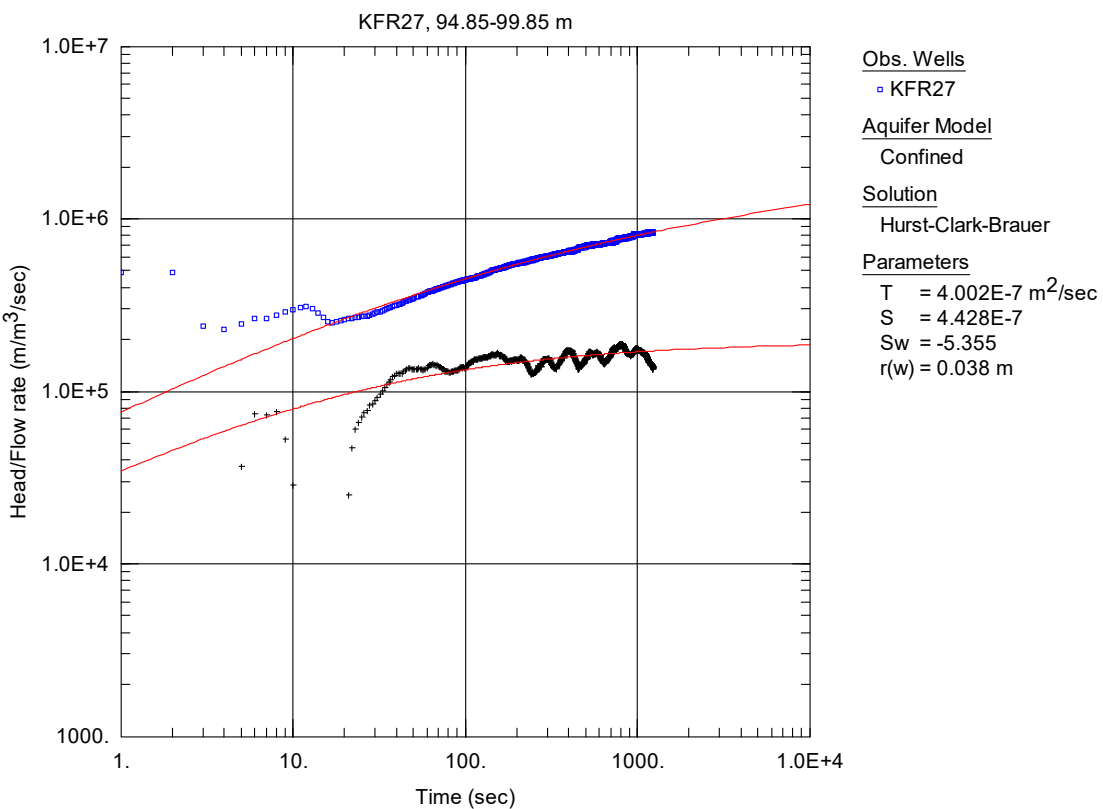


**Figure A2-44.** Log-log plot of head/flow rate (□) and derivative (+) versus time, from the injection test in section 94.85-99.85 m in borehole KFR27.

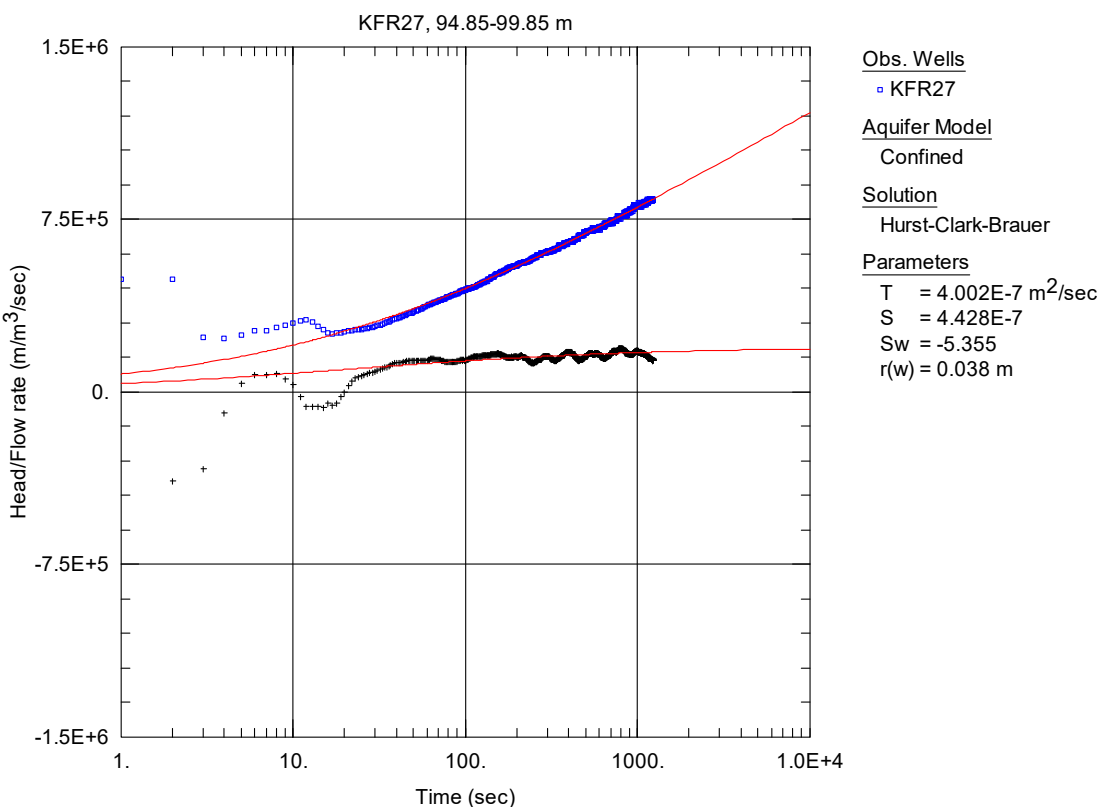


**Figure A2-45.** Lin-log plot of head/flow rate (□) and derivative (+) versus time, from the injection test in section 94.85-99.85 m in borehole KFR27.

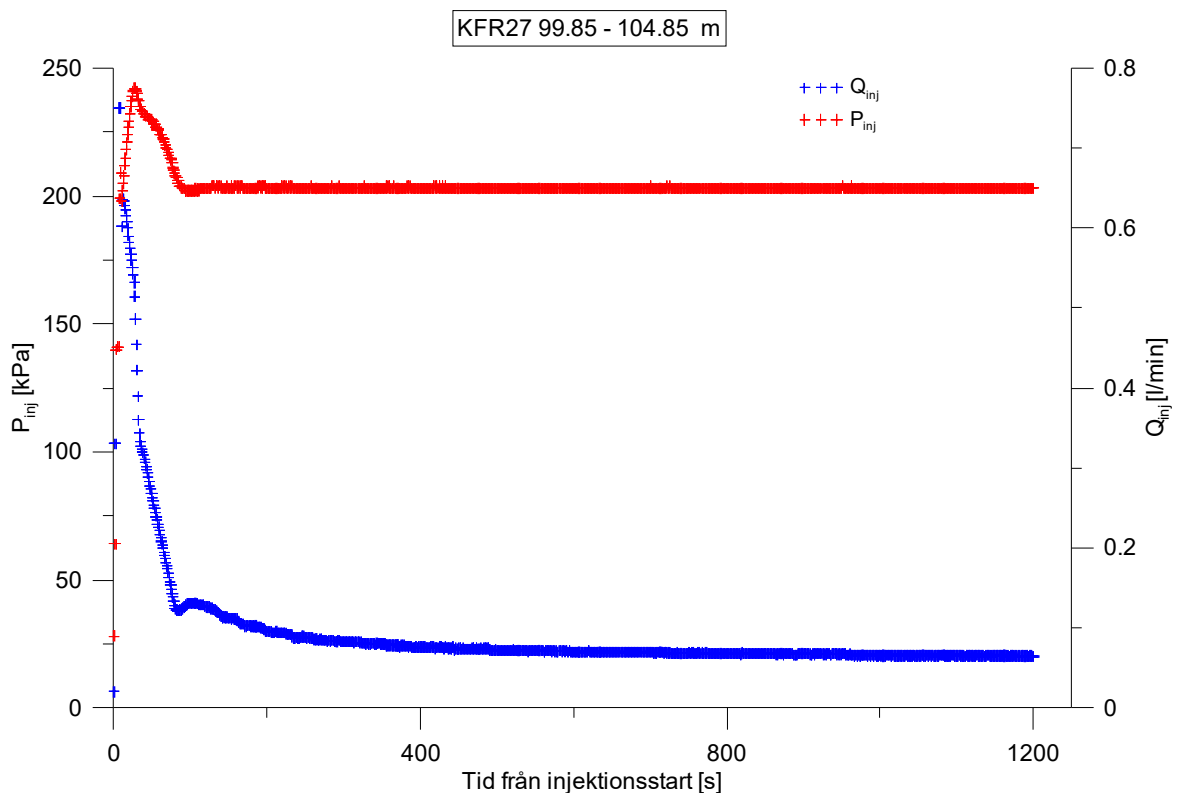


**Figure A2-46.** Linear plot of flow rate ( $Q$ ) and pressure ( $P$ ) versus time from the injection test in section 99.85-104.85 m in borehole KFR27.

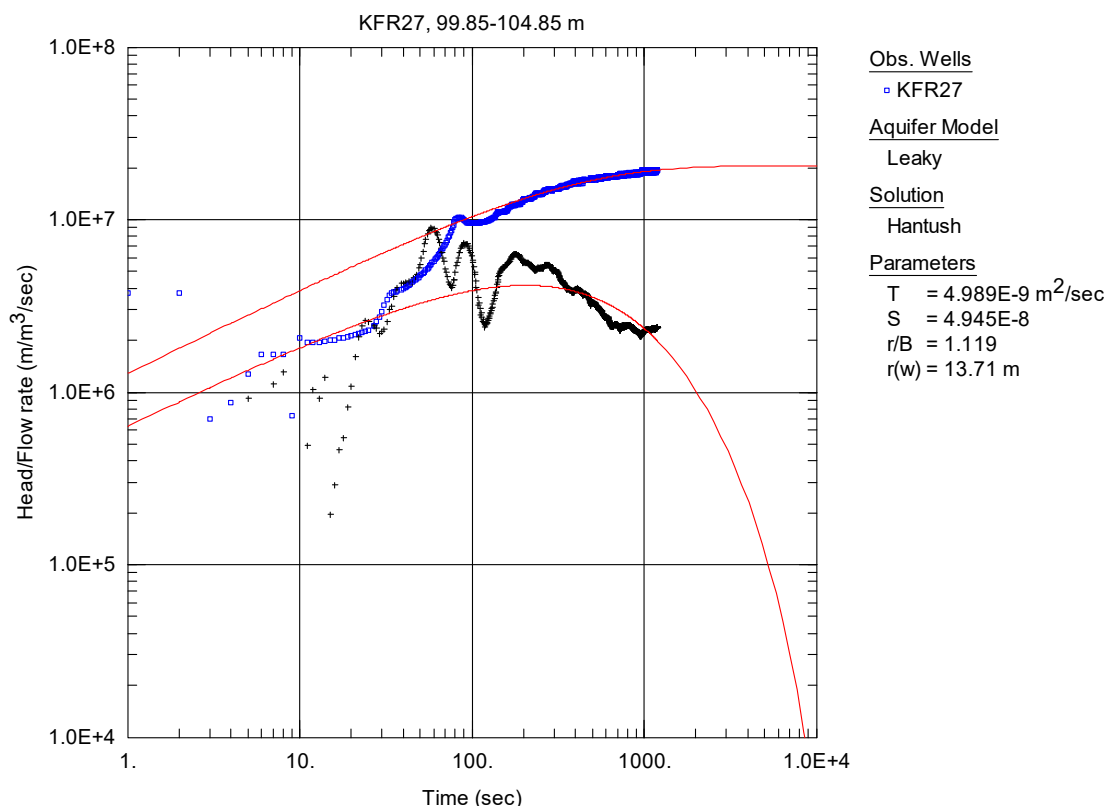


**Figure A2-47.** Log-log plot of head/flow rate (□) and derivative (+) versus time, from the injection test in section 99.85-104.85 m in borehole KFR27.

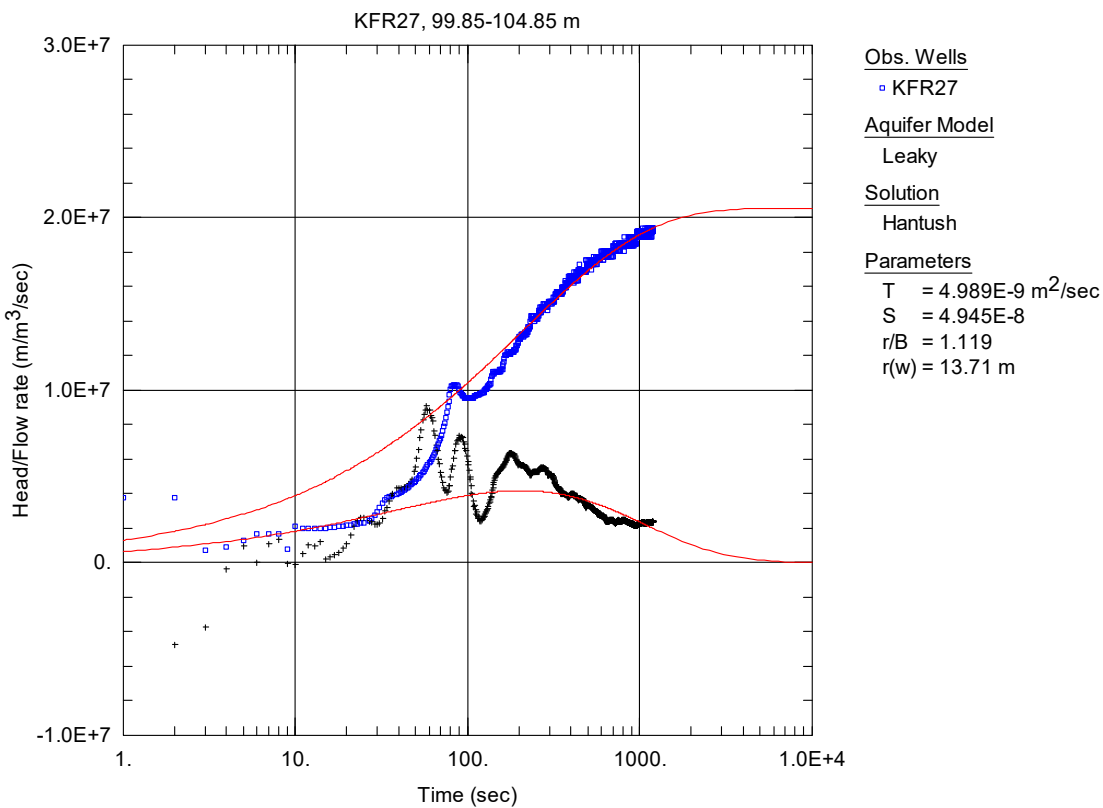


**Figure A2-48.** Lin-log plot of head/flow rate (□) and derivative (+) versus time, from the injection test in section 99.85-104.85 m in borehole KFR27.

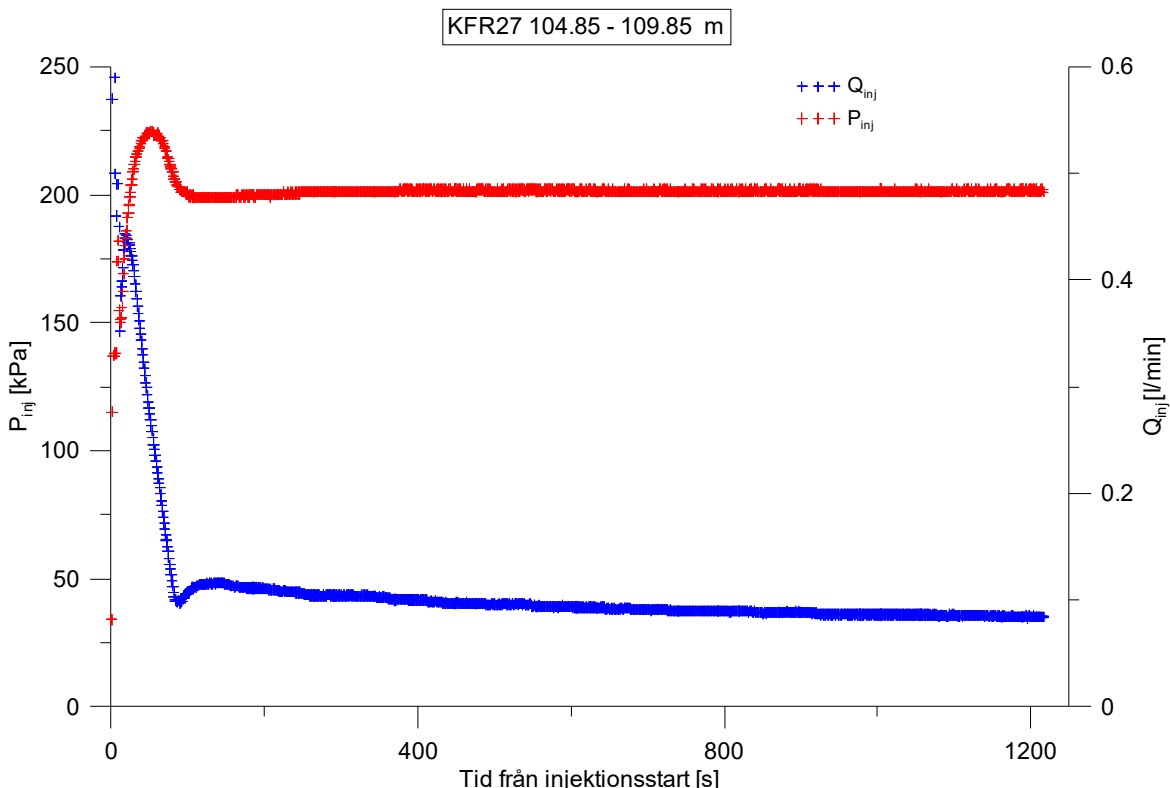


**Figure A2-49.** Linear plot of flow rate ( $Q$ ) and pressure ( $P$ ) versus time from the injection test in section 104.85-109.85 m in borehole KFR27.

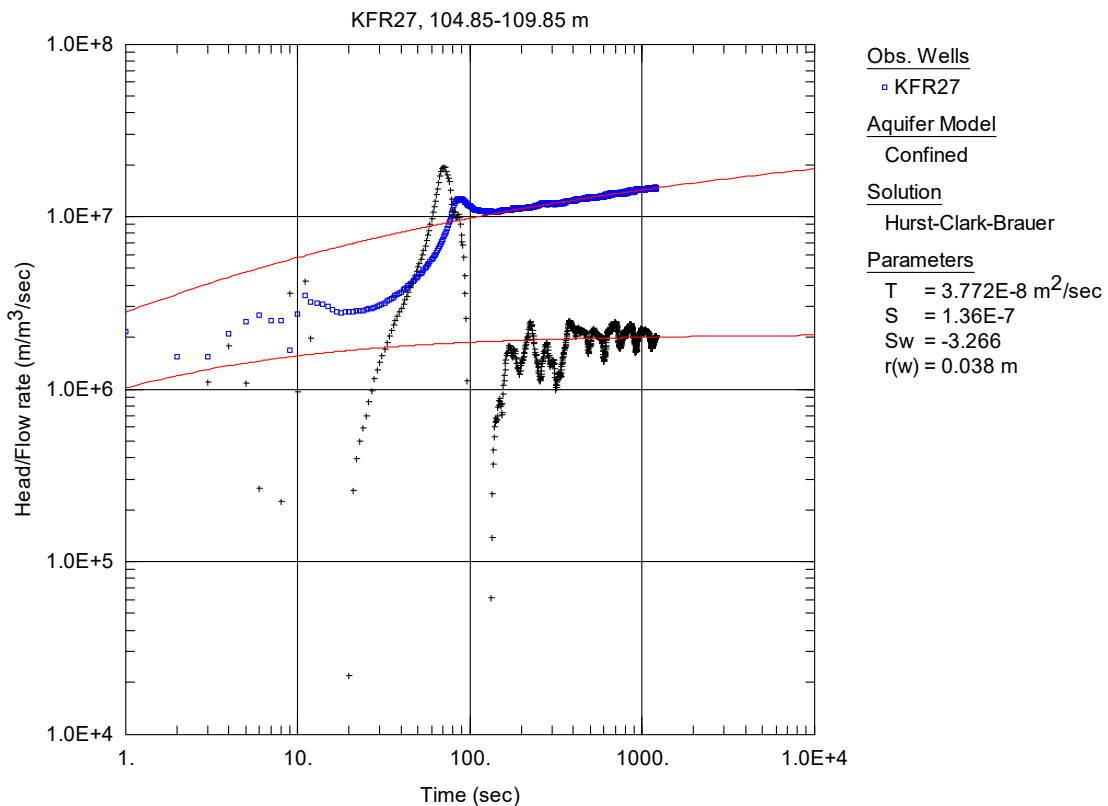


**Figure A2-50.** Log-log plot of head/flow rate (□) and derivative (+) versus time, from the injection test in section 104.85-109.85 m in borehole KFR27.

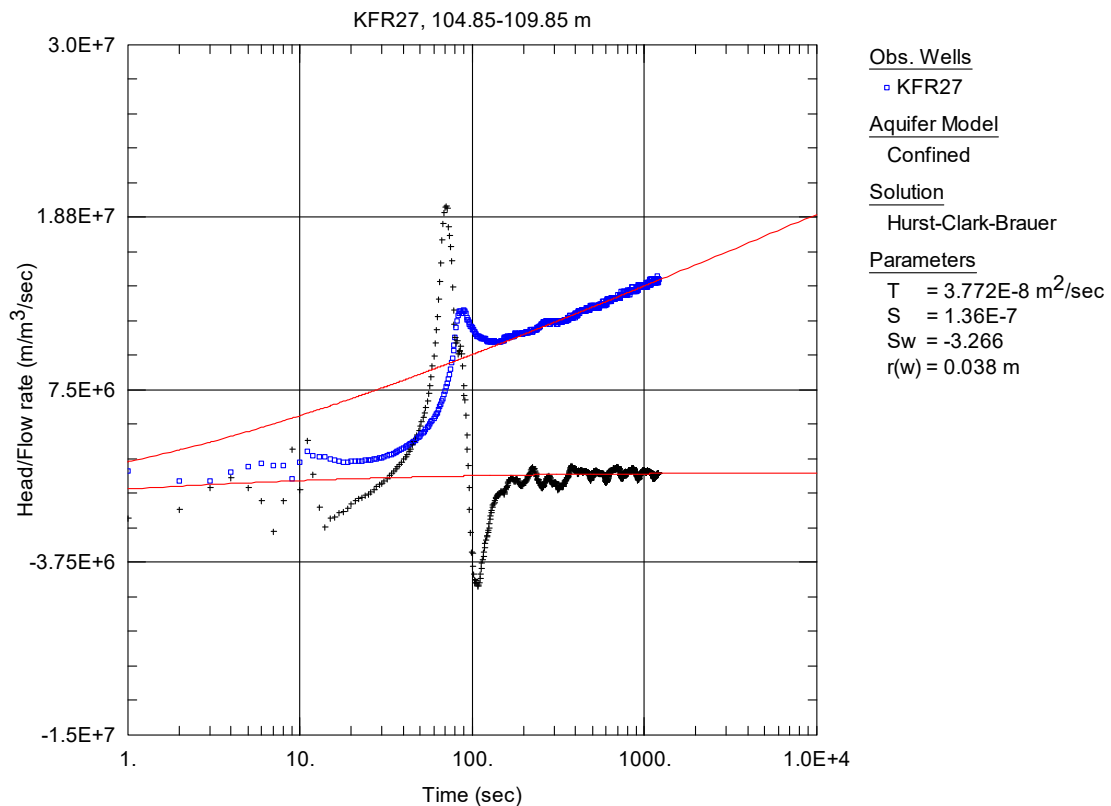


**Figure A2-51.** Lin-log plot of head/flow rate (□) and derivative (+) versus time, from the injection test in section 104.85-109.85 m in borehole KFR27.

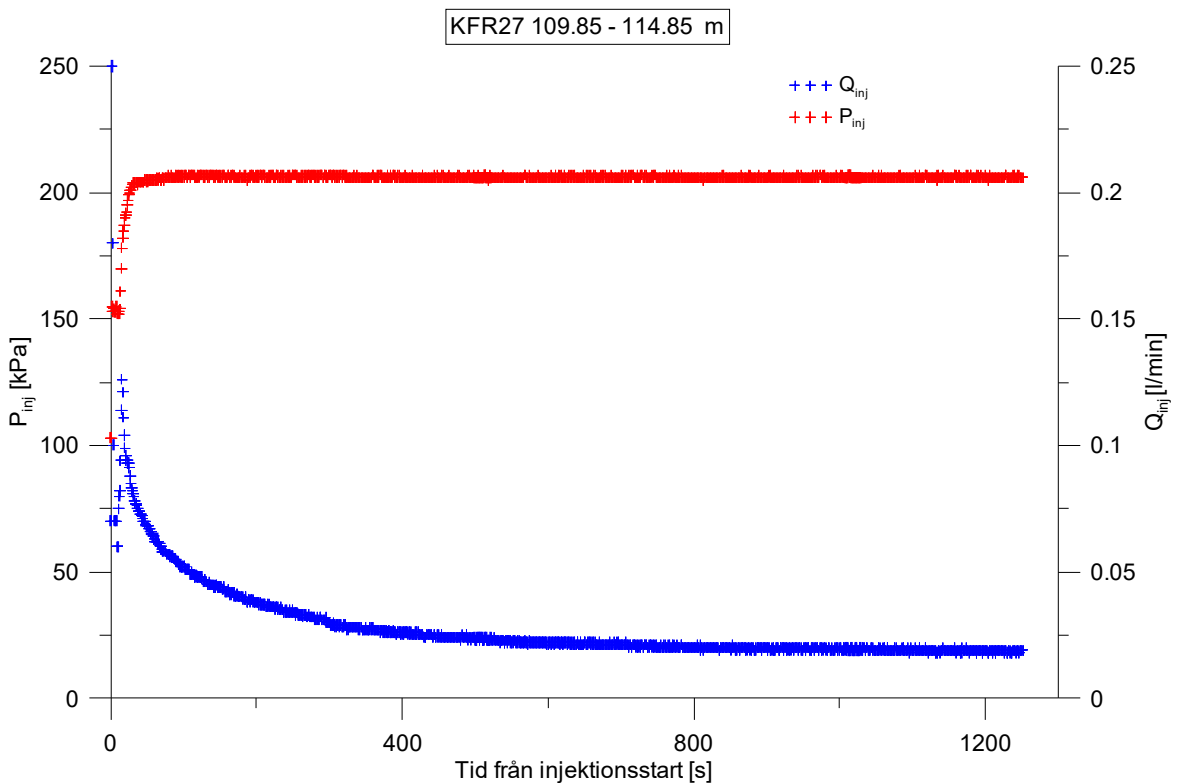


**Figure A2-52.** Linear plot of flow rate ( $Q$ ) and pressure ( $P$ ) versus time from the injection test in section 109.85-114.85 m in borehole KFR27.

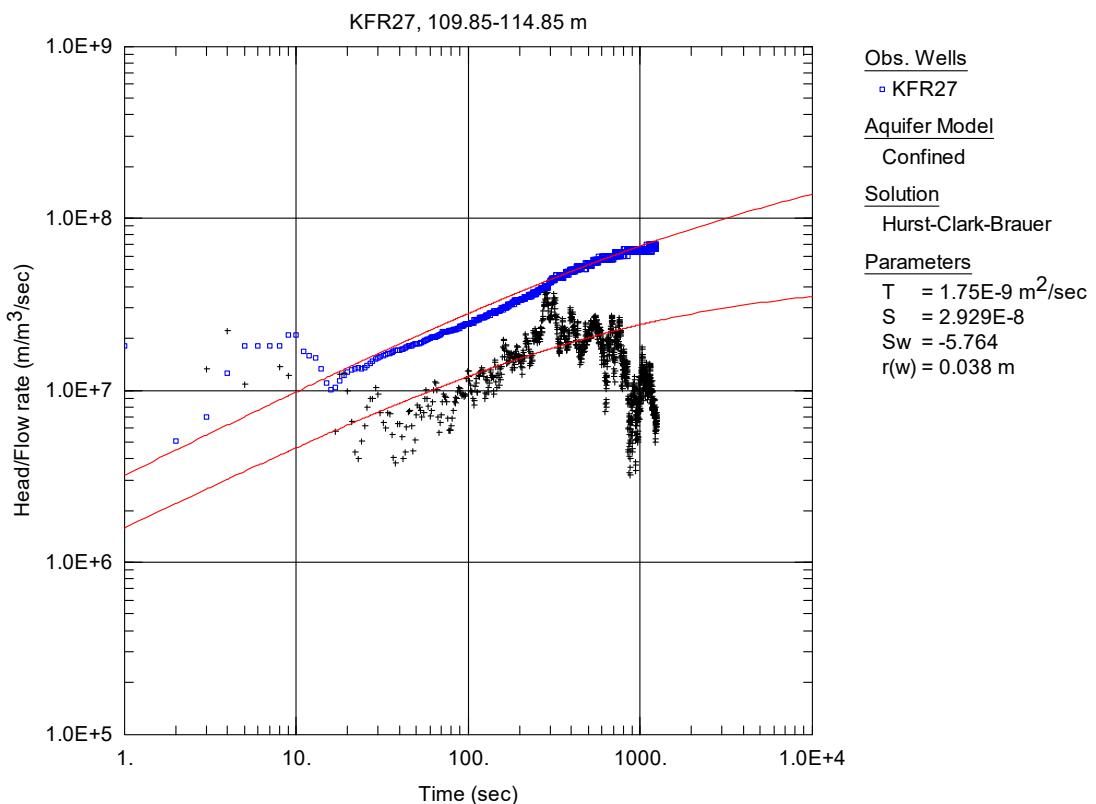


**Figure A2-53.** Log-log plot of head/flow rate ( $\square$ ) and derivative (+) versus time, from the injection test in section 109.85-114.85 m in borehole KFR27.

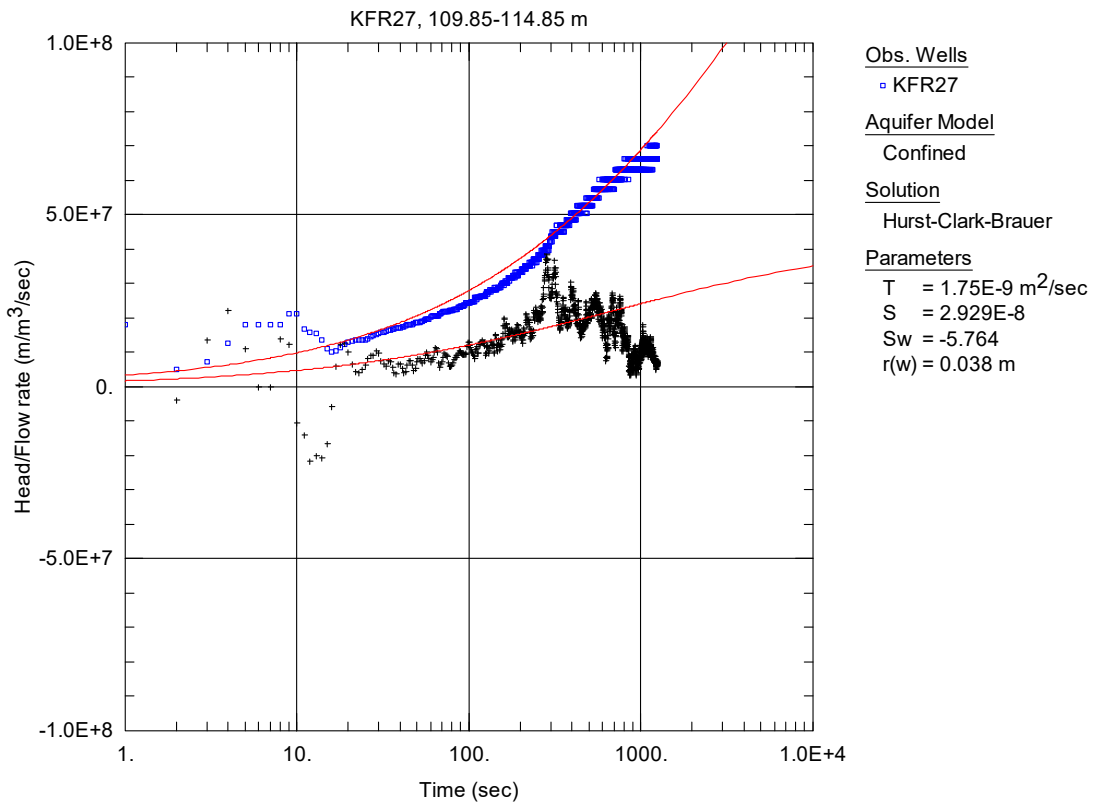


**Figure A2-54.** Lin-log plot of head/flow rate (□) and derivative (+) versus time, from the injection test in section 109.85-114.85 m in borehole KFR27.

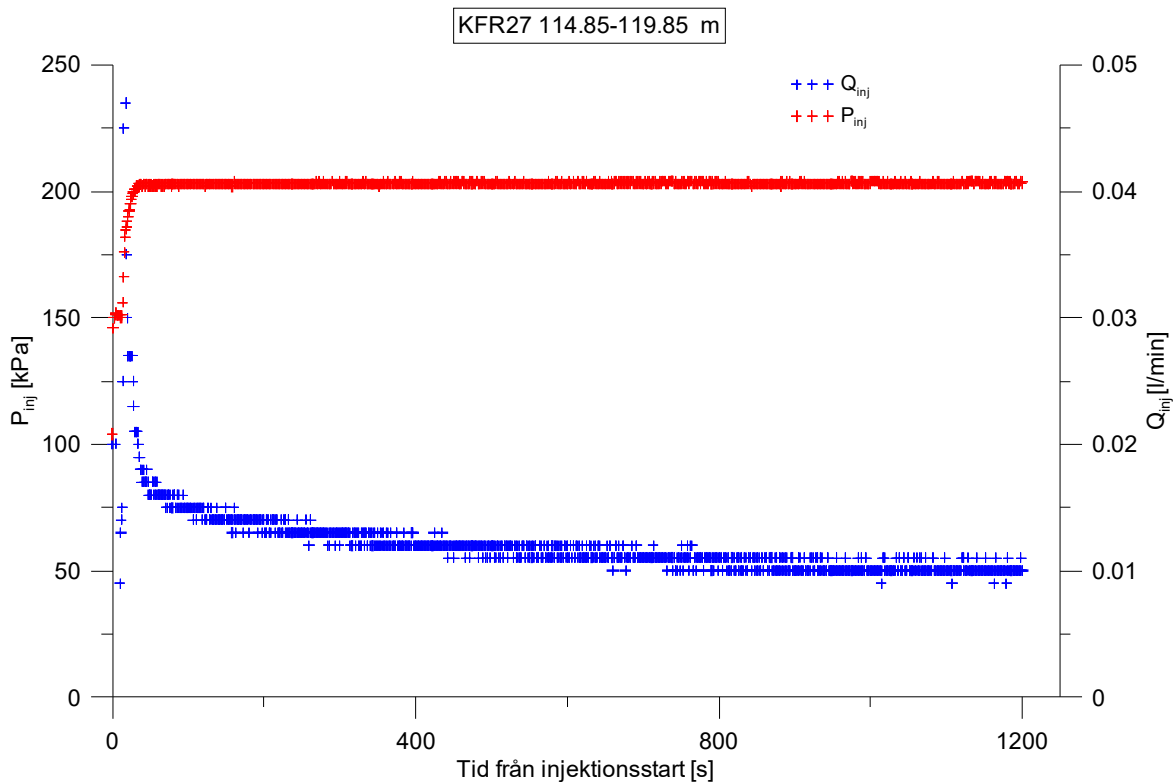


**Figure A2-55.** Linear plot of flow rate ( $Q$ ) and pressure ( $P$ ) versus time from the injection test in section 114.85-119.85 m in borehole KFR27.

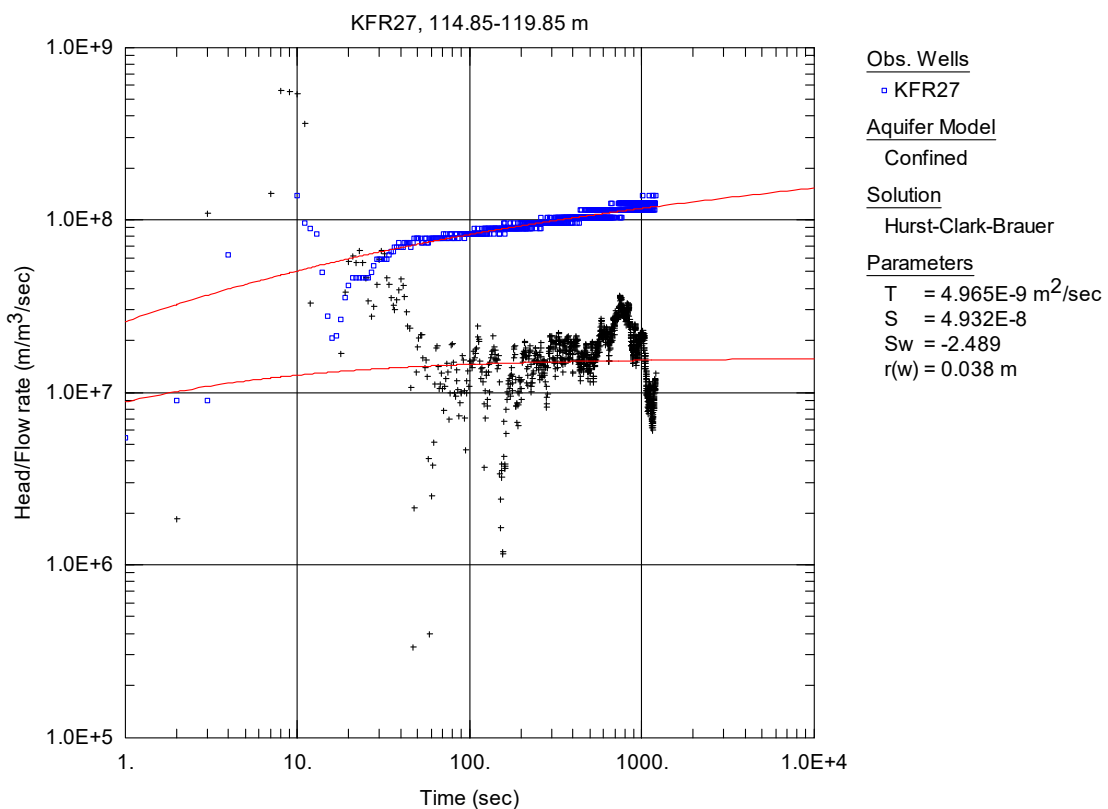


**Figure A2-56.** Log-log plot of head/flow rate ( $\square$ ) and derivative (+) versus time, from the injection test in section 114.85-119.85 m in borehole KFR27.

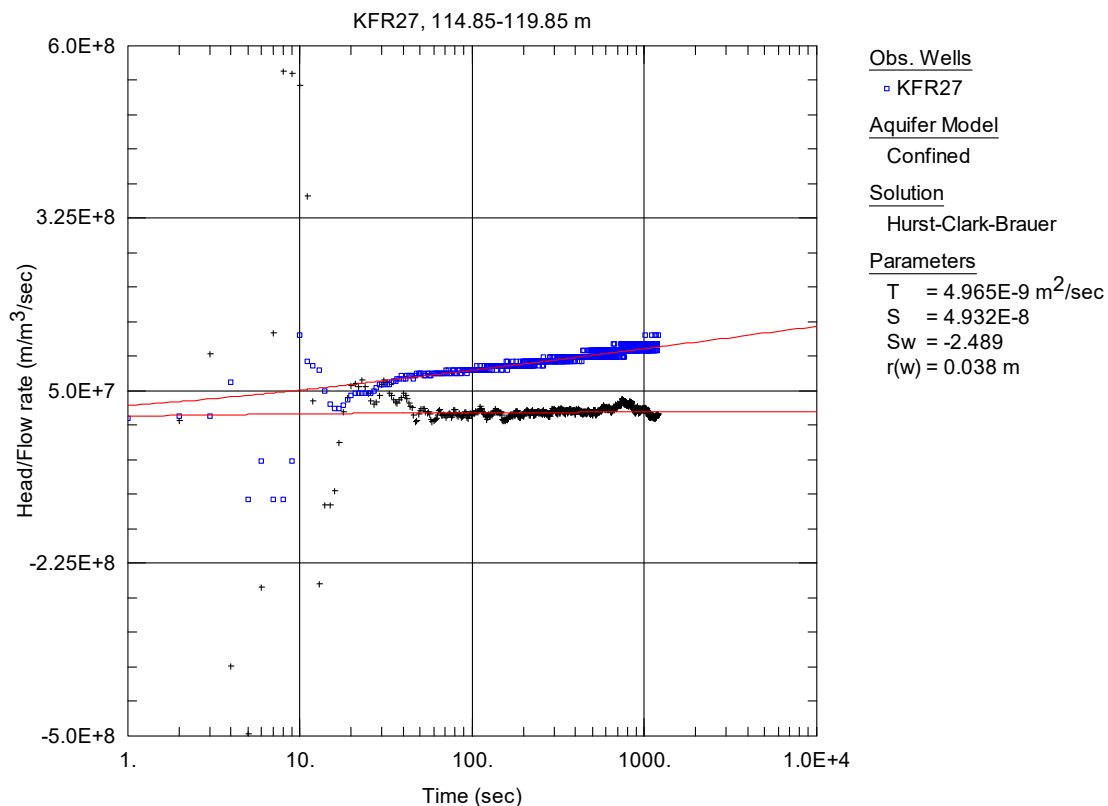


**Figure A2-57.** Lin-log plot of head/flow rate ( $\square$ ) and derivative (+) versus time, from the injection test in section 114.85-119.85 m in borehole KFR27.

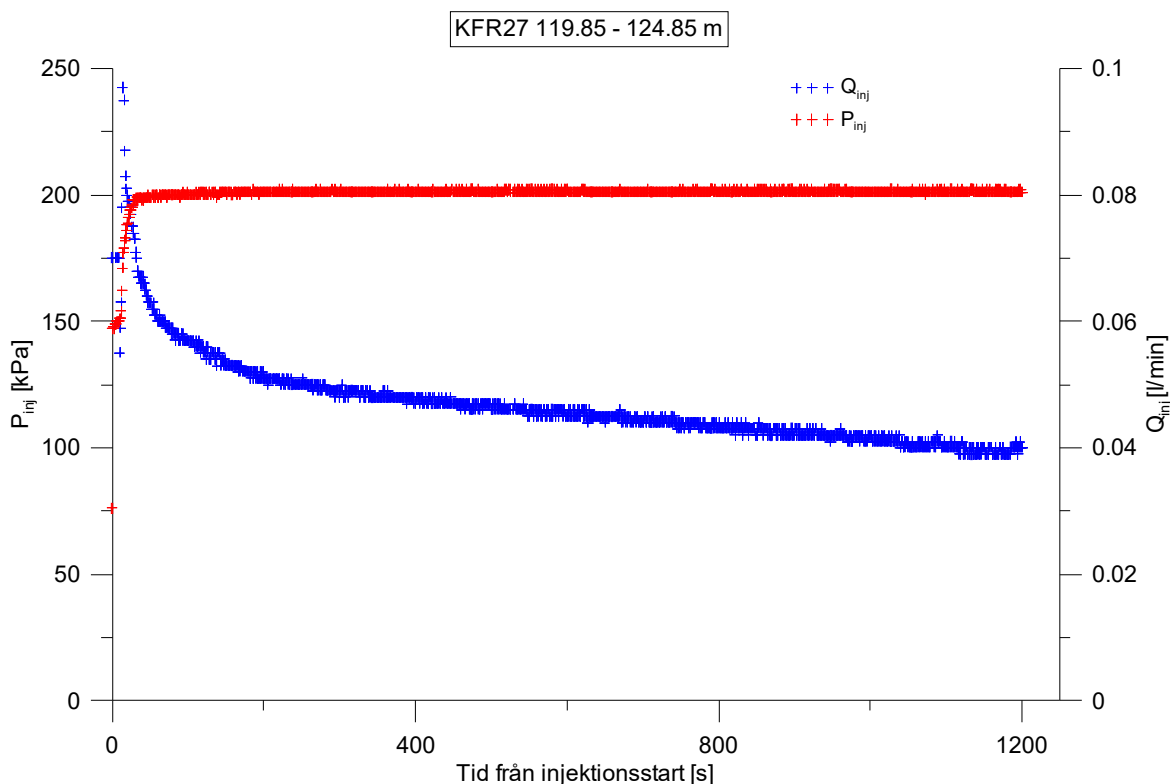


**Figure A2-58.** Linear plot of flow rate ( $Q$ ) and pressure ( $P$ ) versus time from the injection test in section 119.85-124.85 m in borehole KFR27.

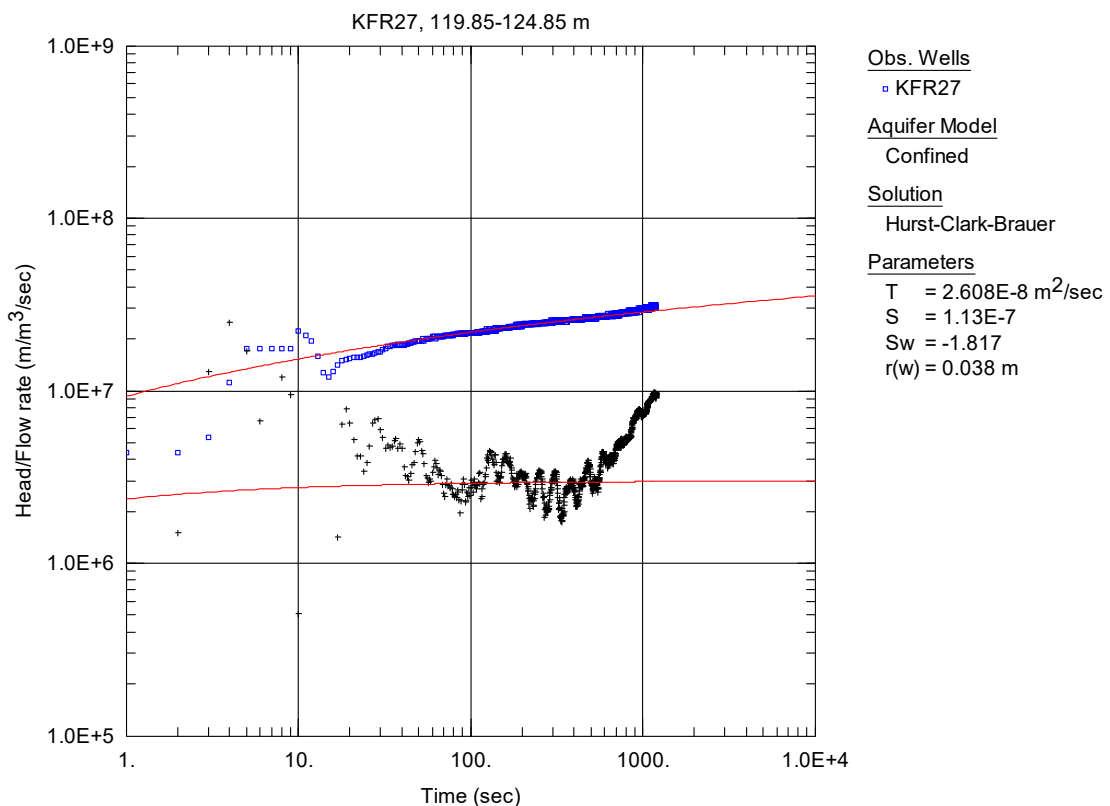


**Figure A2-59.** Log-log plot of head/flow rate (□) and derivative (+) versus time, from the injection test in section 119.85-124.85 m in borehole KFR27.

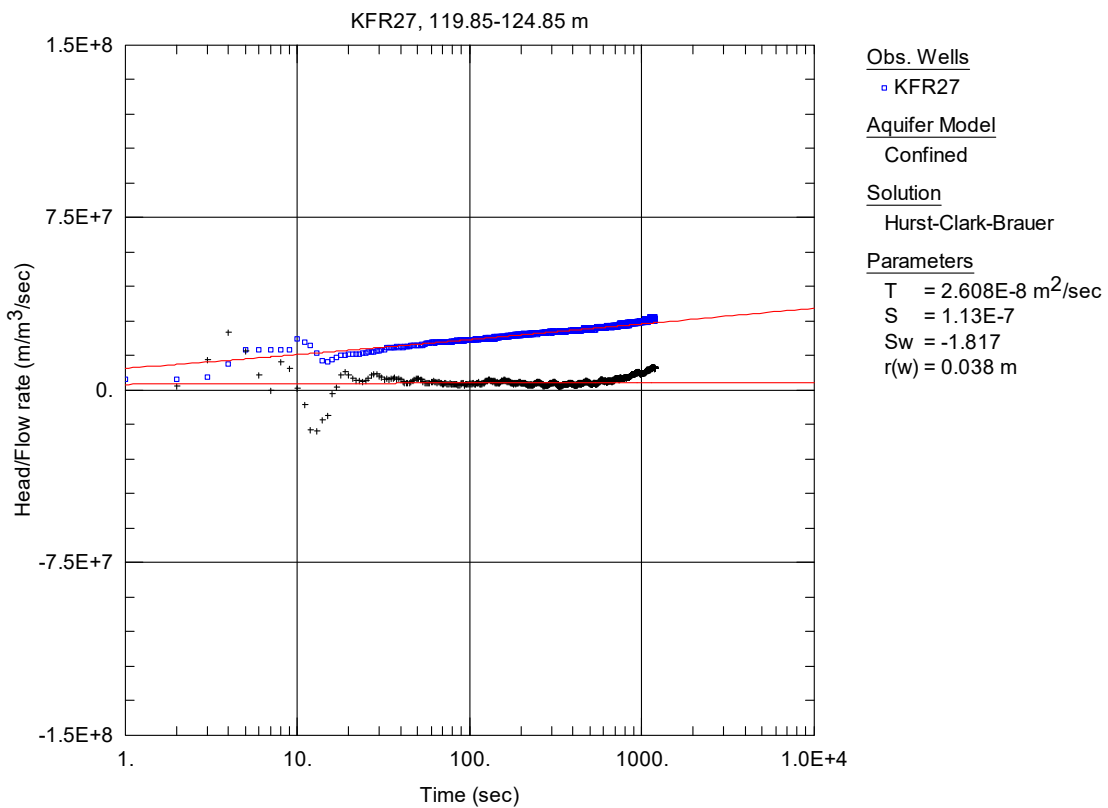


**Figure A2-60.** Lin-log plot of head/flow rate (□) and derivative (+) versus time, from the injection test in section 119.85-124.85 m in borehole KFR27.

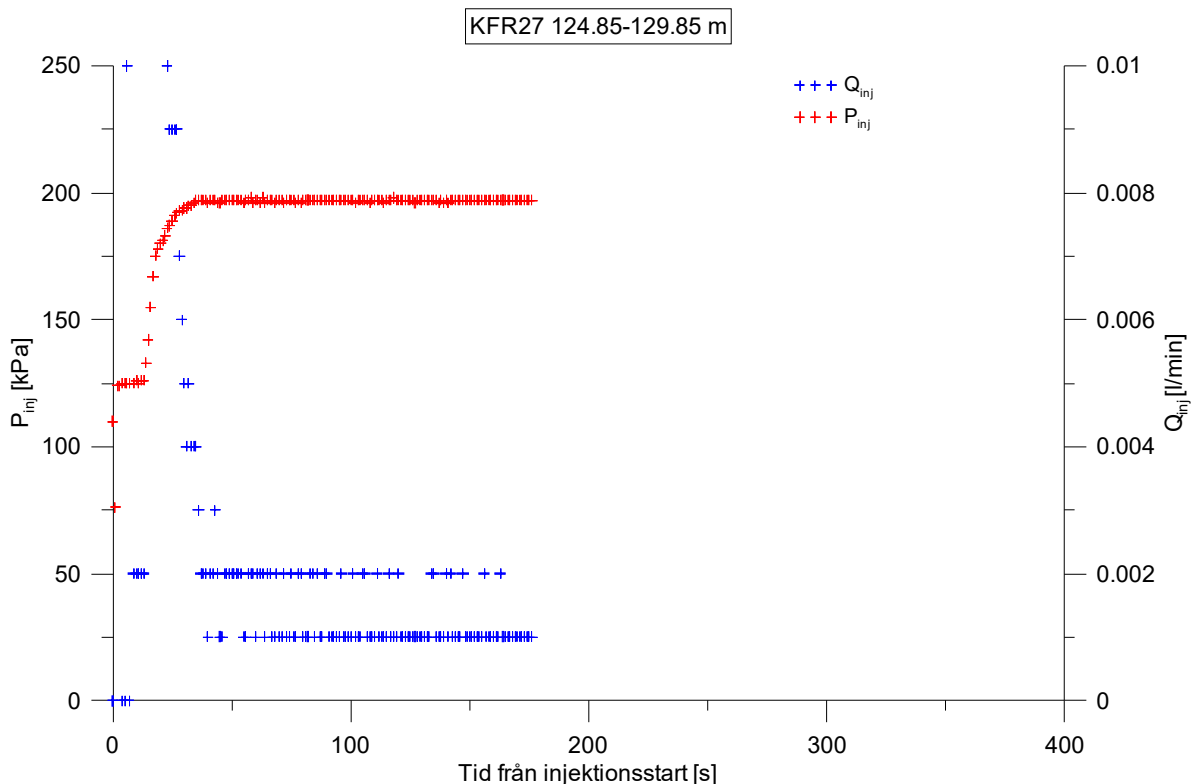


**Figure A2-61.** Linear plot of flow rate (Q) and pressure (P) versus time from the injection test in section 124.85-129.85 m in borehole KFR27.

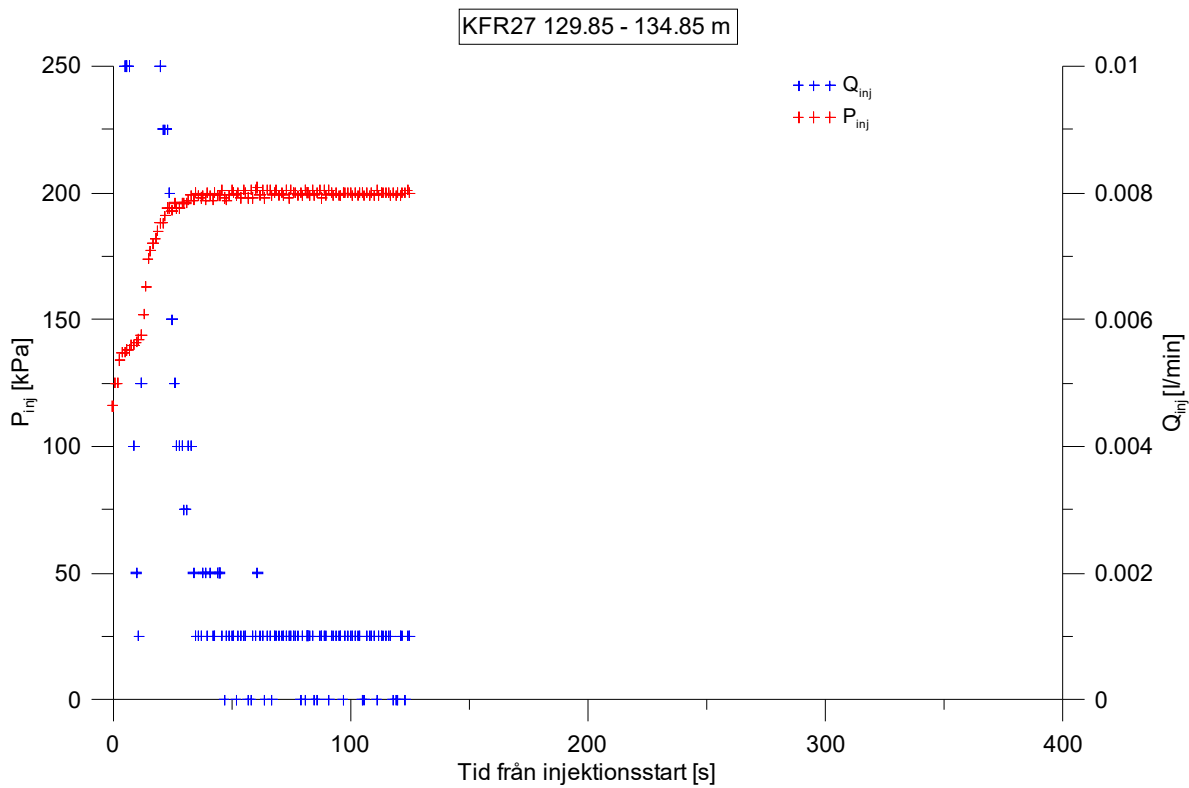


**Figure A2-62.** Linear plot of flow rate ( $Q$ ) and pressure ( $P$ ) versus time from the injection test in section 129.85-134.85 m in borehole KFR27.

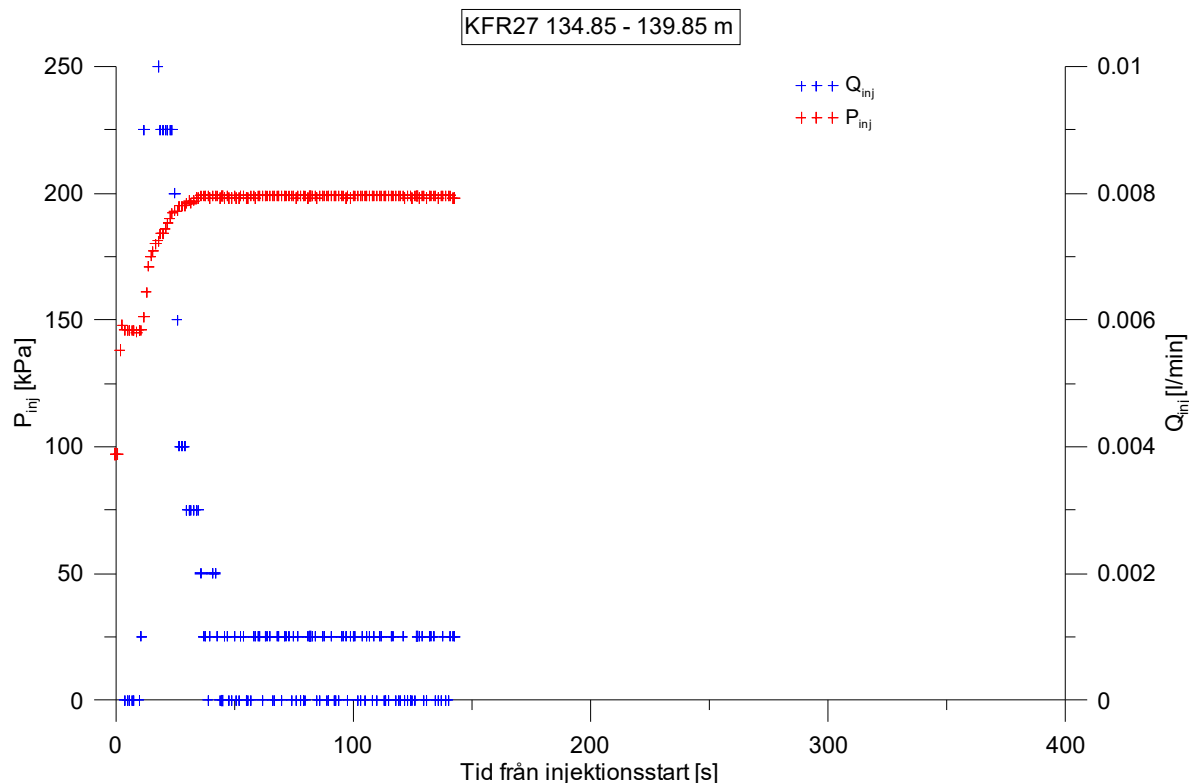


**Figure A2-63.** Linear plot of flow rate ( $Q$ ) and pressure ( $P$ ) versus time from the injection test in section 134.85-139.85 m in borehole KFR27.

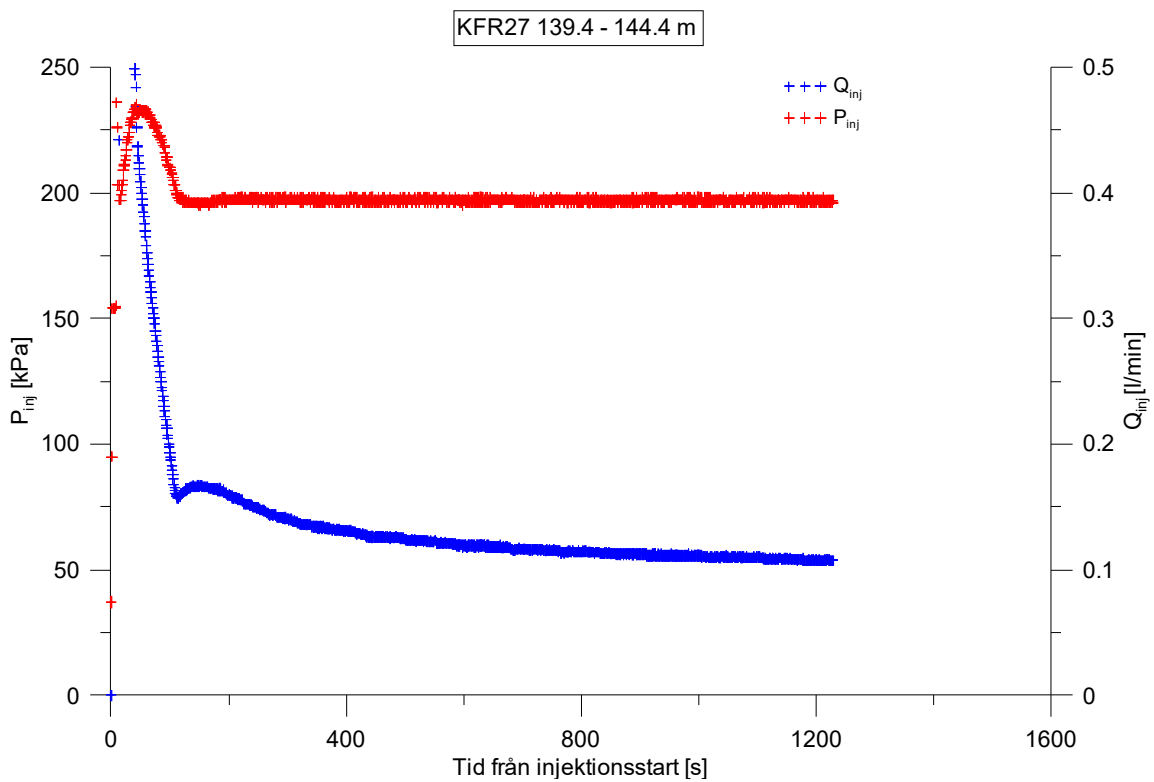


**Figure A2-64.** Linear plot of flow rate ( $Q$ ) and pressure ( $P$ ) versus time from the injection test in section 139.4-144.4 m in borehole KFR27.

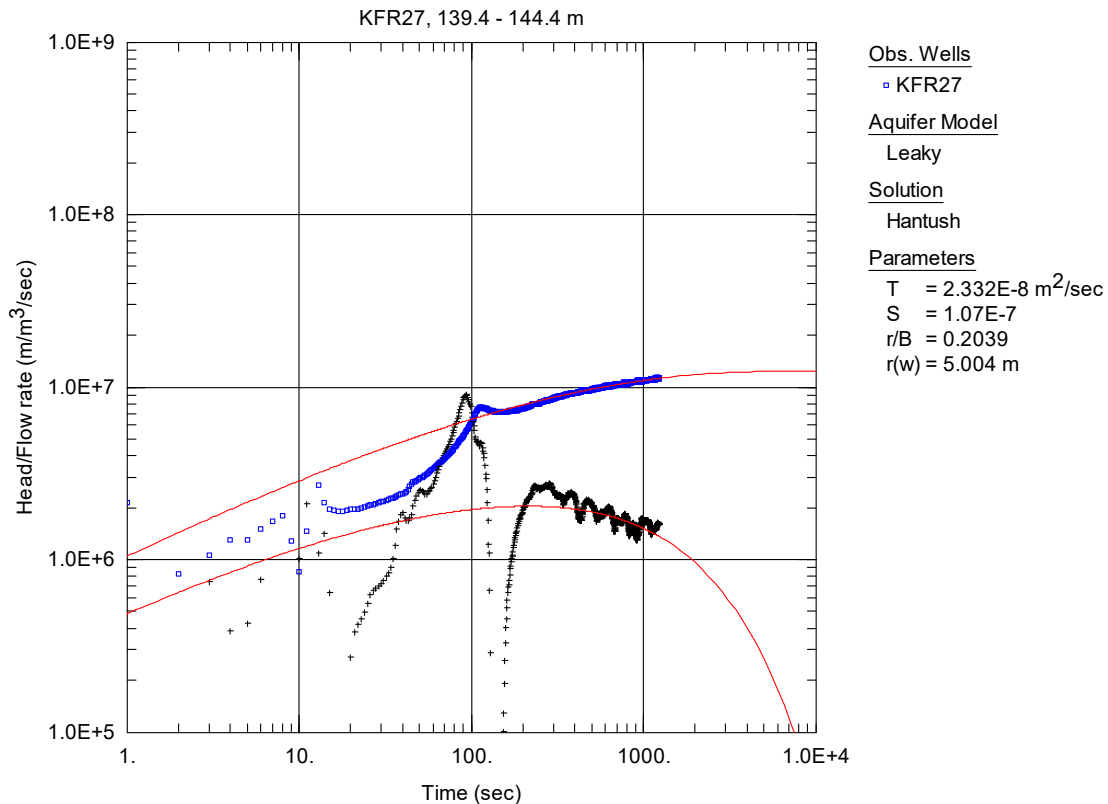


**Figure A2-65.** Log-log plot of head/flow rate ( $\square$ ) and derivative (+) versus time, from the injection test in section 139.4-144.4 m in borehole KFR27.

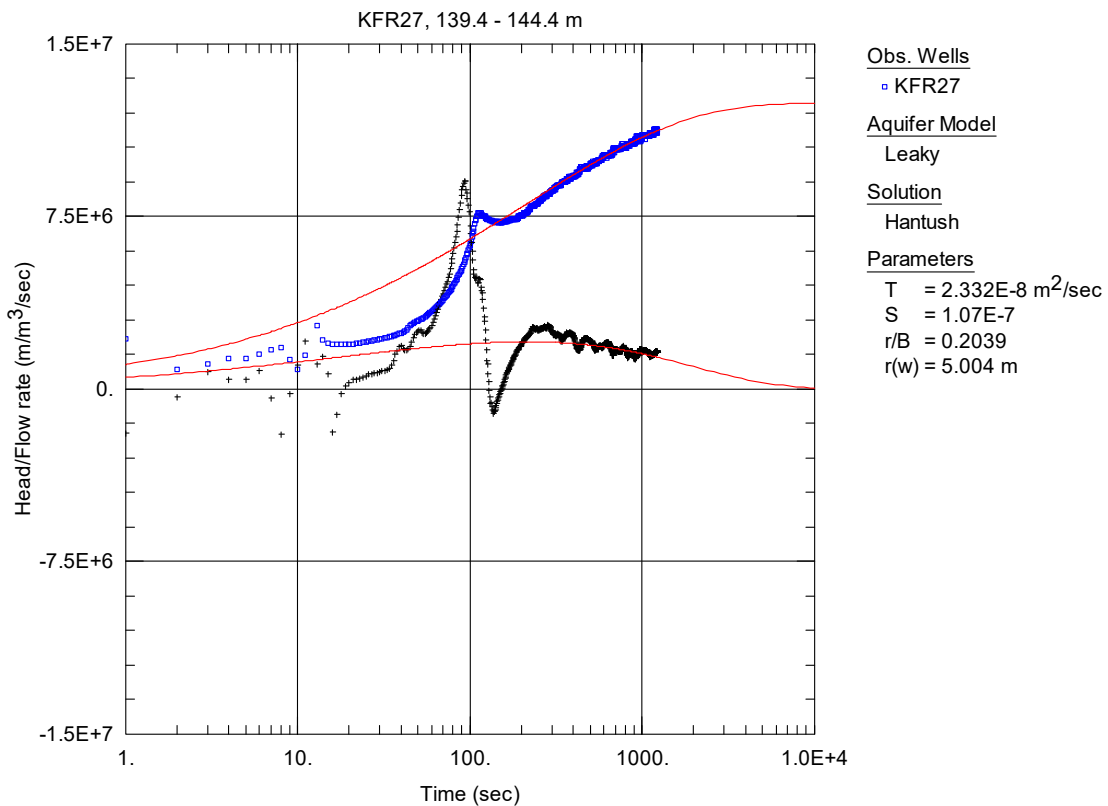


**Figure A2-66.** Lin-log plot of head/flow rate (□) and derivative (+) versus time, from the injection test in section 139.4-144.4 m in borehole KFR27.

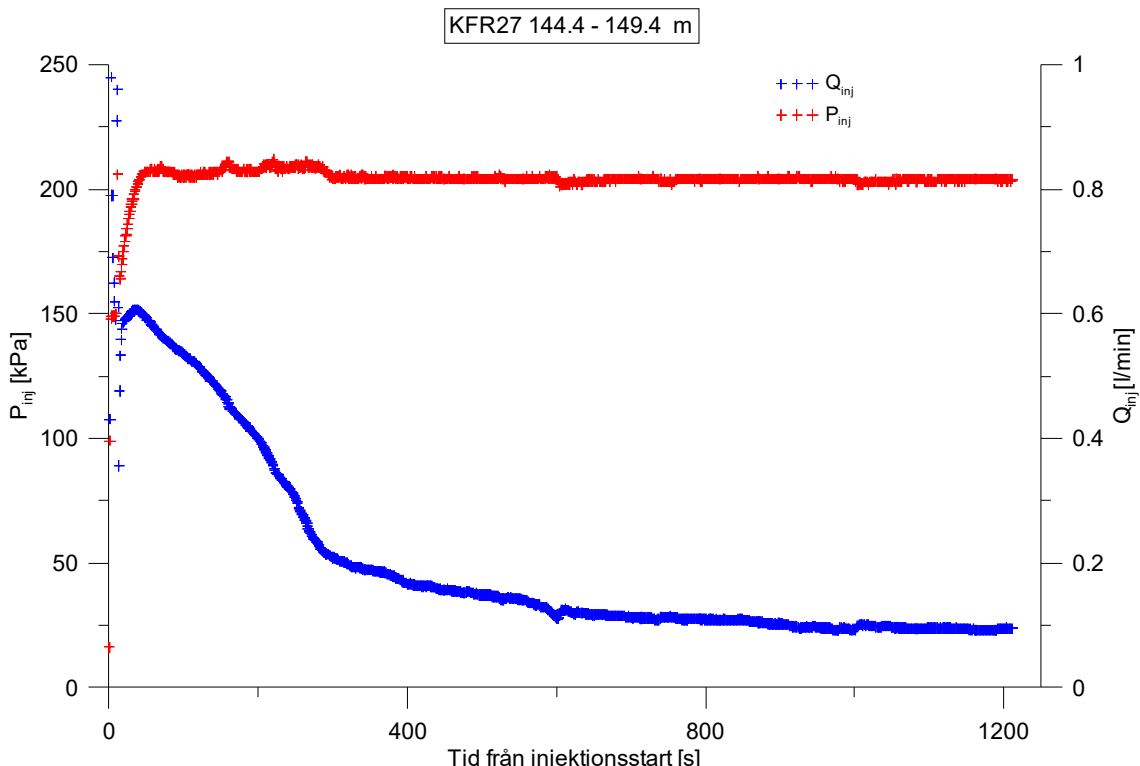


**Figure A2-67.** Linear plot of flow rate (Q) and pressure (P) versus time from the injection test in section 144.4-149.4 m in borehole KFR27.

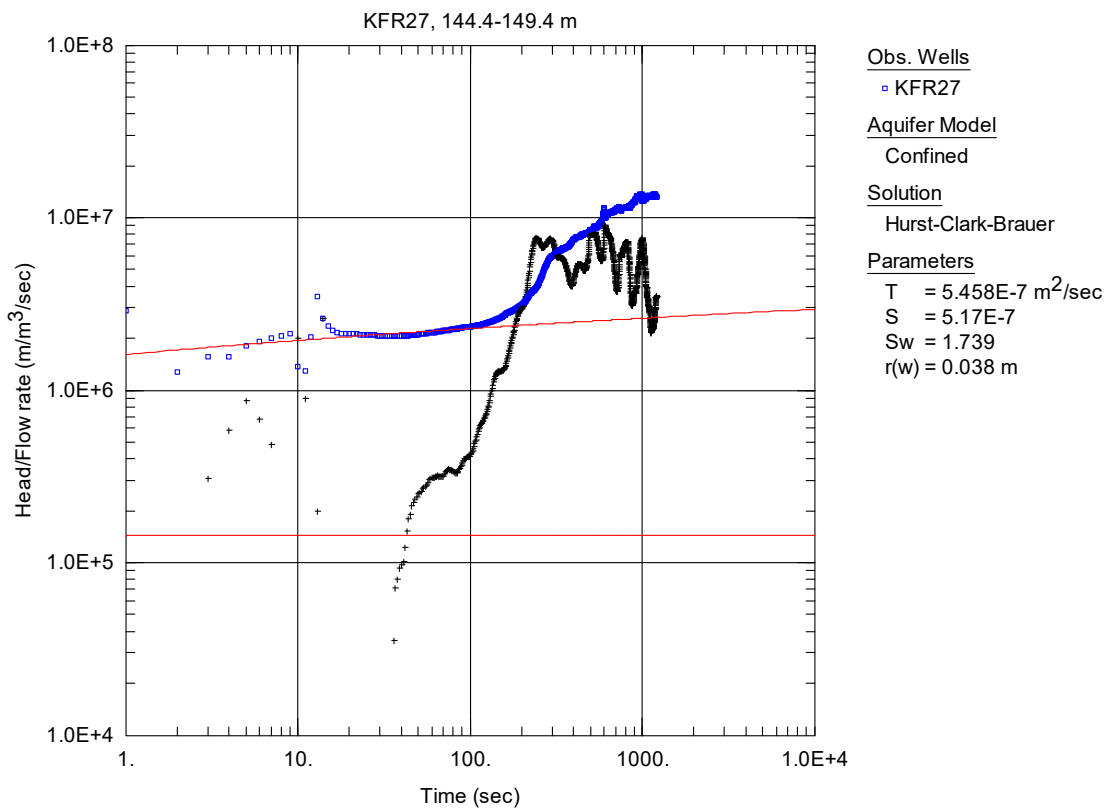


**Figure A2-68.** Log-log plot of head/flow rate (□) and derivative (+) versus time, from the injection test in section 144.4-149.4 m in borehole KFR27.

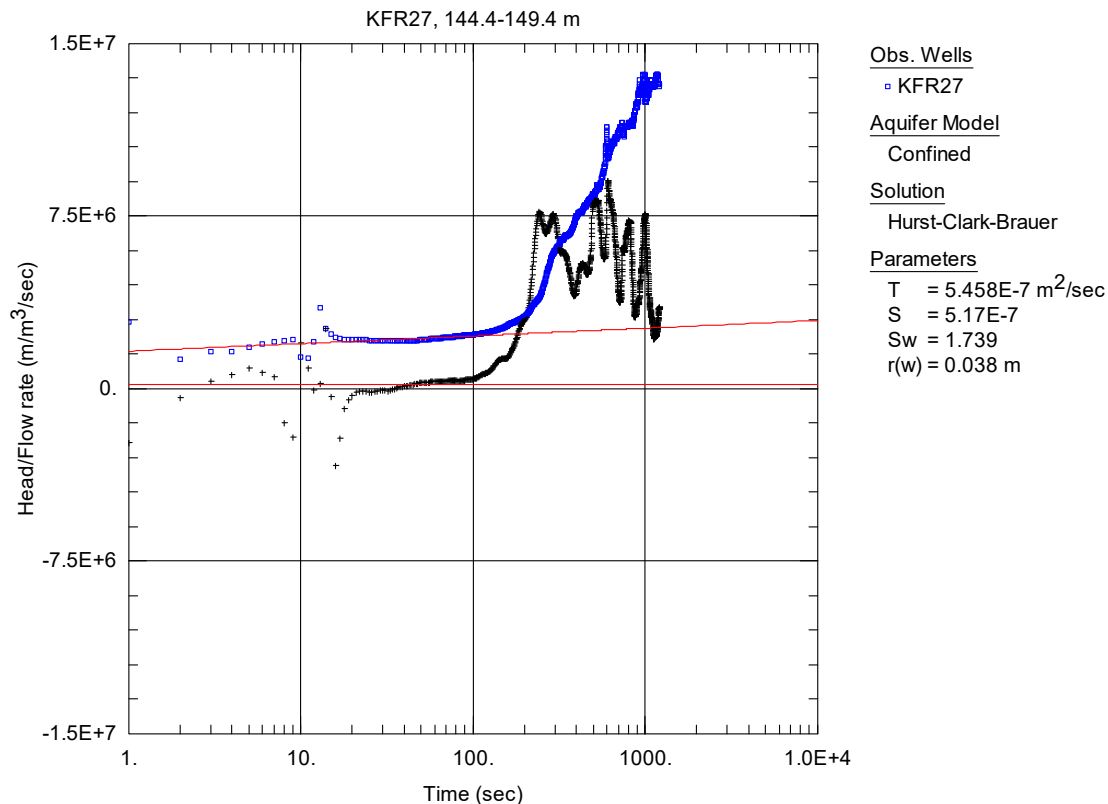


**Figure A2-69.** Lin-log plot of head/flow rate (□) and derivative (+) versus time, from the injection test in section 144.4-149.4 m in borehole KFR27.

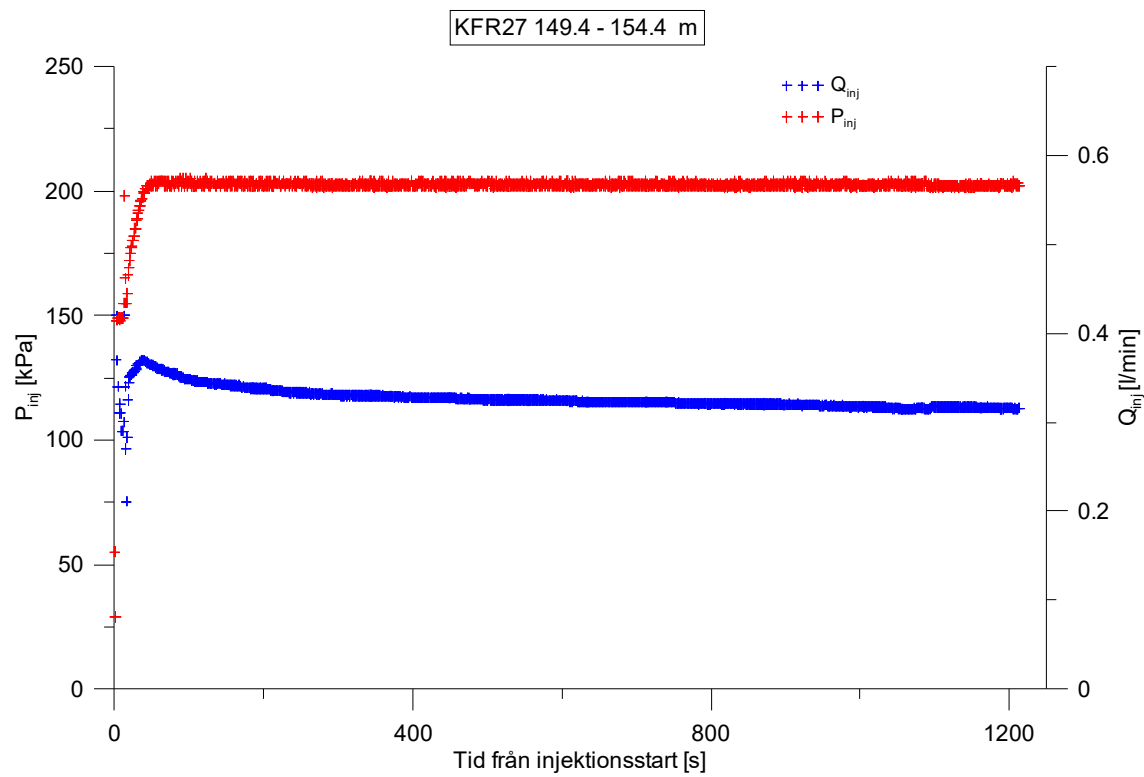


**Figure A2-70.** Linear plot of flow rate ( $Q$ ) and pressure ( $P$ ) versus time from the injection test in section 149.4-154.4 m in borehole KFR27.

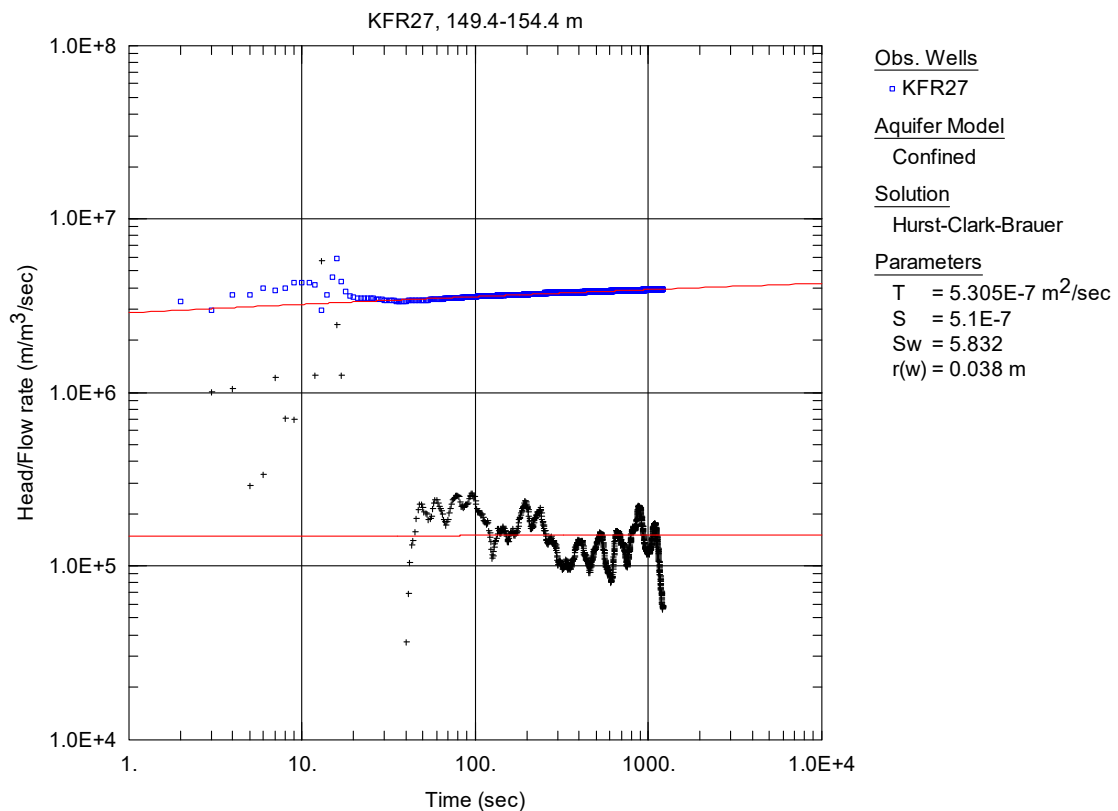


**Figure A2-71.** Log-log plot of head/flow rate ( $\square$ ) and derivative (+) versus time, from the injection test in section 149.4-154.4 m in borehole KFR27.

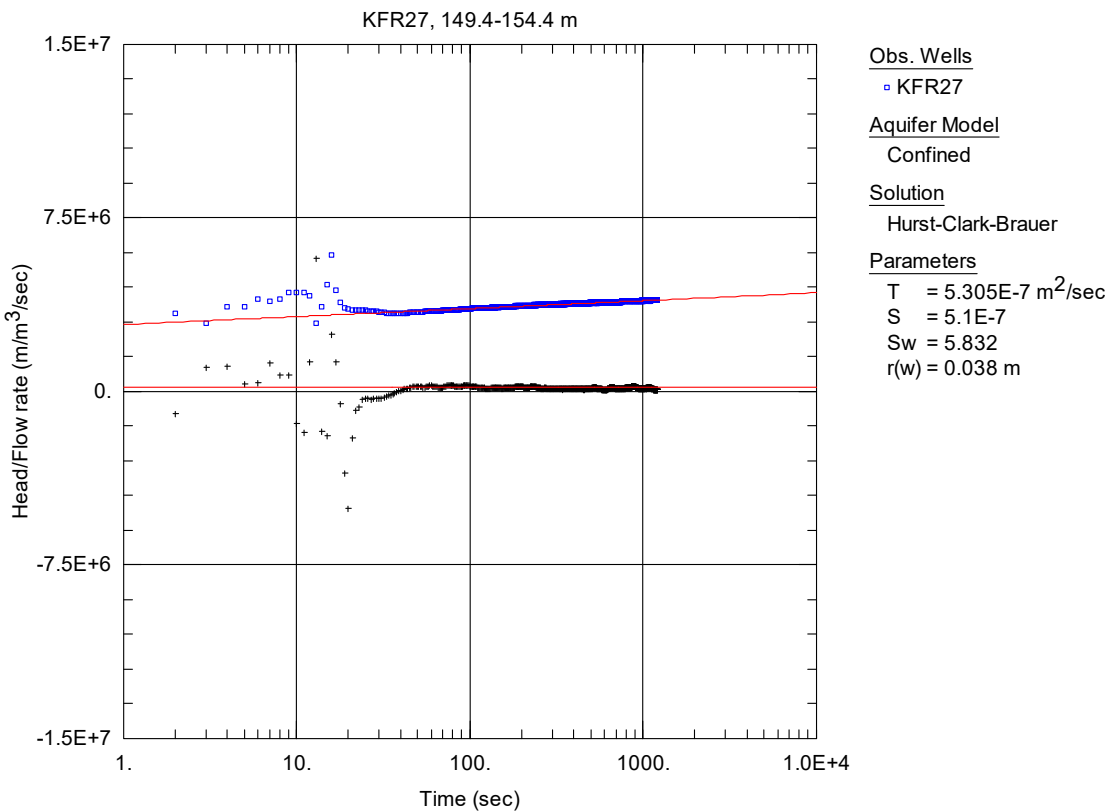


**Figure A2-72.** Lin-log plot of head/flow rate (□) and derivative (+) versus time, from the injection test in section 149.4-154.4 m in borehole KFR27.

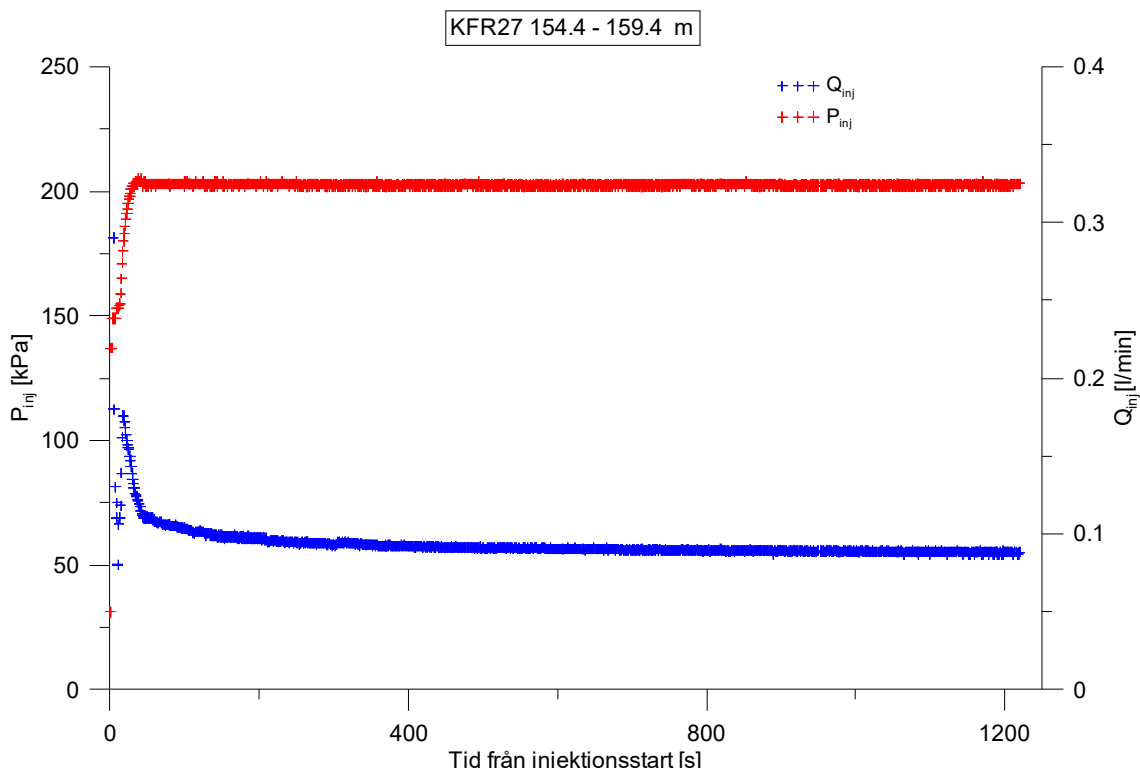


**Figure A2-73.** Linear plot of flow rate ( $Q$ ) and pressure ( $P$ ) versus time from the injection test in section 154.4-159.4 m in borehole KFR27.

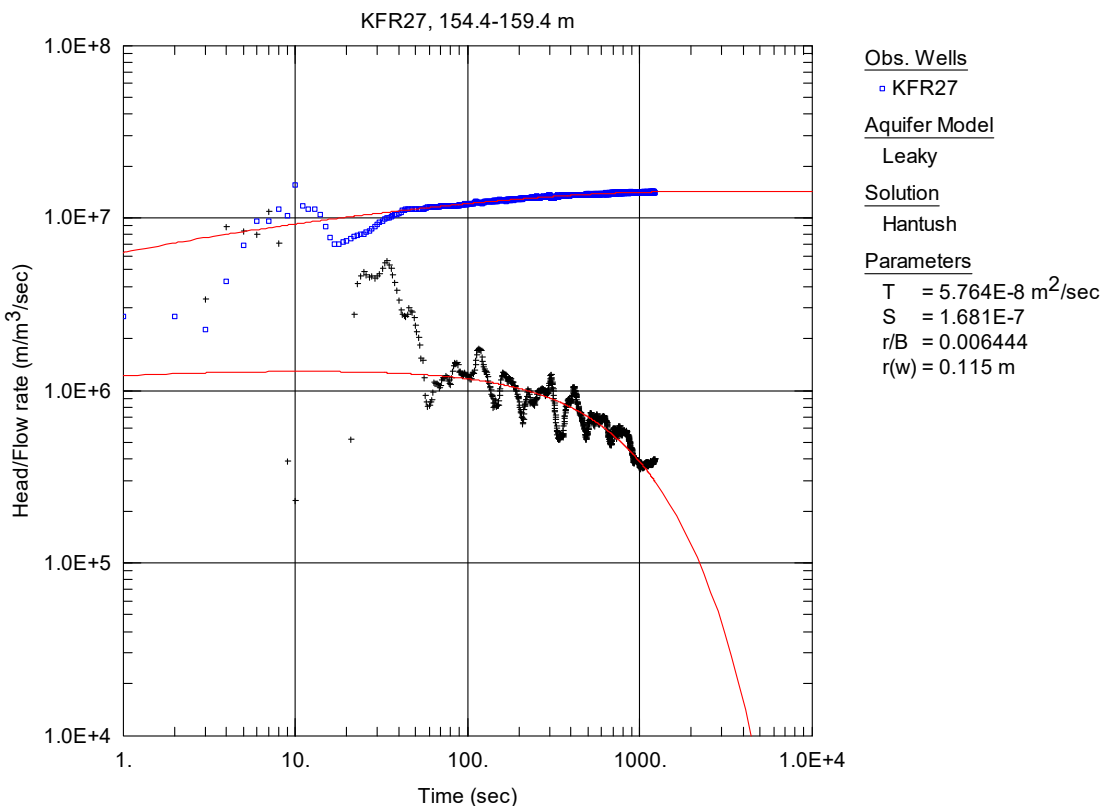


**Figure A2-74.** Log-log plot of head/flow rate (□) and derivative (+) versus time, from the injection test in section 154.4-159.4 m in borehole KFR27.

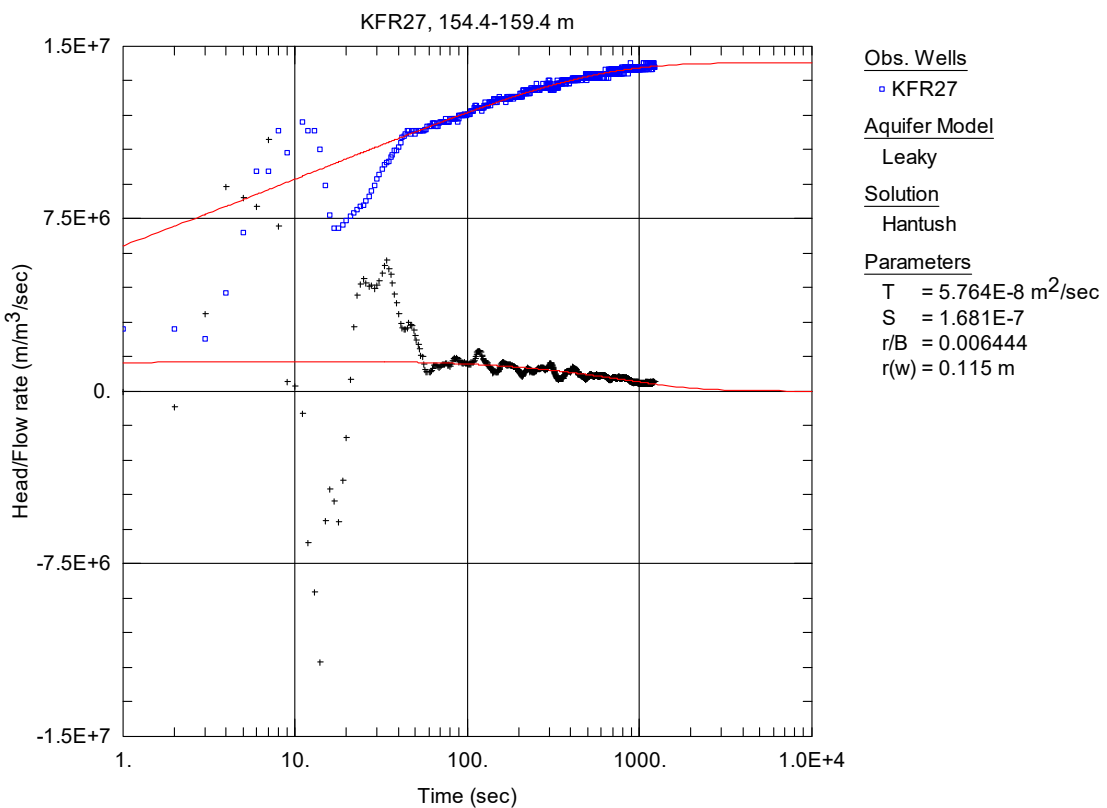


**Figure A2-75.** Lin-log plot of head/flow rate (□) and derivative (+) versus time, from the injection test in section 154.4-159.4 m in borehole KFR27.

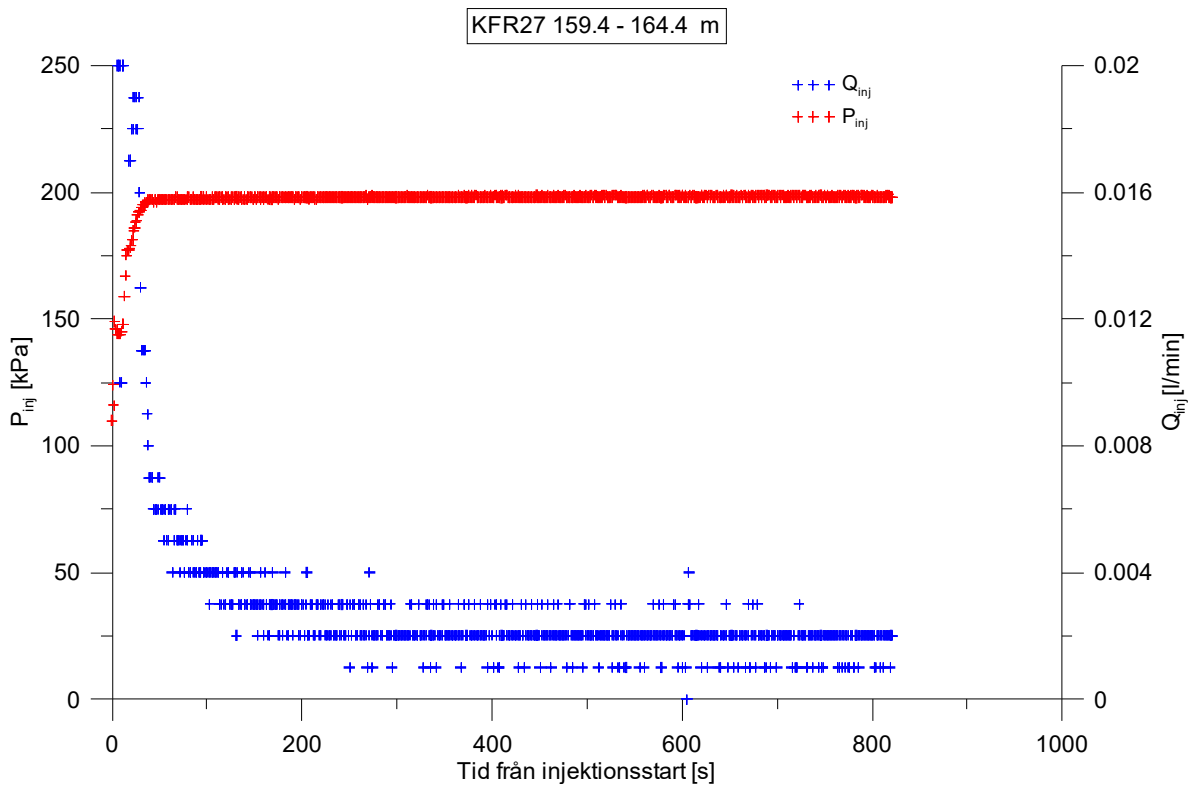


**Figure A2-76.** Linear plot of flow rate ( $Q$ ) and pressure ( $P$ ) versus time from the injection test in section 159.4-164.4 m in borehole KFR27.

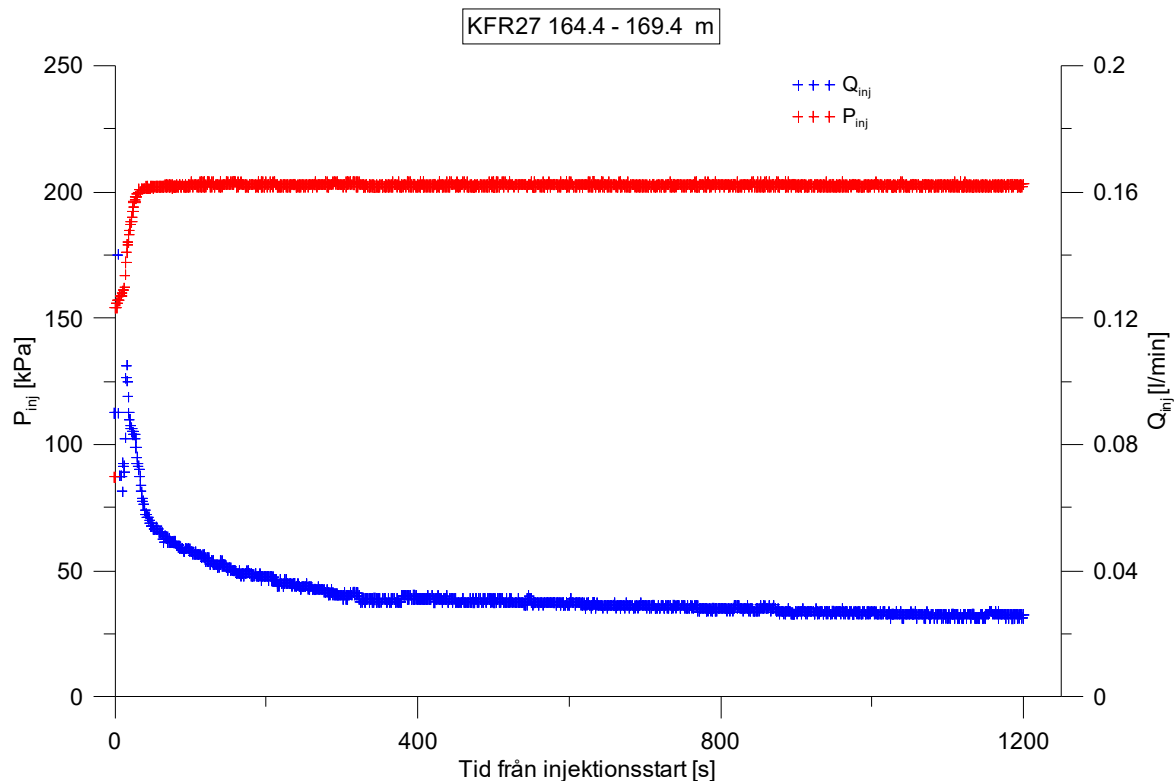


**Figure A2-77.** Linear plot of flow rate ( $Q$ ) and pressure ( $P$ ) versus time from the injection test in section 164.4-169.4 m in borehole KFR27.

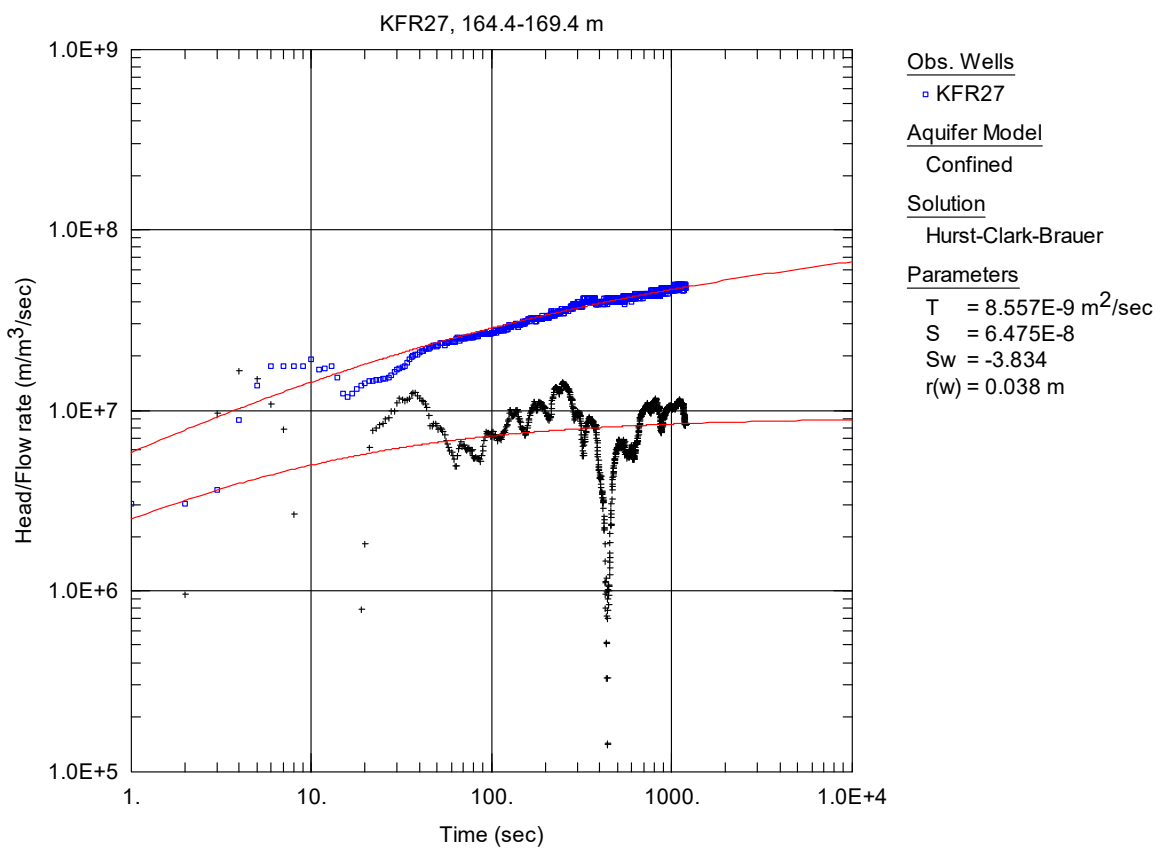


**Figure A2-78.** Log-log plot of head/flow rate (□) and derivative (+) versus time, from the injection test in section 164.4-169.4 m in borehole KFR27.

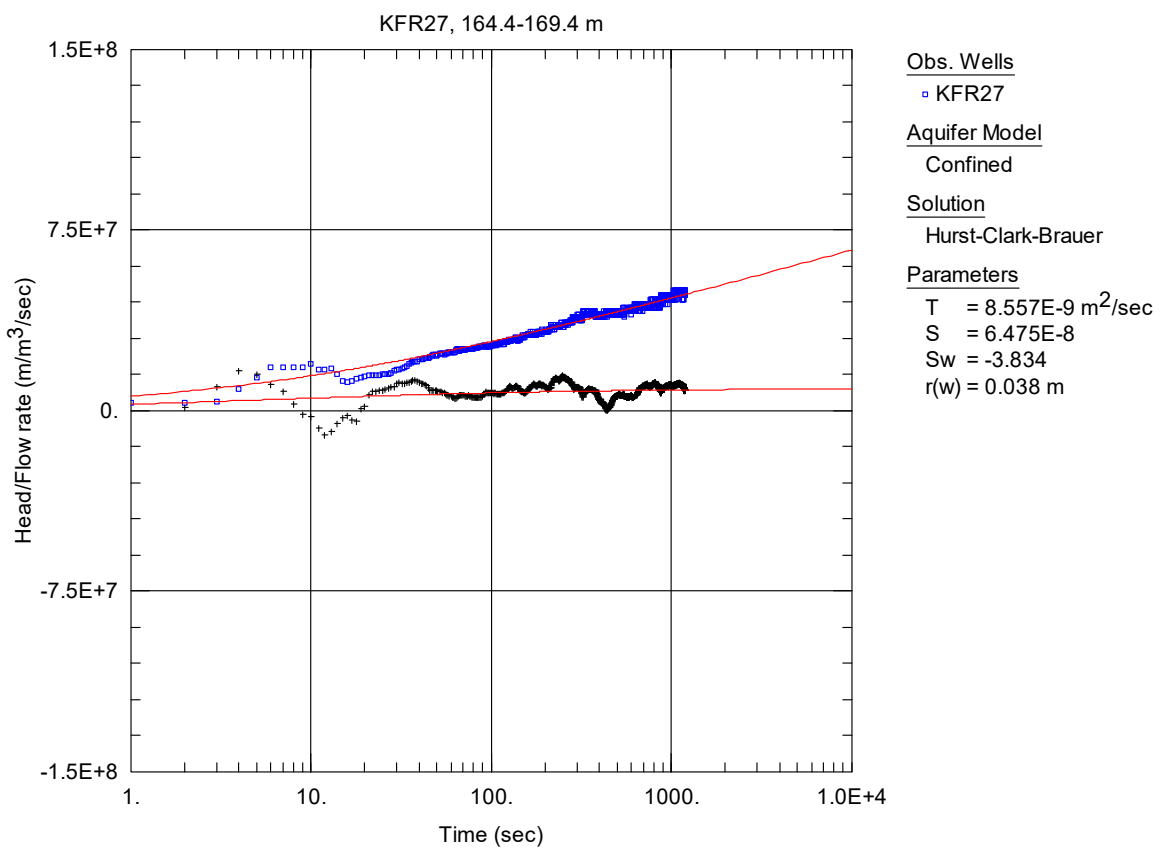


**Figure A2-79.** Lin-log plot of head/flow rate (□) and derivative (+) versus time, from the injection test in section 164.4-169.4 m in borehole KFR27.

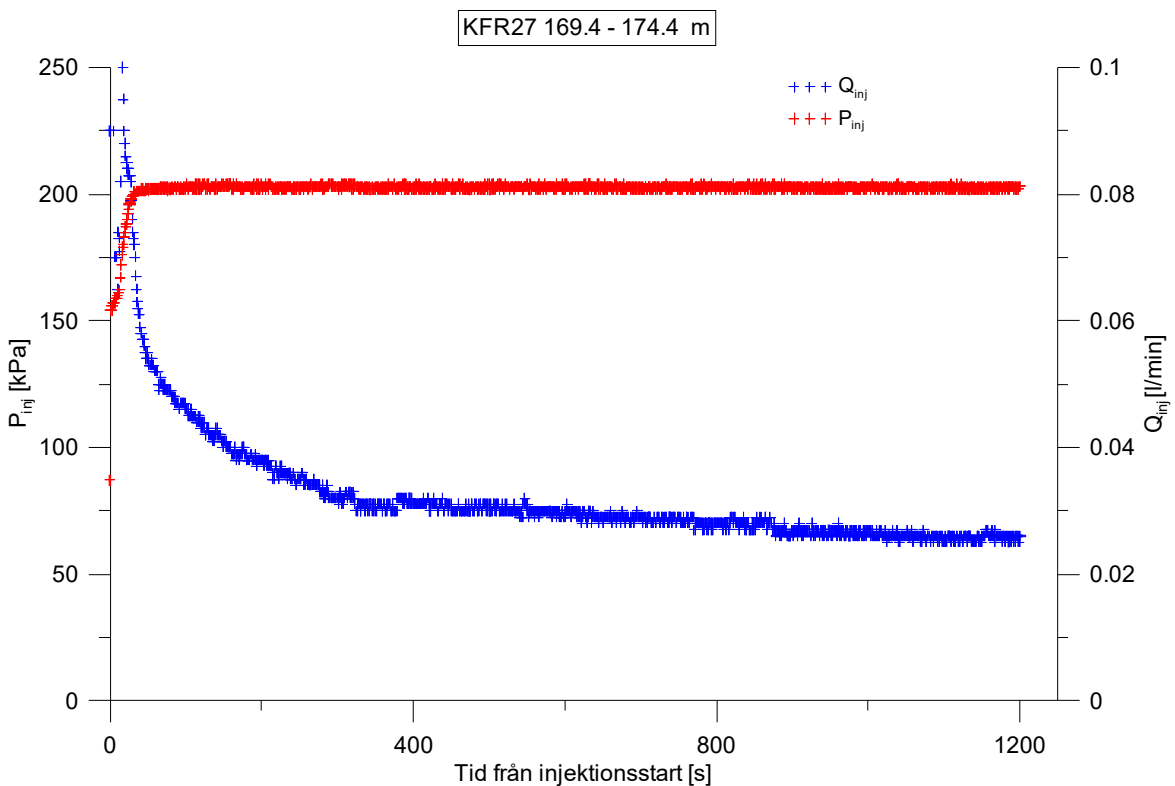


**Figure A2-80.** Linear plot of flow rate ( $Q$ ) and pressure ( $P$ ) versus time from the injection test in section 169.4-174.4 m in borehole KFR27.

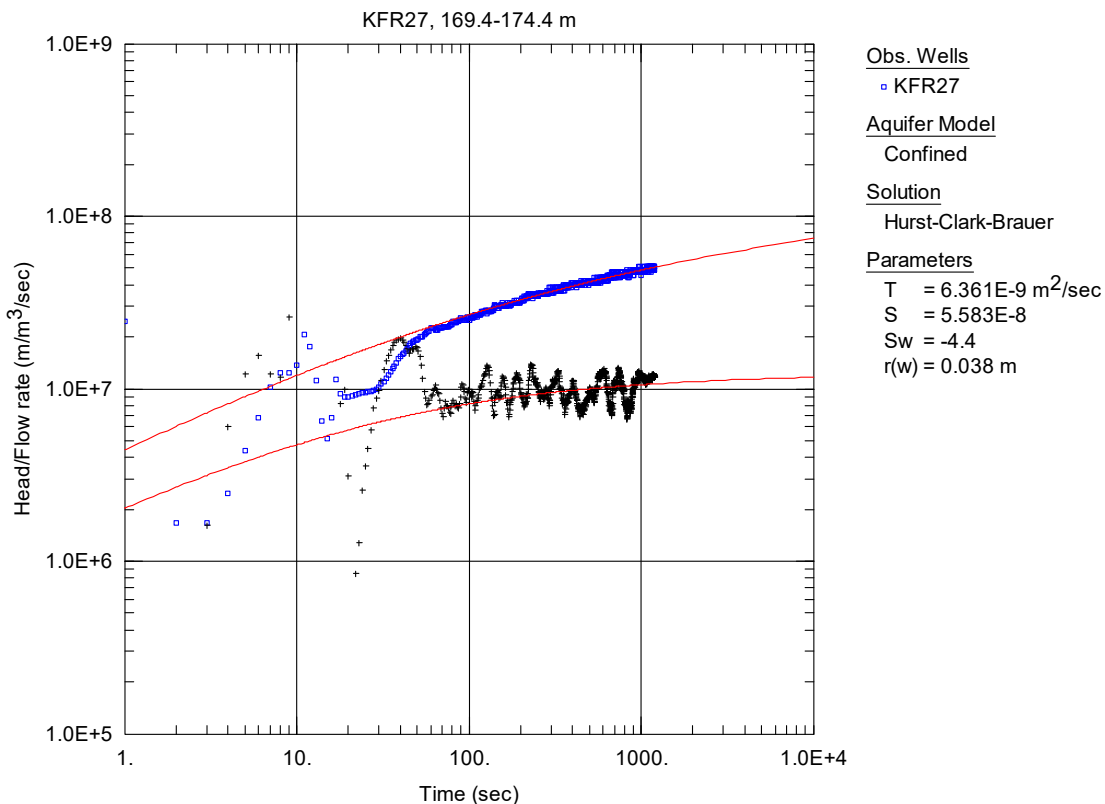


**Figure A2-81.** Log-log plot of head/flow rate (□) and derivative (+) versus time, from the injection test in section 169.4-174.4 m in borehole KFR27.

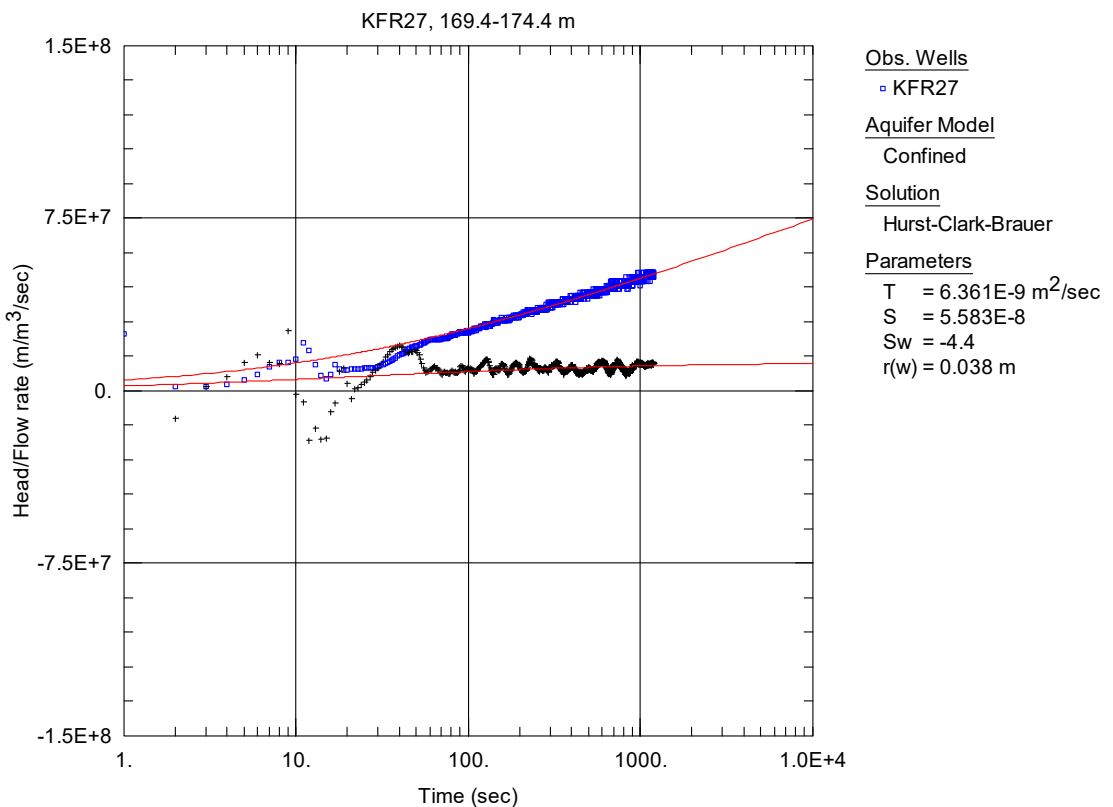


**Figure A2-82.** Lin-log plot of head/flow rate (□) and derivative (+) versus time, from the injection test in section 169.4-174.4 m in borehole KFR27.

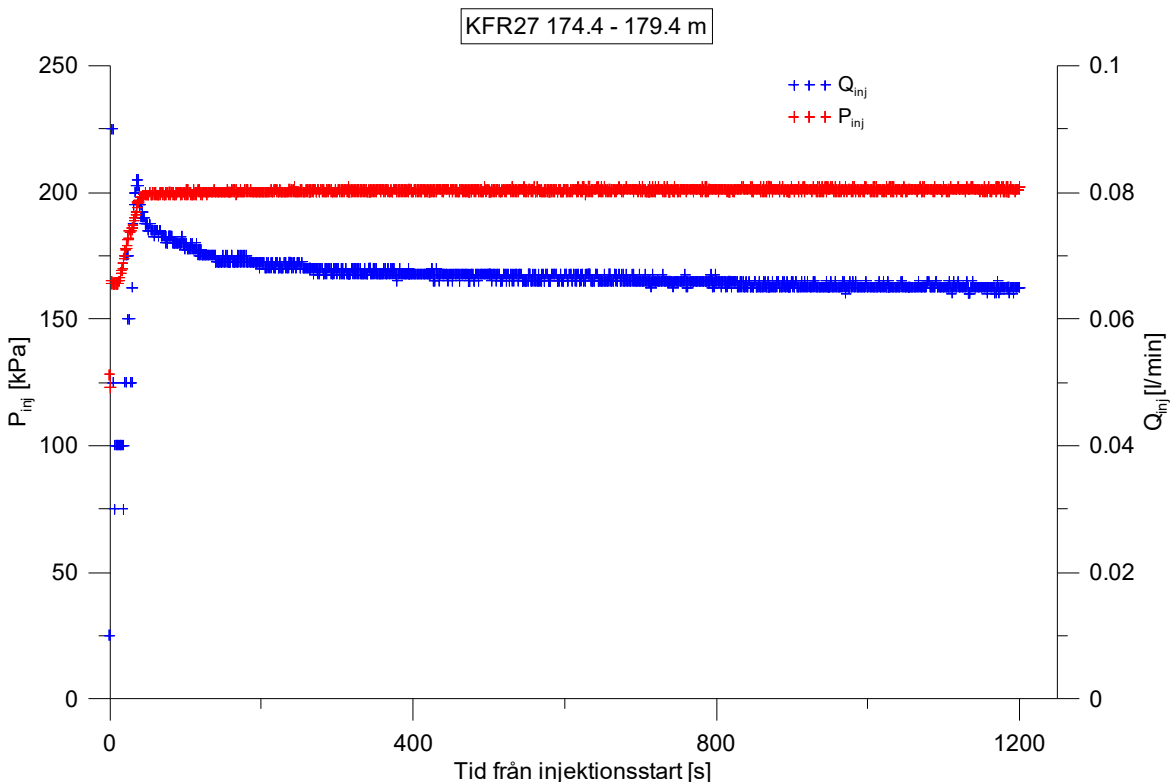


**Figure A2-83.** Linear plot of flow rate ( $Q$ ) and pressure ( $P$ ) versus time from the injection test in section 174.4-179.4 m in borehole KFR27.

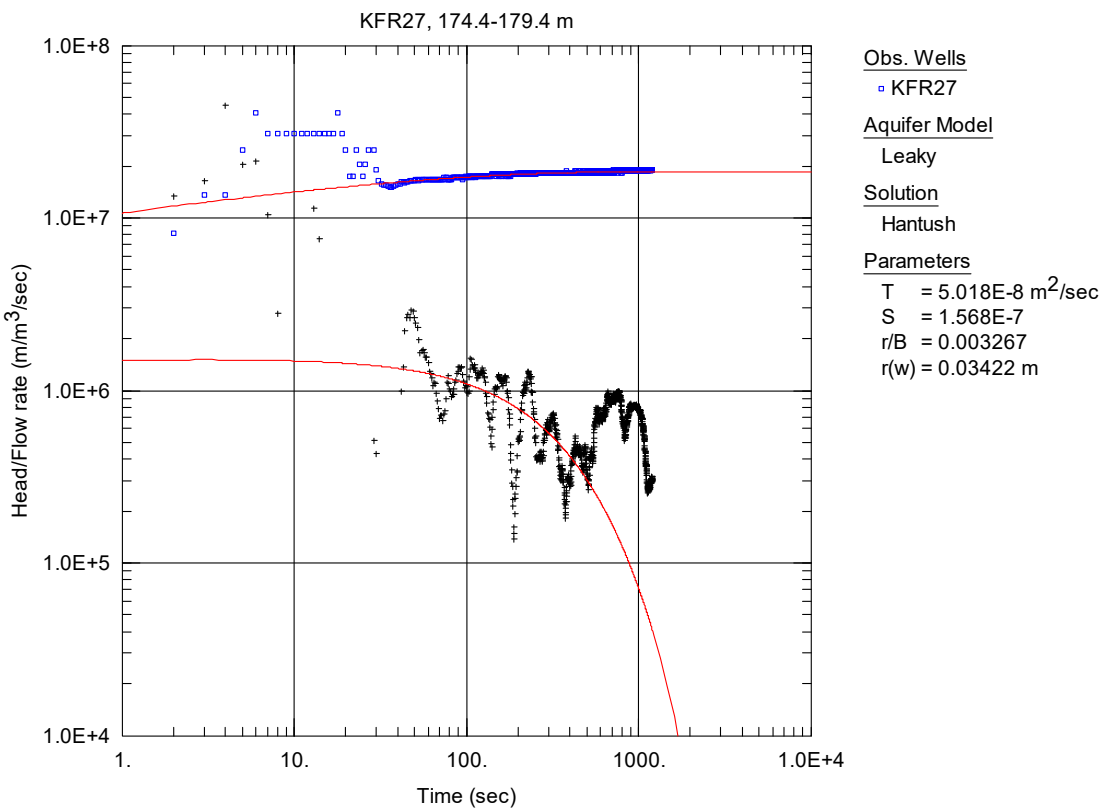


**Figure A2-84.** Log-log plot of head/flow rate (□) and derivative (+) versus time, from the injection test in section 174.4-179.4 m in borehole KFR27.

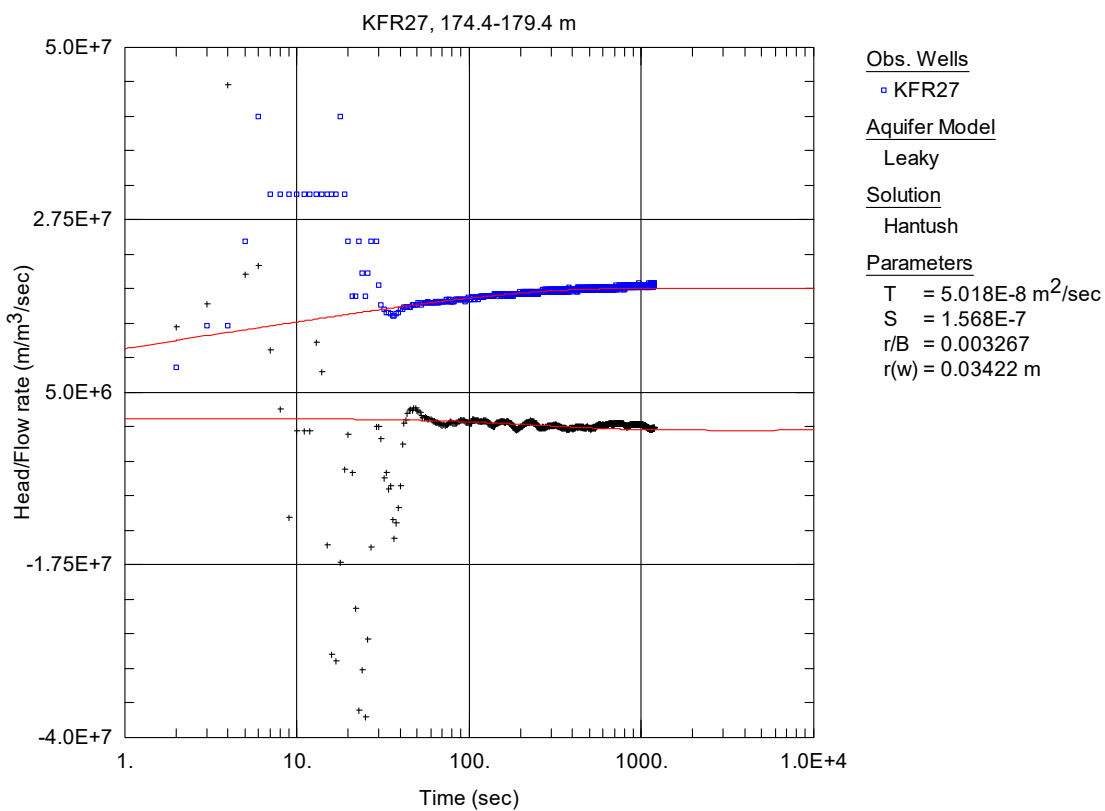


**Figure A2-85.** Lin-log plot of head/flow rate (□) and derivative (+) versus time, from the injection test in section 174.4-179.4 m in borehole KFR27.

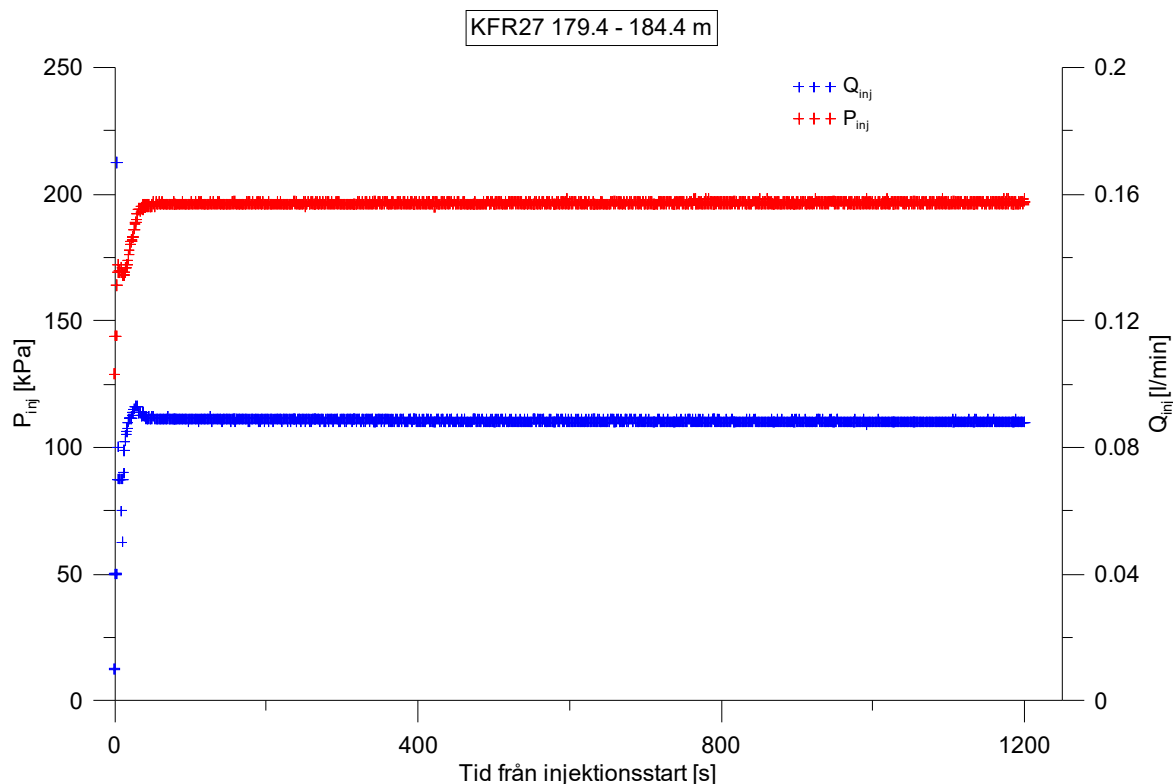


**Figure A2-86.** Linear plot of flow rate ( $Q$ ) and pressure ( $P$ ) versus time from the injection test in section 179.4-184.4 m in borehole KFR27.

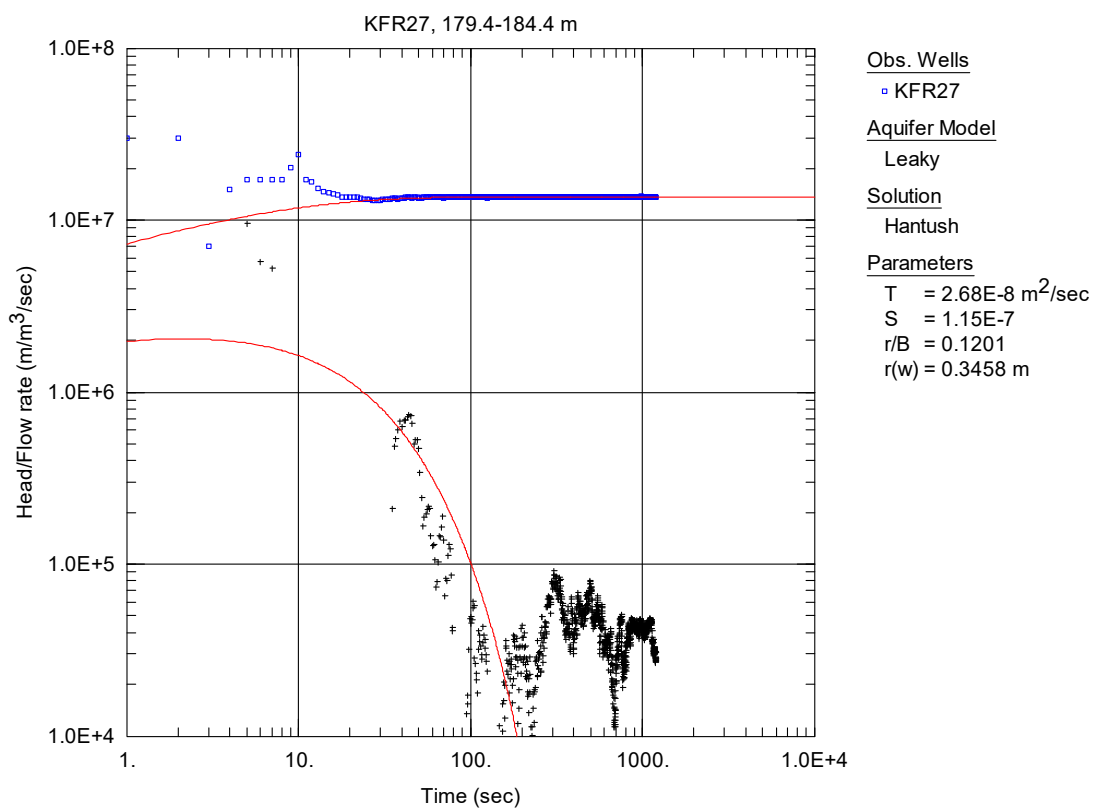


**Figure A2-87.** Log-log plot of head/flow rate (□) and derivative (+) versus time, from the injection test in section 179.4-184.4 m in borehole KFR27.

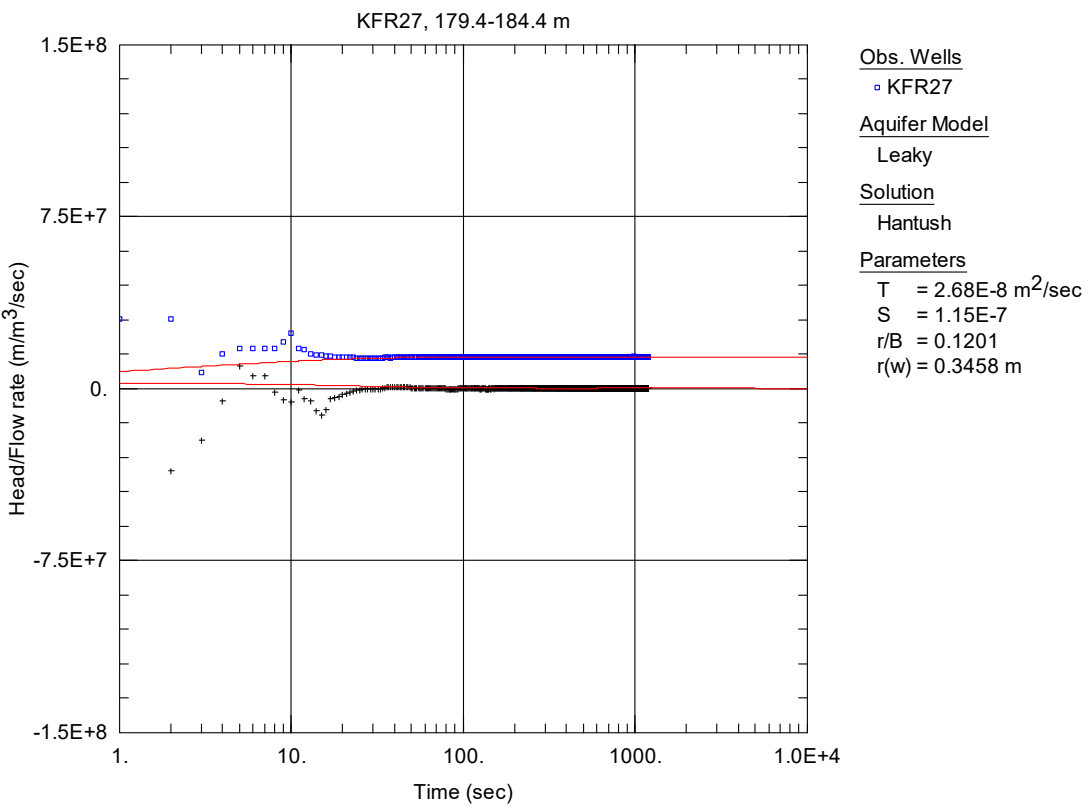


**Figure A2-88.** Lin-log plot of head/flow rate (□) and derivative (+) versus time, from the injection test in section 179.4-184.4 m in borehole KFR27.

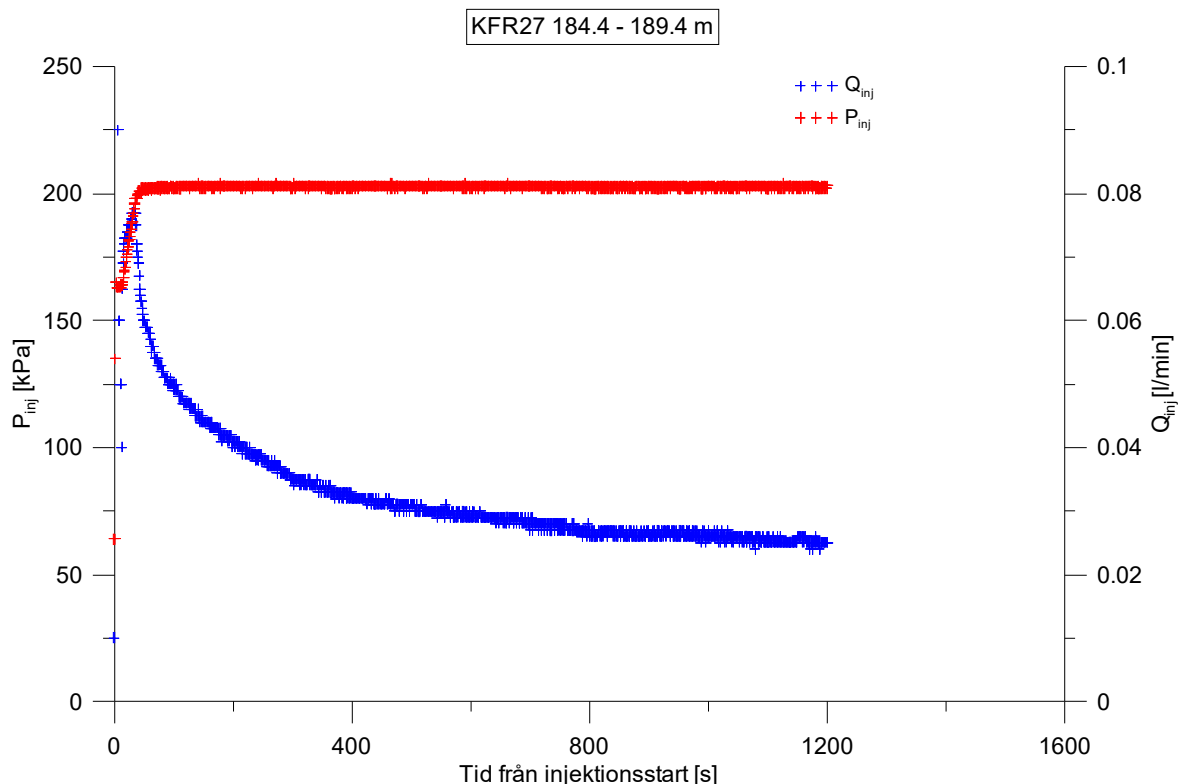


**Figure A2-89.** Linear plot of flow rate ( $Q$ ) and pressure ( $P$ ) versus time from the injection test in section 184.4-189.4 m in borehole KFR27.

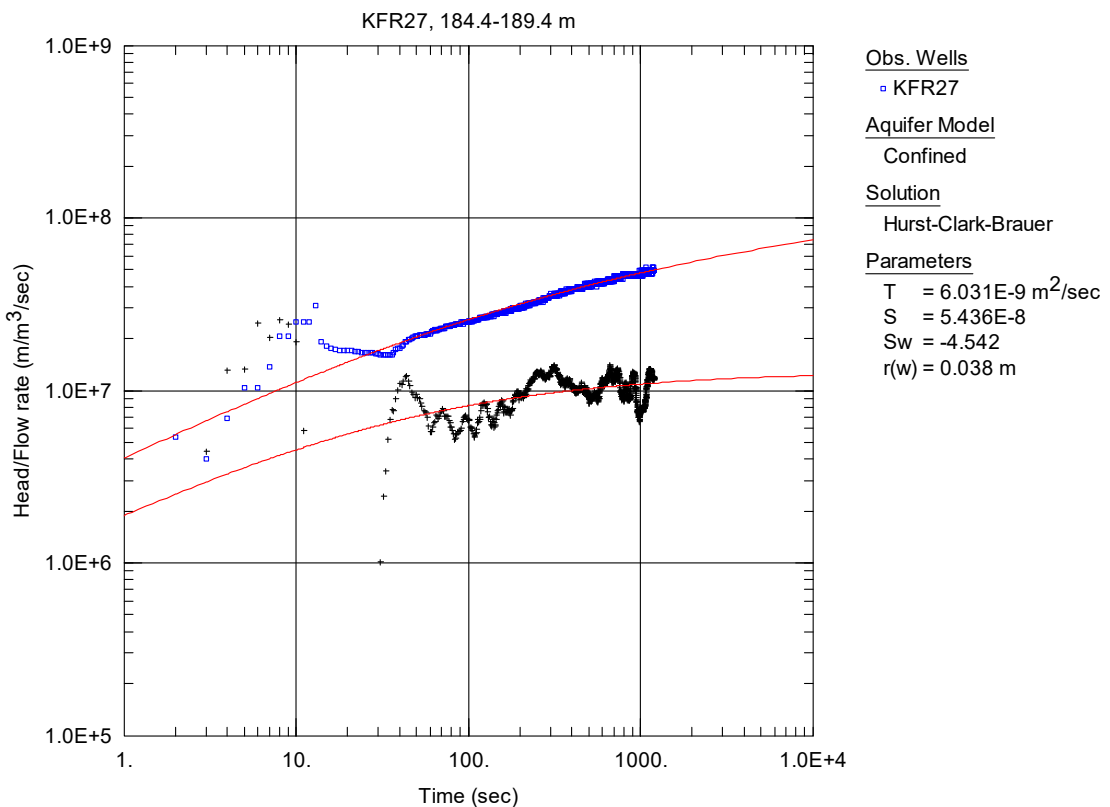


**Figure A2-90.** Log-log plot of head/flow rate (□) and derivative (+) versus time, from the injection test in section 184.4-189.4 m in borehole KFR27.

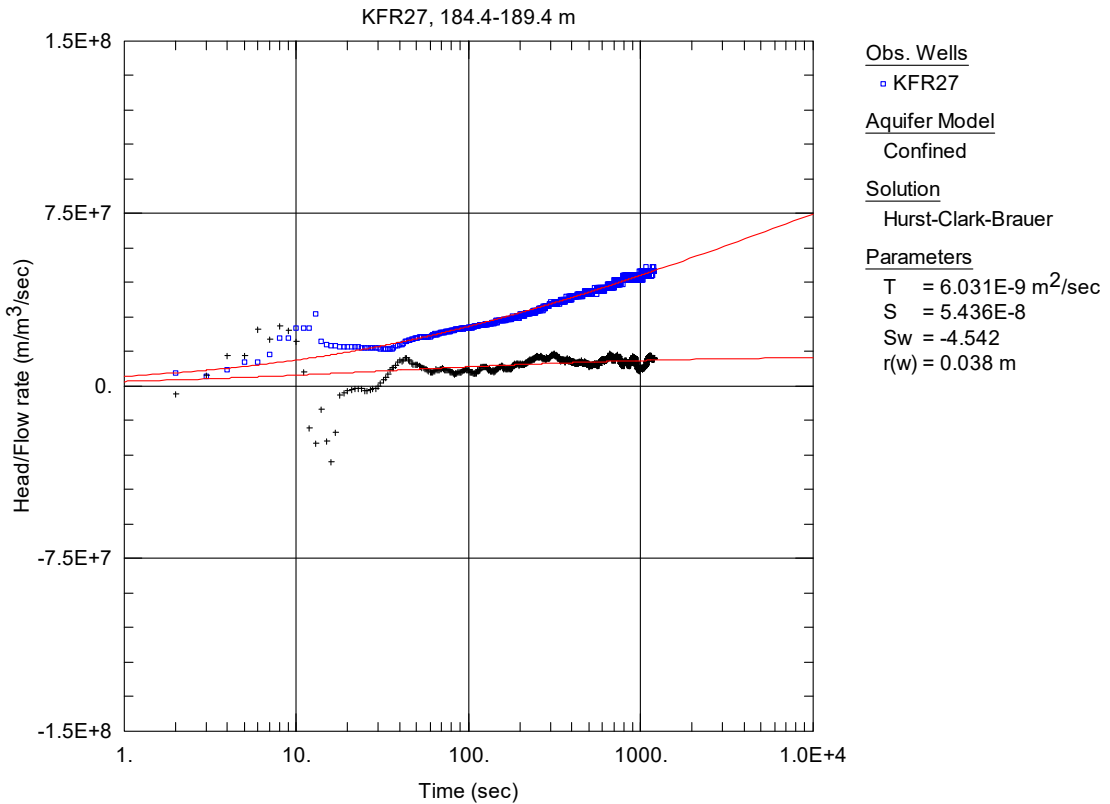


**Figure A2-91.** Lin-log plot of head/flow rate (□) and derivative (+) versus time, from the injection test in section 184.4-189.4 m in borehole KFR27.

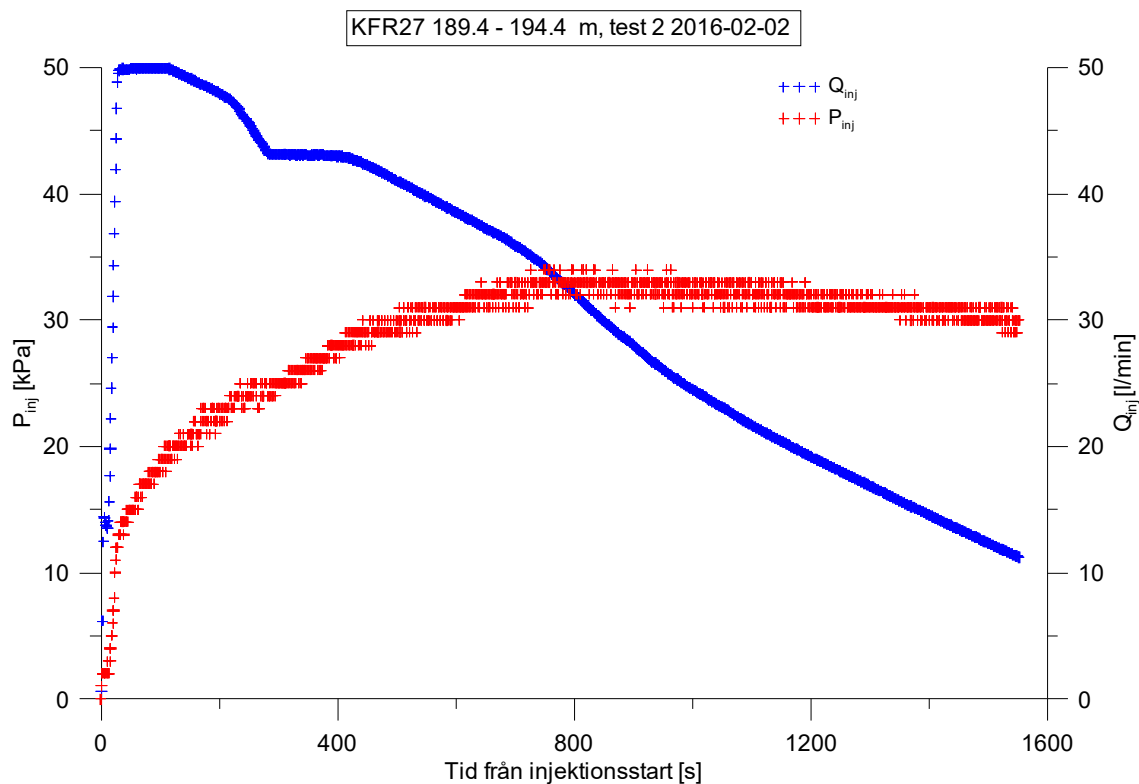


**Figure A2-92.** Linear plot of flow rate ( $Q$ ) and pressure ( $P$ ) versus time from the injection test in section 189.4-194.4 m in borehole KFR27.

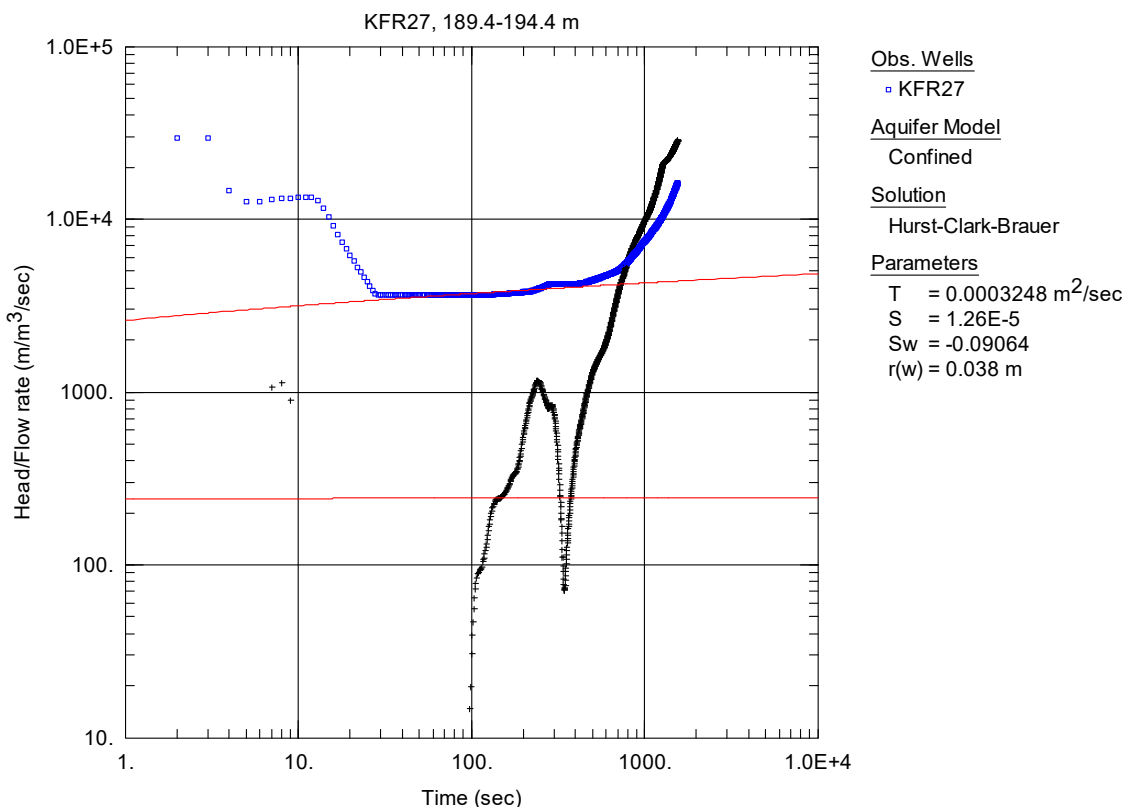


**Figure A2-93.** Log-log plot of head/flow rate (□) and derivative (+) versus time, from the injection test in section 189.4-194.4 m in borehole KFR27.

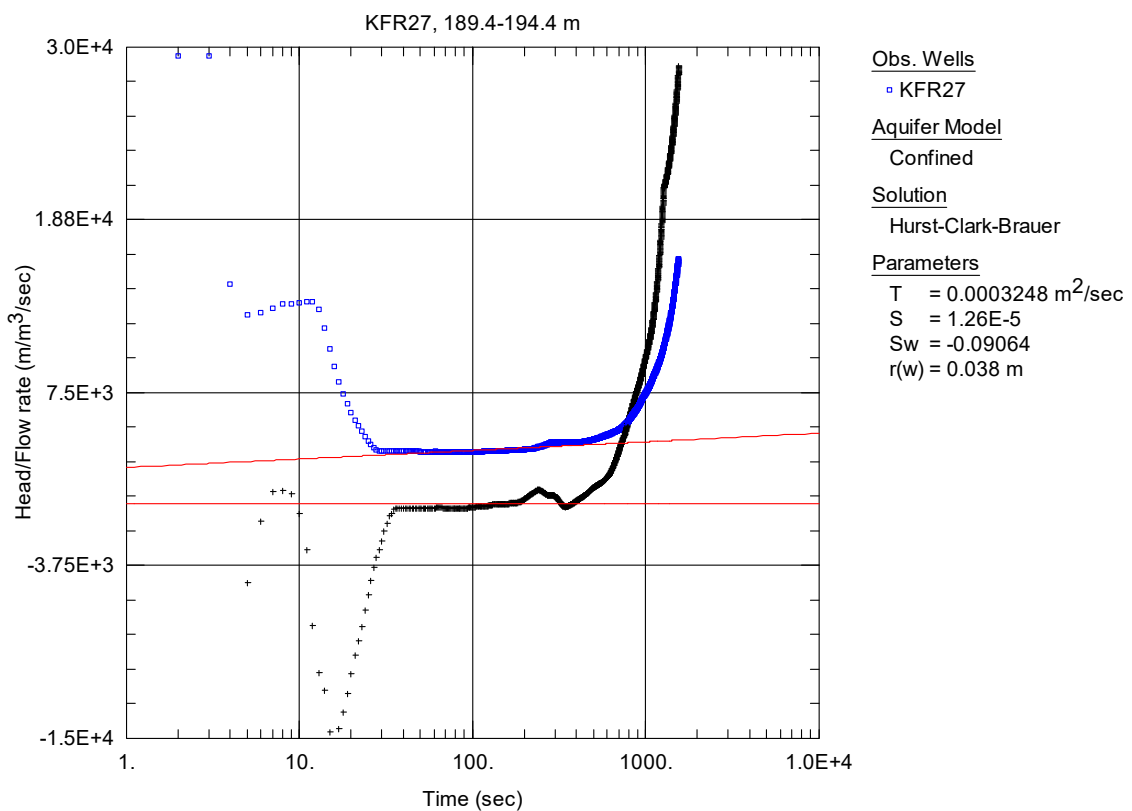


**Figure A2-94.** Lin-log plot of head/flow rate (□) and derivative (+) versus time, from the injection test in section 189.4-194.4 m in borehole KFR27.

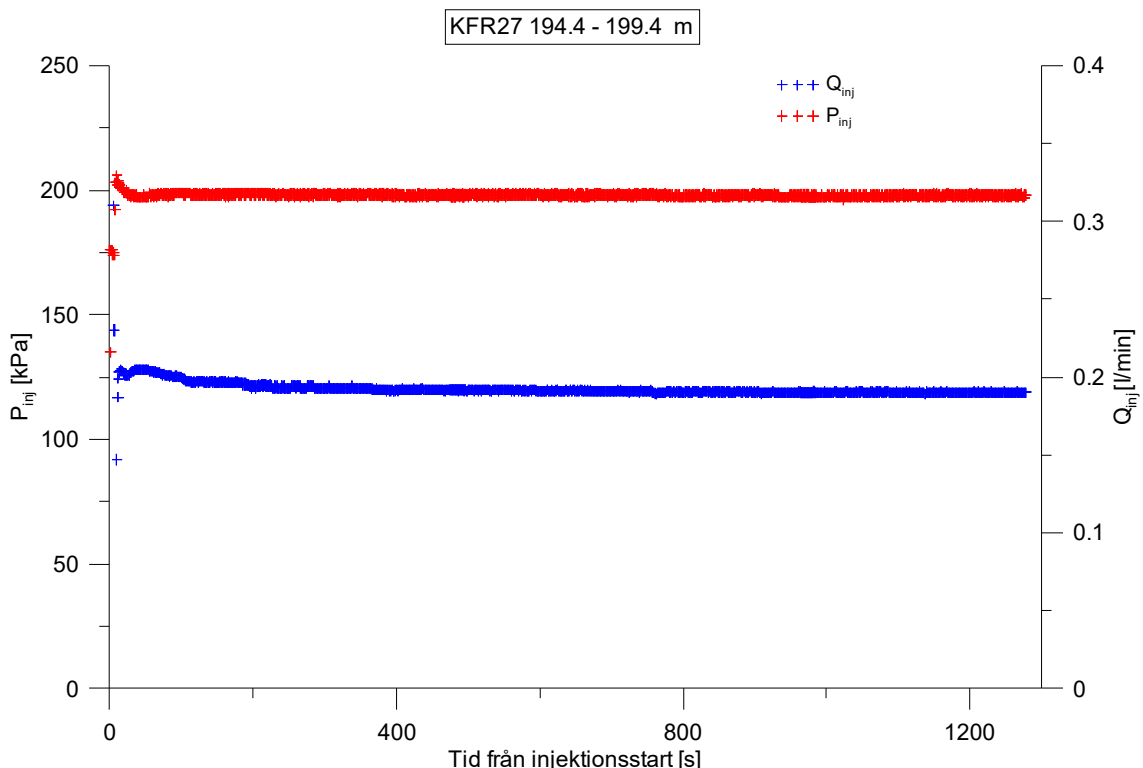


**Figure A2-95.** Linear plot of flow rate ( $Q$ ) and pressure ( $P$ ) versus time from the injection test in section 194.4-199.4 m in borehole KFR27.

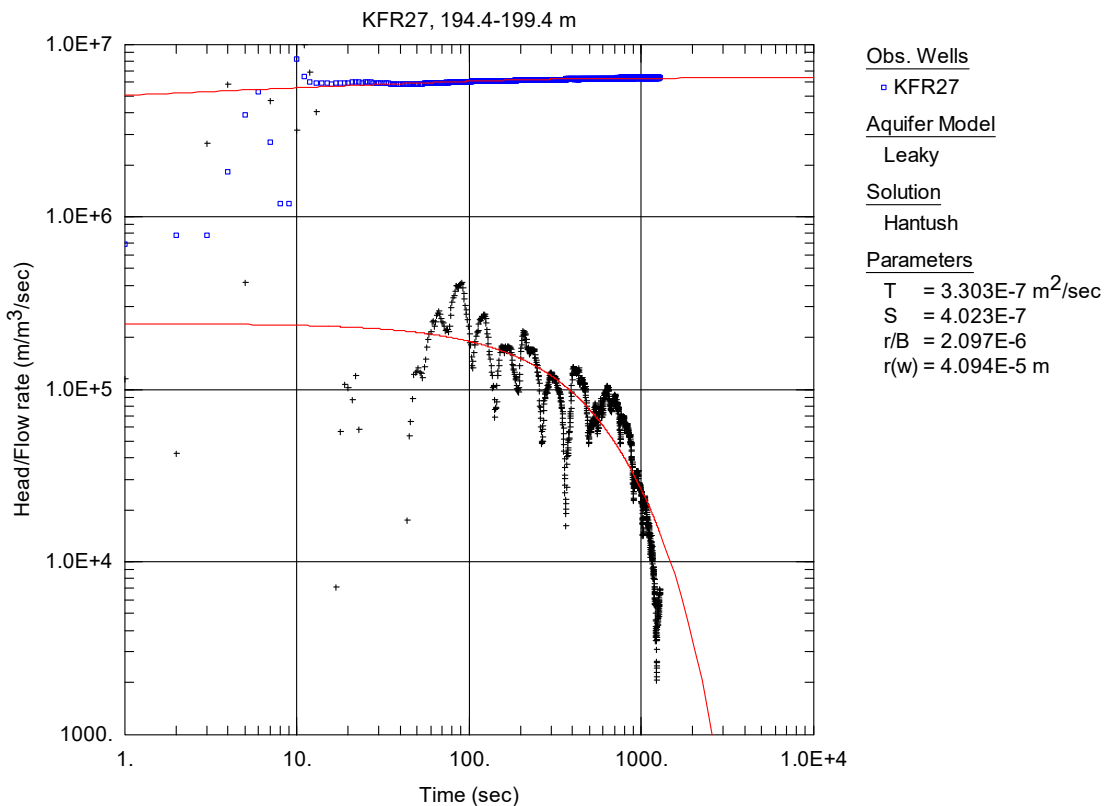


**Figure A2-96.** Log-log plot of head/flow rate (□) and derivative (+) versus time, from the injection test in section 194.4-199.4 m in borehole KFR27.

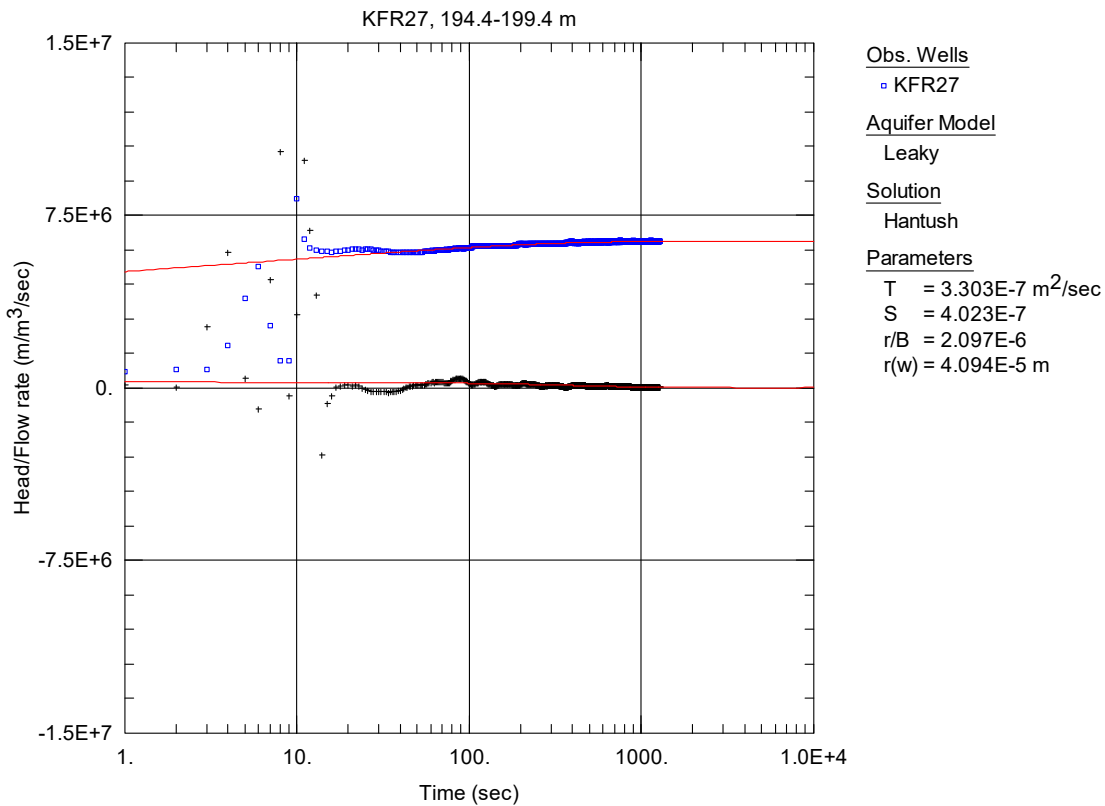


**Figure A2-97.** Lin-log plot of head/flow rate (□) and derivative (+) versus time, from the injection test in section 194.4-199.4 m in borehole KFR27.

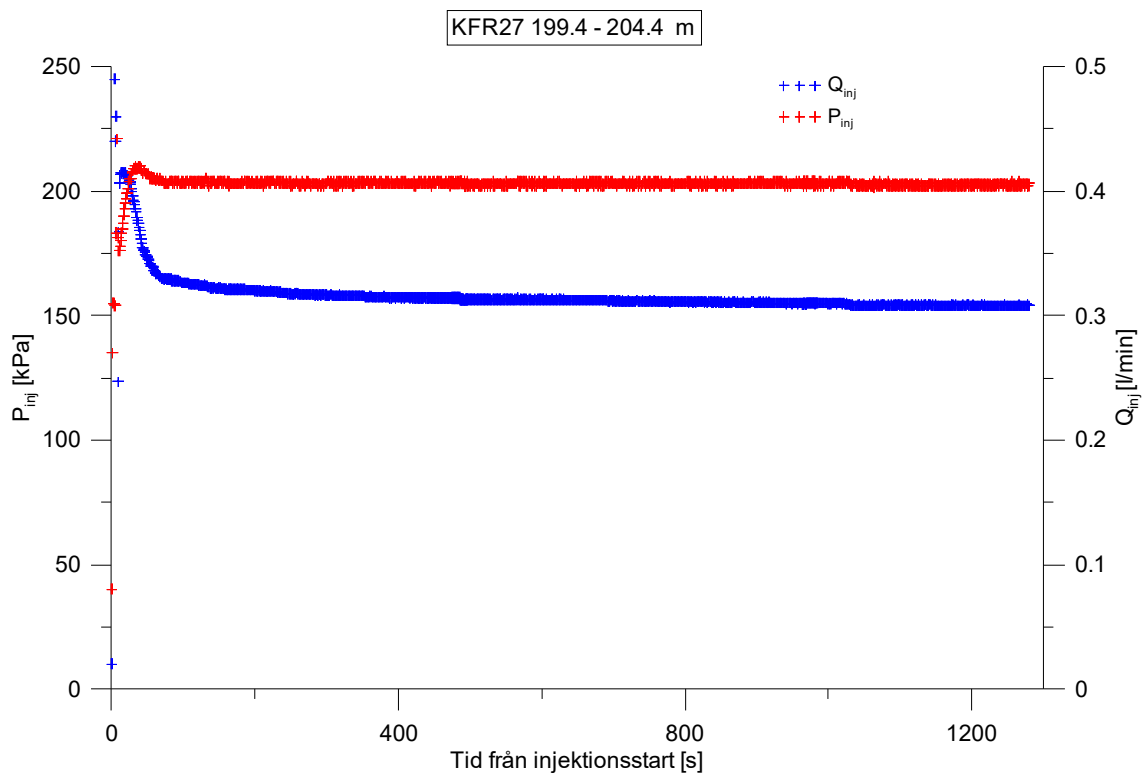


**Figure A2-98.** Linear plot of flow rate ( $Q$ ) and pressure ( $P$ ) versus time from the injection test in section 199.4-204.4 m in borehole KFR27.

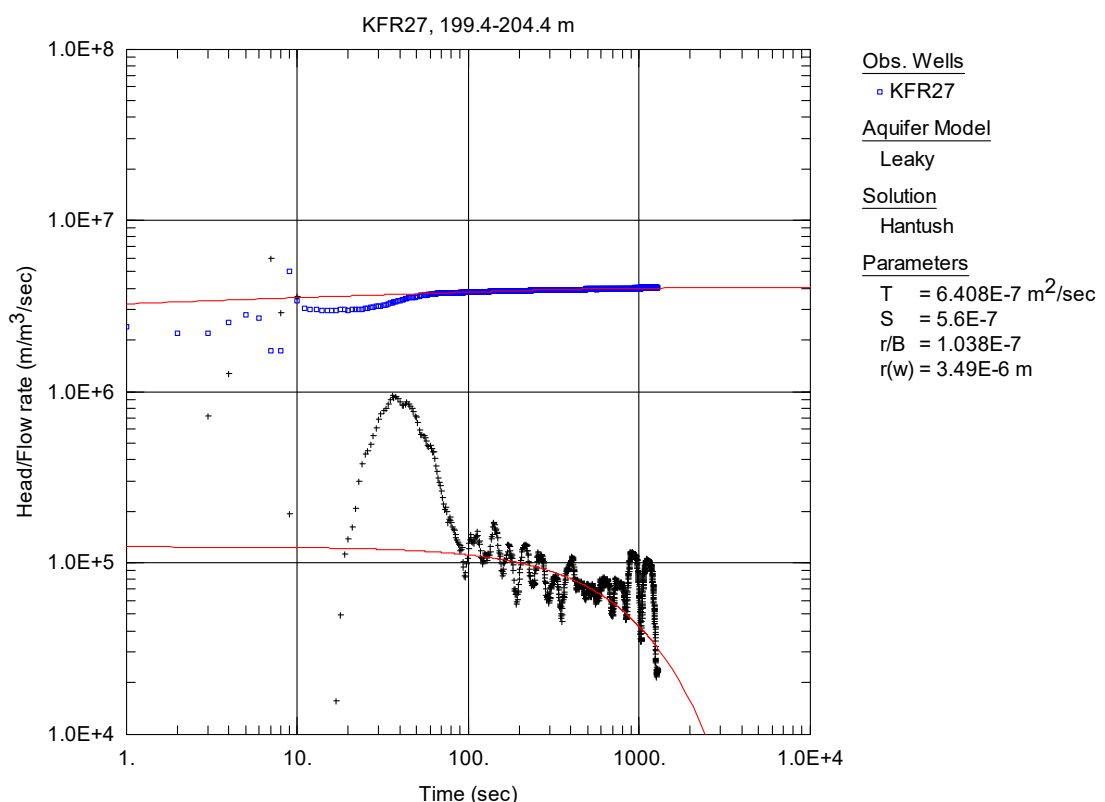


**Figure A2-99.** Log-log plot of head/flow rate ( $\square$ ) and derivative ( $+$ ) versus time, from the injection test in section 199.4-204.4 m in borehole KFR27.

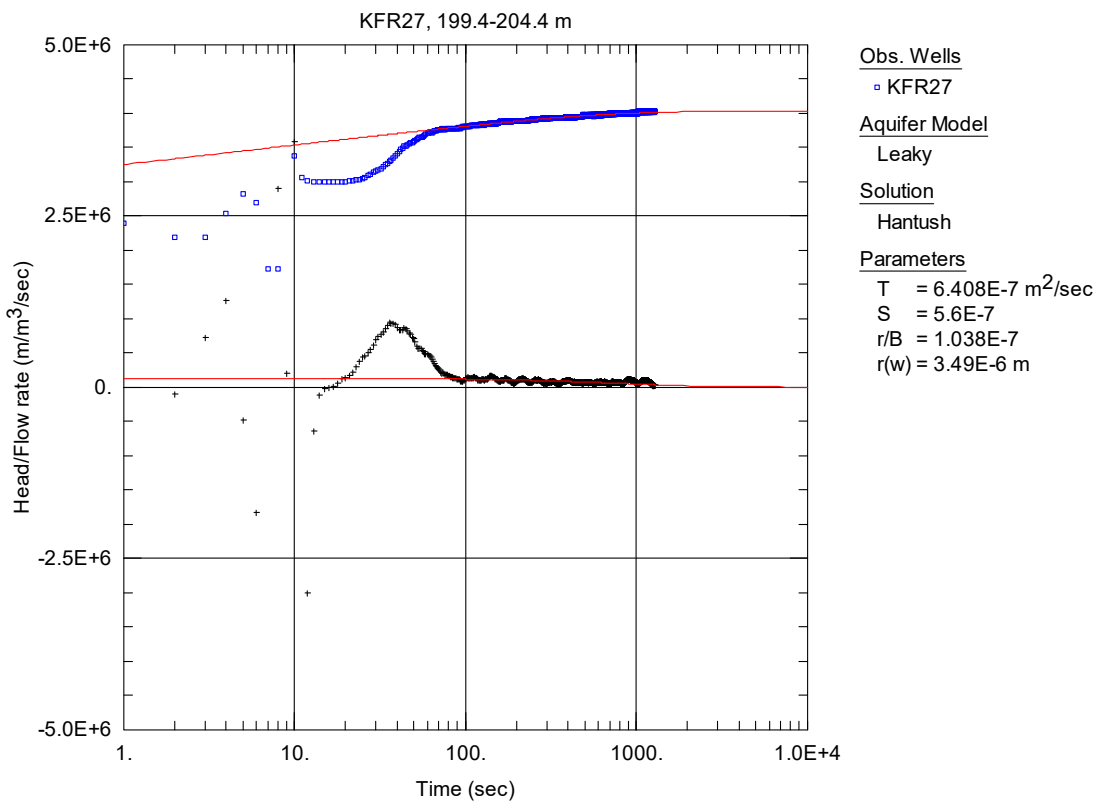


**Figure A2-100.** Lin-log plot of head/flow rate (□) and derivative (+) versus time, from the injection test in section 199.4-204.4 m in borehole KFR27.

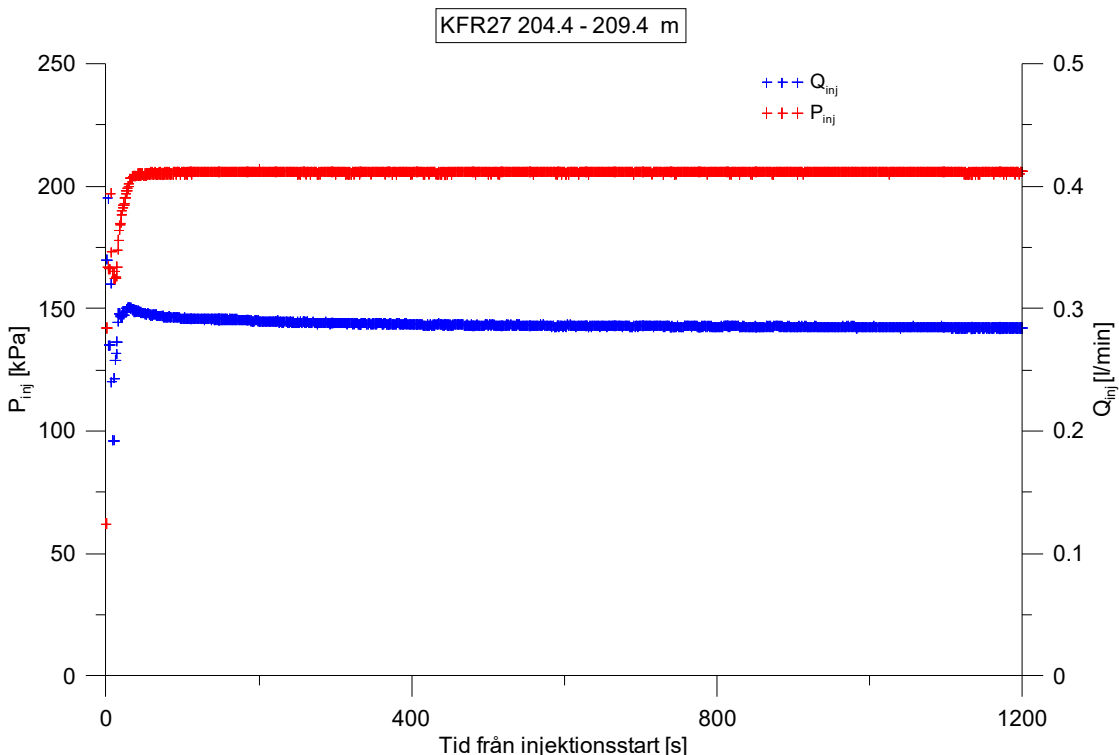


**Figure A2-101.** Linear plot of flow rate ( $Q$ ) and pressure ( $P$ ) versus time from the injection test in section 204.4-209.4 m in borehole KFR27.

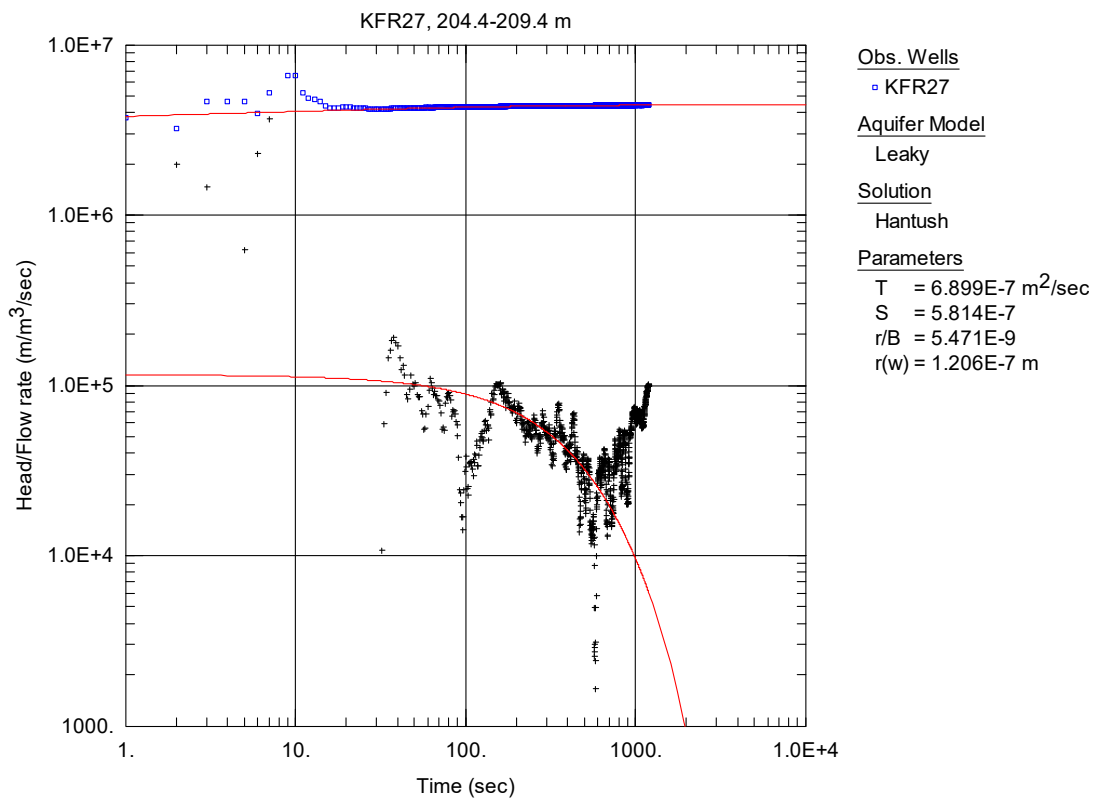


**Figure A2-102.** Log-log plot of head/flow rate (□) and derivative (+) versus time, from the injection test in section 204.4-209.4 m in borehole KFR27.

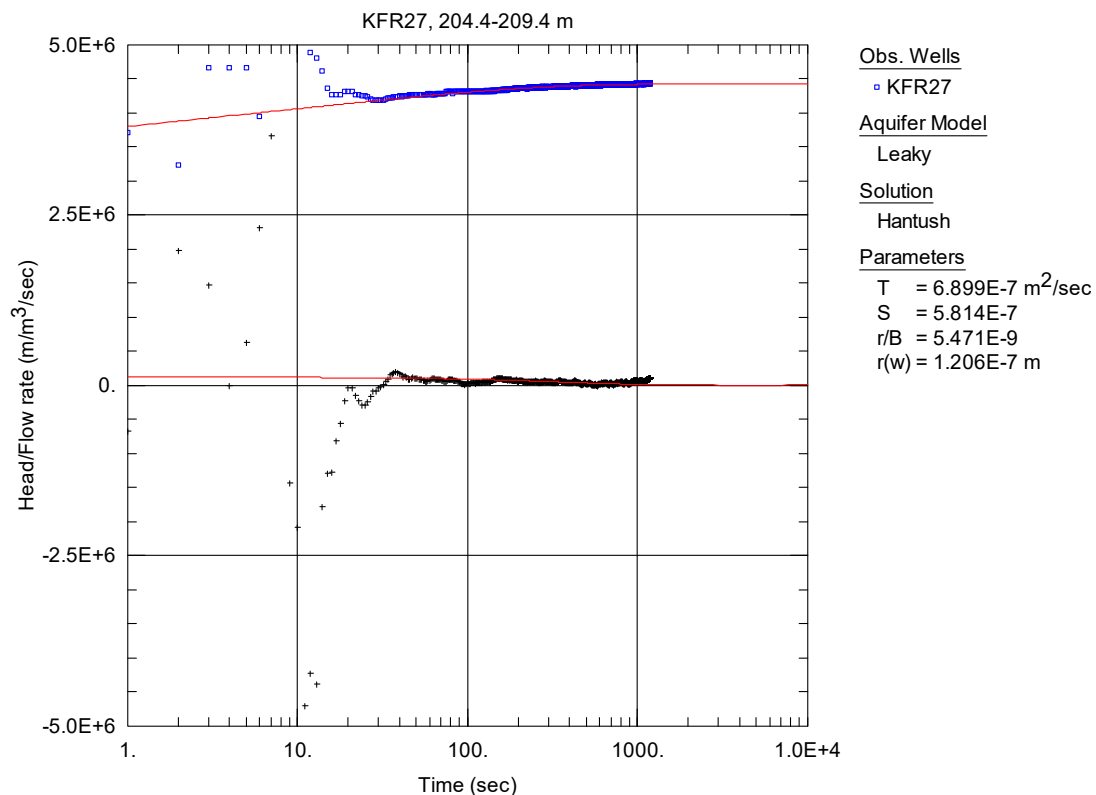


**Figure A2-103.** Lin-log plot of head/flow rate (□) and derivative (+) versus time, from the injection test in section 204.4-209.4 m in borehole KFR27.

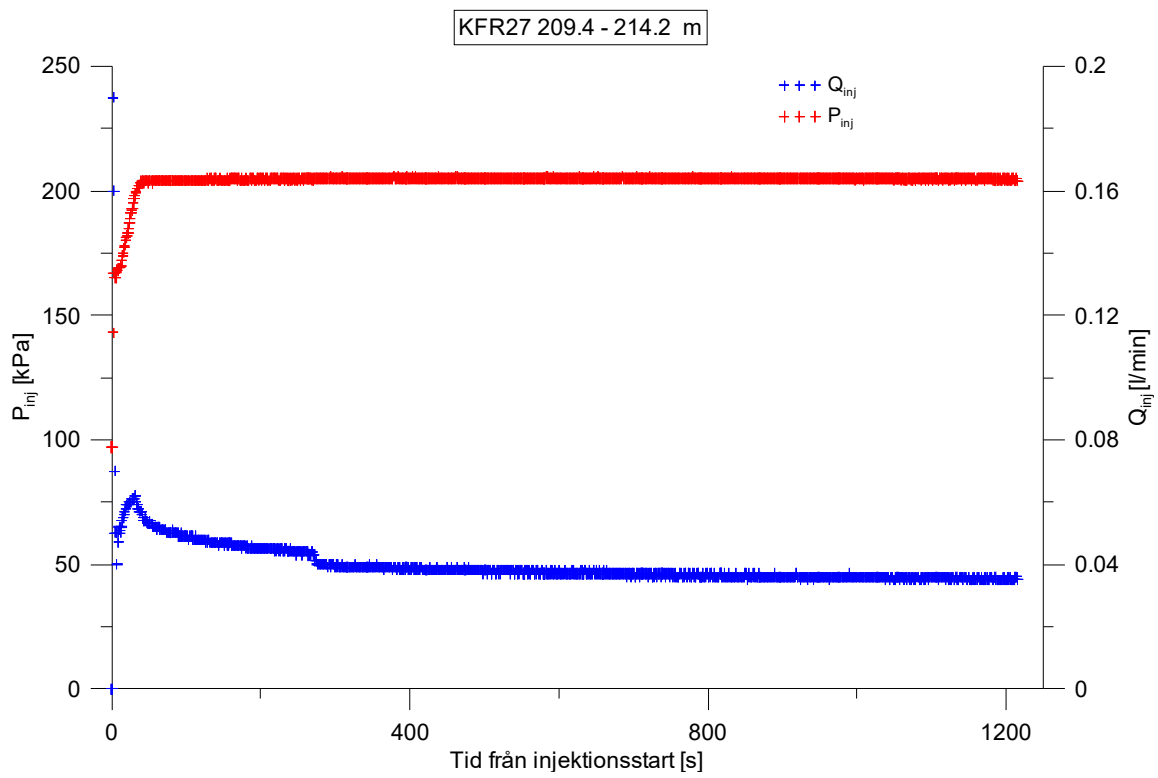


**Figure A2-104.** Linear plot of flow rate ( $Q$ ) and pressure ( $P$ ) versus time from the injection test in section 209.4-214.4 m in borehole KFR27.

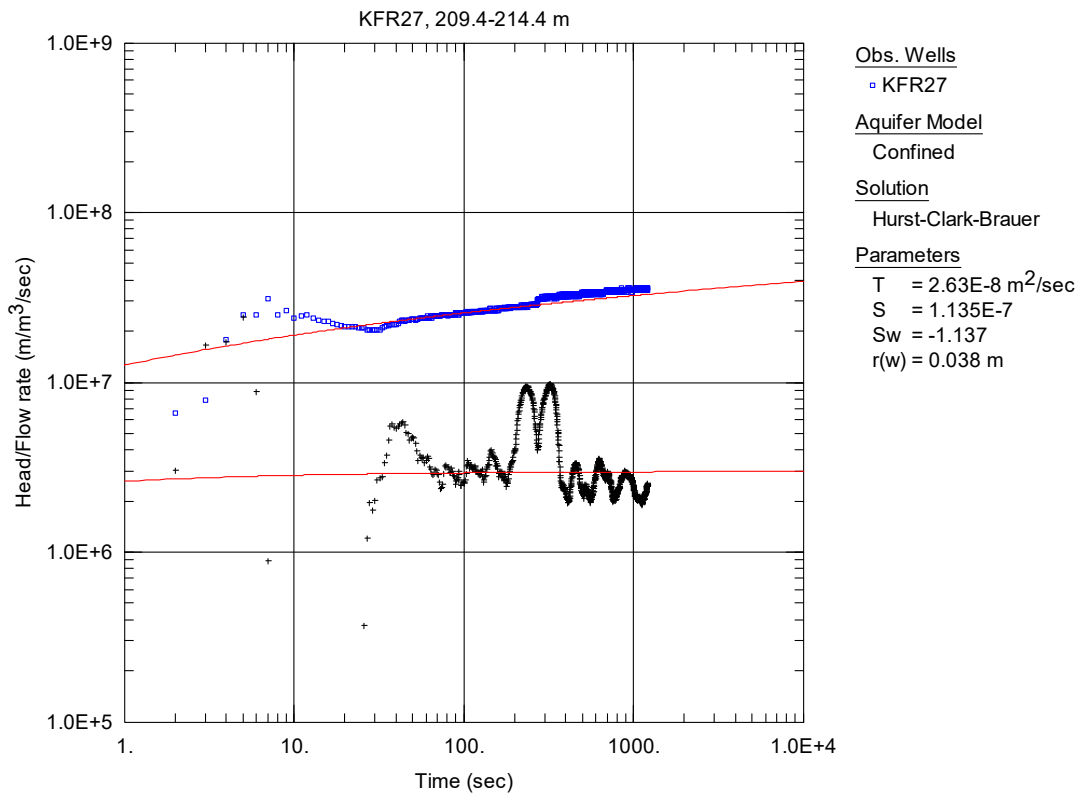


**Figure A2-105.** Log-log plot of head/flow rate ( $\square$ ) and derivative (+) versus time, from the injection test in section 209.4-214.4 m in borehole KFR27.

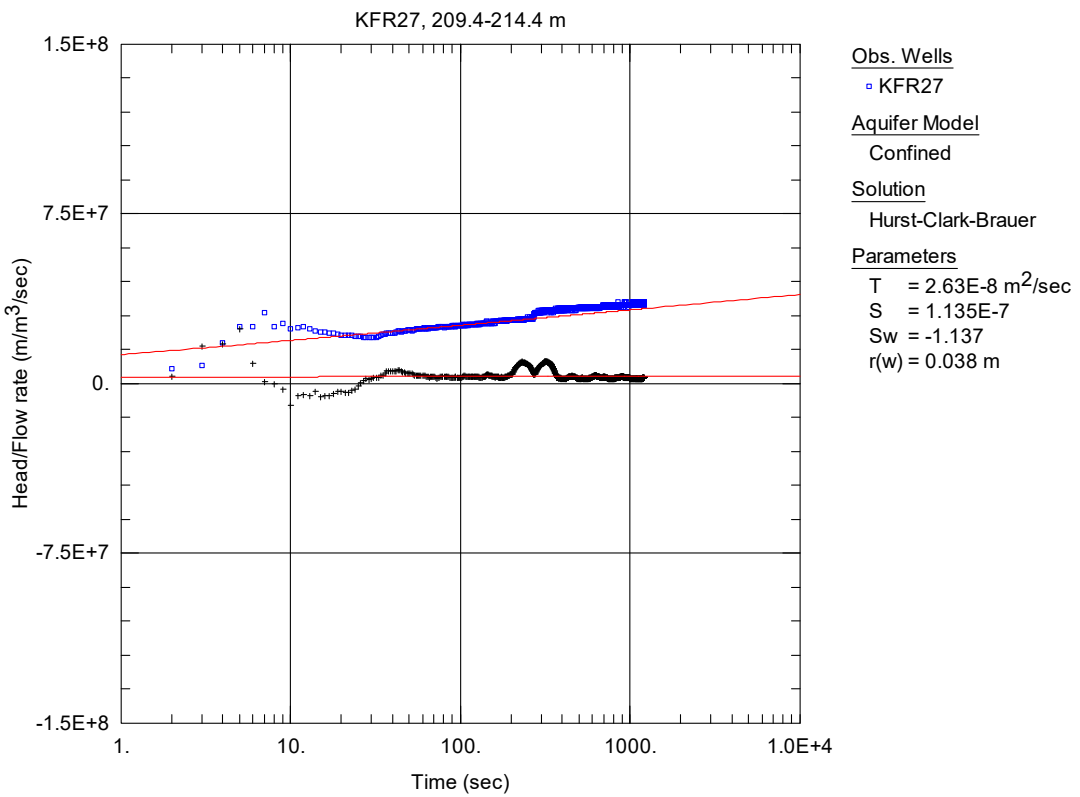


**Figure A2-106.** Lin-log plot of head/flow rate ( $\square$ ) and derivative (+) versus time, from the injection test in section 209.4-214.4 m in borehole KFR27.

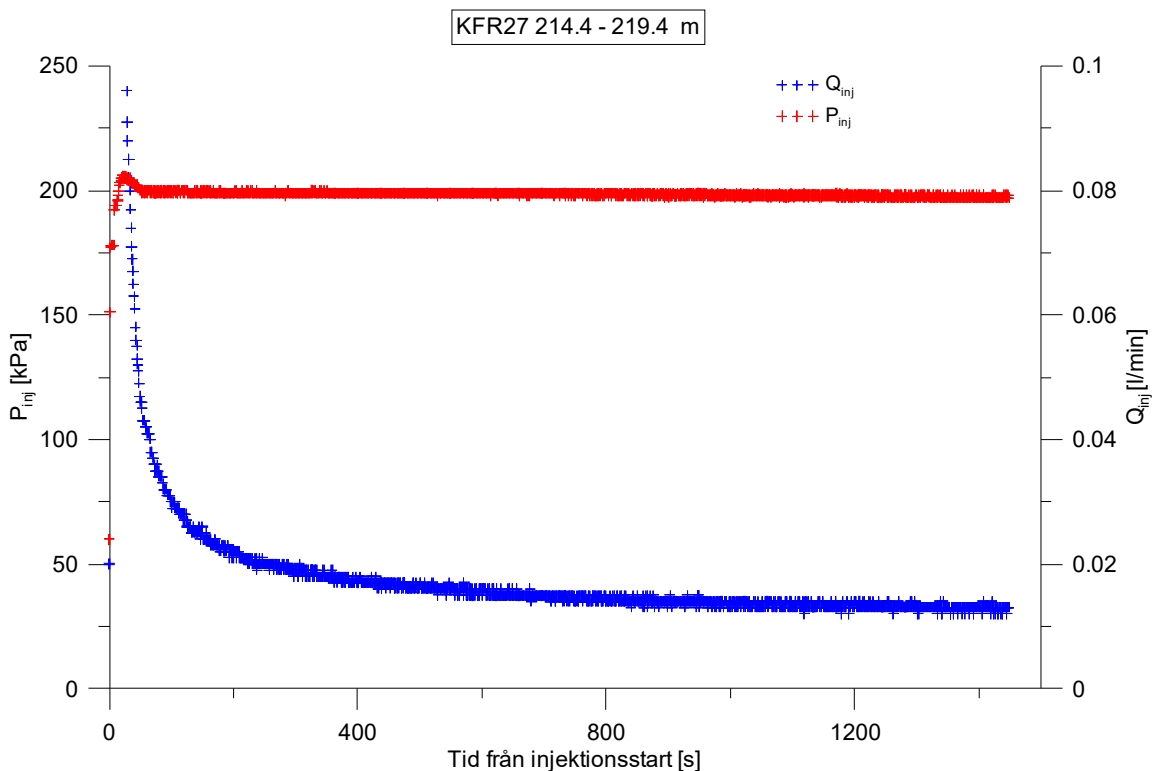


**Figure A2-107.** Linear plot of flow rate ( $Q$ ) and pressure ( $P$ ) versus time from the injection test in section 214.4-219.4 m in borehole KFR27.

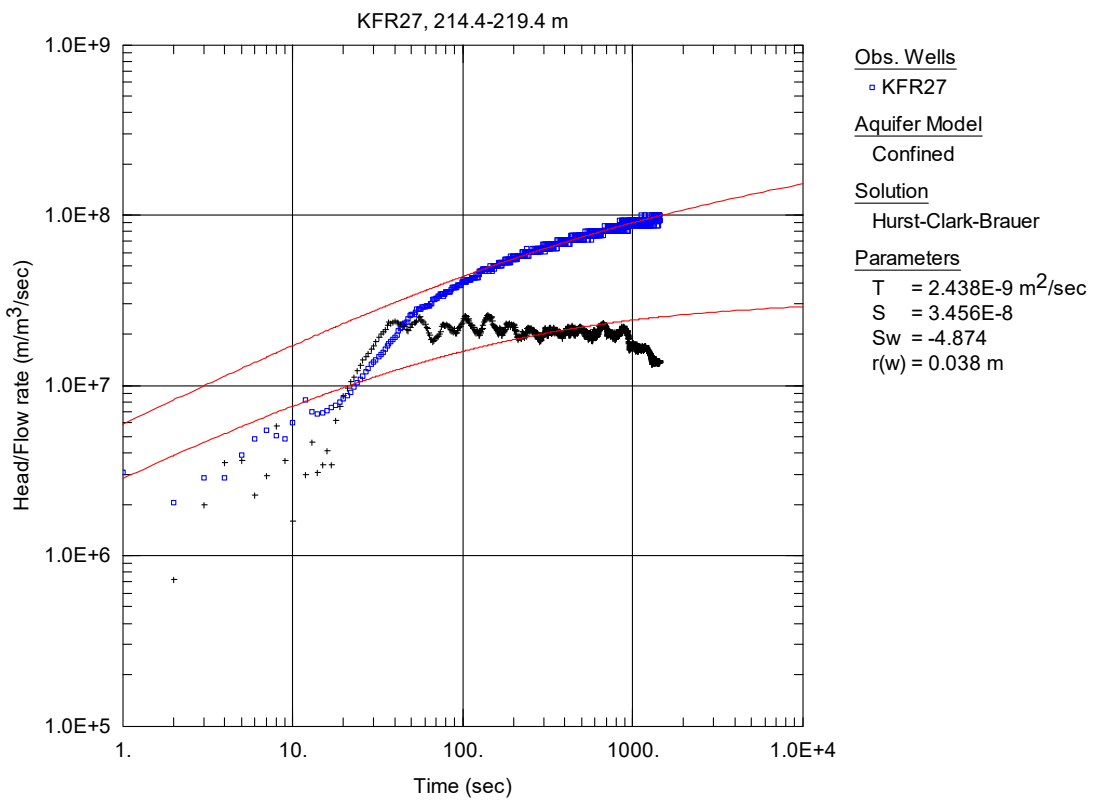


**Figure A2-108.** Log-log plot of head/flow rate (□) and derivative (+) versus time, from the injection test in section 214.4-219.4 m in borehole KFR27.

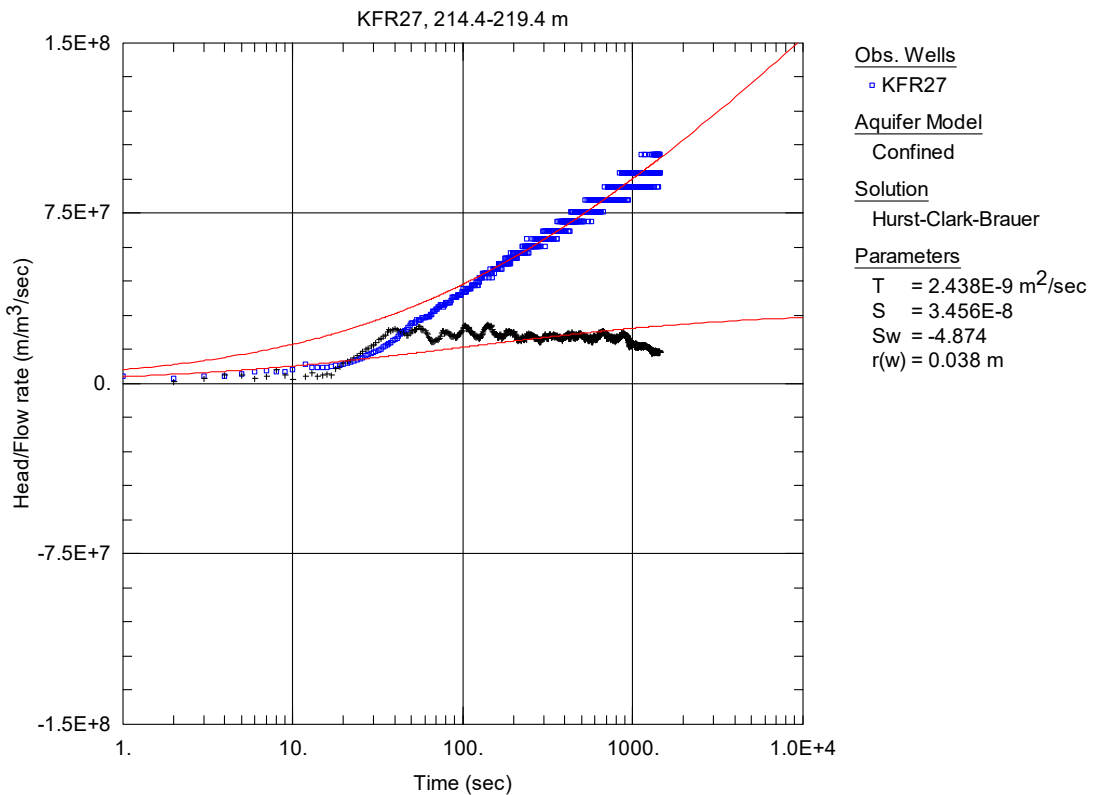


**Figure A2-109.** Lin-log plot of head/flow rate (□) and derivative (+) versus time, from the injection test in section 214.4-219.4 m in borehole KFR27.

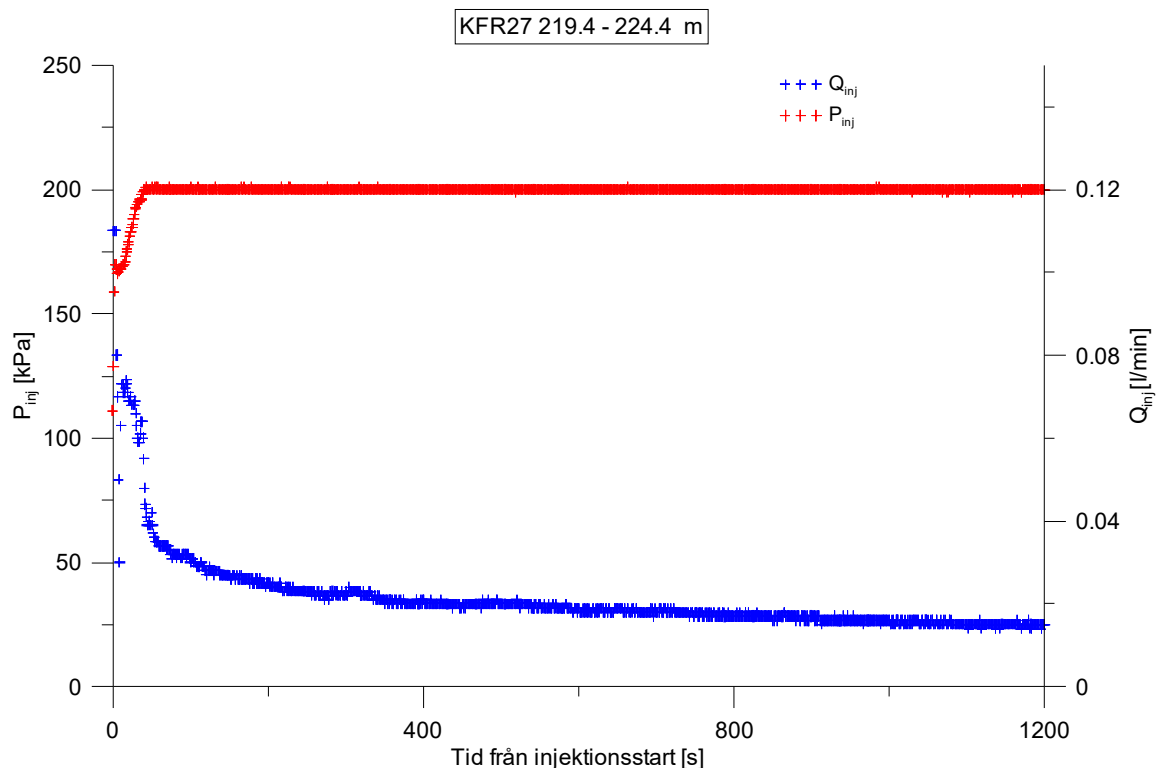


**Figure A2-110.** Linear plot of flow rate ( $Q$ ) and pressure ( $P$ ) versus time from the injection test in section 219.4-224.4 m in borehole KFR27.

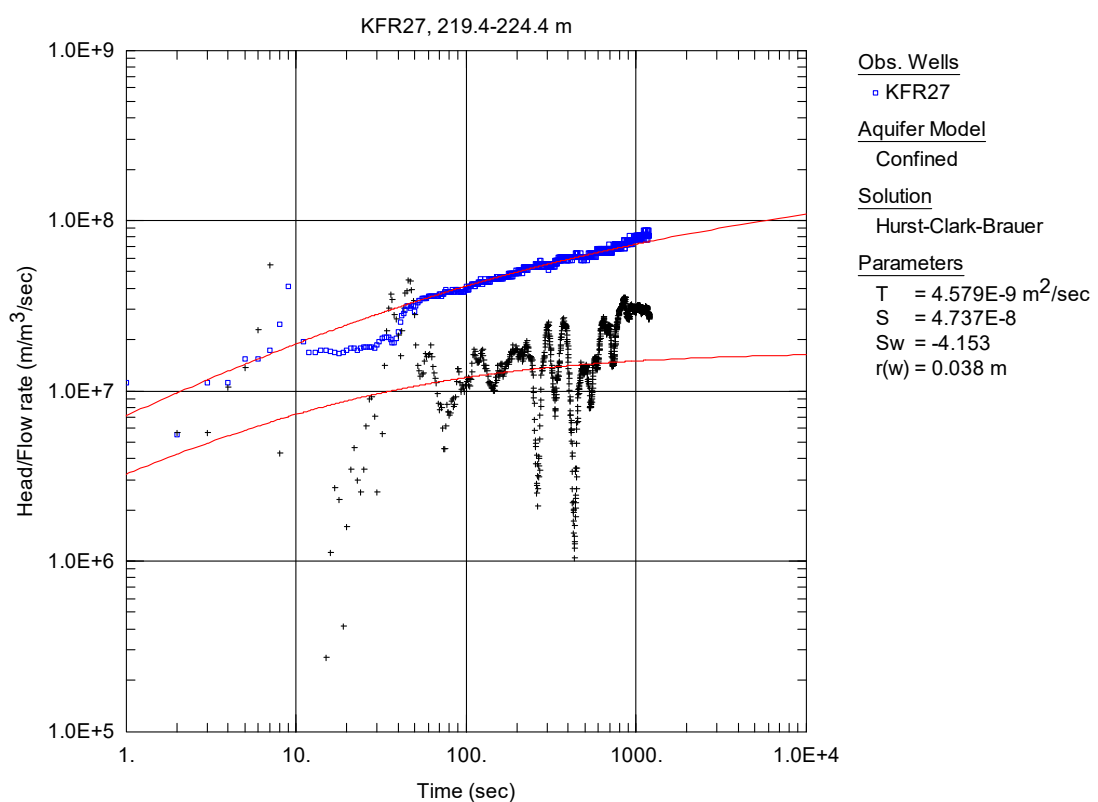


**Figure A2-111.** Log-log plot of head/flow rate ( $\square$ ) and derivative (+) versus time, from the injection test in section 219.4-224.4 m in borehole KFR27.

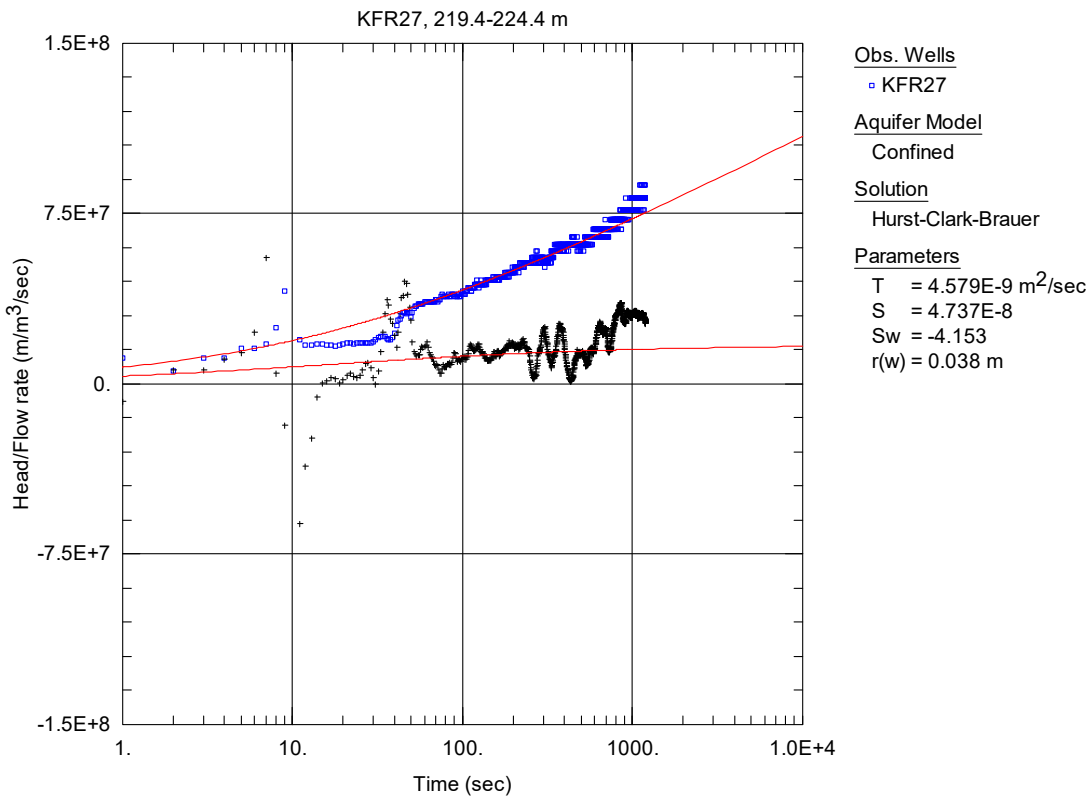


**Figure A2-112.** Lin-log plot of head/flow rate (□) and derivative (+) versus time, from the injection test in section 219.4-224.4 m in borehole KFR27.

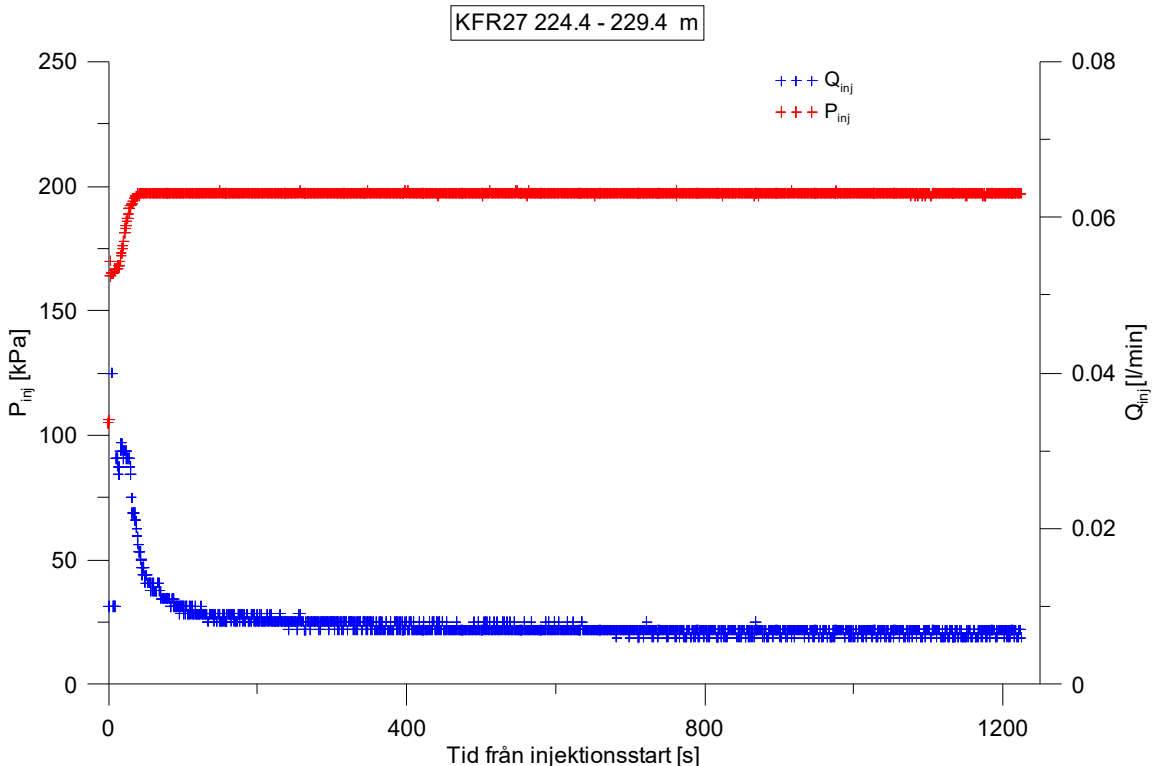


**Figure A2-113.** Linear plot of flow rate ( $Q$ ) and pressure ( $P$ ) versus time from the injection test in section 224.4-229.4 m in borehole KFR27.

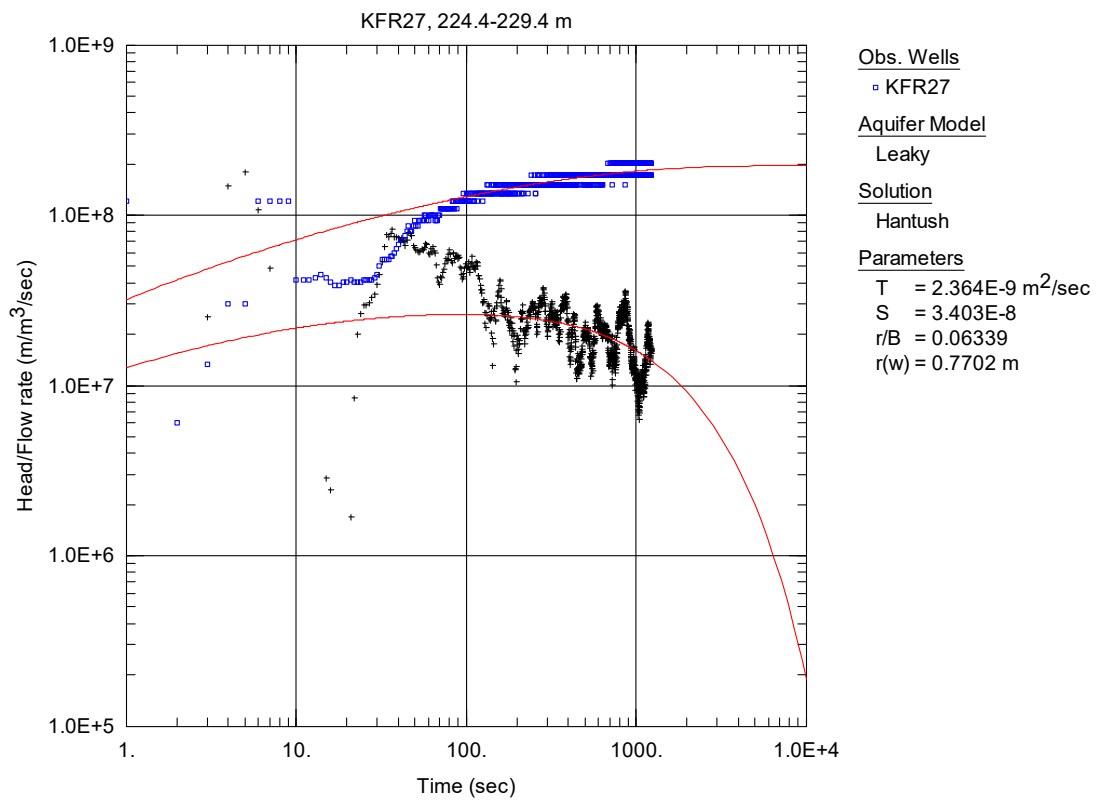


**Figure A2-114.** Log-log plot of head/flow rate (□) and derivative (+) versus time, from the injection test in section 224.4-229.4 m in borehole KFR27.

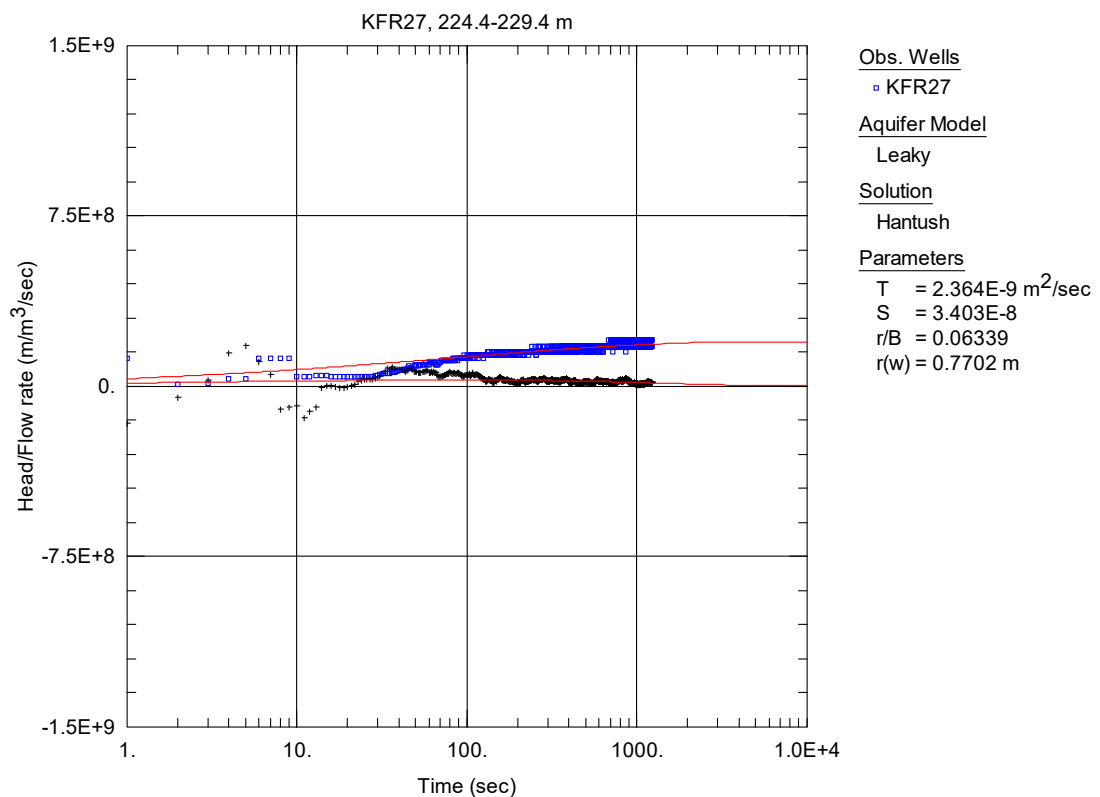


**Figure A2-115.** Lin-log plot of head/flow rate (□) and derivative (+) versus time, from the injection test in section 224.4-229.4 m in borehole KFR27.

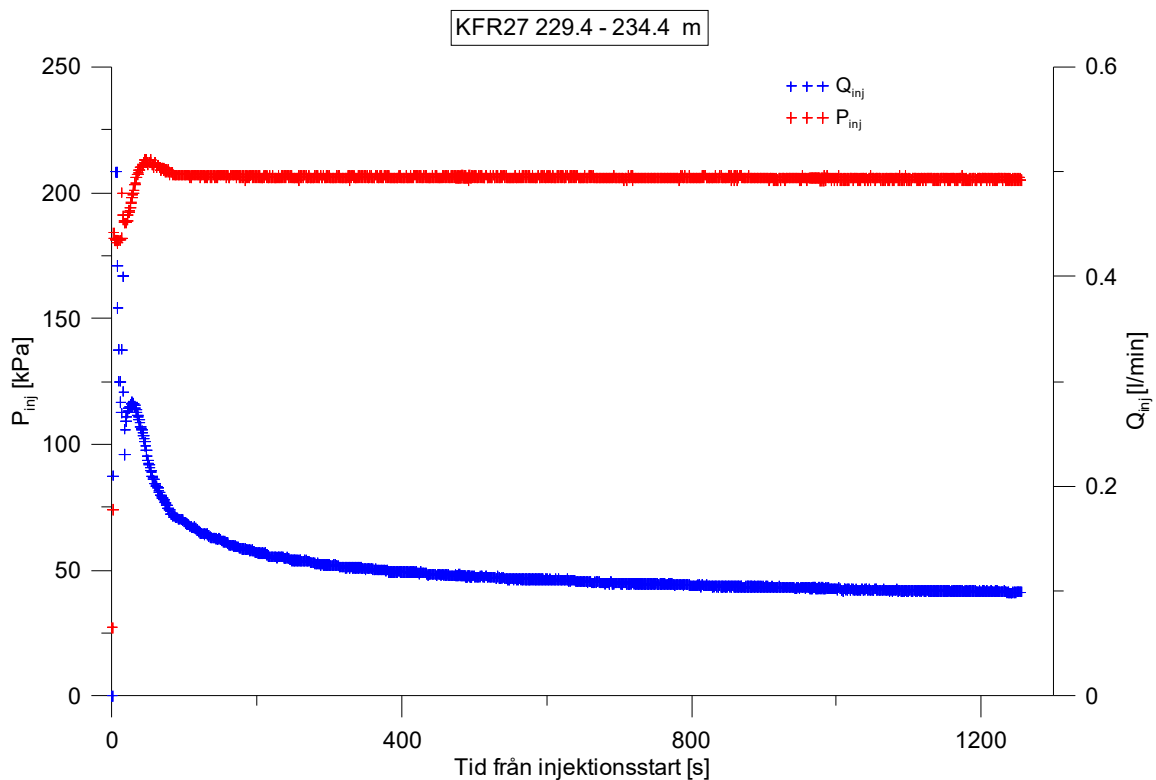


**Figure A2-116.** Linear plot of flow rate ( $Q$ ) and pressure ( $P$ ) versus time from the injection test in section 229.4-234.4 m in borehole KFR27.

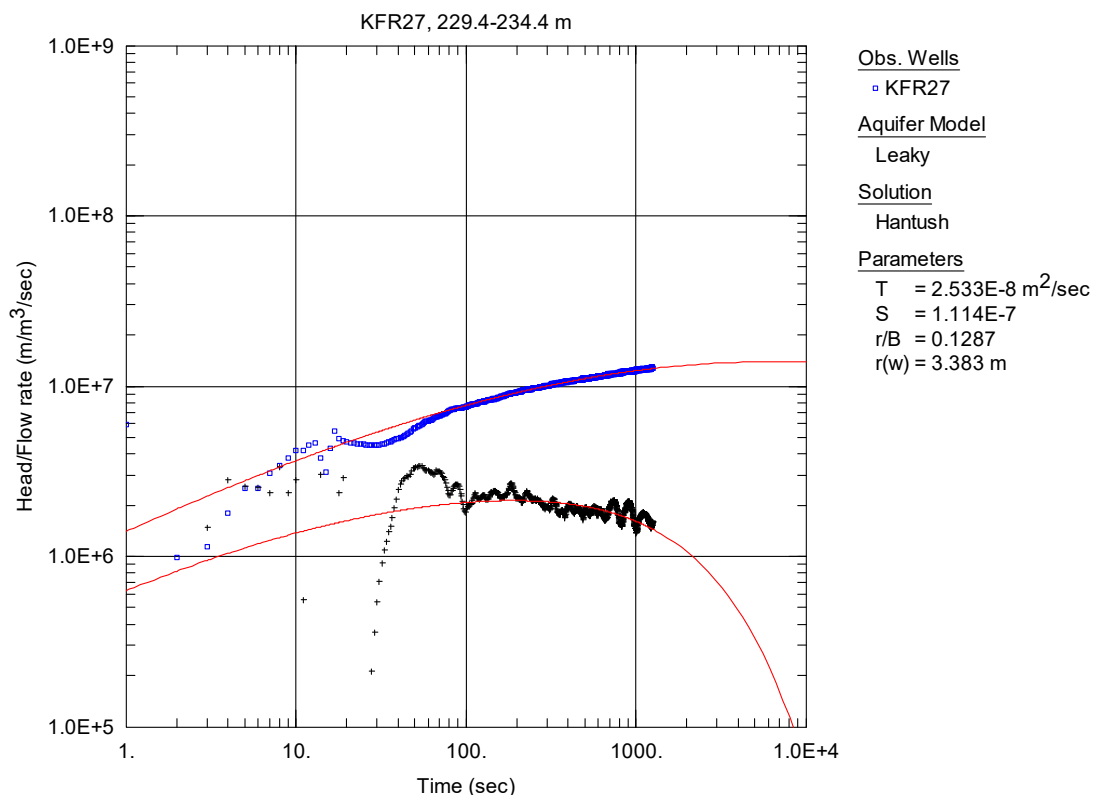


**Figure A2-117.** Log-log plot of head/flow rate ( $\square$ ) and derivative (+) versus time, from the injection test in section 229.4-234.4 m in borehole KFR27.

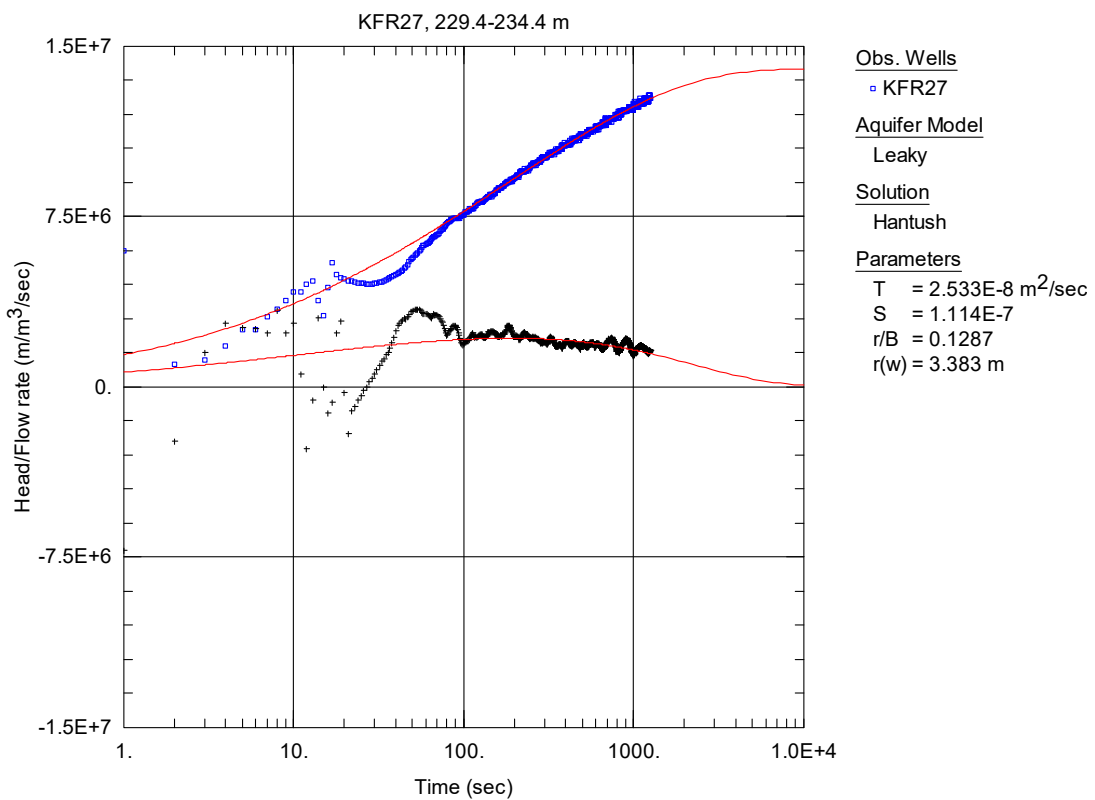


**Figure A2-118.** Lin-log plot of head/flow rate ( $\square$ ) and derivative (+) versus time, from the injection test in section 229.4-234.4 m in borehole KFR27.

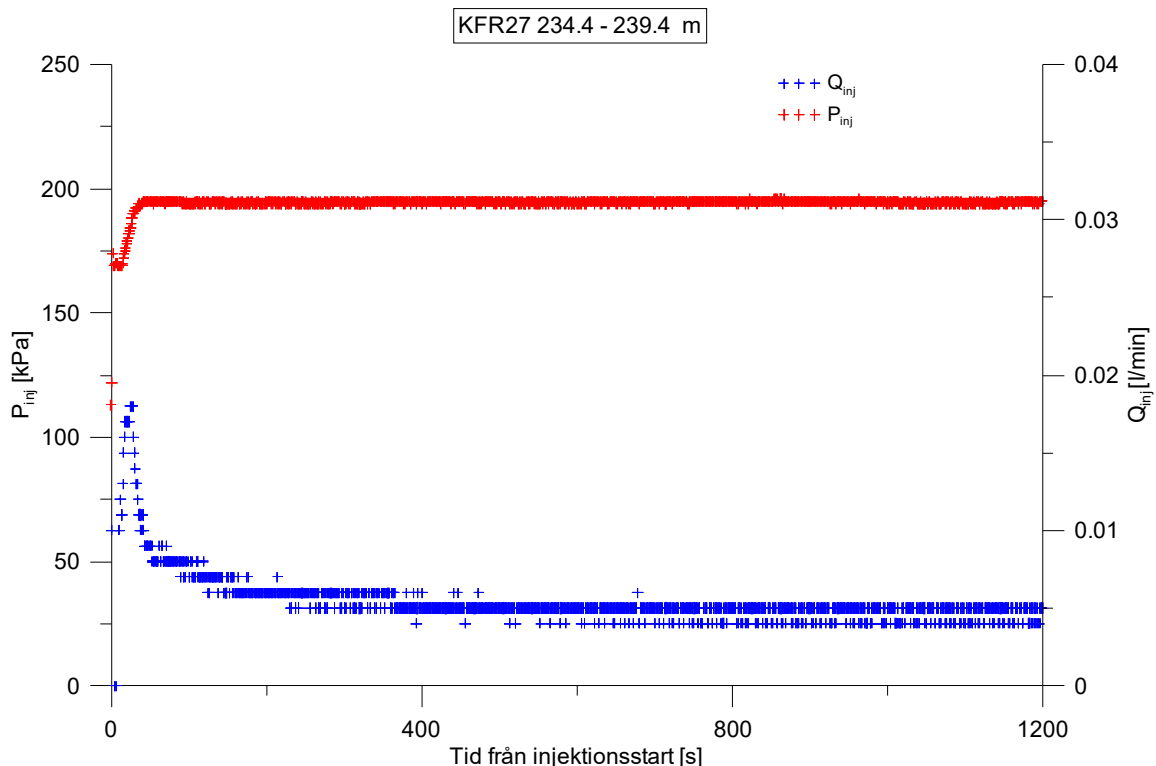


**Figure A2-119.** Linear plot of flow rate ( $Q$ ) and pressure ( $P$ ) versus time from the injection test in section 234.4-239.4 m in borehole KFR27.

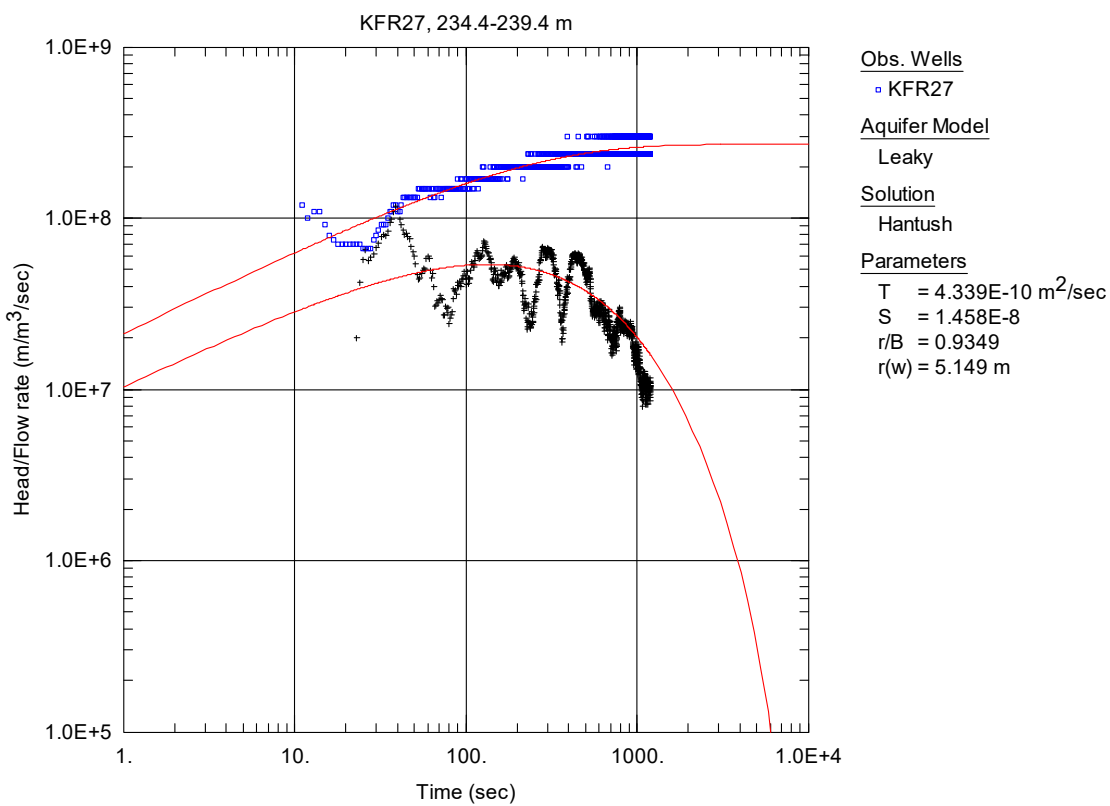


**Figure A2-120.** Log-log plot of head/flow rate (□) and derivative (+) versus time, from the injection test in section 234.4-239.4 m in borehole KFR27.

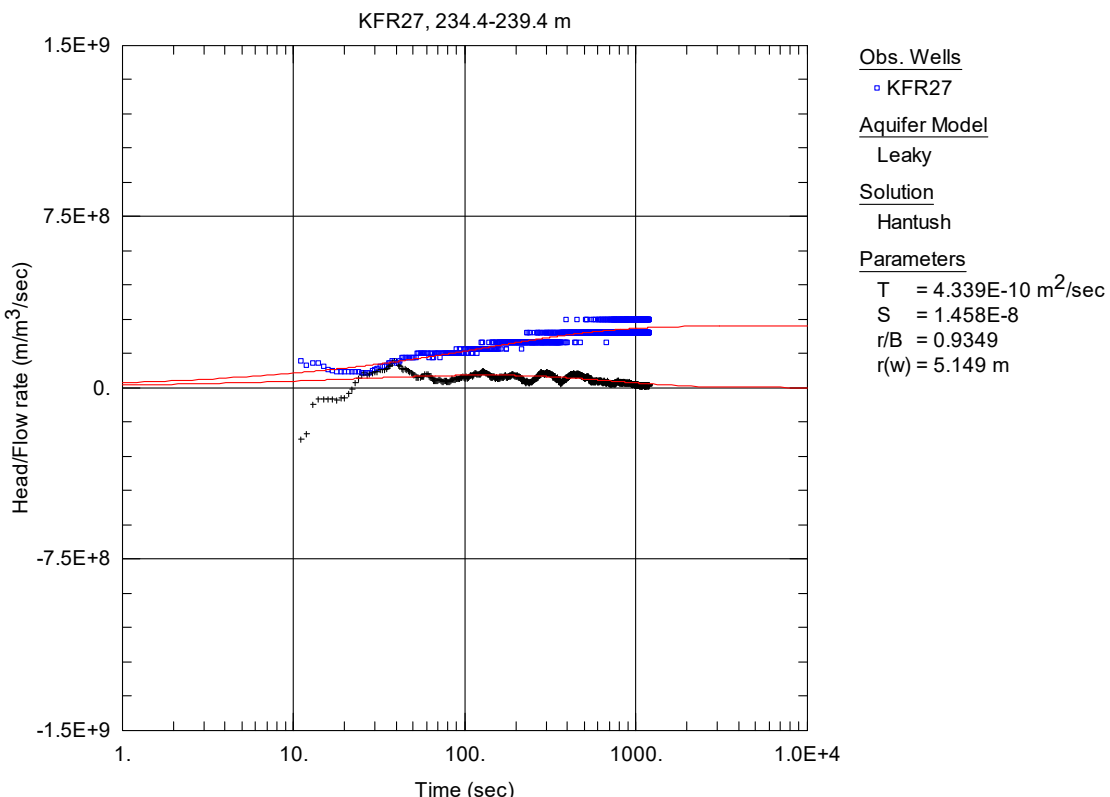


**Figure A2-121.** Lin-log plot of head/flow rate (□) and derivative (+) versus time, from the injection test in section 234.4-239.4 m in borehole KFR27.

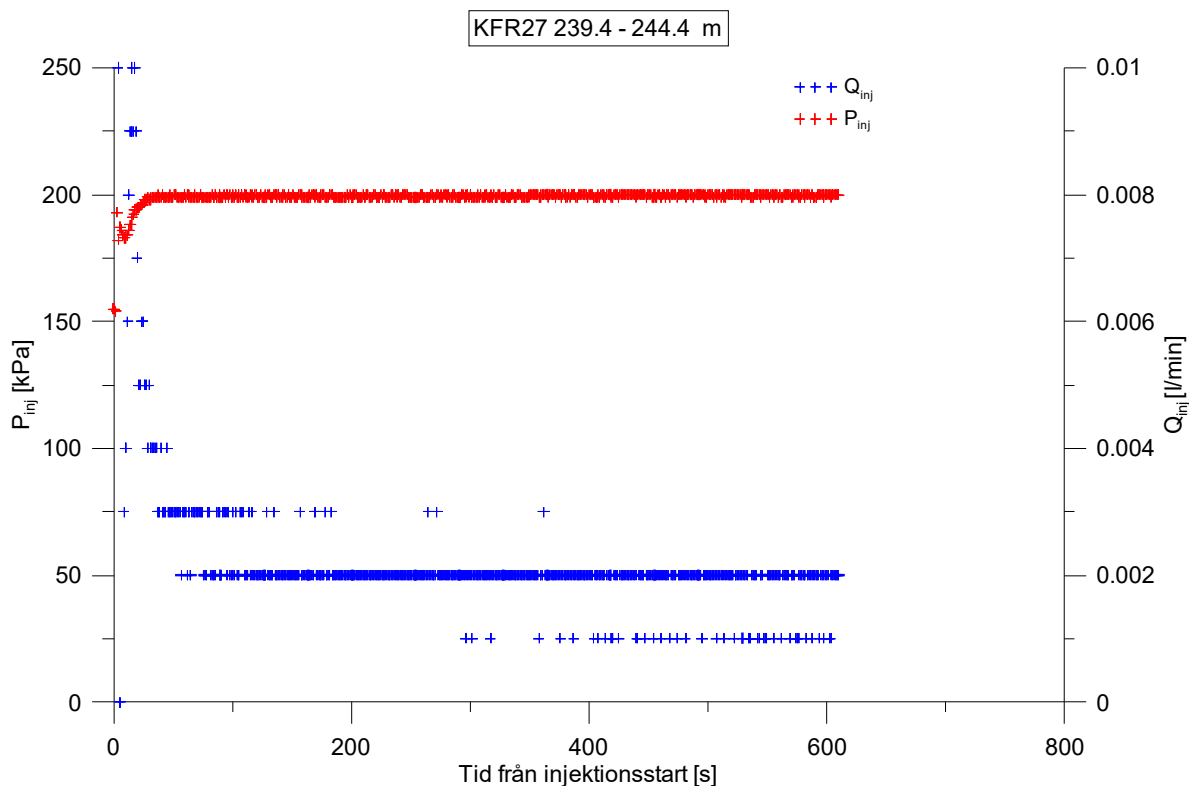


**Figure A2-122.** Linear plot of flow rate ( $Q$ ) and pressure ( $P$ ) versus time from the injection test in section 239.4-244.4 m in borehole KFR27.

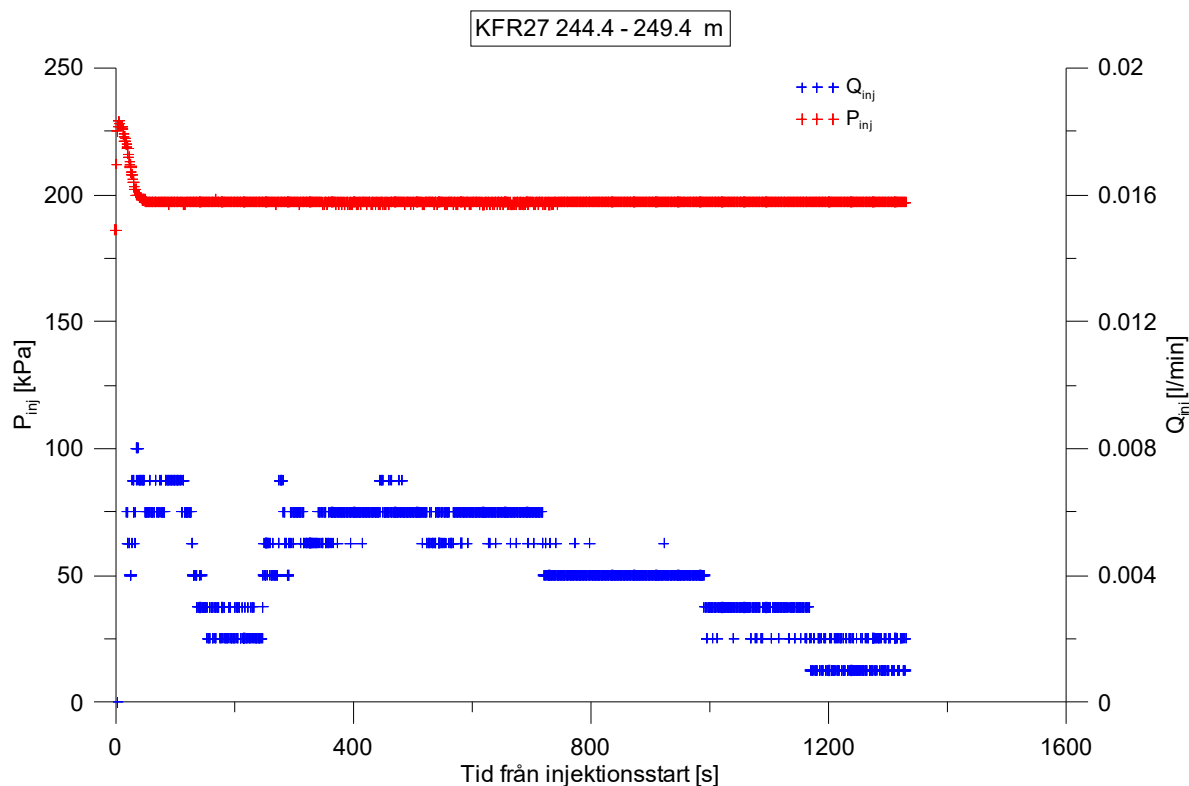


**Figure A2-123.** Linear plot of flow rate ( $Q$ ) and pressure ( $P$ ) versus time from the injection test in section 244.4-249.4 m in borehole KFR27.

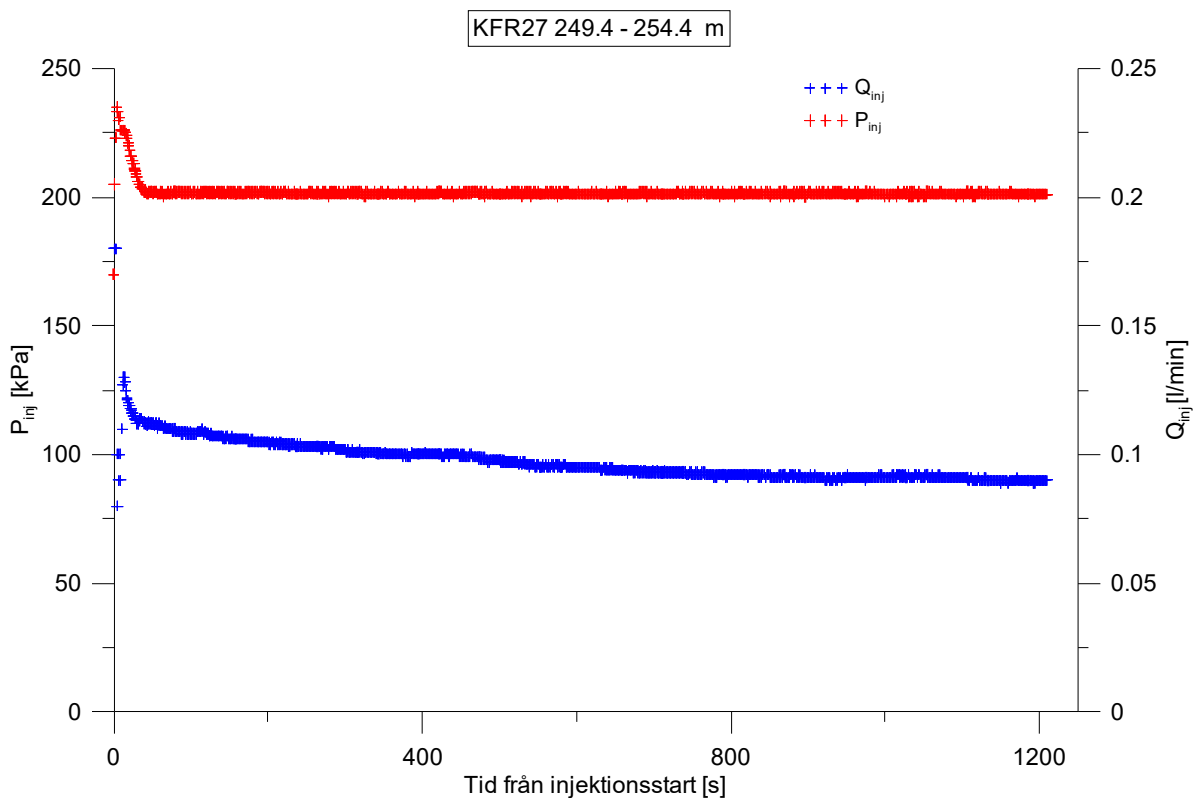


**Figure A2-124.** Linear plot of flow rate ( $Q$ ) and pressure ( $P$ ) versus time from the injection test in section 249.4-254.4 m in borehole KFR27.

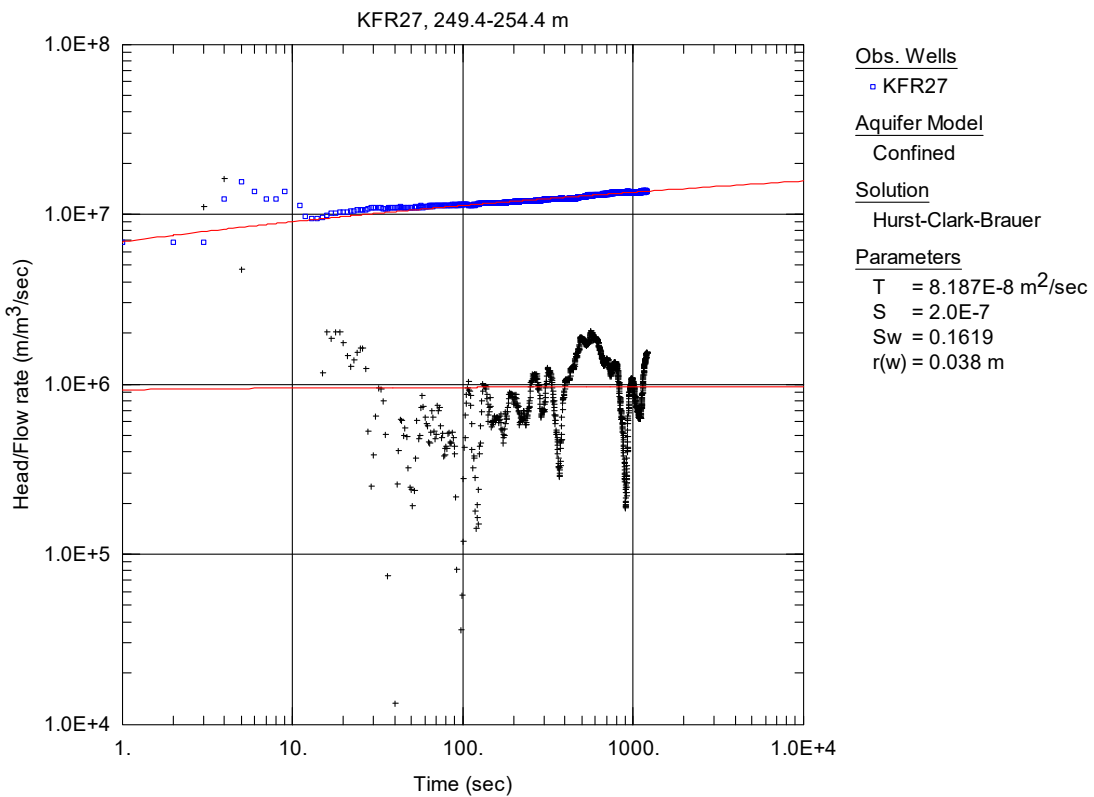


**Figure A2-125.** Log-log plot of head/flow rate (□) and derivative (+) versus time, from the injection test in section 249.4-254.4 m in borehole KFR27.

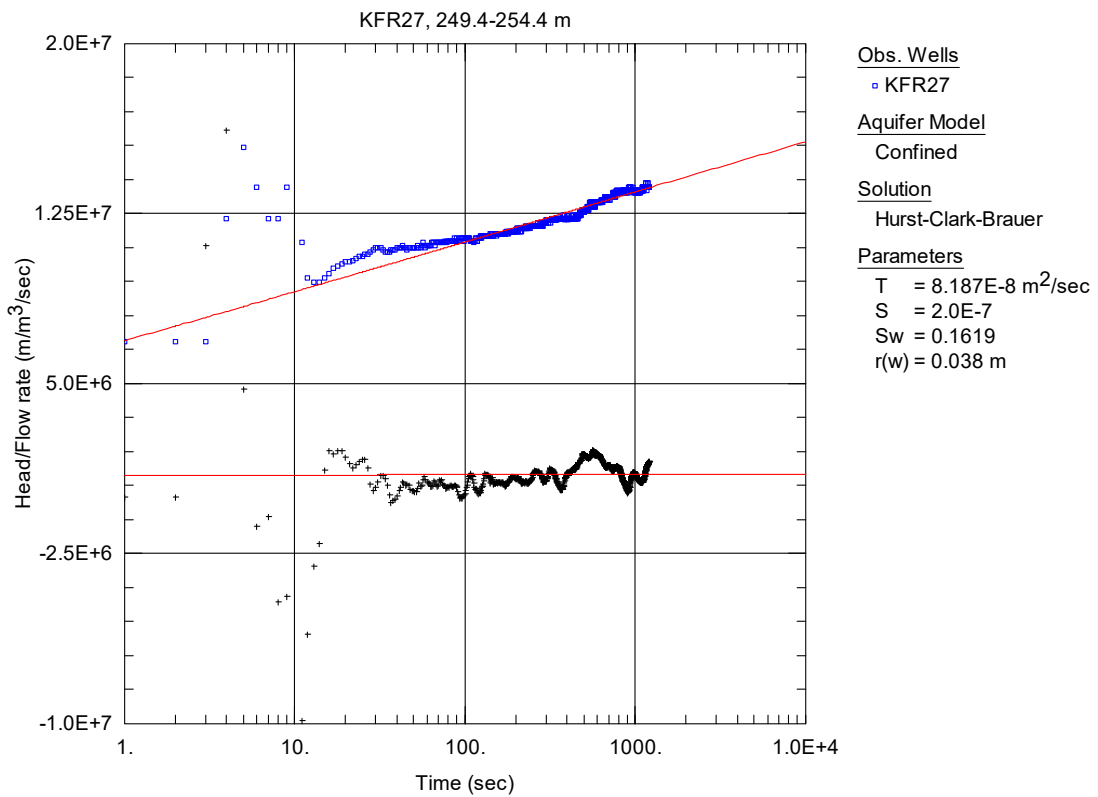


**Figure A2-126.** Lin-log plot of head/flow rate (□) and derivative (+) versus time, from the injection test in section 249.4-254.4 m in borehole KFR27.

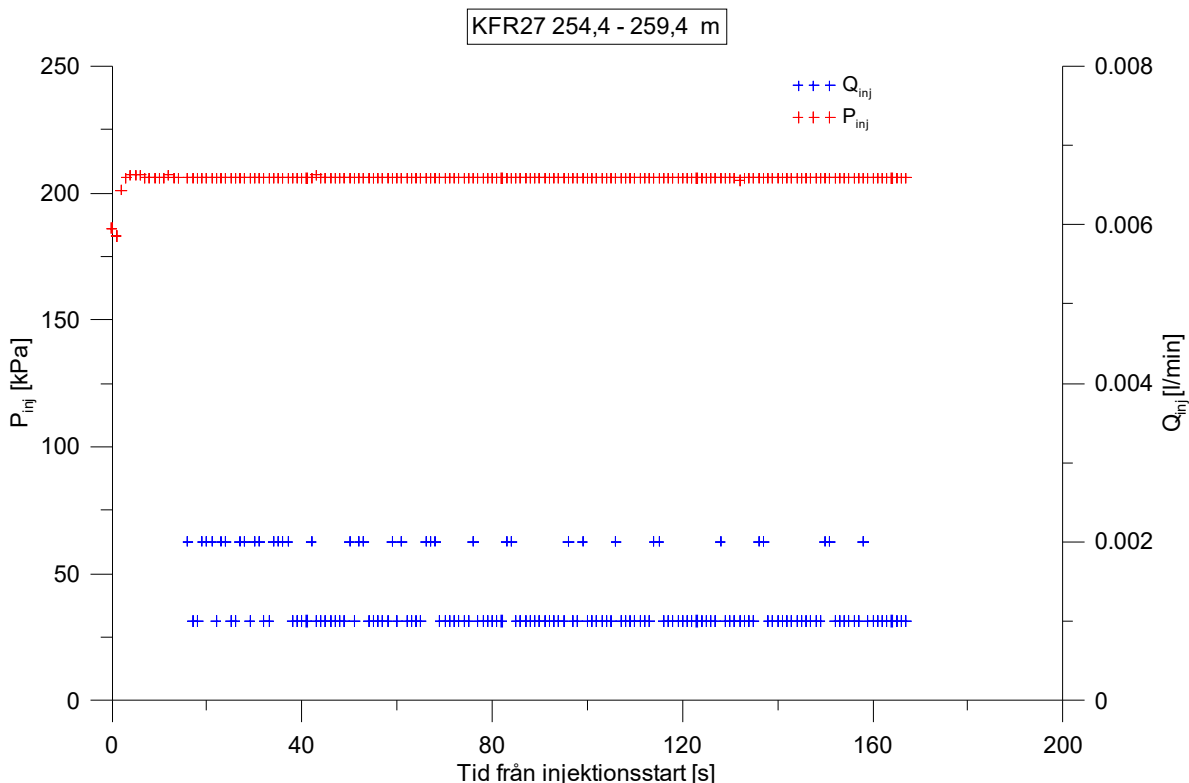


**Figure A2-127.** Linear plot of flow rate ( $Q$ ) and pressure ( $P$ ) versus time from the injection test in section 254.4-259.4 m in borehole KFR27.

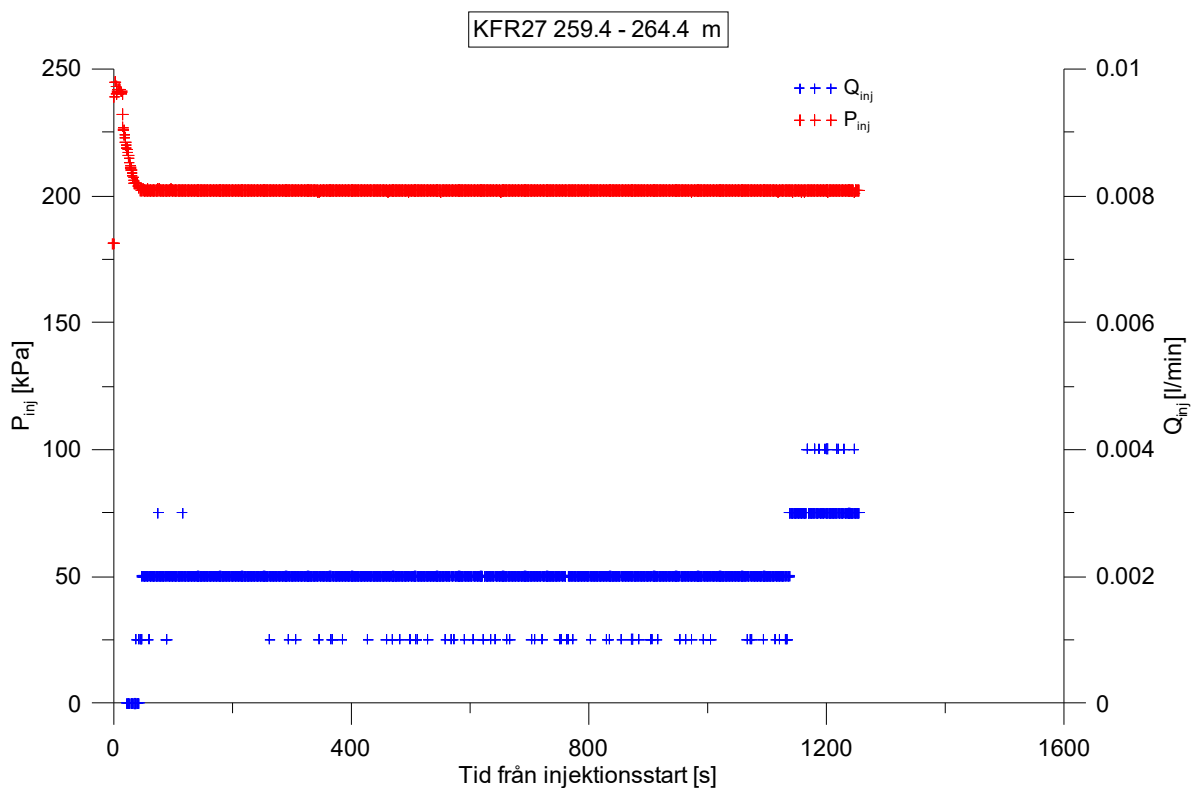


**Figure A2-128.** Linear plot of flow rate ( $Q$ ) and pressure ( $P$ ) versus time from the injection test in section 259.4-264.4 m in borehole KFR27.

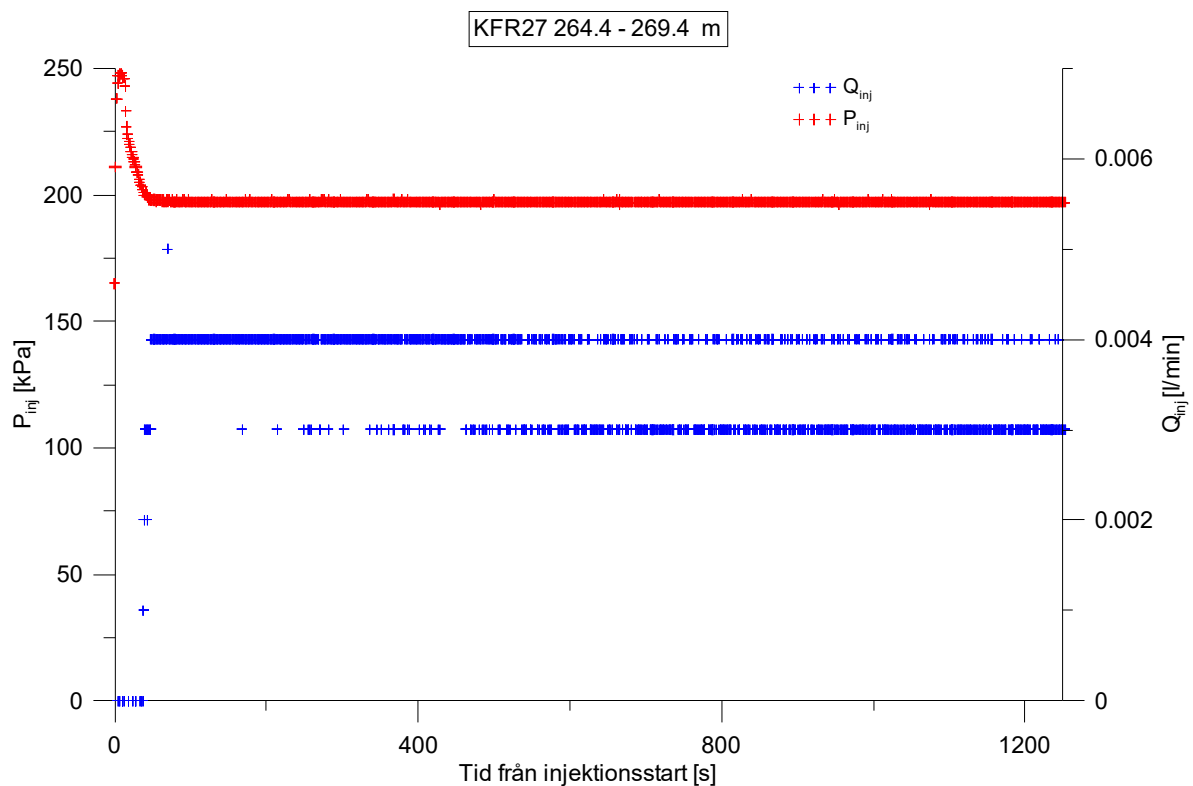


**Figure A2-129.** Linear plot of flow rate ( $Q$ ) and pressure ( $P$ ) versus time from the injection test in section 264.4-269.4 m in borehole KFR27.

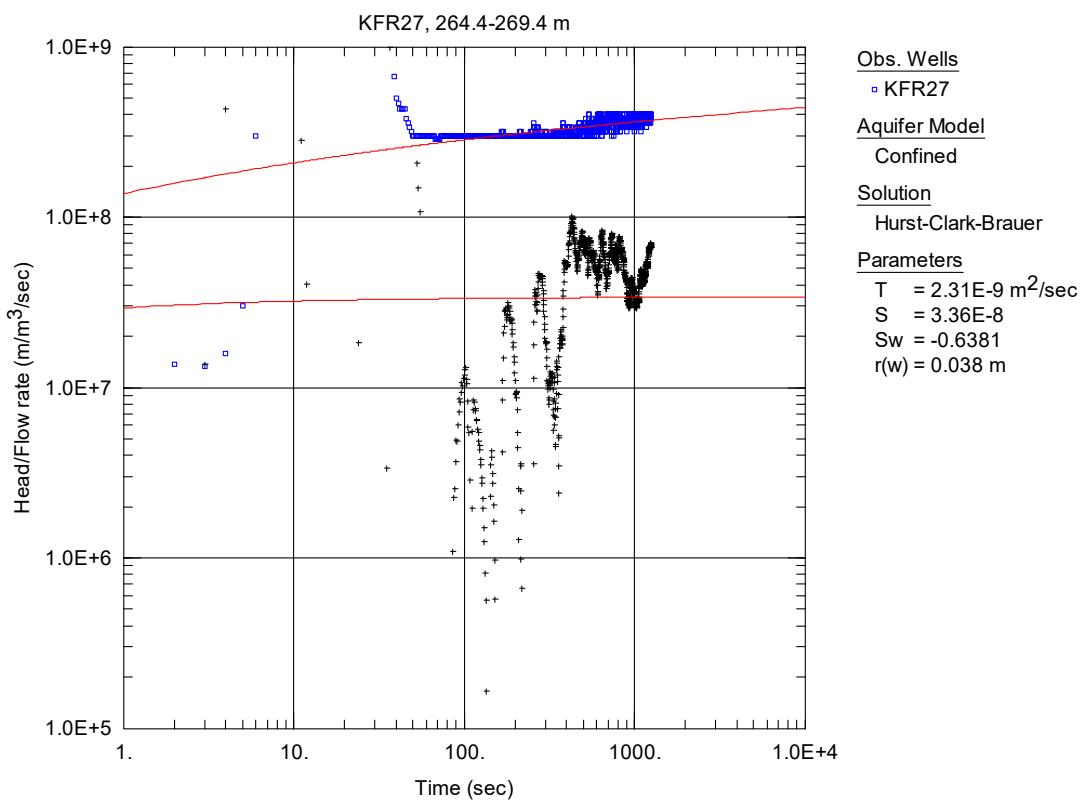


**Figure A2-130.** Log-log plot of head/flow rate (□) and derivative (+) versus time, from the injection test in section 264.4-269.4 m in borehole KFR27.

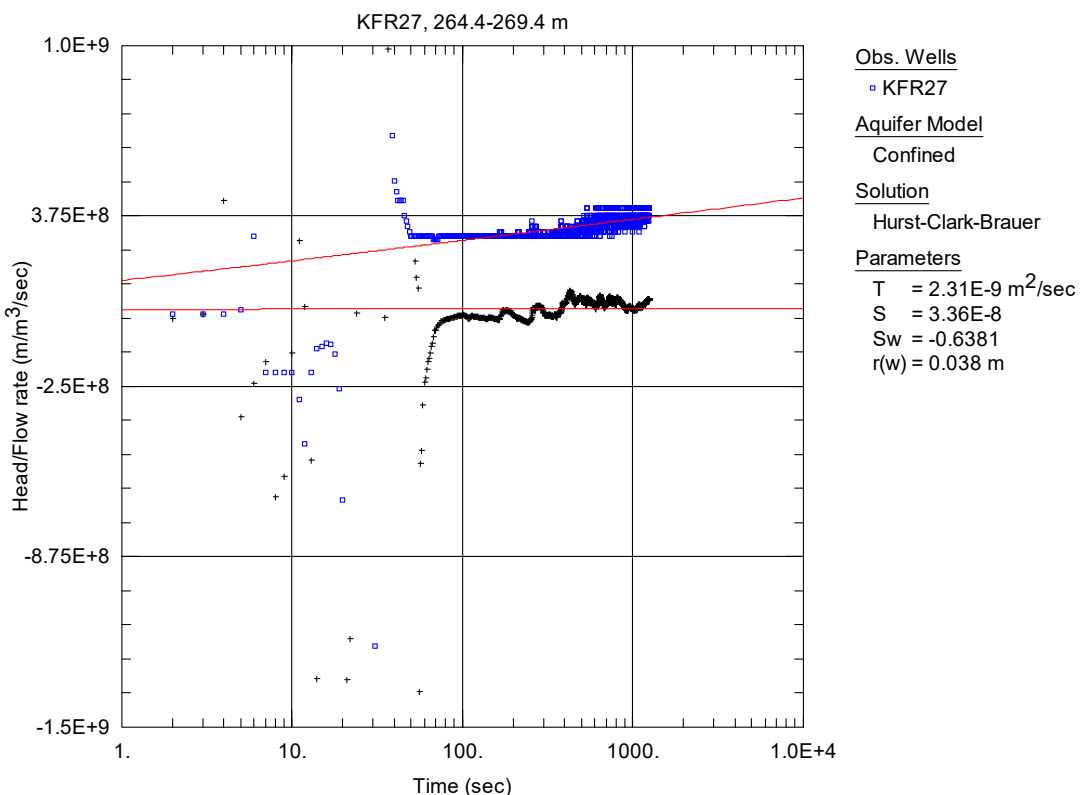


**Figure A2-131.** Lin-log plot of head/flow rate (□) and derivative (+) versus time, from the injection test in section 264.4-269.4 m in borehole KFR27.

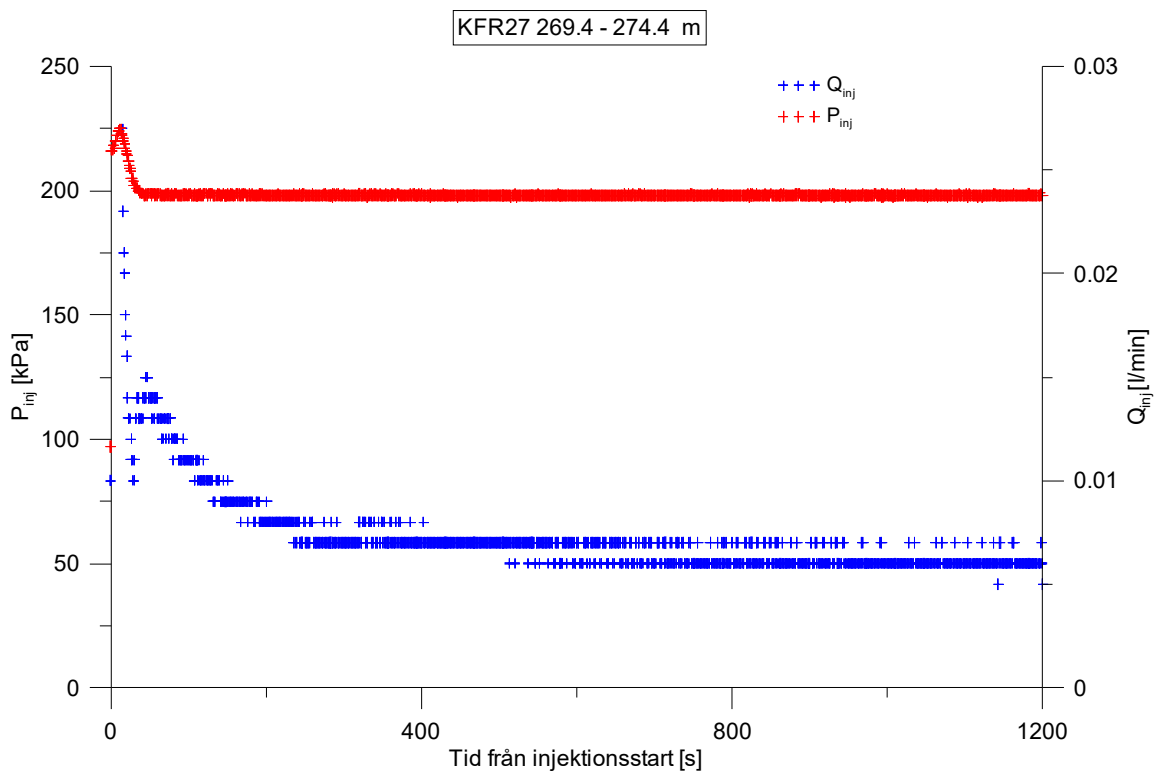


**Figure A2-132.** Linear plot of flow rate ( $Q$ ) and pressure ( $P$ ) versus time from the injection test in section 269.4-274.4 m in borehole KFR27.

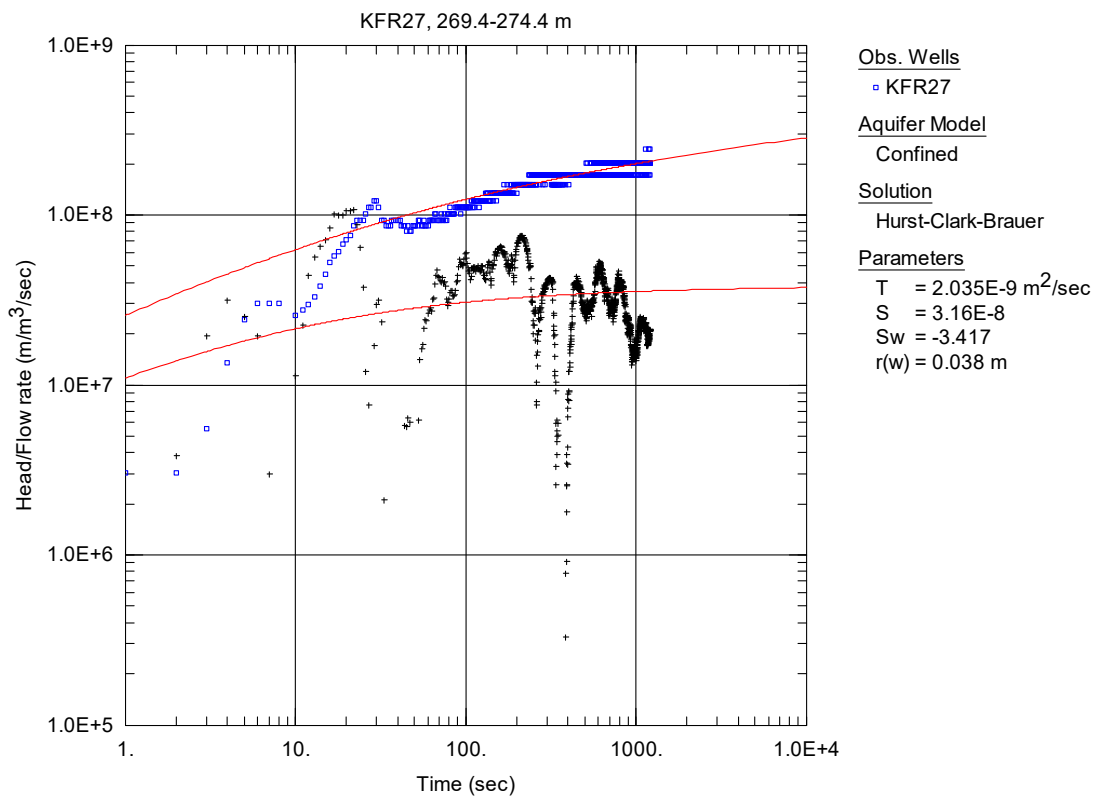


**Figure A2-133.** Log-log plot of head/flow rate (□) and derivative (+) versus time, from the injection test in section 269.4-274.4 m in borehole KFR27.

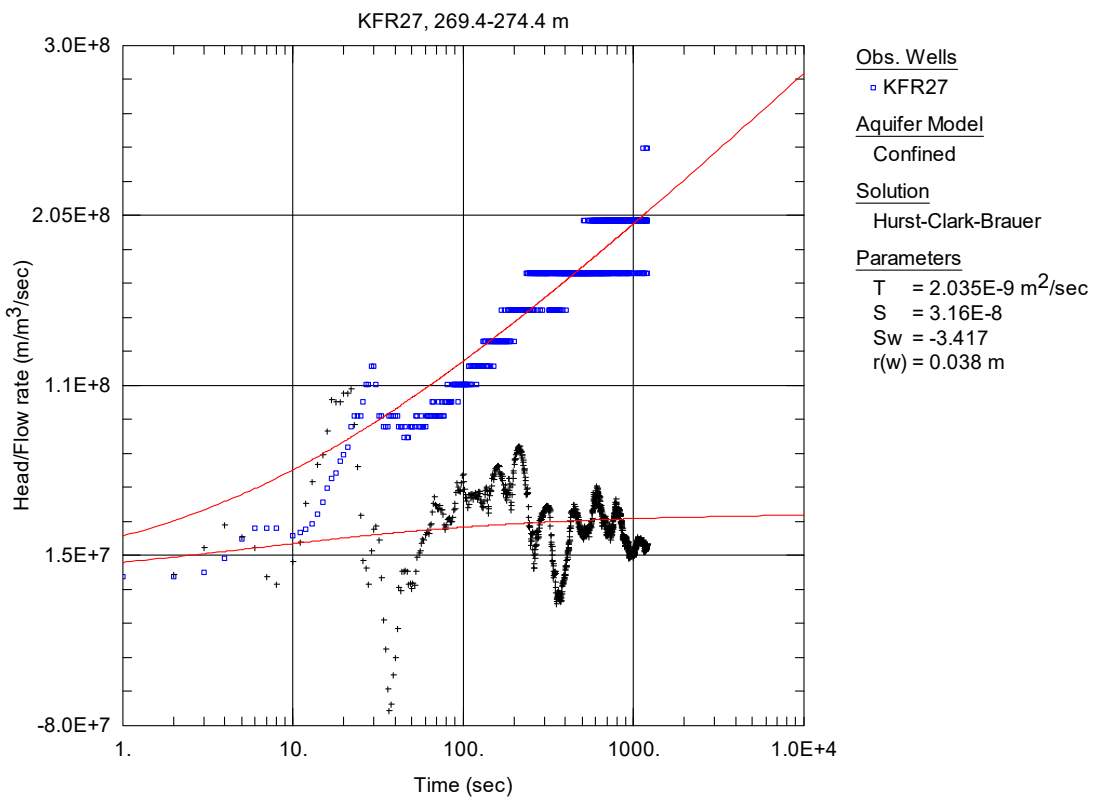


**Figure A2-134.** Lin-log plot of head/flow rate ( $\square$ ) and derivative (+) versus time, from the injection test in section 269.4-274.4 m in borehole KFR27.

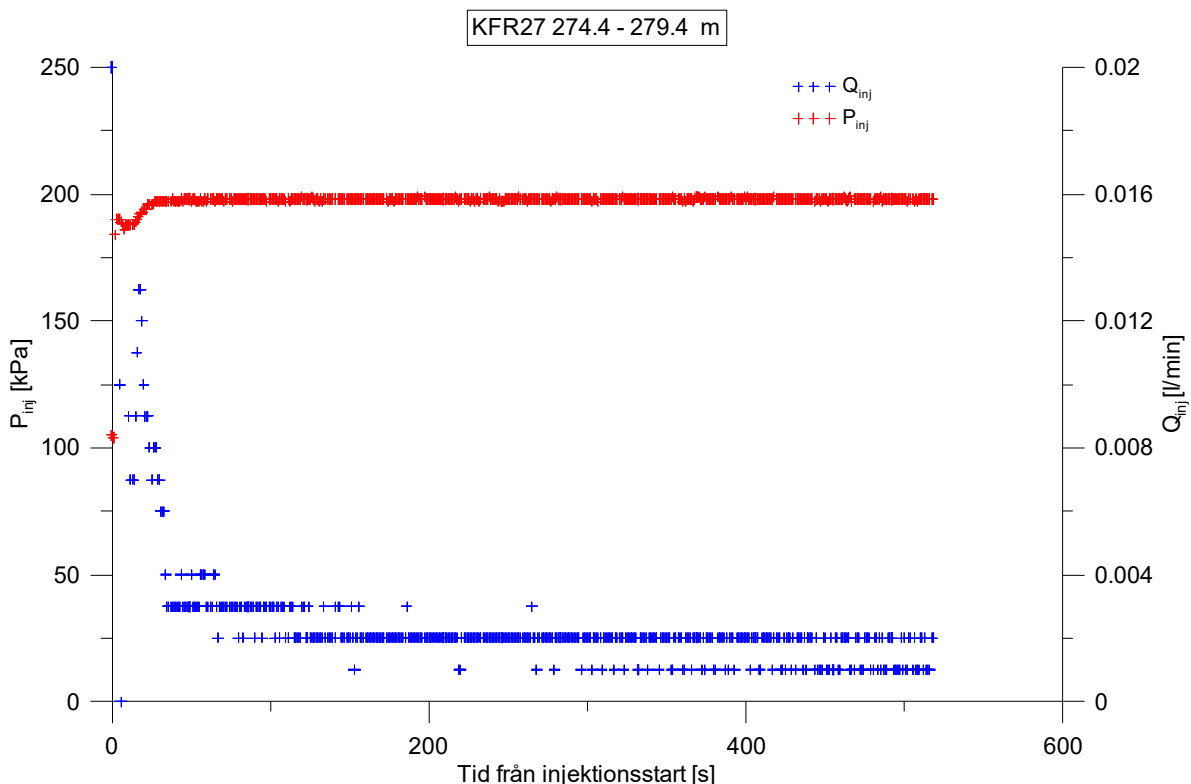


**Figure A2-135.** Linear plot of flow rate ( $Q$ ) and pressure ( $P$ ) versus time from the injection test in section 274.4-279.4 m in borehole KFR27.

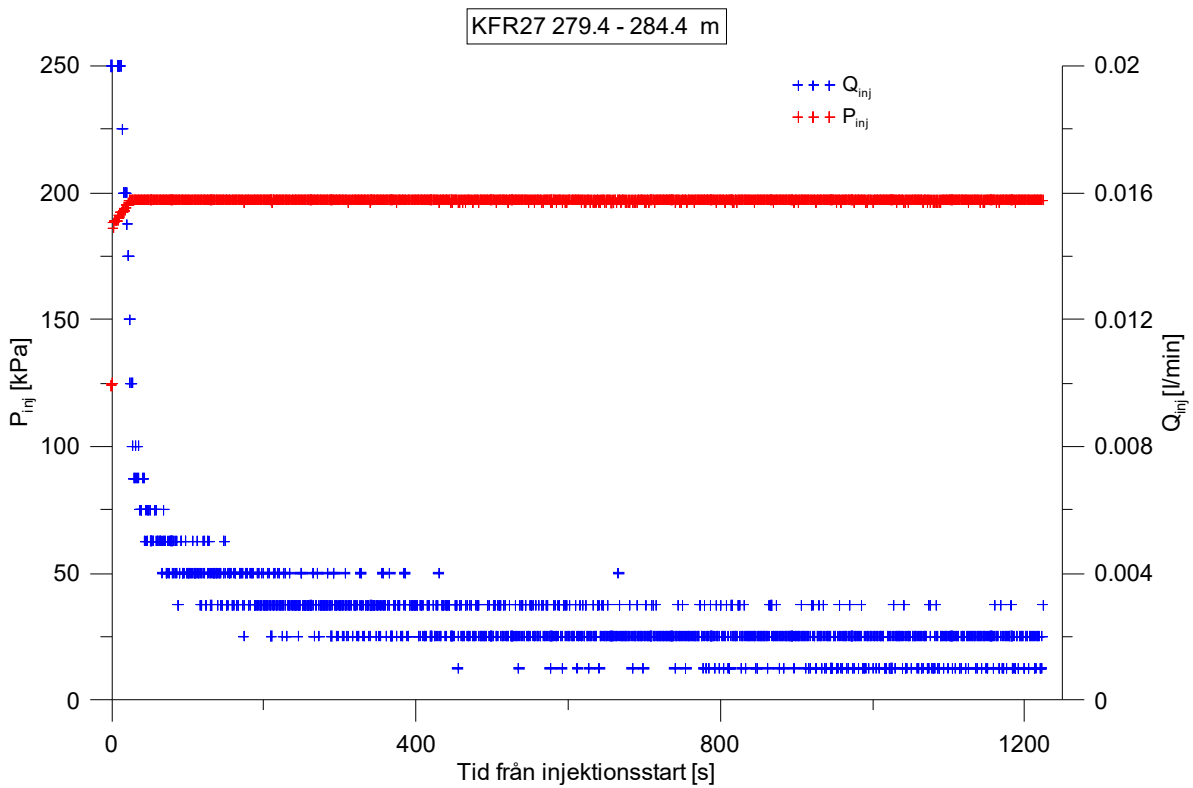


**Figure A2-136.** Linear plot of flow rate ( $Q$ ) and pressure ( $P$ ) versus time from the injection test in section 279.4-284.4 m in borehole KFR27.

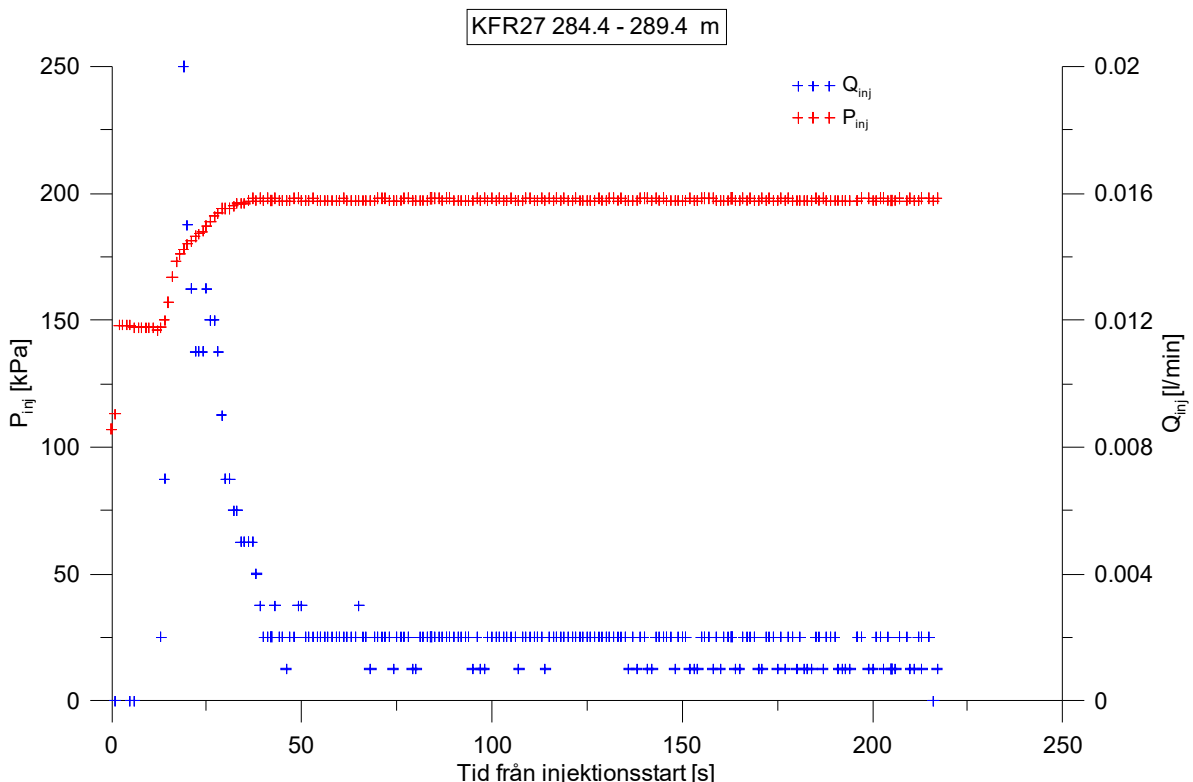


**Figure A2-137.** Linear plot of flow rate ( $Q$ ) and pressure ( $P$ ) versus time from the injection test in section 284.4-289.4 m in borehole KFR27.

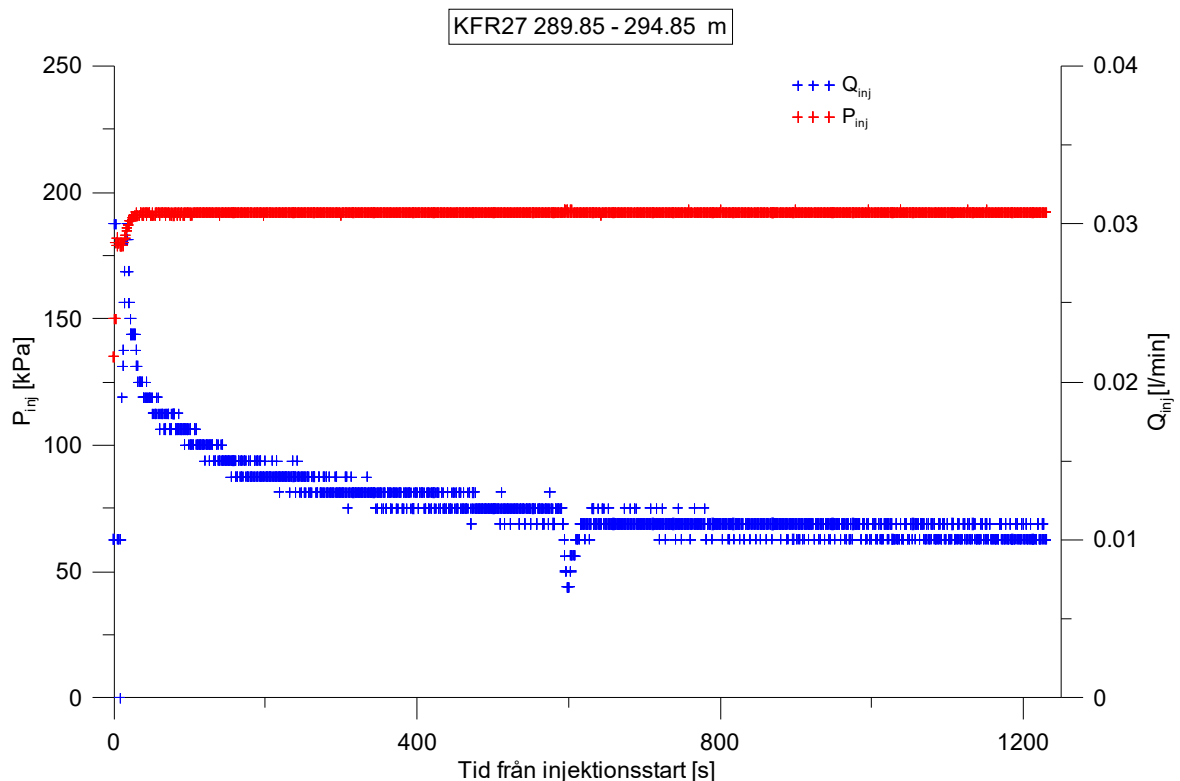


**Figure A2-138.** Linear plot of flow rate ( $Q$ ) and pressure ( $P$ ) versus time from the injection test in section 289.4-294.4 m in borehole KFR27.

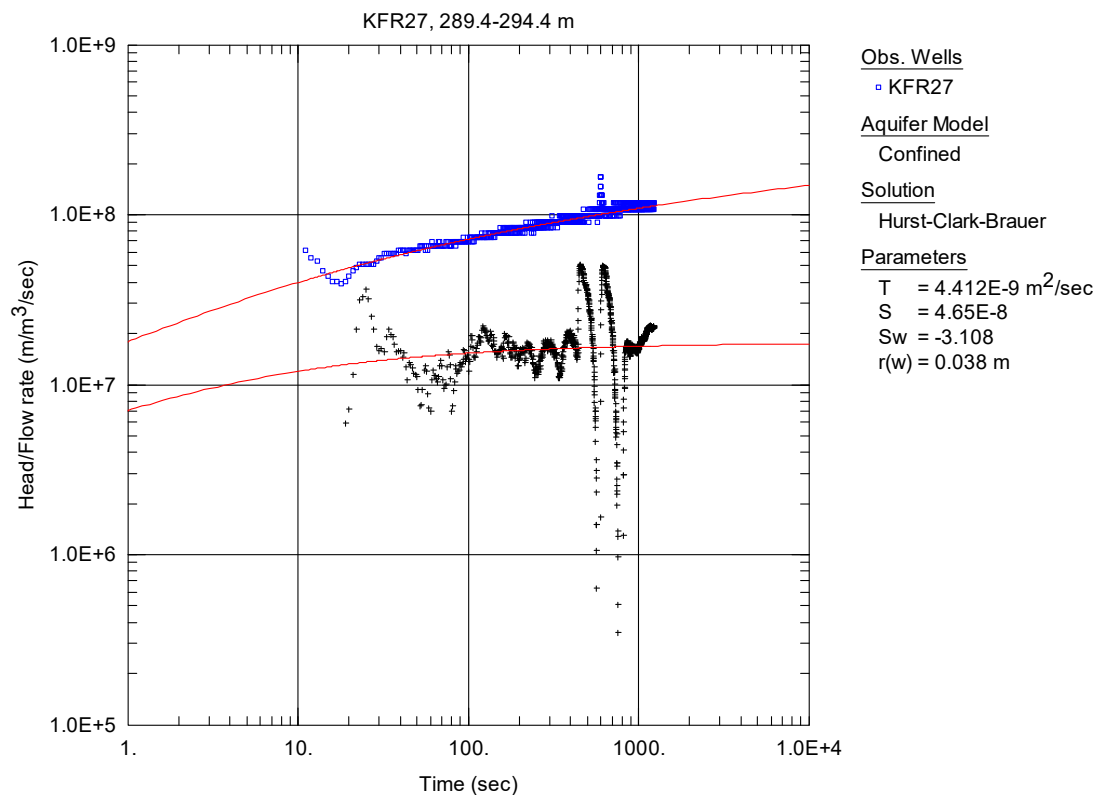


**Figure A2-139.** Log-log plot of head/flow rate ( $\square$ ) and derivative ( $+$ ) versus time, from the injection test in section 289.4-294.4 m in borehole KFR27.

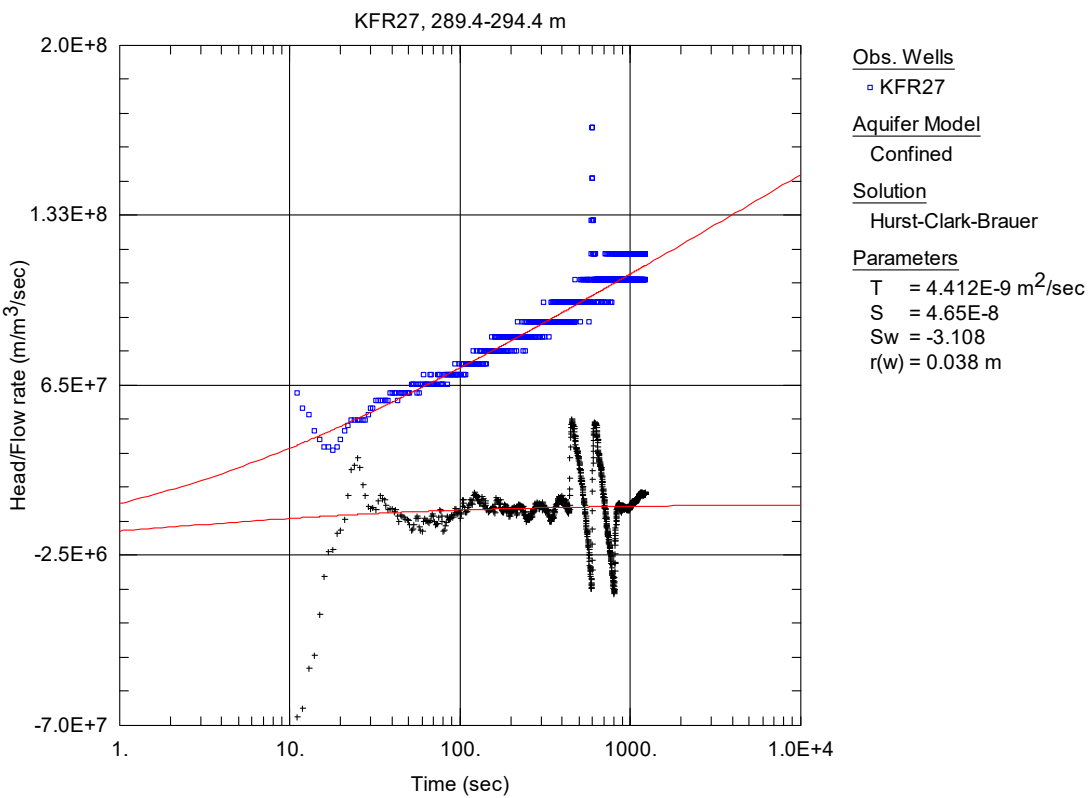


**Figure A2-140.** Lin-log plot of head/flow rate (□) and derivative (+) versus time, from the injection test in section 289.4-294.4 m in borehole KFR27.

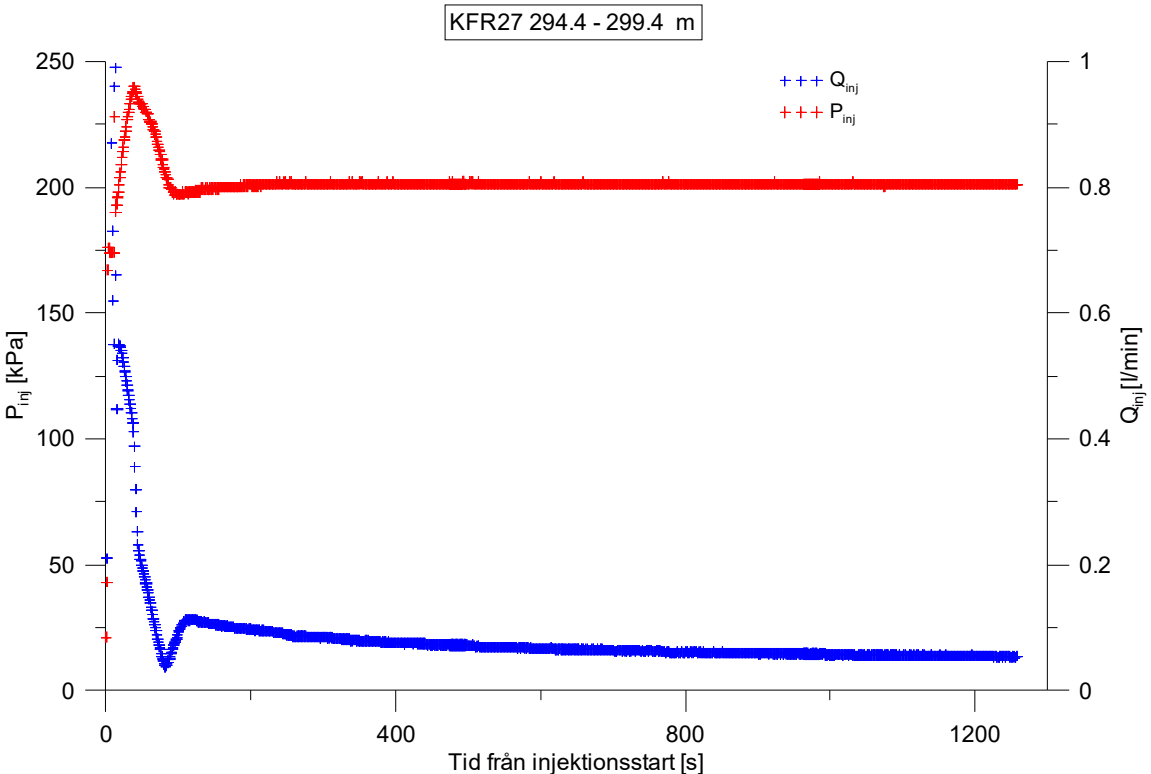


**Figure A2-141.** Linear plot of flow rate ( $Q$ ) and pressure ( $P$ ) versus time from the injection test in section 294.4-299.4 m in borehole KFR27.

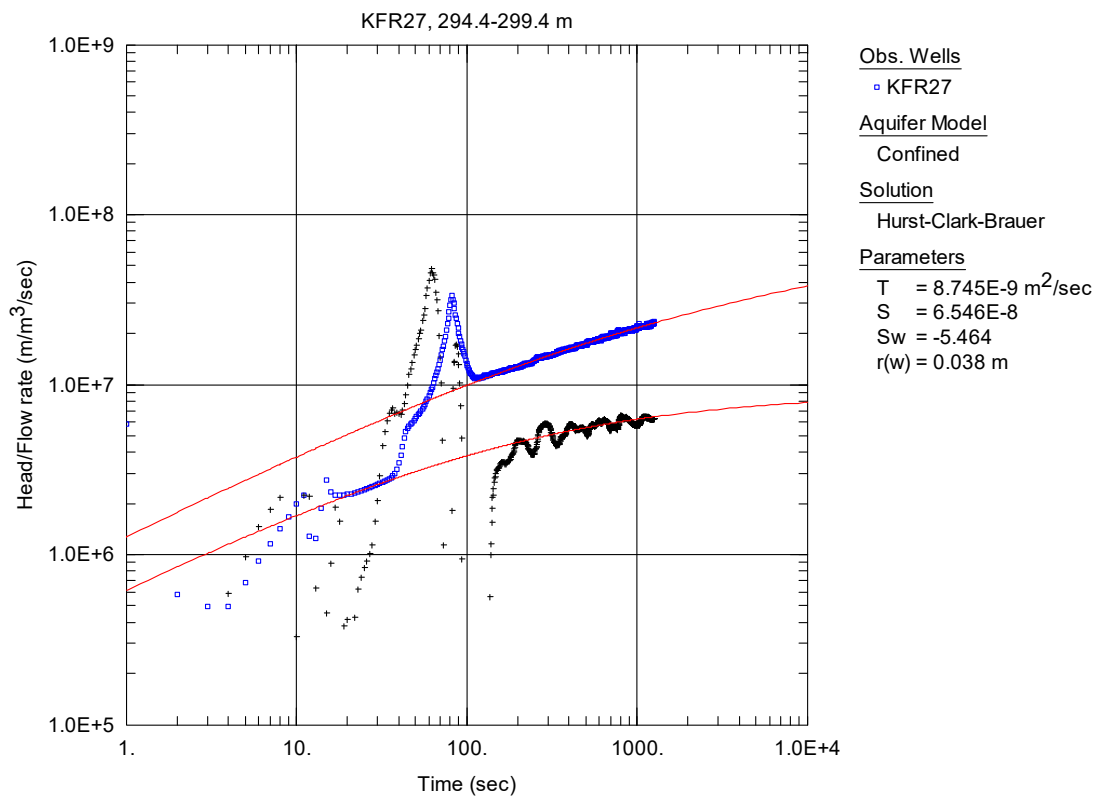


**Figure A2-142.** Log-log plot of head/flow rate ( $\square$ ) and derivative (+) versus time, from the injection test in section 294.4-299.4 m in borehole KFR27.

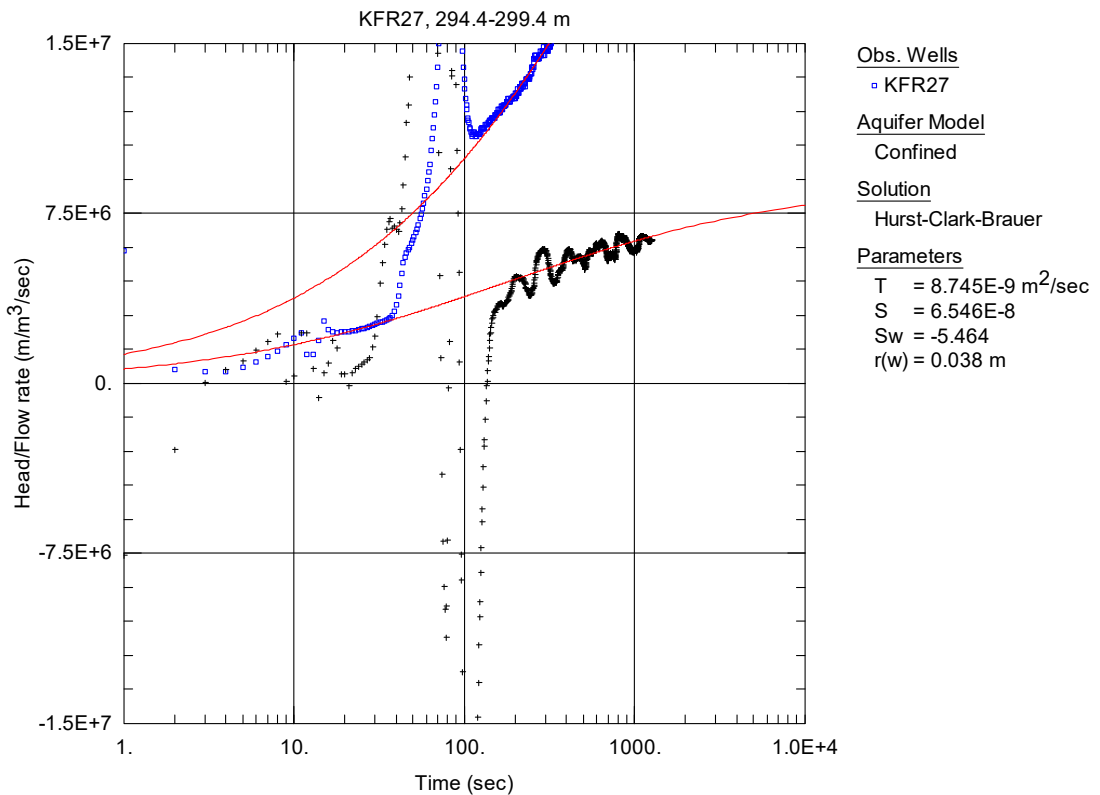


**Figure A2-143.** Lin-log plot of head/flow rate ( $\square$ ) and derivative (+) versus time, from the injection test in section 294.4-299.4 m in borehole KFR27.

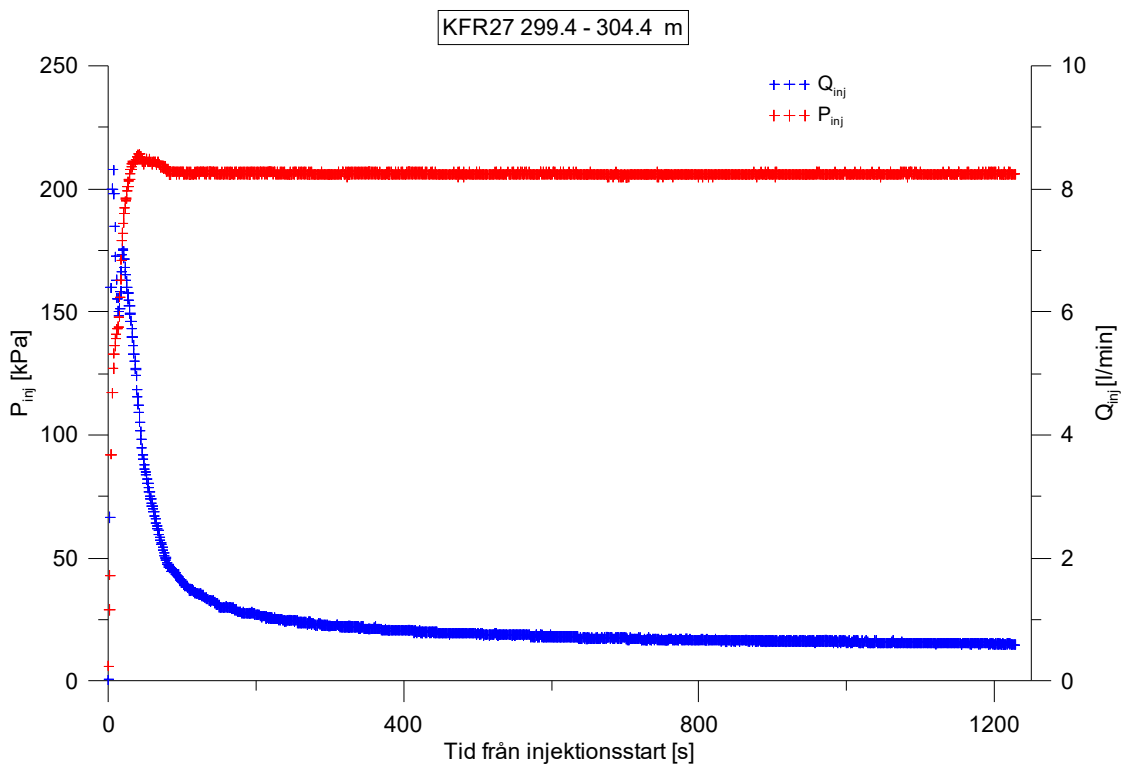


**Figure A2-144.** Linear plot of flow rate ( $Q$ ) and pressure ( $P$ ) versus time from the injection test in section 299.4-304.4 m in borehole KFR27.

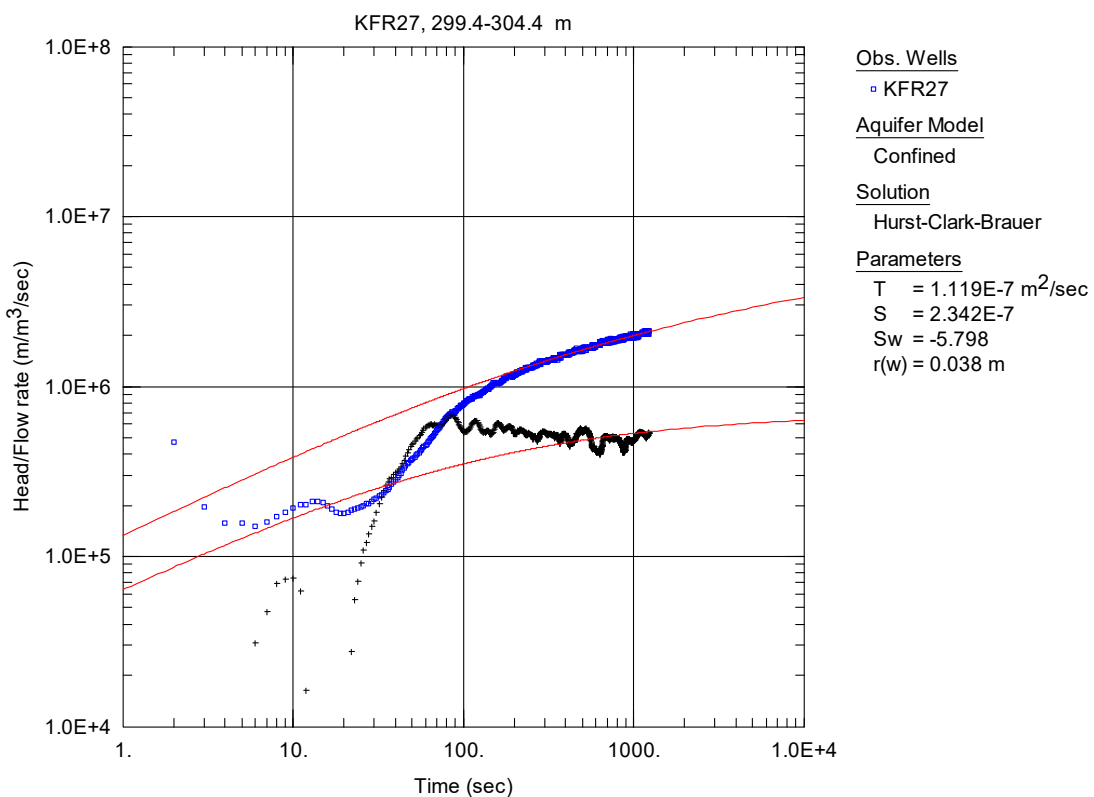


**Figure A2-145.** Log-log plot of head/flow rate ( $\square$ ) and derivative (+) versus time, from the injection test in section 299.4-304.4 m in borehole KFR27.

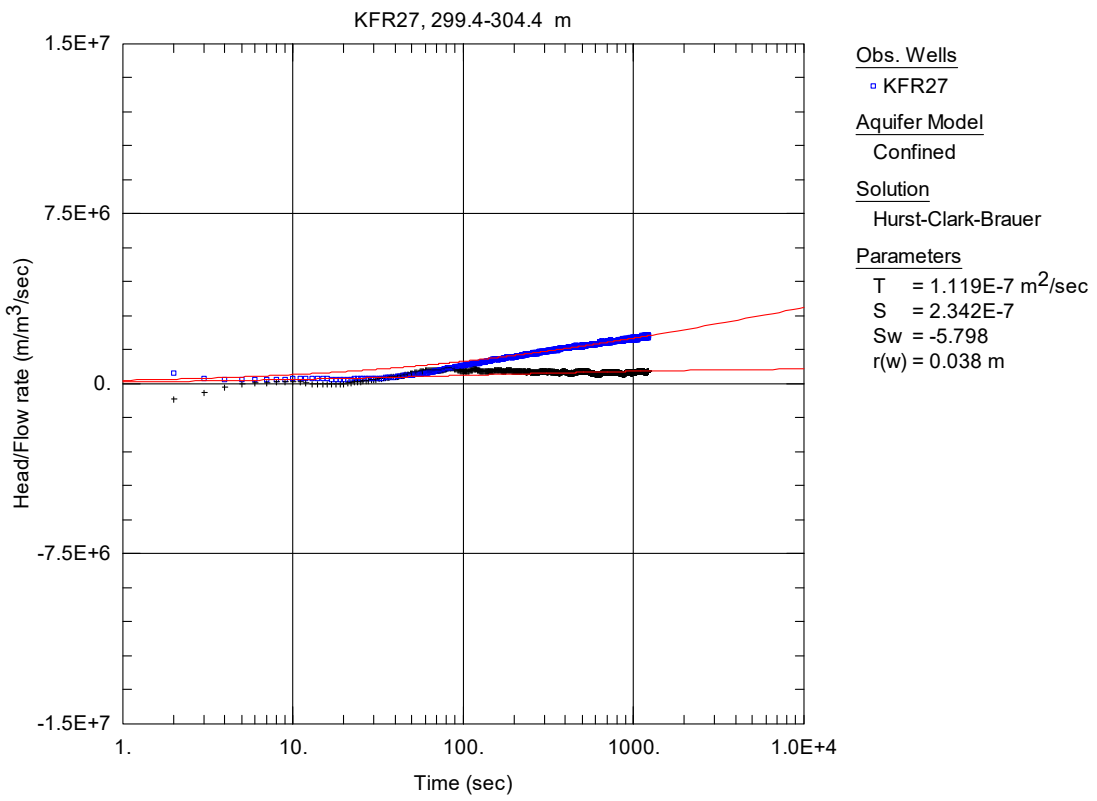


**Figure A2-146.** Lin-log plot of head/flow rate ( $\square$ ) and derivative (+) versus time, from the injection test in section 299.4-304.4 m in borehole KFR27.

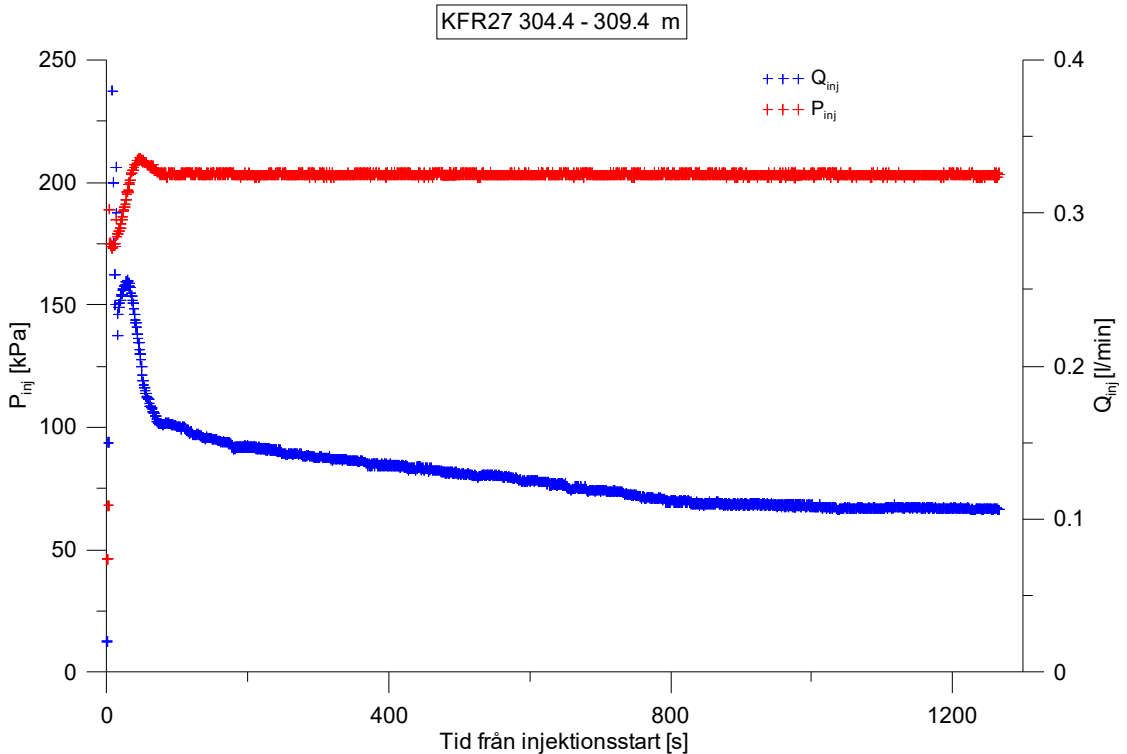


**Figure A2-147.** Linear plot of flow rate ( $Q$ ) and pressure ( $P$ ) versus time from the injection test in section 304.4-309.4 m in borehole KFR27.

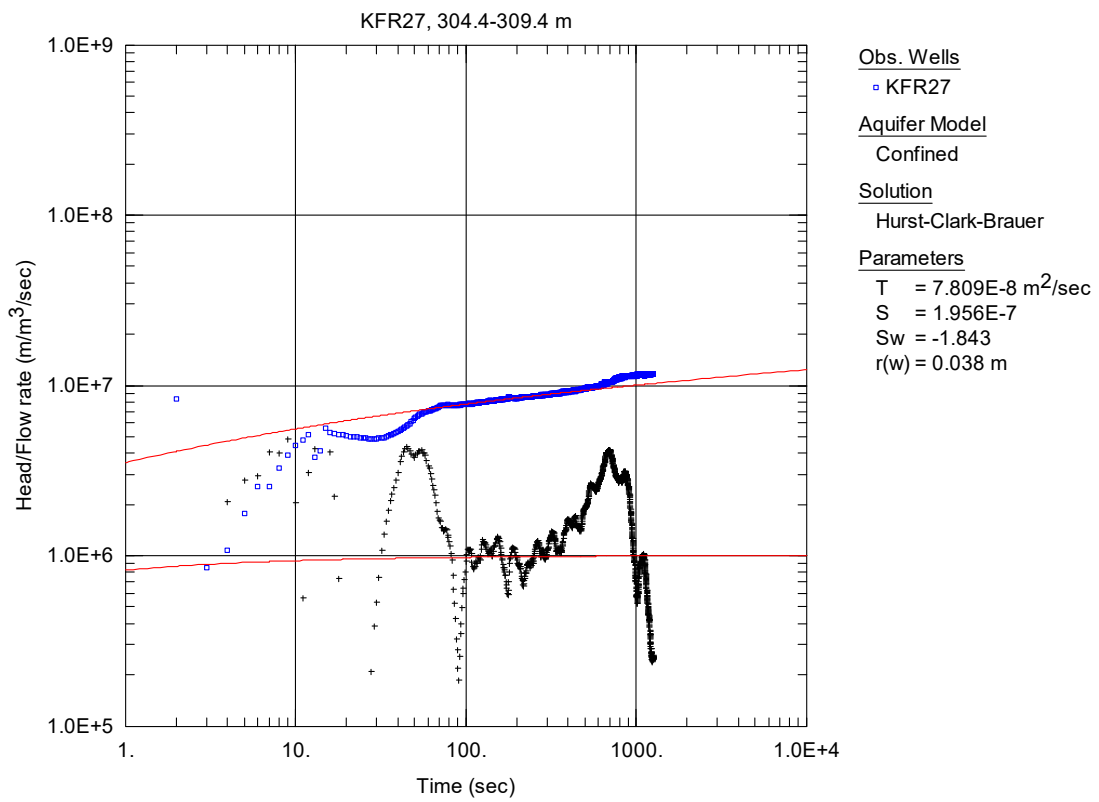


**Figure A2-148.** Log-log plot of head/flow rate (□) and derivative (+) versus time, from the injection test in section 304.4-309.4 m in borehole KFR27.

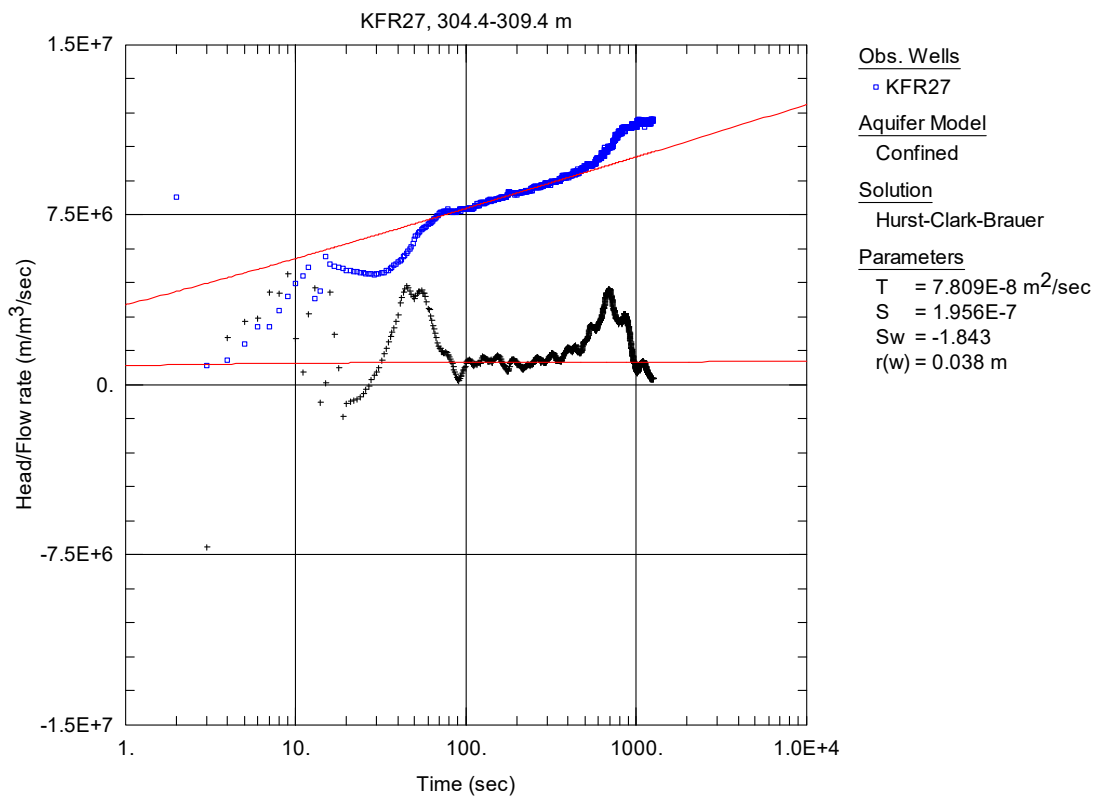


**Figure A2-149.** Lin-log plot of head/flow rate (□) and derivative (+) versus time, from the injection test in section 304.4-309.4 m in borehole KFR27.

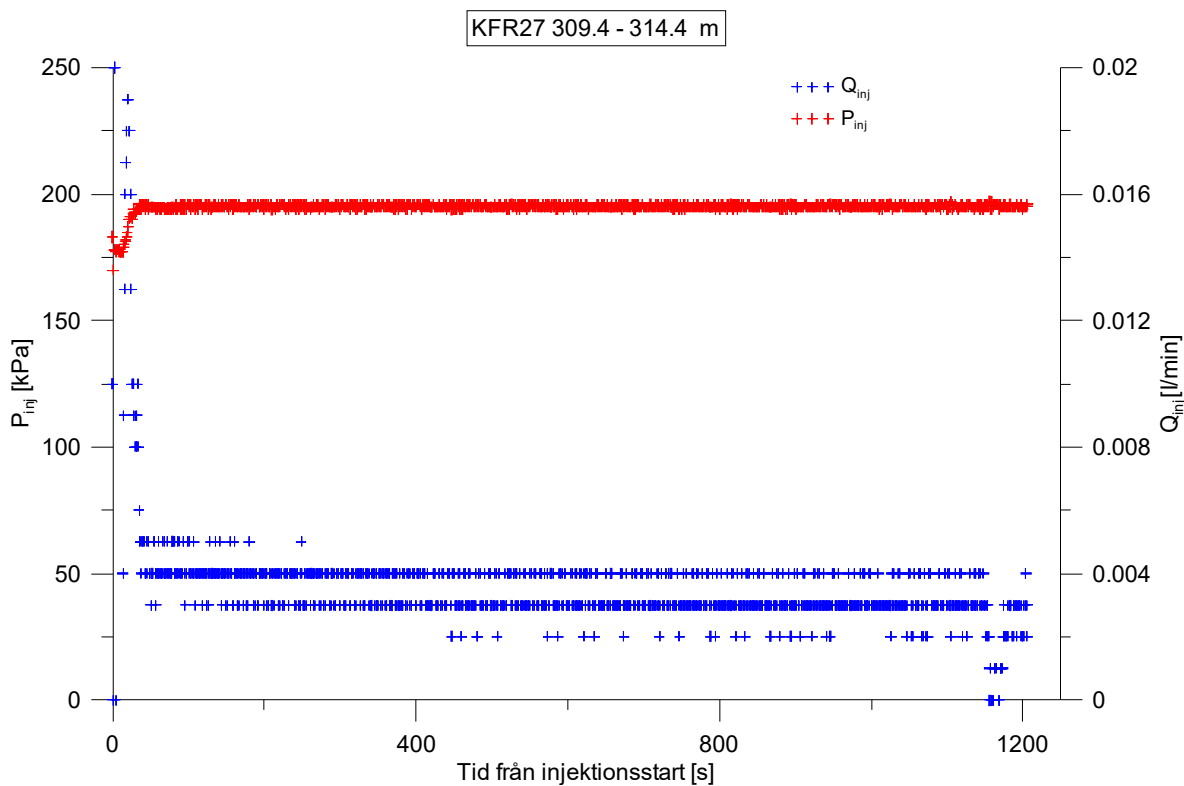


**Figure A2-150.** Linear plot of flow rate ( $Q$ ) and pressure ( $P$ ) versus time from the injection test in section 309.4-314.4 m in borehole KFR27.

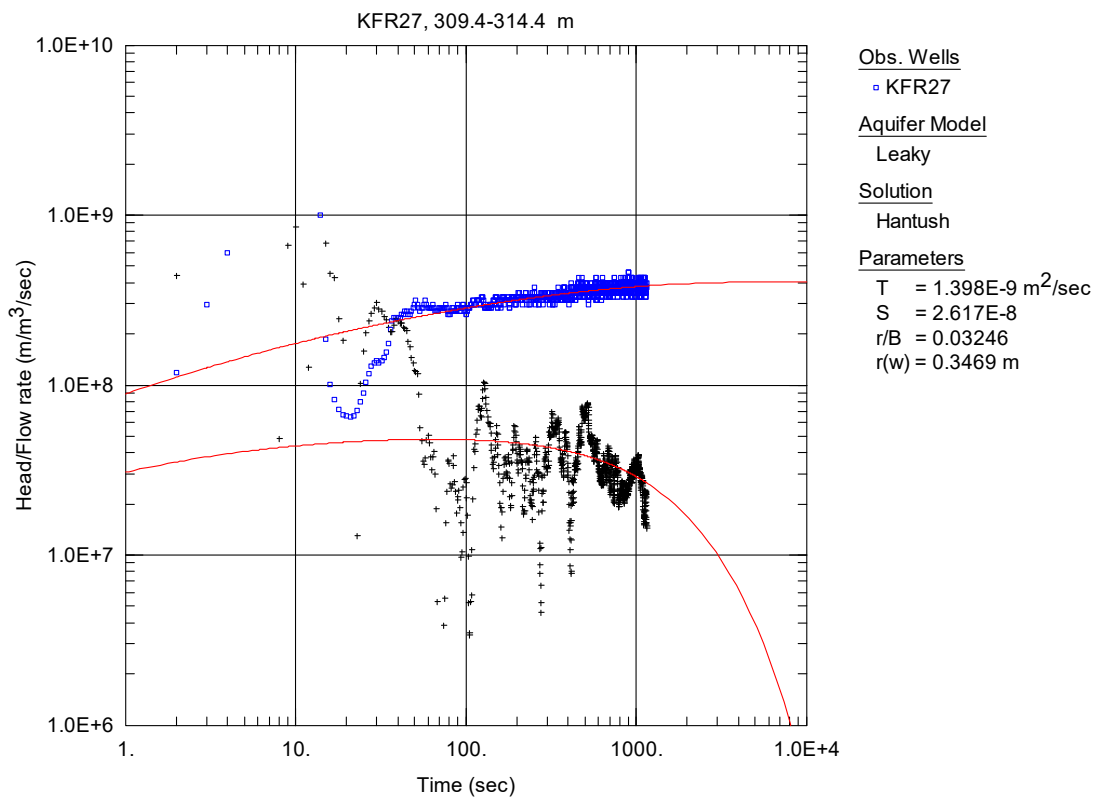


**Figure A2-151.** Log-log plot of head/flow rate ( $\square$ ) and derivative (+) versus time, from the injection test in section 309.4-314.4 m in borehole KFR27.

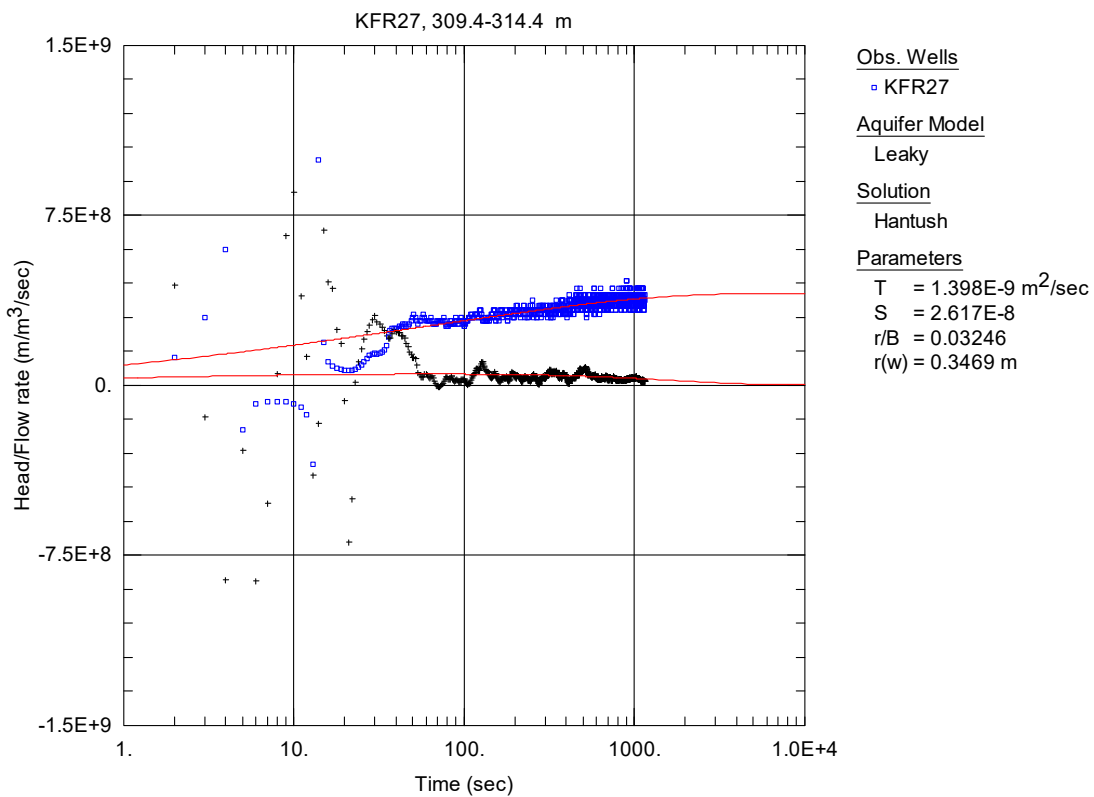


**Figure A2-152.** Lin-log plot of head/flow rate (□) and derivative (+) versus time, from the injection test in section 309.4-314.4 m in borehole KFR27.

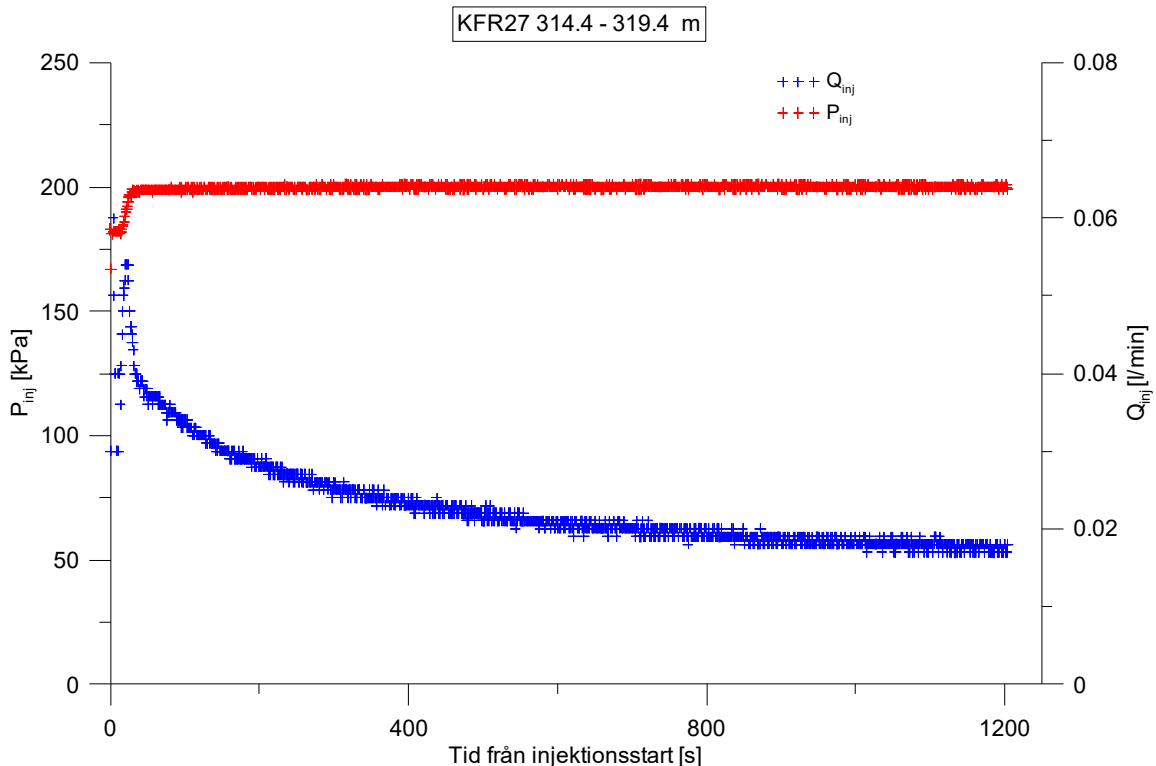


**Figure A2-153.** Linear plot of flow rate ( $Q$ ) and pressure ( $P$ ) versus time from the injection test in section 314.4-319.4 m in borehole KFR27.

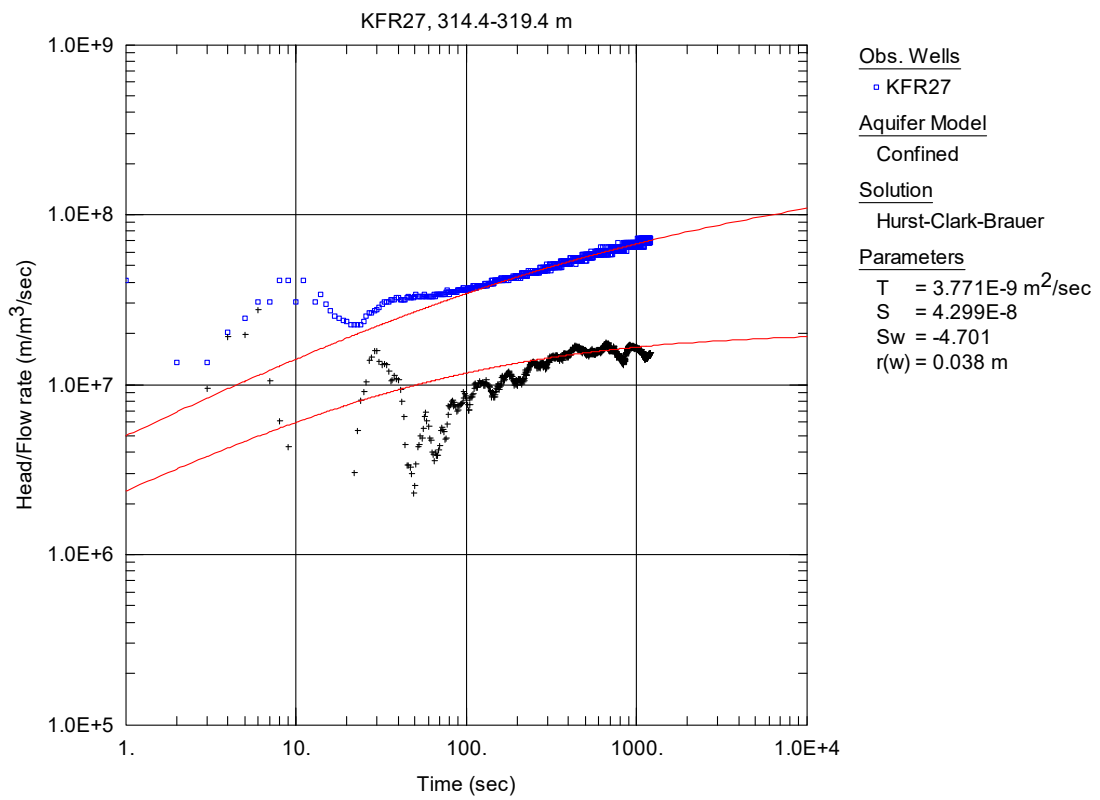


**Figure A2-154.** Log-log plot of head/flow rate (□) and derivative (+) versus time, from the injection test in section 314.4-319.4 m in borehole KFR27.

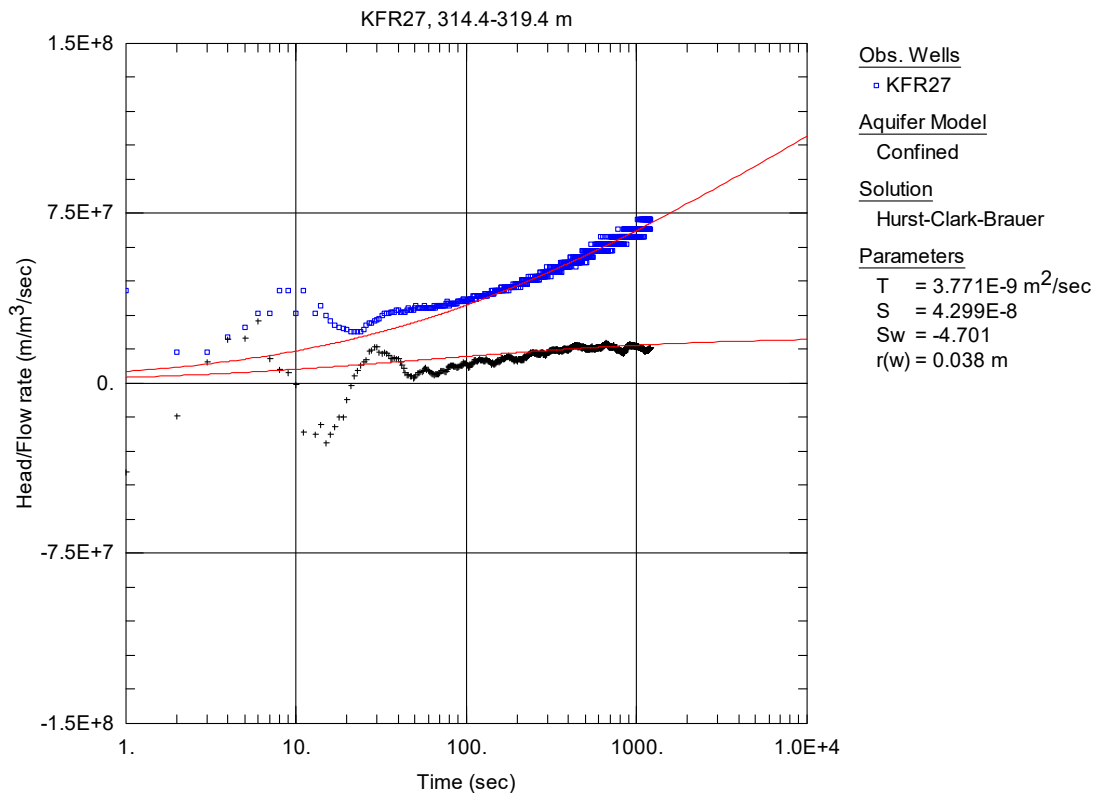


**Figure A2-155.** Lin-log plot of head/flow rate (□) and derivative (+) versus time, from the injection test in section 314.4-319.4 m in borehole KFR27.

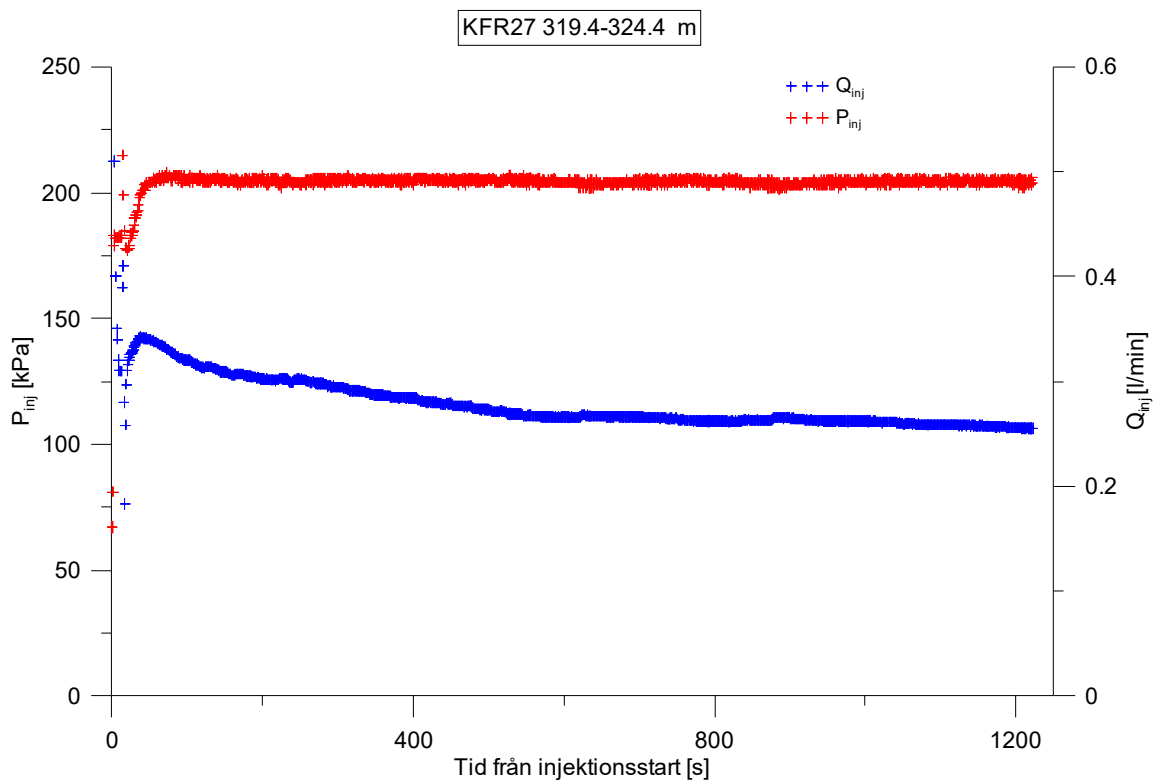


**Figure A2-156.** Linear plot of flow rate ( $Q$ ) and pressure ( $P$ ) versus time from the injection test in section 319.4-324.4 m in borehole KFR27.

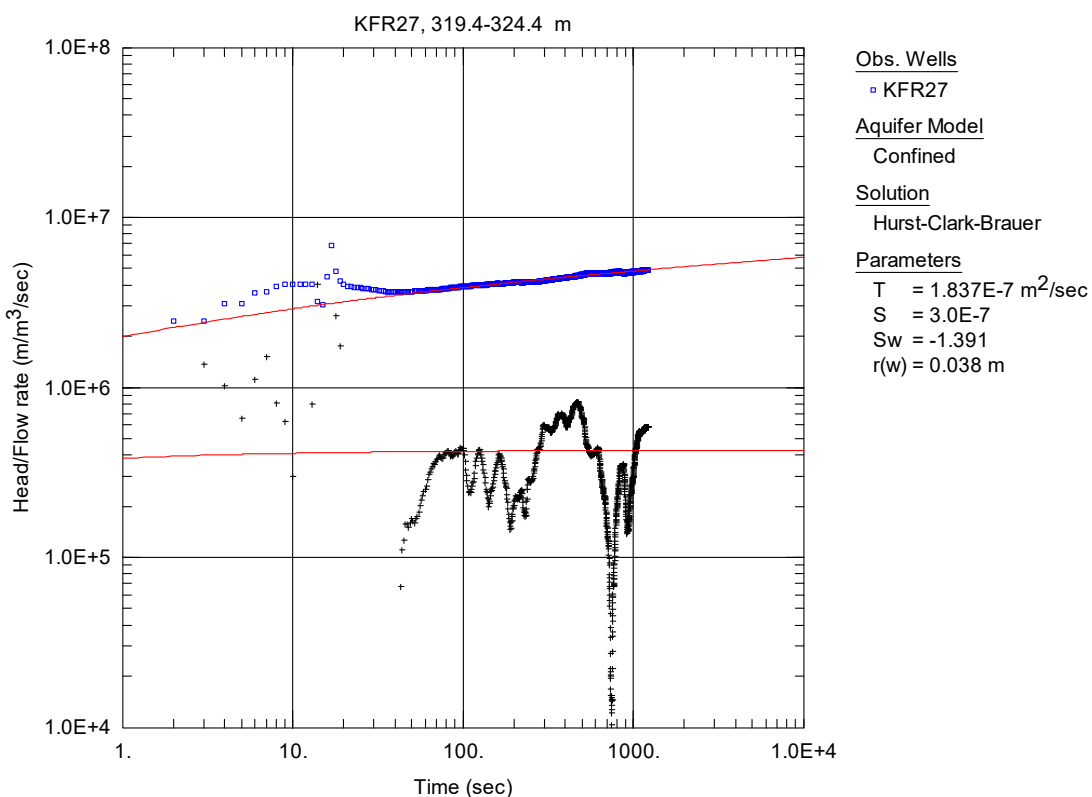


**Figure A2-157.** Log-log plot of head/flow rate (□) and derivative (+) versus time, from the injection test in section 319.4-324.4 m in borehole KFR27.

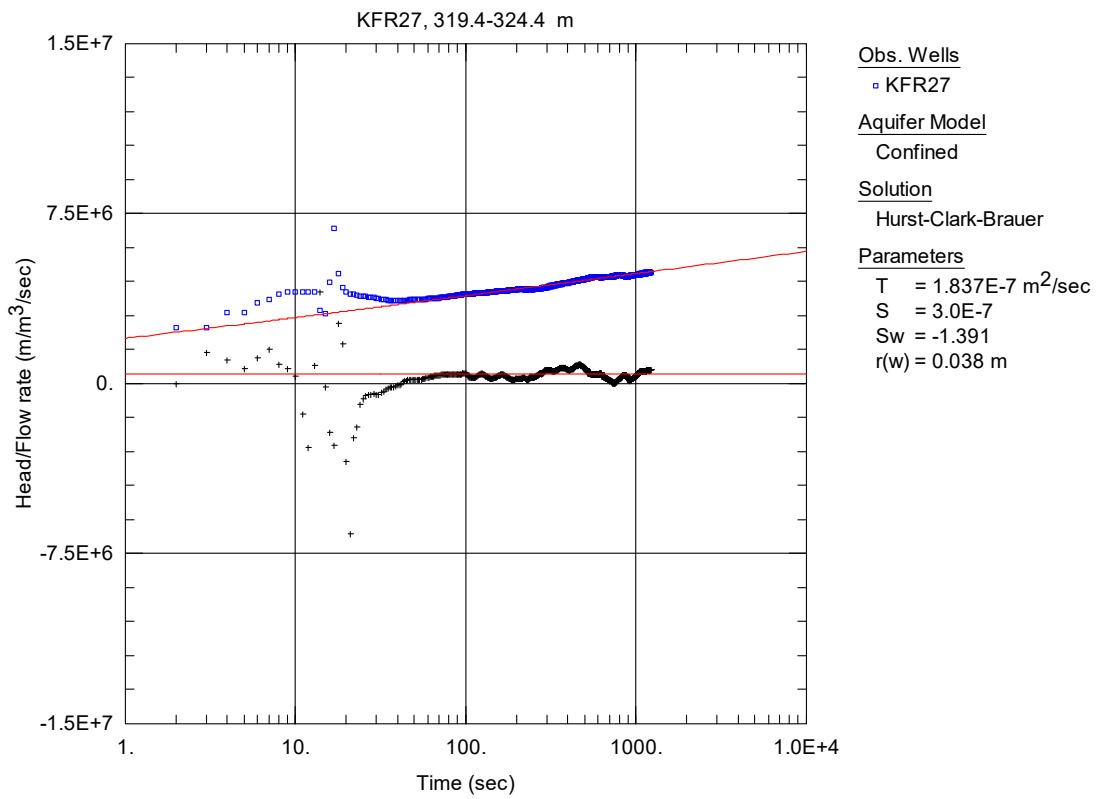


**Figure A2-158.** Lin-log plot of head/flow rate (□) and derivative (+) versus time, from the injection test in section 319.4-324.4 m in borehole KFR27.

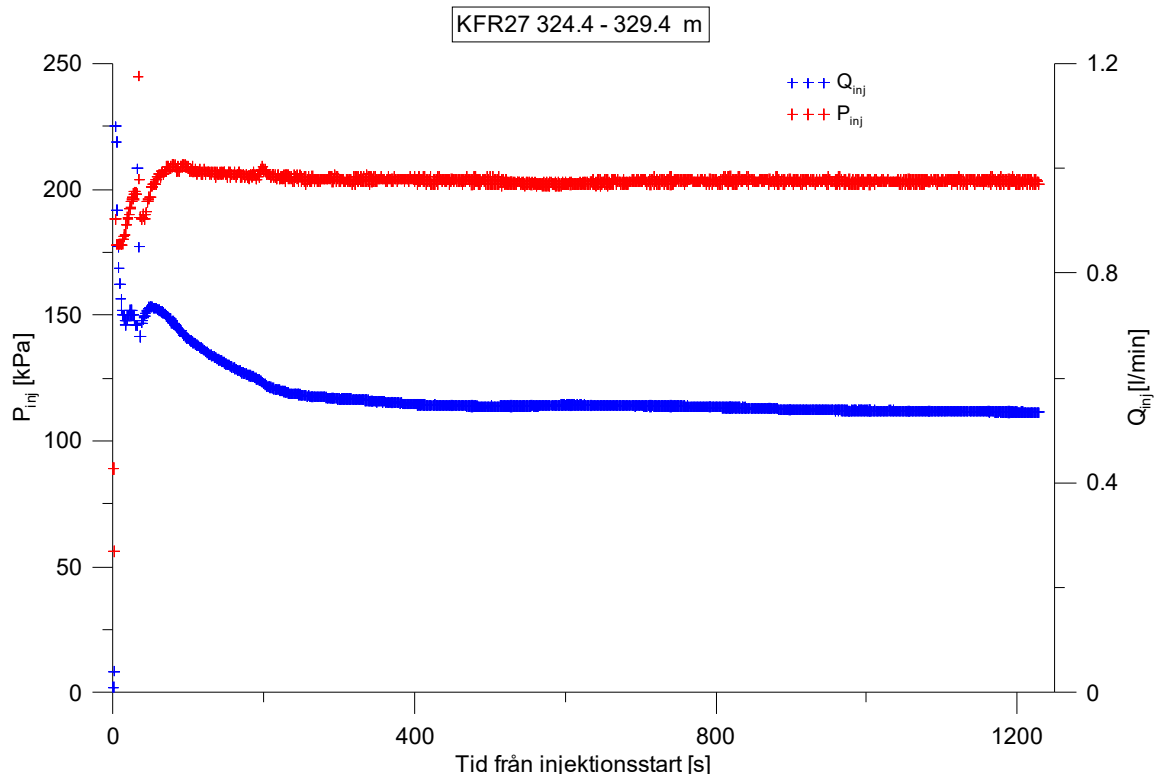


**Figure A2-159.** Linear plot of flow rate ( $Q$ ) and pressure ( $P$ ) versus time from the injection test in section 324.4-329.4 m in borehole KFR27.

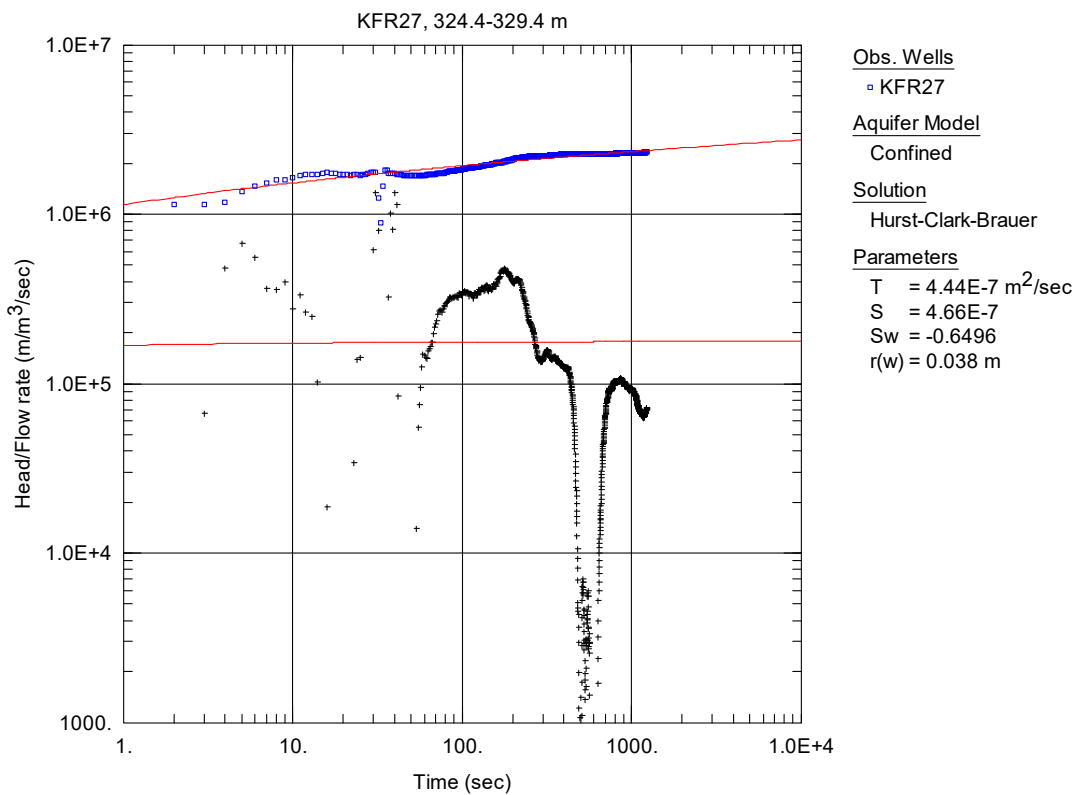


**Figure A2-160.** Log-log plot of head/flow rate (□) and derivative (+) versus time, from the injection test in section 324.4-329.4 m in borehole KFR27.

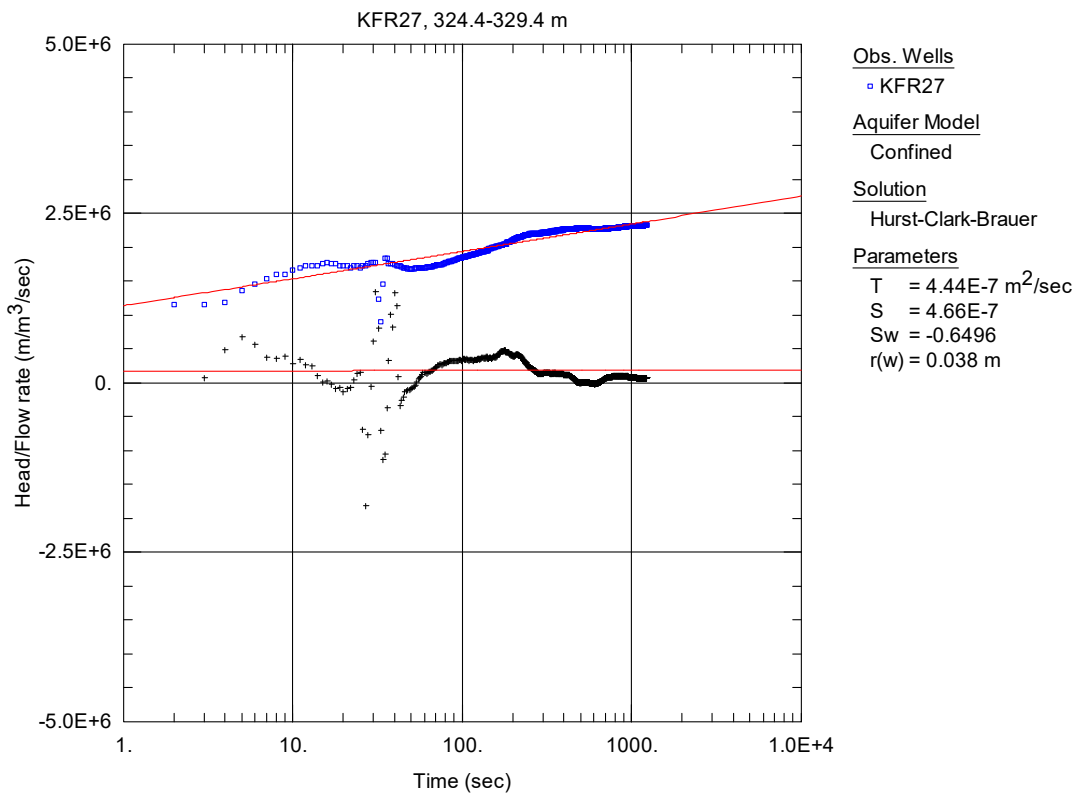


**Figure A2-161.** Lin-log plot of head/flow rate (□) and derivative (+) versus time, from the injection test in section 324.4-329.4 m in borehole KFR27.

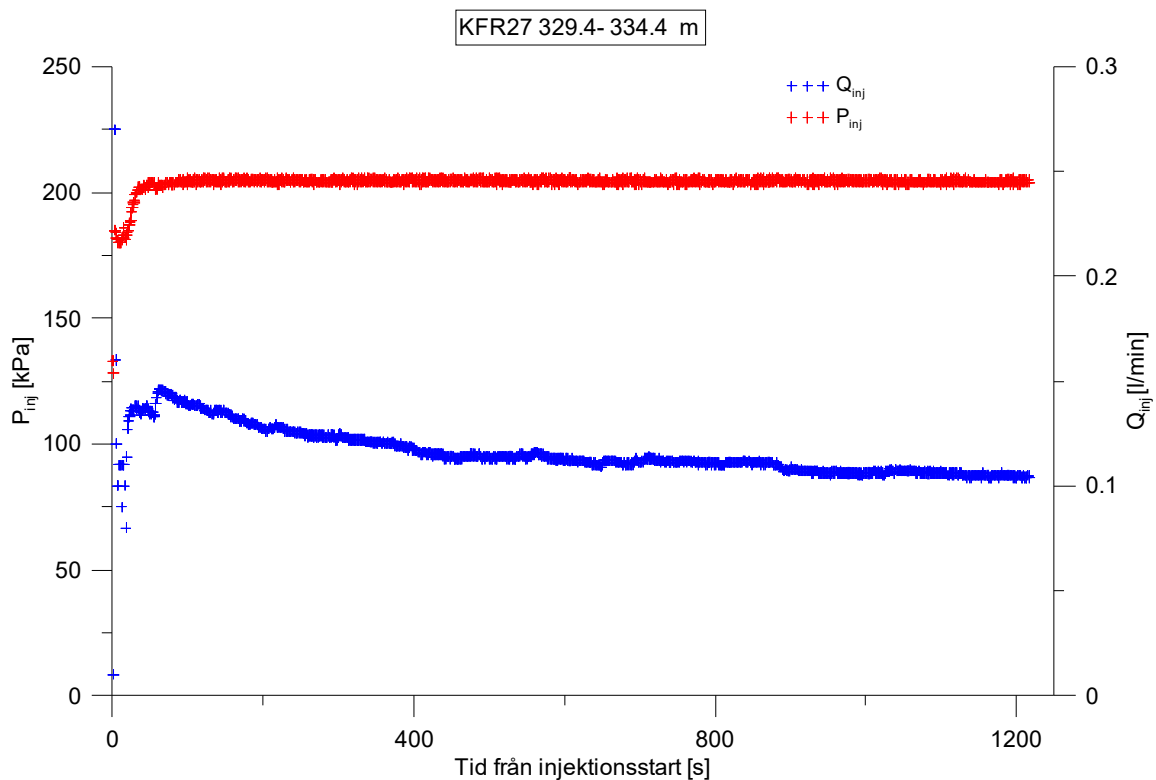


**Figure A2-162.** Linear plot of flow rate ( $Q$ ) and pressure ( $P$ ) versus time from the injection test in section 329.4-334.4 m in borehole KFR27.

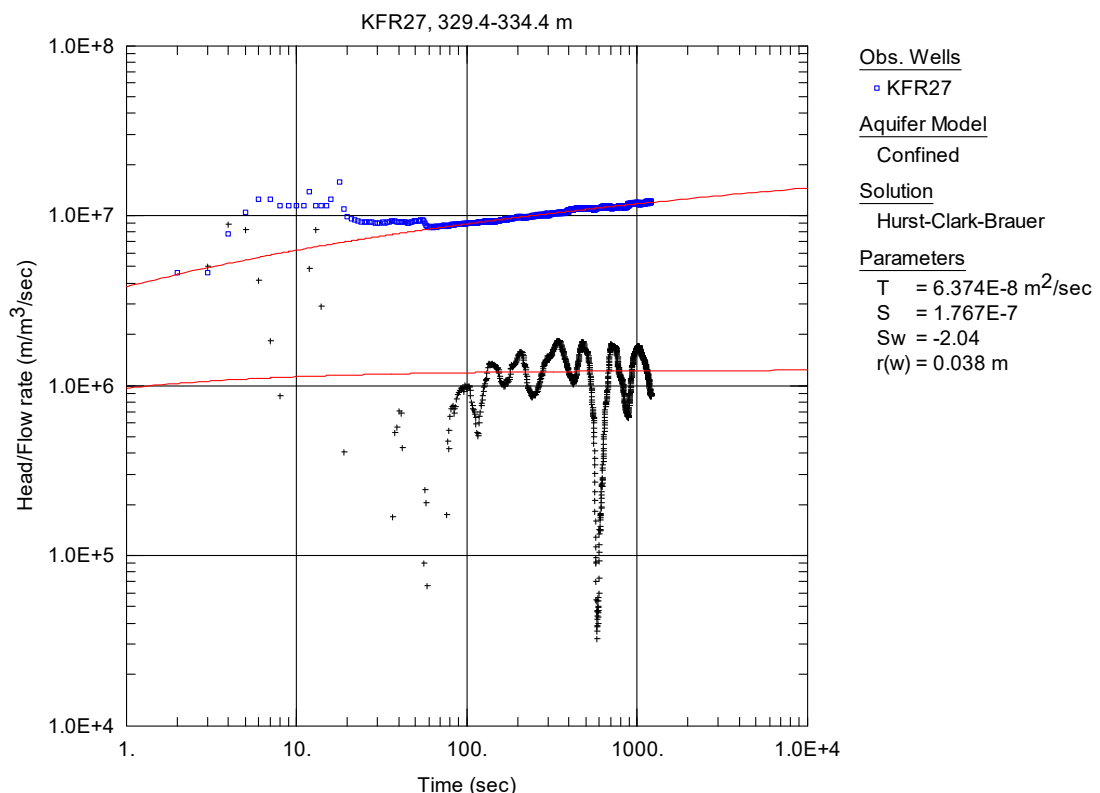


**Figure A2-163.** Log-log plot of head/flow rate (□) and derivative (+) versus time, from the injection test in section 329.4-334.4 m in borehole KFR27.

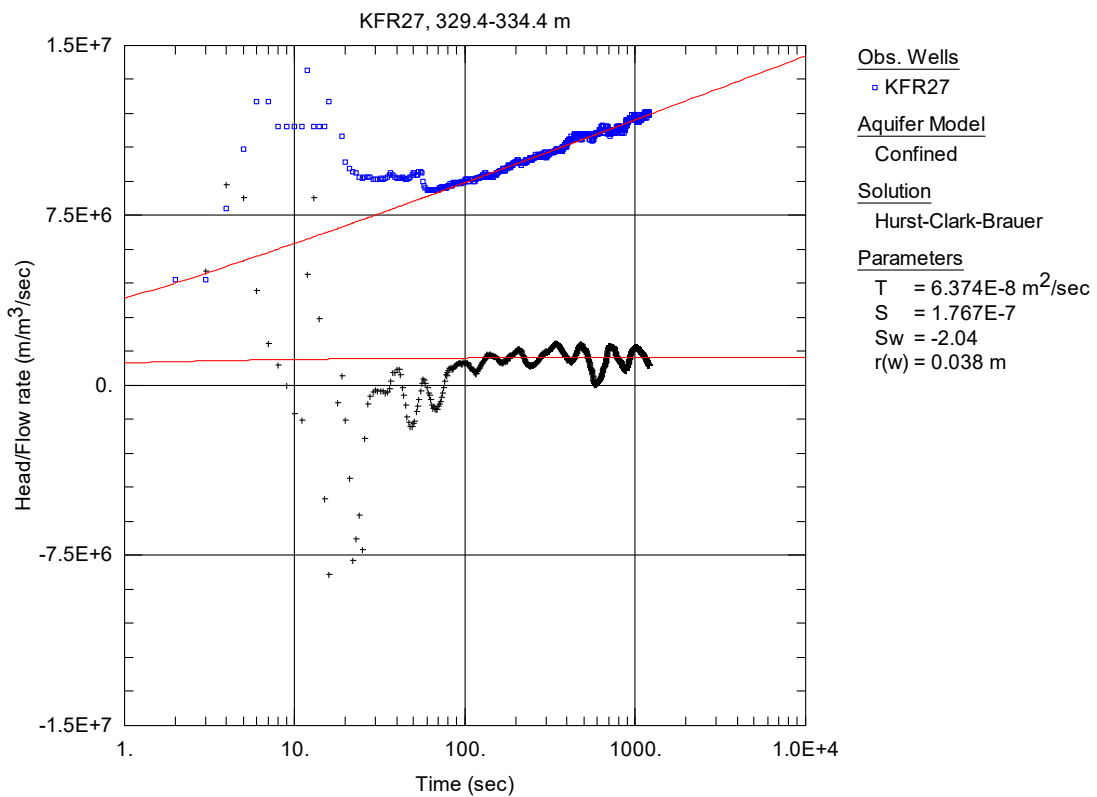


**Figure A2-164.** Lin-log plot of head/flow rate (□) and derivative (+) versus time, from the injection test in section 329.4-334.4 m in borehole KFR27.

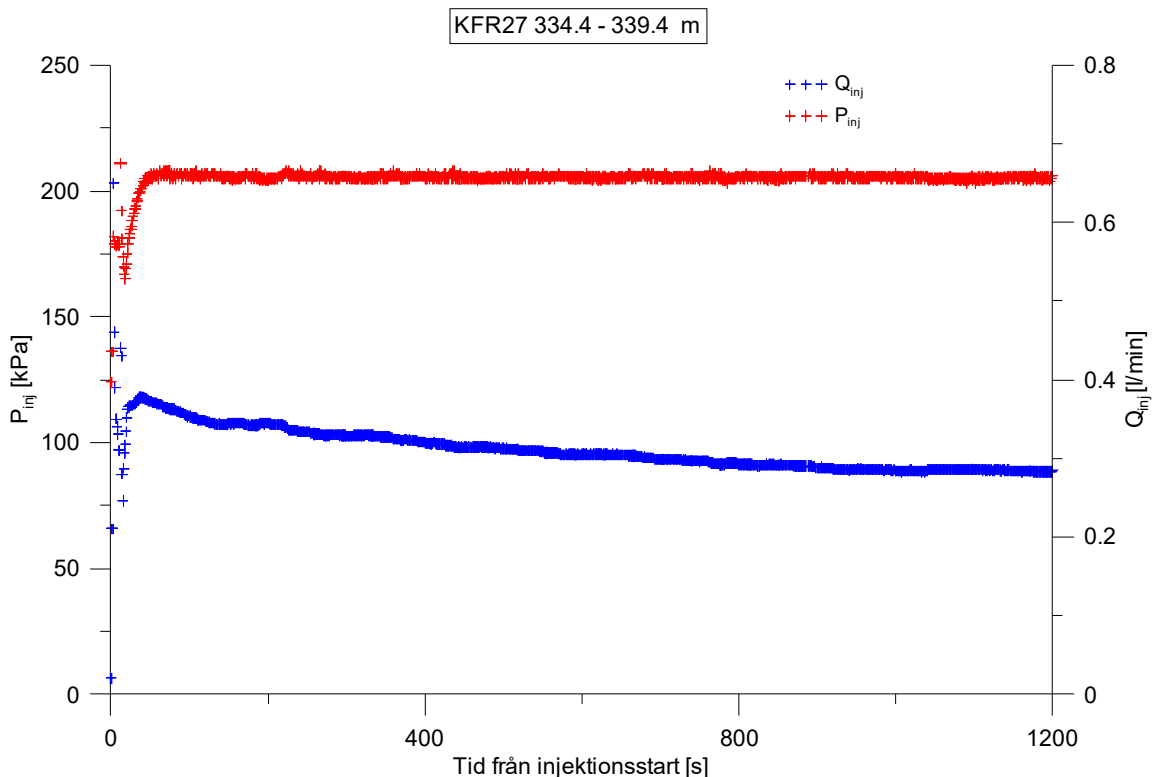


**Figure A2-165.** Linear plot of flow rate ( $Q$ ) and pressure ( $P$ ) versus time from the injection test in section 334.4-339.4 m in borehole KFR27.

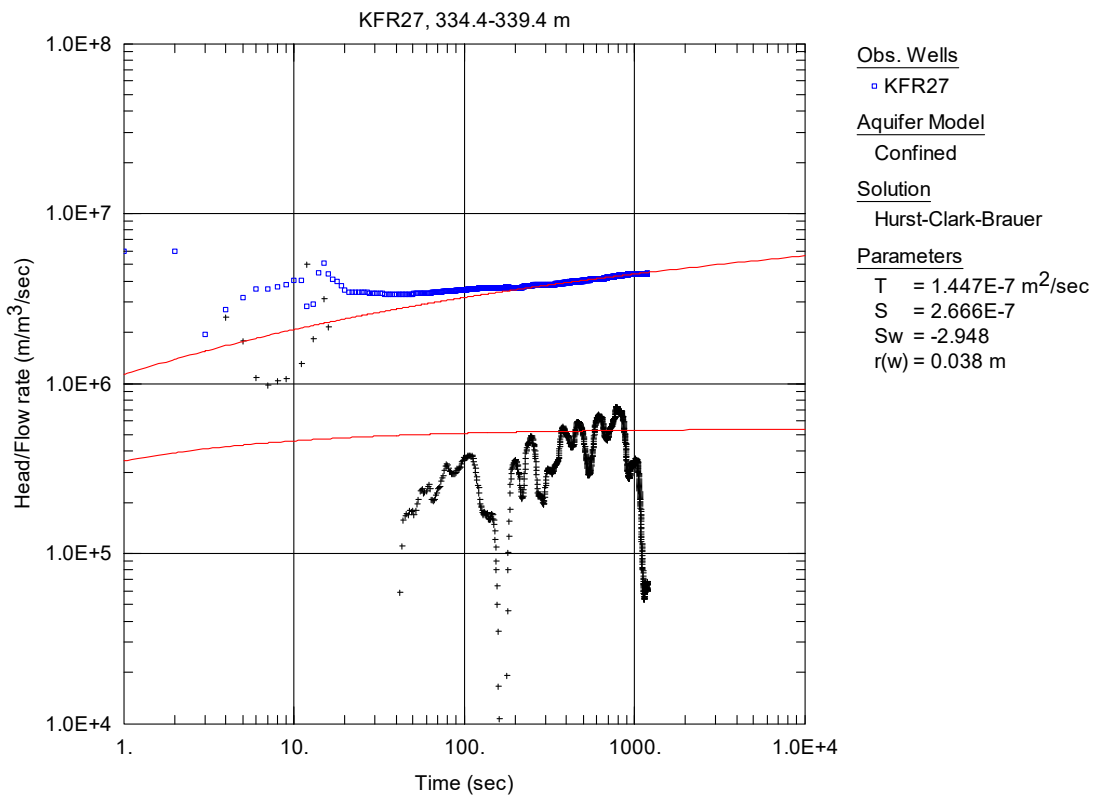


**Figure A2-166.** Log-log plot of head/flow rate (□) and derivative (+) versus time, from the injection test in section 334.4-339.4 m in borehole KFR27.

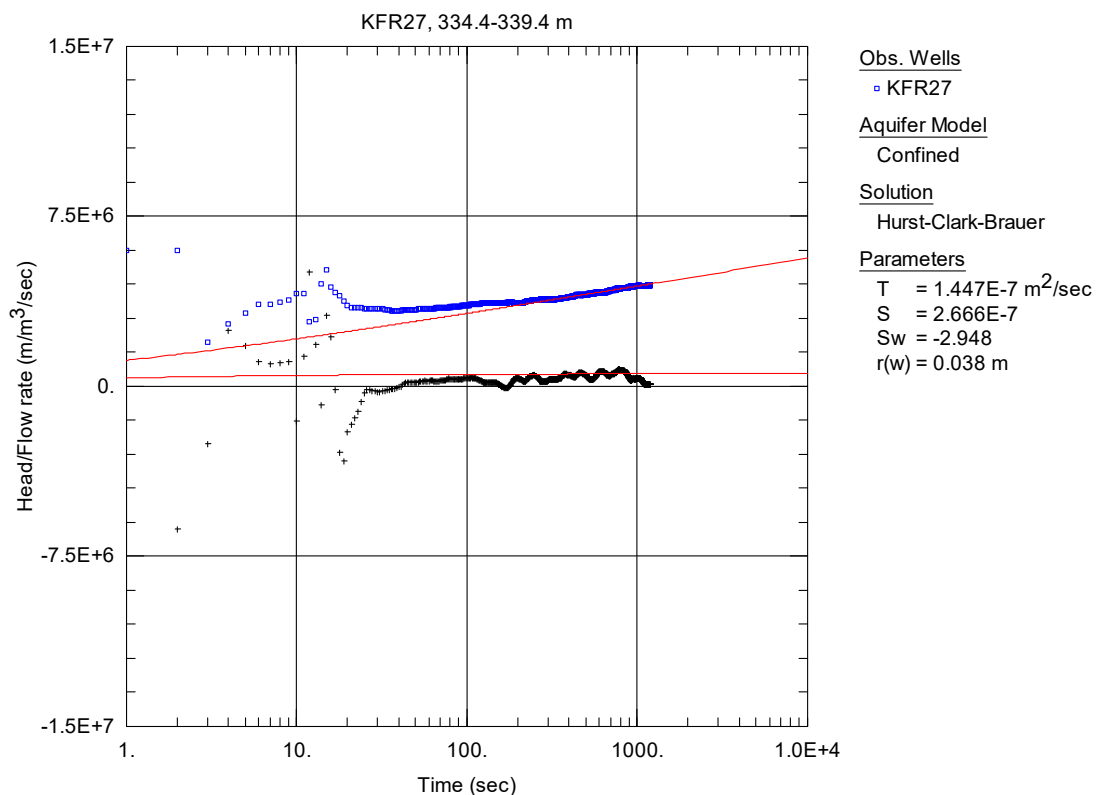


**Figure A2-167.** Lin-log plot of head/flow rate (□) and derivative (+) versus time, from the injection test in section 334.4-339.4 m in borehole KFR27.

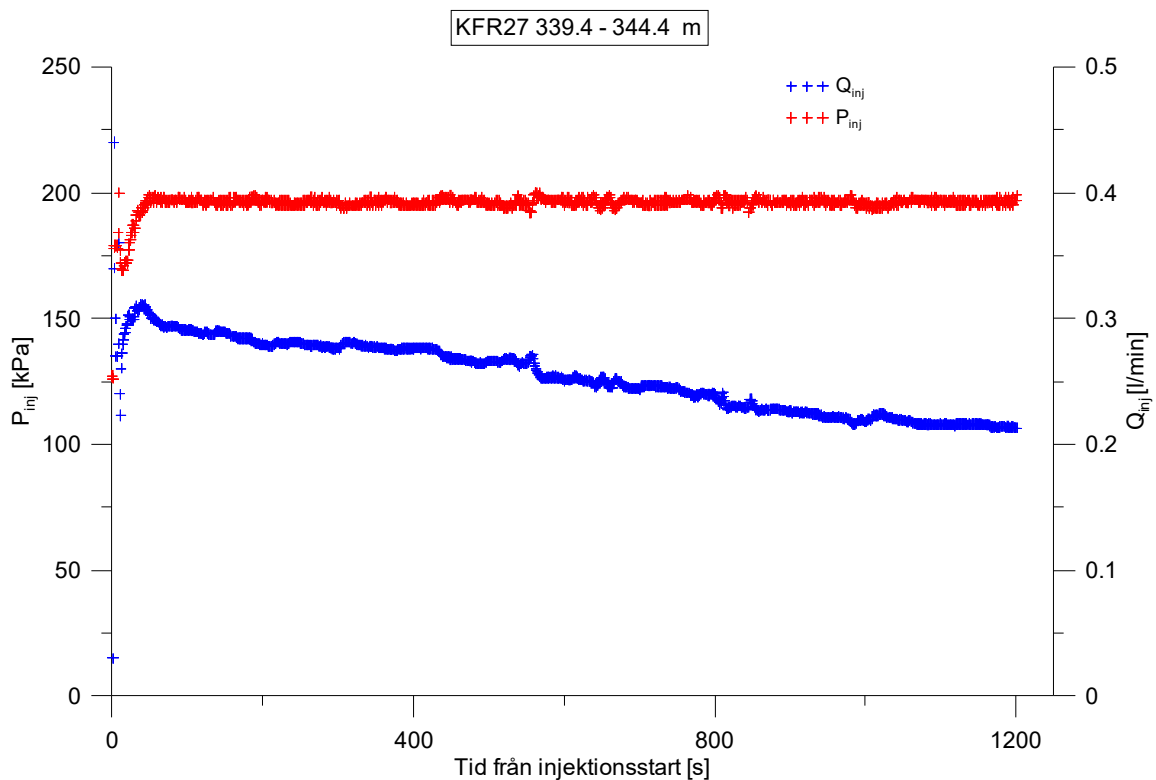


**Figure A2-168.** Linear plot of flow rate ( $Q$ ) and pressure ( $P$ ) versus time from the injection test in section 339.4-344.4 m in borehole KFR27.

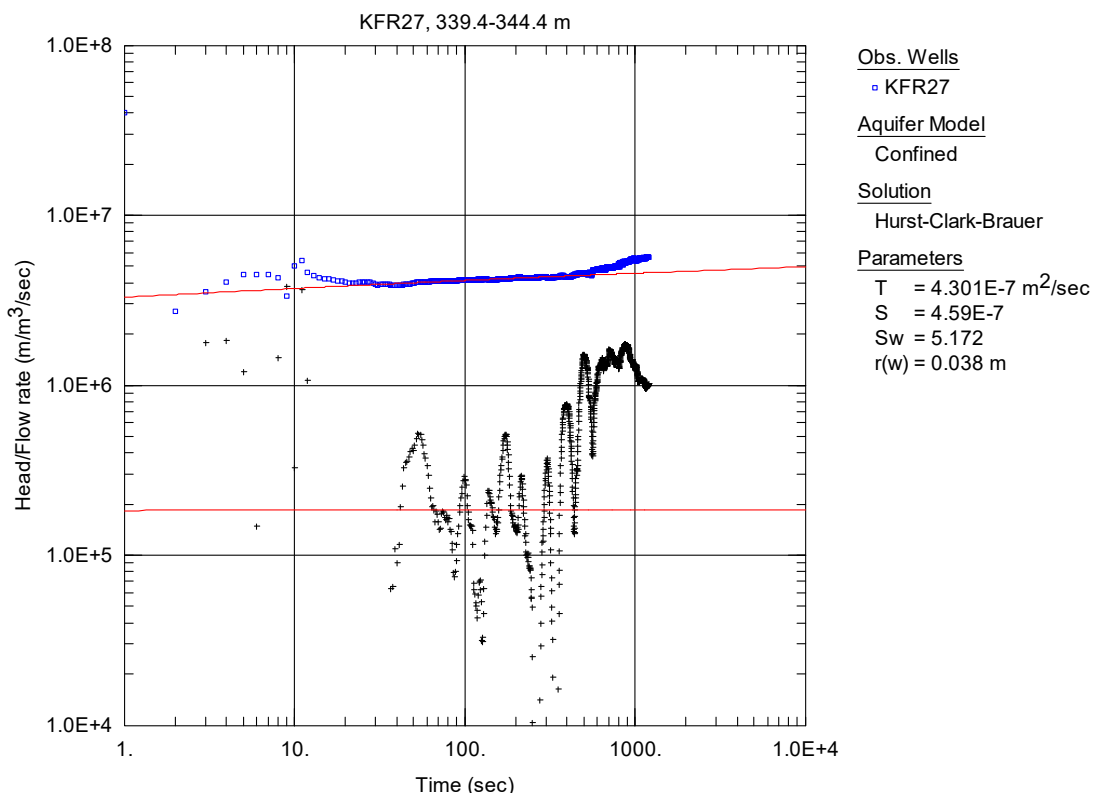


**Figure A2-169.** Log-log plot of head/flow rate ( $\square$ ) and derivative (+) versus time, from the injection test in section 339.4-344.4 m in borehole KFR27.

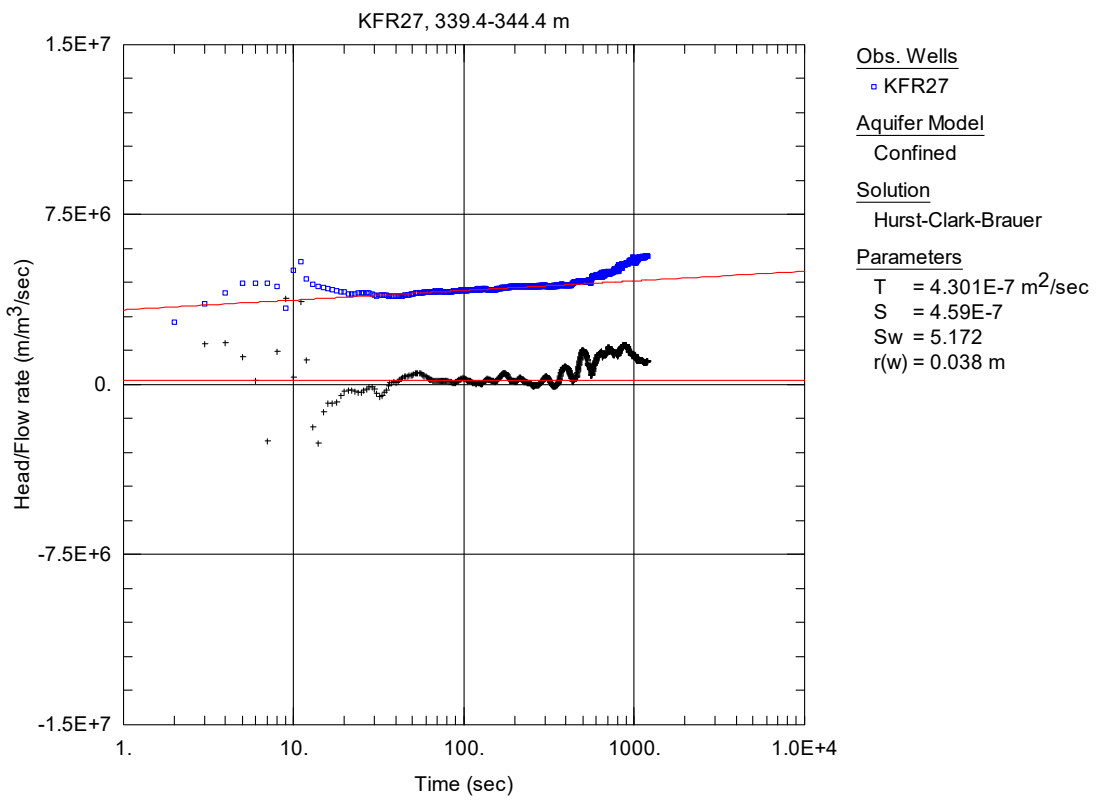


**Figure A2-170.** Lin-log plot of head/flow rate ( $\square$ ) and derivative (+) versus time, from the injection test in section 339.4-344.4 m in borehole KFR27.

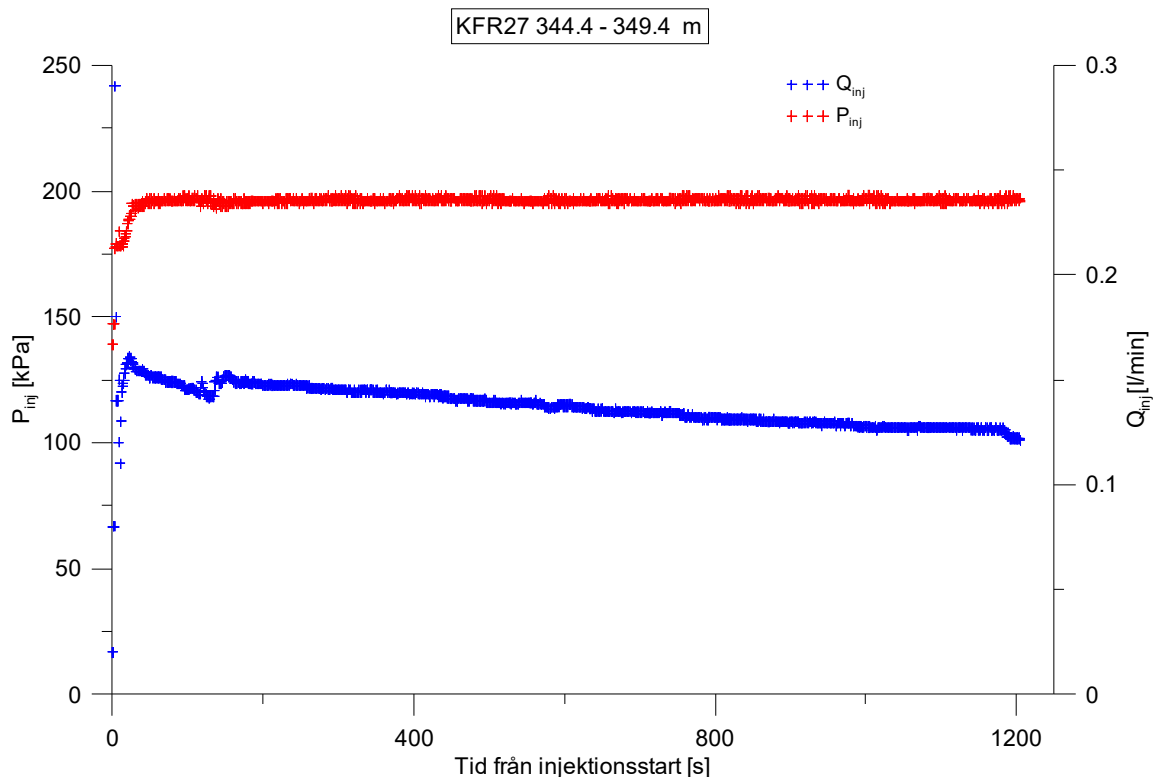


**Figure A2-171.** Linear plot of flow rate ( $Q$ ) and pressure ( $P$ ) versus time from the injection test in section 344.4-349.4 m in borehole KFR27.

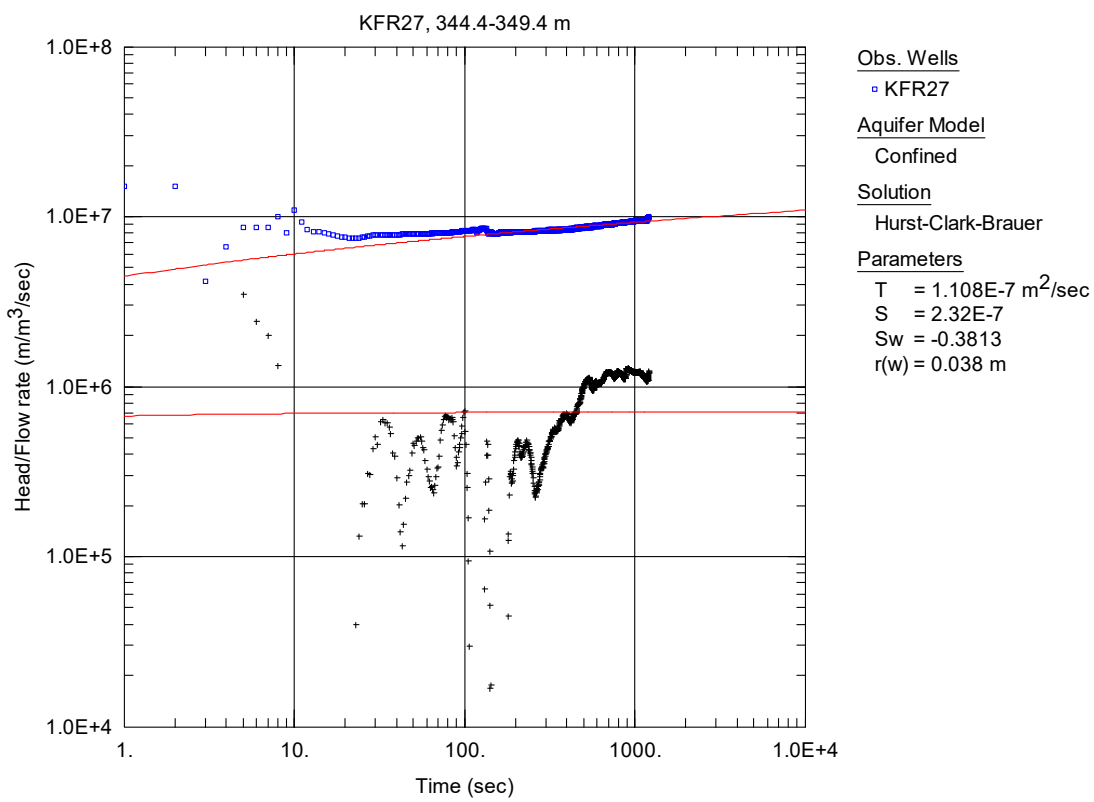


**Figure A2-172.** Log-log plot of head/flow rate (□) and derivative (+) versus time, from the injection test in section 344.4-349.4 m in borehole KFR27.

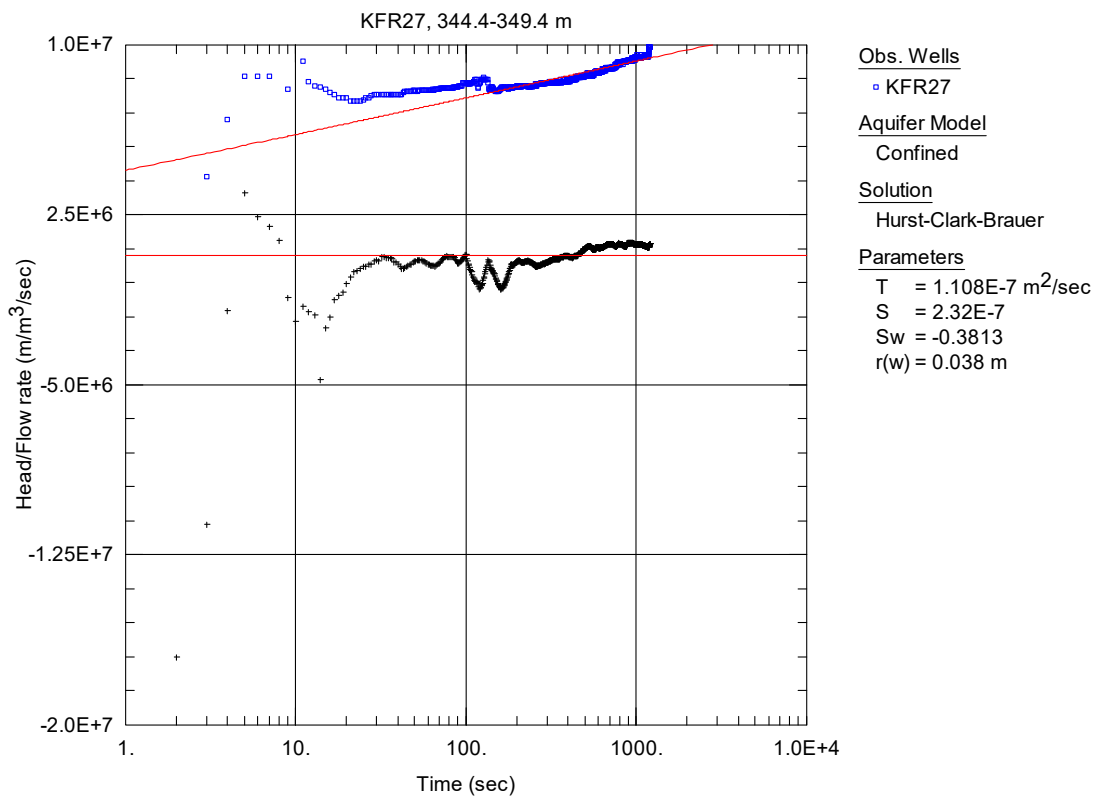


**Figure A2-173.** Lin-log plot of head/flow rate (□) and derivative (+) versus time, from the injection test in section 344.4-349.4 m in borehole KFR27.

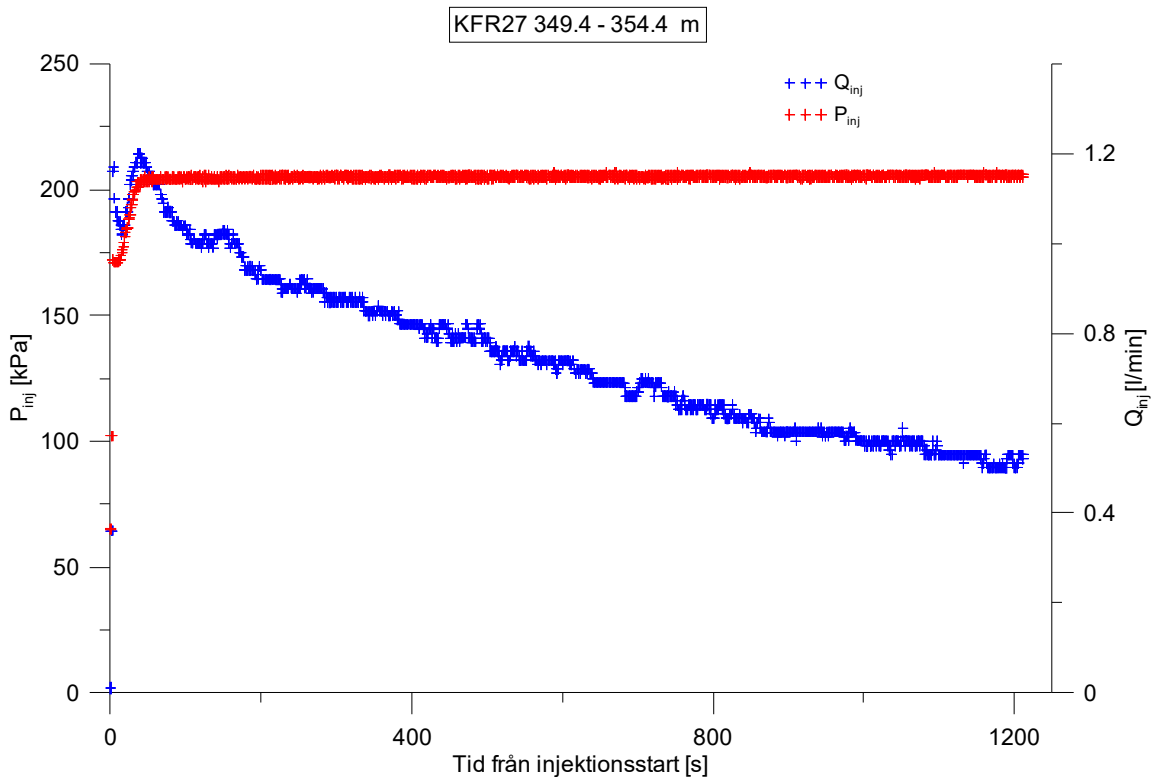


**Figure A2-174.** Linear plot of flow rate ( $Q$ ) and pressure ( $P$ ) versus time from the injection test in section 349.4-354.4 m in borehole KFR27.

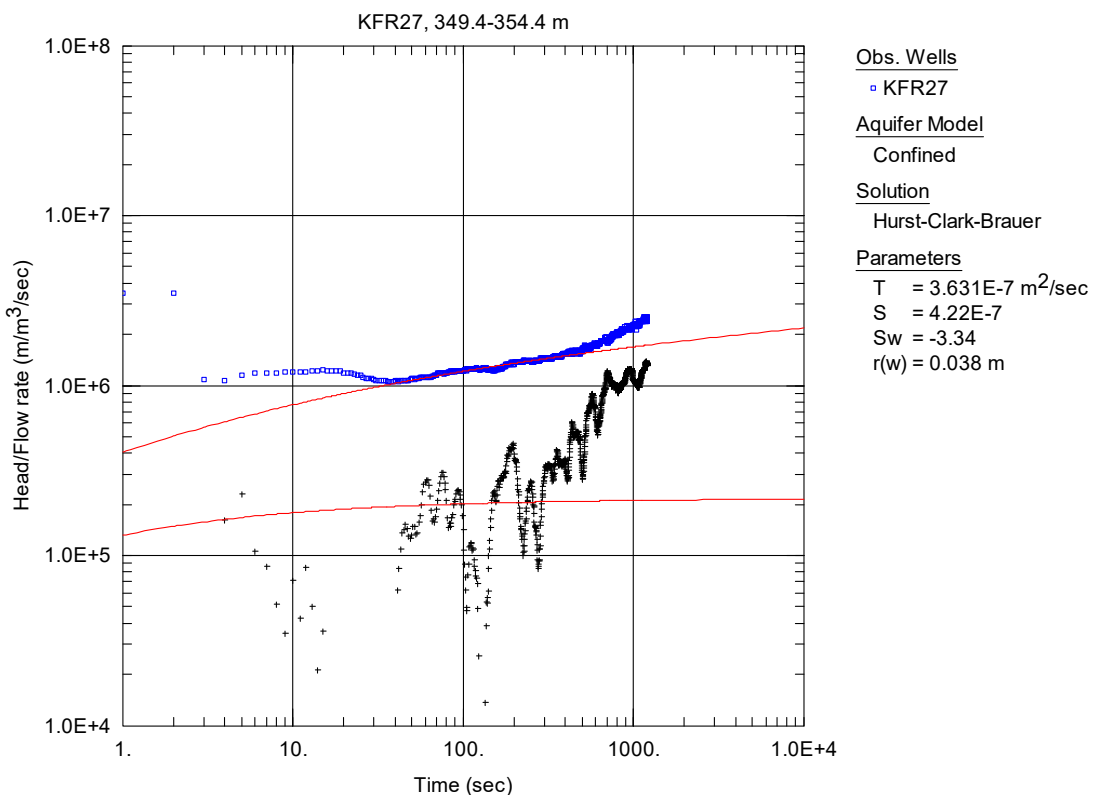


**Figure A2-175.** Log-log plot of head/flow rate ( $\square$ ) and derivative (+) versus time, from the injection test in section 349.4-354.4 m in borehole KFR27.

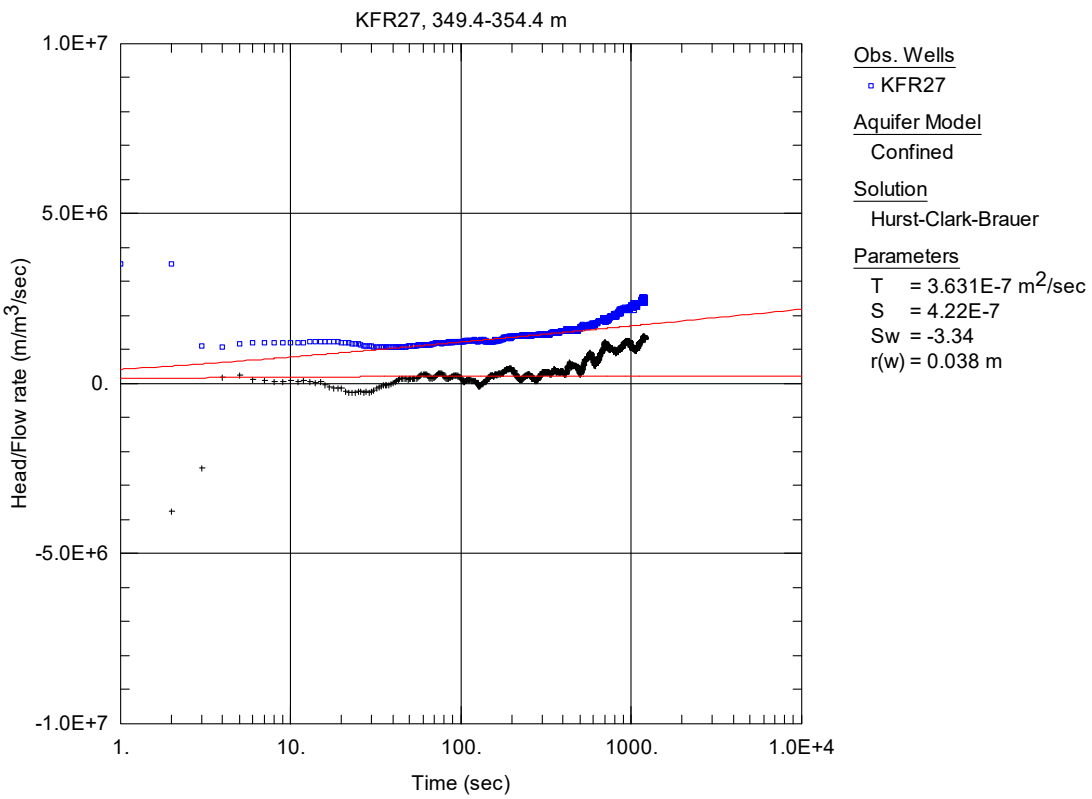


**Figure A2-176.** Lin-log plot of head/flow rate (□) and derivative (+) versus time, from the injection test in section 349.4-354.4 m in borehole KFR27.

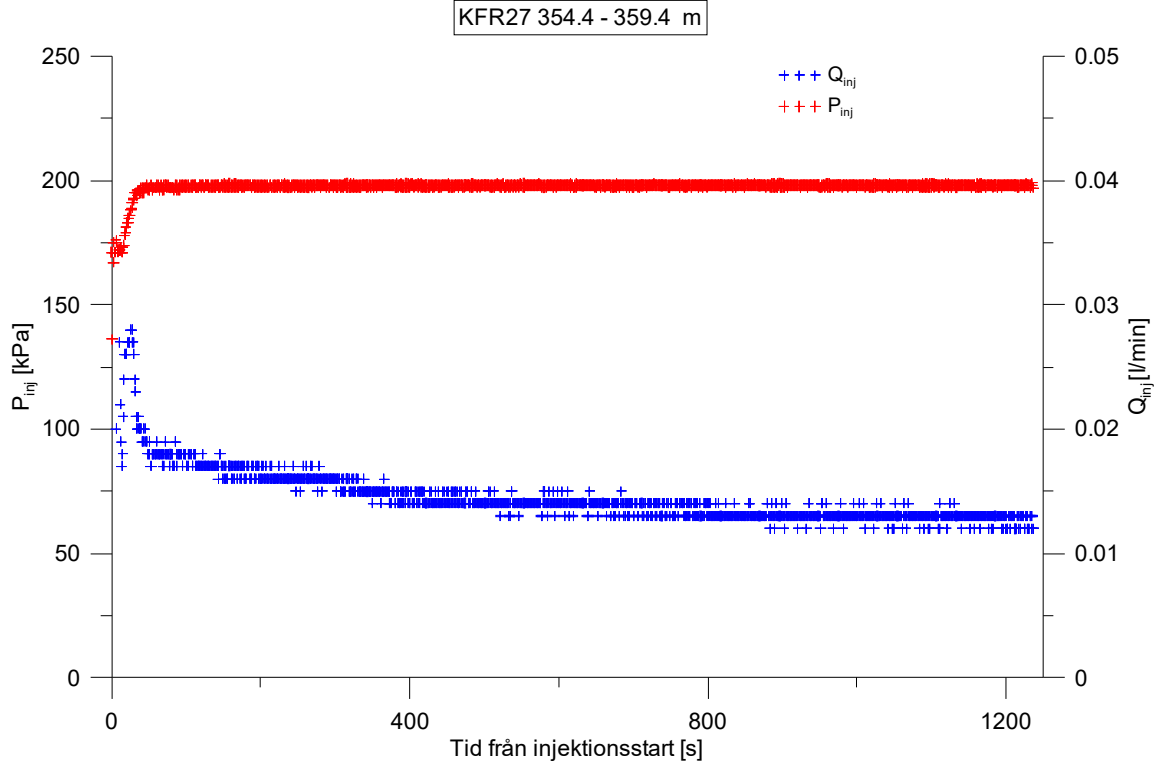


**Figure A2-177.** Linear plot of flow rate ( $Q$ ) and pressure ( $P$ ) versus time from the injection test in section 354.4-359.4 m in borehole KFR27.

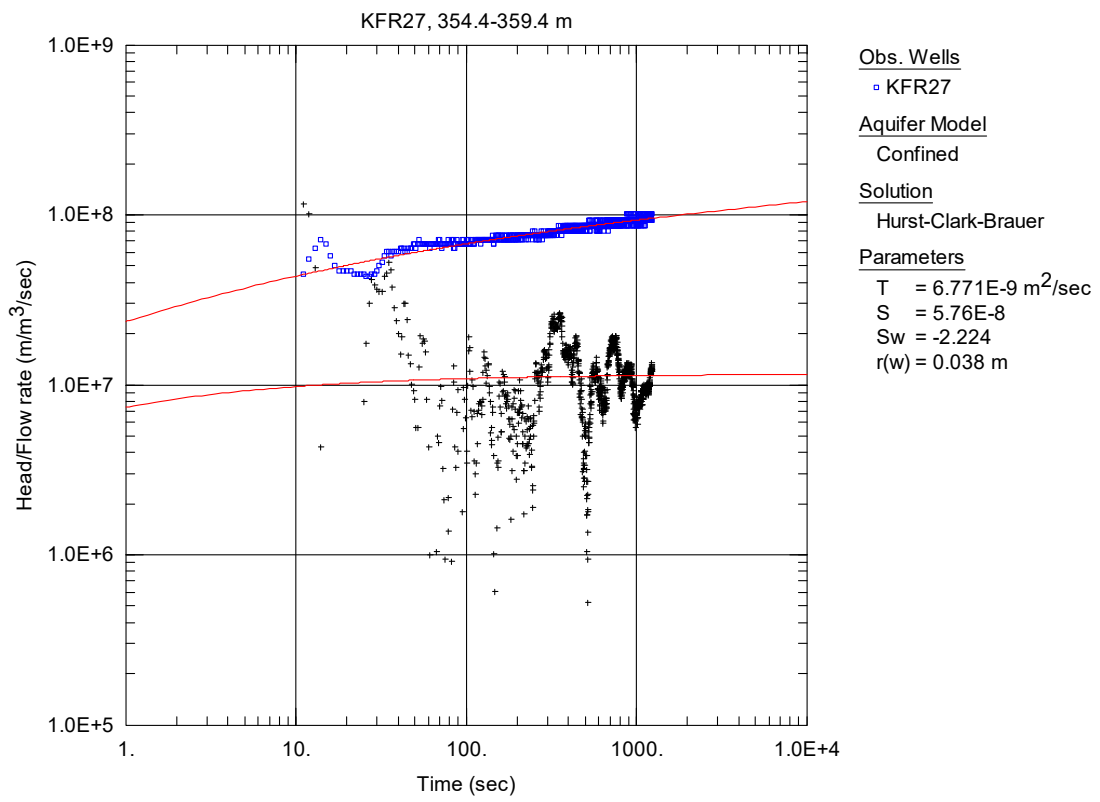


**Figure A2-178.** Log-log plot of head/flow rate (□) and derivative (+) versus time, from the injection test in section 354.4-359.4 m in borehole KFR27.

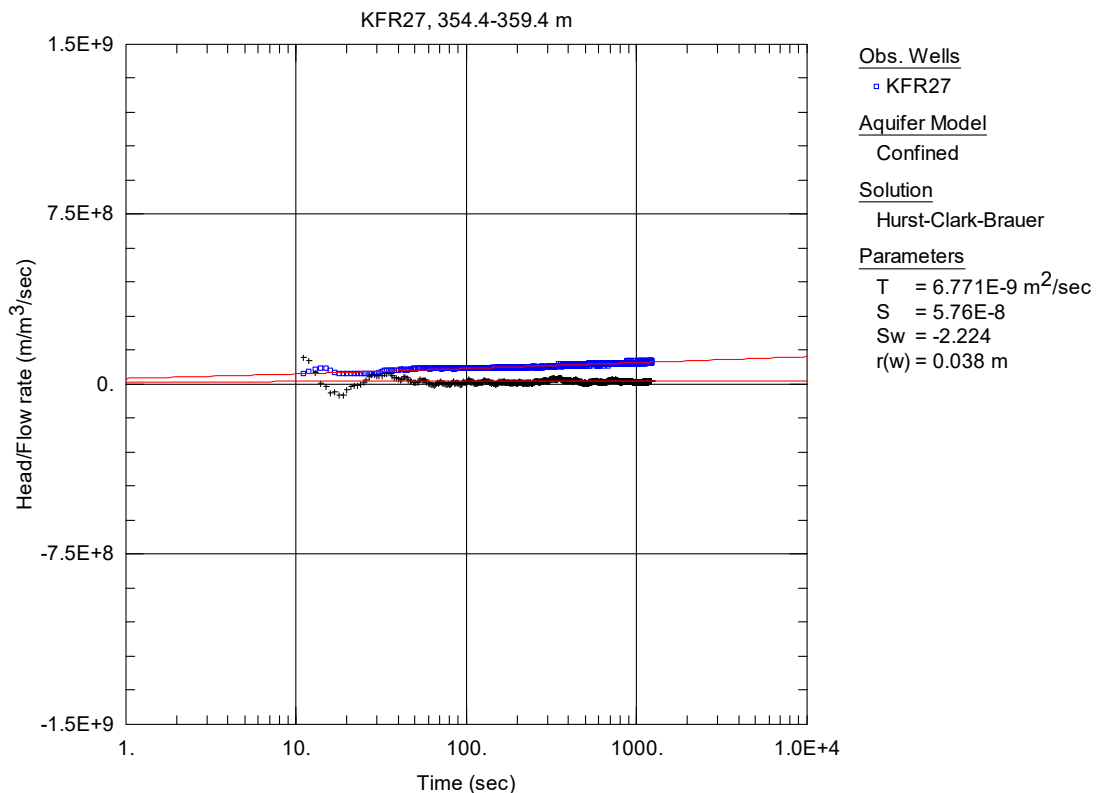


**Figure A2-179.** Lin-log plot of head/flow rate (□) and derivative (+) versus time, from the injection test in section 354.4-359.4 m in borehole KFR27.

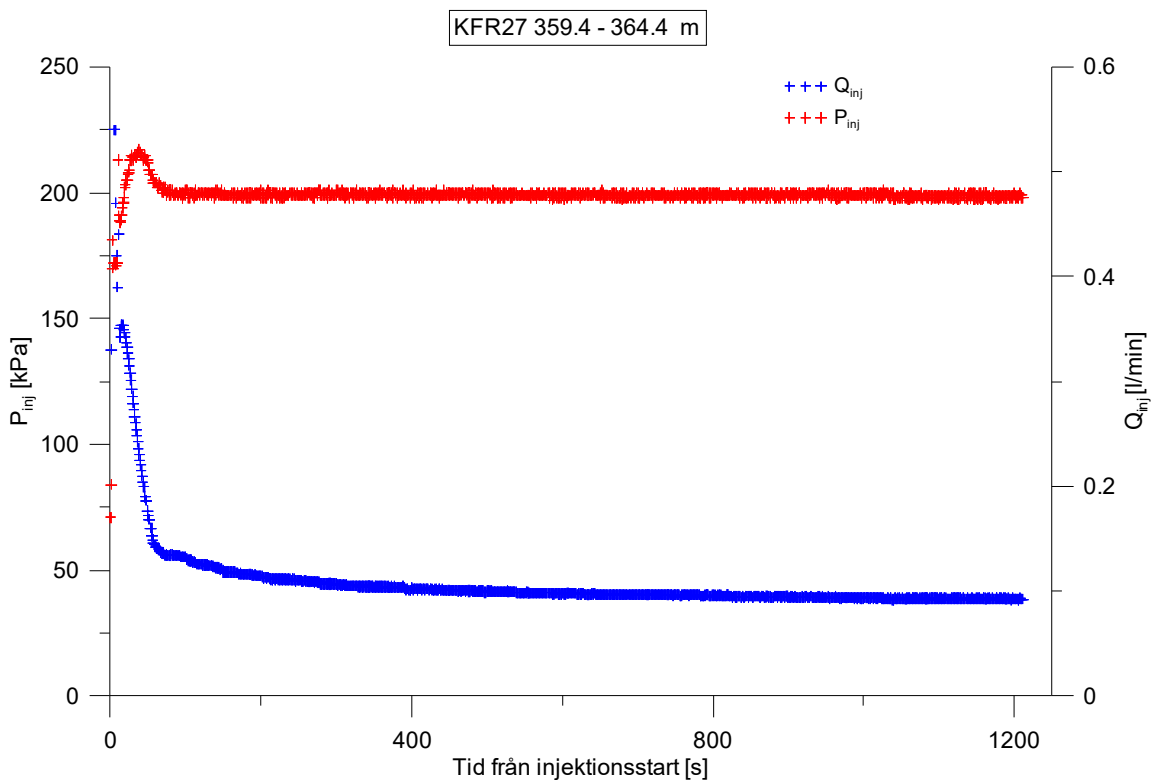


**Figure A2-180.** Linear plot of flow rate ( $Q$ ) and pressure ( $P$ ) versus time from the injection test in section 359.4-364.4 m in borehole KFR27.

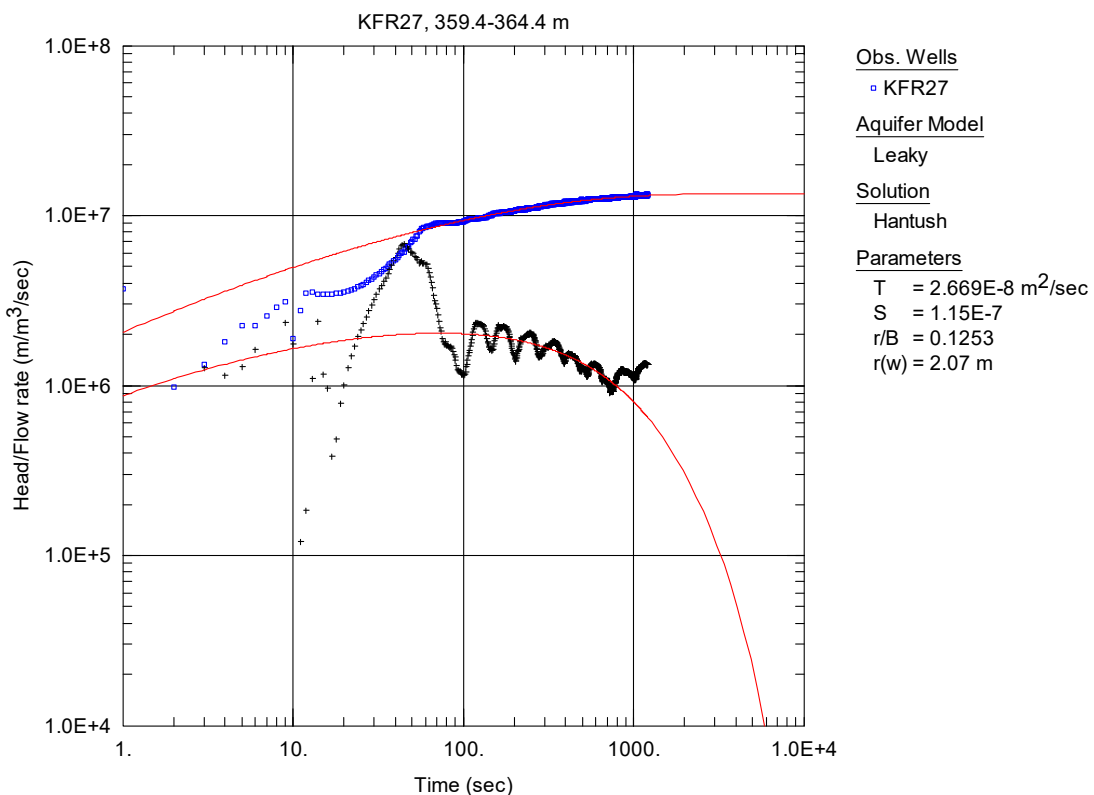


**Figure A2-181.** Log-log plot of head/flow rate ( $\square$ ) and derivative ( $+$ ) versus time, from the injection test in section 359.4-364.4 m in borehole KFR27.

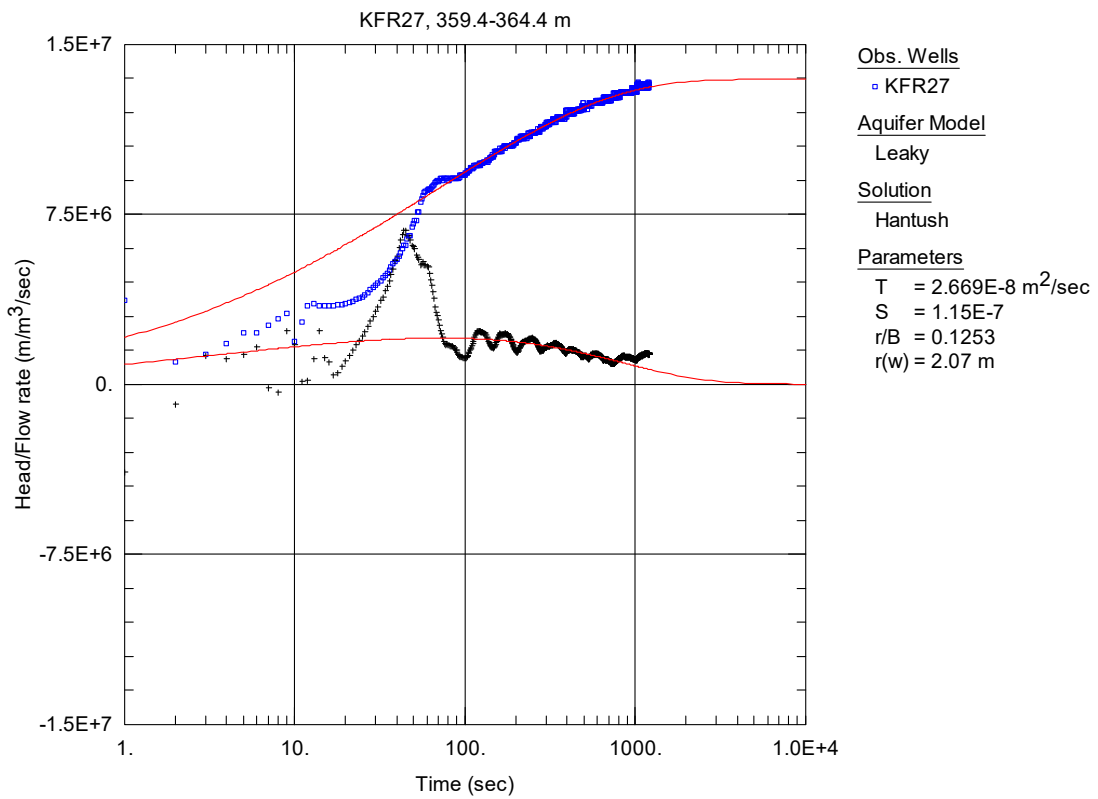


**Figure A2-182.** Lin-log plot of head/flow rate (□) and derivative (+) versus time, from the injection test in section 359.4-364.4 m in borehole KFR27.

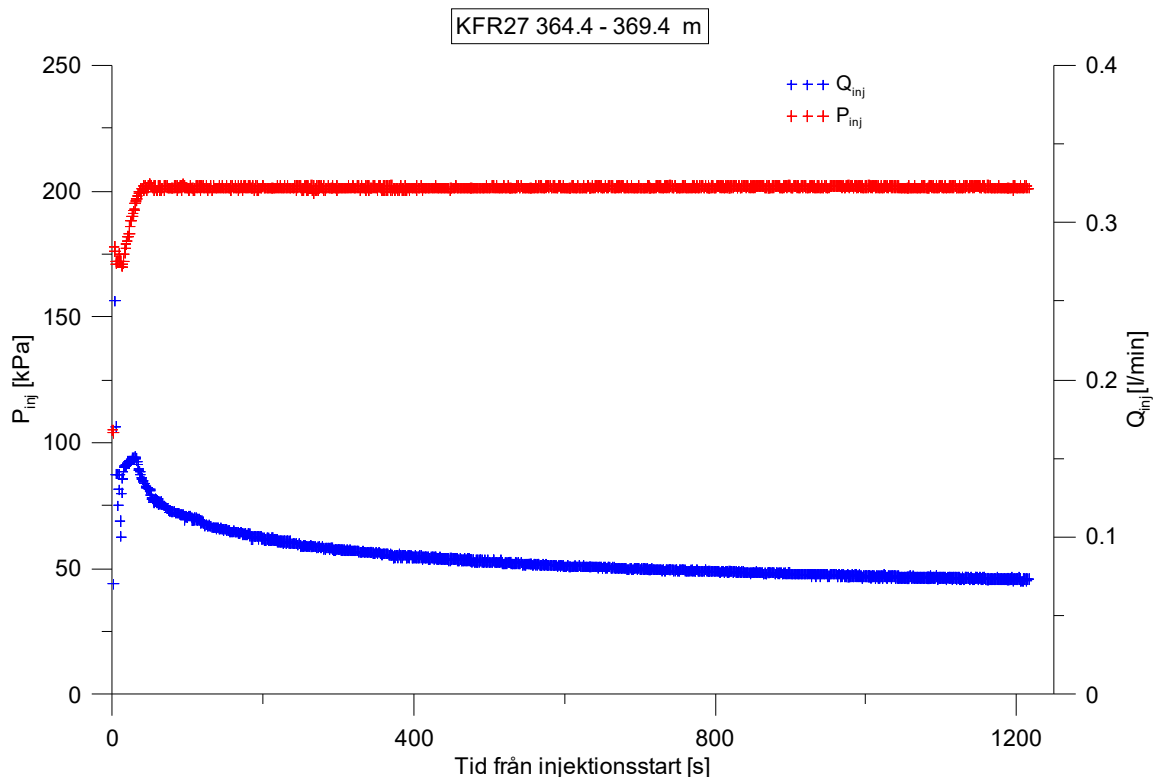


**Figure A2-183.** Linear plot of flow rate ( $Q$ ) and pressure ( $P$ ) versus time from the injection test in section 364.4-369.4 m in borehole KFR27.

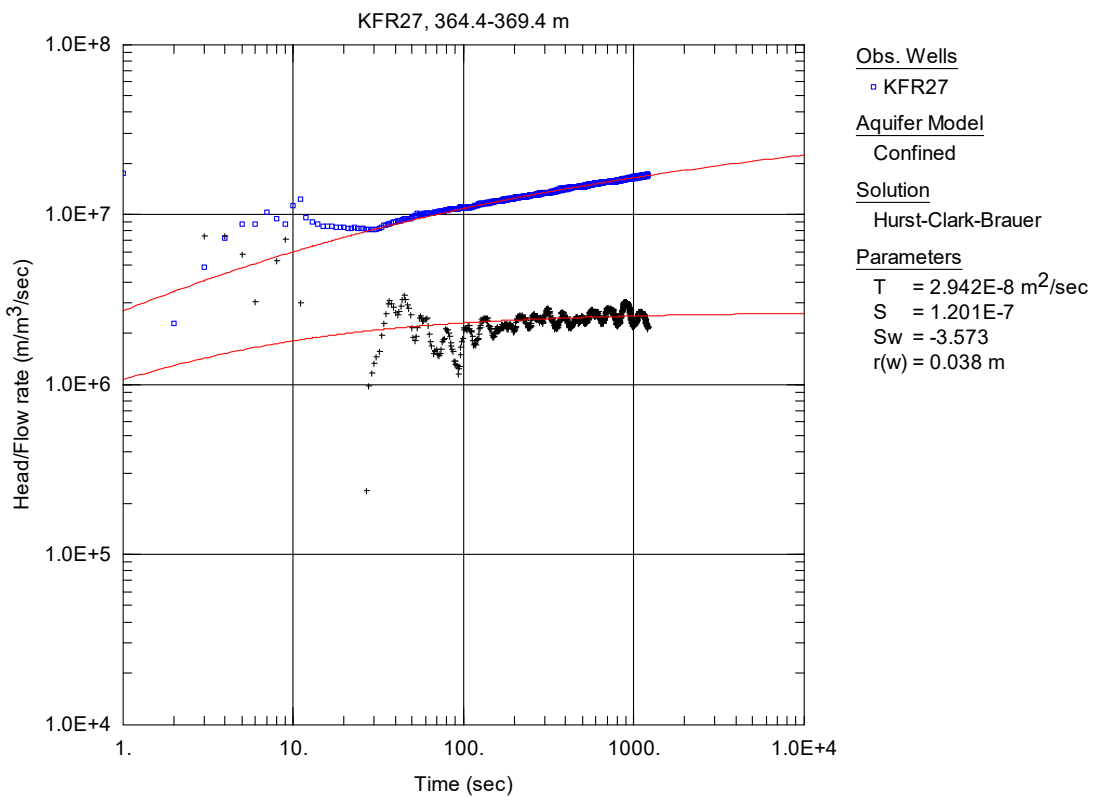


**Figure A2-184.** Log-log plot of head/flow rate ( $\square$ ) and derivative (+) versus time, from the injection test in section 364.4-369.4 m in borehole KFR27.

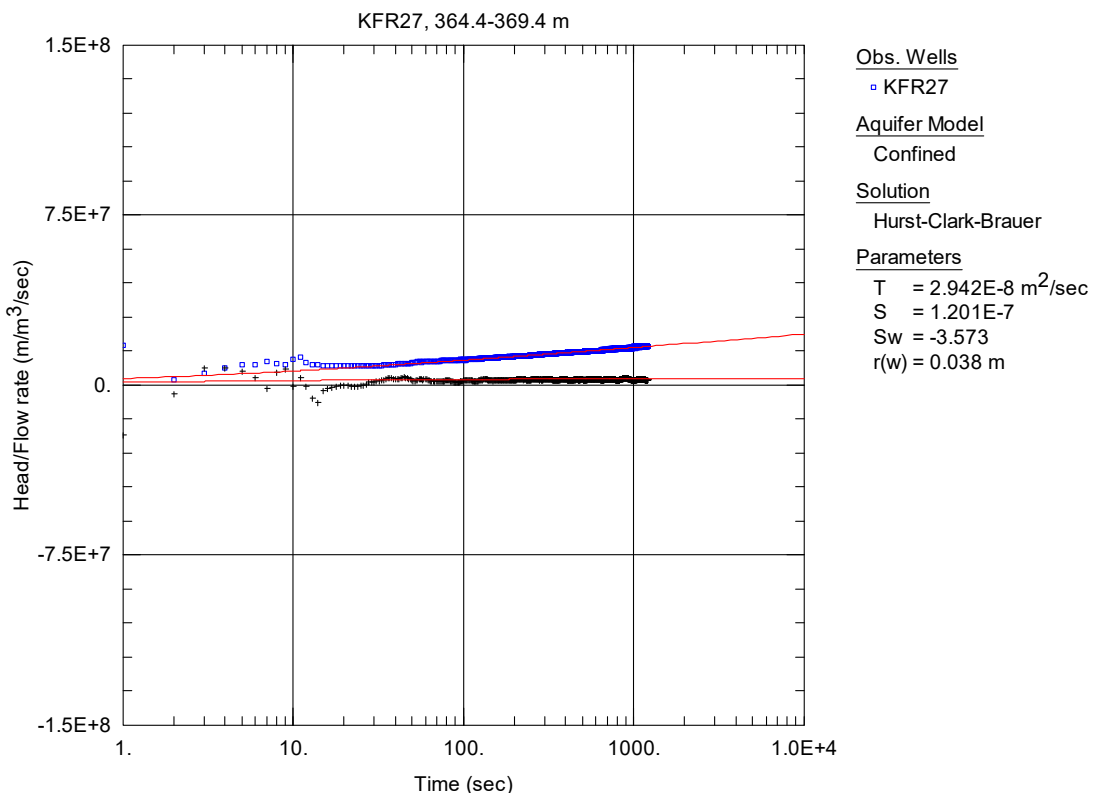


**Figure A2-185.** Lin-log plot of head/flow rate ( $\square$ ) and derivative (+) versus time, from the injection test in section 364.4-369.4 m in borehole KFR27.

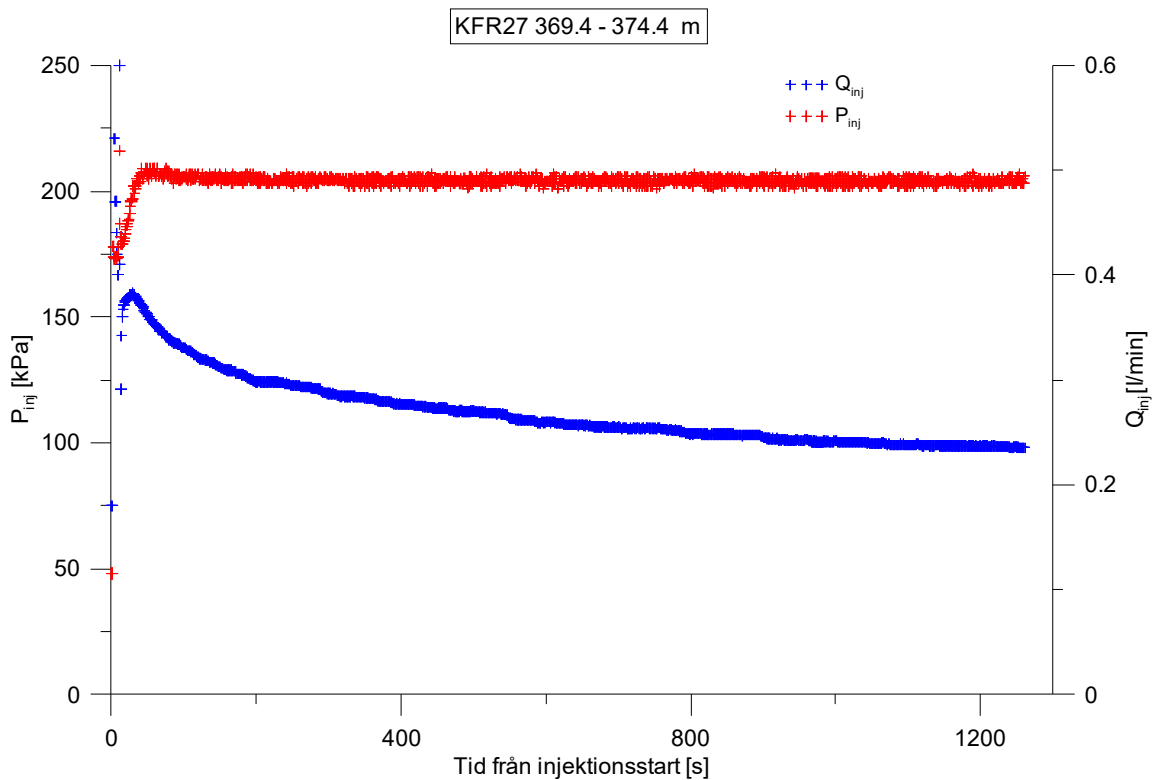


**Figure A2-186.** Linear plot of flow rate ( $Q$ ) and pressure ( $P$ ) versus time from the injection test in section 369.4-374.4 m in borehole KFR27.

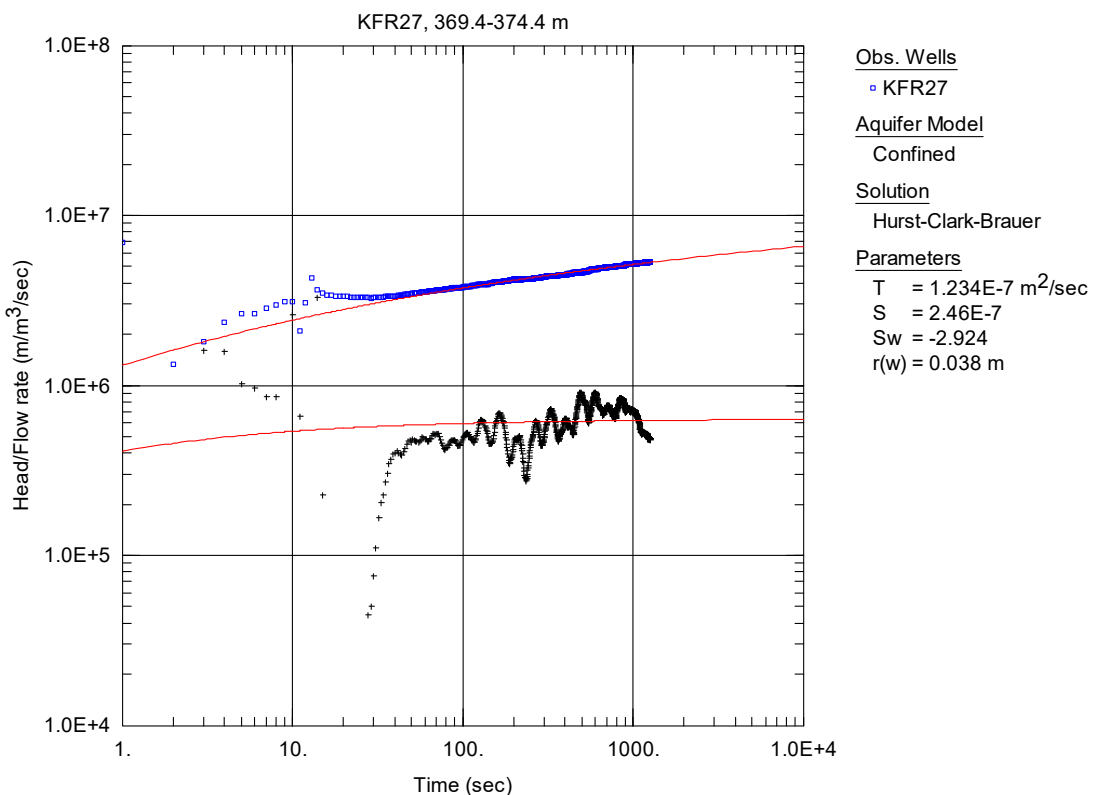


**Figure A2-187.** Log-log plot of head/flow rate ( $\square$ ) and derivative (+) versus time, from the injection test in section 369.4-374.4 m in borehole KFR27.

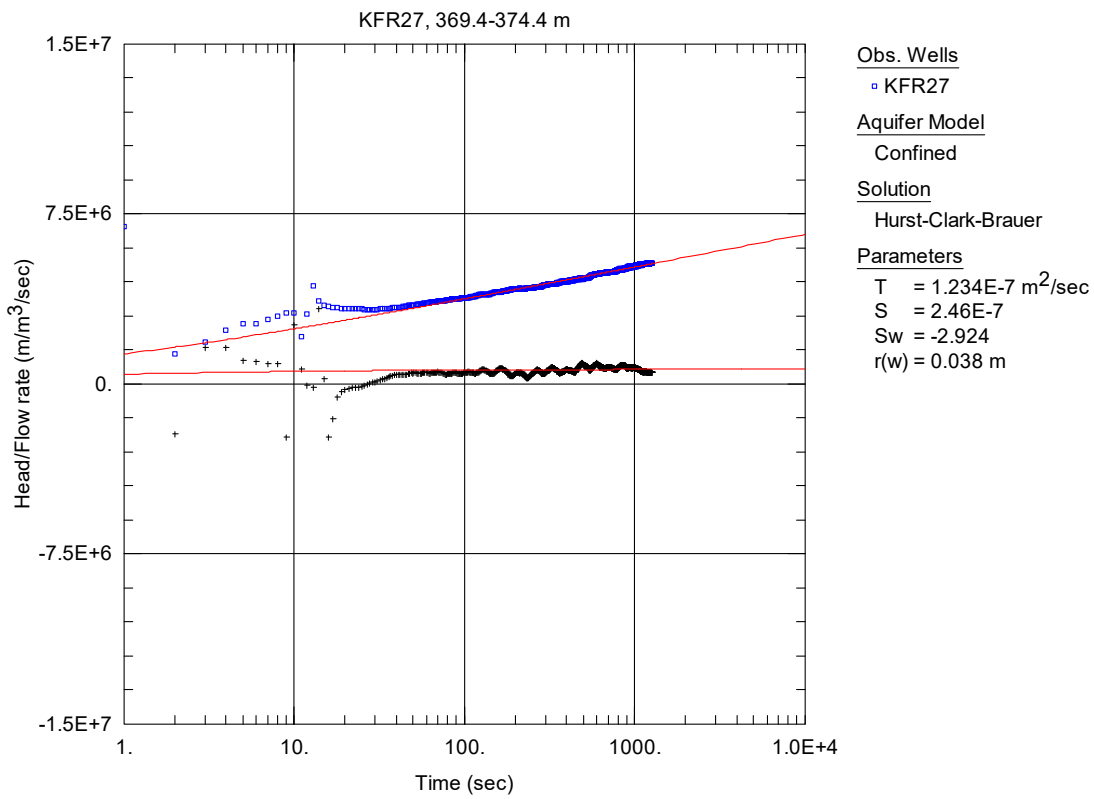


**Figure A2-188.** Lin-log plot of head/flow rate (□) and derivative (+) versus time, from the injection test in section 369.4-374.4 m in borehole KFR27.

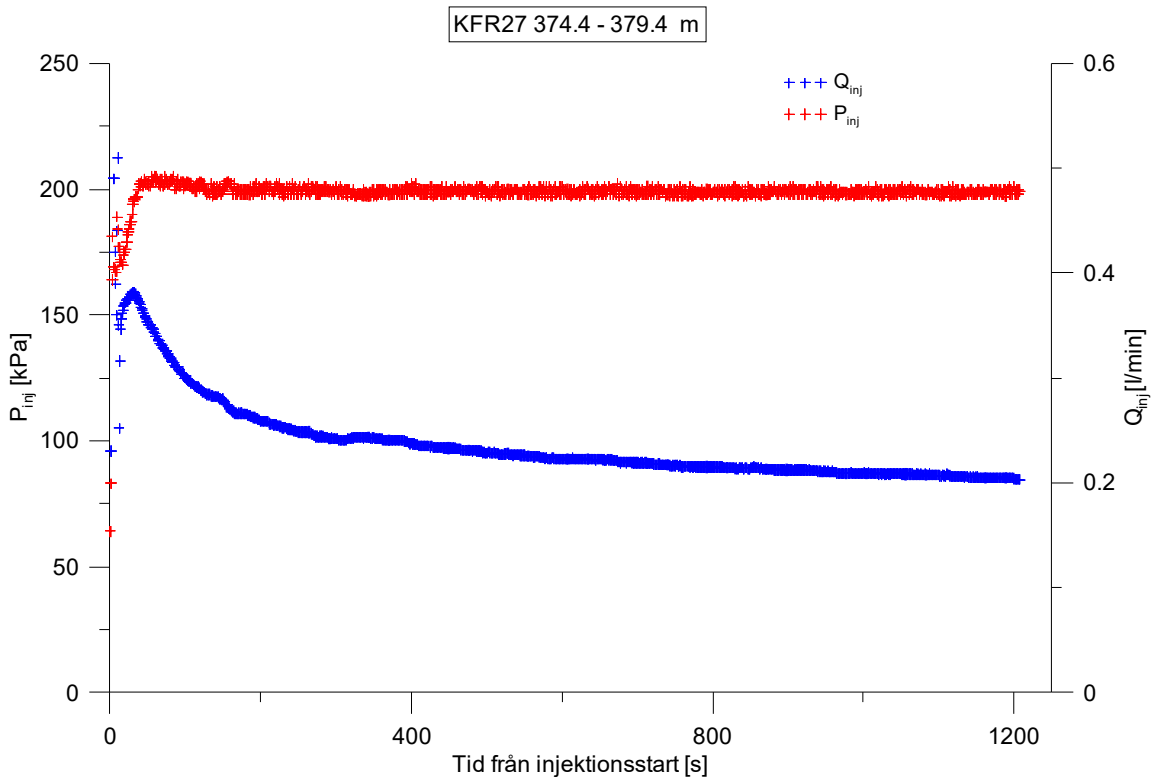


**Figure A2-189.** Linear plot of flow rate ( $Q$ ) and pressure ( $P$ ) versus time from the injection test in section 374.4-379.4 m in borehole KFR27.

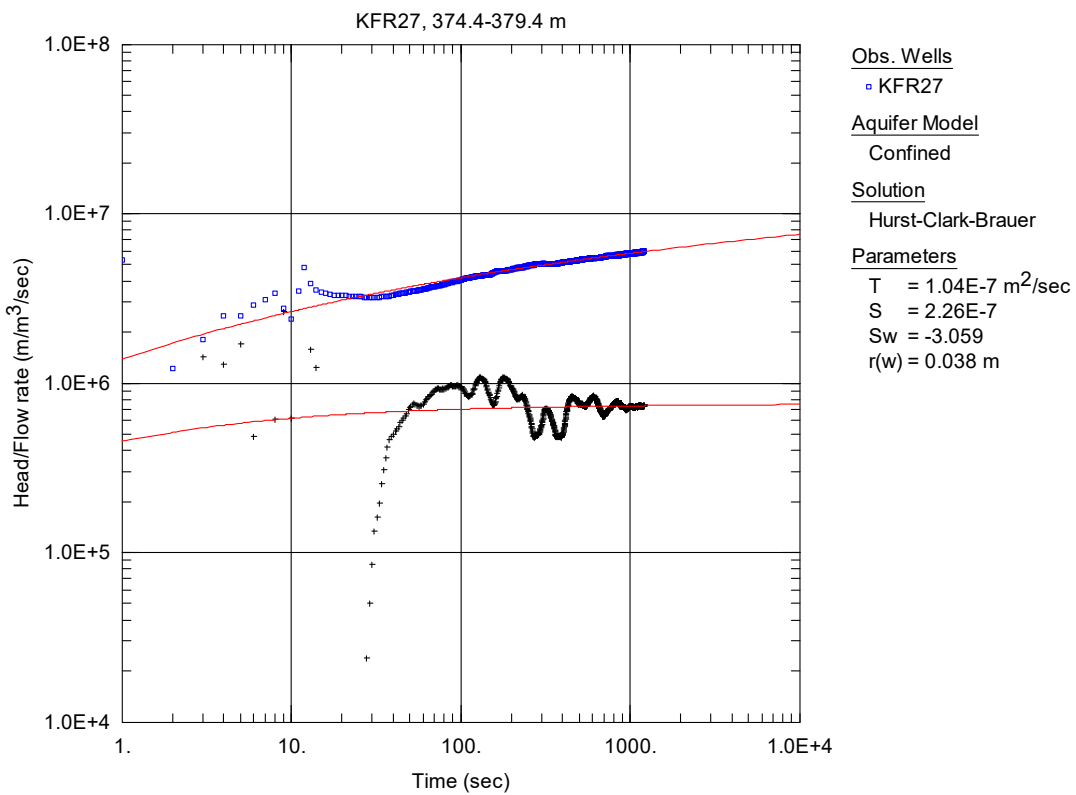


**Figure A2-190.** Log-log plot of head/flow rate (□) and derivative (+) versus time, from the injection test in section 374.4-379.4 m in borehole KFR27.

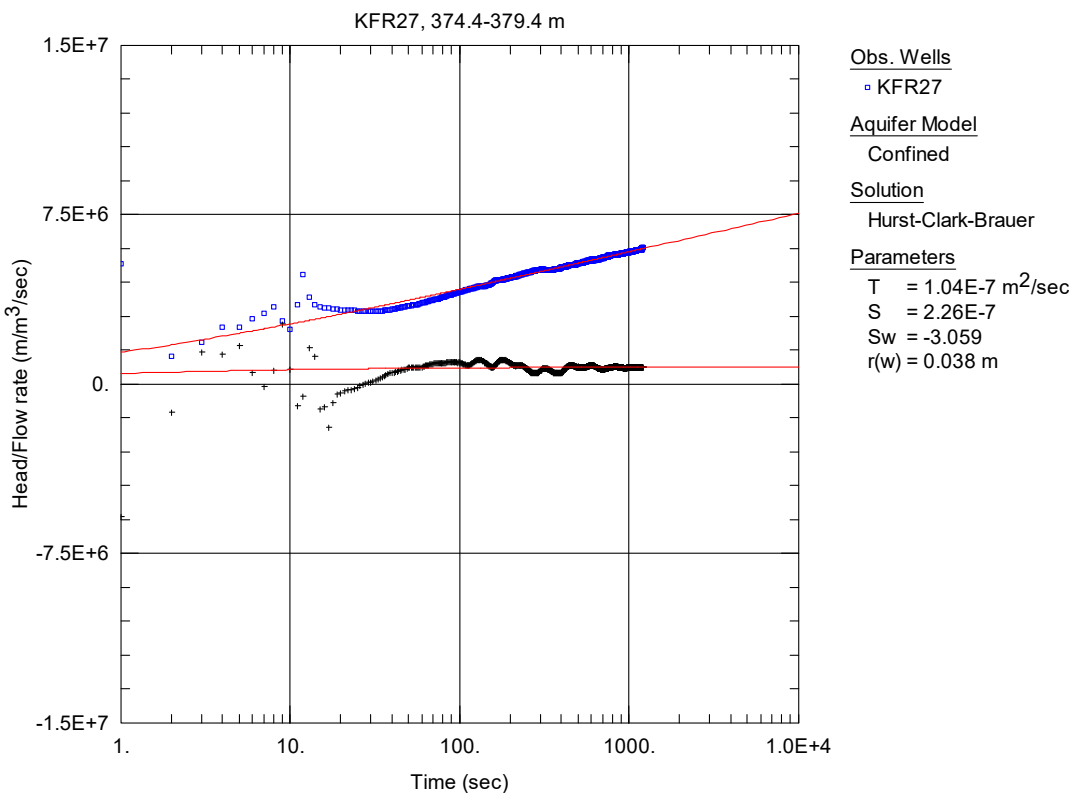


**Figure A2-191.** Lin-log plot of head/flow rate (□) and derivative (+) versus time, from the injection test in section 374.4-379.4 m in borehole KFR27.

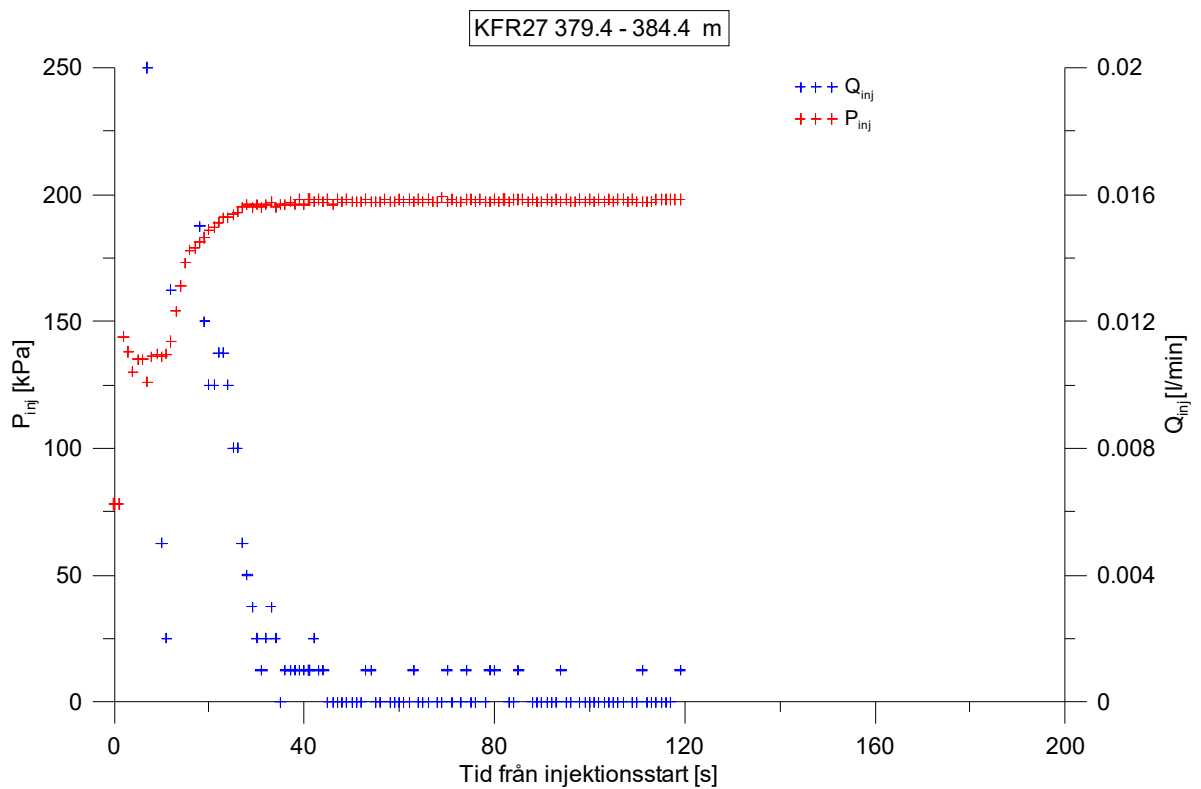


**Figure A2-192.** Linear plot of flow rate ( $Q$ ) and pressure ( $P$ ) versus time from the injection test in section 379.4-384.4 m in borehole KFR27.

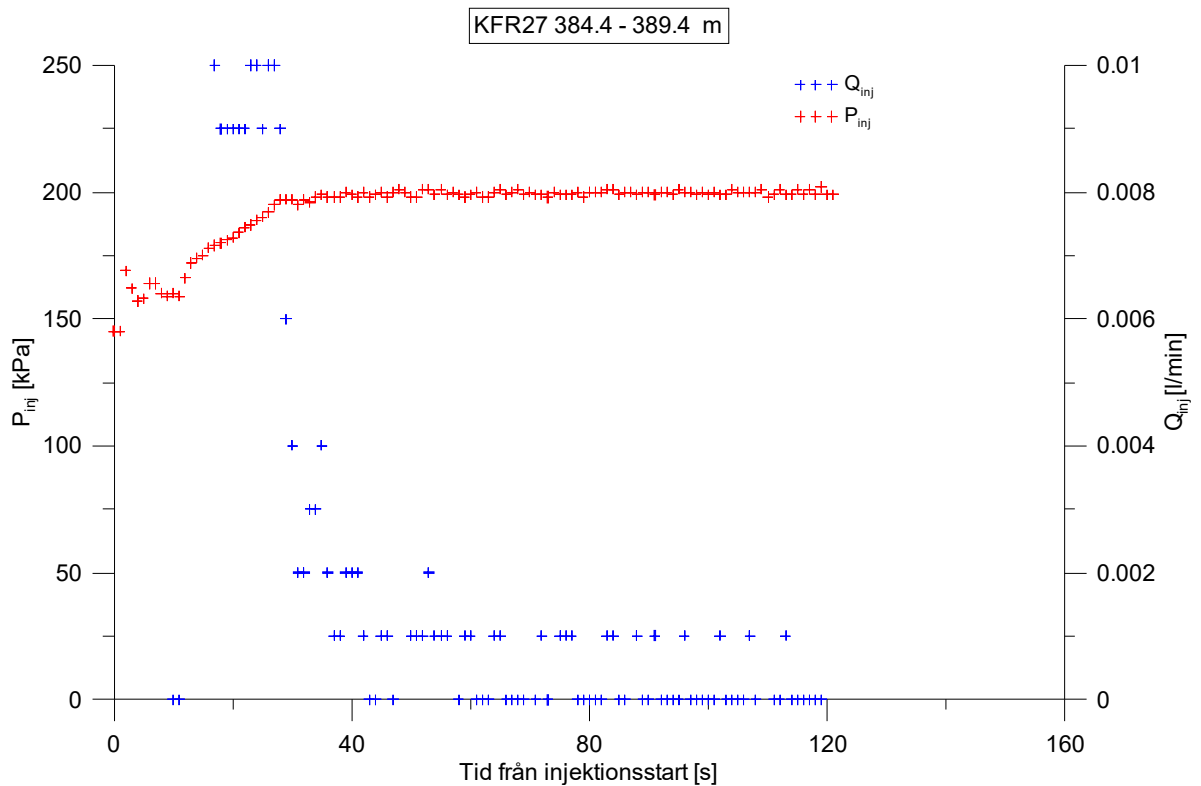


**Figure A2-193.** Linear plot of flow rate ( $Q$ ) and pressure ( $P$ ) versus time from the injection test in section 384.4-389.4 m in borehole KFR27.

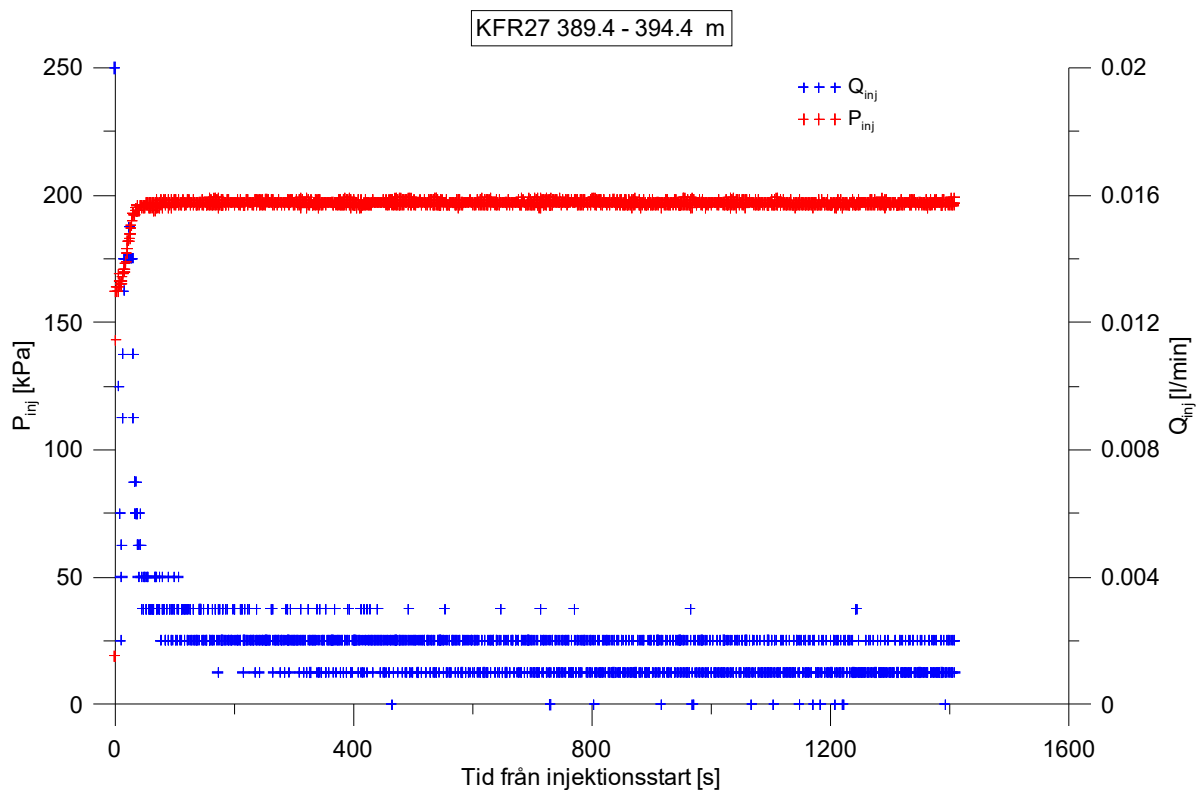


**Figure A2-194.** Linear plot of flow rate ( $Q$ ) and pressure ( $P$ ) versus time from the injection test in section 389.4-394.4 m in borehole KFR27.

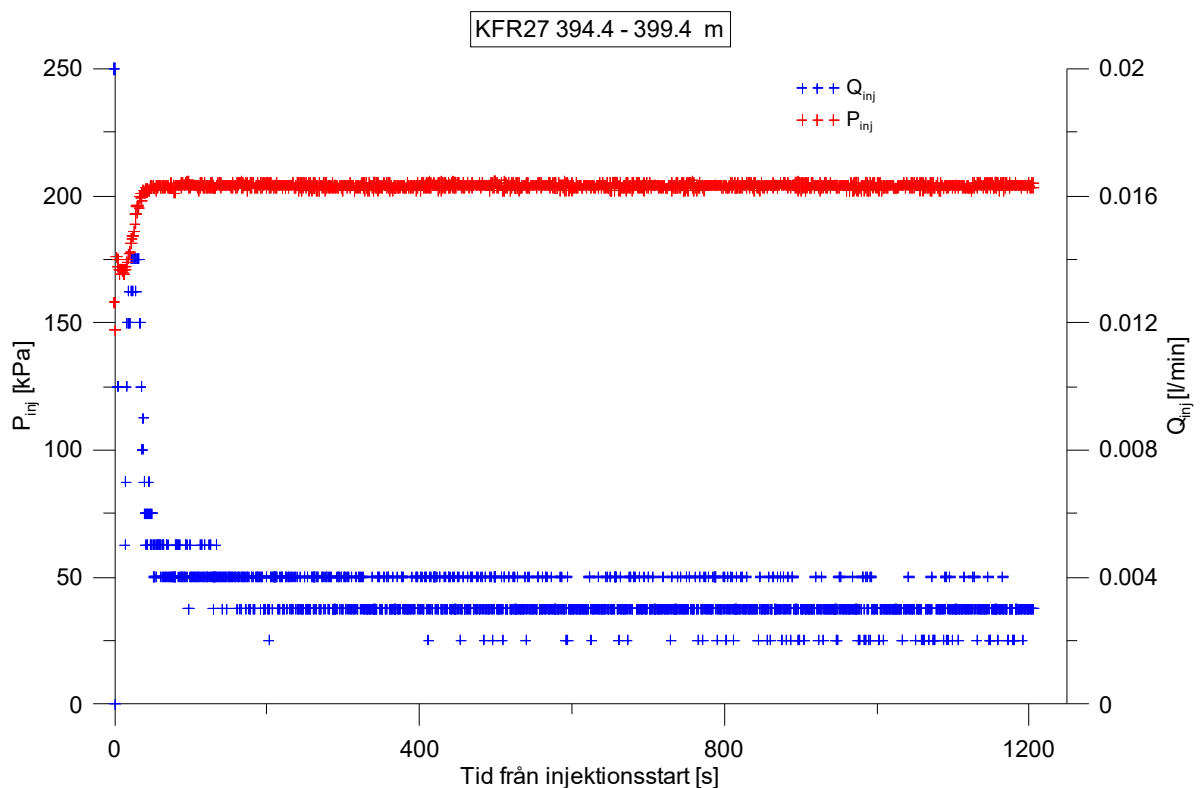


**Figure A2-195.** Linear plot of flow rate ( $Q$ ) and pressure ( $P$ ) versus time from the injection test in section 394.4-399.4 m in borehole KFR27.

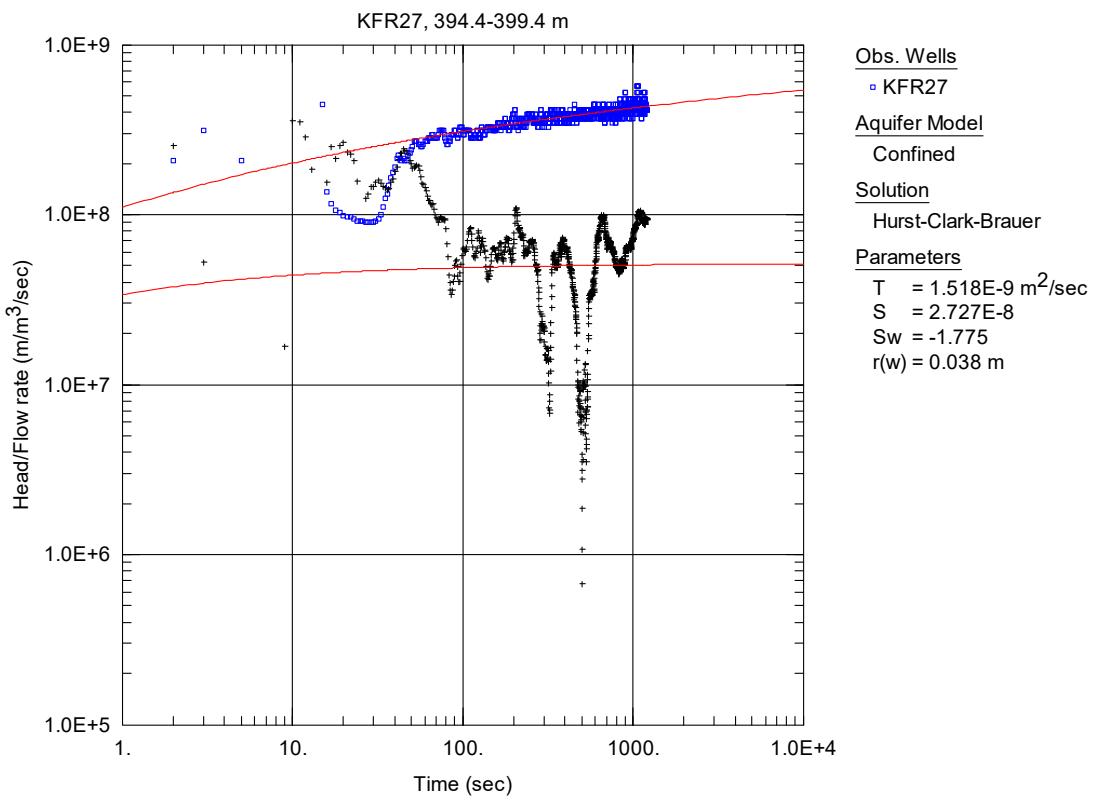


**Figure A2-196.** Log-log plot of head/flow rate (□) and derivative (+) versus time, from the injection test in section 394.4-399.4 m in borehole KFR27.

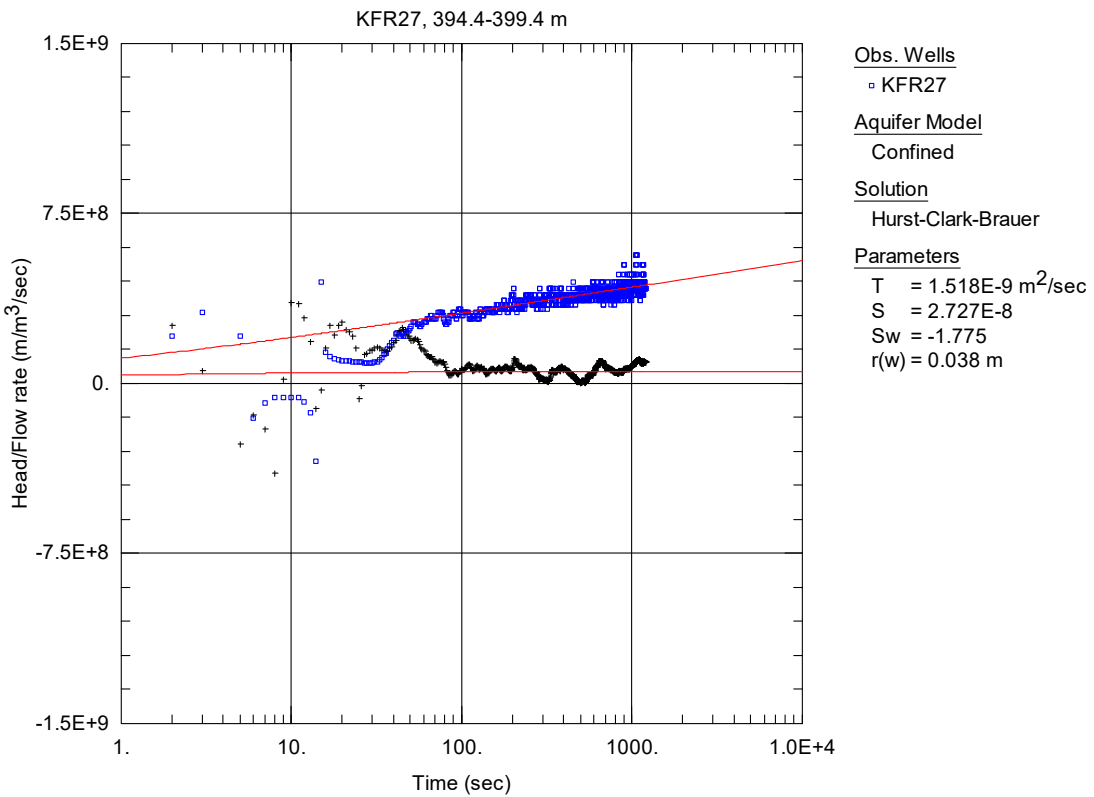


**Figure A2-197.** Lin-log plot of head/flow rate (□) and derivative (+) versus time, from the injection test in section 394.4-399.4 m in borehole KFR27.

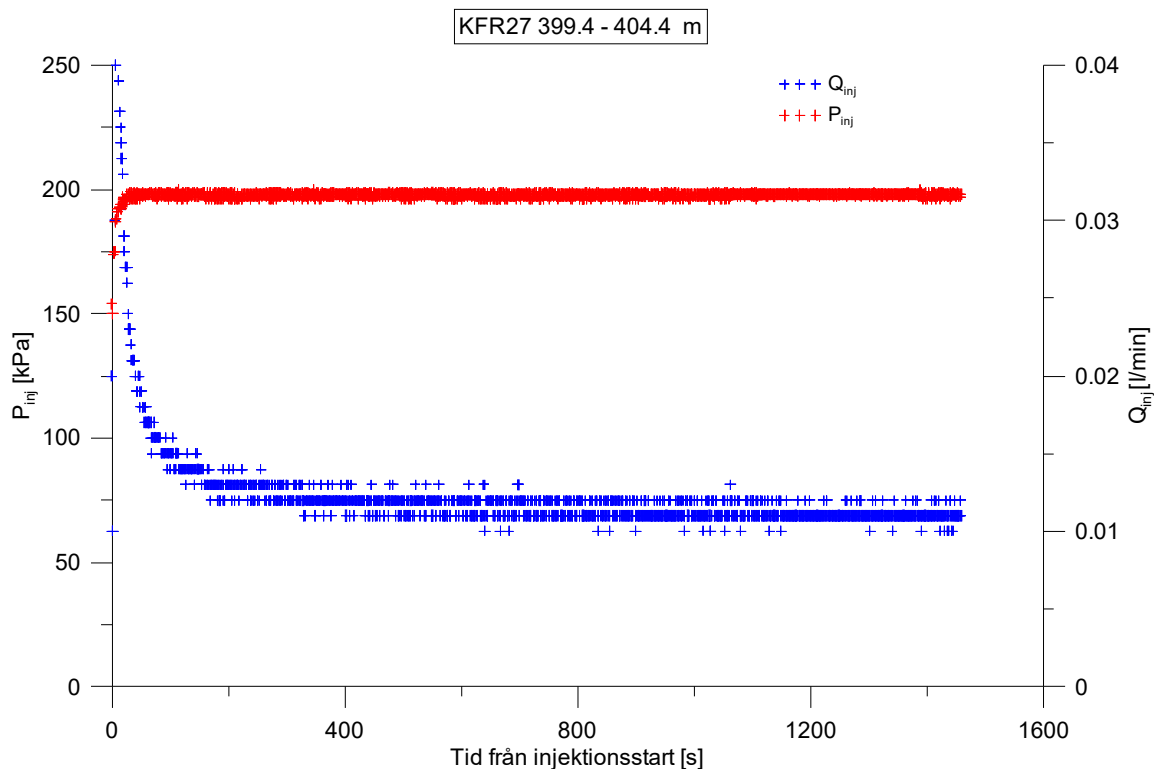


**Figure A2-198.** Linear plot of flow rate ( $Q$ ) and pressure ( $P$ ) versus time from the injection test in section 399.4-404.4 m in borehole KFR27.

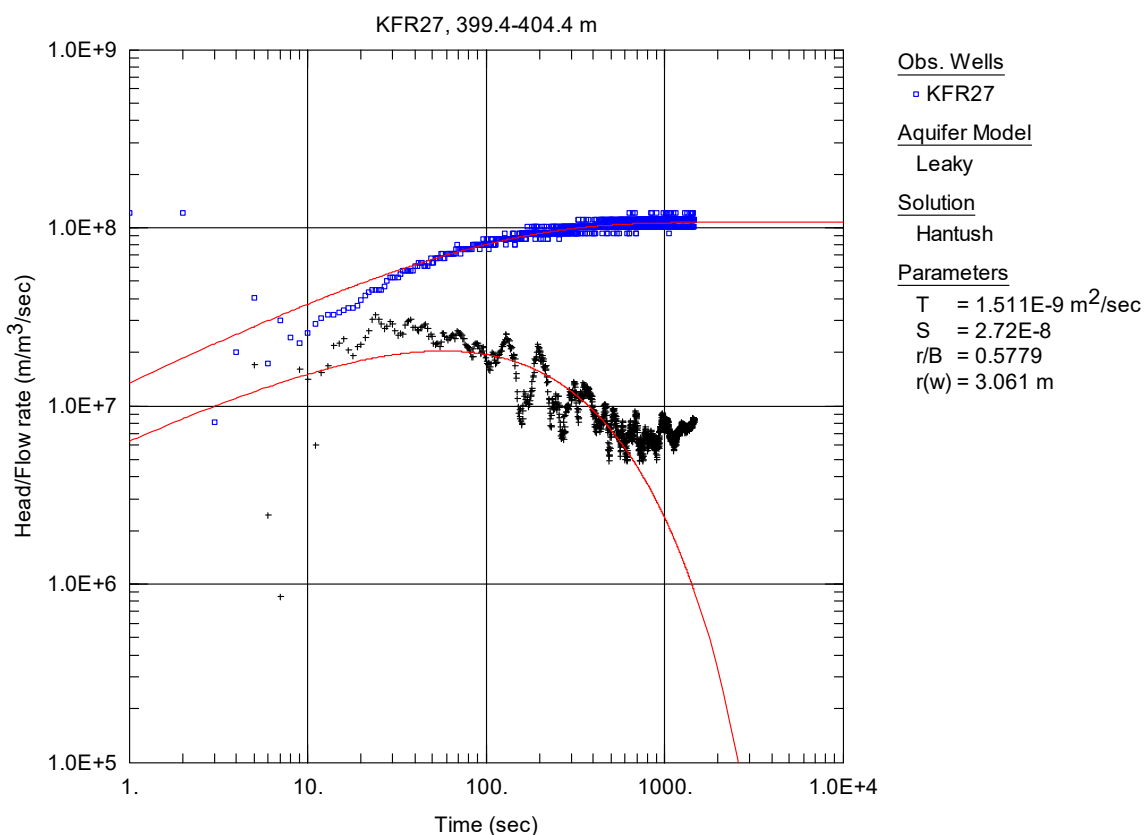


**Figure A2-199.** Log-log plot of head/flow rate (□) and derivative (+) versus time, from the injection test in section 399.4-404.4 m in borehole KFR27.

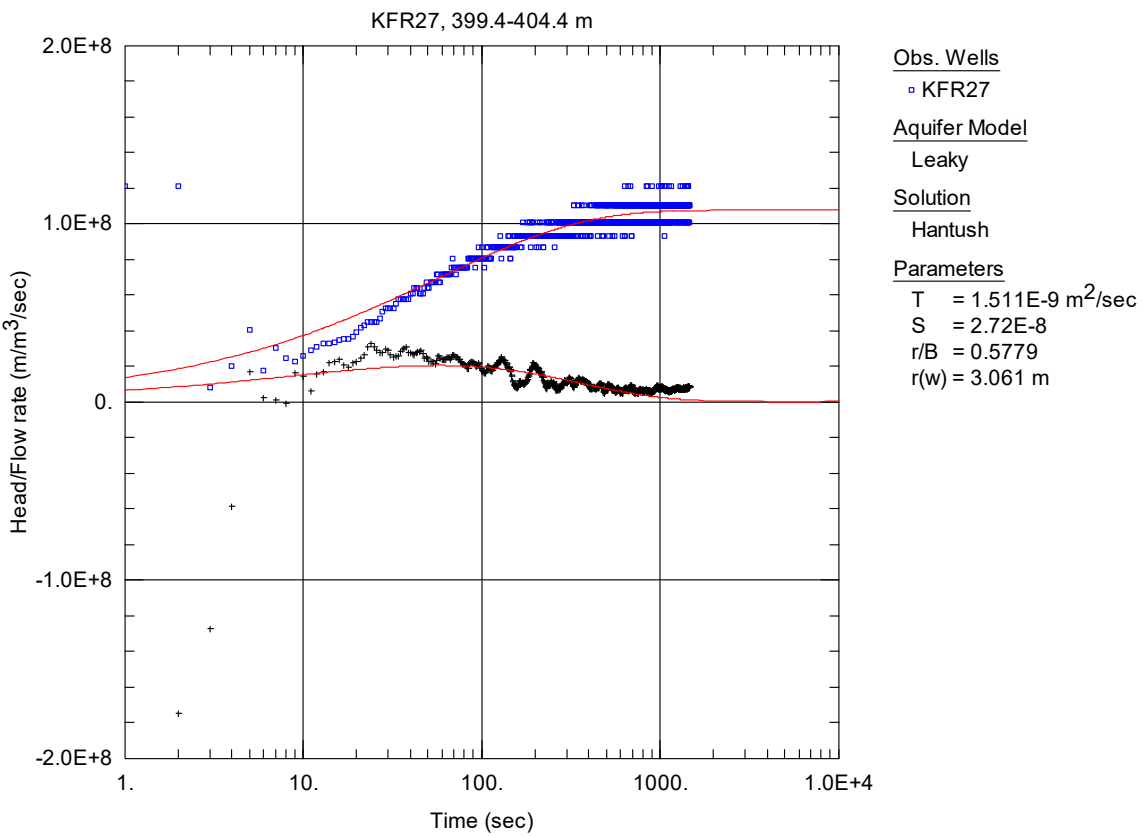


**Figure A2-200.** Lin-log plot of head/flow rate (□) and derivative (+) versus time, from the injection test in section 399.4-404.4 m in borehole KFR27.

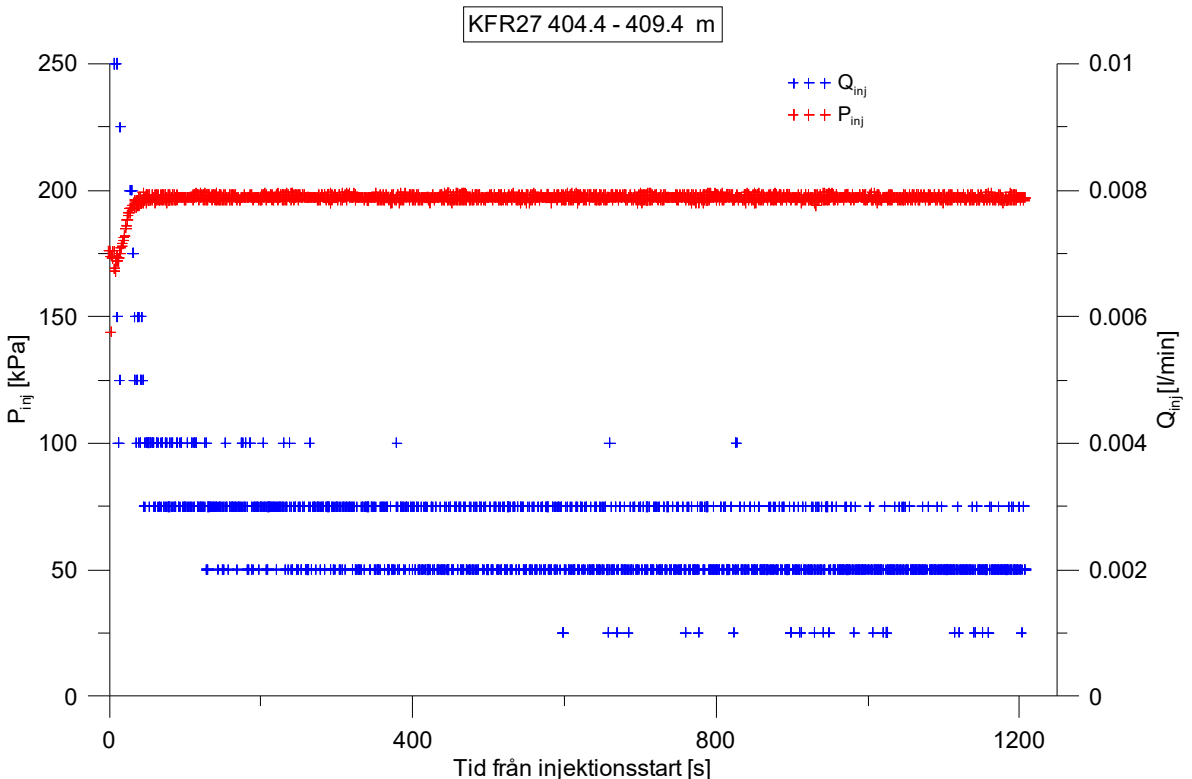


**Figure A2-201.** Linear plot of flow rate ( $Q$ ) and pressure ( $P$ ) versus time from the injection test in section 404.4-409.4 m in borehole KFR27.

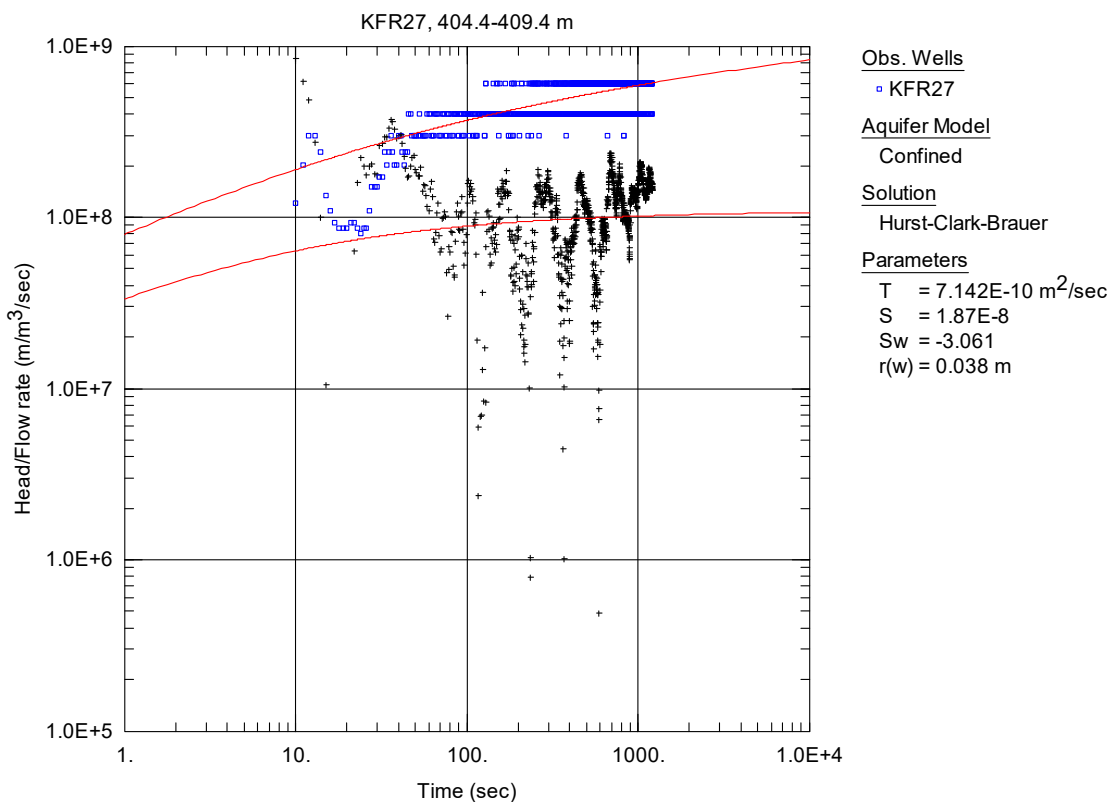


**Figure A2-202.** Log-log plot of head/flow rate (□) and derivative (+) versus time, from the injection test in section 404.4-409.4 m in borehole KFR27.

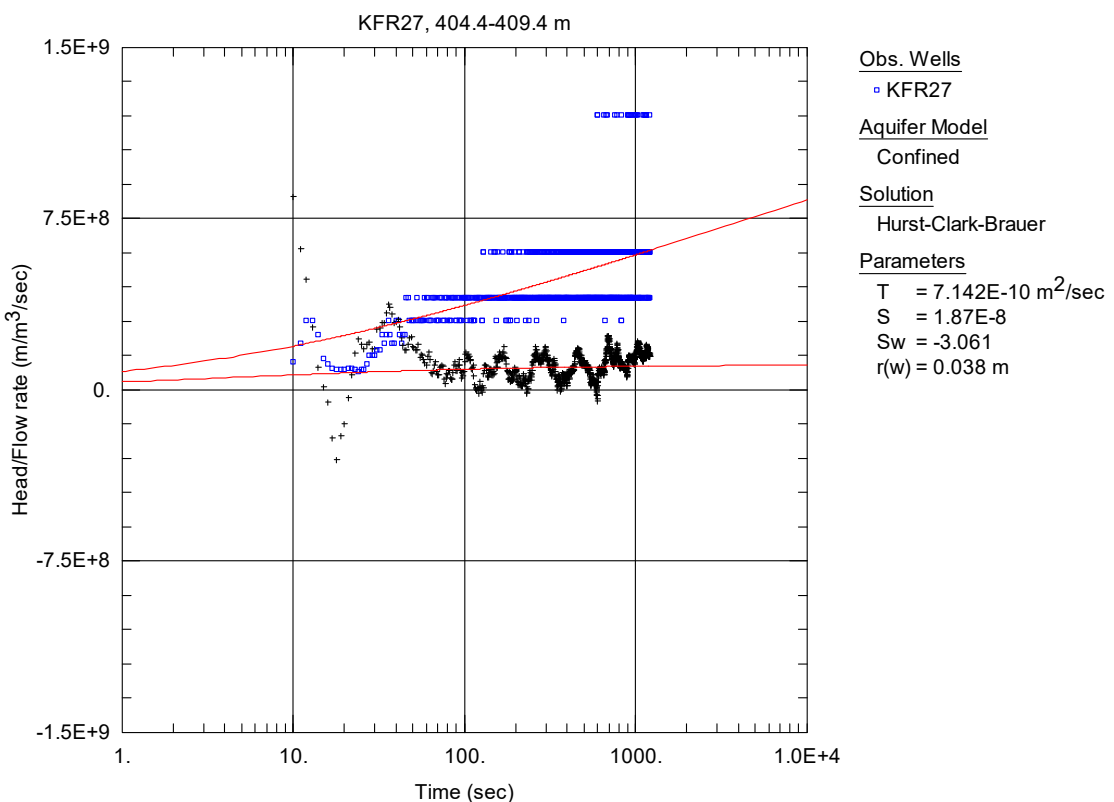


**Figure A2-203.** Lin-log plot of head/flow rate (□) and derivative (+) versus time, from the injection test in section 404.4-409.4 m in borehole KFR27.

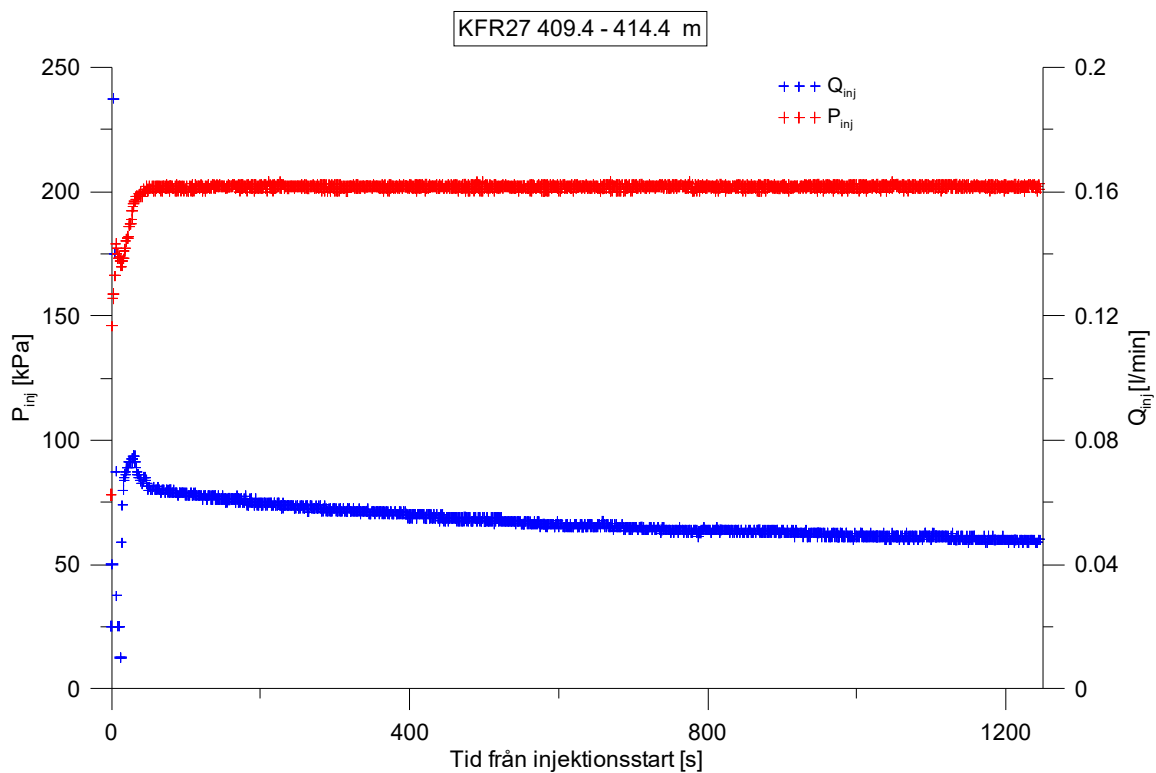


**Figure A2-204.** Linear plot of flow rate ( $Q$ ) and pressure ( $P$ ) versus time from the injection test in section 409.4-414.4 m in borehole KFR27.

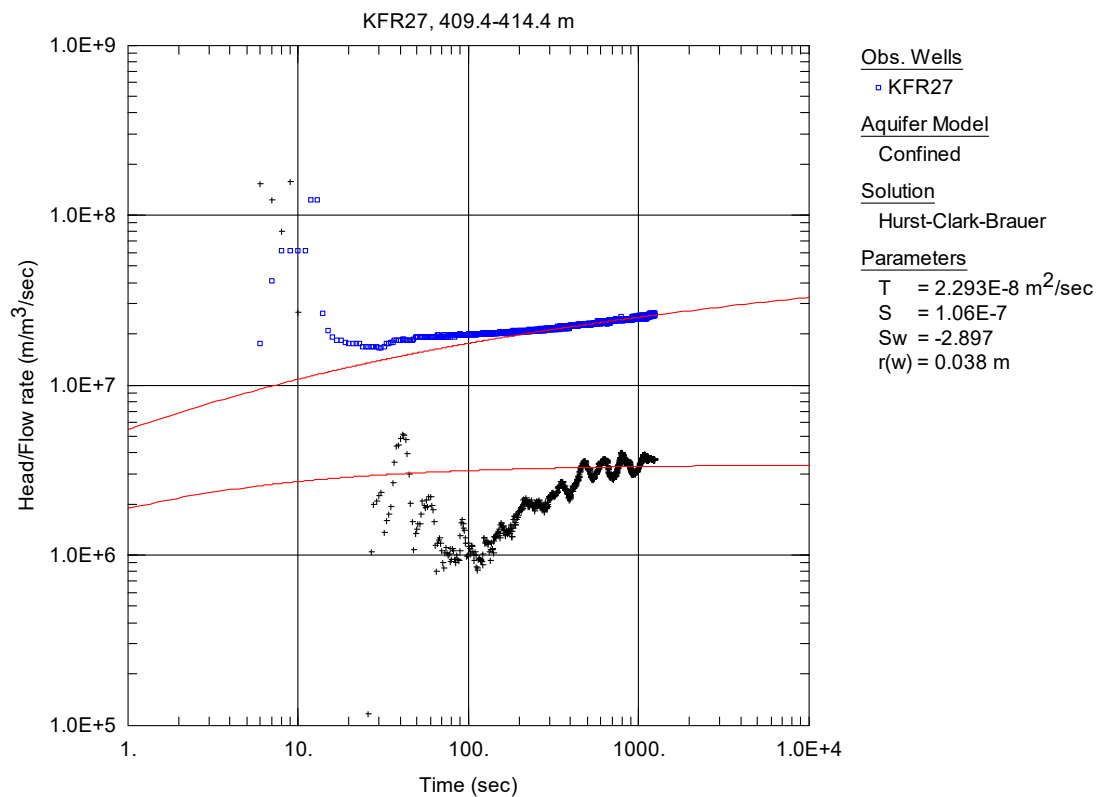


**Figure A2-205.** Log-log plot of head/flow rate (□) and derivative (+) versus time, from the injection test in section 409.4-414.4 m in borehole KFR27.

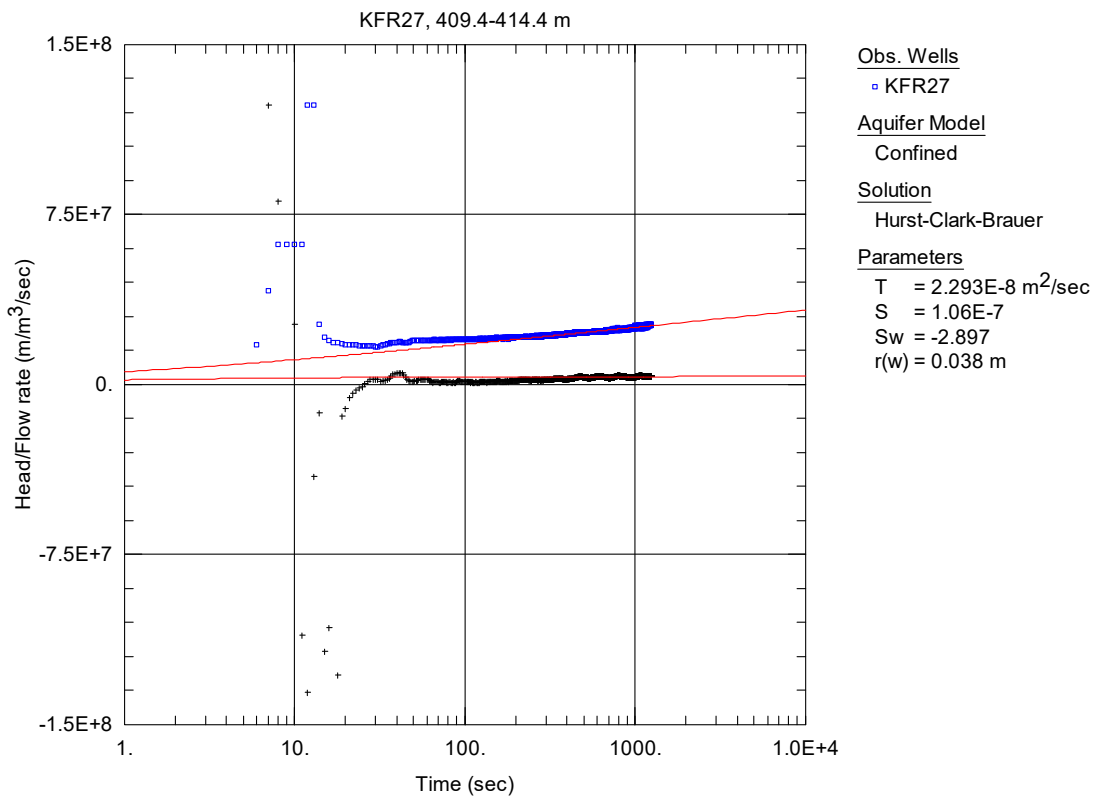


**Figure A2-206.** Lin-log plot of head/flow rate ( $\square$ ) and derivative (+) versus time, from the injection test in section 409.4-414.4 m in borehole KFR27.

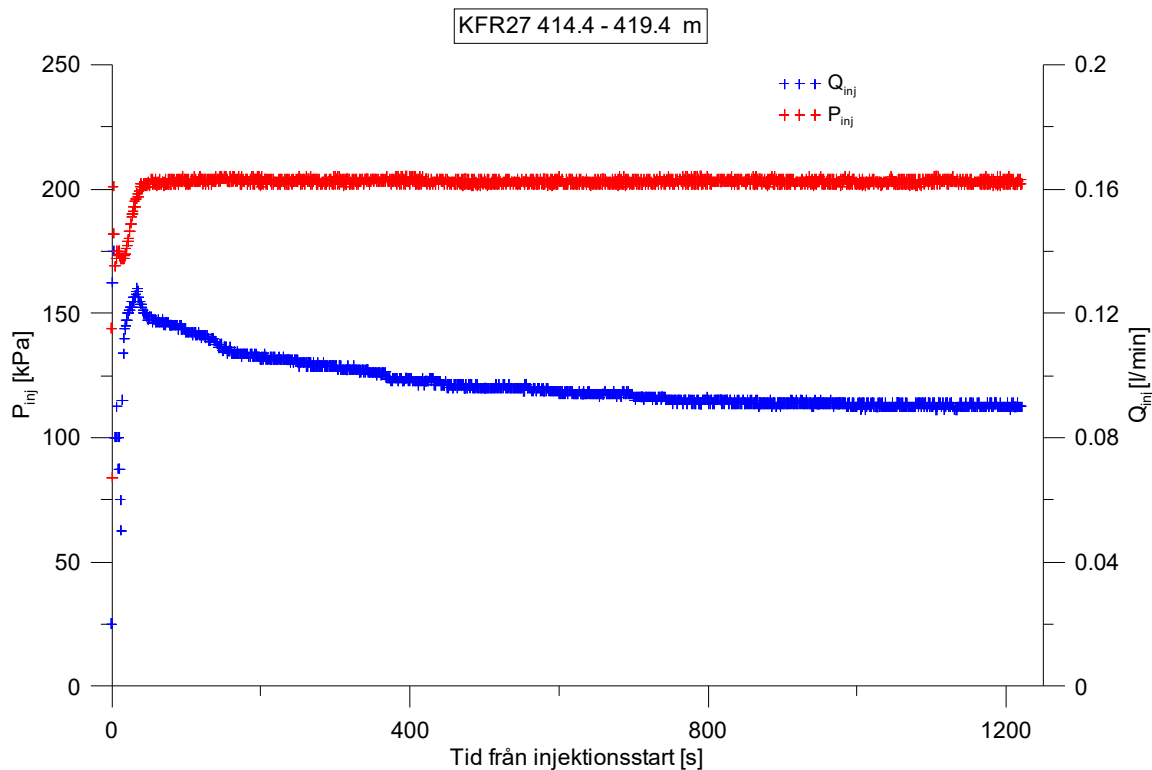


**Figure A2-207.** Linear plot of flow rate ( $Q$ ) and pressure ( $P$ ) versus time from the injection test in section 414.4-419.4 m in borehole KFR27.

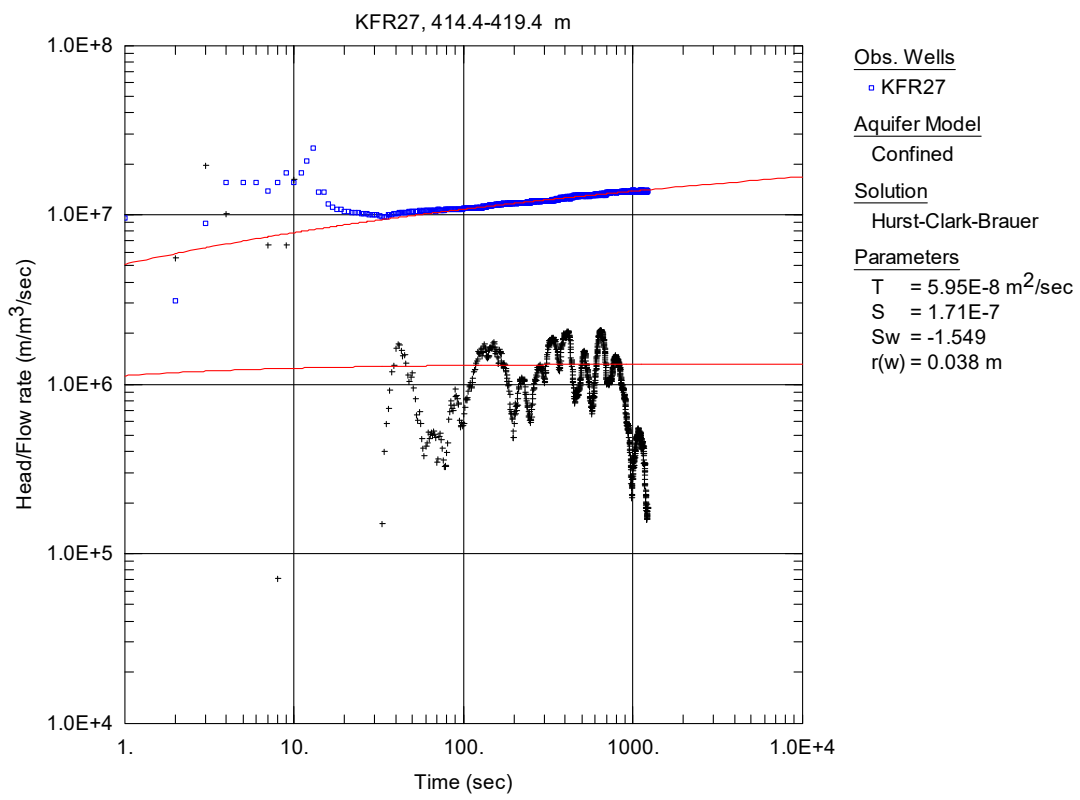


**Figure A2-208.** Log-log plot of head/flow rate (□) and derivative (+) versus time, from the injection test in section 414.4-419.4 m in borehole KFR27.

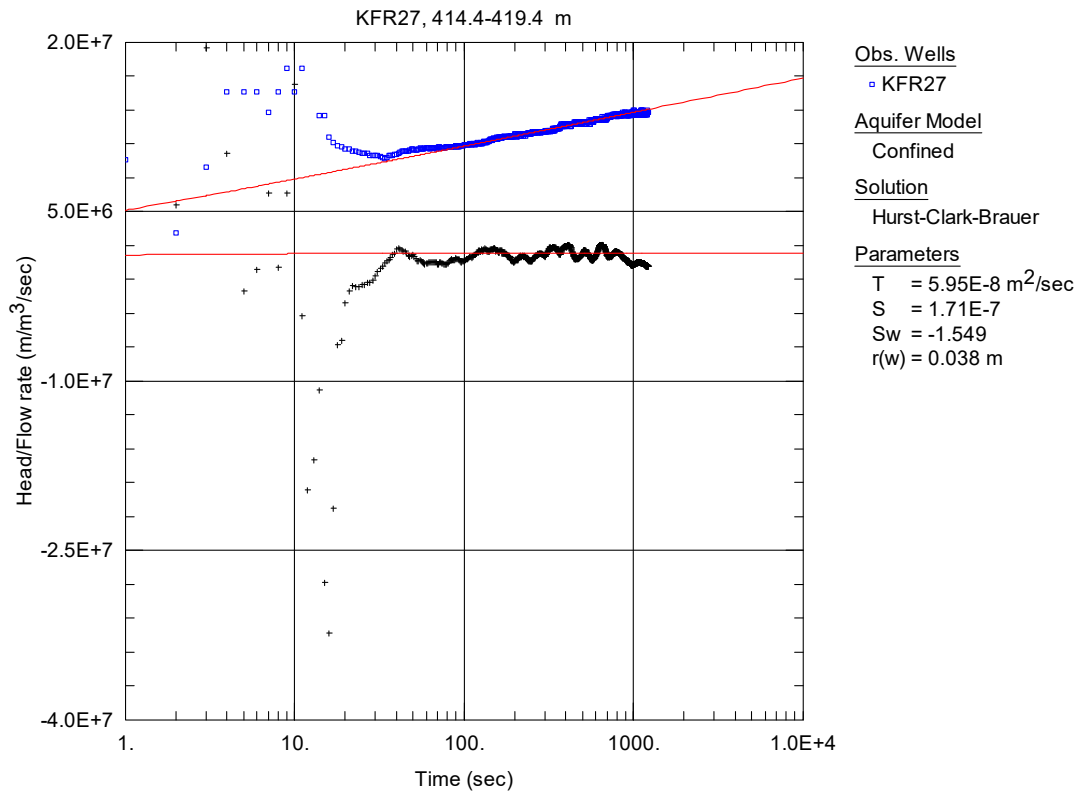


**Figure A2-209.** Lin-log plot of head/flow rate (□) and derivative (+) versus time, from the injection test in section 414.4-419.4 m in borehole KFR27.

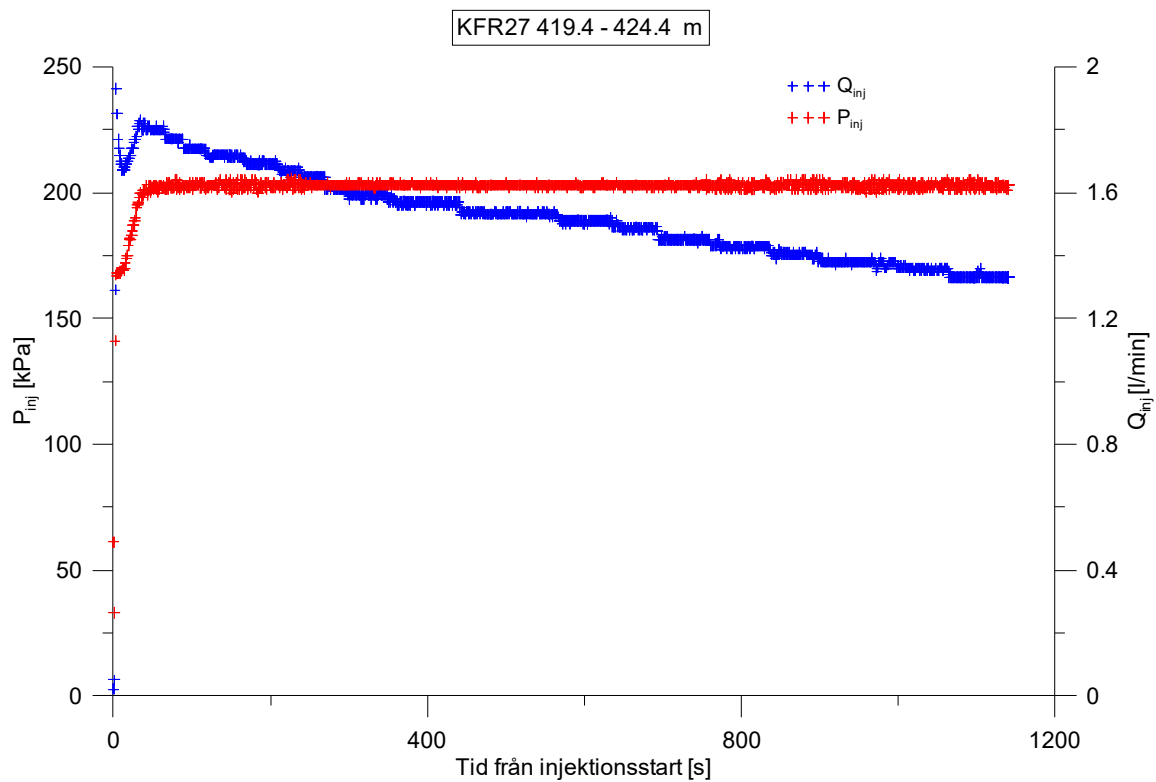


**Figure A2-210.** Linear plot of flow rate ( $Q$ ) and pressure ( $P$ ) versus time from the injection test in section 419.4-424.4 m in borehole KFR27.

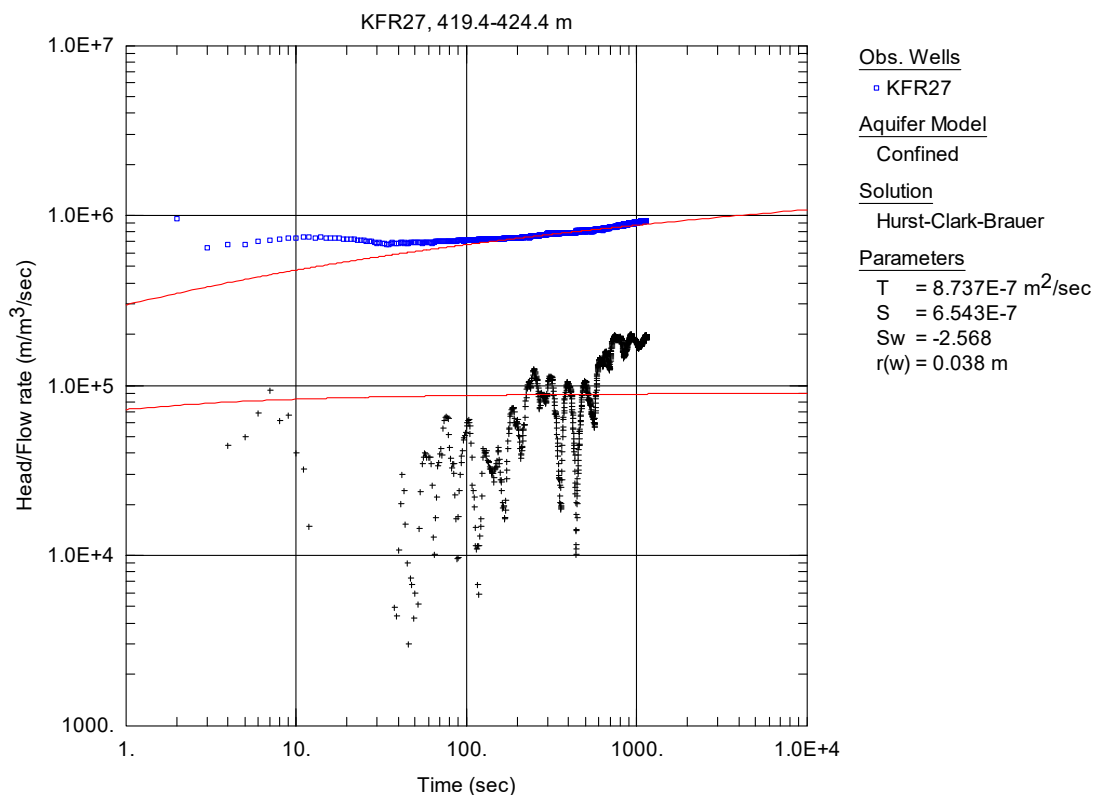


**Figure A2-211.** Log-log plot of head/flow rate (□) and derivative (+) versus time, from the injection test in section 419.4-424.4 m in borehole KFR27.

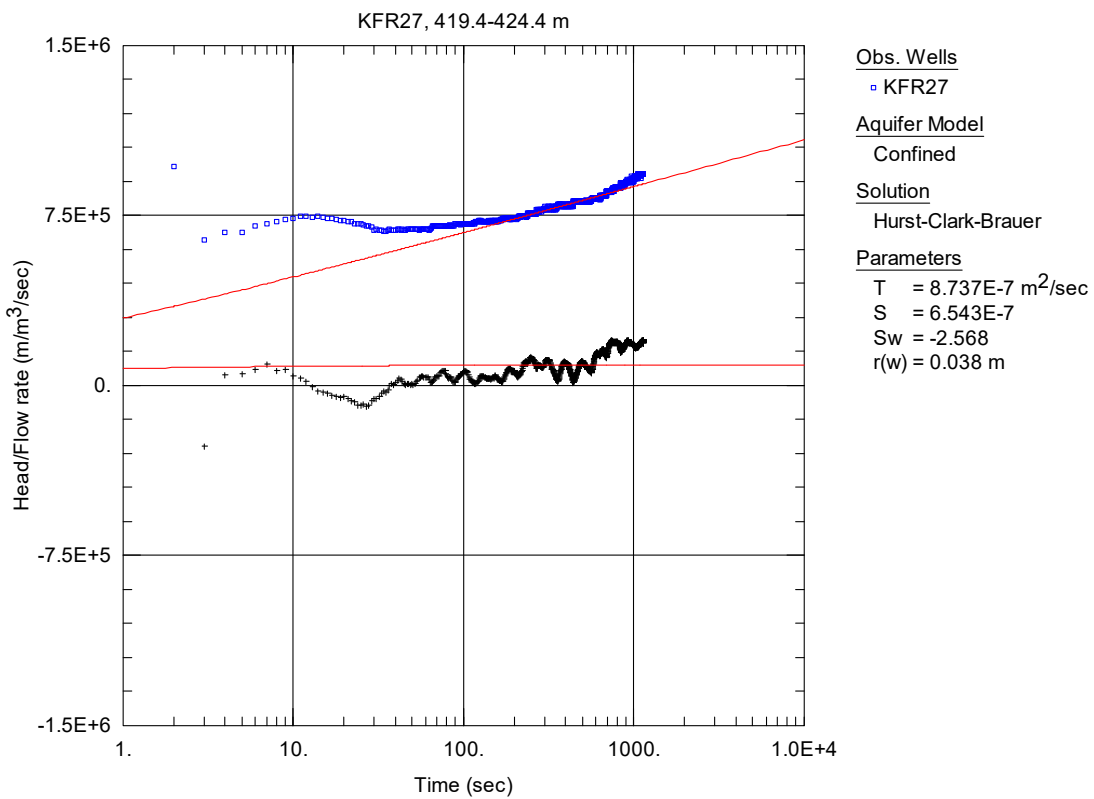


**Figure A2-212.** Lin-log plot of head/flow rate (□) and derivative (+) versus time, from the injection test in section 419.4-424.4 m in borehole KFR27.

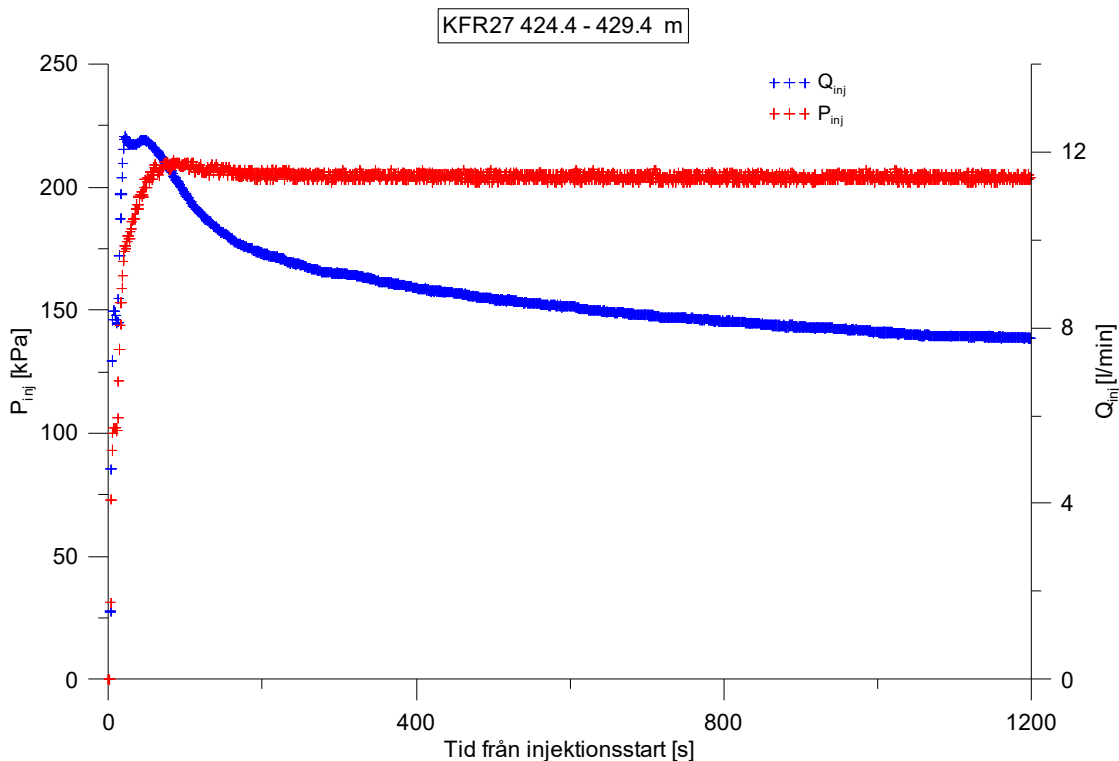


**Figure A2-213.** Linear plot of flow rate ( $Q$ ) and pressure ( $P$ ) versus time from the injection test in section 424.4-429.4 m in borehole KFR27.

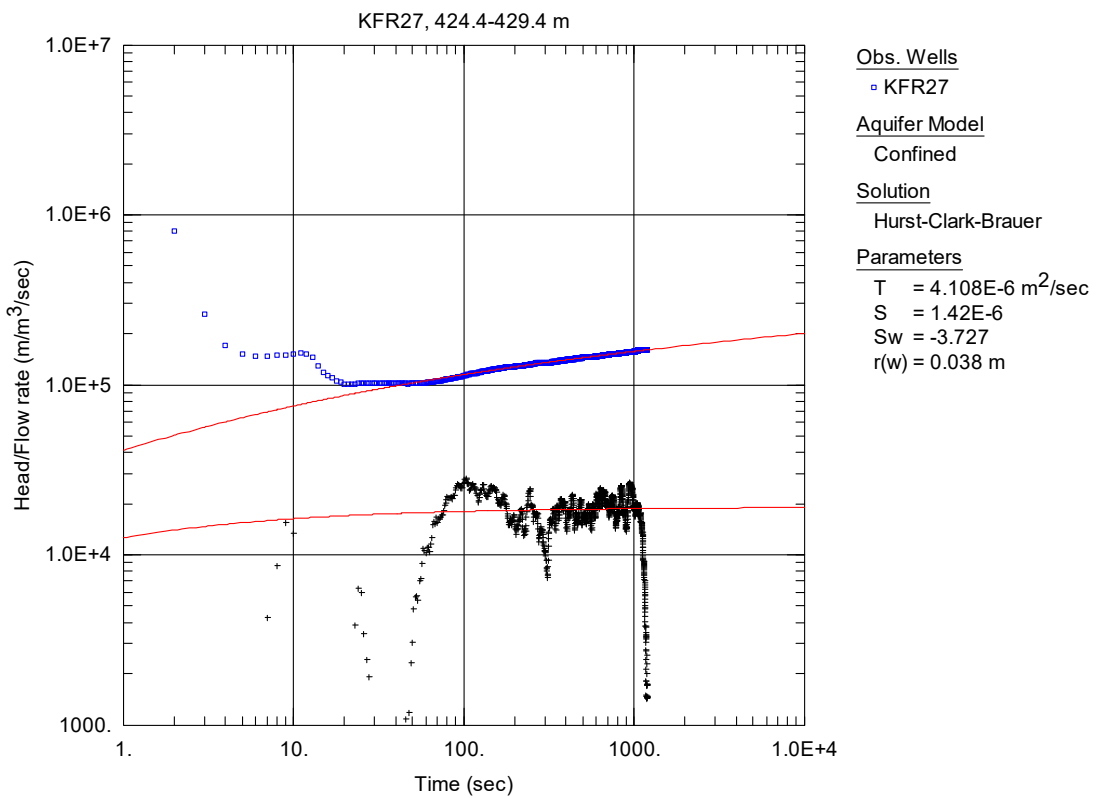


**Figure A2-214.** Log-log plot of head/flow rate (□) and derivative (+) versus time, from the injection test in section 424.4-429.4 m in borehole KFR27.

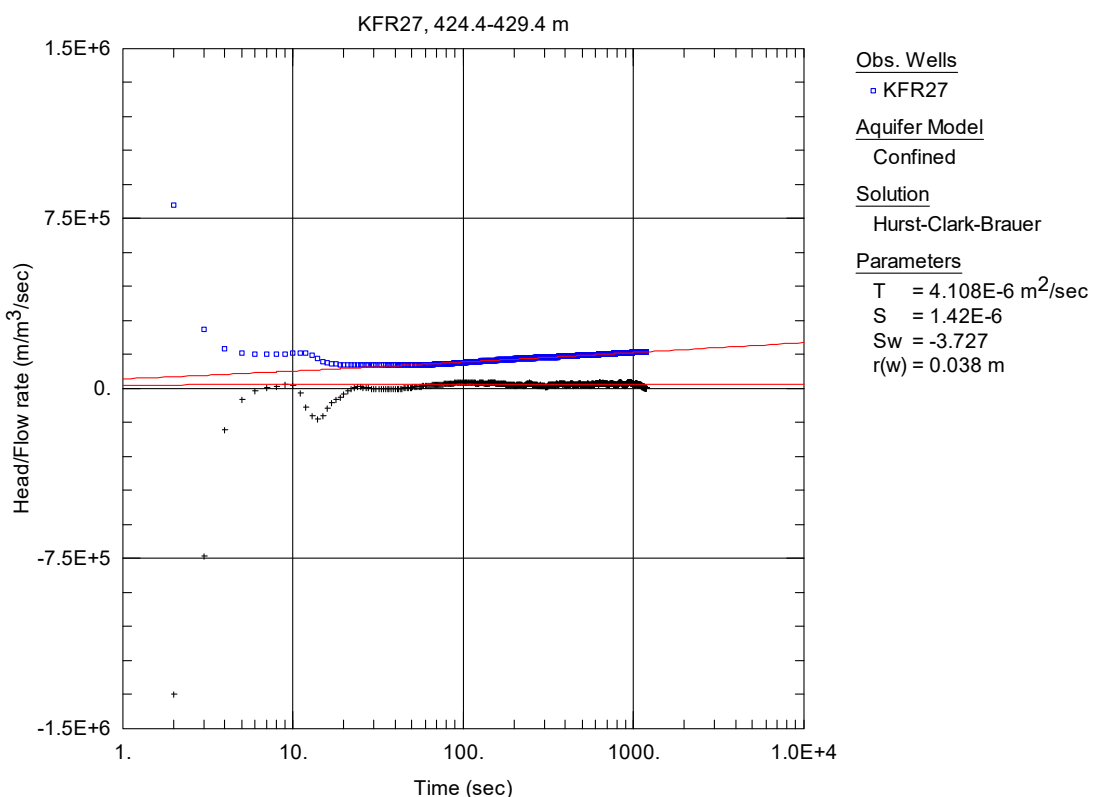


**Figure A2-215.** Lin-log plot of head/flow rate (□) and derivative (+) versus time, from the injection test in section 424.4-429.4 m in borehole KFR27.

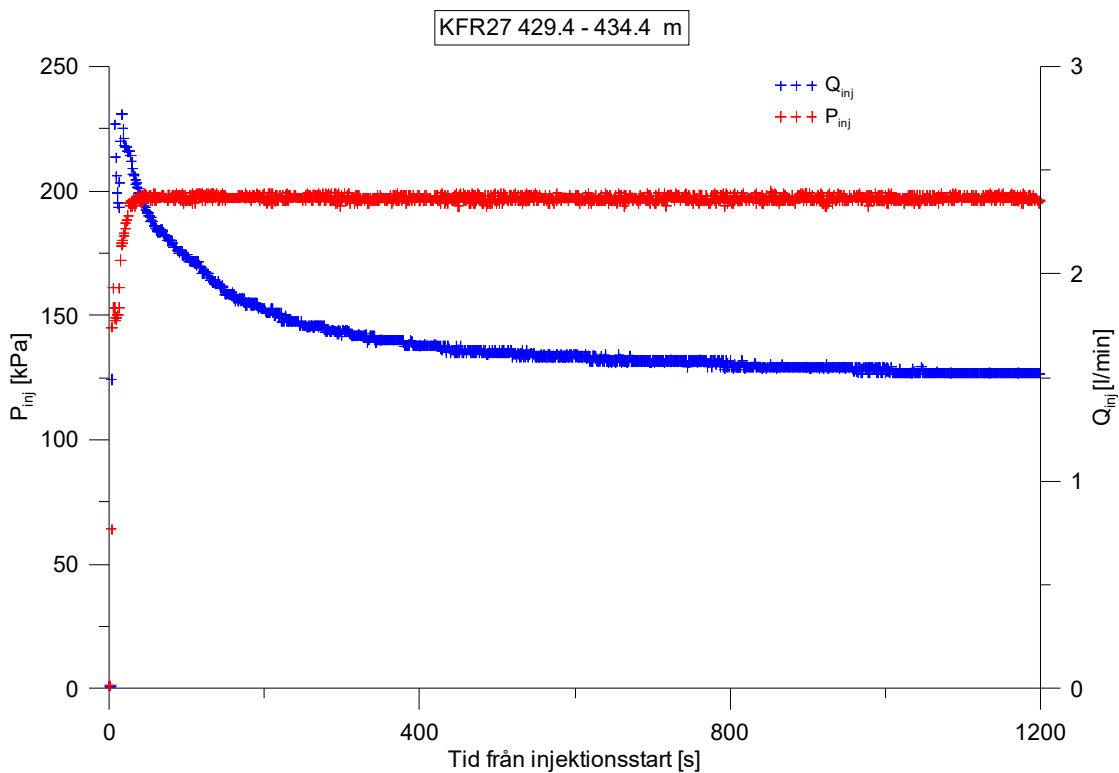


**Figure A2-216.** Linear plot of flow rate ( $Q$ ) and pressure ( $P$ ) versus time from the injection test in section 429.4-434.4 m in borehole KFR27.

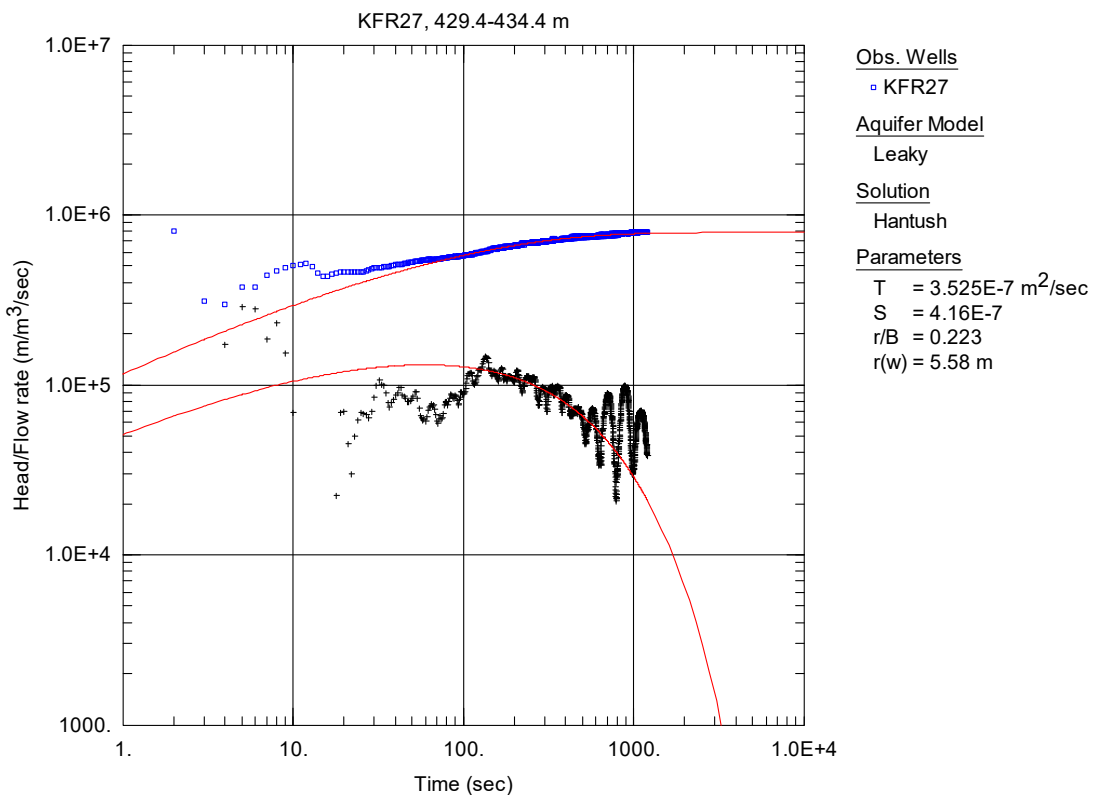


**Figure A2-217.** Log-log plot of head/flow rate (□) and derivative (+) versus time, from the injection test in section 429.4-434.4 m in borehole KFR27.

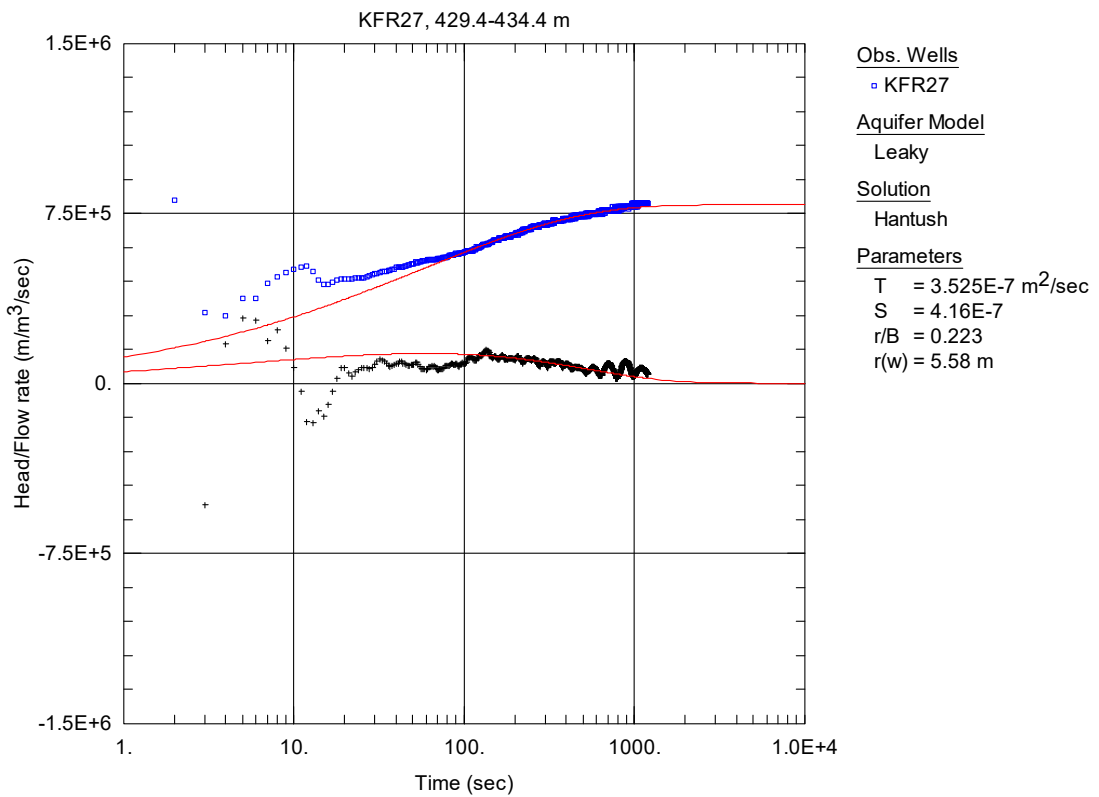


**Figure A2-218.** Lin-log plot of head/flow rate (□) and derivative (+) versus time, from the injection test in section 429.4-434.4 m in borehole KFR27.

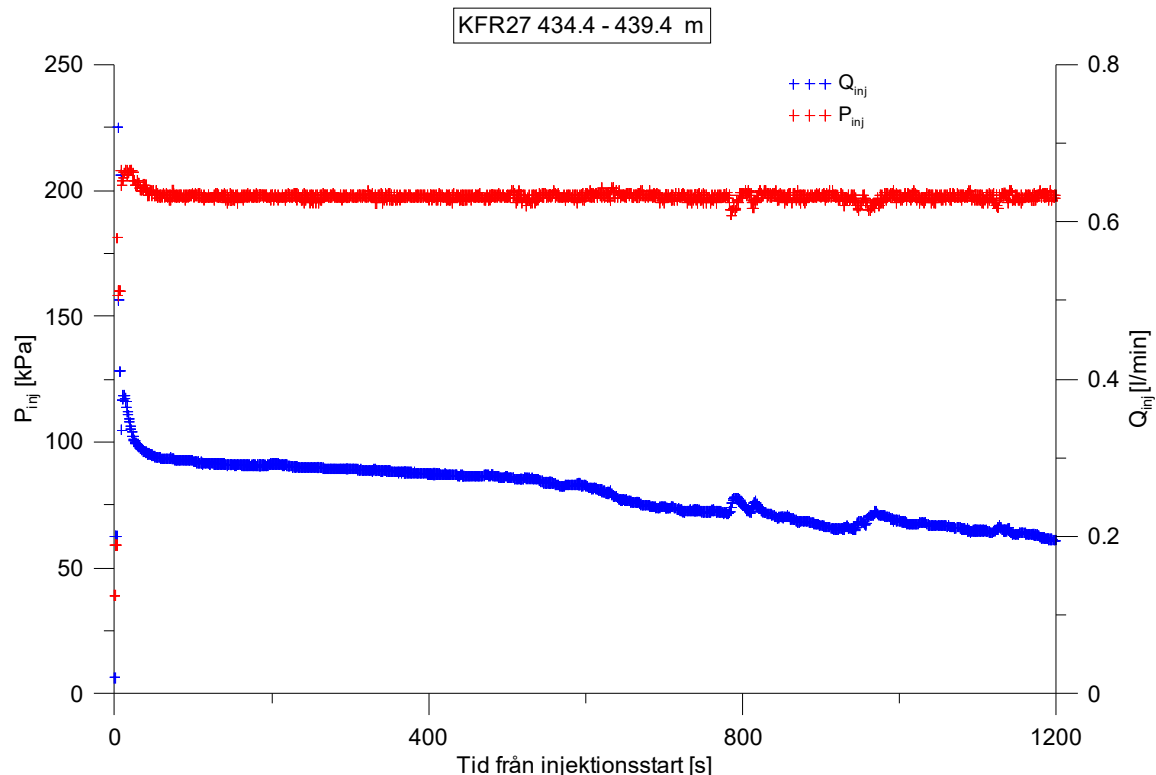


**Figure A2-219.** Linear plot of flow rate ( $Q$ ) and pressure ( $P$ ) versus time from the injection test in section 434.4-439.4 m in borehole KFR27.

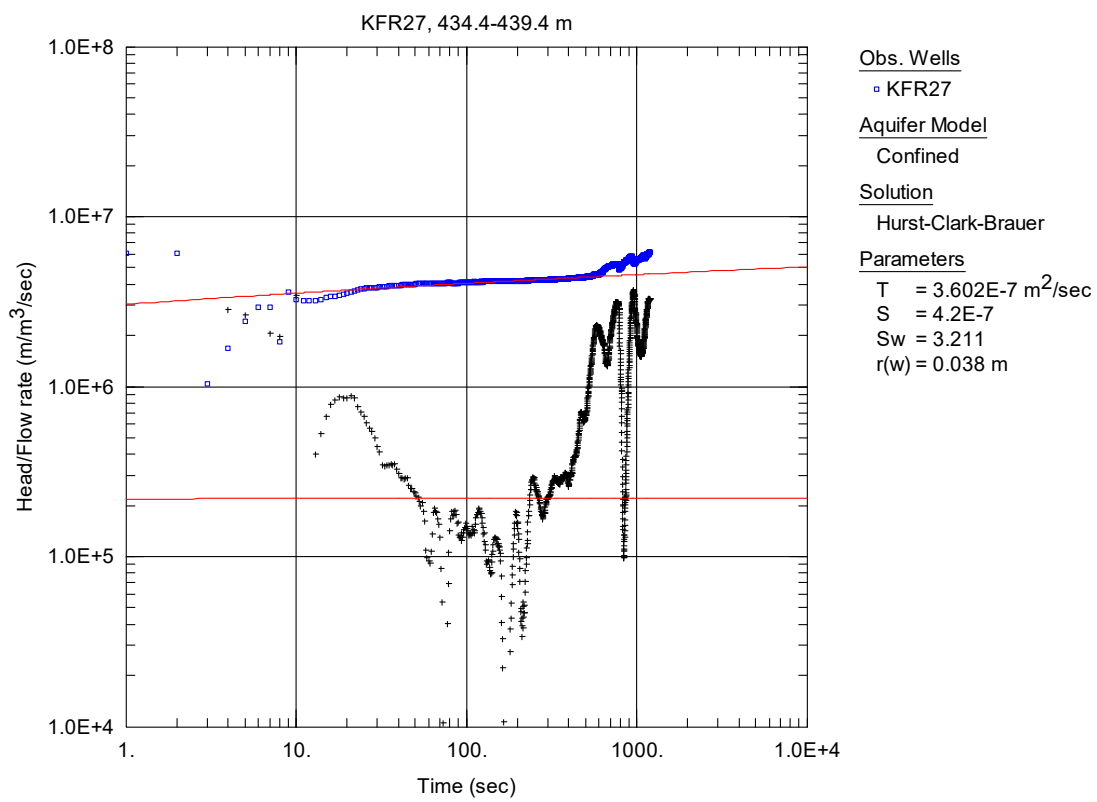


**Figure A2-220.** Log-log plot of head/flow rate (□) and derivative (+) versus time, from the injection test in section 434.4-439.4 m in borehole KFR27.

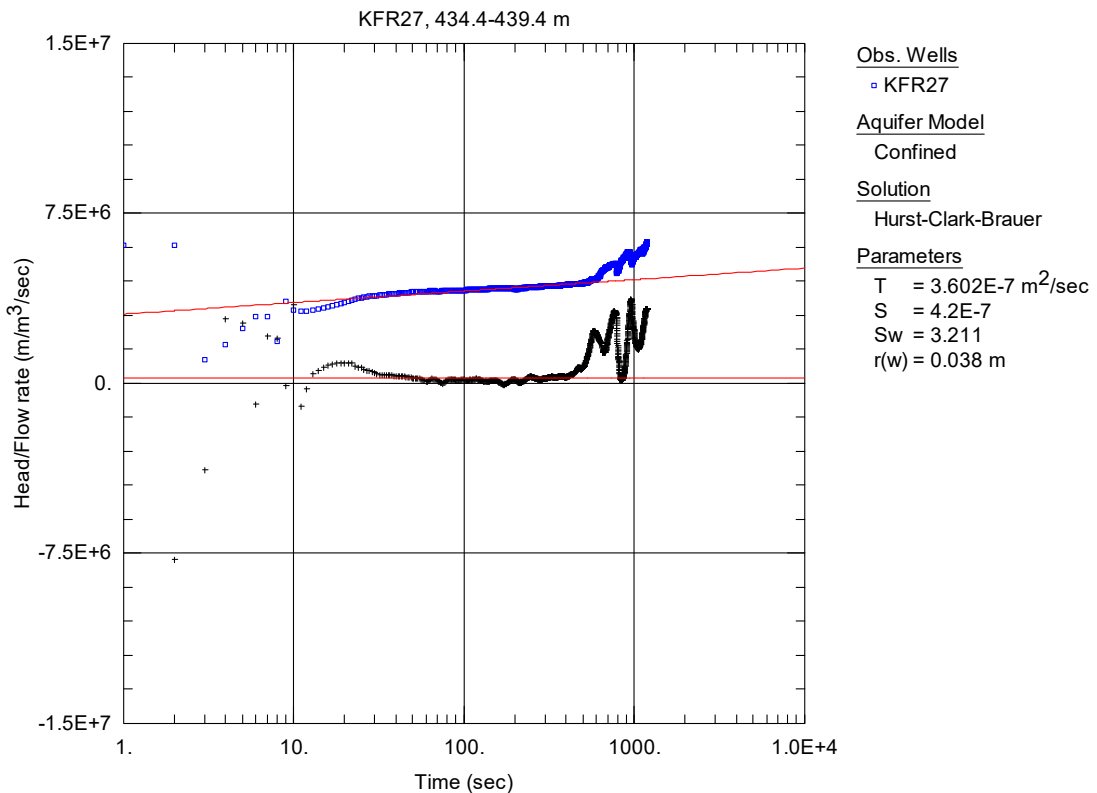


**Figure A2-221.** Lin-log plot of head/flow rate (□) and derivative (+) versus time, from the injection test in section 434.4-439.4 m in borehole KFR27.

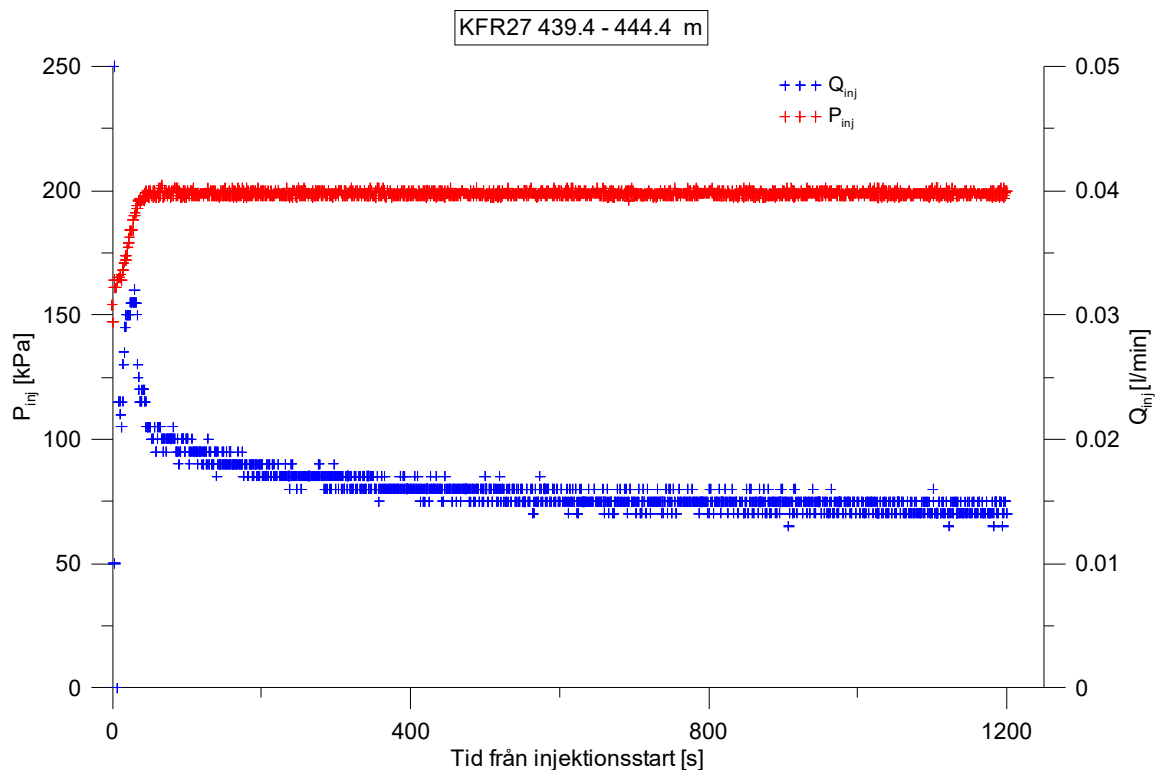


**Figure A2-222.** Linear plot of flow rate ( $Q$ ) and pressure ( $P$ ) versus time from the injection test in section 439.4-444.4 m in borehole KFR27.

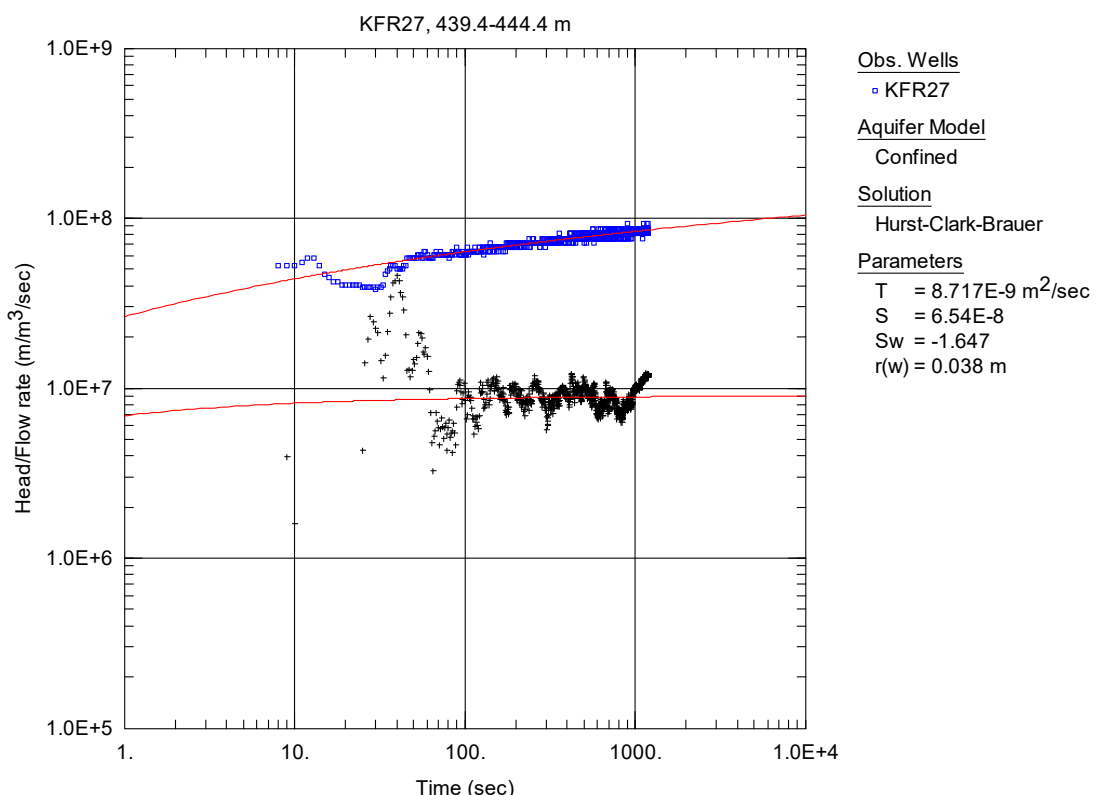


**Figure A2-223.** Log-log plot of head/flow rate (□) and derivative (+) versus time, from the injection test in section 439.4-444.4 m in borehole KFR27.

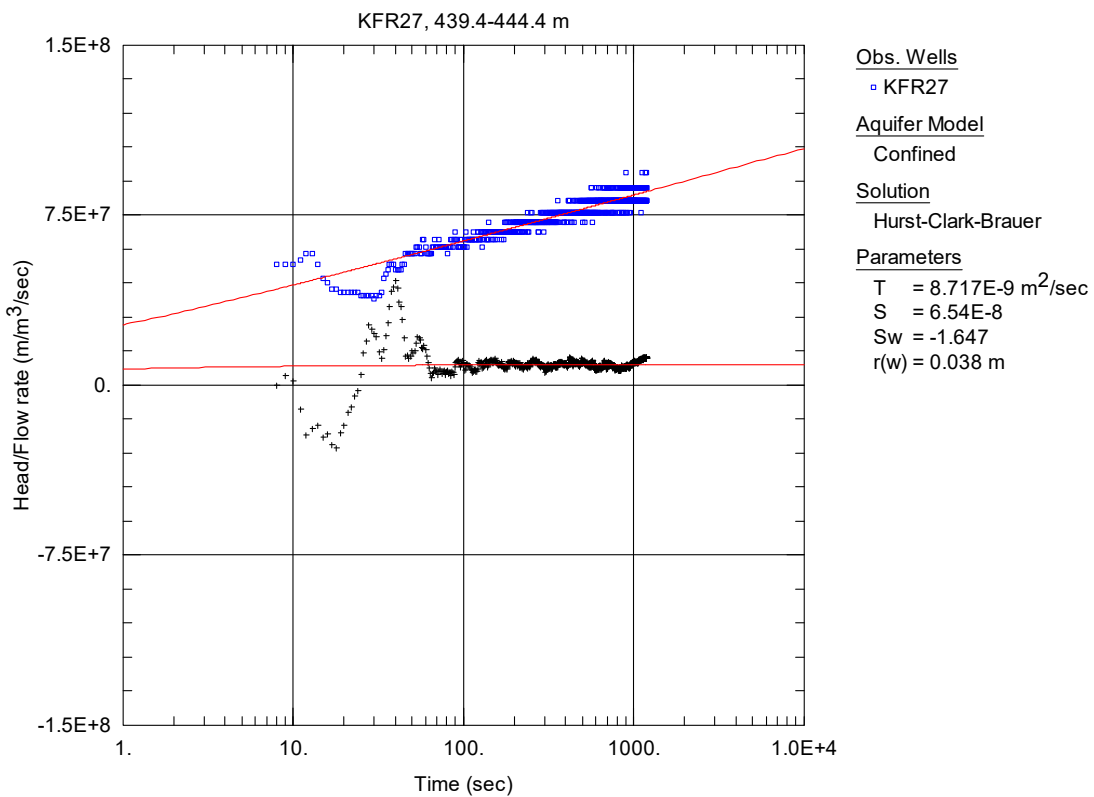


**Figure A2-224.** Lin-log plot of head/flow rate (□) and derivative (+) versus time, from the injection test in section 439.4-444.4 m in borehole KFR27.

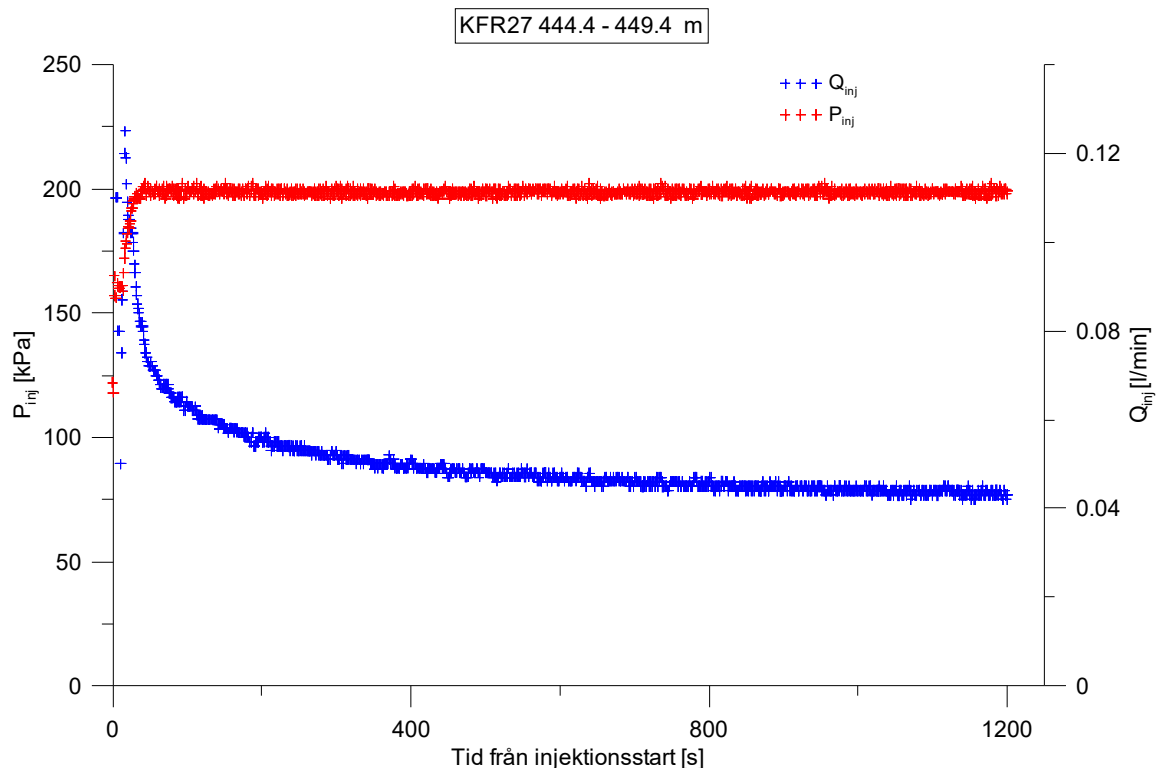


**Figure A2-225.** Linear plot of flow rate ( $Q$ ) and pressure ( $P$ ) versus time from the injection test in section 444.4-449.4 m in borehole KFR27.

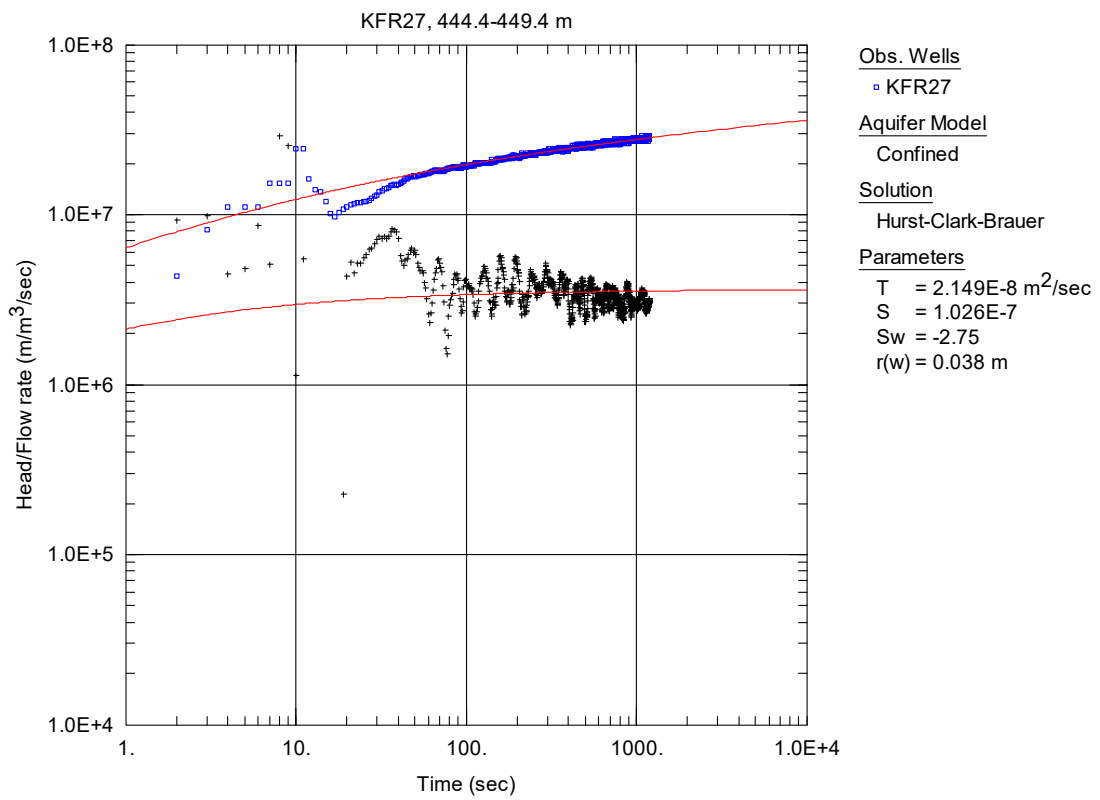


**Figure A2-226.** Log-log plot of head/flow rate (□) and derivative (+) versus time, from the injection test in section 444.4-449.4 m in borehole KFR27.

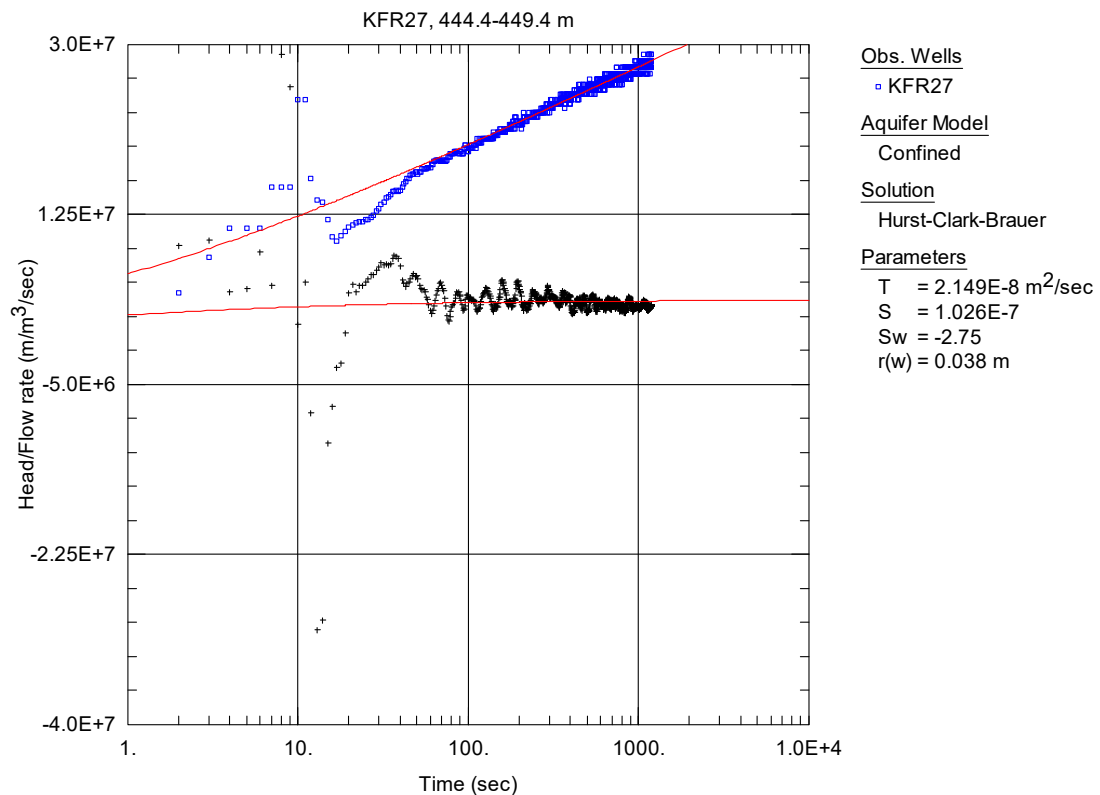


**Figure A2-227.** Lin-log plot of head/flow rate (□) and derivative (+) versus time, from the injection test in section 444.4-449.4 m in borehole KFR27.

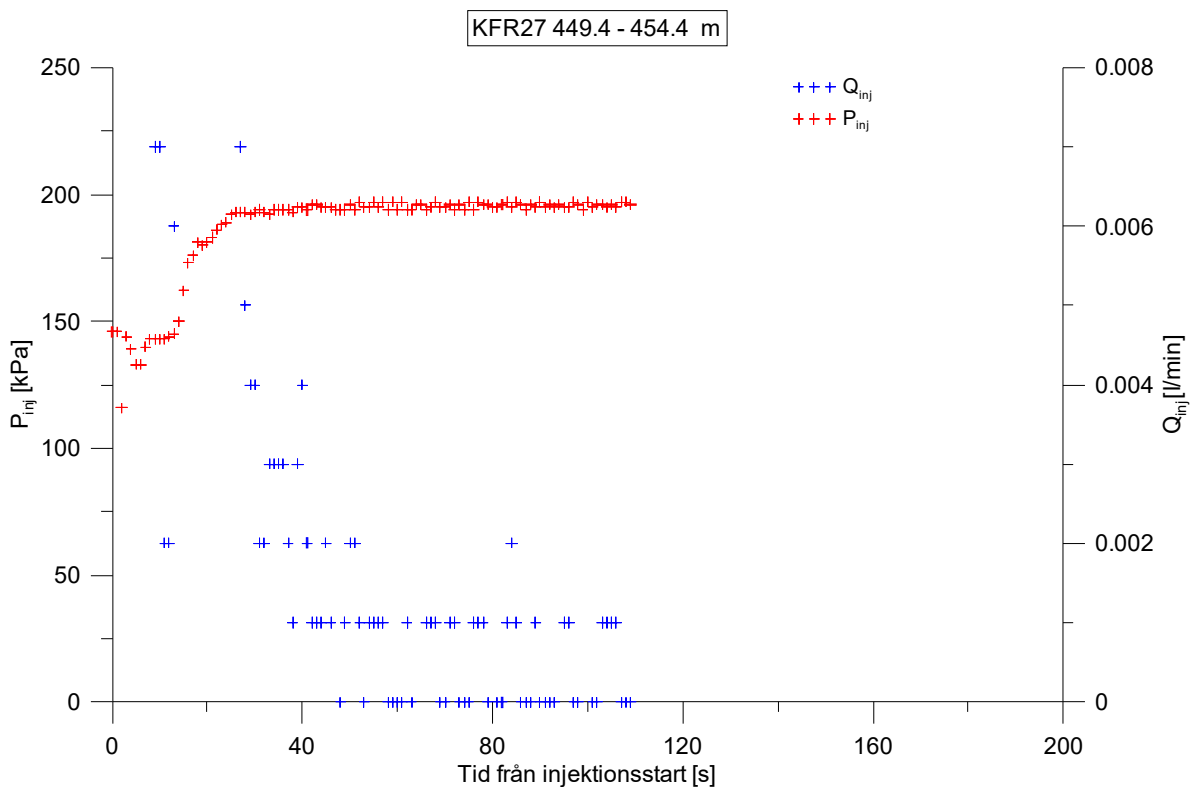


**Figure A2-228.** Linear plot of flow rate ( $Q$ ) and pressure ( $P$ ) versus time from the injection test in section 449.4-454.4 m in borehole KFR27.

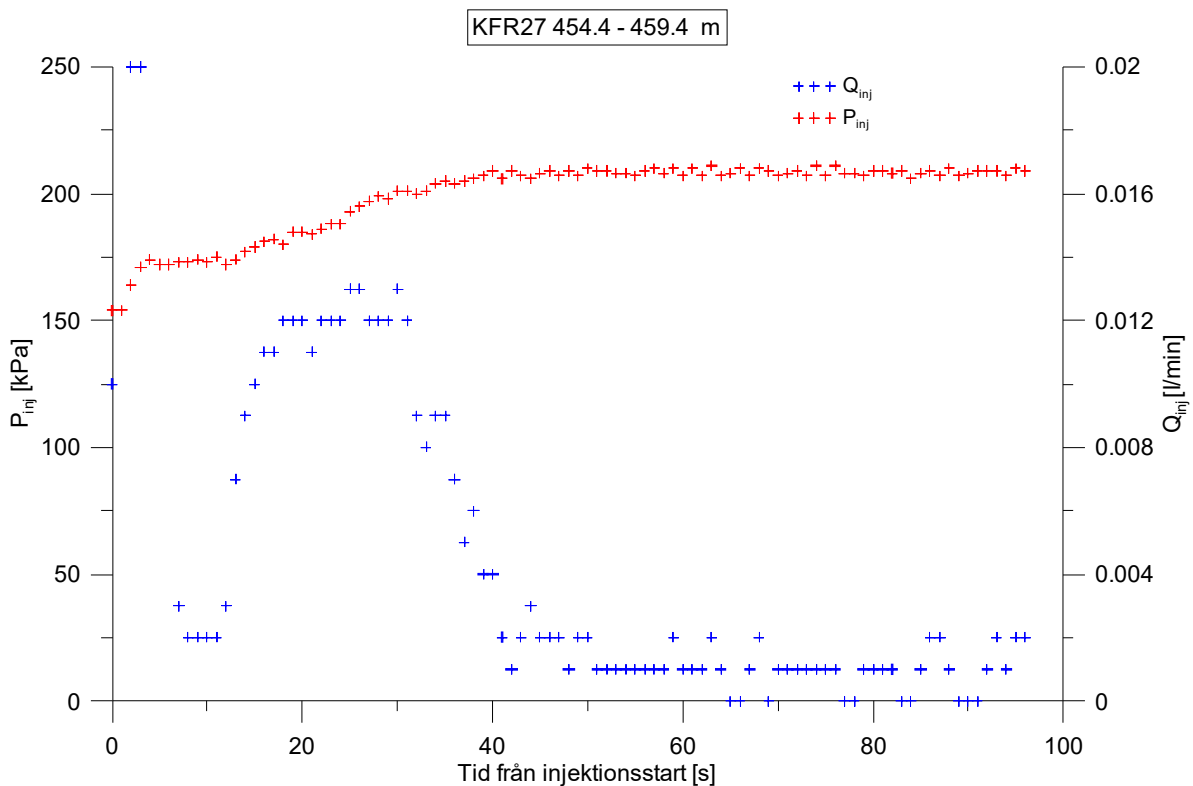


**Figure A2-229.** Linear plot of flow rate ( $Q$ ) and pressure ( $P$ ) versus time from the injection test in section 454.4-459.4 m in borehole KFR27.

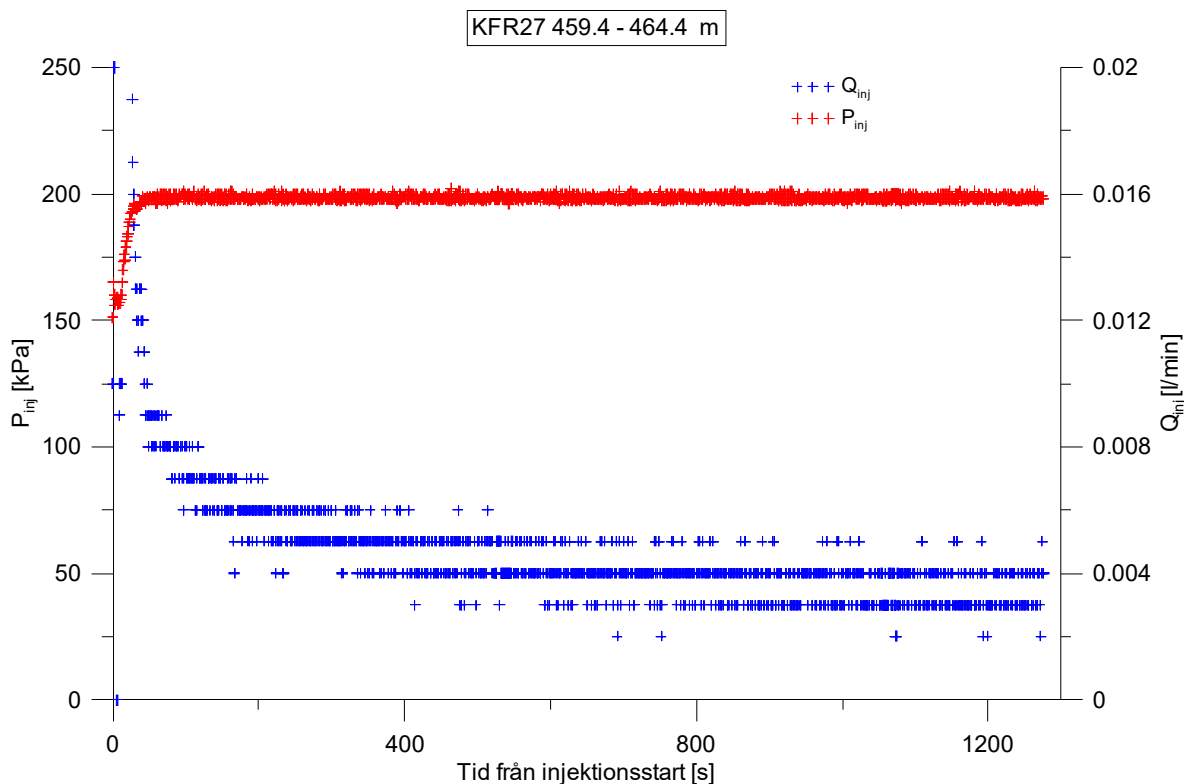


**Figure A2-230.** Linear plot of flow rate ( $Q$ ) and pressure ( $P$ ) versus time from the injection test in section 459.4-464.4 m in borehole KFR27.

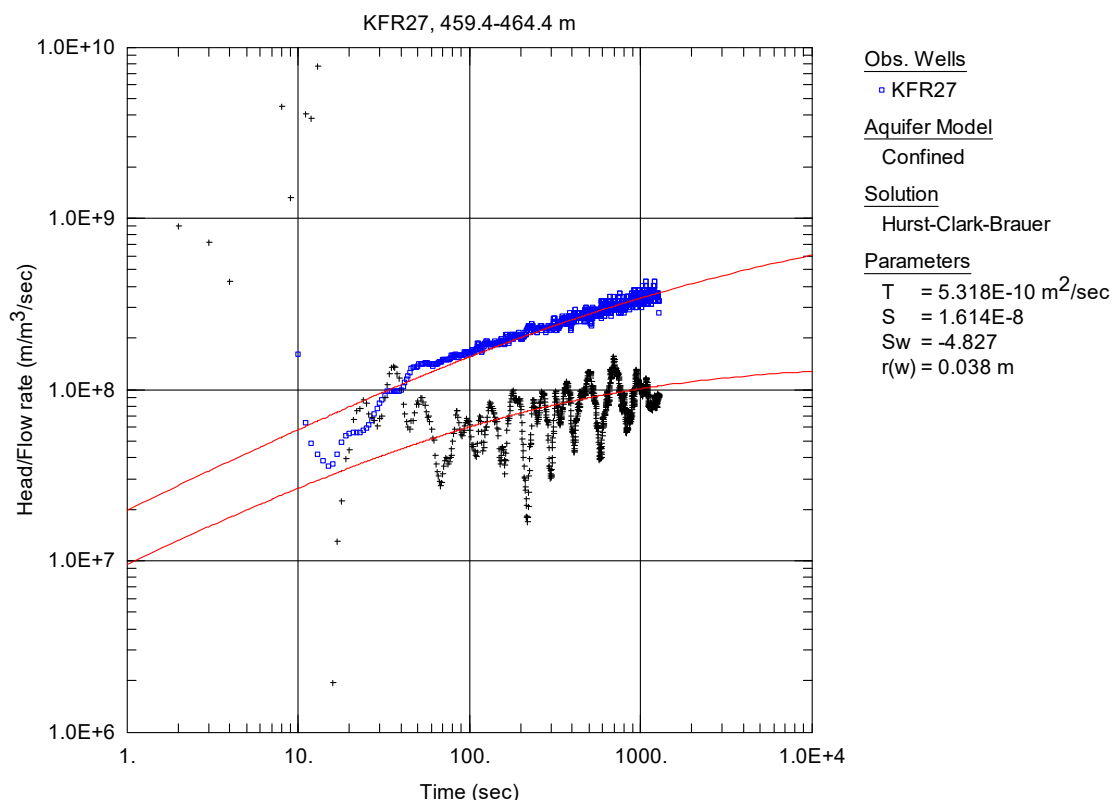


**Figure A2-231.** Log-log plot of head/flow rate (□) and derivative (+) versus time, from the injection test in section 459.4-464.4 m in borehole KFR27.

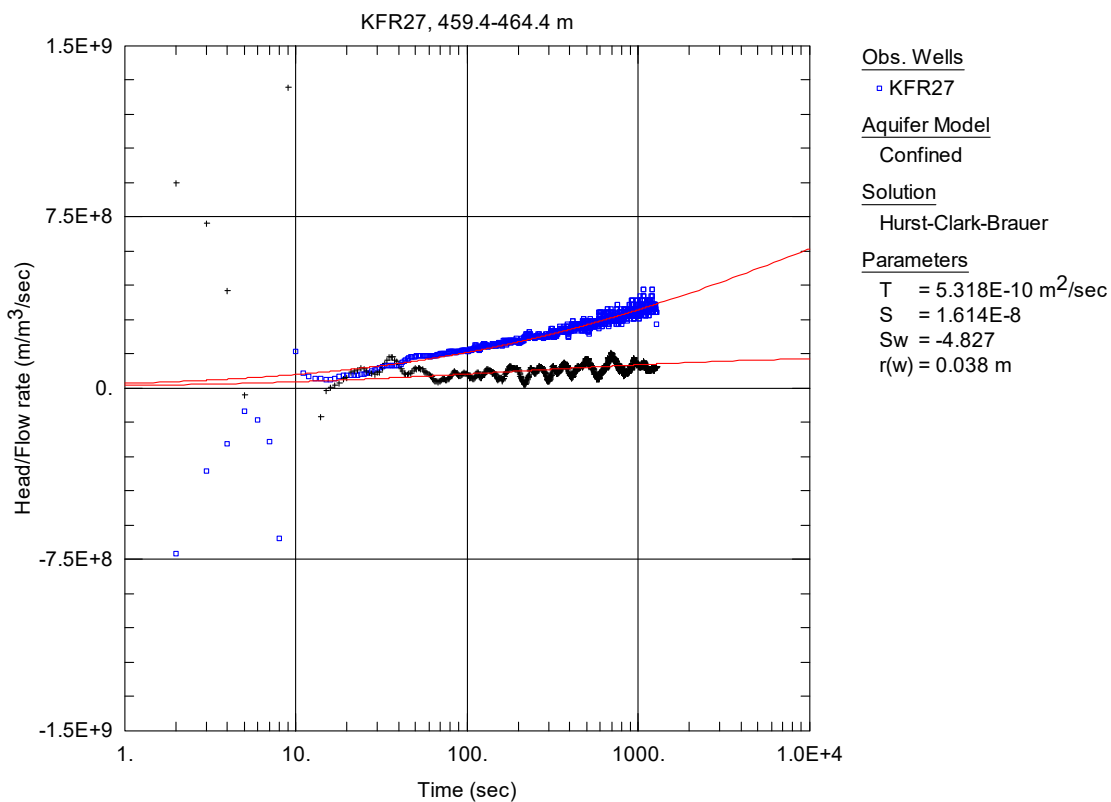


**Figure A2-232.** Lin-log plot of head/flow rate (□) and derivative (+) versus time, from the injection test in section 459.4-464.4 m in borehole KFR27.

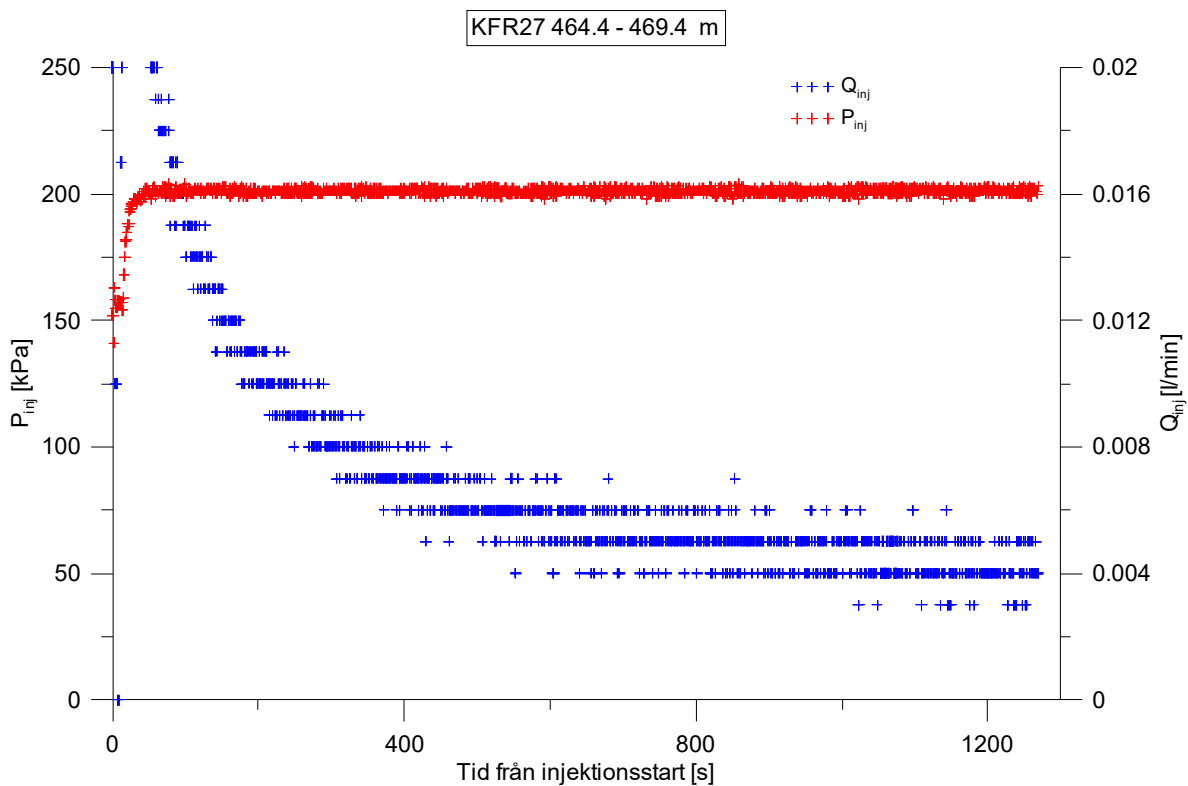


**Figure A2-233.** Linear plot of flow rate (Q) and pressure (P) versus time from the injection test in section 464.4-469.4 m in borehole KFR27.

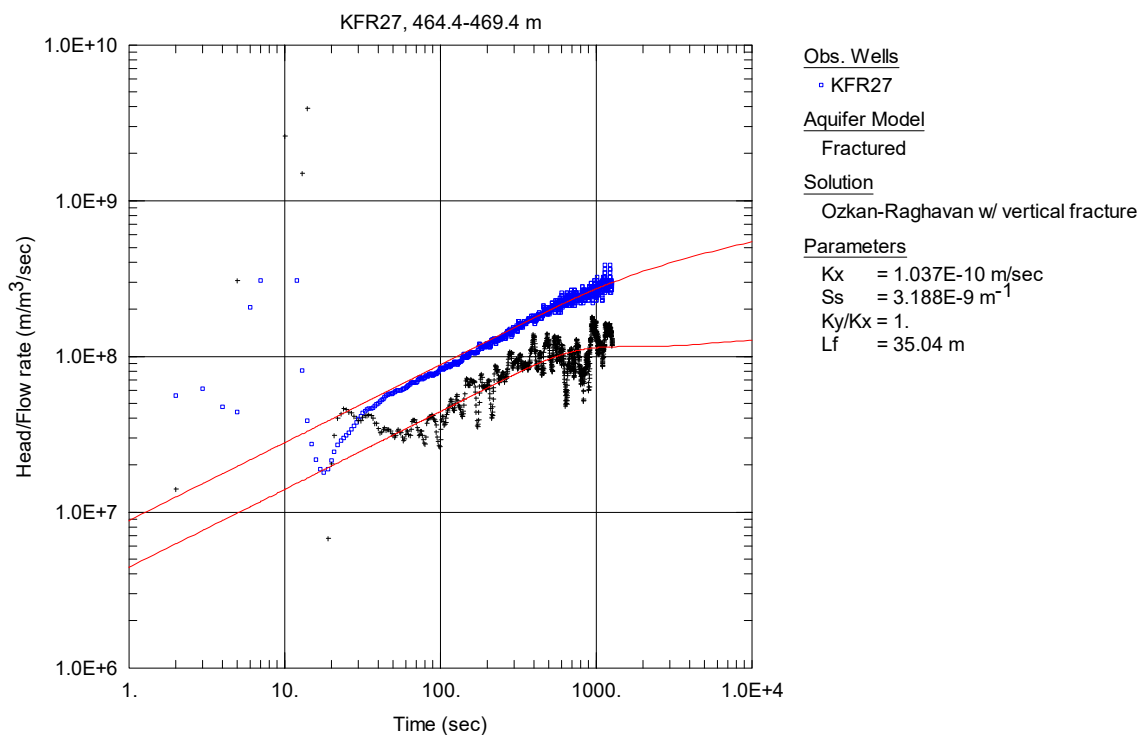


**Figure A2-234.** Log-log plot of head/flow rate (□) and derivative (+) versus time, from the injection test in section 464.4-469.4 m in borehole KFR27.

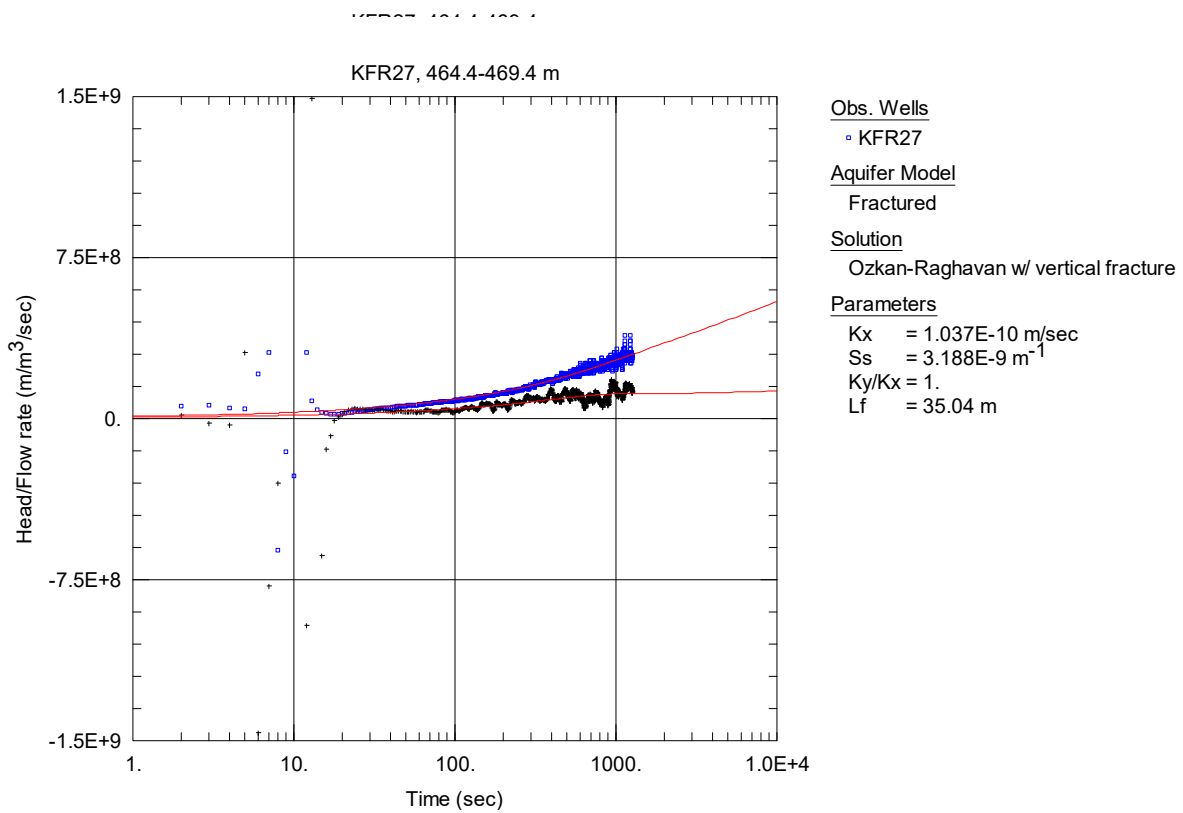


**Figure A2-235.** Lin-log plot of head/flow rate (□) and derivative (+) versus time, from the injection test in section 464.4-469.4 m in borehole KFR27.

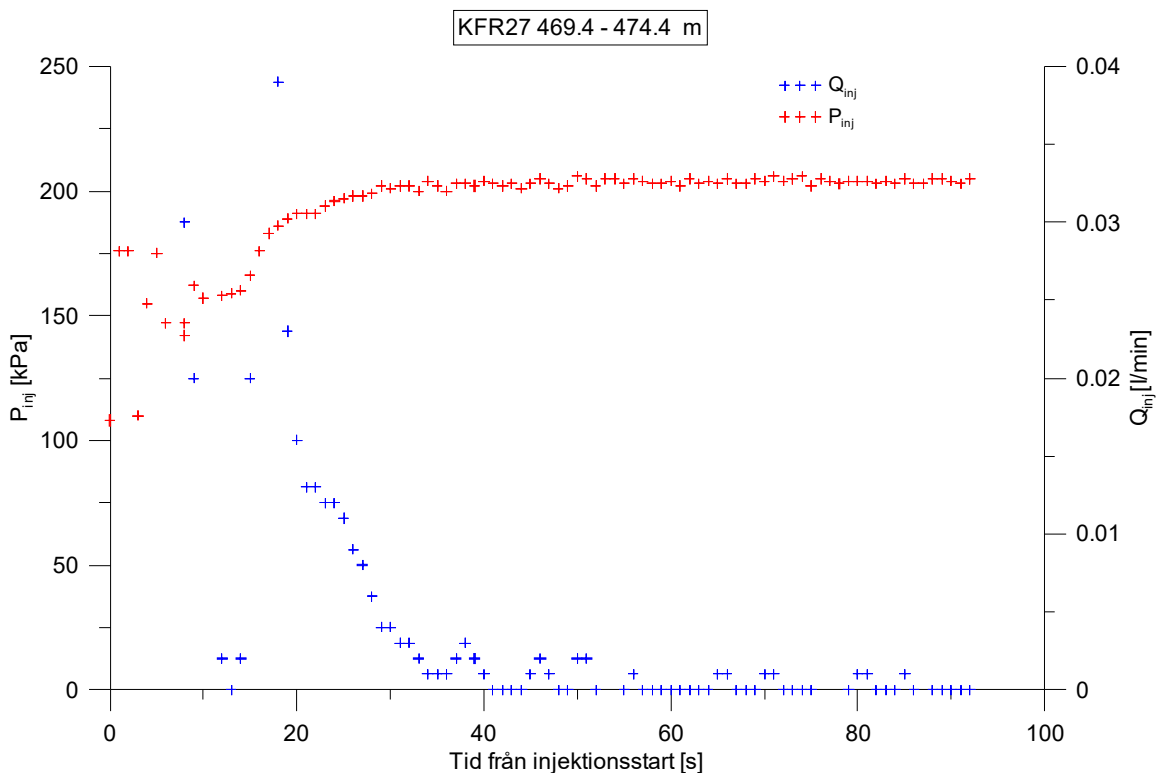


**Figure A2-236.** Linear plot of flow rate ( $Q$ ) and pressure ( $P$ ) versus time from the injection test in section 469.4-474.4 m in borehole KFR27.

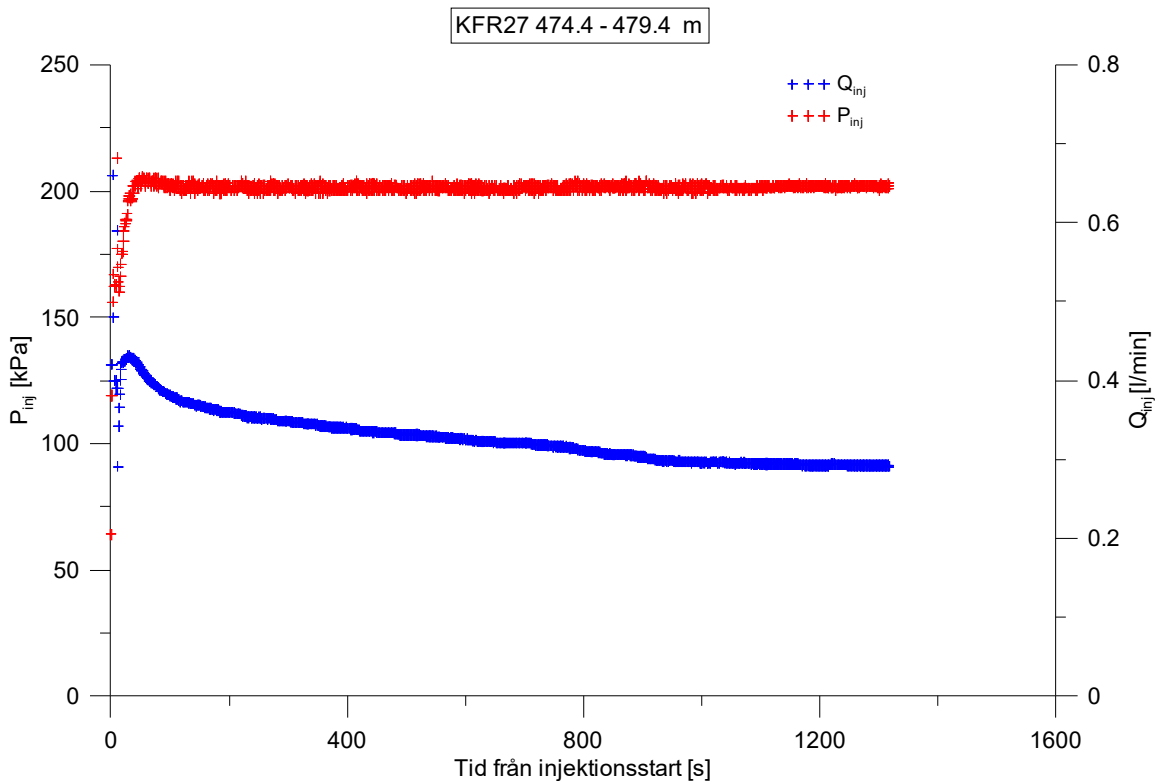


**Figure A2-237.** Linear plot of flow rate ( $Q$ ) and pressure ( $P$ ) versus time from the injection test in section 474.4-479.4 m in borehole KFR27.

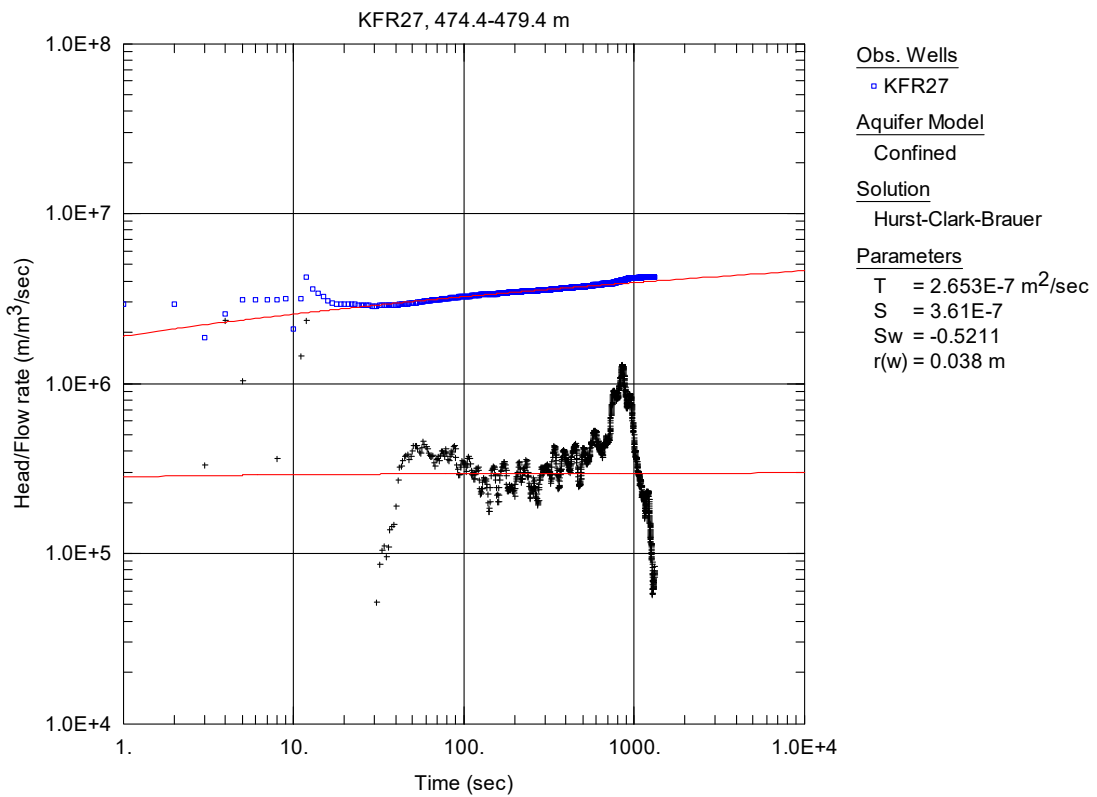


**Figure A2-238.** Log-log plot of head/flow rate (□) and derivative (+) versus time, from the injection test in section 474.4-479.4 m in borehole KFR27.

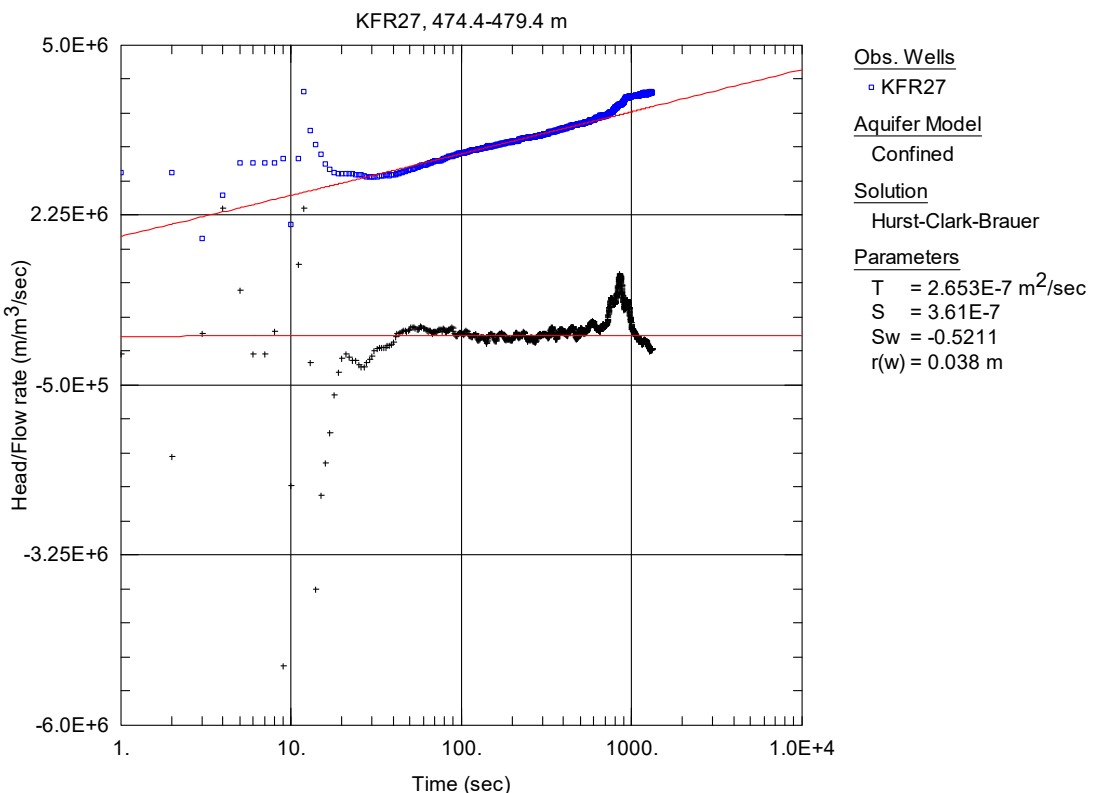


**Figure A2-239.** Lin-log plot of head/flow rate (□) and derivative (+) versus time, from the injection test in section 474.4-479.4 m in borehole KFR27.

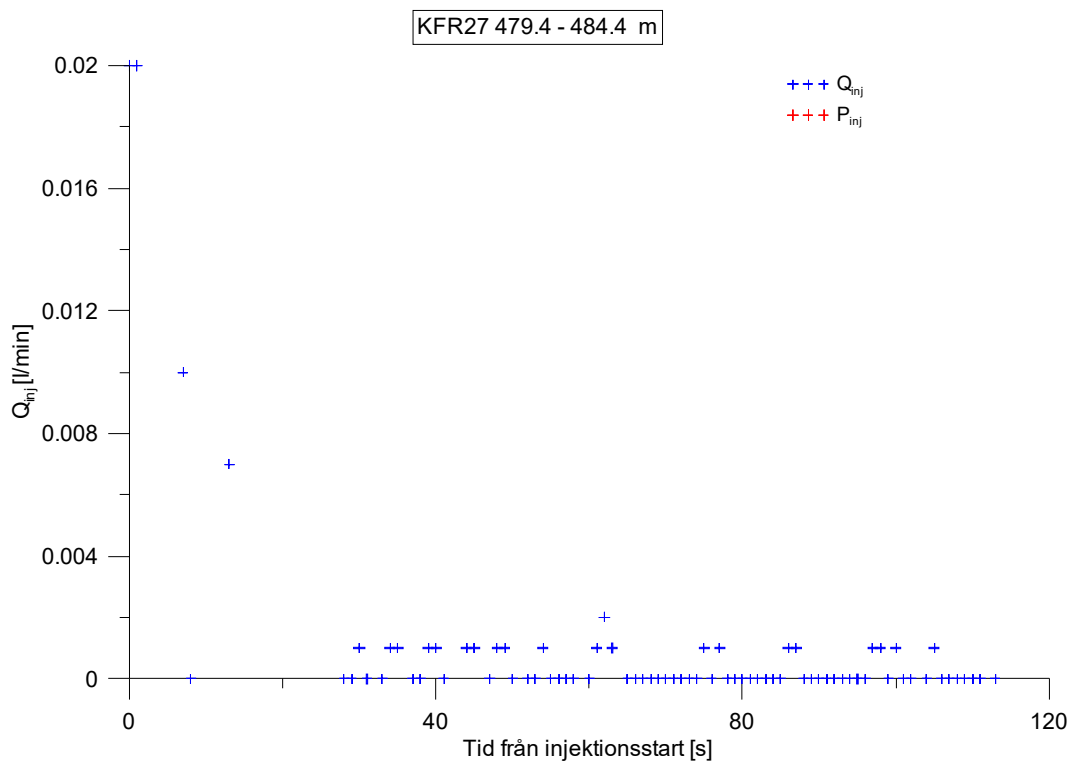


**Figure A2-240.** Linear plot of flow rate ( $Q$ ) and pressure ( $P$ ) versus time from the injection test in section 479.4-484.4 m in borehole KFR27. Pressure in section above measuring limit for pressure transducer in borehole. Injection test was performed with internal pressure transducer in WIC.

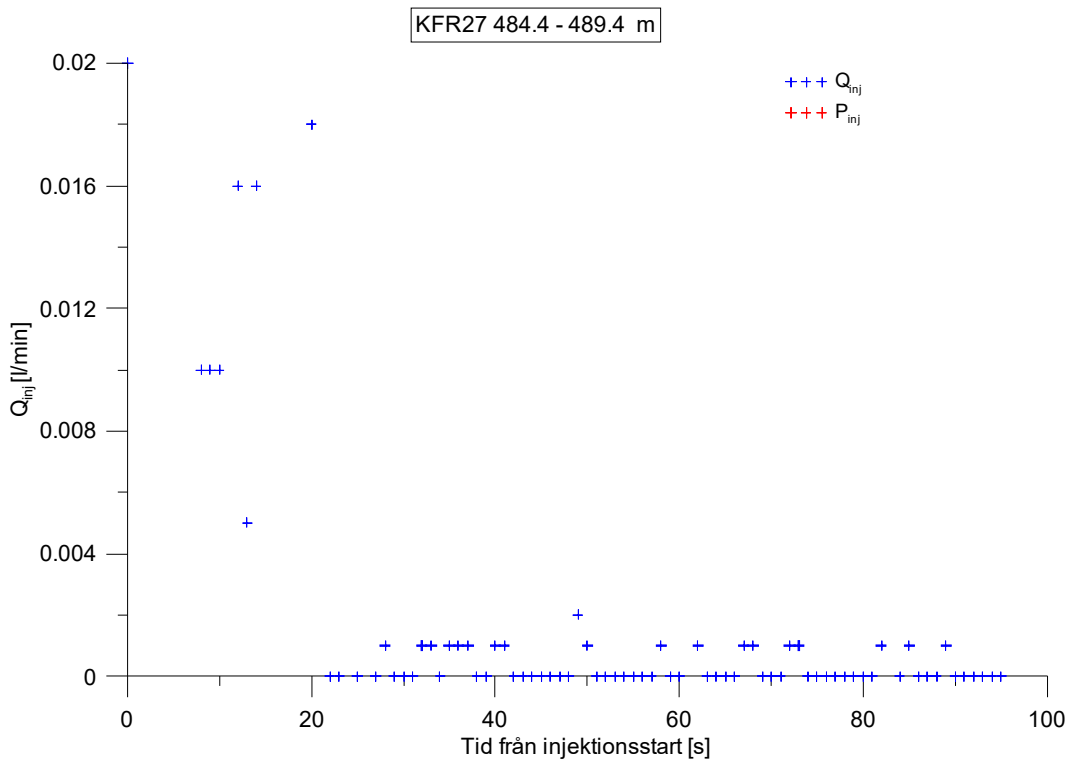


**Figure A2-241.** Linear plot of flow rate ( $Q$ ) and pressure ( $P$ ) versus time from the injection test in section 484.4-489.4 m in borehole KFR27. Pressure in section above measuring limit for pressure transducer in borehole. Injection test was performed with internal pressure transducer in WIC.

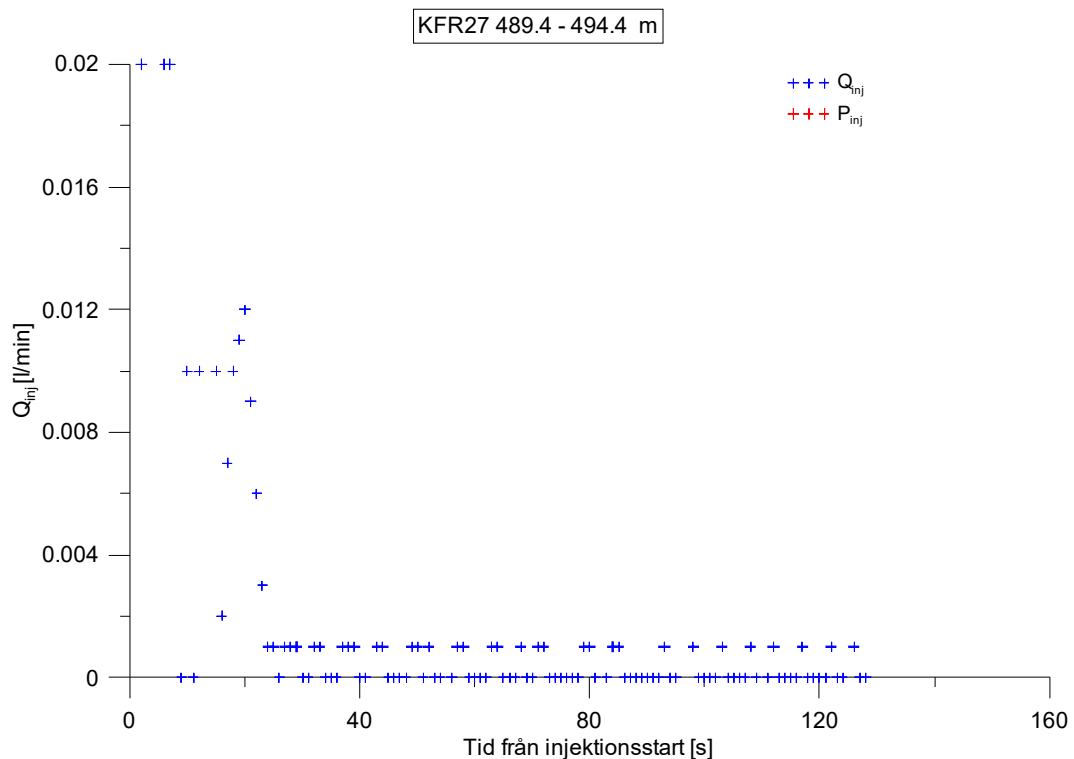


**Figure A2-242.** Linear plot of flow rate ( $Q$ ) and pressure ( $P$ ) versus time from the injection test in section 489.4-494.4 m in borehole KFR27. Pressure in section above measuring limit for pressure transducer in borehole. Injection test was performed with internal pressure transducer in WIC.

## Appendix 3

### Test diagrams – Injection tests in KFR105

In the following pages the selected test diagrams are presented for all test sections. A linear diagram of pressure and flow rate is presented for each test. For most tests are log-log diagrams presented, from injection and recovery period respectively. From the tests with a flow rate below the estimated lower measurement limit for the specific test, only the linear diagram is presented. Additionally, for a few tests, the fit are judged as non-representative. For these tests, the type curve fit is not presentet.

Nomenclature for Aquasolv:

T = transmissivity ( $\text{m}^2/\text{s}$ )

S = storativity (-)

$K_z/K_r$  = ratio of hydraulic conductivities in the vertical and radial direction (set to 1)

Sw = skin factor

r(w) = borehole radius (m)

r(c) = effective casing radius (m)

C = well loss constant (set to 0)

r/B = leakage factor (-)

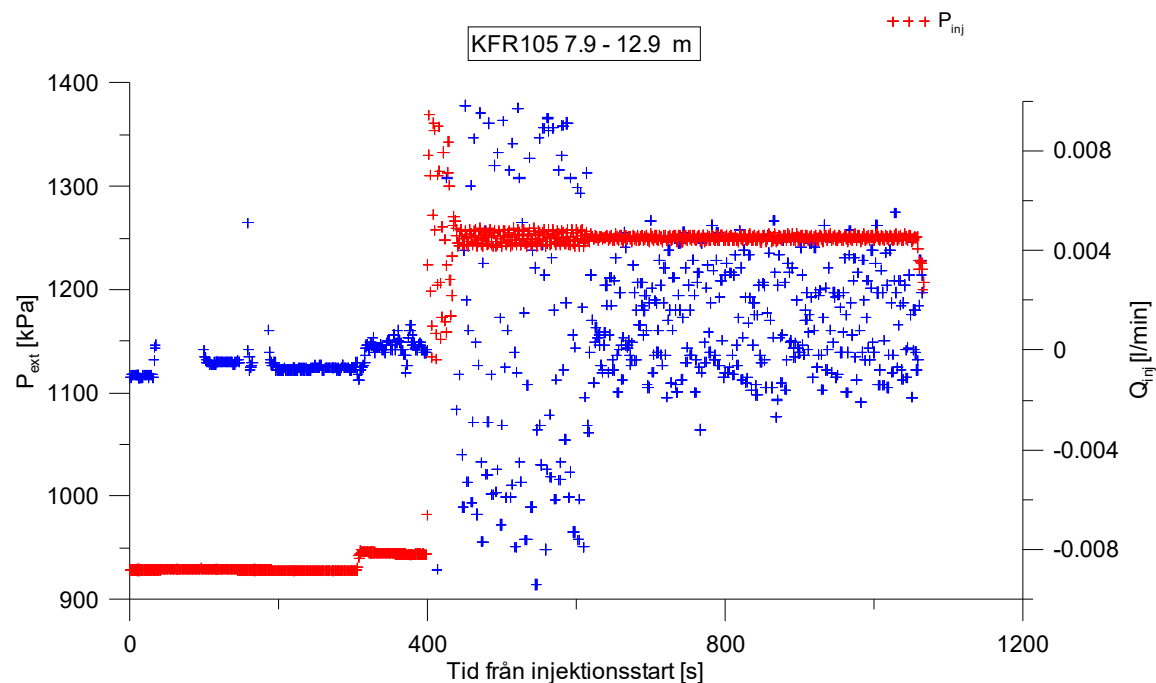


**Figure A3-1.** Linear plot of flow rate ( $Q$ ) and pressure ( $P$ ) versus time from the injection test in section 7.9-12.9 m in borehole KFR105.

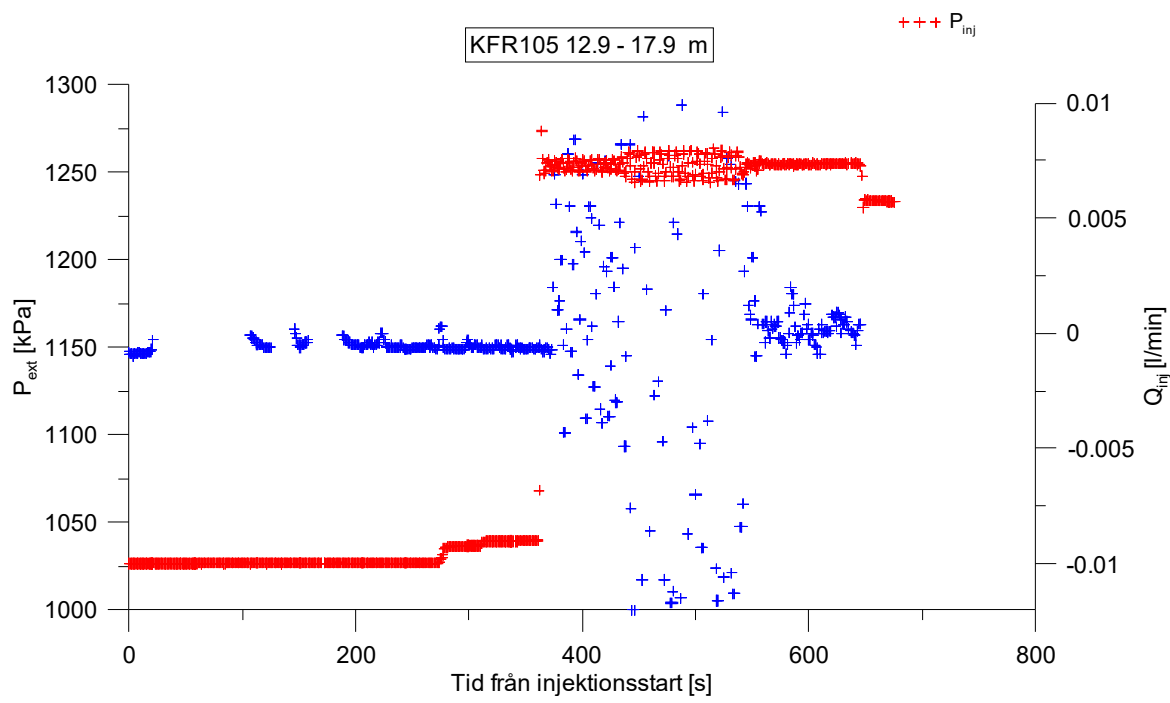


**Figure A3-2.** Linear plot of flow rate ( $Q$ ) and pressure ( $P$ ) versus time from the injection test in section 12.9-17.9 m in borehole KFR105.

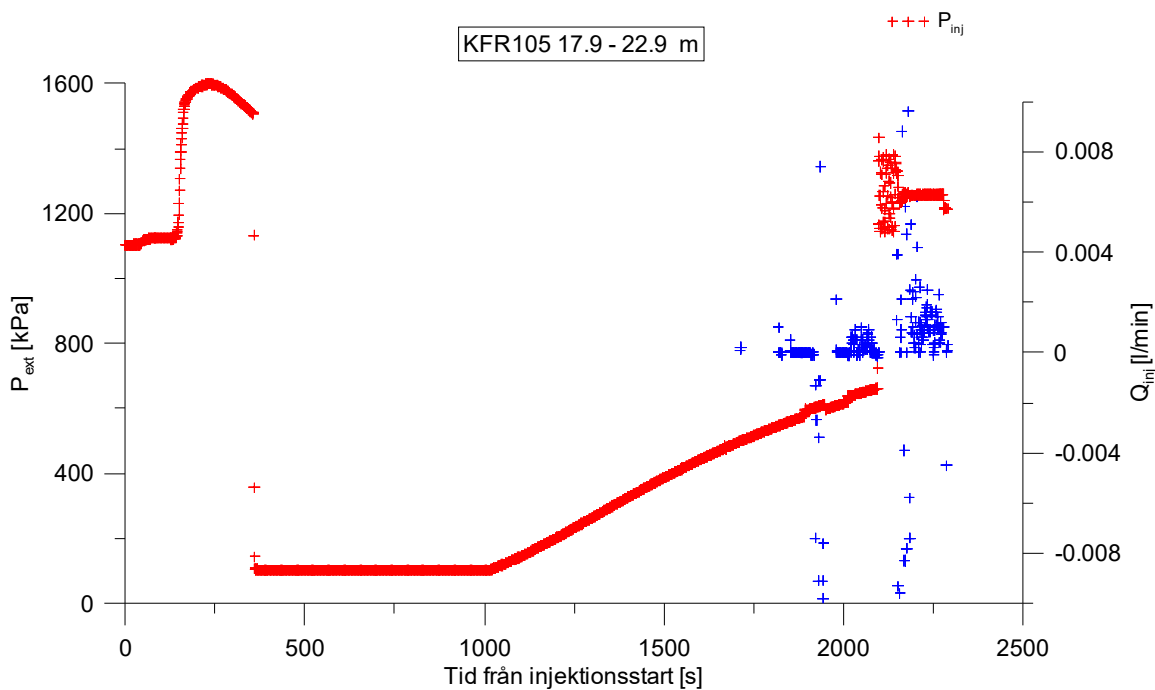


**Figure A3-3.** Linear plot of flow rate ( $Q$ ) and pressure ( $P$ ) versus time from the injection test in section 17.9-22.9 m in borehole KFR105.

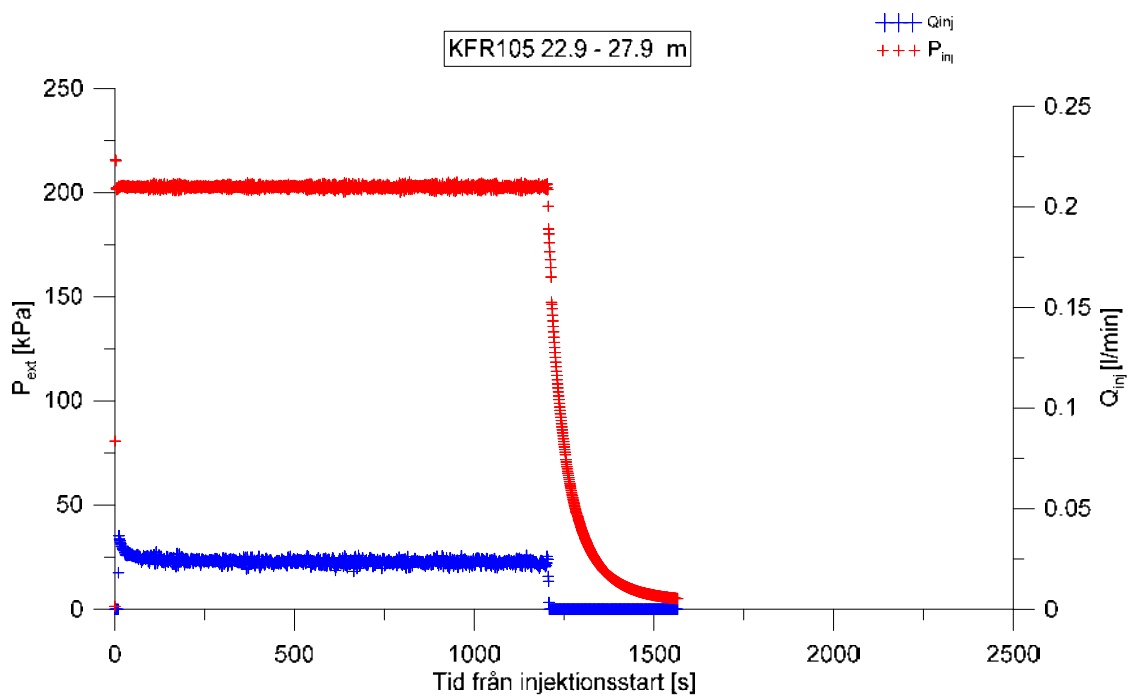


**Figure A3-4.** Linear plot of flow rate ( $Q$ ) and pressure ( $P$ ) versus time from the injection test in section 22.9-27.9 m in borehole KFR105.

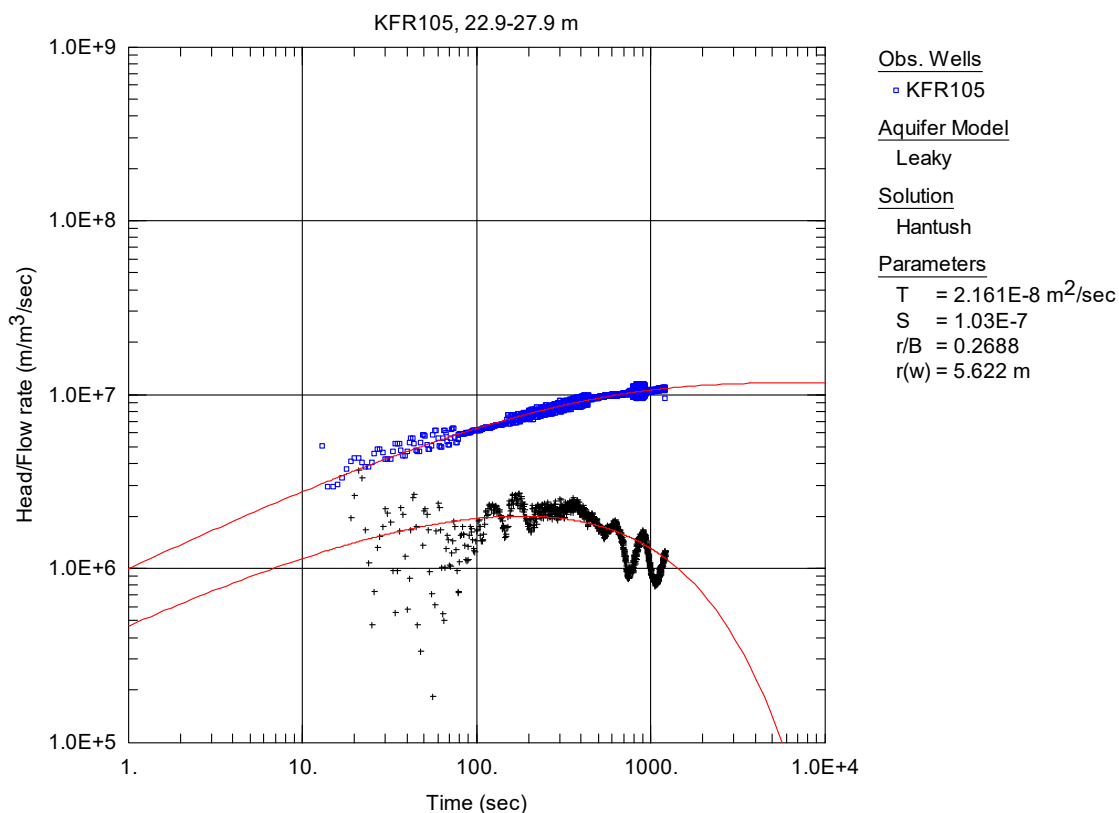


**Figure A3-5.** Log-log plot of head/flow rate ( $\square$ ) and derivative (+) versus time, from the injection test in section 22.9-27.9 m in KFR105.

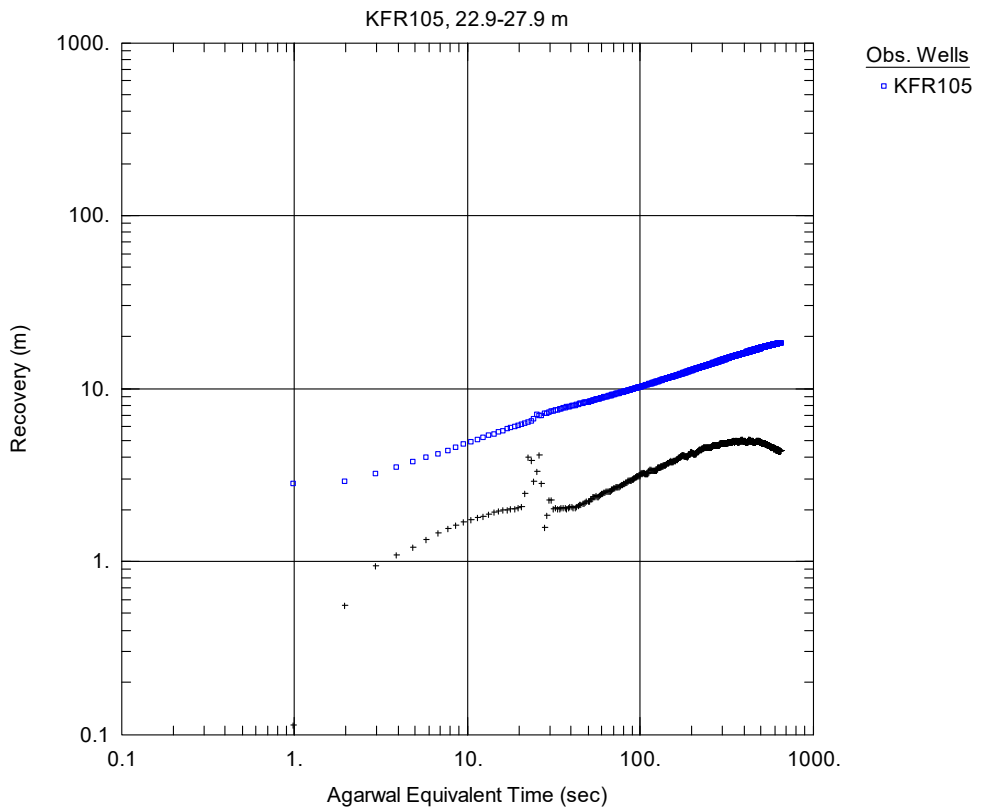


**Figure A3-6.** Log-log plot of recovery (□) and derivative (+) versus equivalent time, from the injection test in section 22.9-27.9 m in KFR105. No satisfying solution was found.

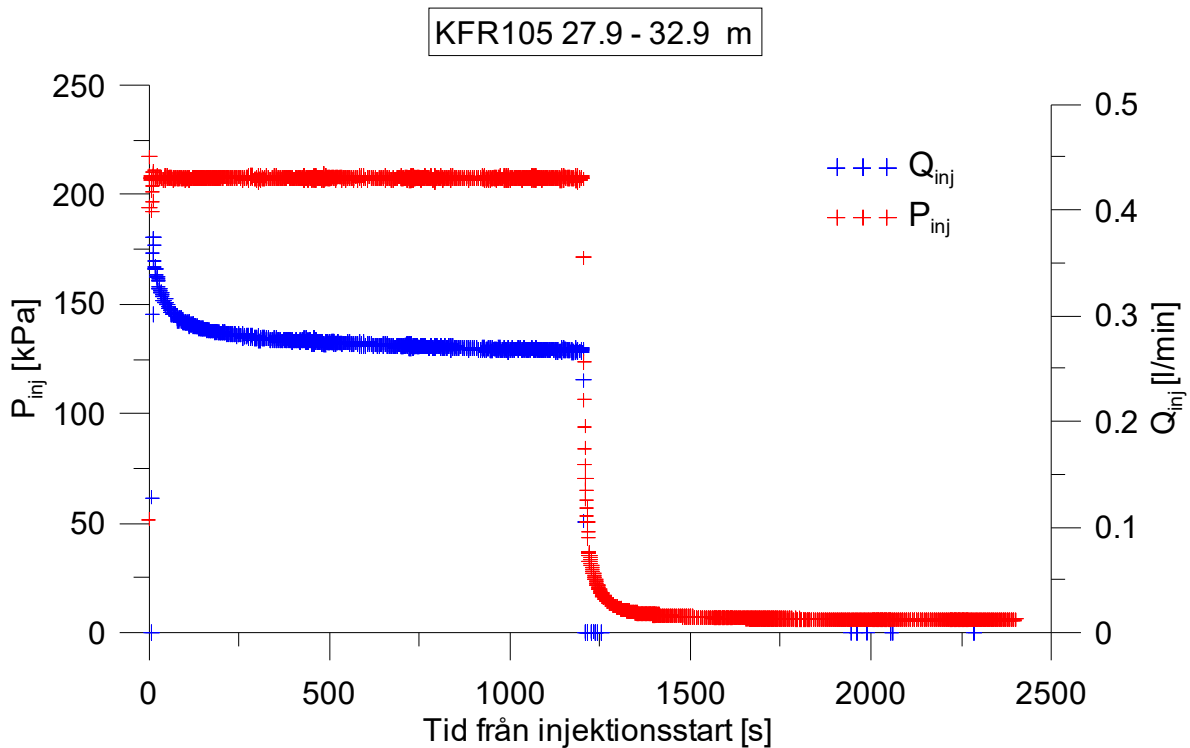


**Figure A3-7.** Linear plot of flow rate ( $Q$ ) and pressure ( $P$ ) versus time from the injection test in section 27.9-32.9 m in borehole KFR105.

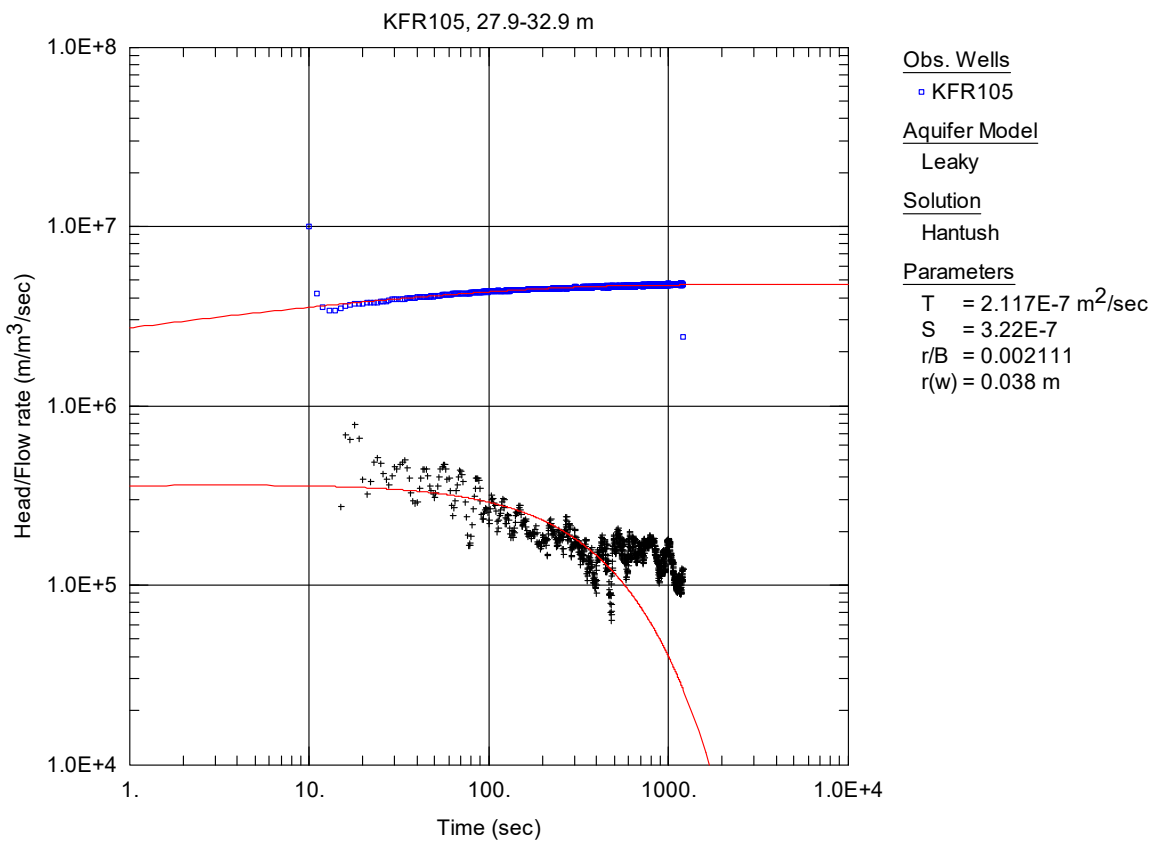


**Figure A3-8.** Log-log plot of head/flow rate (□) and derivative (+) versus time, from the injection test in section 27.9-32.9 m in KFR105.

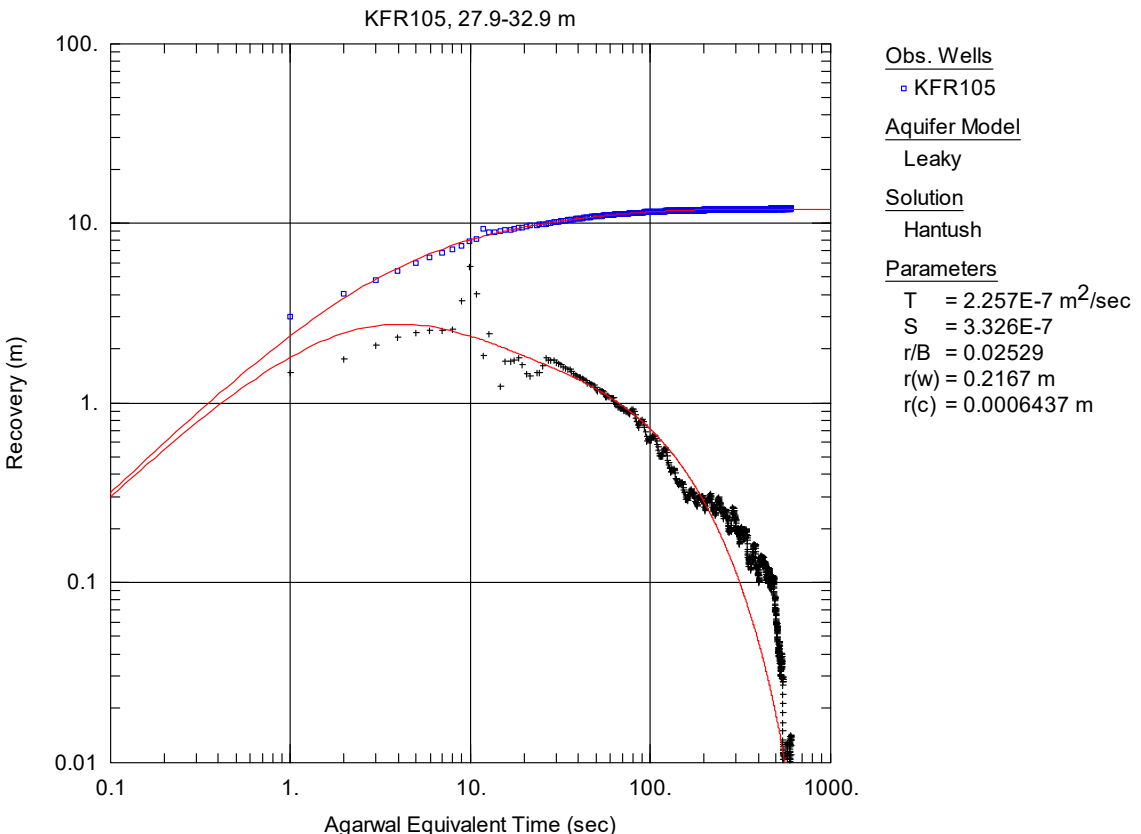


**Figure A3-9.** Log-log plot of recovery (□) and derivative (+) versus equivalent time, from the injection test in section 27.9-32.9 m in KFR105.

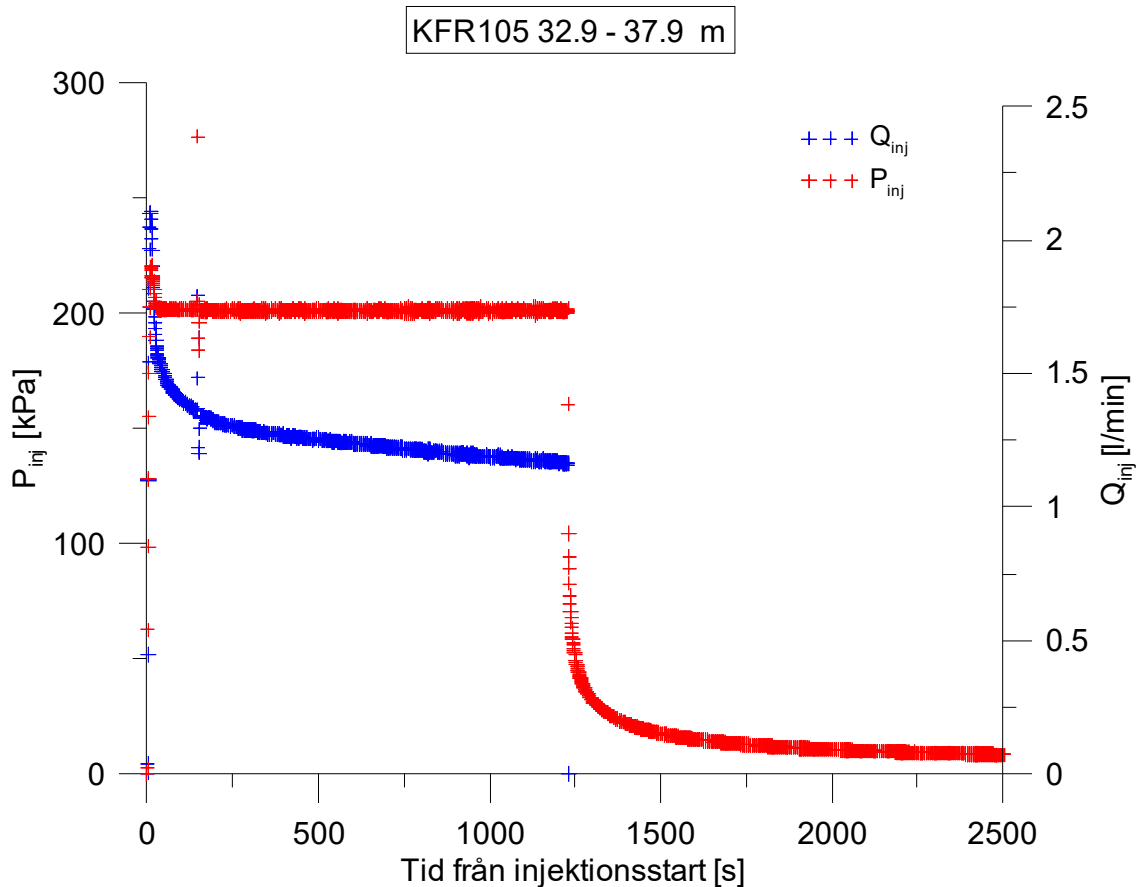


**Figure A3-10.** Linear plot of flow rate ( $Q$ ) and pressure ( $P$ ) versus time from the injection test in section 32.9-37.9 m in borehole KFR105.

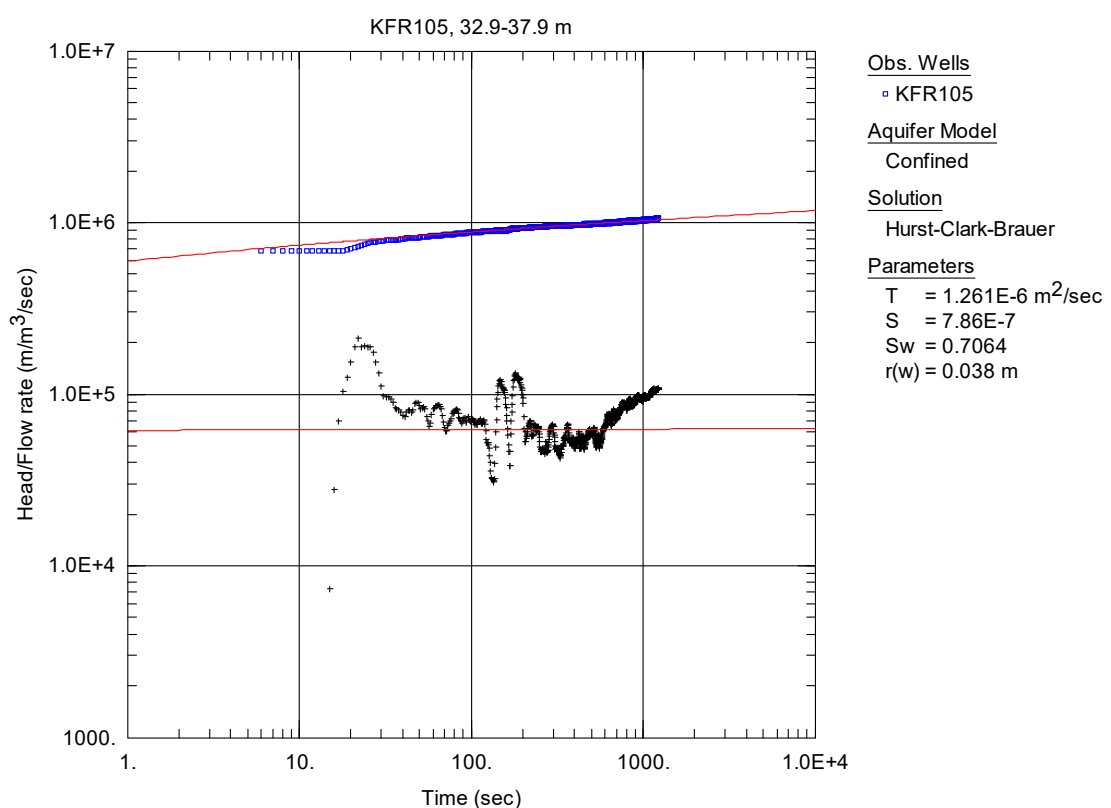


**Figure A3-11.** Log-log plot of head/flow rate (□) and derivative (+) versus time, from the injection test in section 32.9-37.9 m in KFR105.

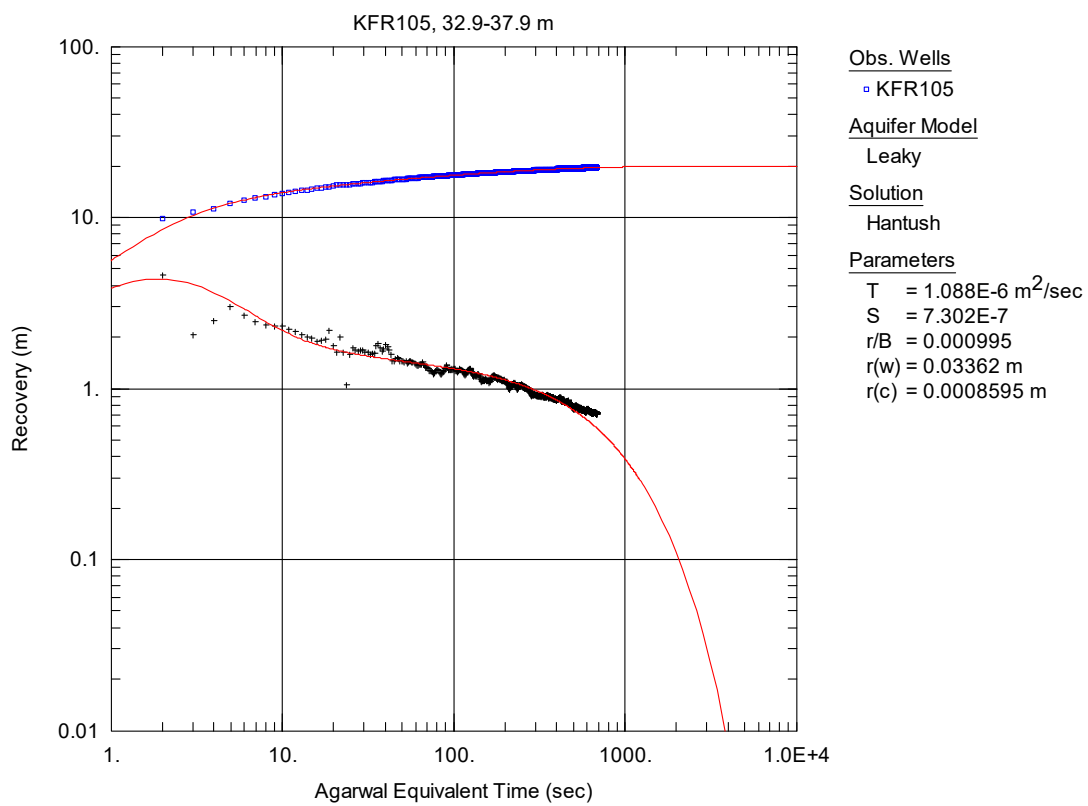


**Figure A3-12.** Log-log plot of recovery (□) and derivative (+) versus equivalent time, from the injection test in section 32.9-37.9 m in KFR105.

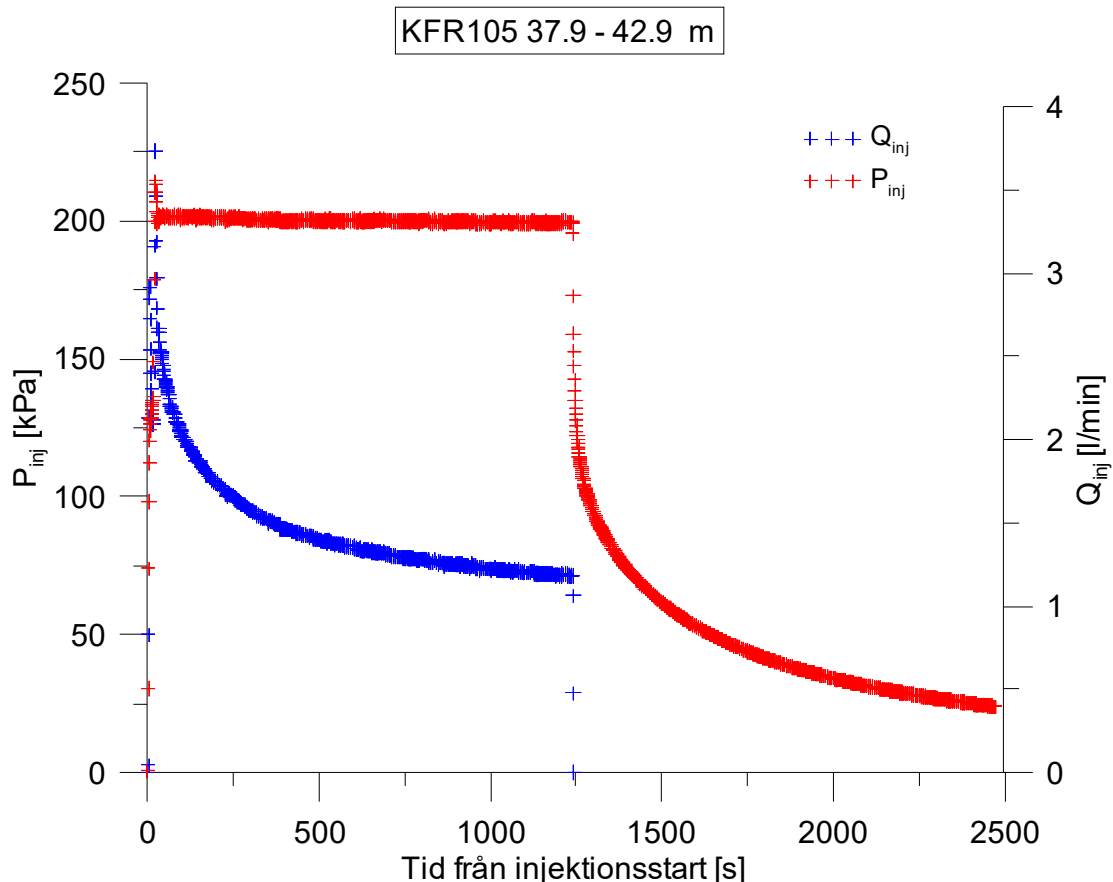


**Figure A3-13.** Linear plot of flow rate (Q) and pressure (P) versus time from the injection test in section 37.9-42.9 m in borehole KFR105.

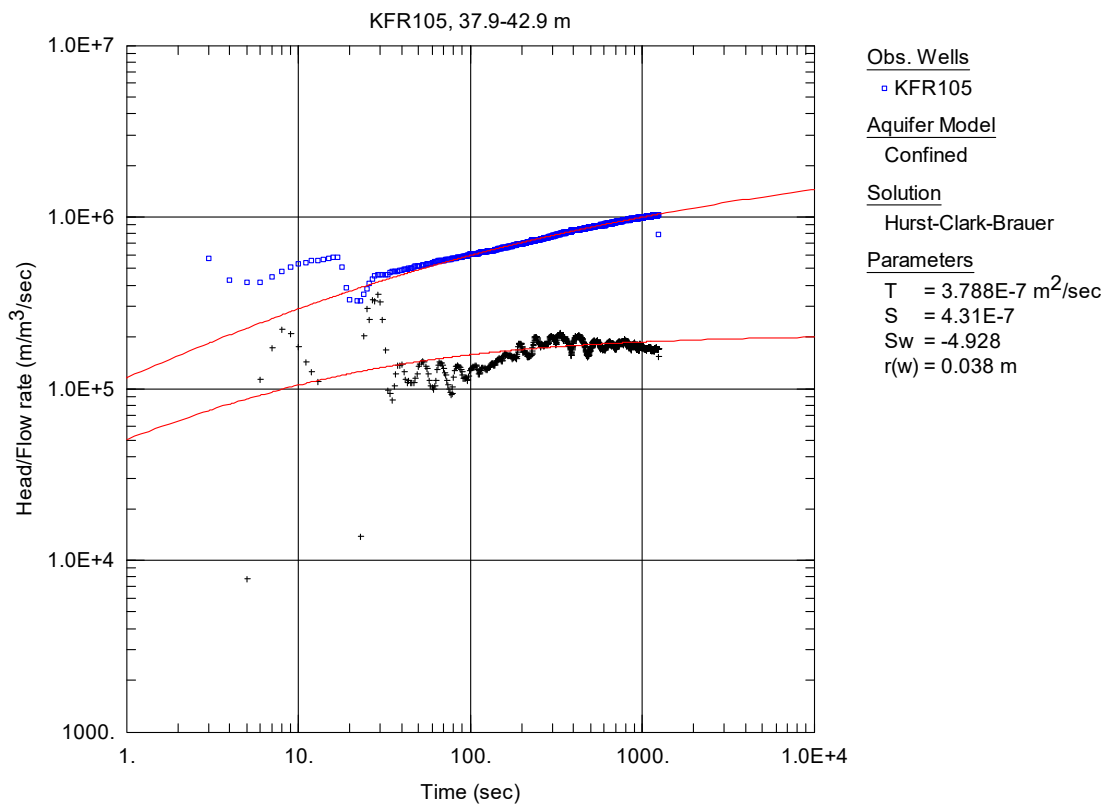


**Figure A3-14.** Log-log plot of head/flow rate (□) and derivative (+) versus time, from the injection test in section 37.9-42.9 m in KFR105.

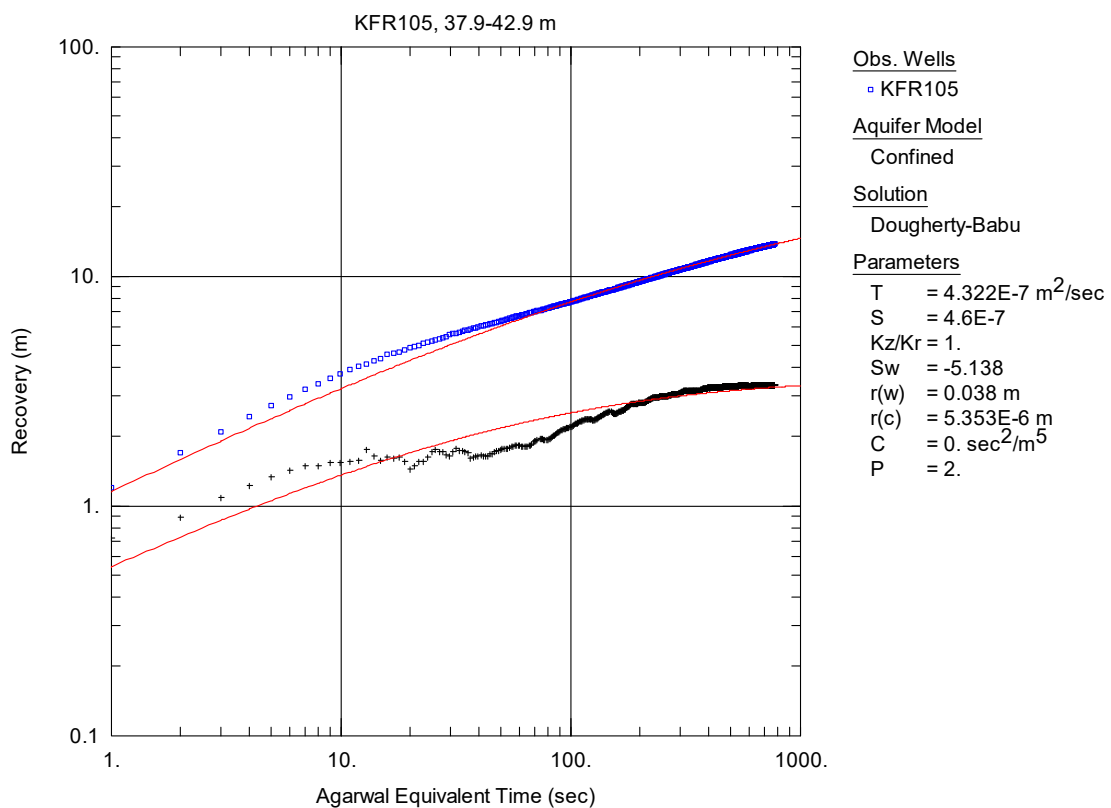


**Figure A3-15.** Log-log plot of recovery (□) and derivative (+) versus equivalent time, from the injection test in section 37.9-42.9 m in KFR105.

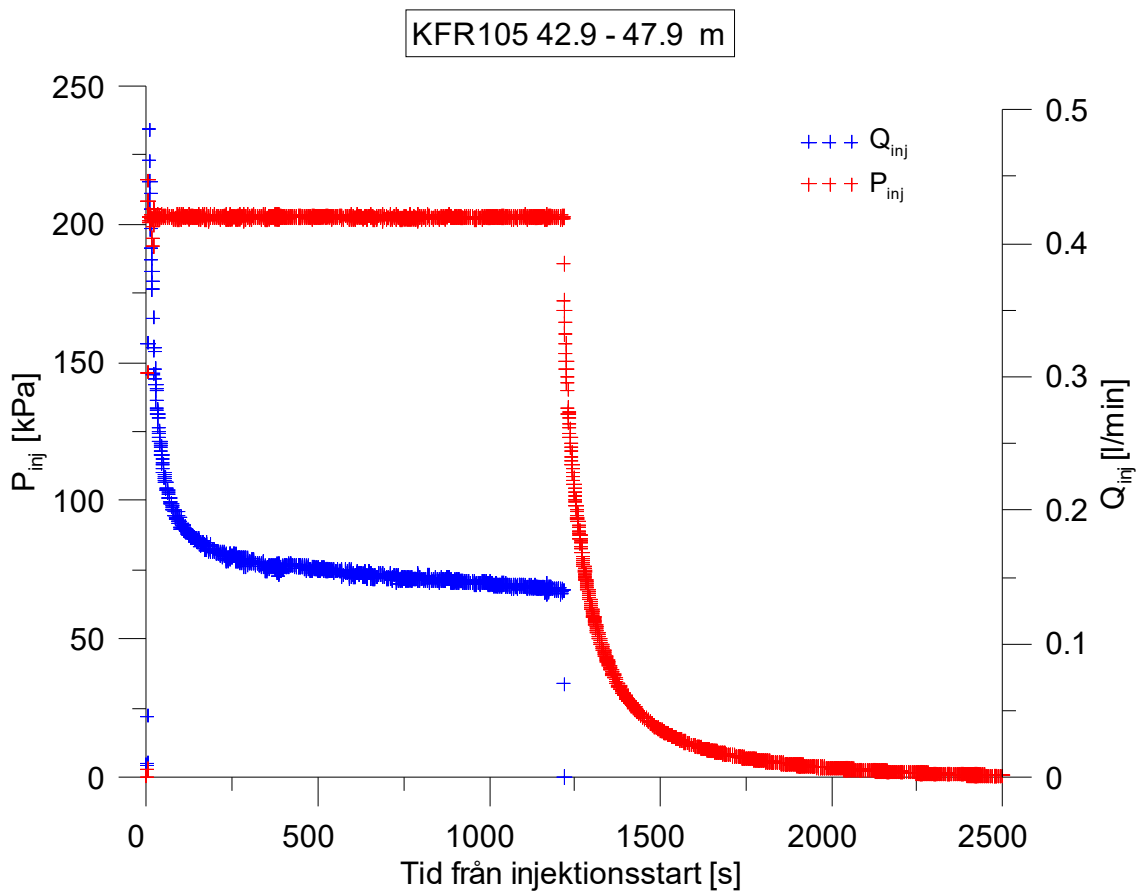


**Figure A3-16.** Linear plot of flow rate ( $Q$ ) and pressure ( $P$ ) versus time from the injection test in section 42.9-47.9 m in borehole KFR105.

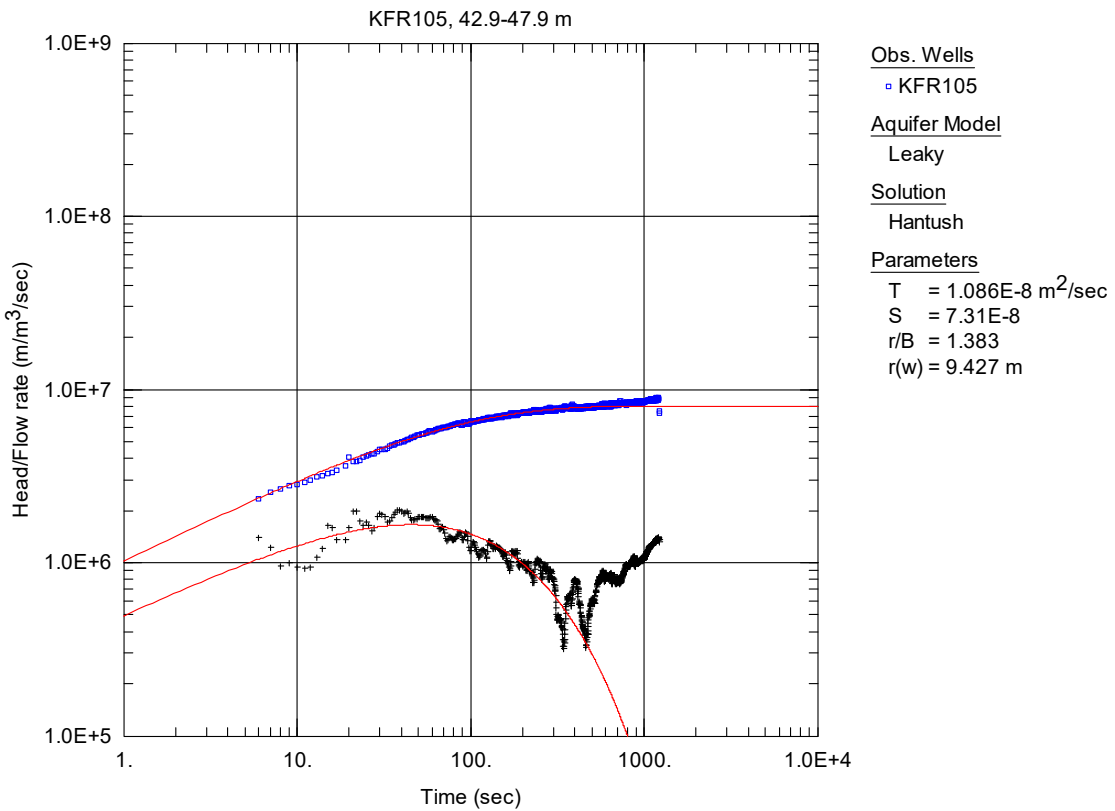


**Figure A3-17.** Log-log plot of head/flow rate (□) and derivative (+) versus time, from the injection test in section 42.9-47.9 m in KFR105.

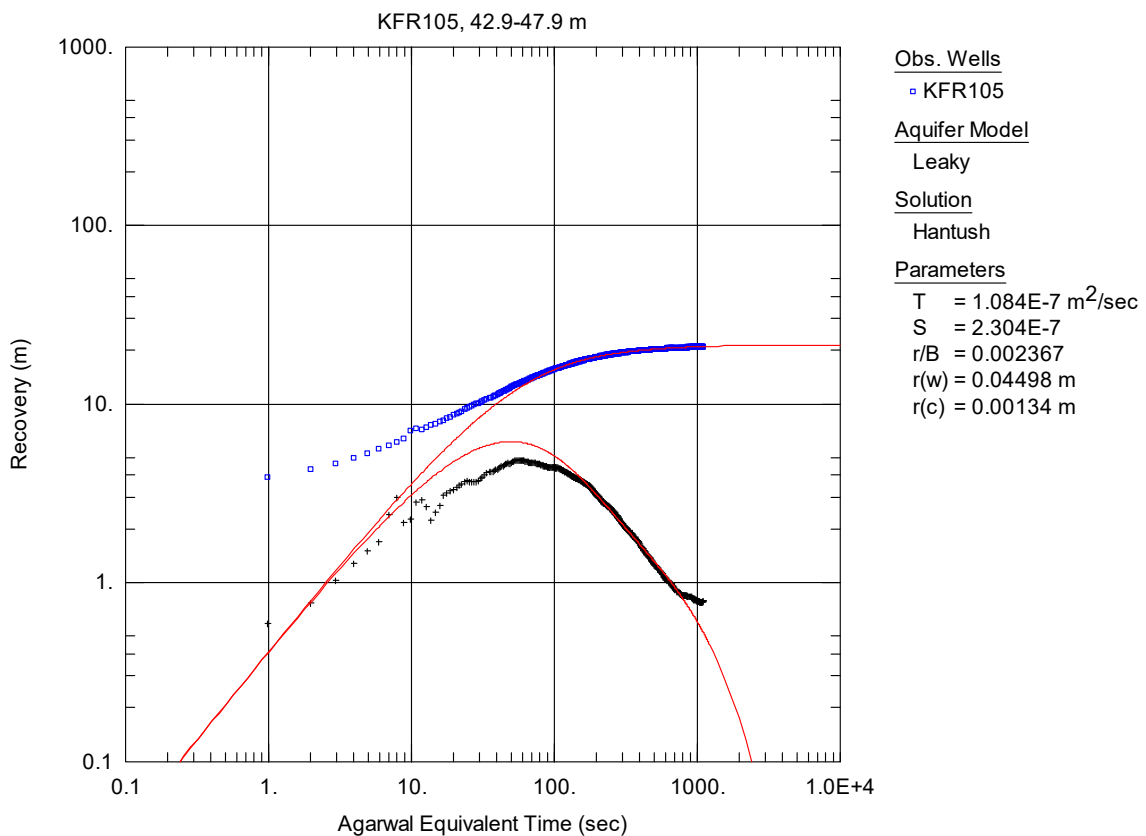


**Figure A3-18.** Log-log plot of recovery (□) and derivative (+) versus equivalent time, from the injection test in section 42.9-47.9 m in KFR105.

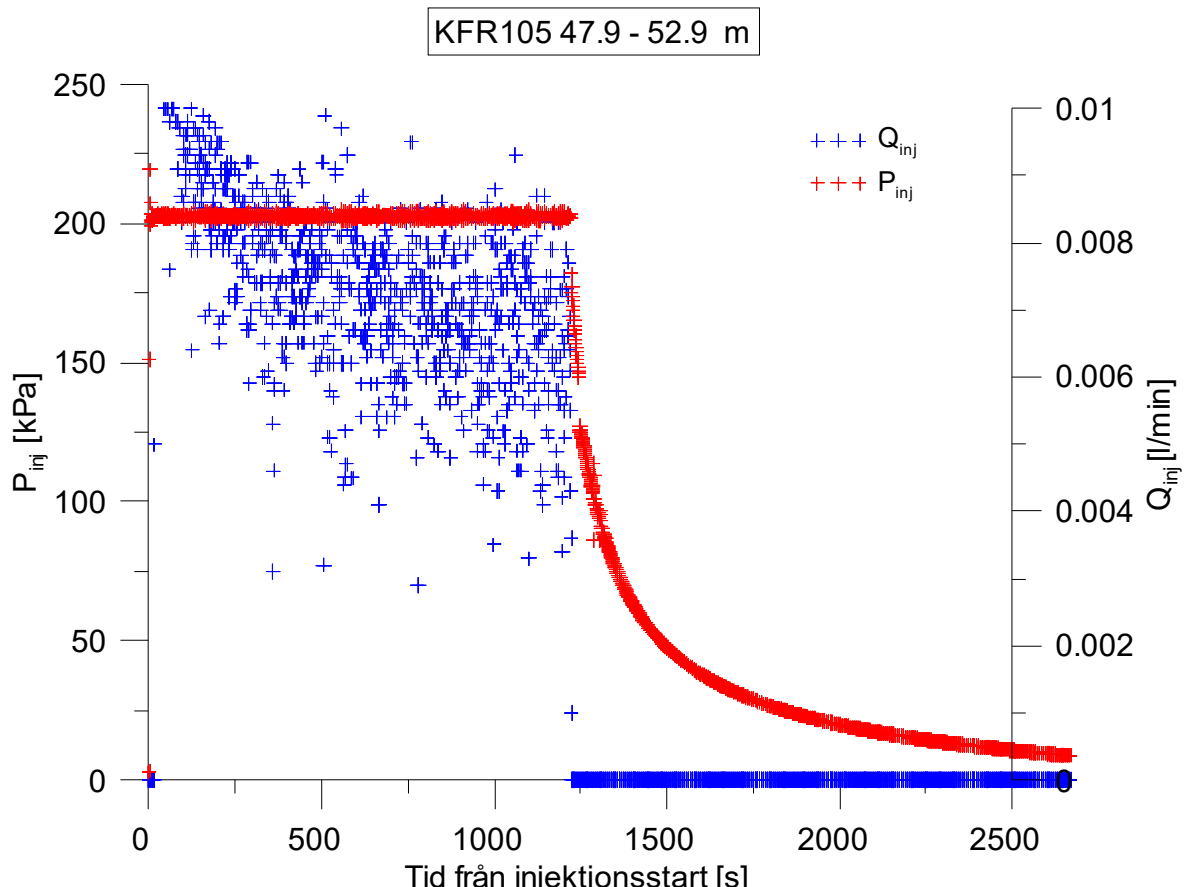


**Figure A3-19.** Linear plot of flow rate ( $Q$ ) and pressure ( $P$ ) versus time from the injection test in section 47.9-52.9 m in borehole KFR105.

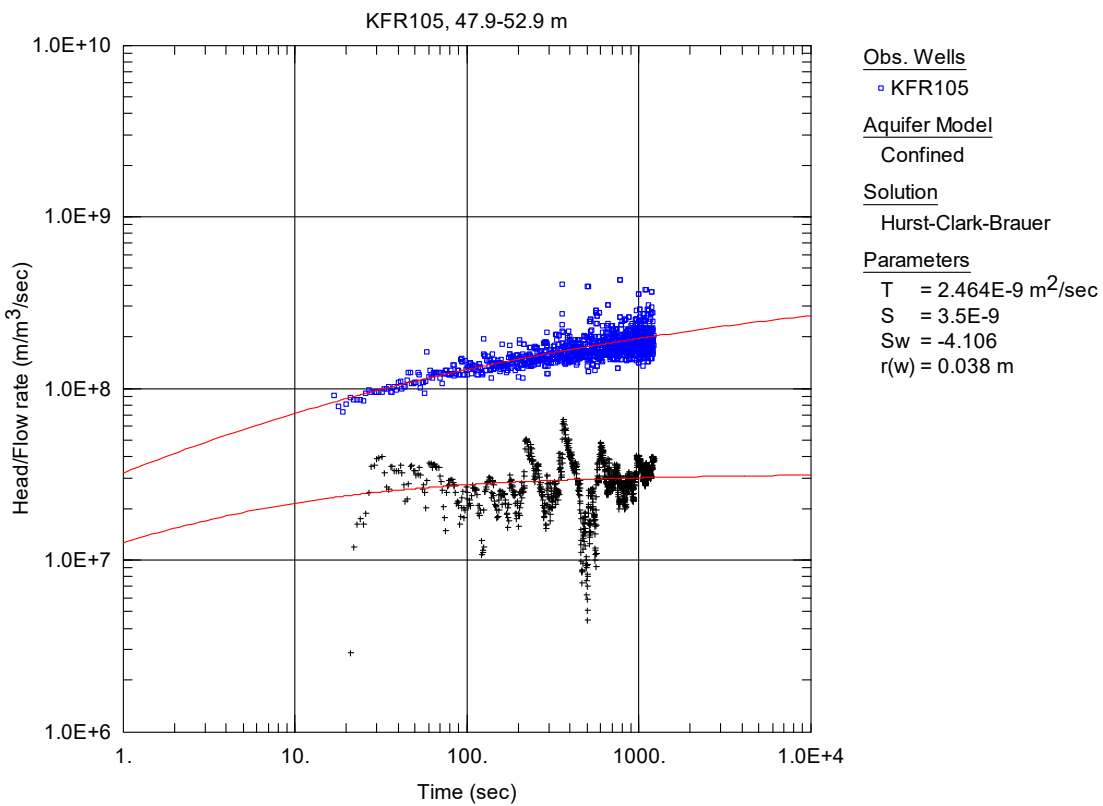


**Figure A3-20.** Log-log plot of head/flow rate (□) and derivative (+) versus time, from the injection test in section 47.9-52.9 m in KFR105.

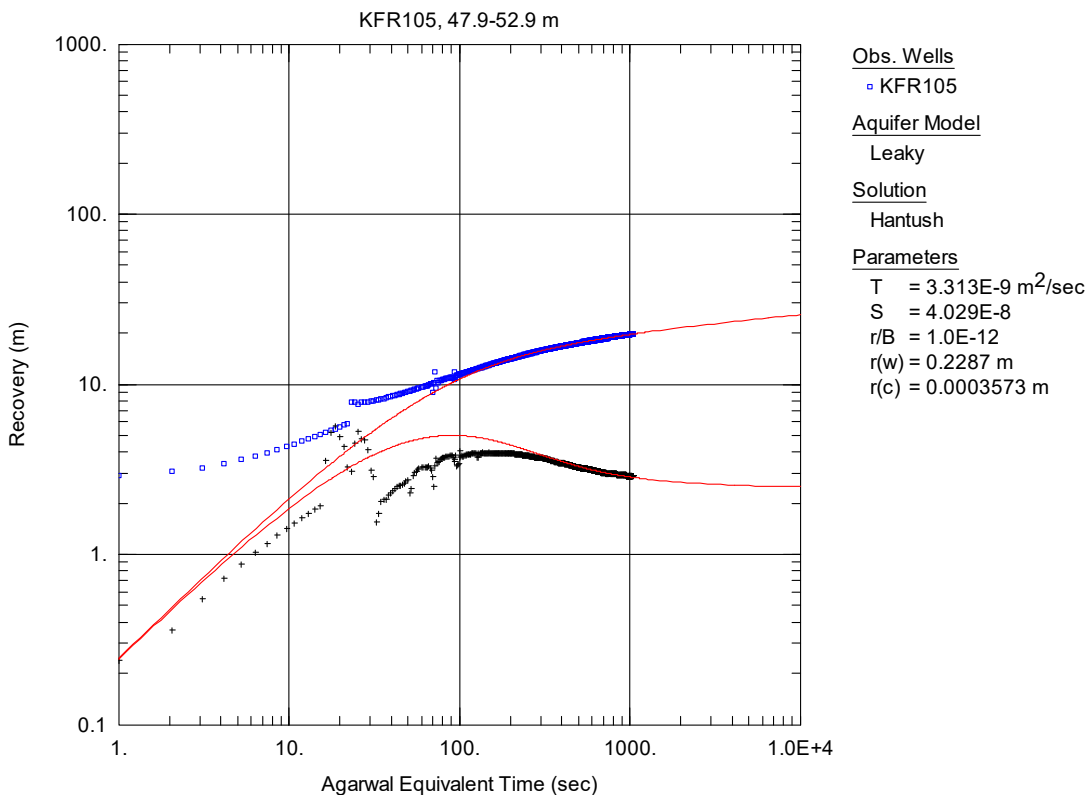


**Figure A3-21.** Log-log plot of recovery (□) and derivative (+) versus equivalent time, from the injection test in section 47.9-52.9 m in KFR105.

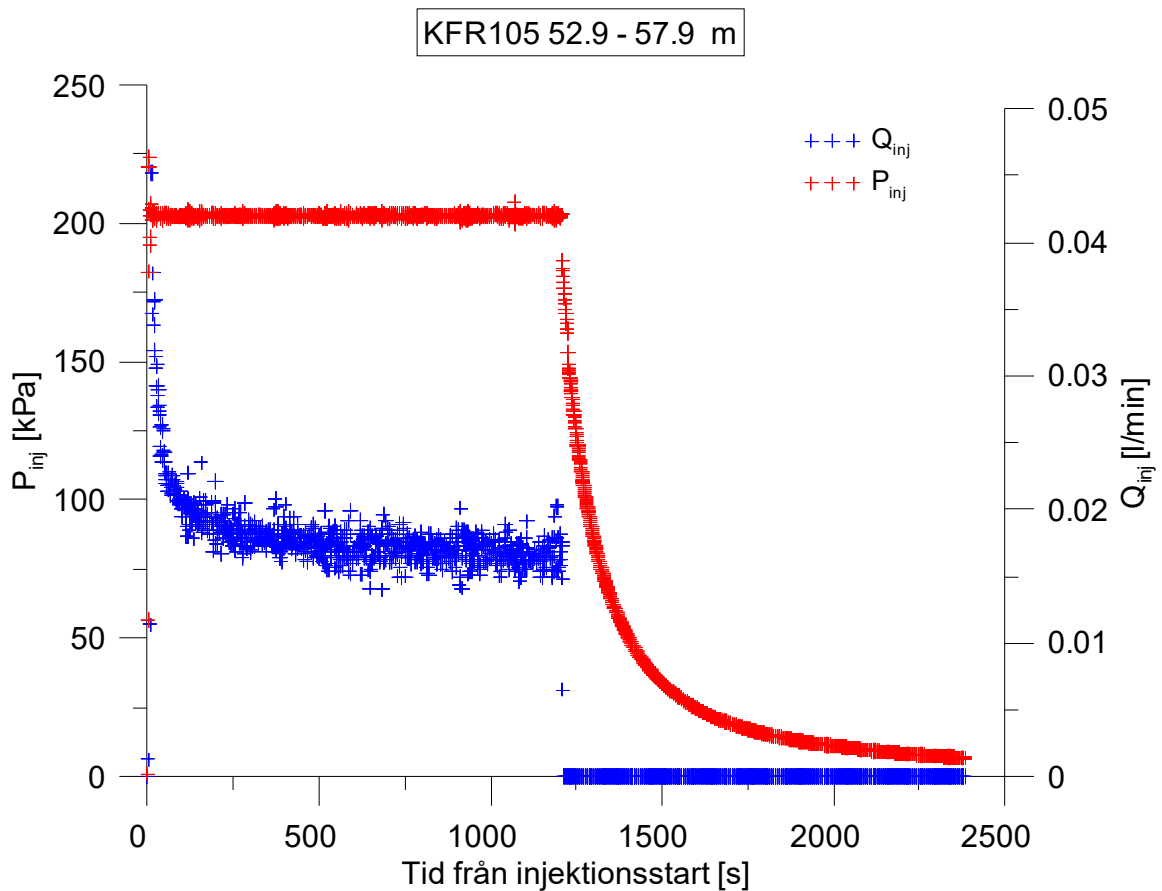


**Figure A3-22.** Linear plot of flow rate ( $Q$ ) and pressure ( $P$ ) versus time from the injection test in section 52.9-57.9 m in borehole KFR105.

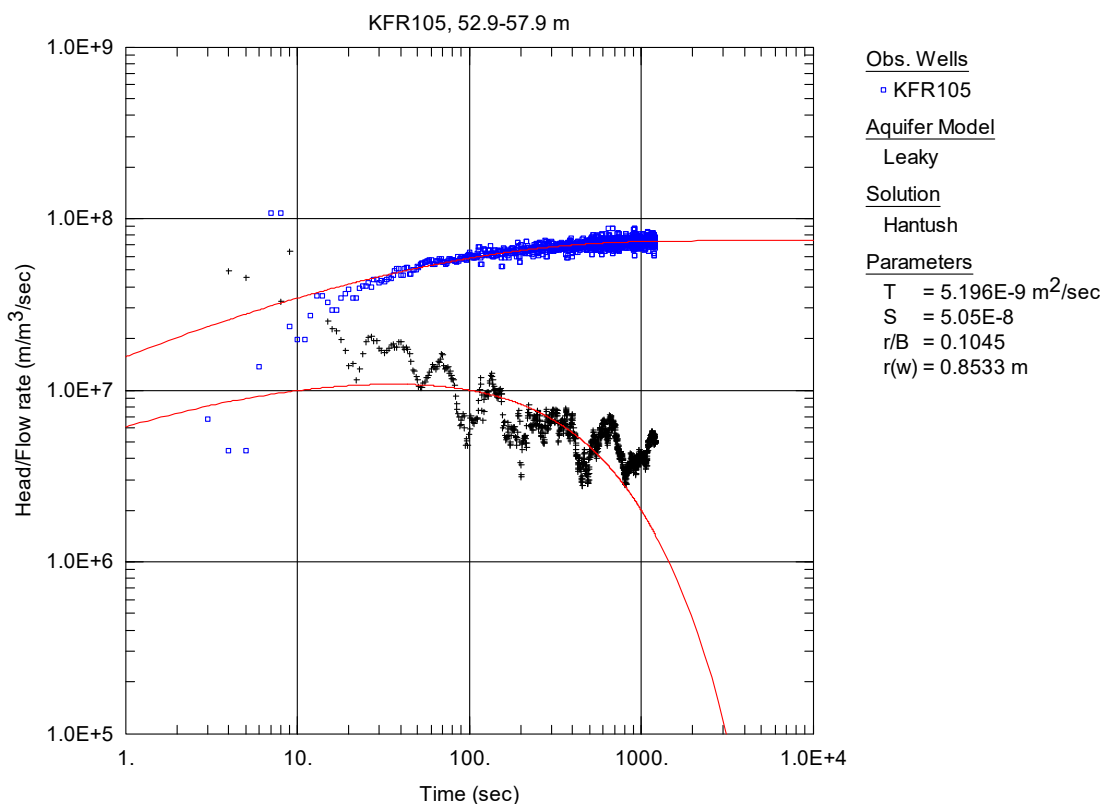


**Figure A3-23.** Log-log plot of head/flow rate (□) and derivative (+) versus time, from the injection test in section 52.9-57.9 m in KFR105.

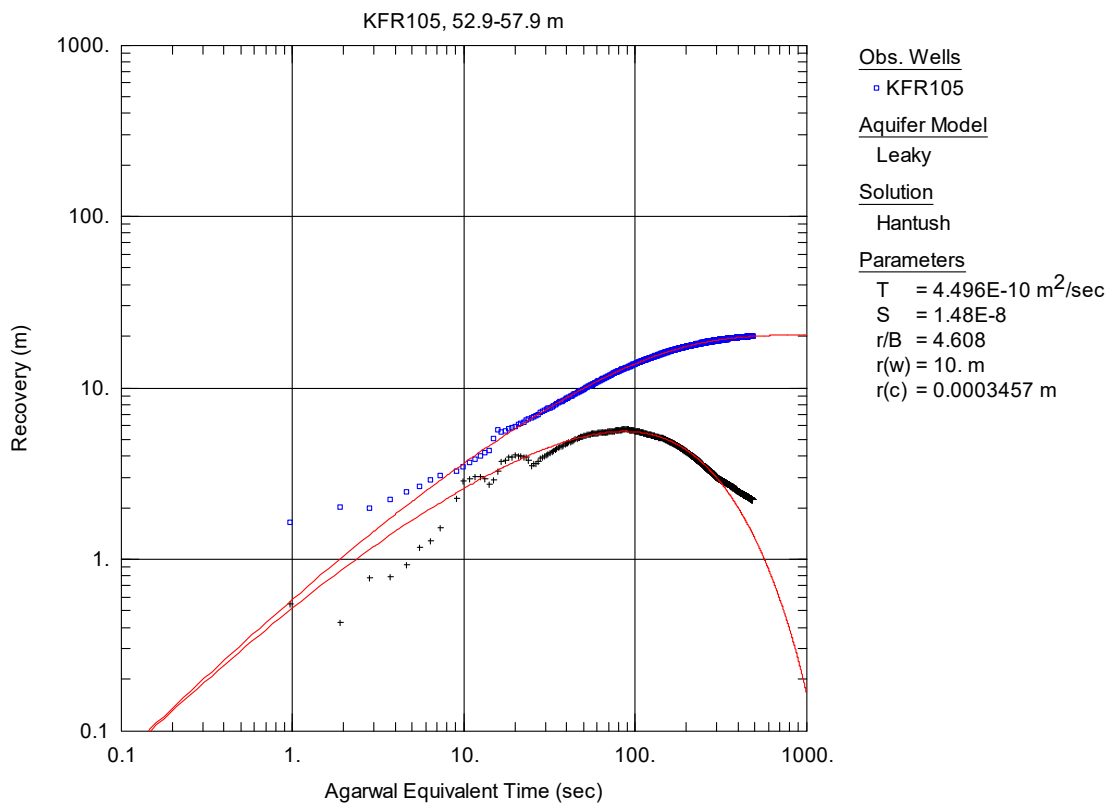


**Figure A3-24.** Log-log plot of recovery (□) and derivative (+) versus equivalent time, from the injection test in section 52.9-57.9 m in KFR105.

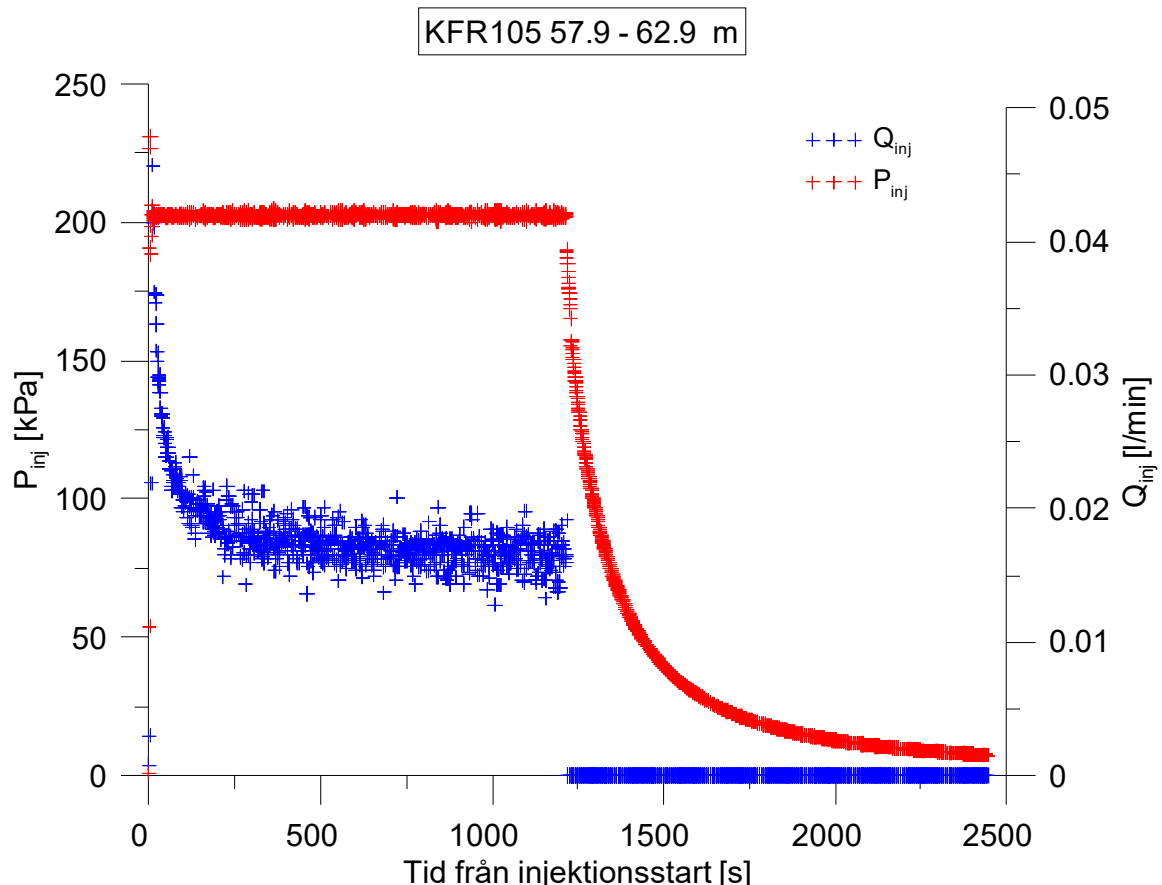


**Figure A3-25.** Linear plot of flow rate ( $Q$ ) and pressure ( $P$ ) versus time from the injection test in section 57.9-62.9 m in borehole KFR105.

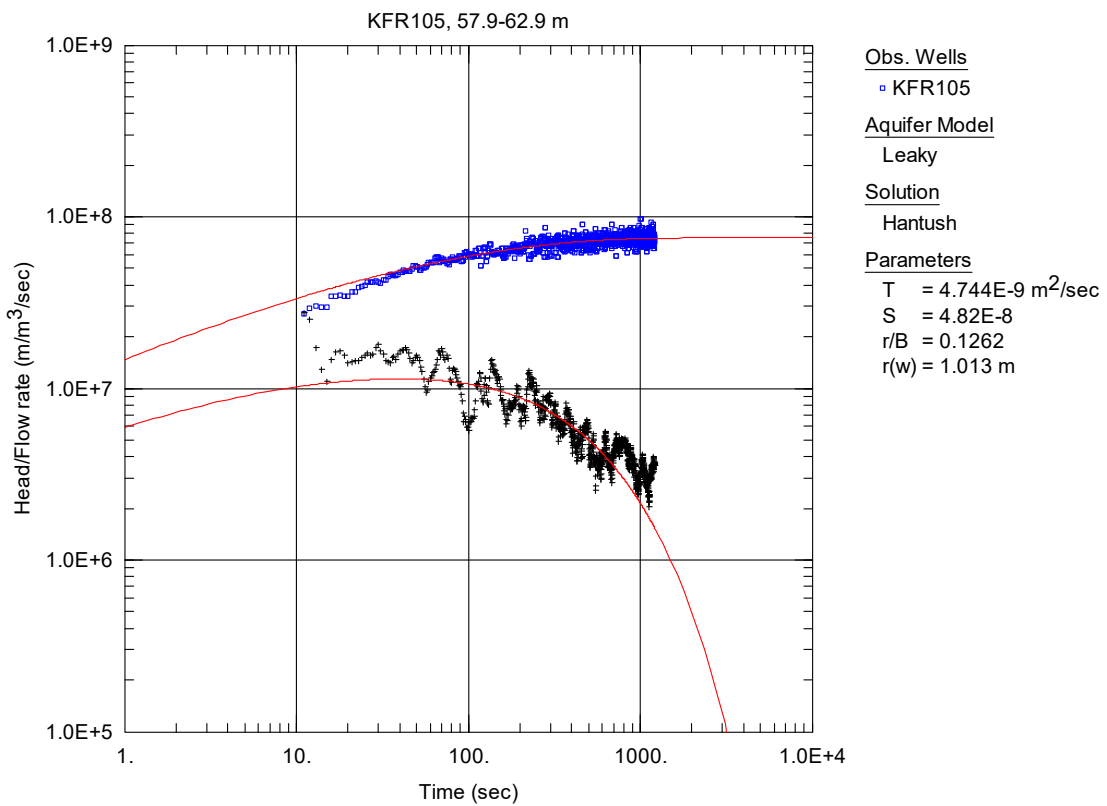


**Figure A3-26.** Log-log plot of head/flow rate (□) and derivative (+) versus time, from the injection test in section 57.9-62.9 m in KFR105.

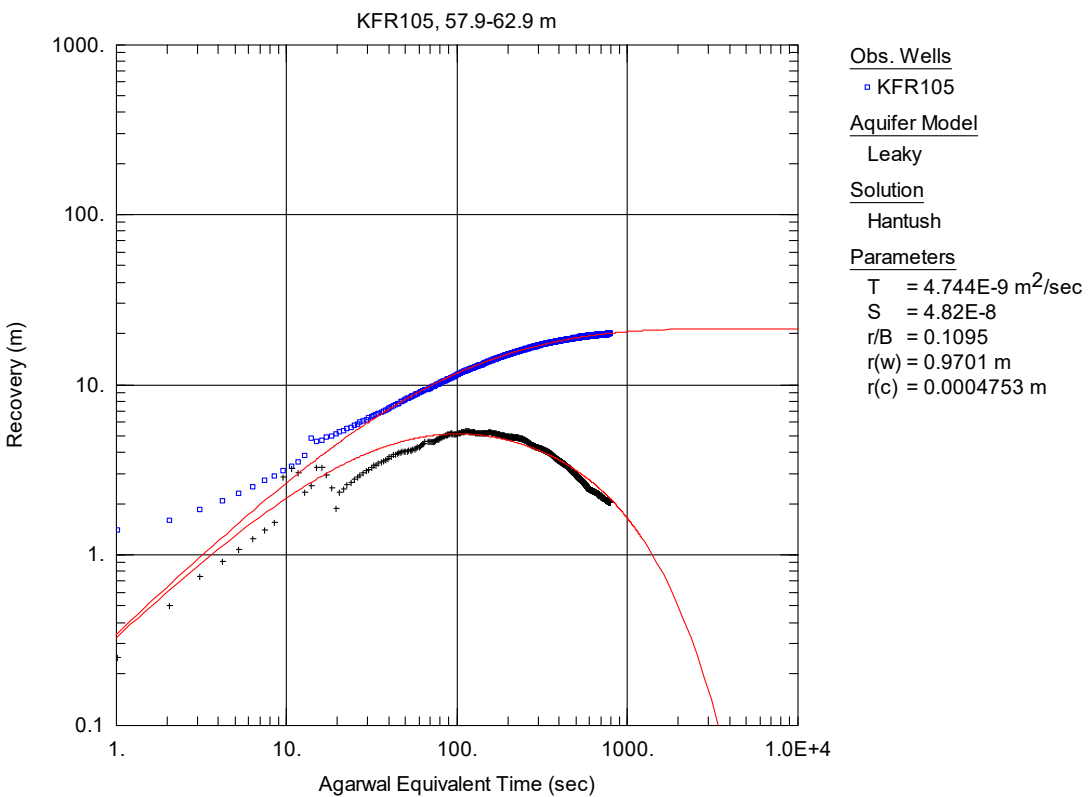


**Figure A3-27.** Log-log plot of recovery (□) and derivative (+) versus equivalent time, from the injection test in section 57.9-62.9 m in KFR105.

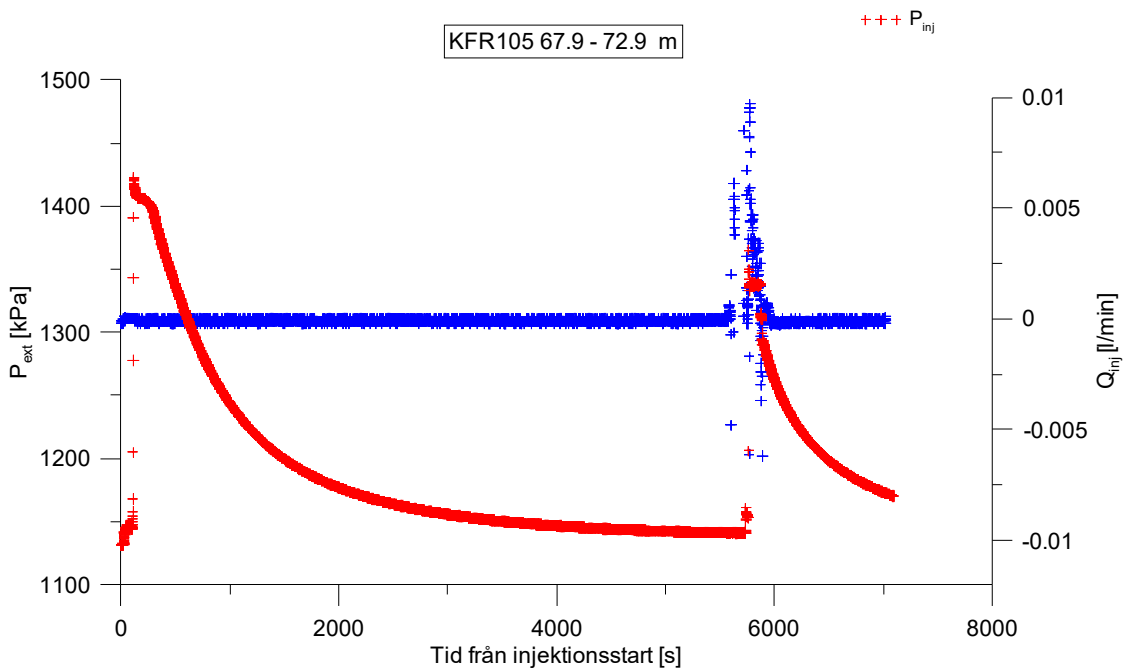


**Figure A3-28.** Linear plot of flow rate ( $Q$ ) and pressure ( $P$ ) versus time from the injection test in section 67.9-72.9 m in borehole KFR105.

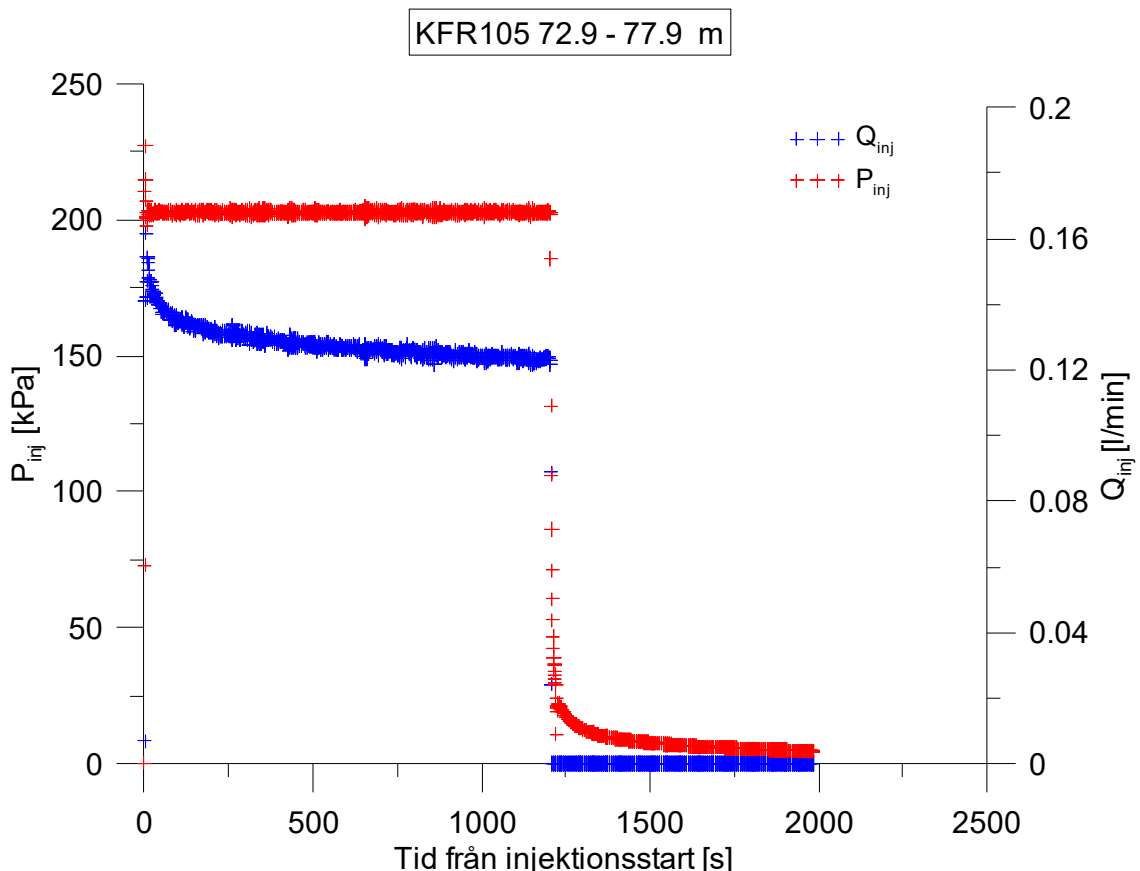


**Figure A3-29.** Linear plot of flow rate ( $Q$ ) and pressure ( $P$ ) versus time from the injection test in section 72.9-77.9 m in borehole KFR105.

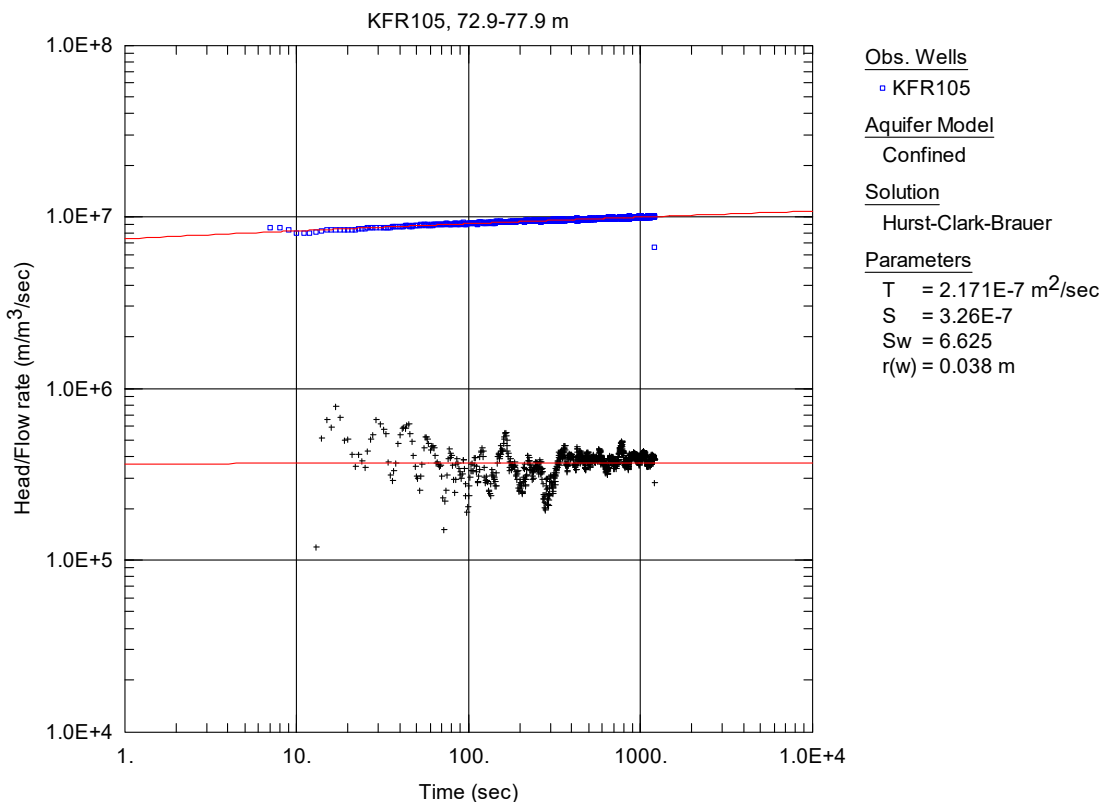


**Figure A3-30.** Log-log plot of head/flow rate (□) and derivative (+) versus time, from the injection test in section 72.9-77.9 m in KFR105.

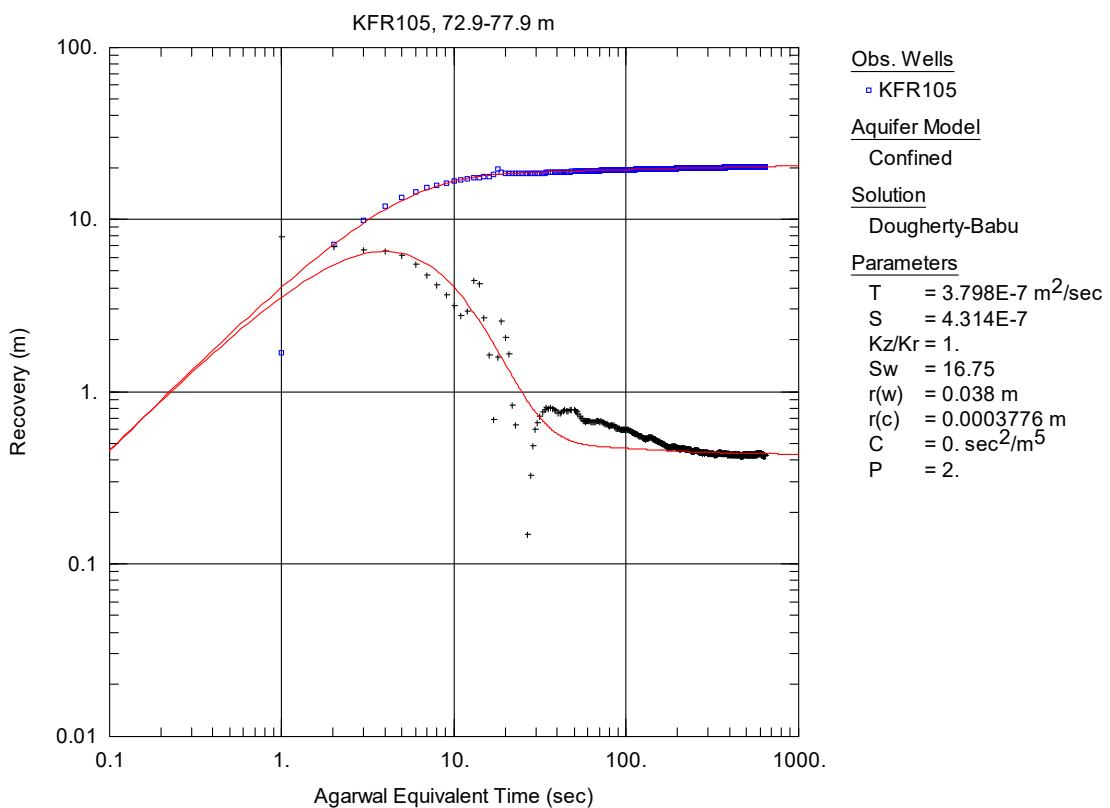


**Figure A3-31.** Log-log plot of recovery (□) and derivative (+) versus equivalent time, from the injection test in section 72.9-77.9 m in KFR105.

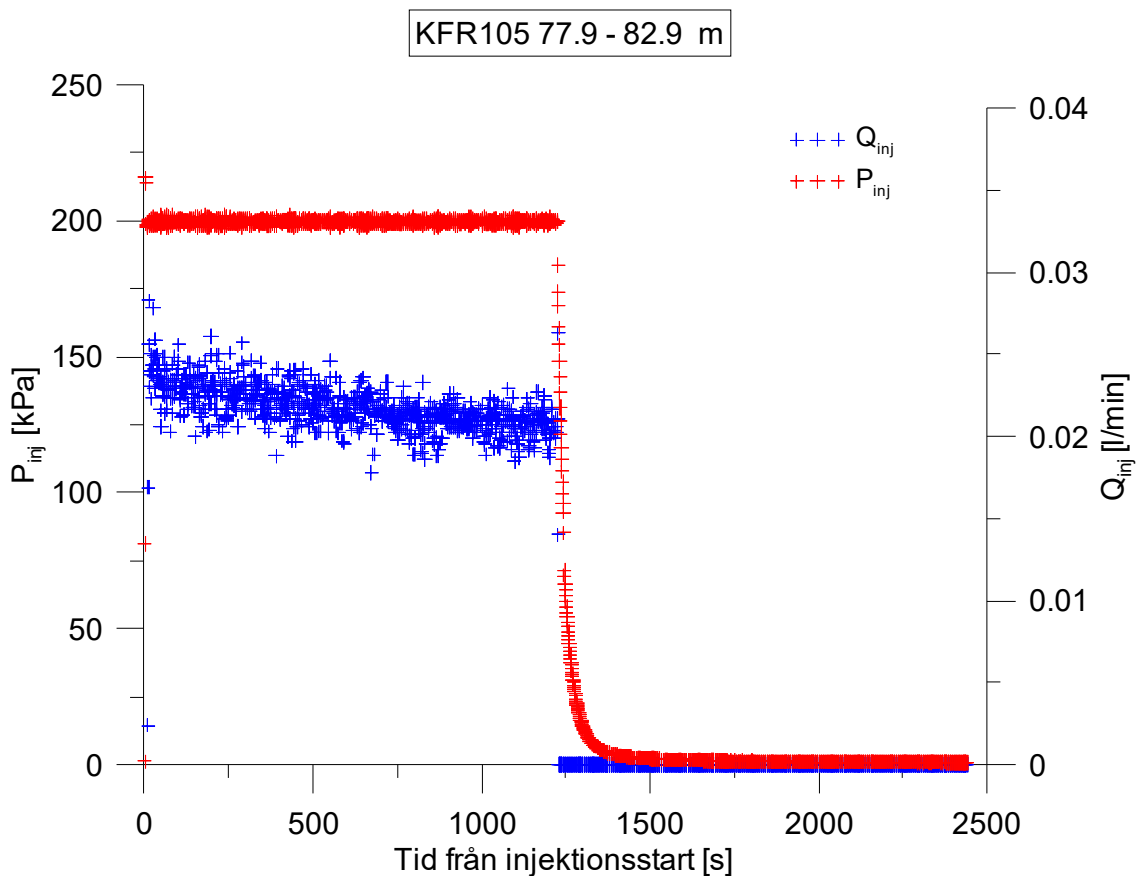


**Figure A3-32.** Linear plot of flow rate ( $Q$ ) and pressure ( $P$ ) versus time from the injection test in section 77.9-82.9 m in borehole KFR105.

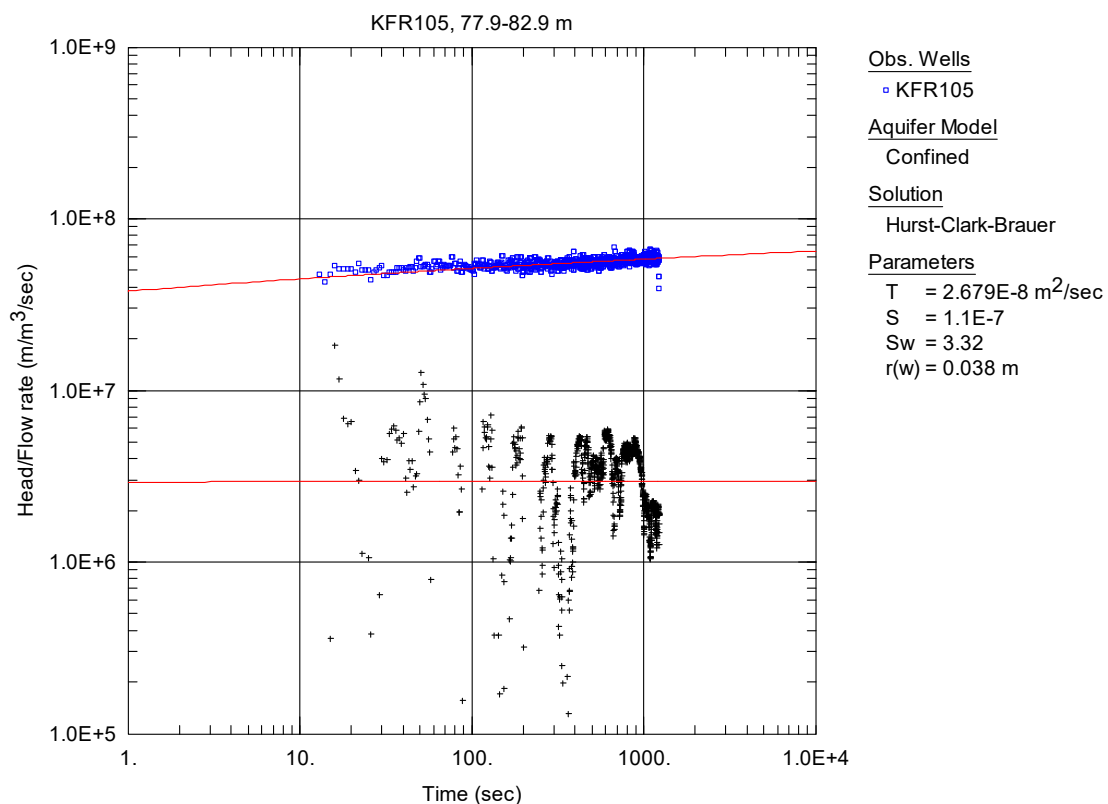


**Figure A3-33.** Log-log plot of head/flow rate ( $\square$ ) and derivative (+) versus time, from the injection test in section 77.9-82.9 m in KFR105.

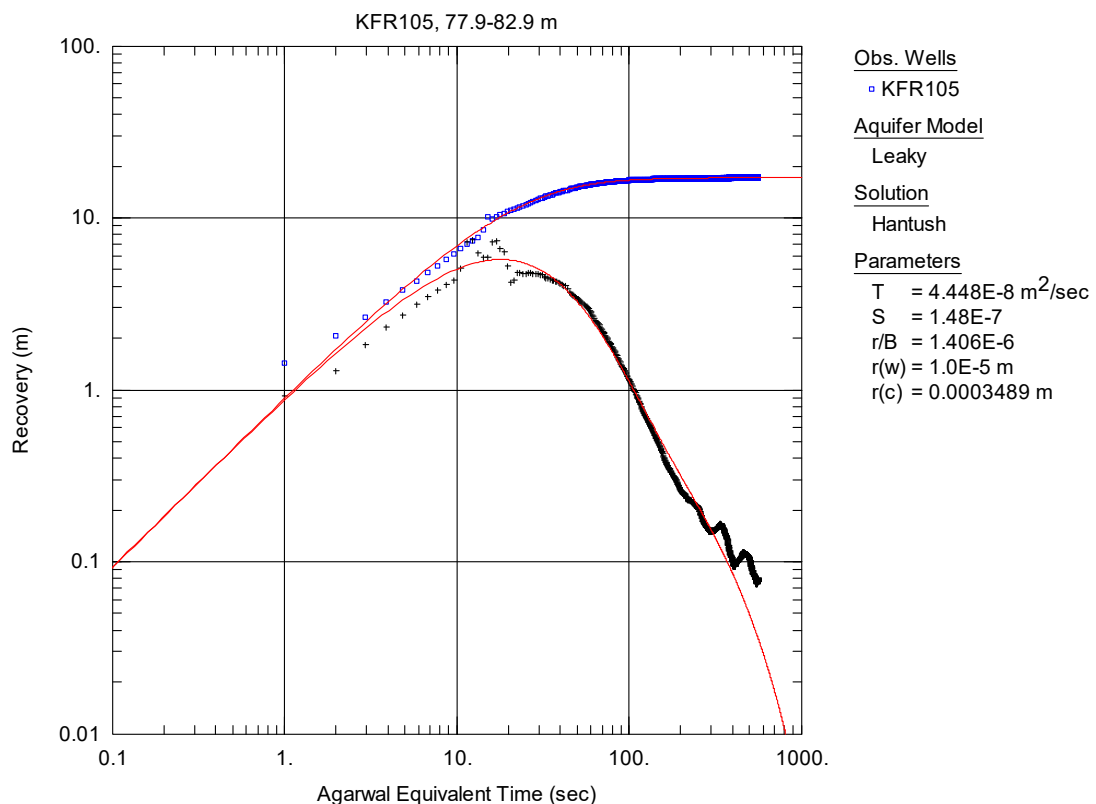


**Figure A3-34.** Log-log plot of recovery (□) and derivative (+) versus equivalent time, from the injection test in section 77.9-82.9 m in KFR105.

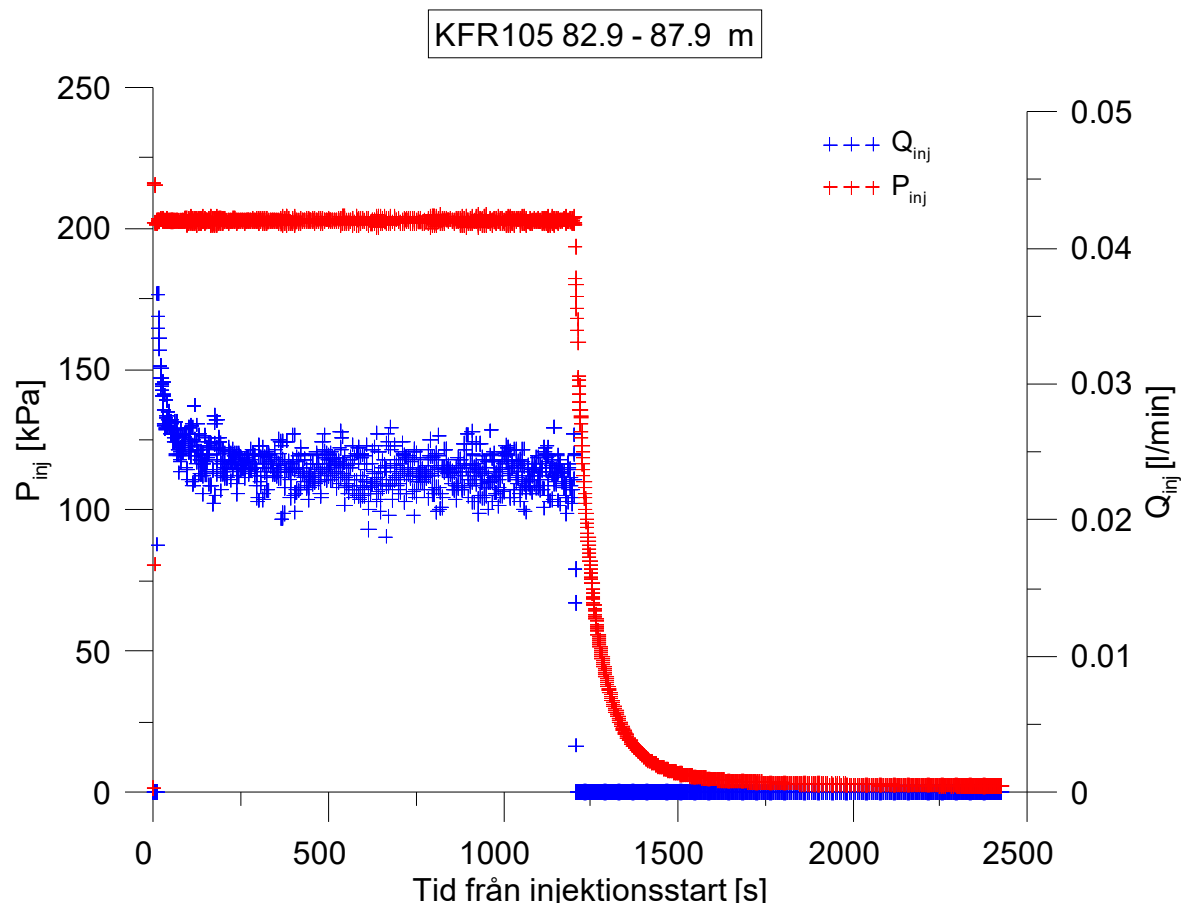


**Figure A3-35.** Linear plot of flow rate ( $Q$ ) and pressure ( $P$ ) versus time from the injection test in section 82.9-87.9 m in borehole KFR105.

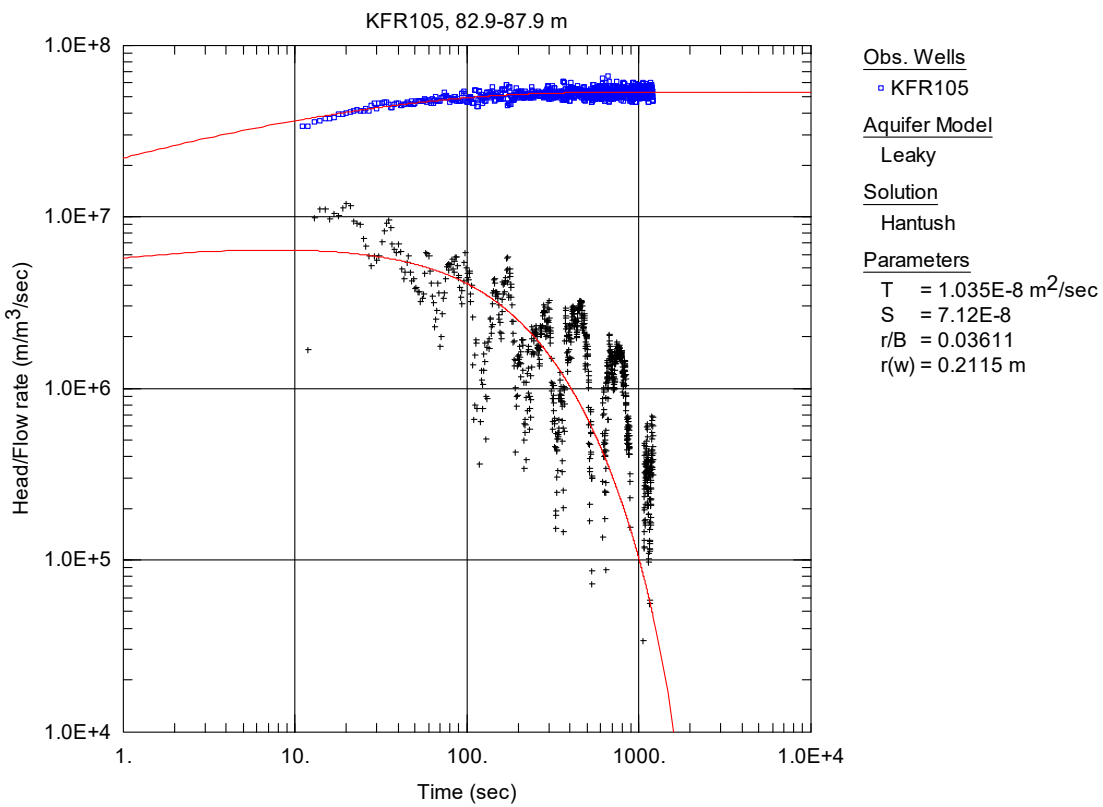


**Figure A3-36.** Log-log plot of head/flow rate ( $\square$ ) and derivative (+) versus time, from the injection test in section 82.9-87.9 m in KFR105.

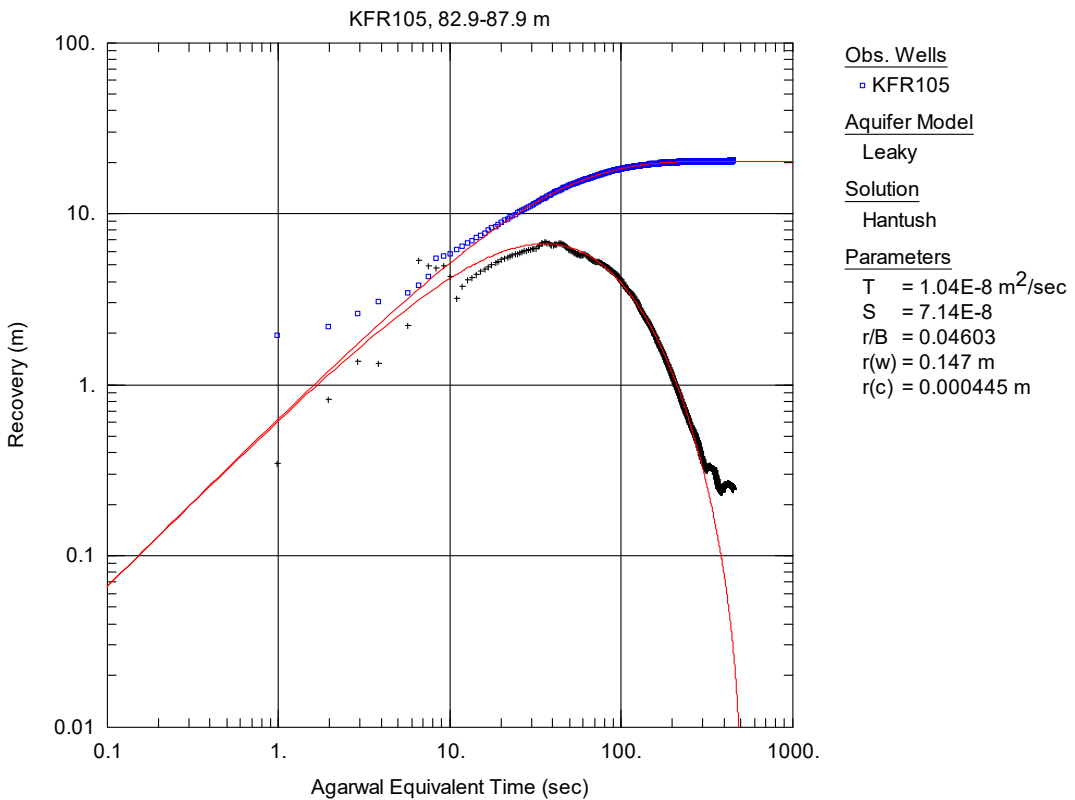


**Figure A3-37.** Log-log plot of recovery ( $\square$ ) and derivative (+) versus equivalent time, from the injection test in section 82.9-87.9 m in KFR105.

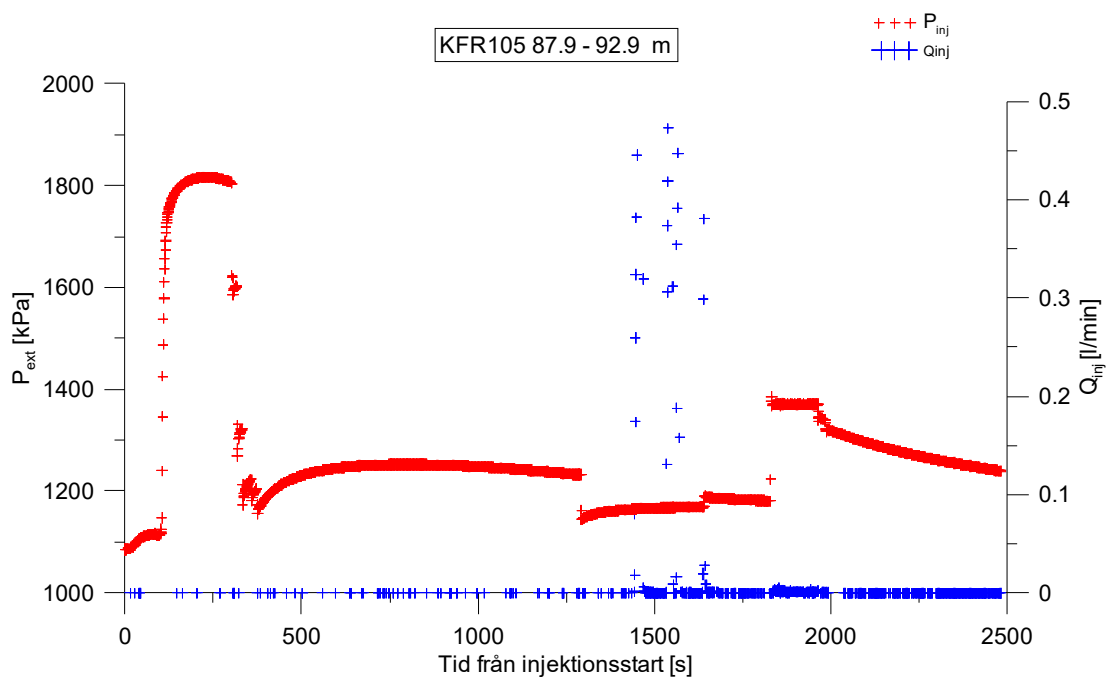


**Figure A3-38.** Linear plot of flow rate ( $Q$ ) and pressure ( $P$ ) versus time from the injection test in section 87.9-92.9 m in borehole KFR105.

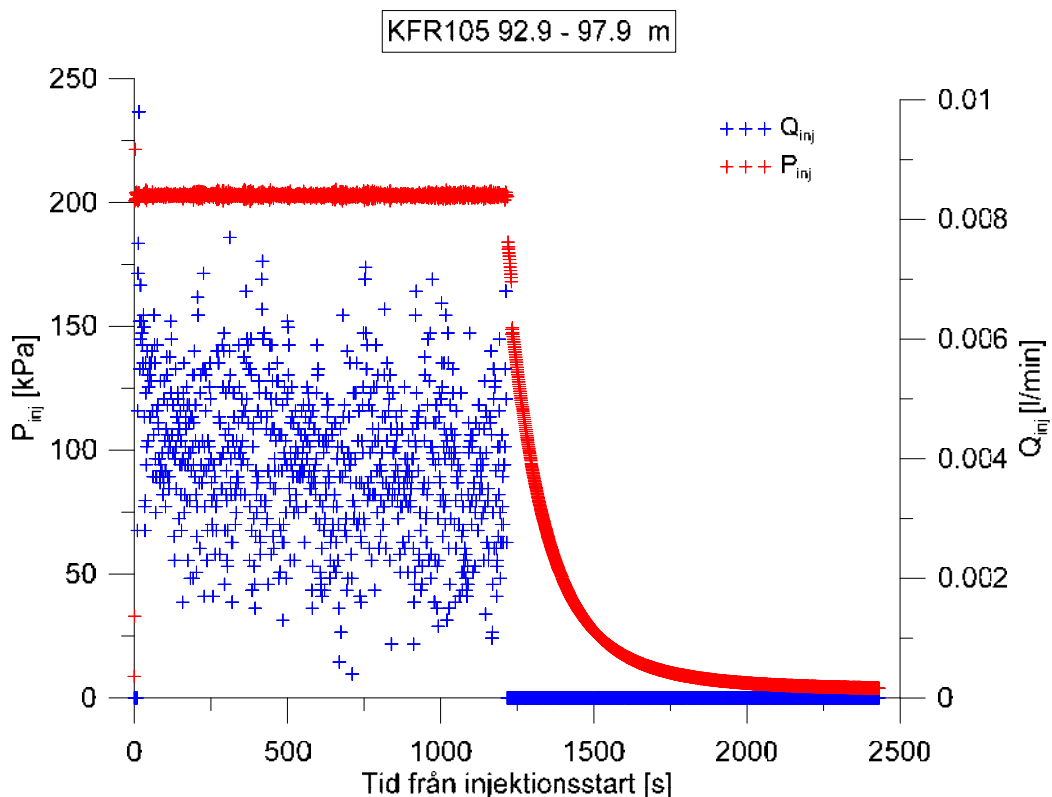


**Figure A3-39.** Linear plot of flow rate ( $Q$ ) and pressure ( $P$ ) versus time from the injection test in section 92.9-97.9 m in borehole KFR105.

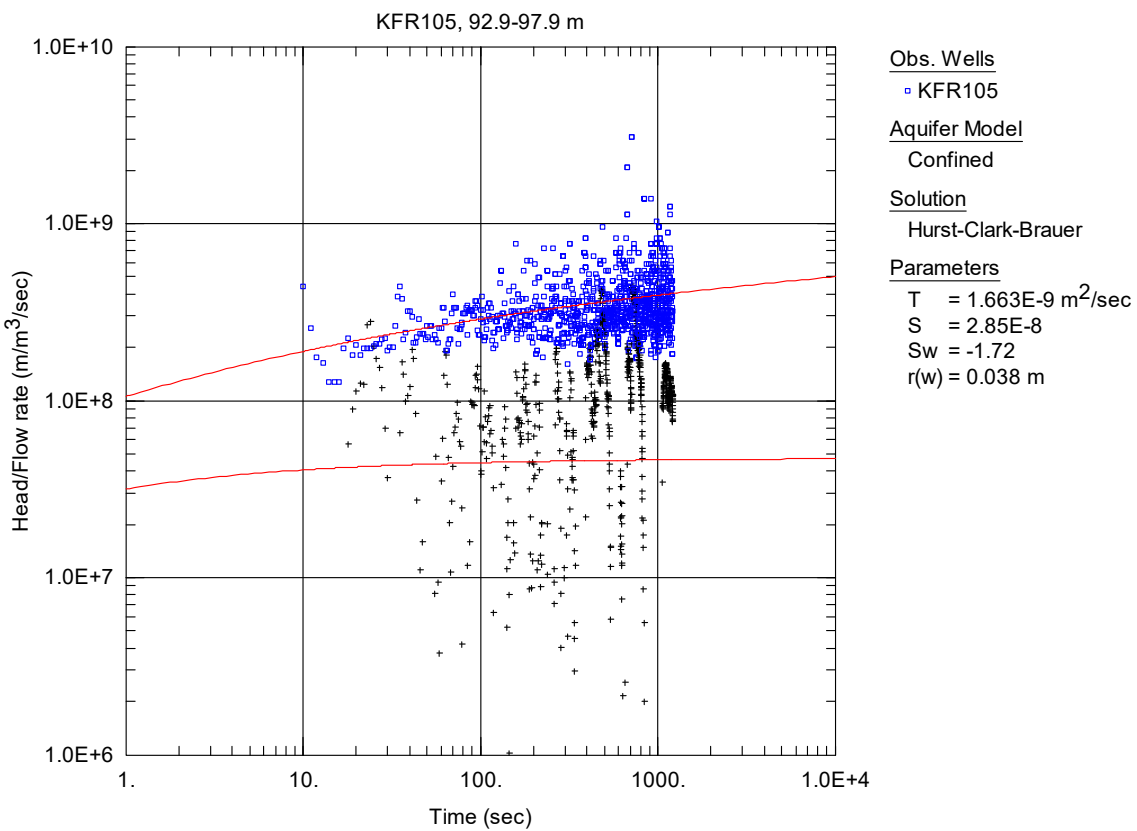


**Figure A3-40.** Log-log plot of head/flow rate ( $\square$ ) and derivative (+) versus time, from the injection test in section 92.9-97.9 m in KFR105.

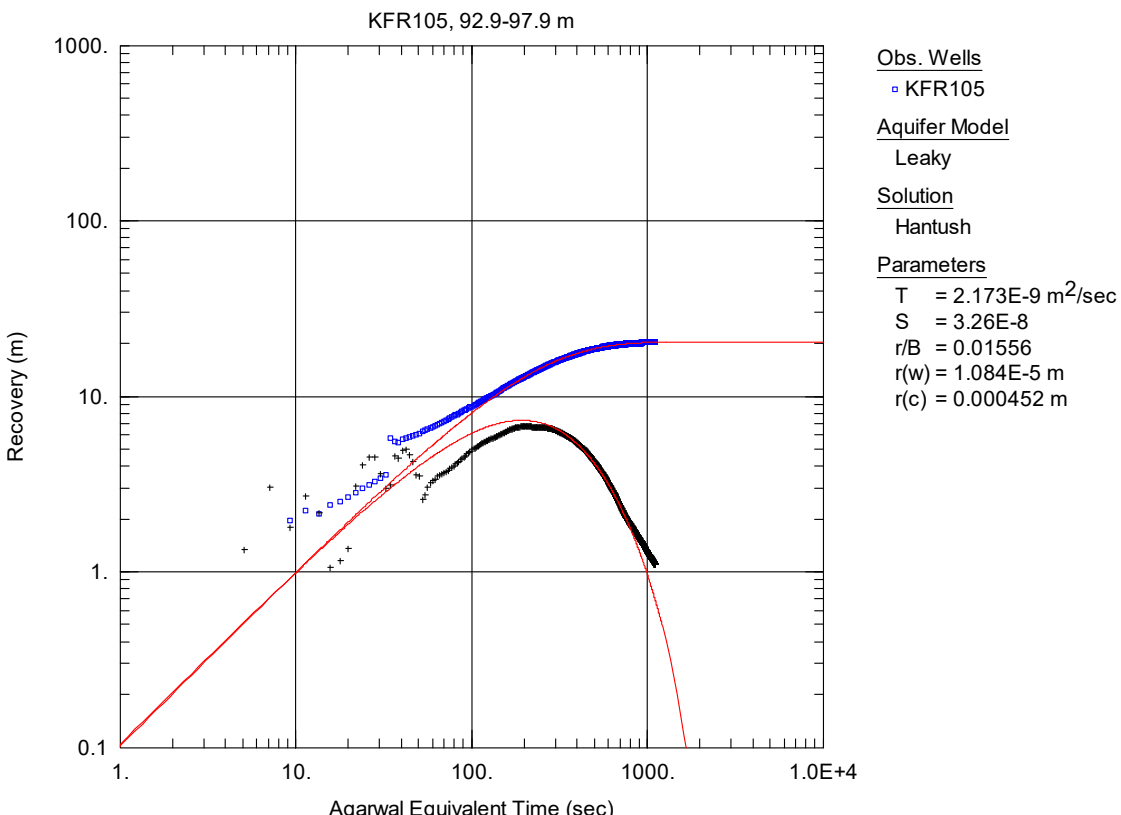


**Figure A3-41.** Log-log plot of recovery ( $\square$ ) and derivative (+) versus equivalent time, from the injection test in section 92.9-97.9 m in KFR105.

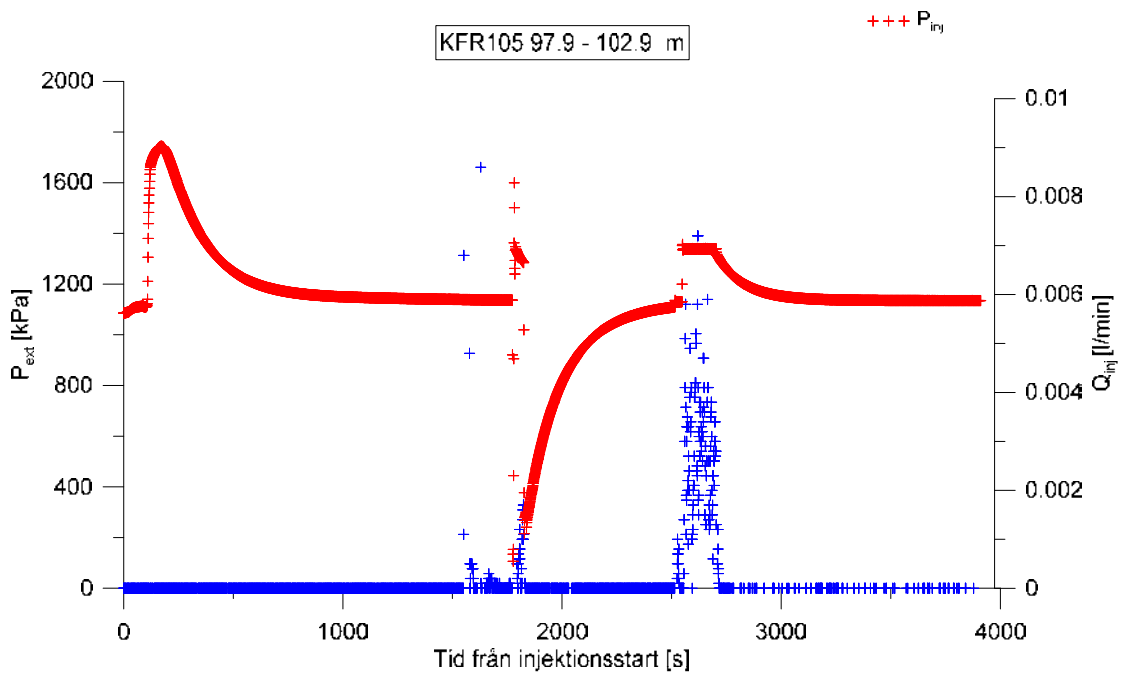


**Figure A3-42.** Linear plot of flow rate ( $Q$ ) and pressure ( $P$ ) versus time from the injection test in section 97.9-102.9 m in borehole KFR105.

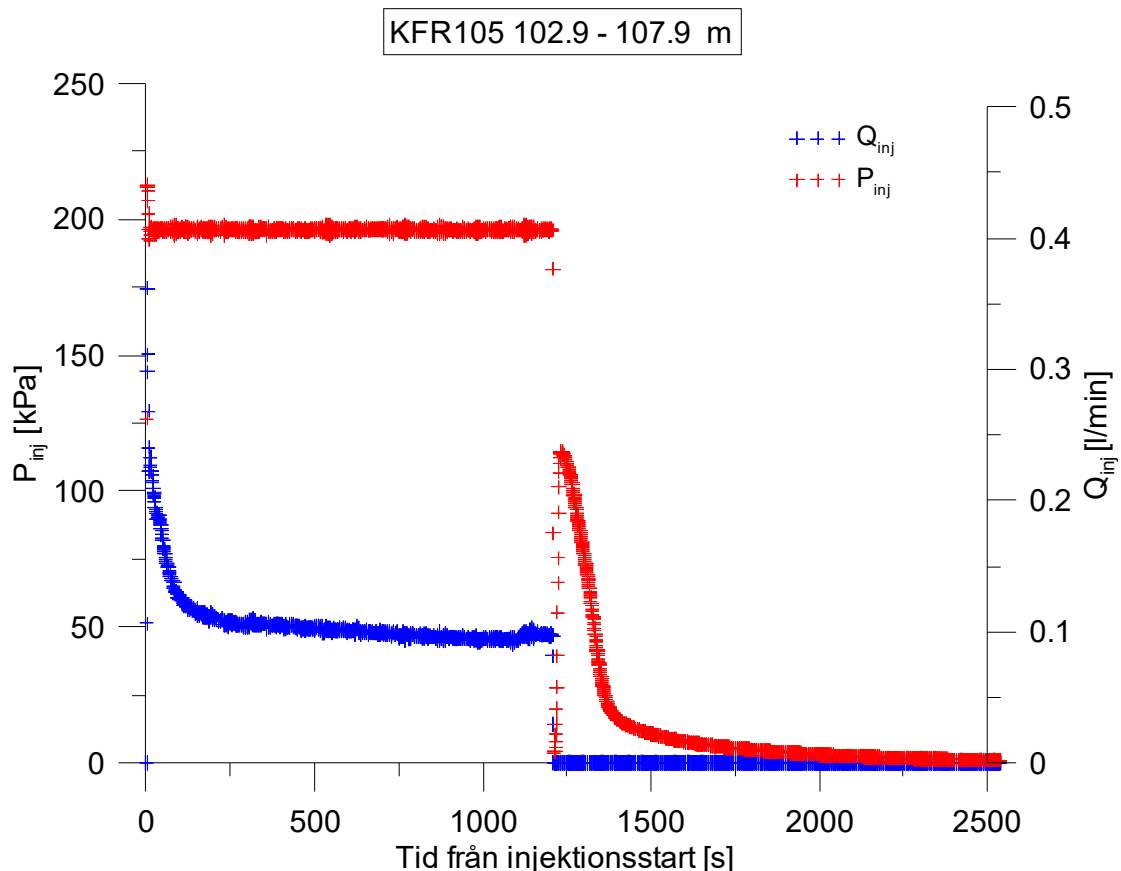


**Figure A3-43.** Linear plot of flow rate ( $Q$ ) and pressure ( $P$ ) versus time from the injection test in section 102.9-107.9 m in borehole KFR105.

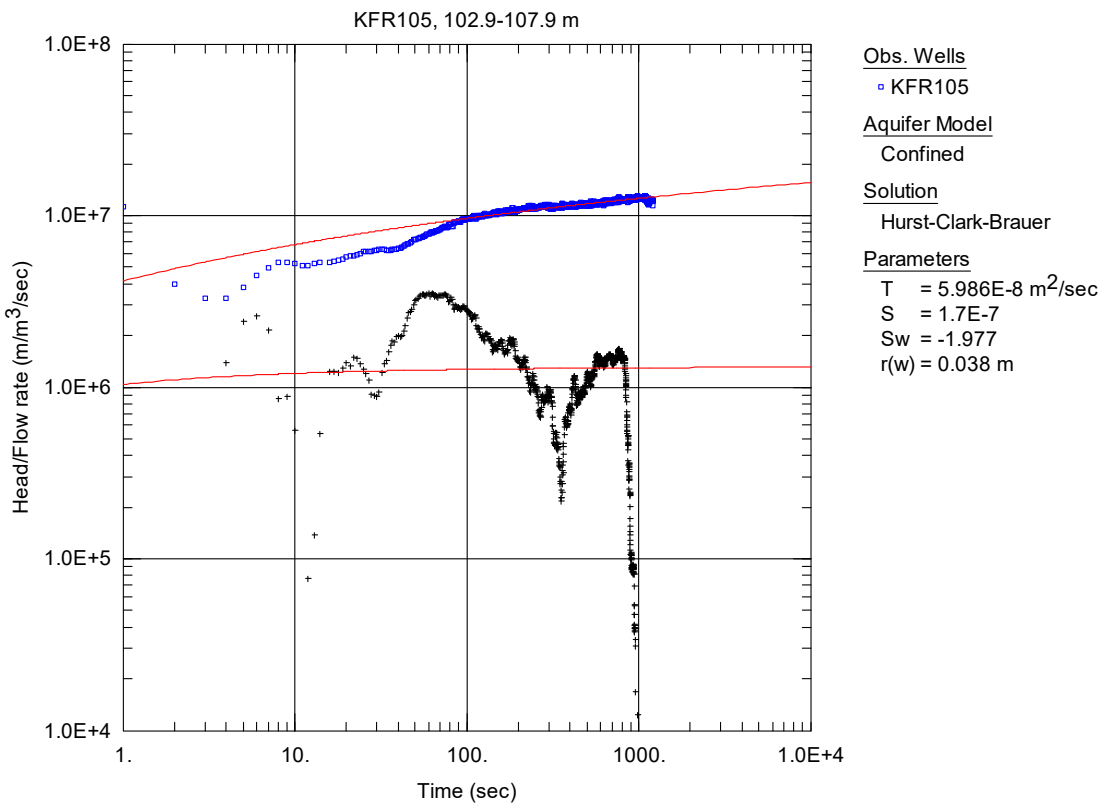


**Figure A3-44.** Log-log plot of head/flow rate (□) and derivative (+) versus time, from the injection test in section 102.9-107.9 m in KFR105.

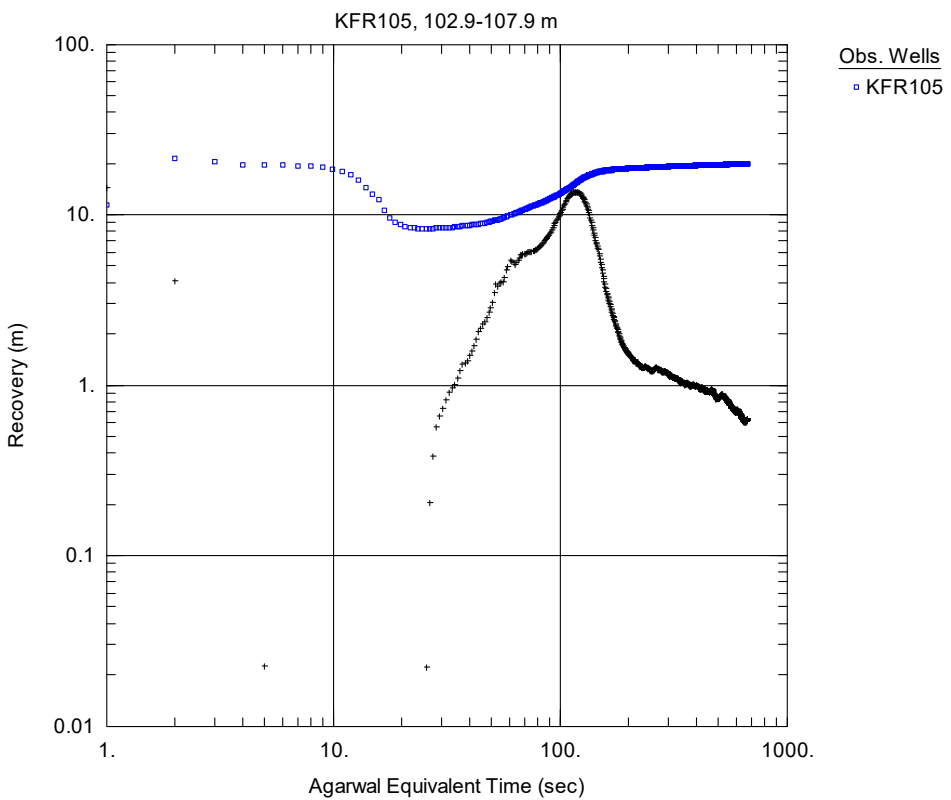


**Figure A3-45.** Log-log plot of recovery (□) and derivative (+) versus equivalent time, from the injection test in section 102.9-107.9 m in KFR105. No satisfying solution was found.

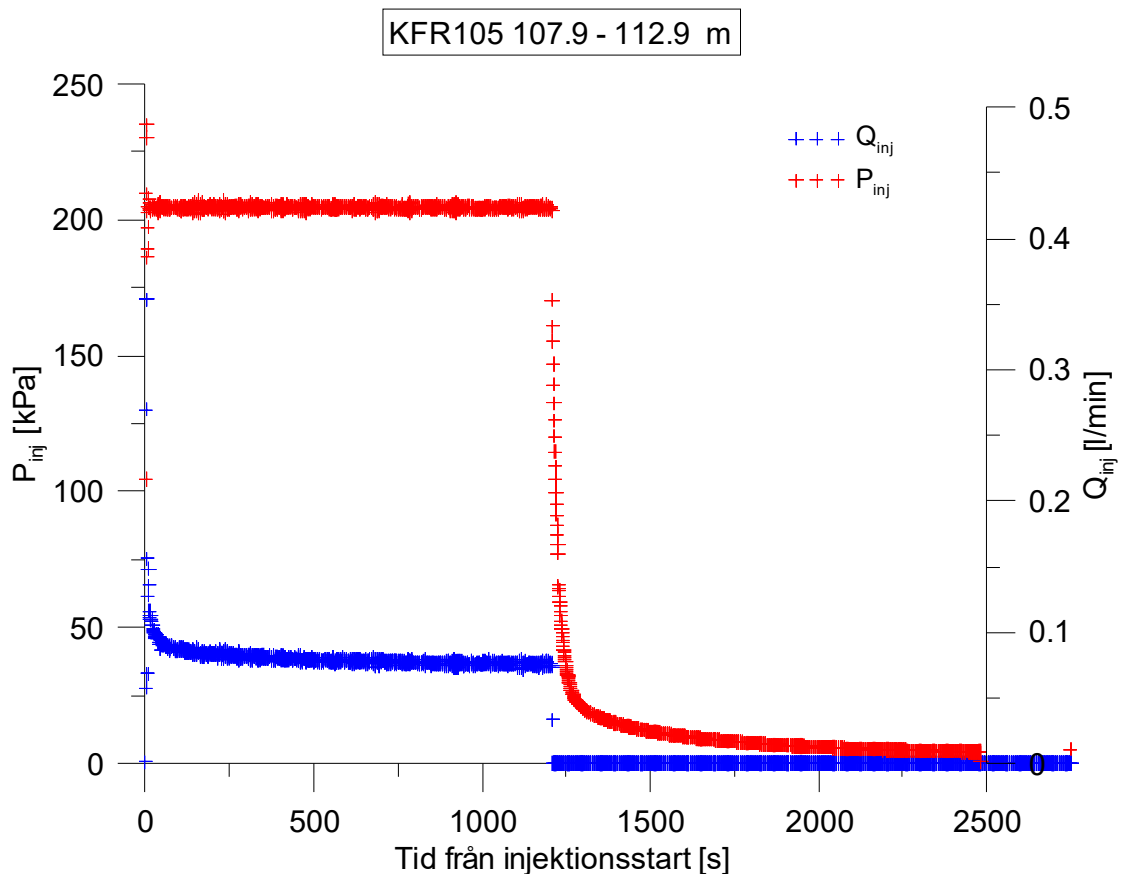


**Figure A3-46.** Linear plot of flow rate ( $Q$ ) and pressure ( $P$ ) versus time from the injection test in section 107.9-112.9 m in borehole KFR105.

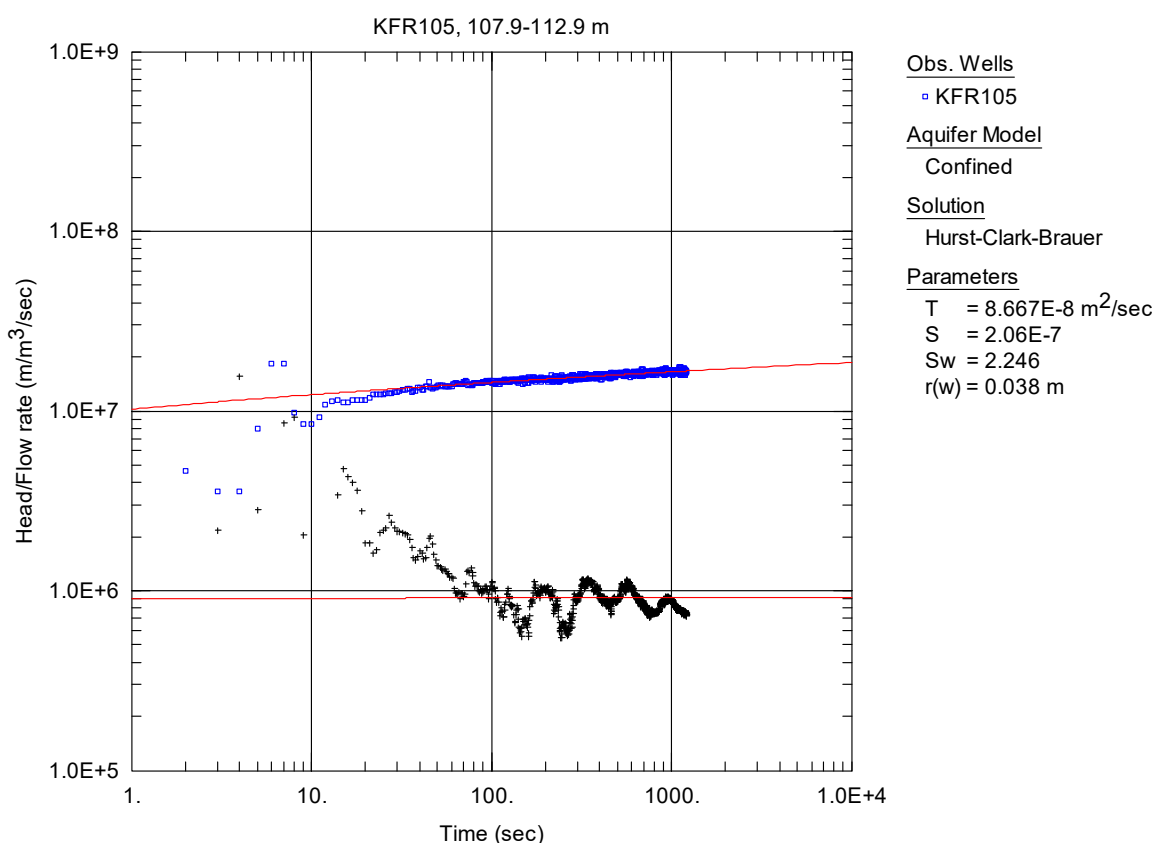


**Figure A3-47.** Log-log plot of head/flow rate (□) and derivative (+) versus time, from the injection test in section 107.9-112.9 m in KFR105.

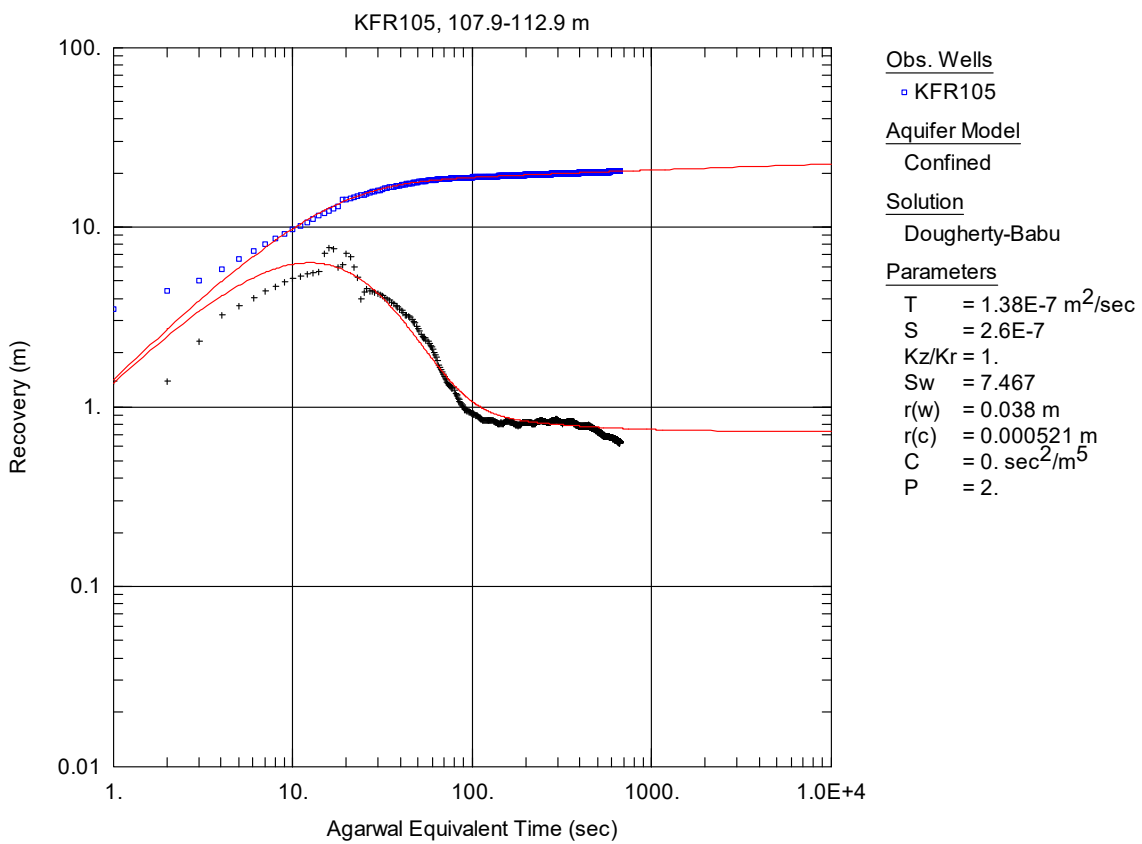


**Figure A3-48.** Log-log plot of recovery (□) and derivative (+) versus equivalent time, from the injection test in section 107.9-112.9 m in KFR105. No satisfying solution was found.

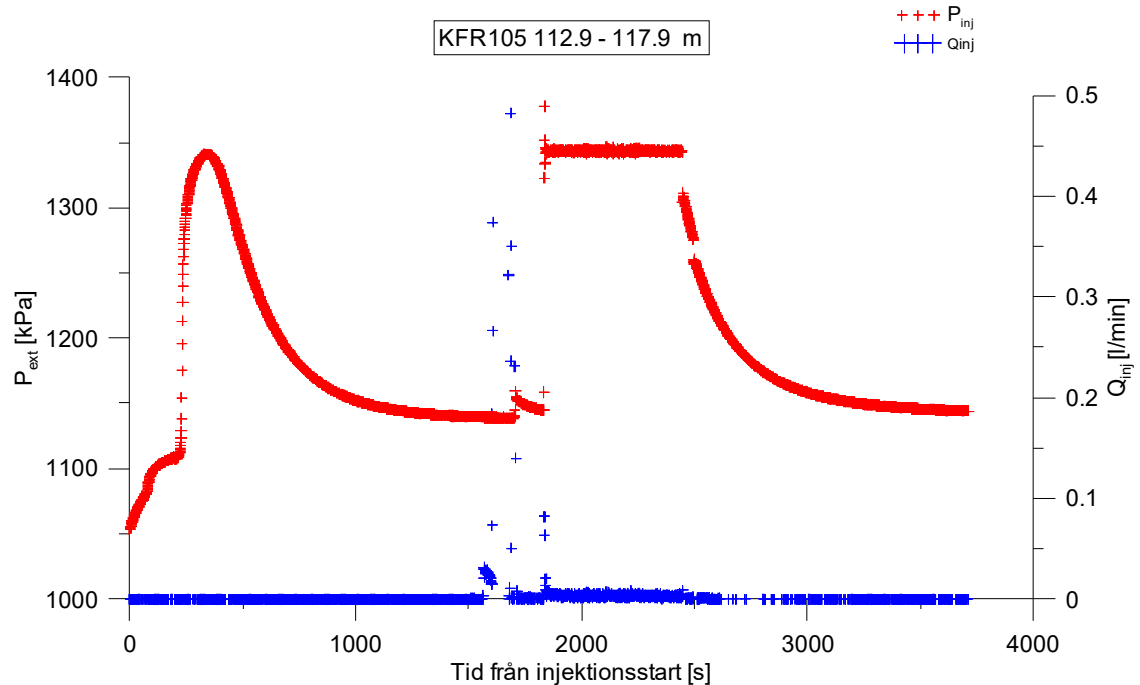


**Figure A3-49.** Linear plot of flow rate ( $Q$ ) and pressure ( $P$ ) versus time from the injection test in section 112.9-117.9 m in borehole KFR105.

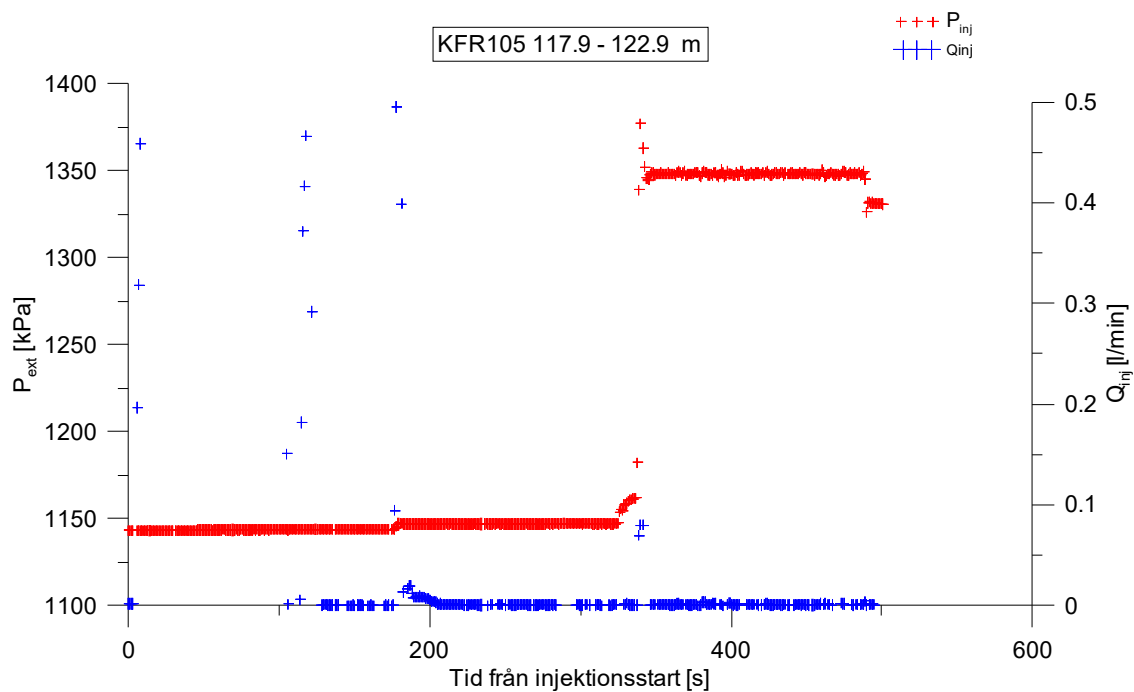


**Figure A3-50.** Linear plot of flow rate ( $Q$ ) and pressure ( $P$ ) versus time from the injection test in section 117.9-122.9 m in borehole KFR105.

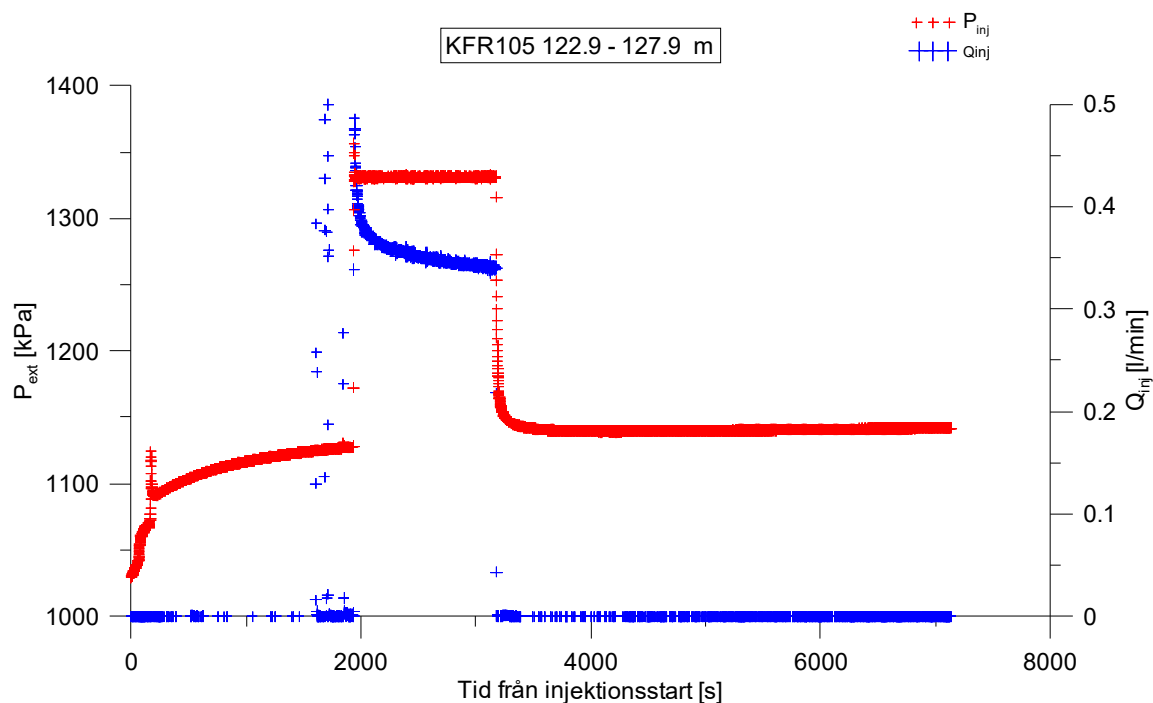


**Figure A3-51.** Linear plot of flow rate ( $Q$ ) and pressure ( $P$ ) versus time from the injection test in section 122.9-127.9 m in borehole KFR105.

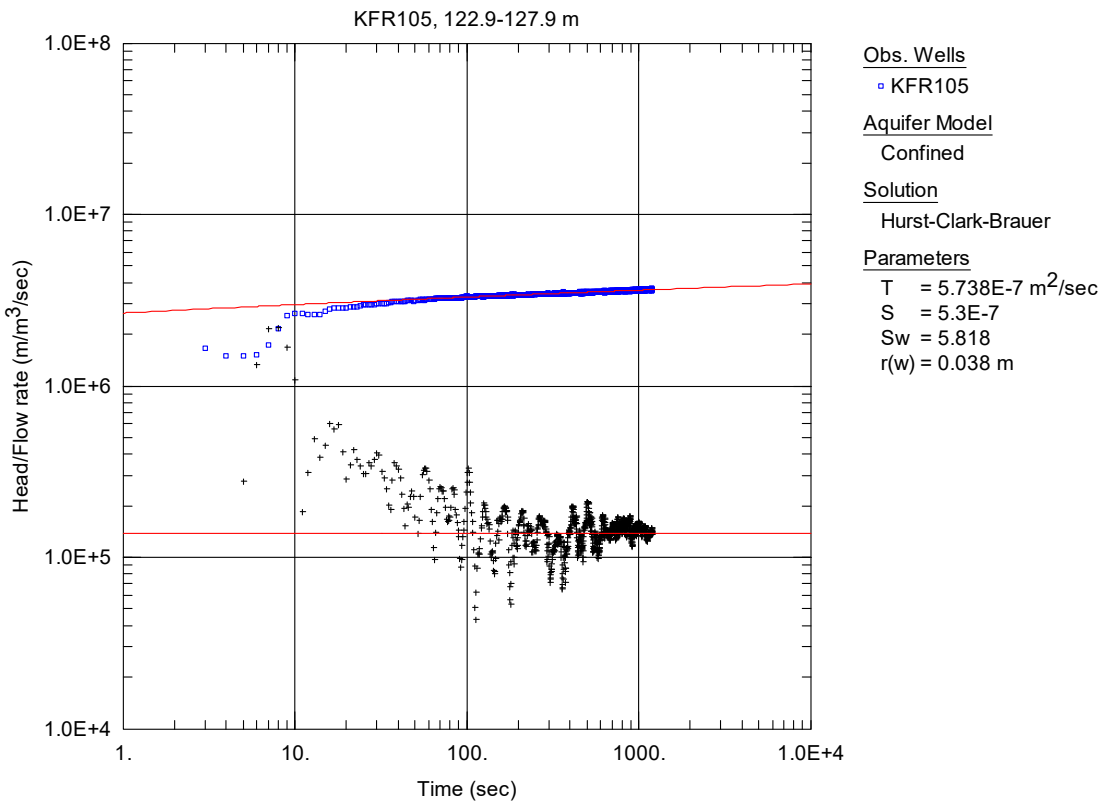


**Figure A3-52.** Log-log plot of head/flow rate (□) and derivative (+) versus time, from the injection test in section 122.9-127.9 m in KFR105.

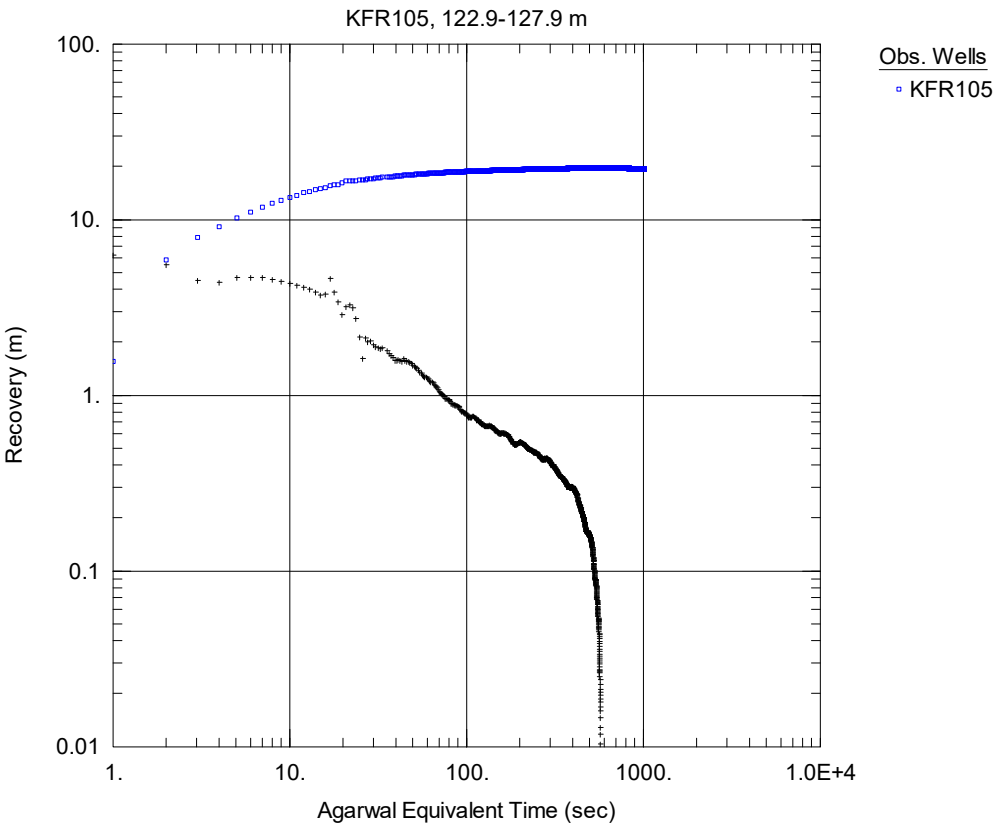


**Figure A3-53.** Log-log plot of recovery (□) and derivative (+) versus equivalent time, from the injection test in section 122.9-127.9 m in KFR105. No satisfying solution was found.

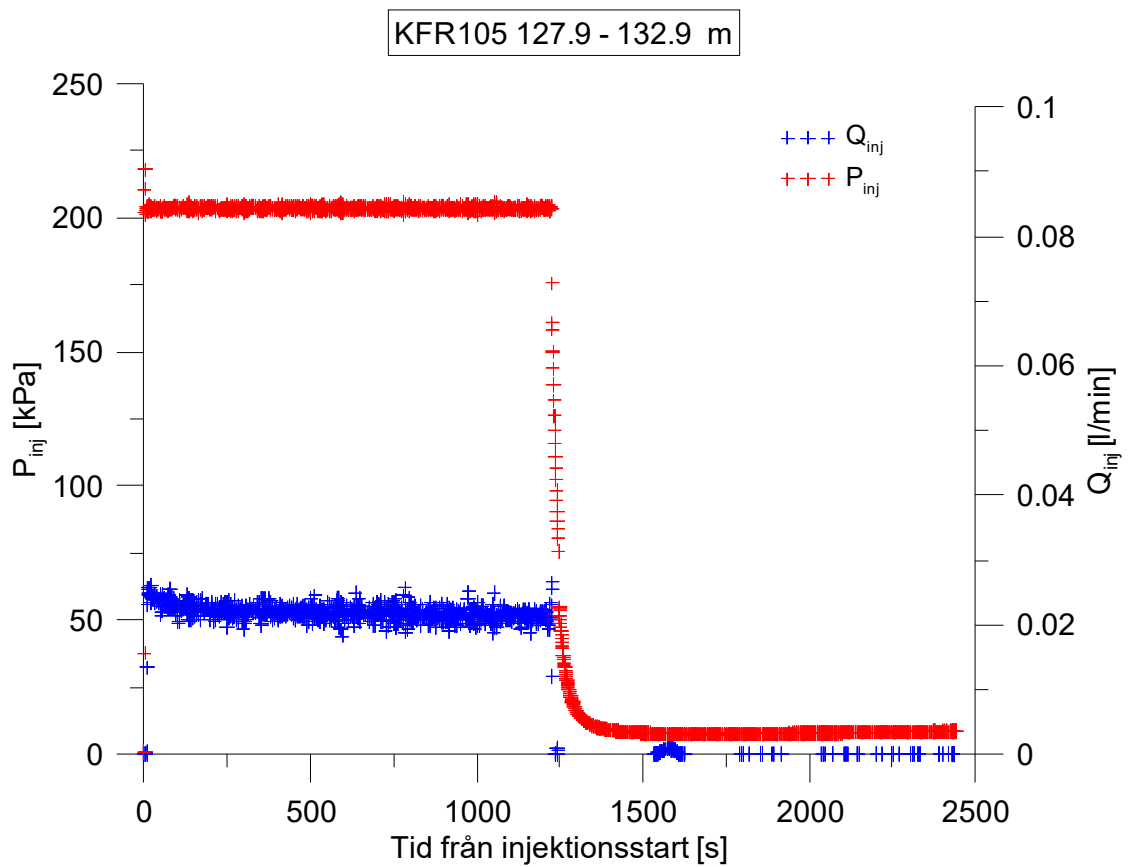


**Figure A3-54.** Linear plot of flow rate ( $Q$ ) and pressure ( $P$ ) versus time from the injection test in section 127.9-132.9 m in borehole KFR105.

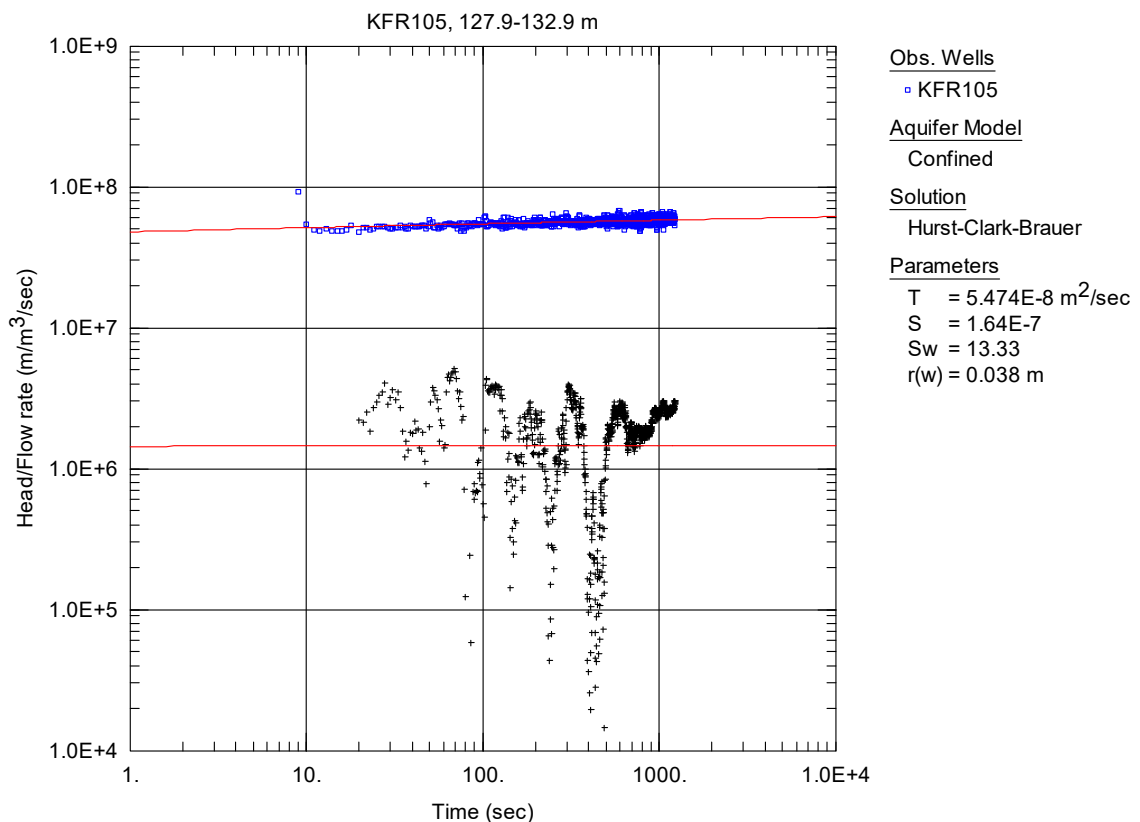


**Figure A3-55.** Log-log plot of head/flow rate (□) and derivative (+) versus time, from the injection test in section 127.9-132.9 m in KFR105.

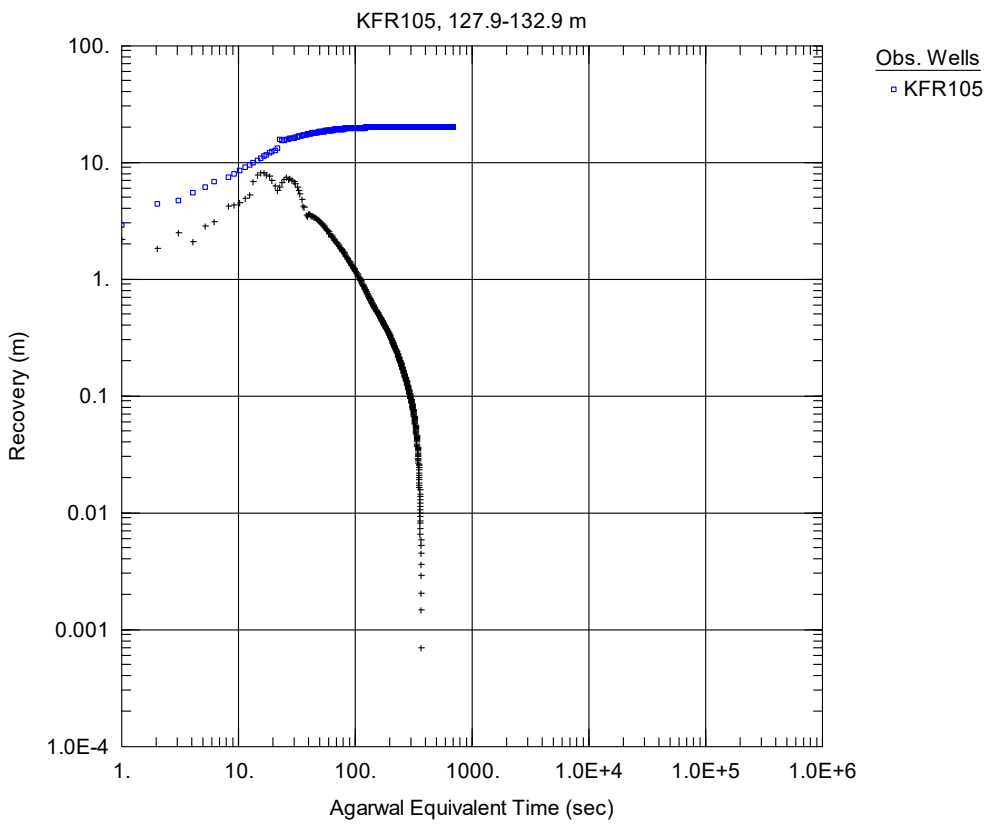


**Figure A3-56.** Log-log plot of recovery (□) and derivative (+) versus equivalent time, from the injection test in section 127.9-132.9 m in KFR105. No satisfying solution was found.

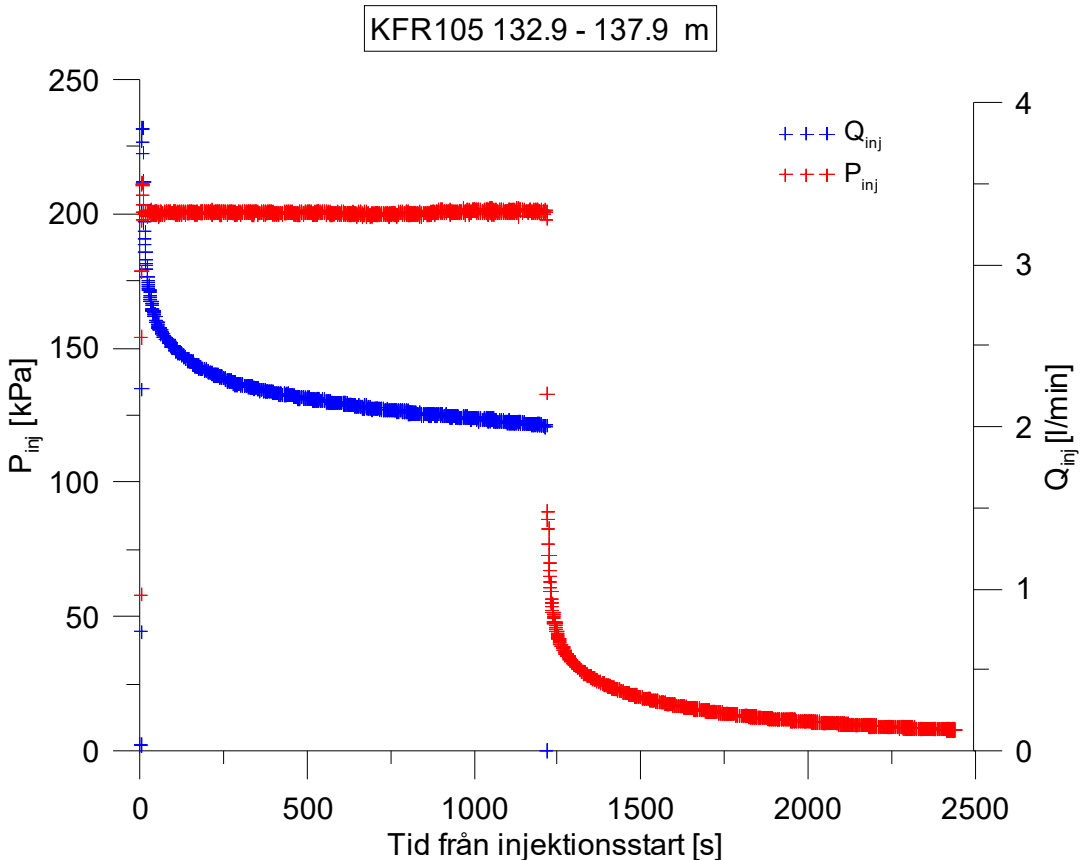


**Figure A3-57.** Linear plot of flow rate ( $Q$ ) and pressure ( $P$ ) versus time from the injection test in section 132.9-137.9 m in borehole KFR105.

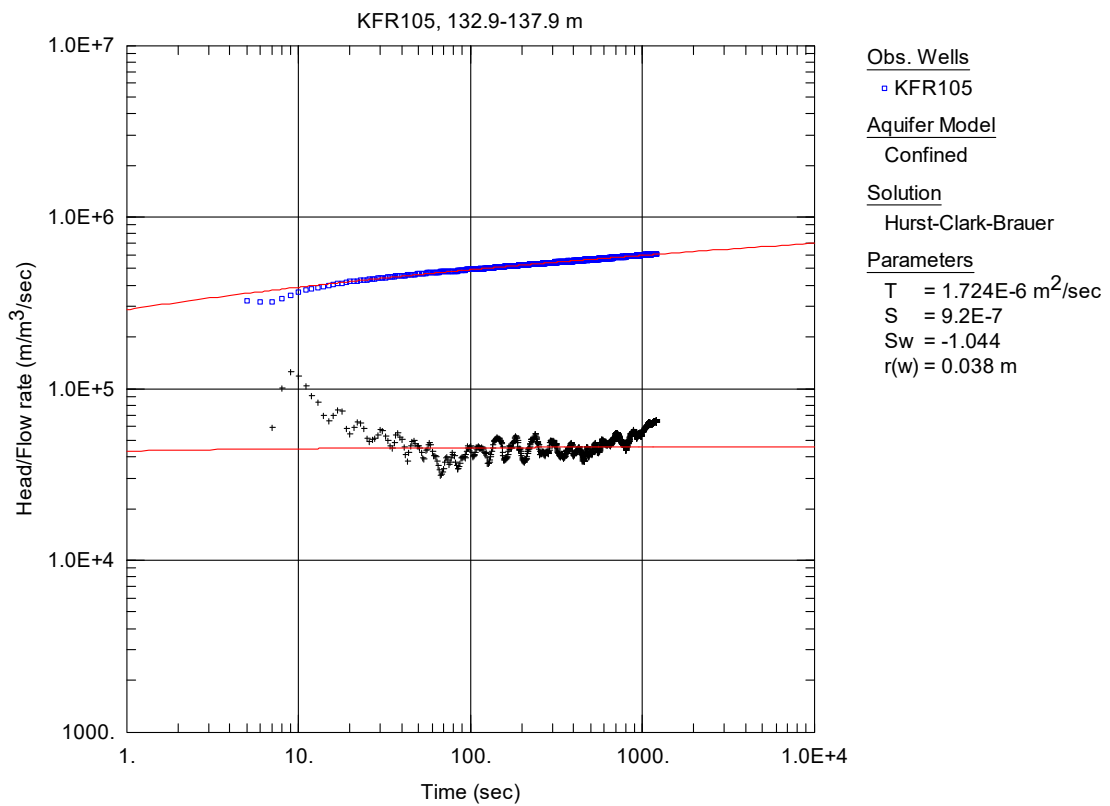


**Figure A3-58.** Log-log plot of head/flow rate (□) and derivative (+) versus time, from the injection test in section 132.9-137.9 m in KFR105.

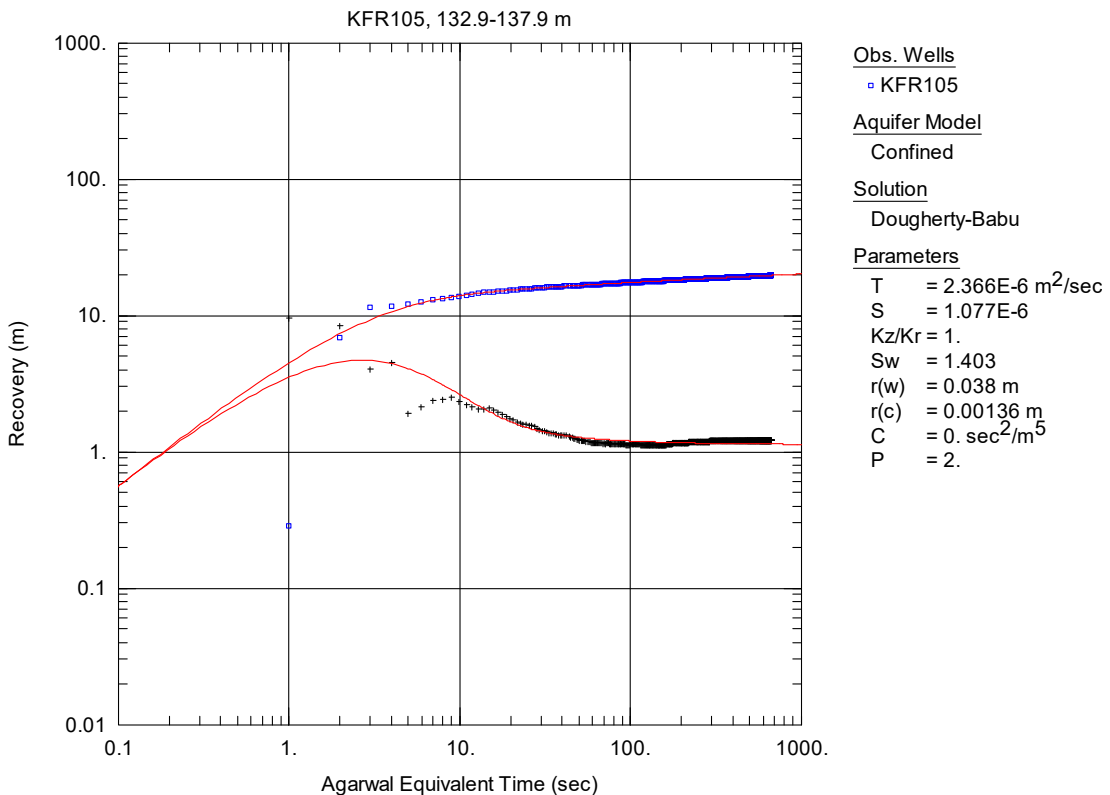


**Figure A3-59.** Log-log plot of recovery (□) and derivative (+) versus equivalent time, from the injection test in section 132.9-137.9 m in KFR105.

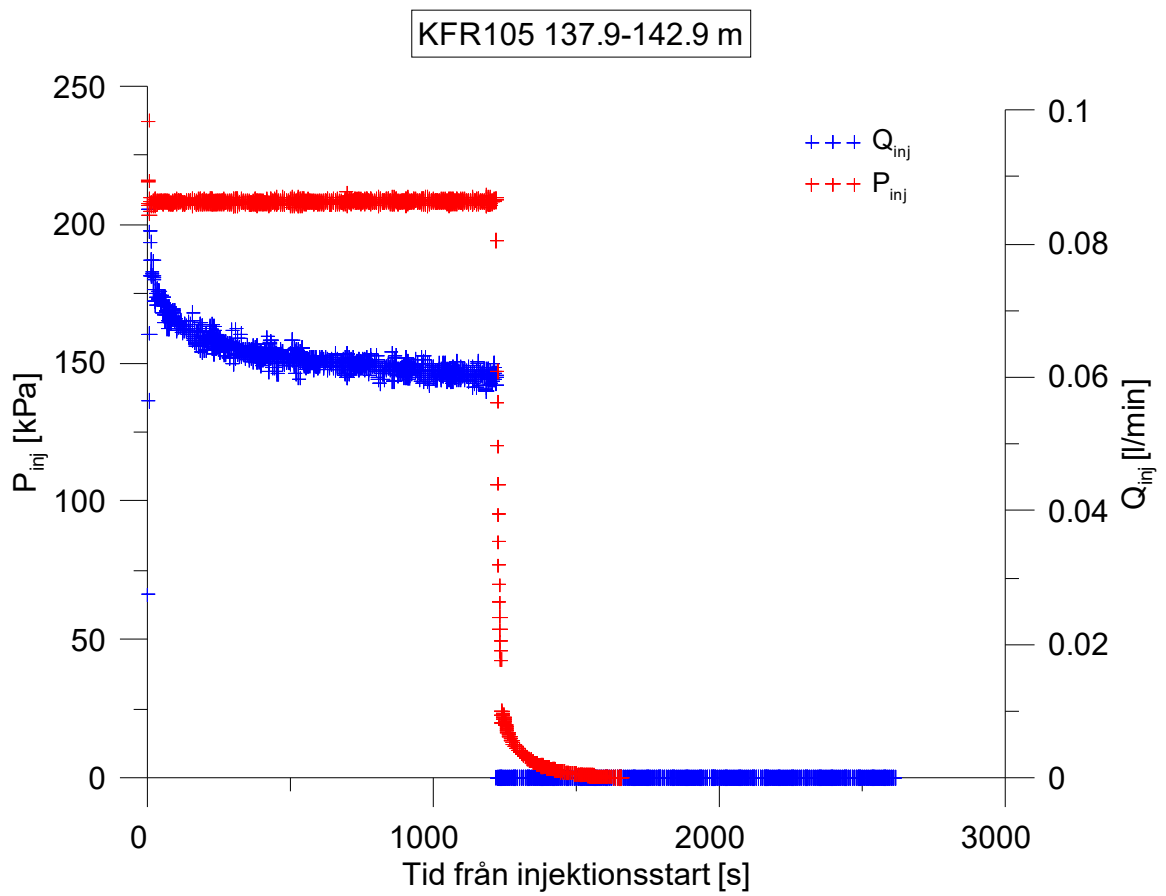


**Figure A3-60.** Linear plot of flow rate ( $Q$ ) and pressure ( $P$ ) versus time from the injection test in section 137.9-142.9 m in borehole KFR105.

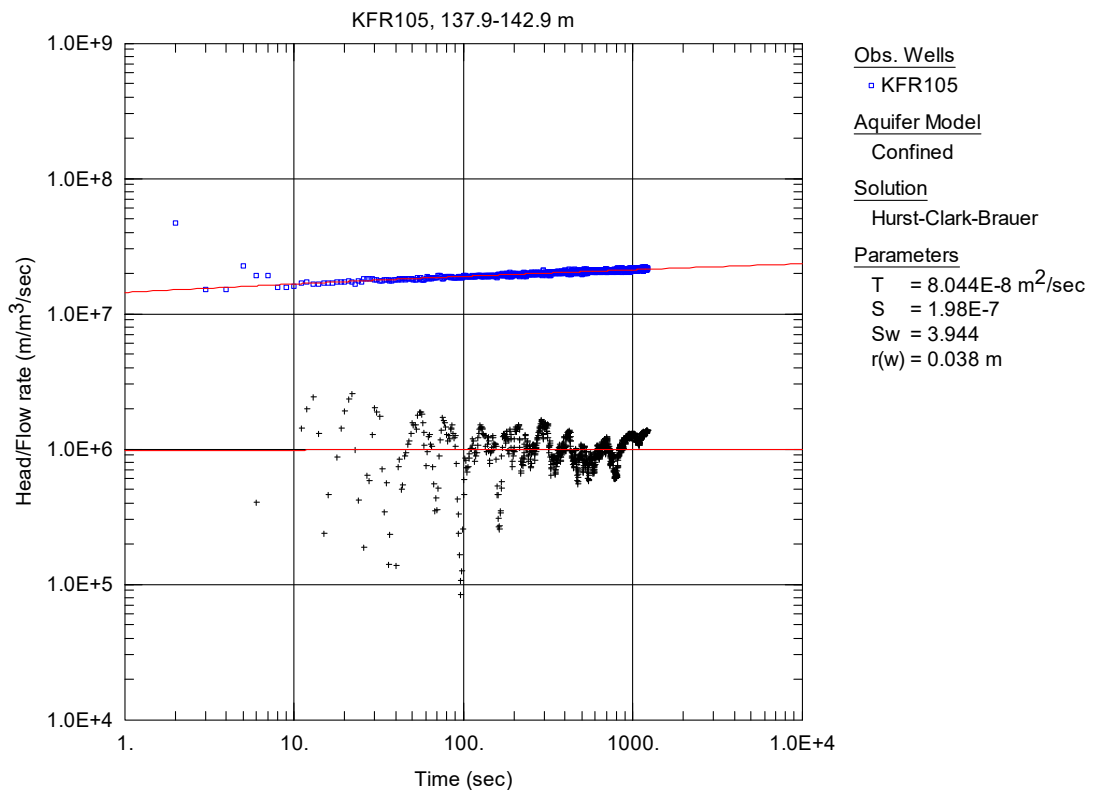


**Figure A3-61.** Log-log plot of head/flow rate (□) and derivative (+) versus time, from the injection test in section 137.9-142.9 m in KFR105.

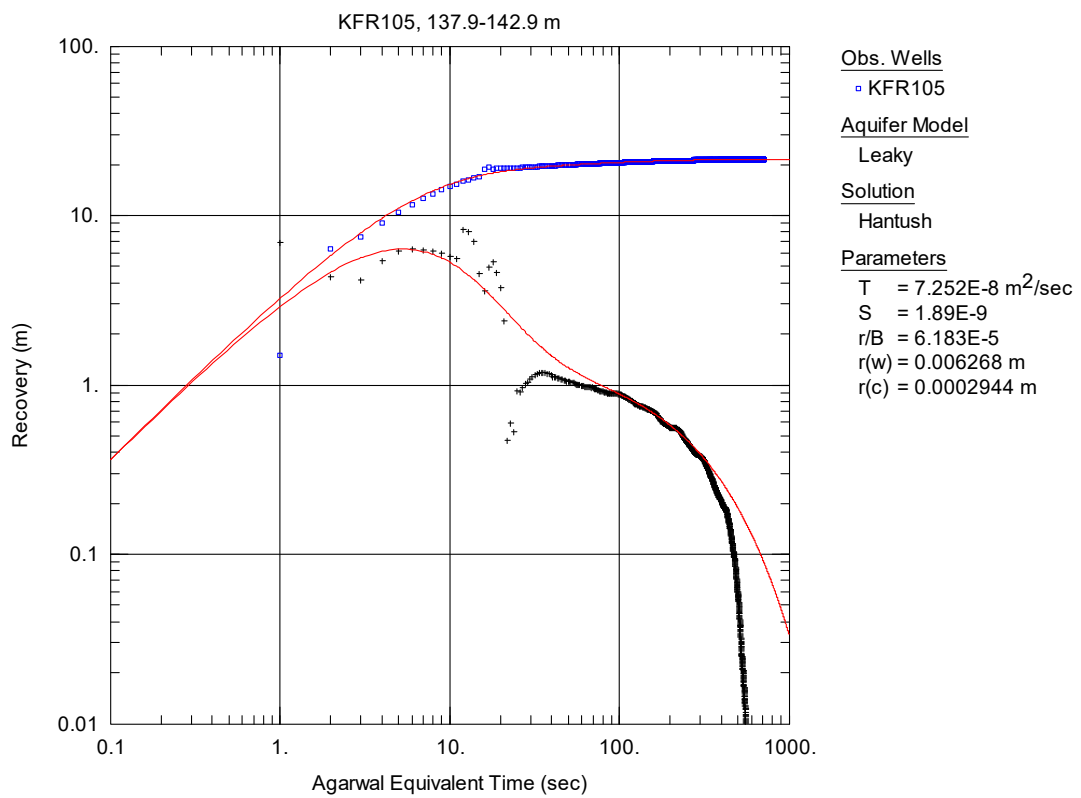


**Figure A3-62.** Log-log plot of recovery (□) and derivative (+) versus equivalent time, from the injection test in section 137.9-142.9 m in KFR105.

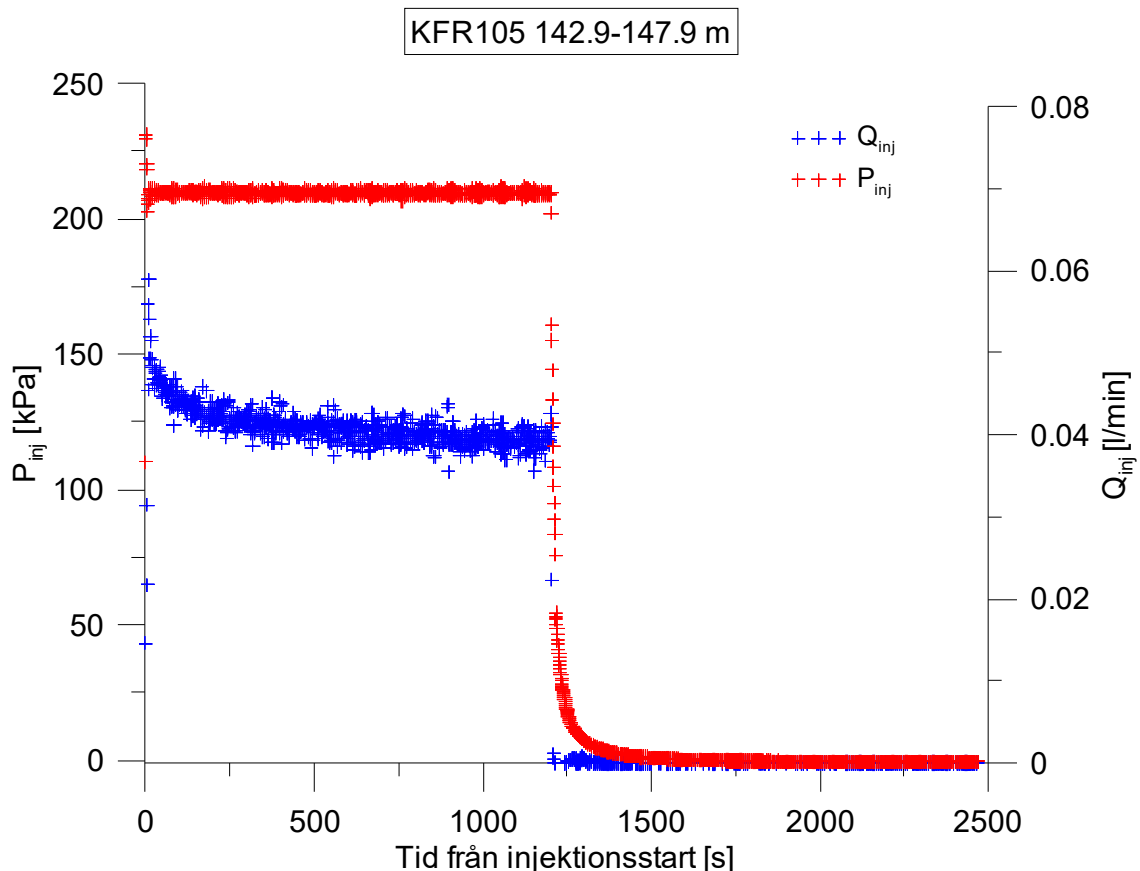


**Figure A3-63.** Linear plot of flow rate ( $Q$ ) and pressure ( $P$ ) versus time from the injection test in section 142.9-147.9 m in borehole KFR105.

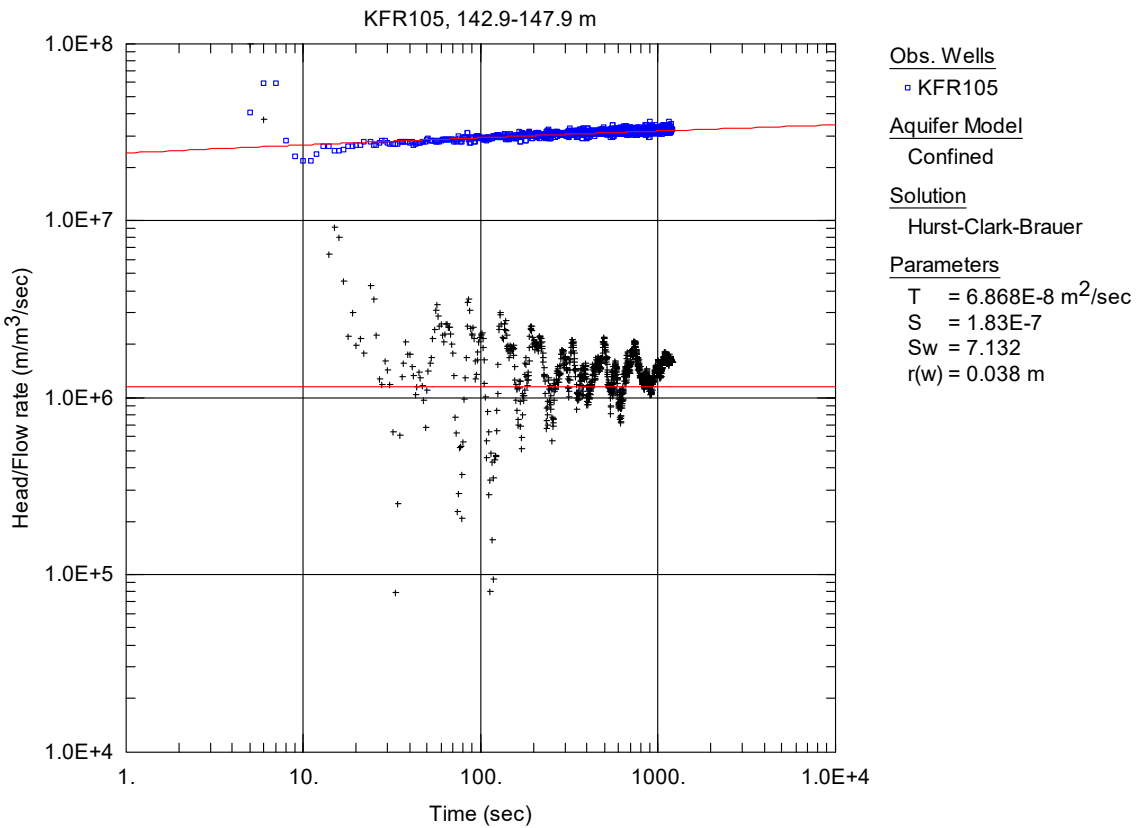


**Figure A3-64.** Log-log plot of head/flow rate (□) and derivative (+) versus time, from the injection test in section 142.9-147.9 m in KFR105.

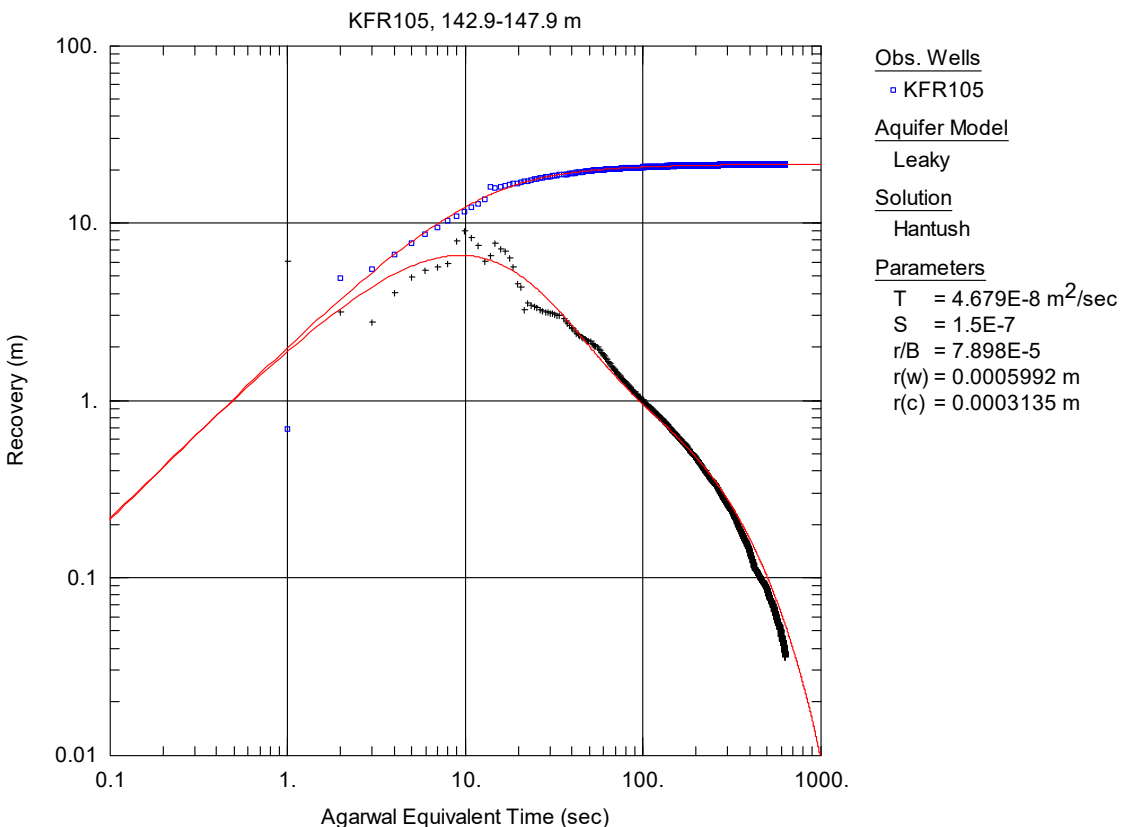


**Figure A3-65.** Log-log plot of recovery (□) and derivative (+) versus equivalent time, from the injection test in section 142.9-147.9 m in KFR105.

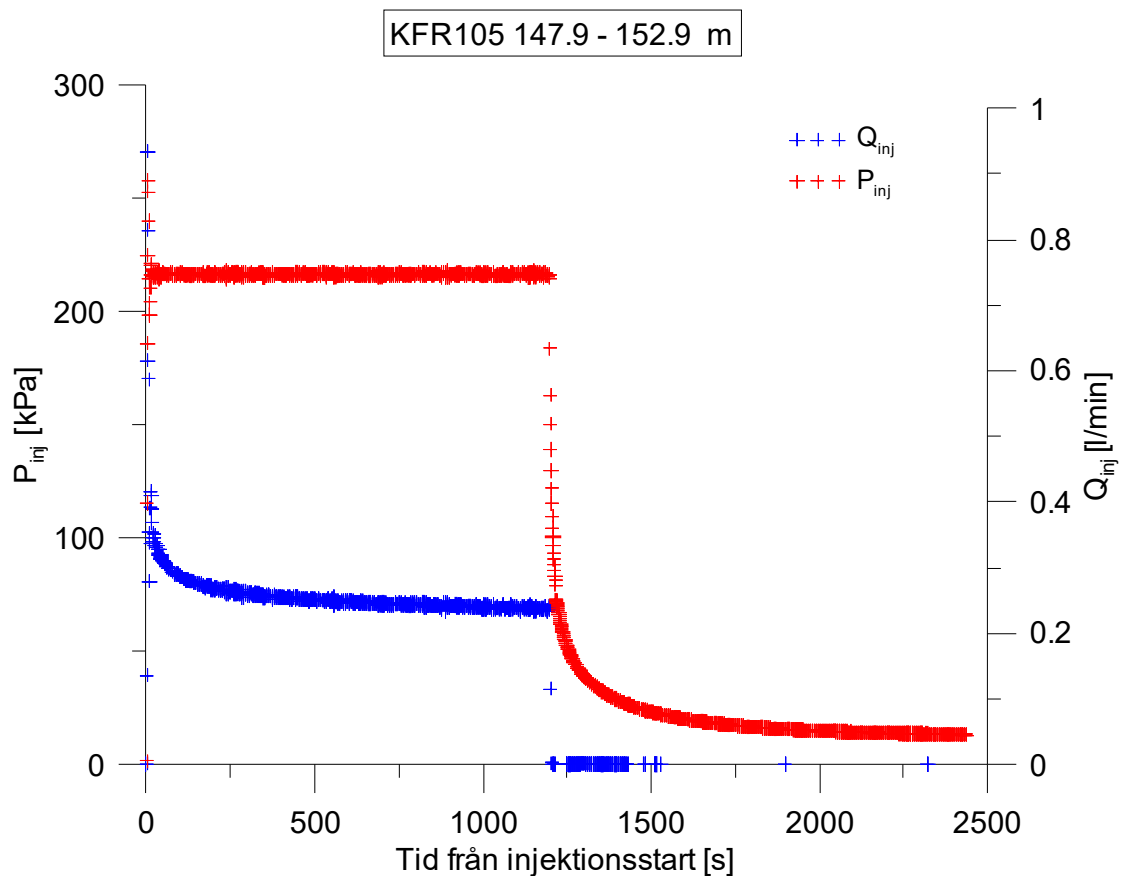


**Figure A3-66.** Linear plot of offflow rate ( $Q$ ) and pressure ( $P$ ) versus time from the injection test in section 147.9-152.9 m in borehole KFR105.

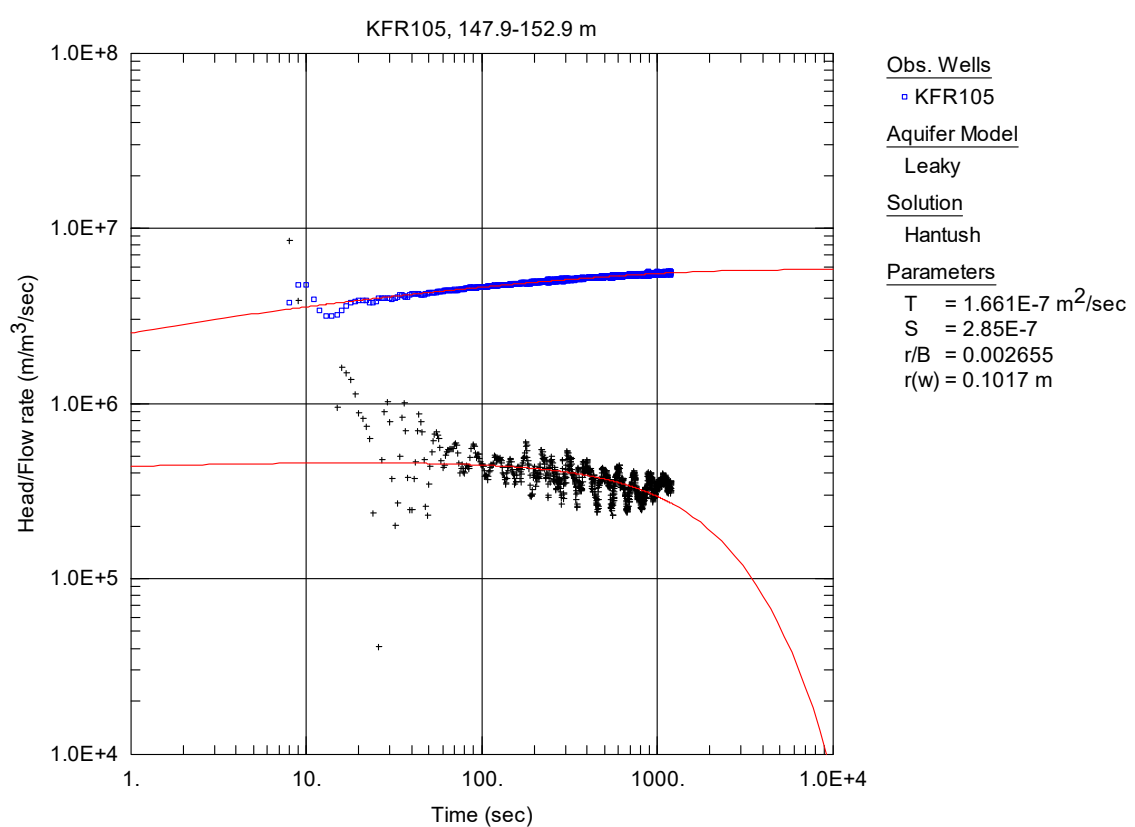


**Figure A3-67.** Log-log plot of head/flow rate (□) and derivative (+) versus time, from the injection test in section 147.9-152.9 m in KFR105.

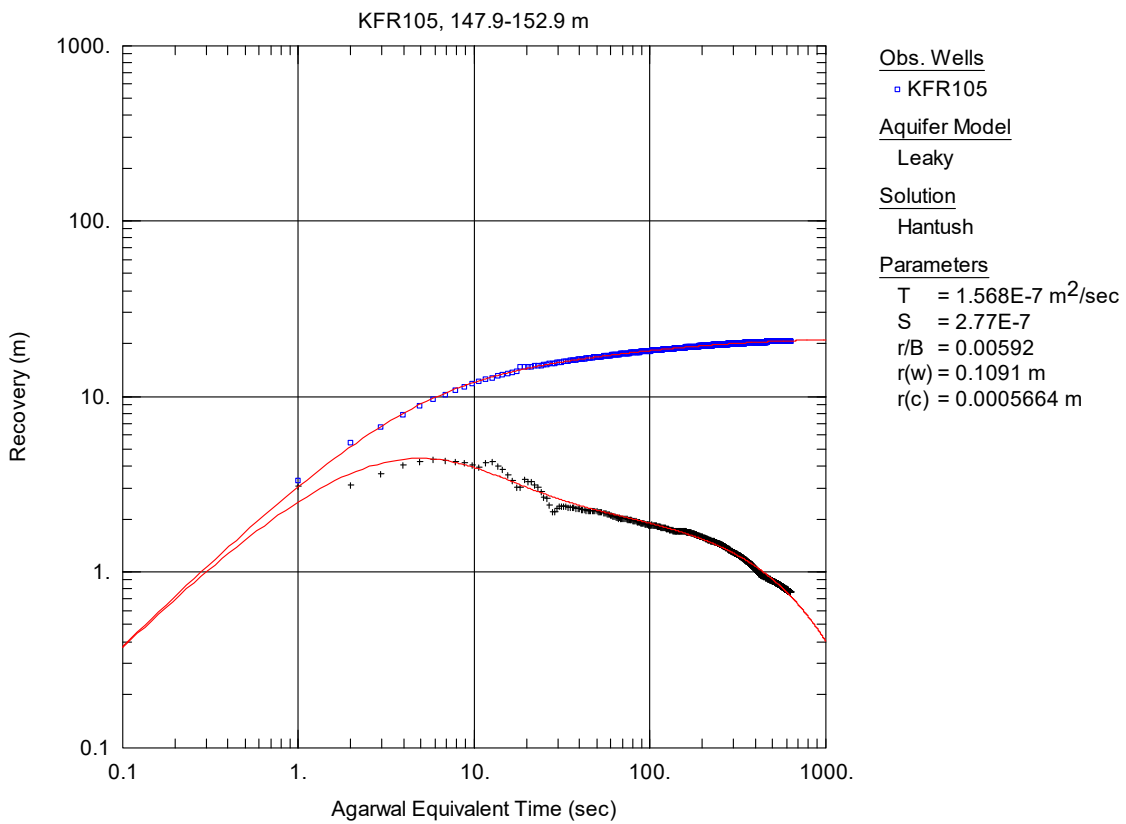


**Figure A3-68.** Log-log plot of recovery (□) and derivative (+) versus equivalent time, from the injection test in section 147.9-152.9 m in KFR105.

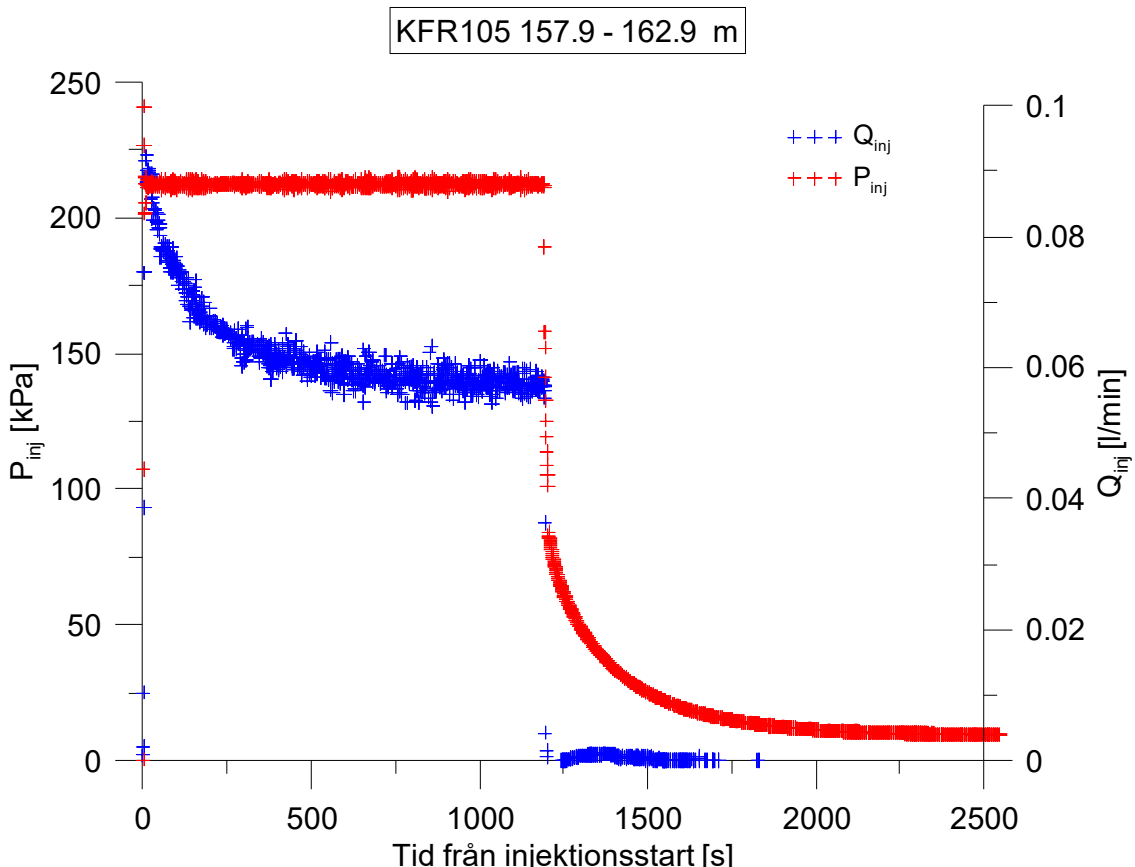


**Figure A3-69.** Linear plot of flow rate ( $Q$ ) and pressure ( $P$ ) versus time from the injection test in section 157.9-162.9 m in borehole KFR105.

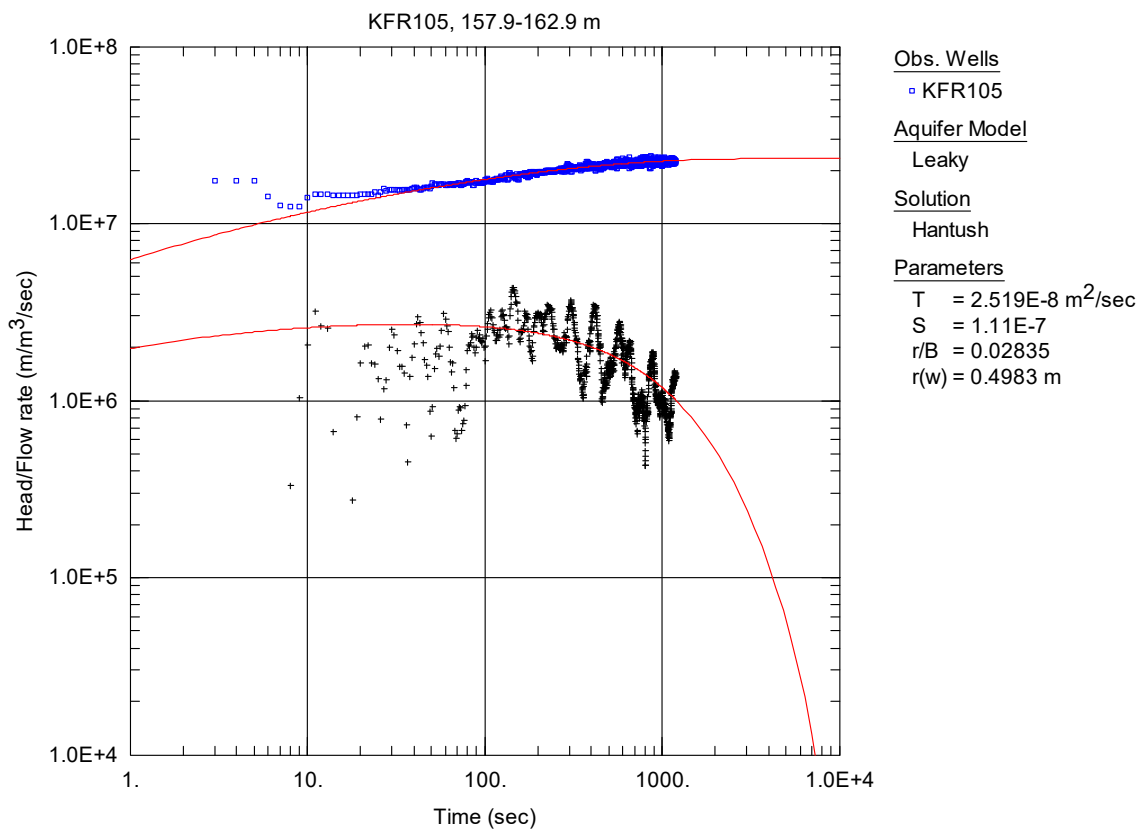


**Figure A3-70.** Log-log plot of head/flow rate (□) and derivative (+) versus time, from the injection test in section 157.9-162.9 m in KFR105.

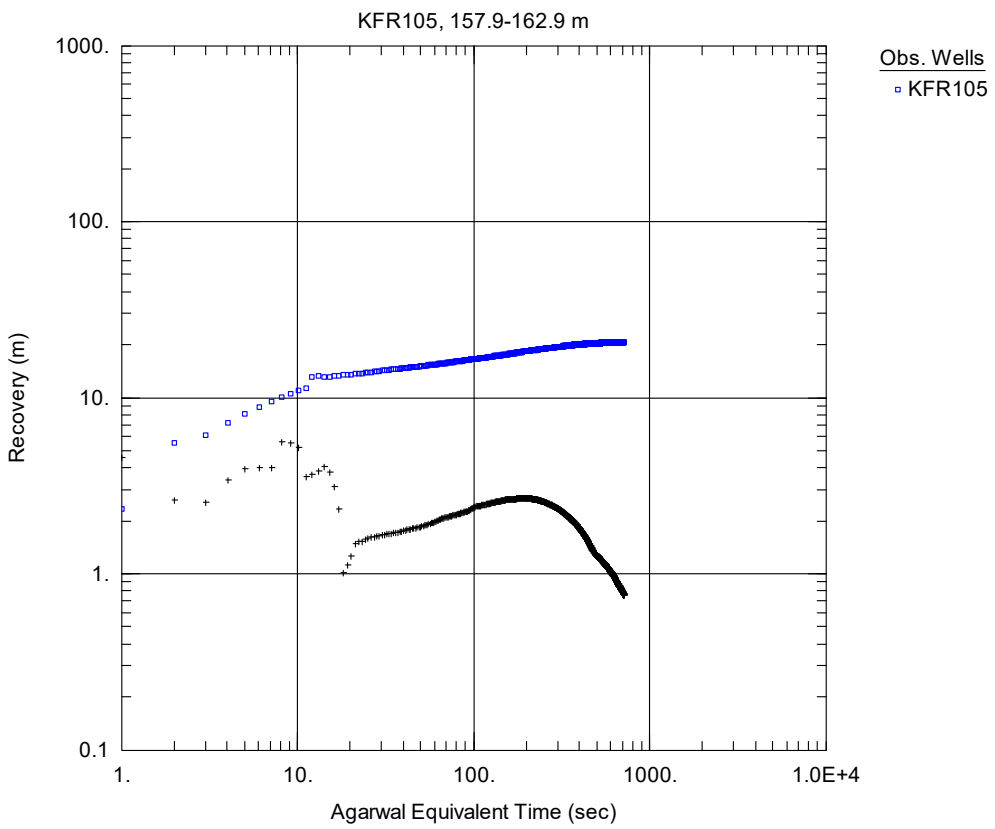


**Figure A3-71.** Log-log plot of recovery (□) and derivative (+) versus equivalent time, from the injection test in section 157.9-162.9 m in KFR105. No satisfying solution was found.

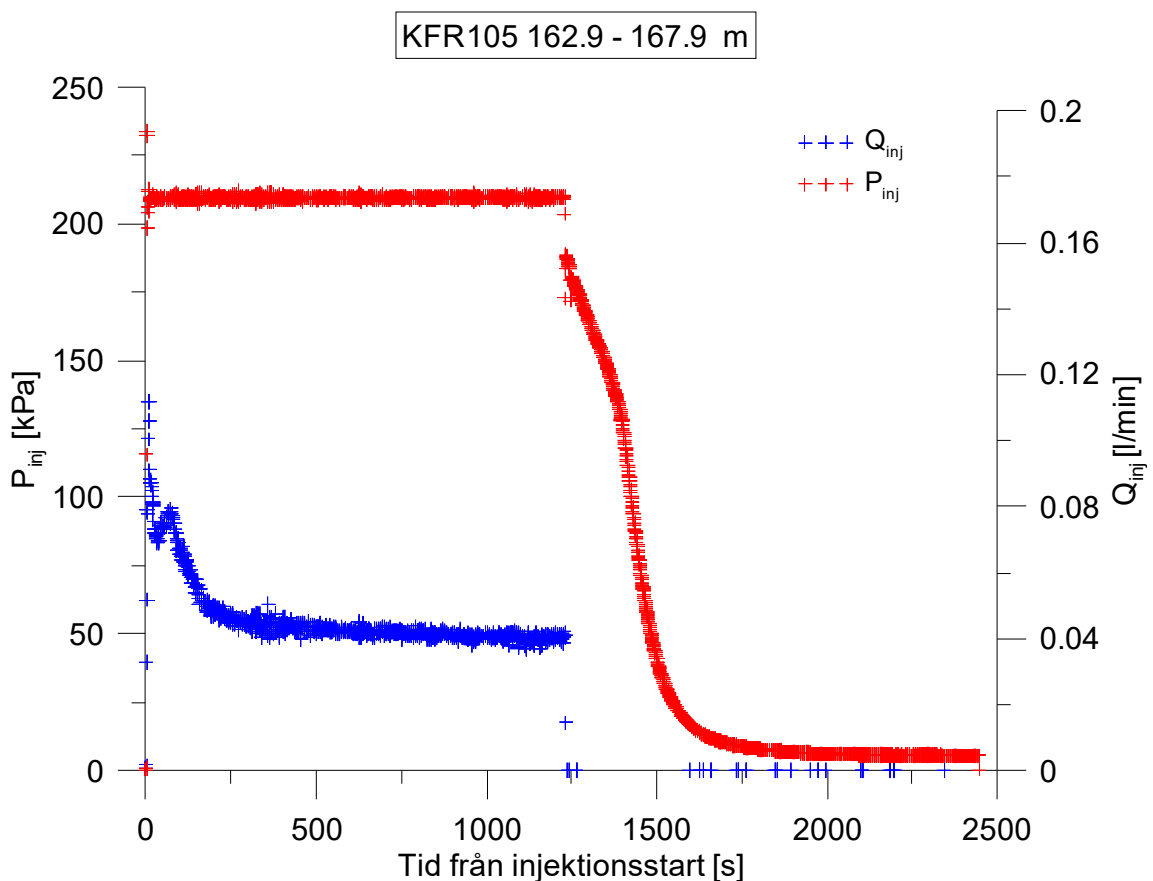


**Figure A3-72.** Linear plot of flow rate ( $Q$ ) and pressure ( $P$ ) versus time from the injection test in section 162.9-167.9 m in borehole KFR105.

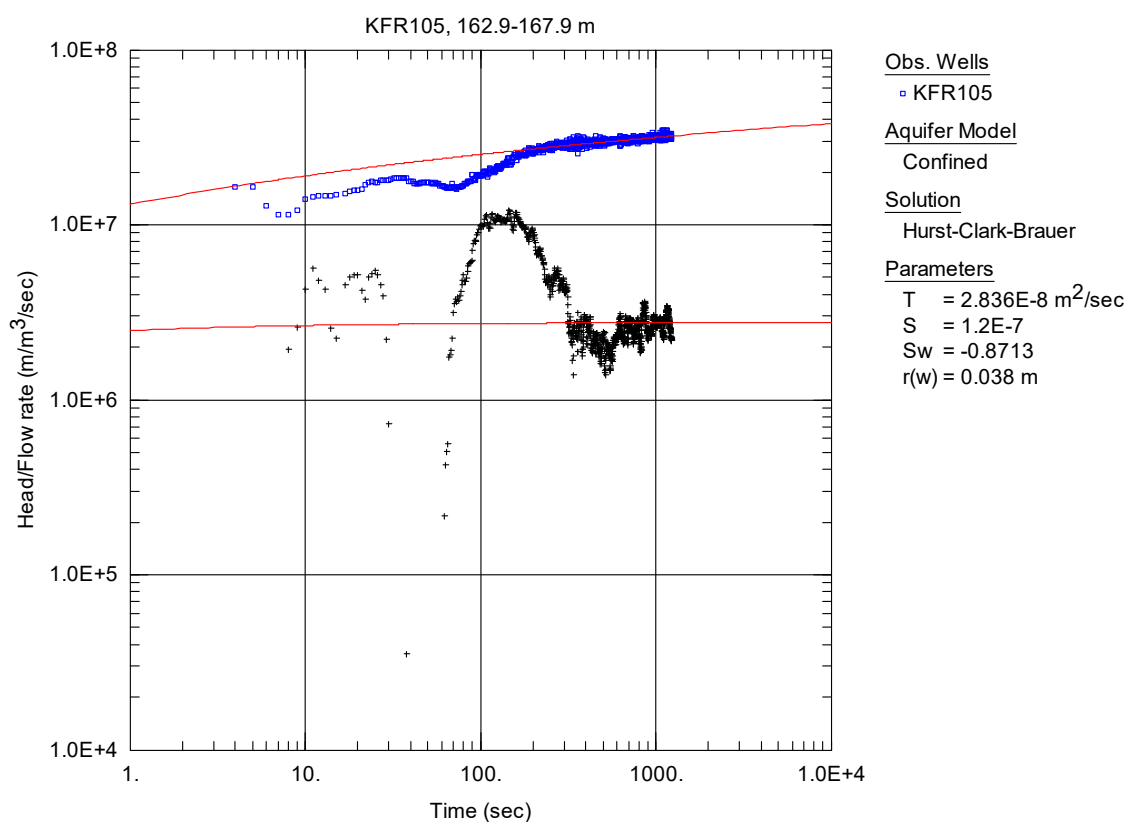


**Figure A3-73.** Log-log plot of head/flow rate (□) and derivative (+) versus time, from the injection test in section 162.9-167.9 m in KFR105.

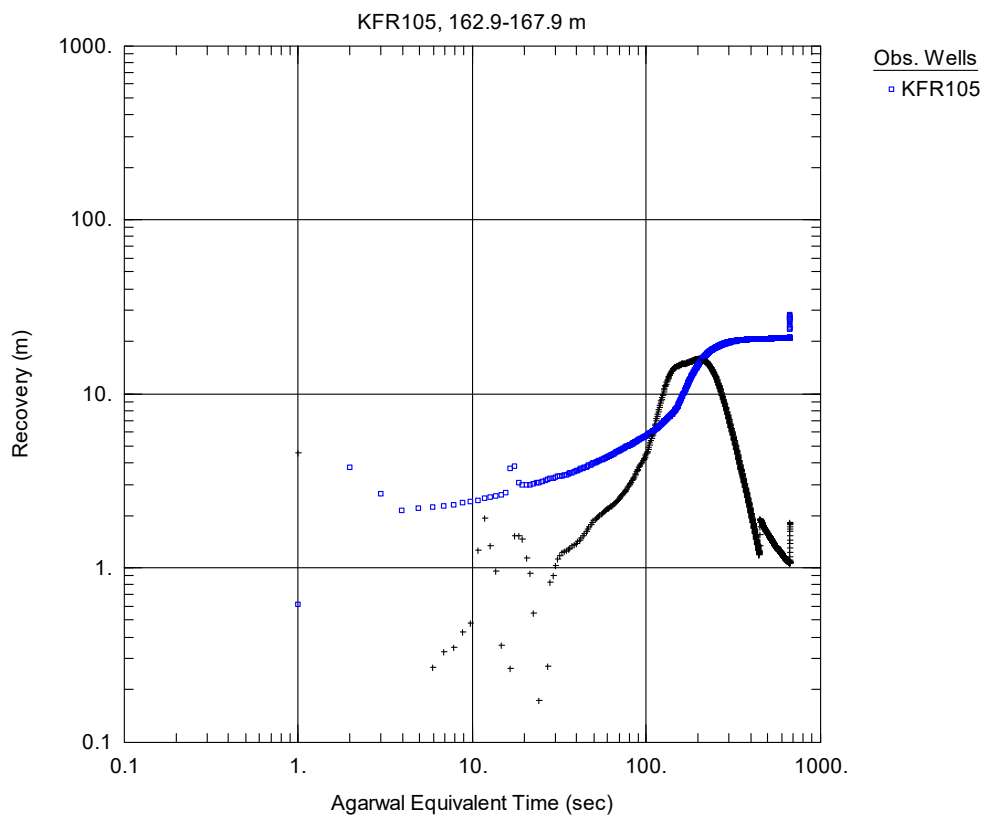


**Figure A3-74.** Log-log plot of recovery (□) and derivative (+) versus equivalent time, from the injection test in section 162.9-167.9 m in KFR105. No satisfying solution was found.

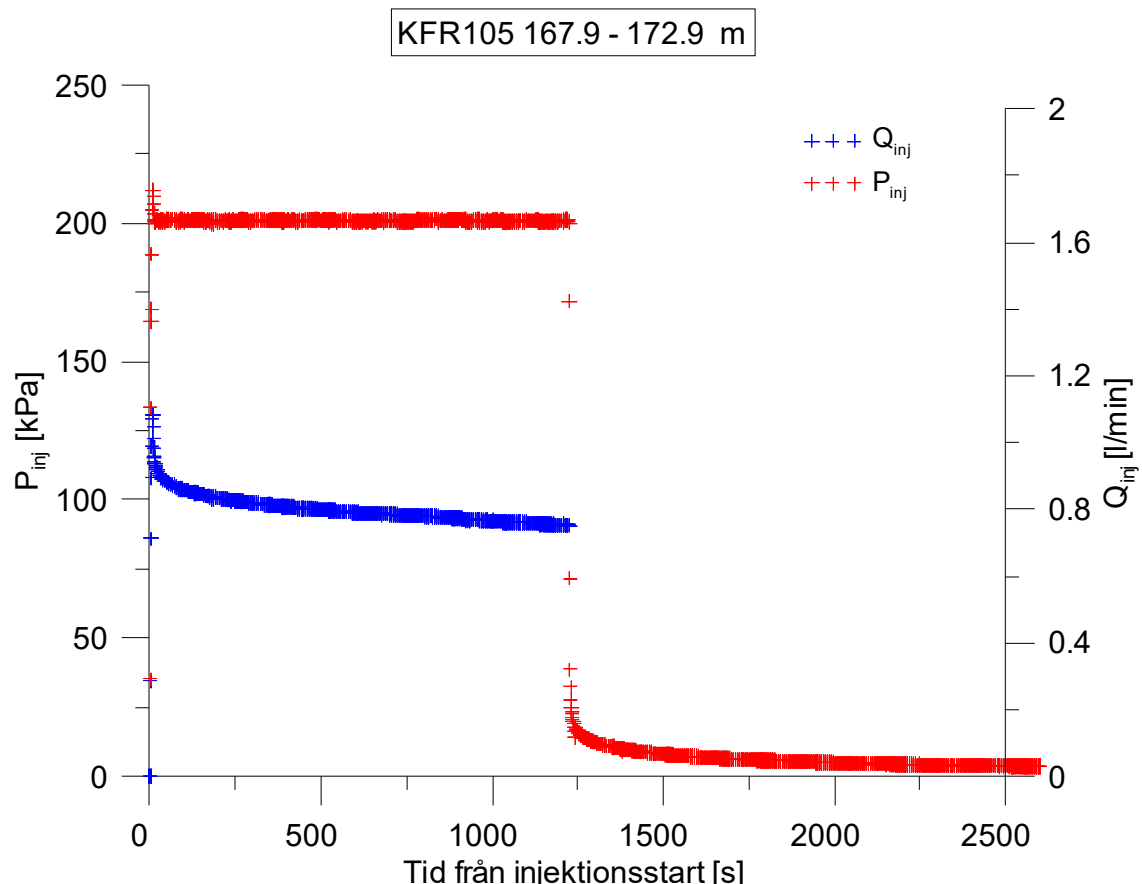


**Figure A3-75.** Linear plot of flow rate ( $Q$ ) and pressure ( $P$ ) versus time from the injection test in section 167.9-172.9 m in borehole KFR105.

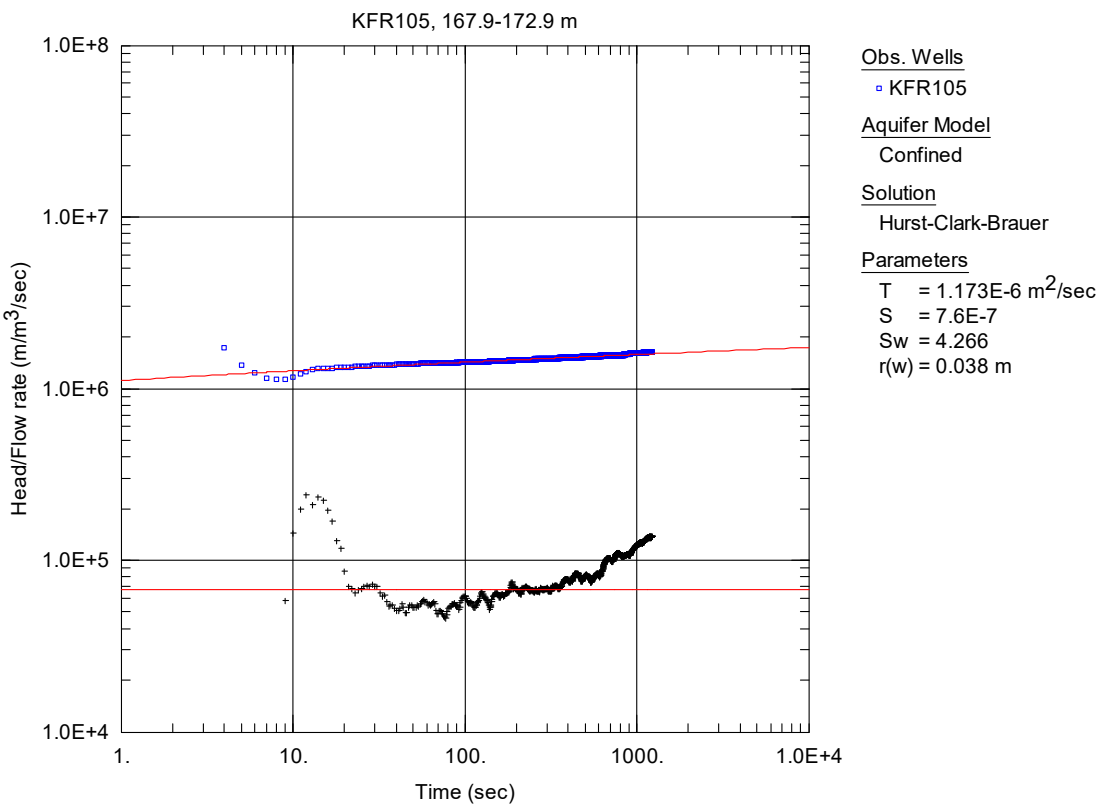


**Figure A3-76.** Log-log plot of head/flow rate (□) and derivative (+) versus time, from the injection test in section 167.9-172.9 m in KFR105.

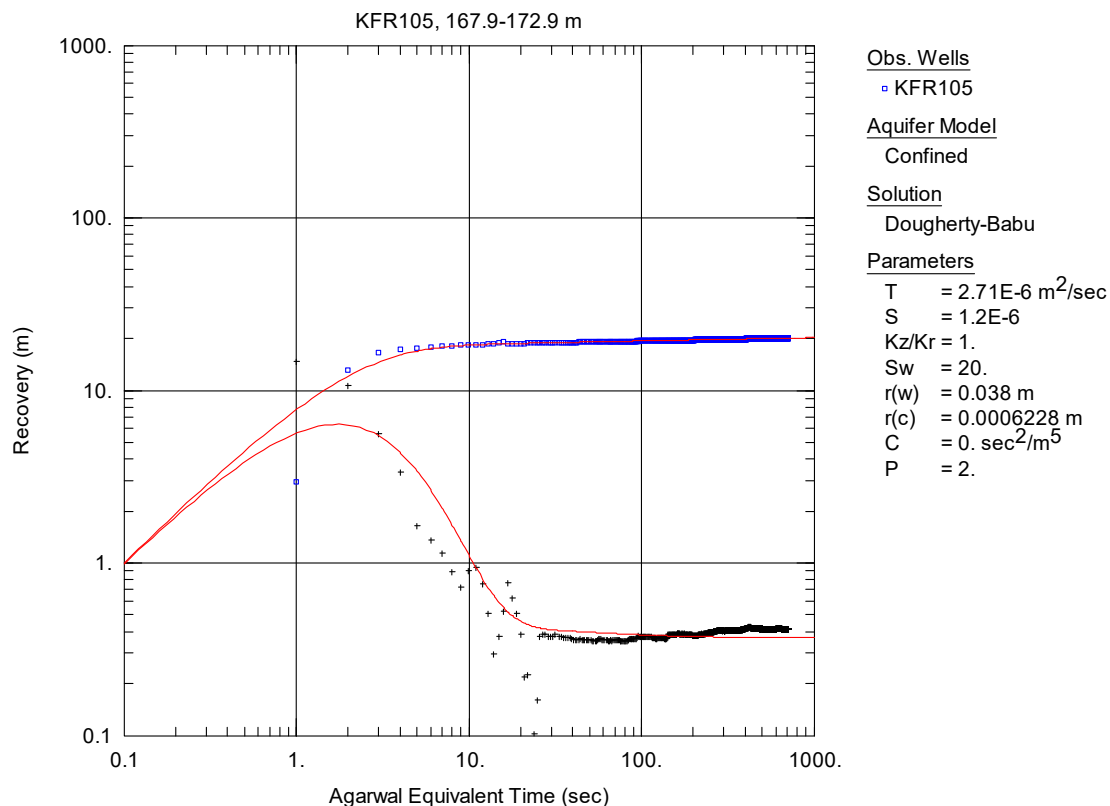


**Figure A3-77.** Log-log plot of recovery (□) and derivative (+) versus equivalent time, from the injection test in section 167.9-172.9 m in KFR105.

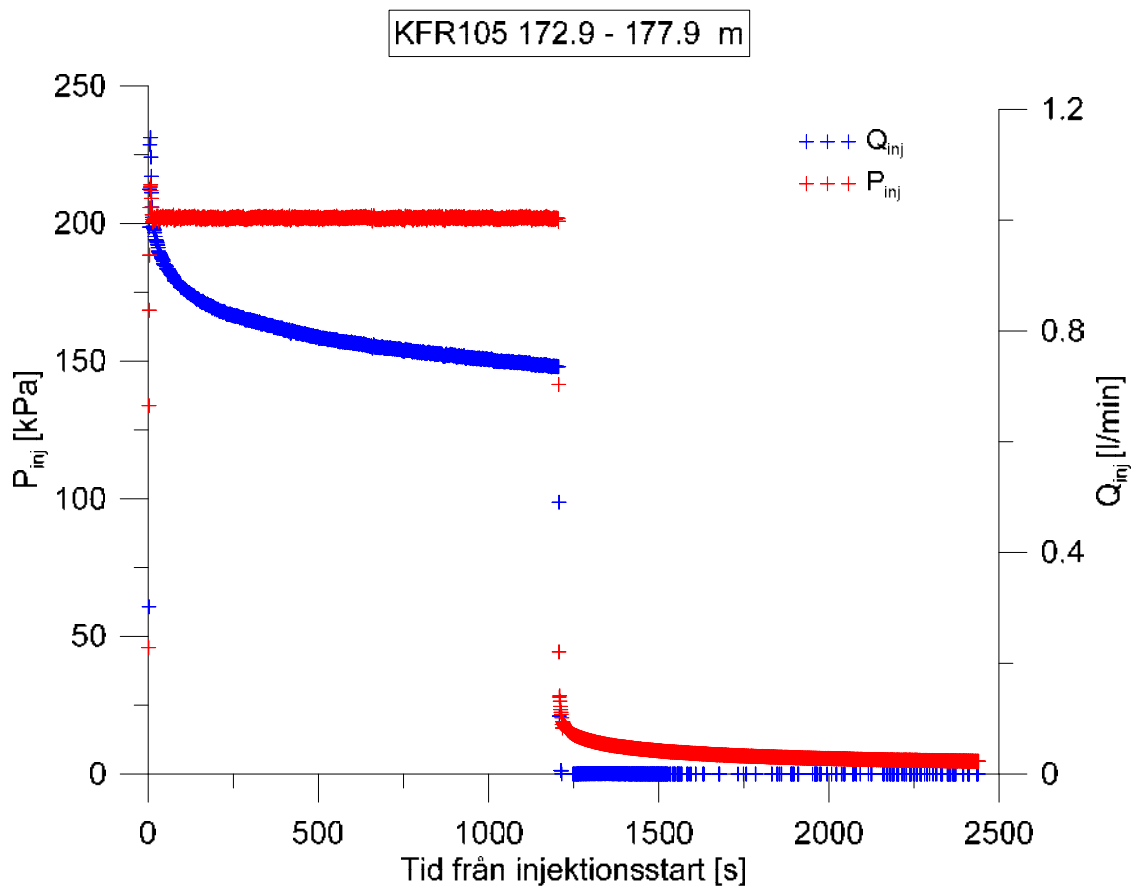


**Figure A3-78.** Linear plot of flow rate ( $Q$ ) and pressure ( $P$ ) versus time from the injection test in section 172.9-177.9 m in borehole KFR105.

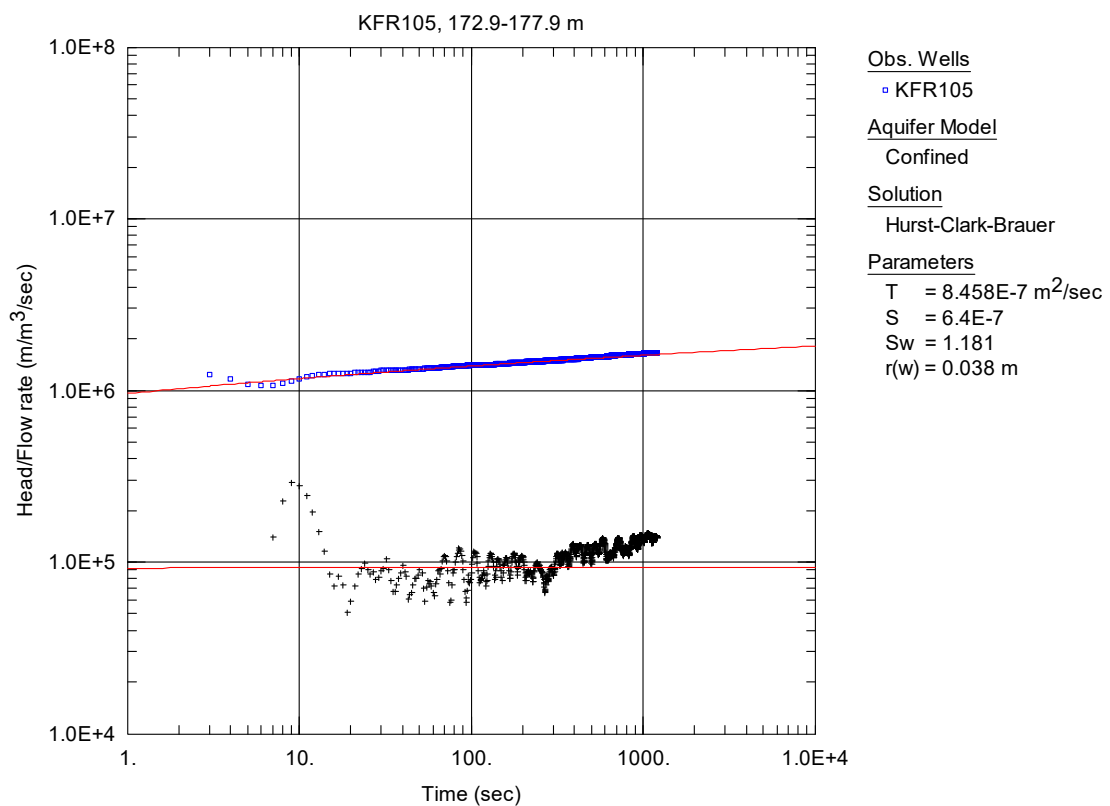


**Figure A3-79.** Log-log plot of head/flow rate ( $\square$ ) and derivative (+) versus time, from the injection test in section 172.9-177.9 m in KFR105.

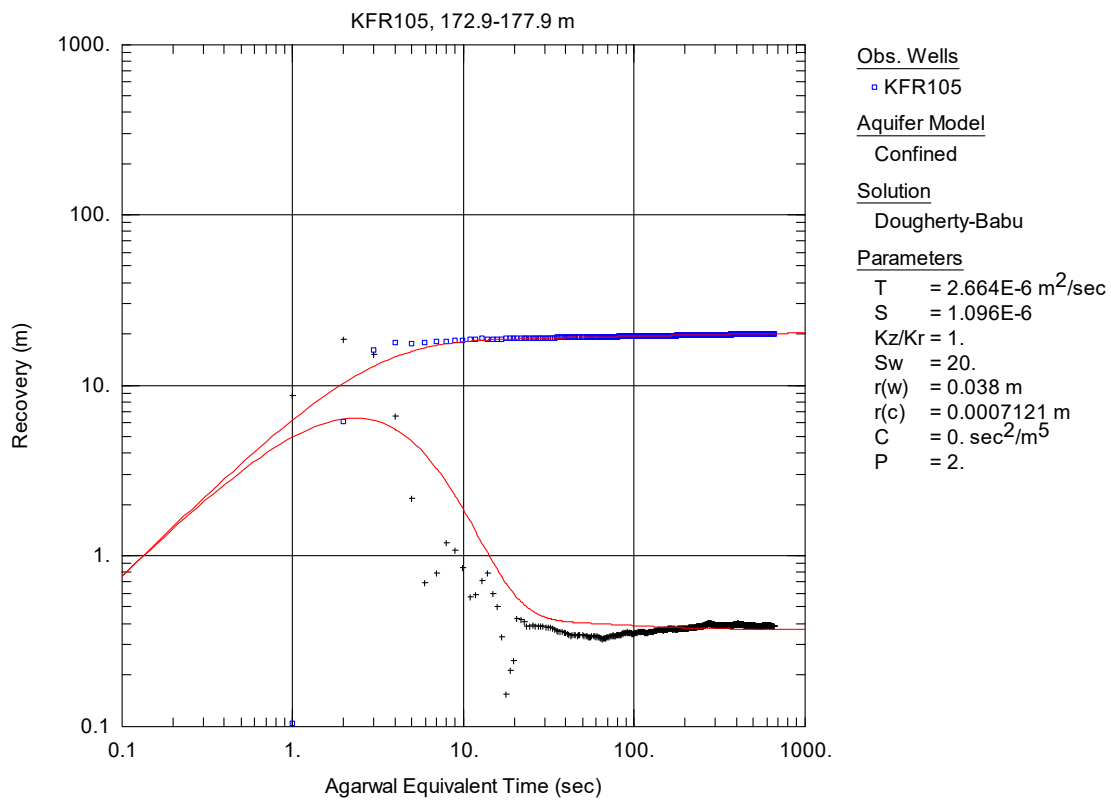


**Figure A3-80.** Log-log plot of recovery (□) and derivative (+) versus equivalent time, from the injection test in section 172.9-177.9 m in KFR105.

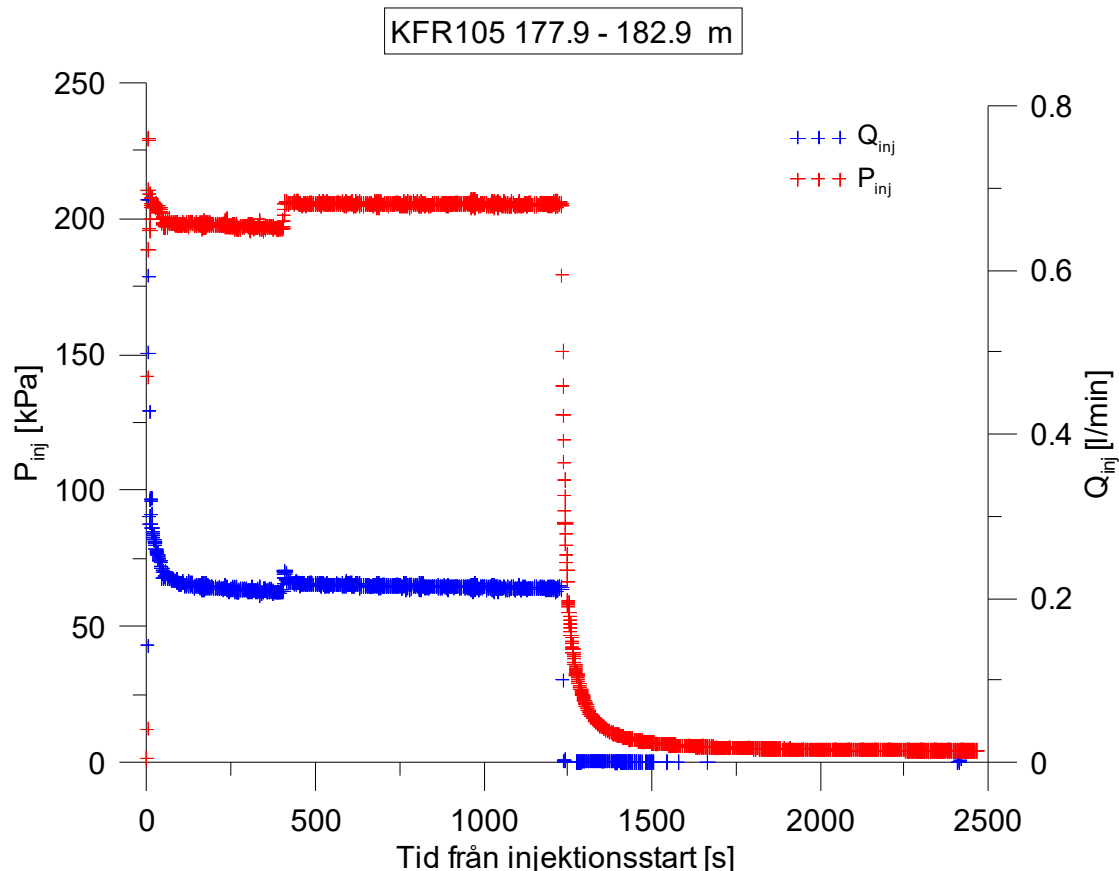


**Figure A3-81.** Linear plot of flow rate ( $Q$ ) and pressure ( $P$ ) versus time from the injection test in section 177.9-182.9 m in borehole KFR105.

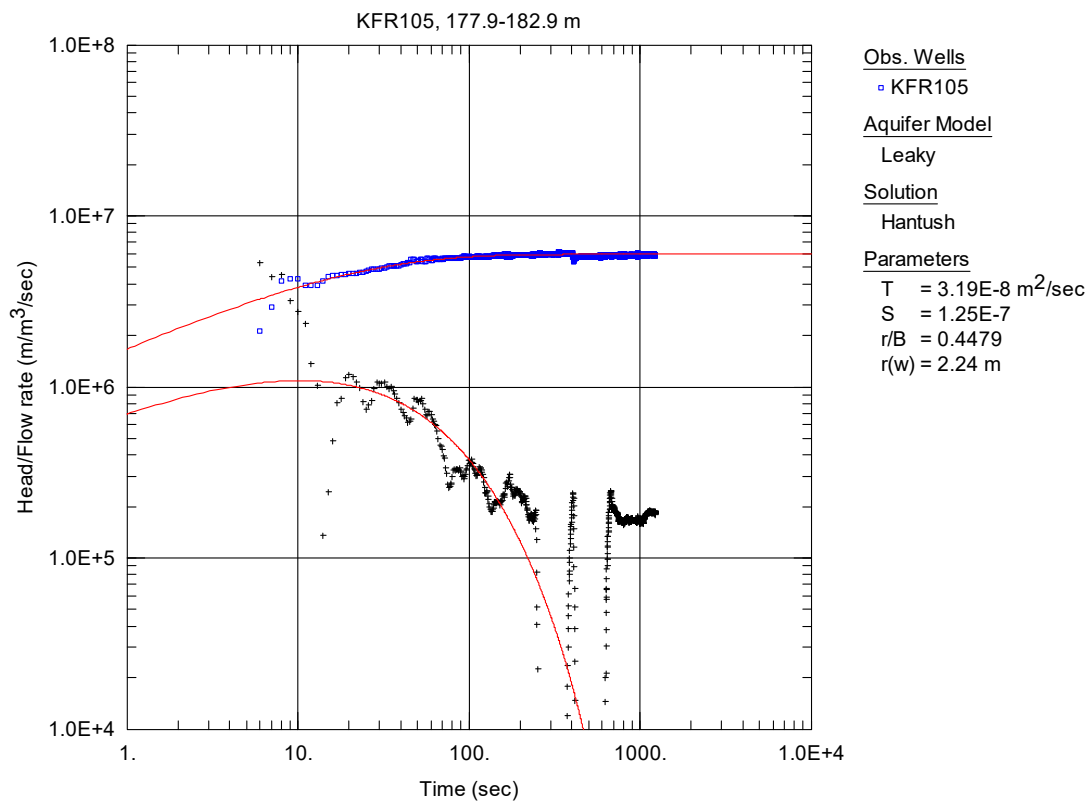


**Figure A3-82.** Log-log plot of head/flow rate (□) and derivative (+) versus time, from the injection test in section 177.9-182.9 m in KFR105.

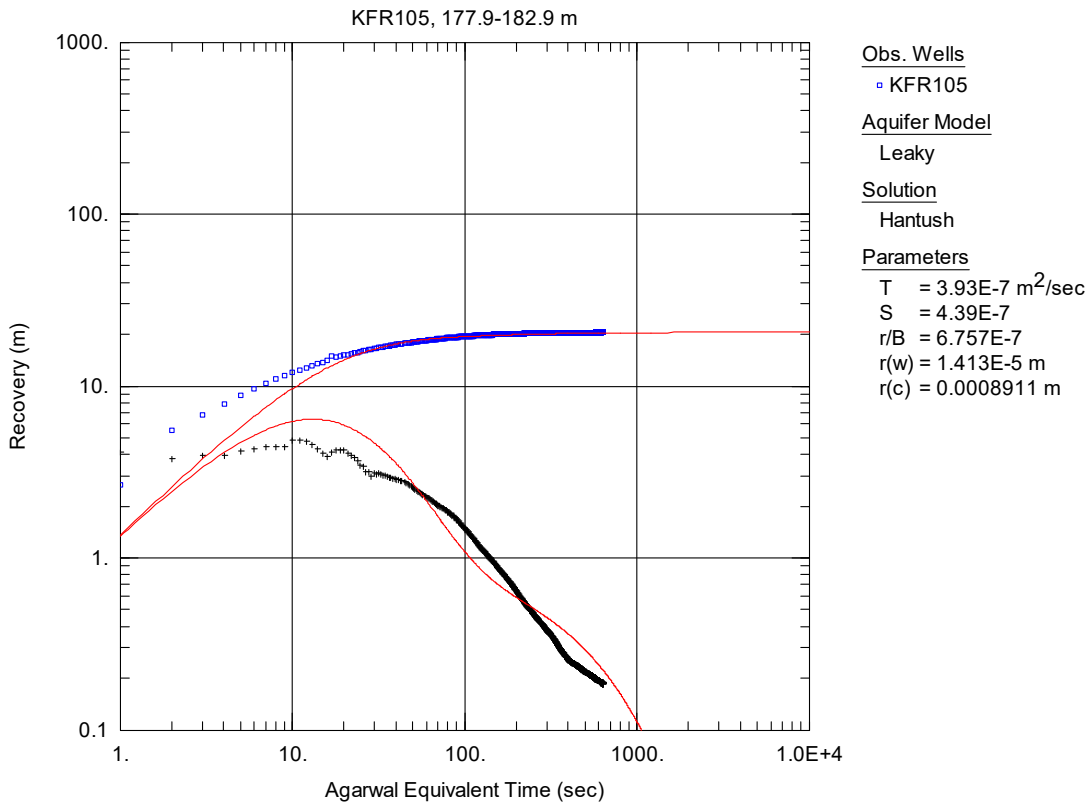


**Figure A3-83.** Log-log plot of recovery (□) and derivative (+) versus equivalent time, from the injection test in section 177.9-182.9 m in KFR105.

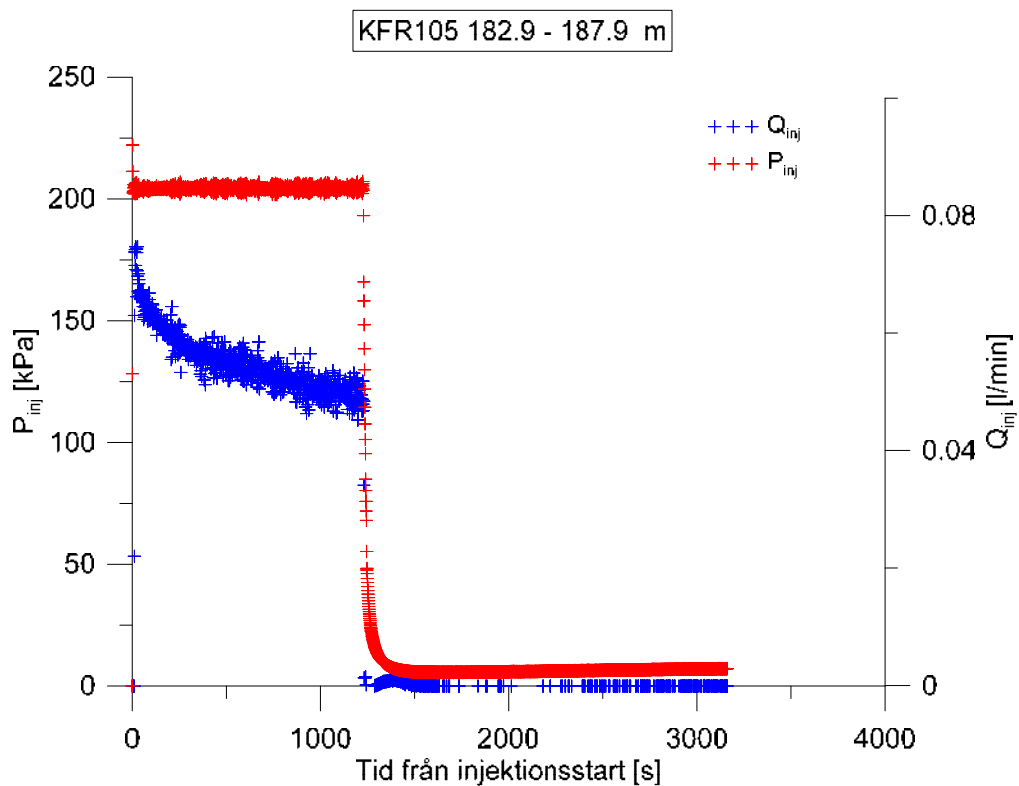


**Figure A3-84.** Linear plot of flow rate ( $Q$ ) and pressure ( $P$ ) versus time from the injection test in section 182.9-187.9 m in borehole KFR105.

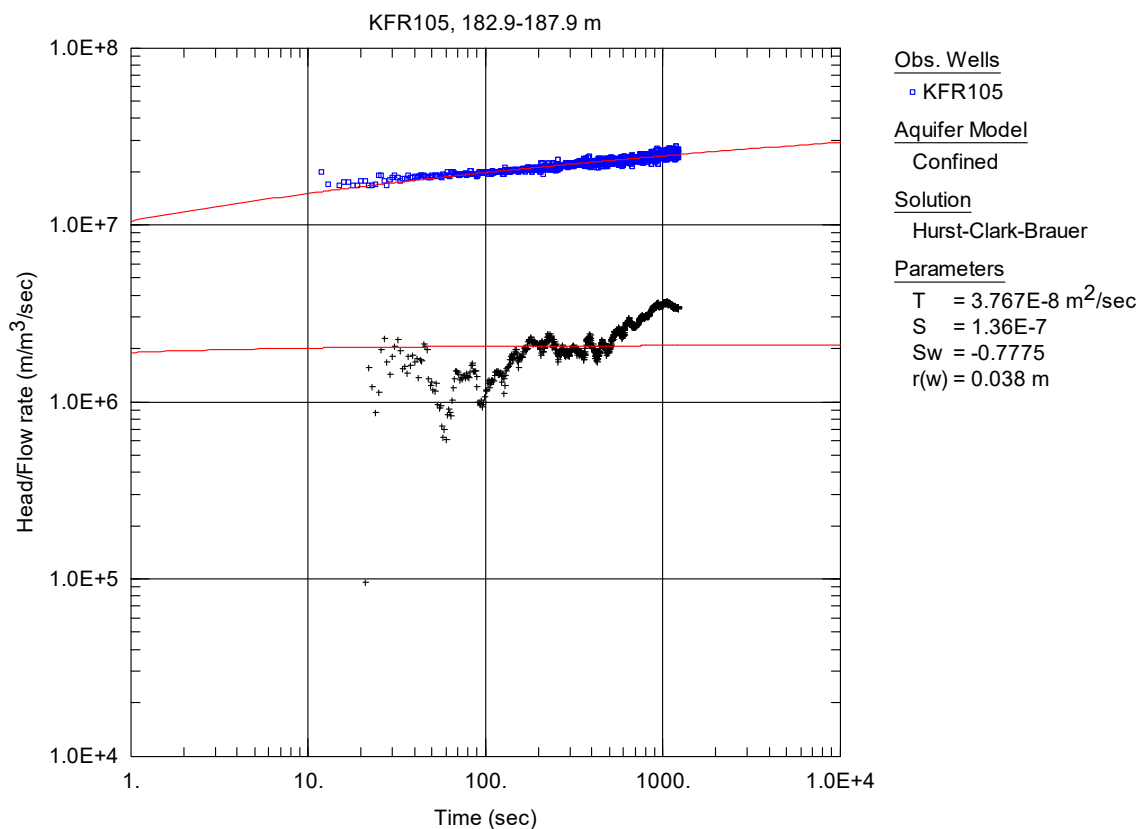


**Figure A3-85.** Log-log plot of head/flow rate (□) and derivative (+) versus time, from the injection test in section 182.9-187.9 m in KFR105.

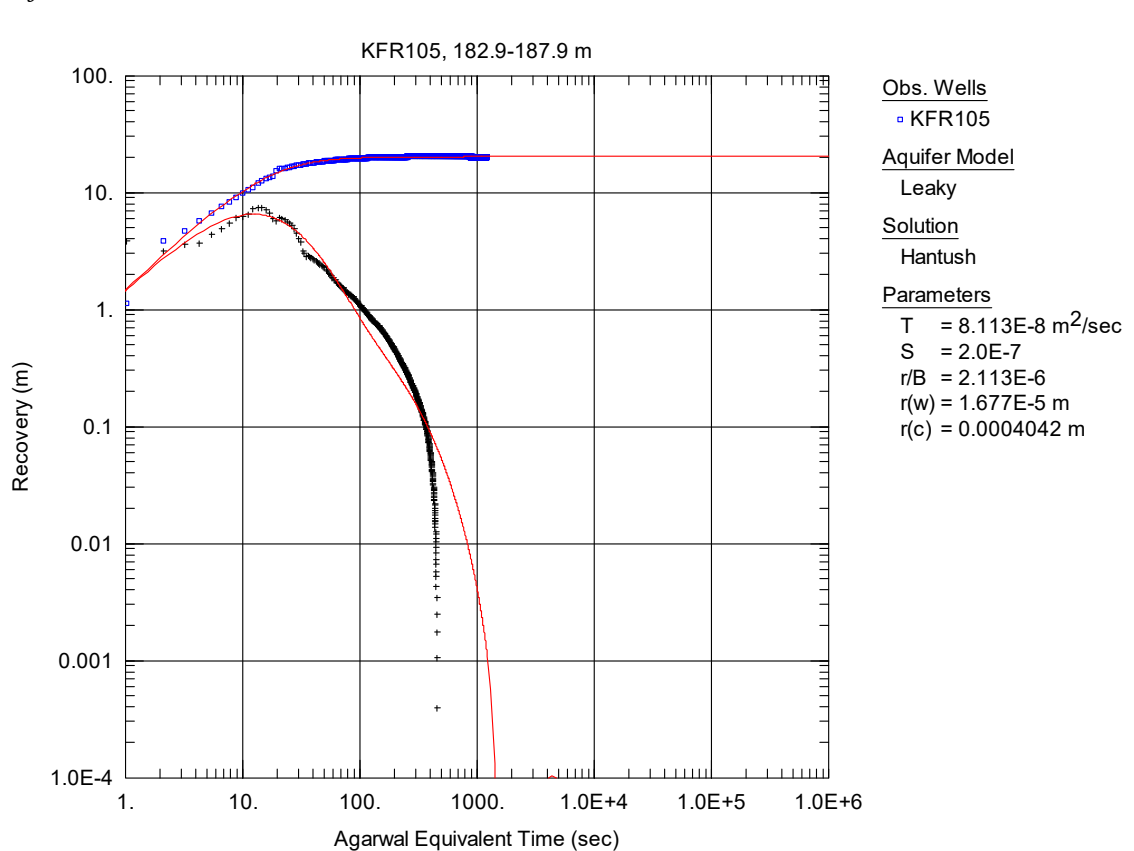


**Figure A3-86.** Log-log plot of recovery (□) and derivative (+) versus equivalent time, from the injection test in section 182.9-187.9 m in KFR105.

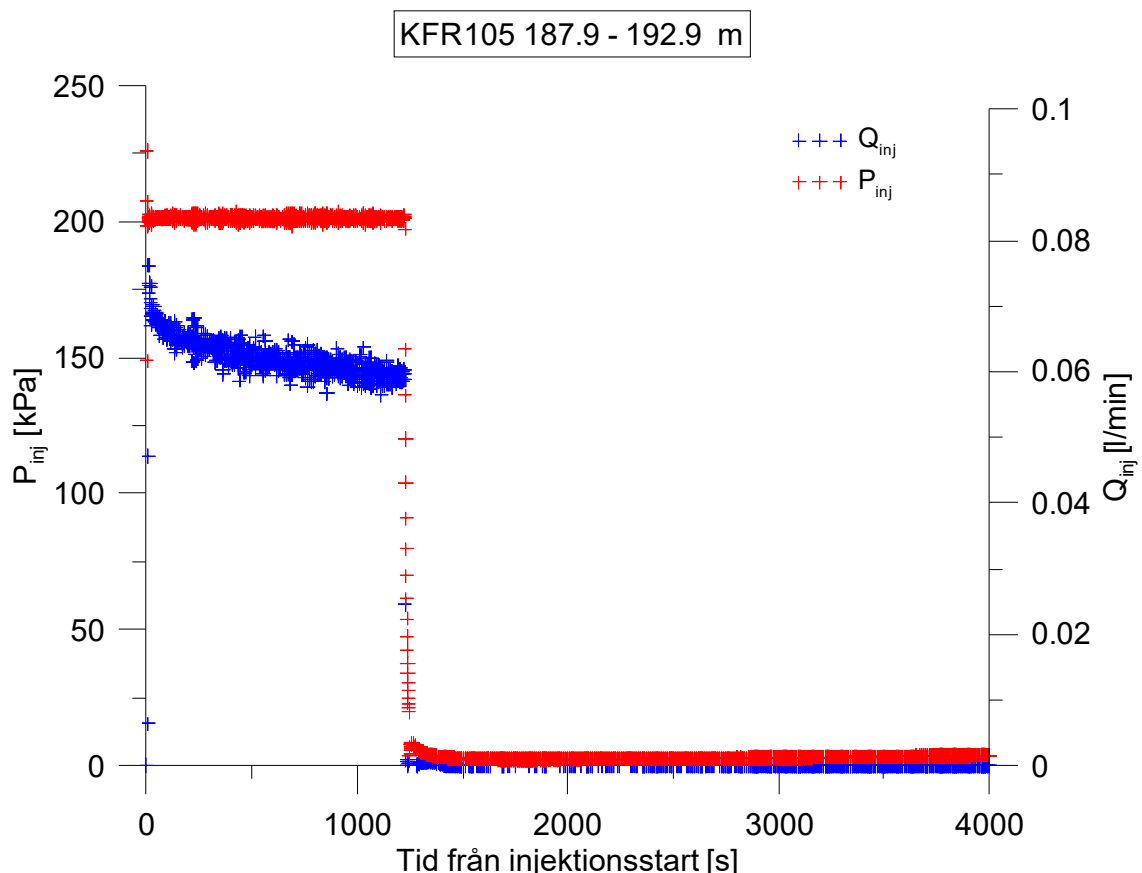


**Figure A3-87.** Linear plot of flow rate ( $Q$ ) and pressure ( $P$ ) versus time from the injection test in section 187.9-192.9 m in borehole KFR105.

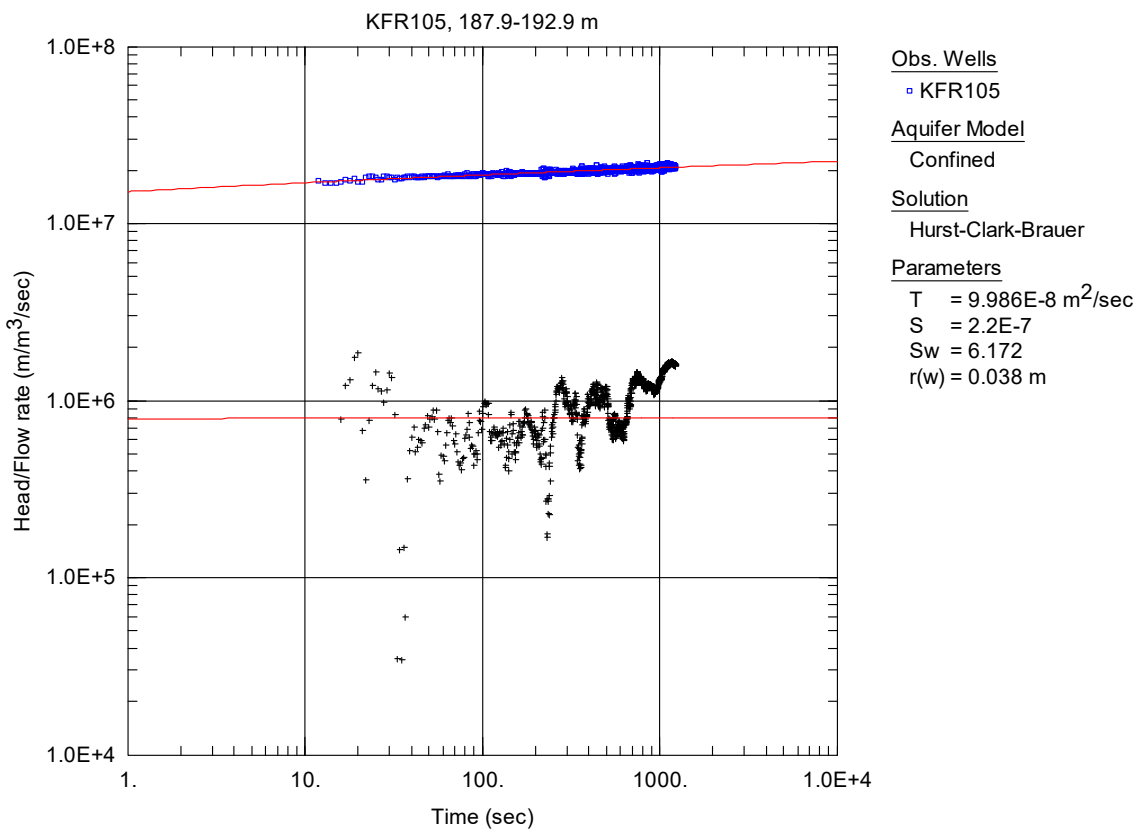


**Figure A3-88.** Log-log plot of head/flow rate ( $\square$ ) and derivative (+) versus time, from the injection test in section 187.9-192.9 m in KFR105.

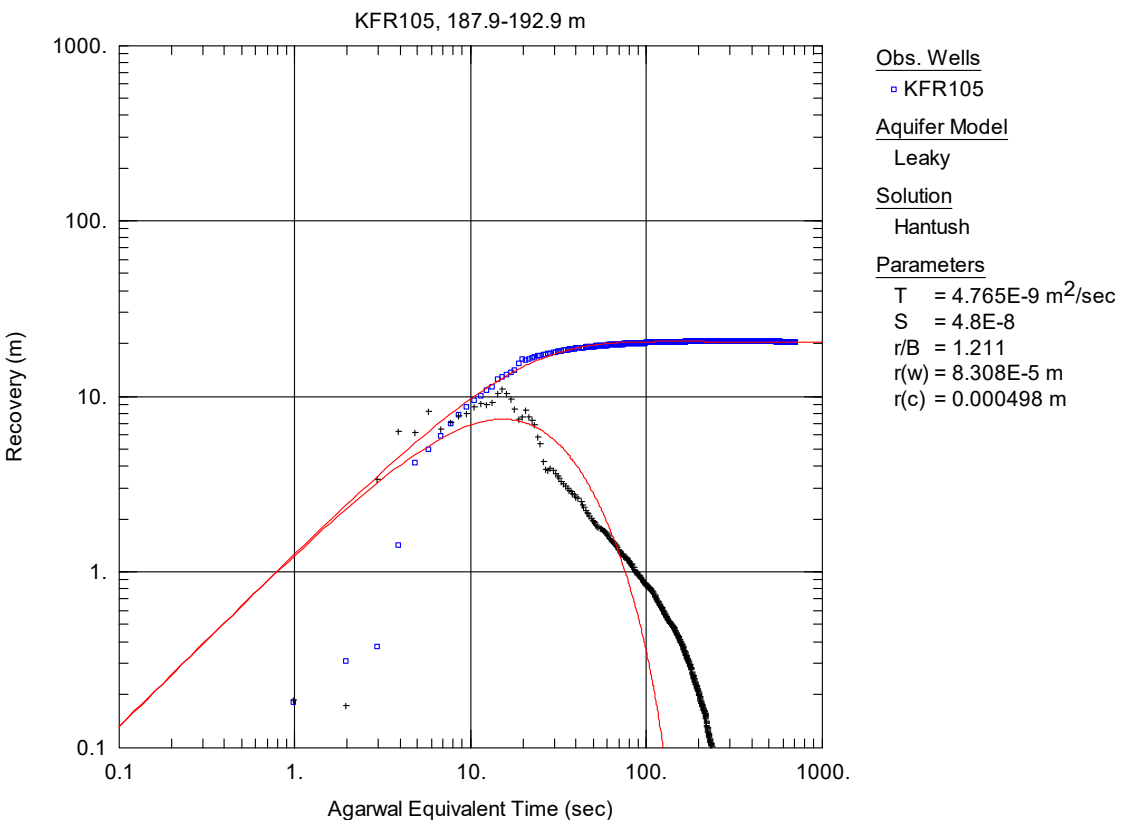


**Figure A3-89.** Log-log plot of recovery ( $\square$ ) and derivative (+) versus equivalent time, from the injection test in section 187.9-192.9 m in KFR105.

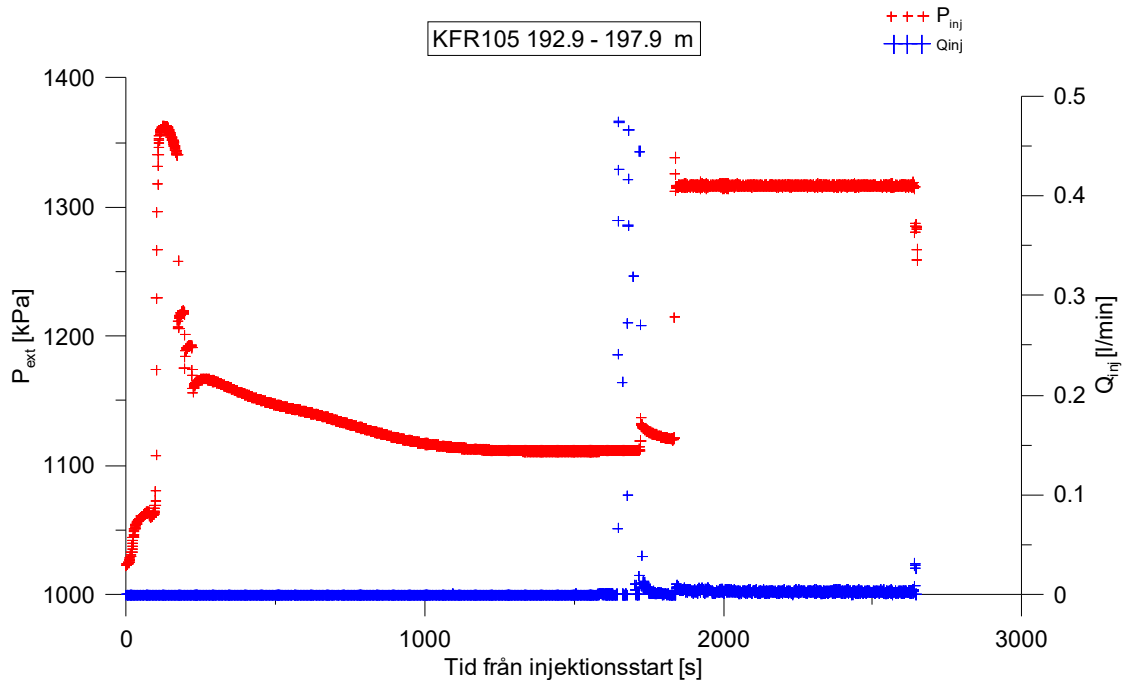


**Figure A3-90.** Linear plot of flow rate ( $Q$ ) and pressure ( $P$ ) versus time from the injection test in section 192.9-197.9 m in borehole KFR105.

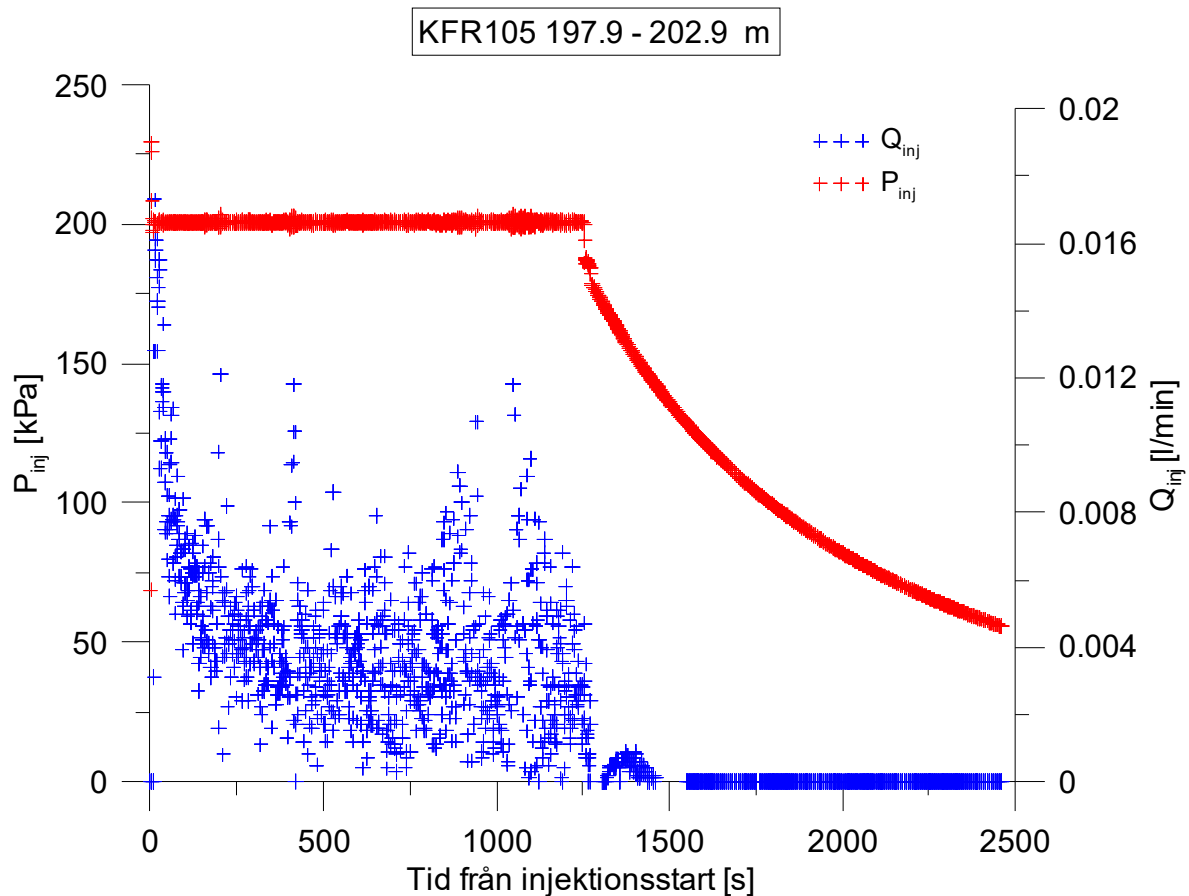


**Figure A3-91.** Linear plot of flow rate ( $Q$ ) and pressure ( $P$ ) versus time from the injection test in section 197.9-202.9 m in borehole KFR105.

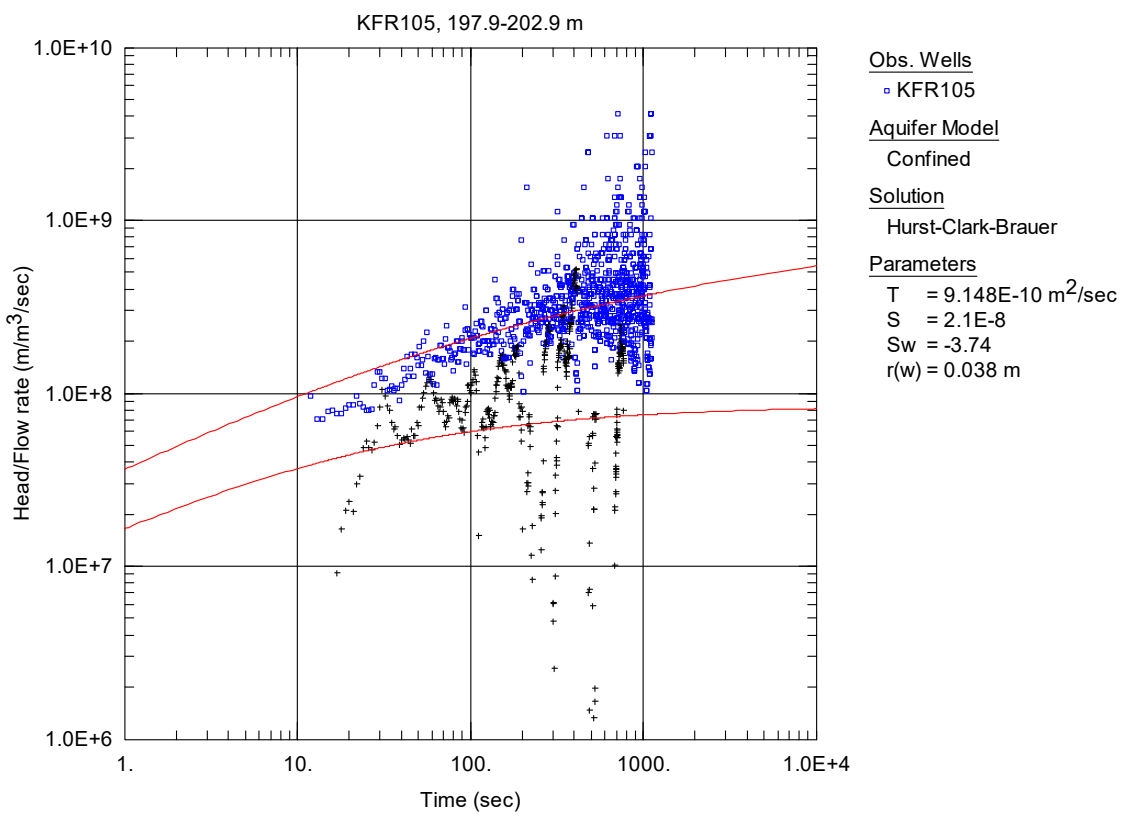


**Figure A3-92.** Log-log plot of head/flow rate (□) and derivative (+) versus time, from the injection test in section 197.9-202.9 m in KFR105.

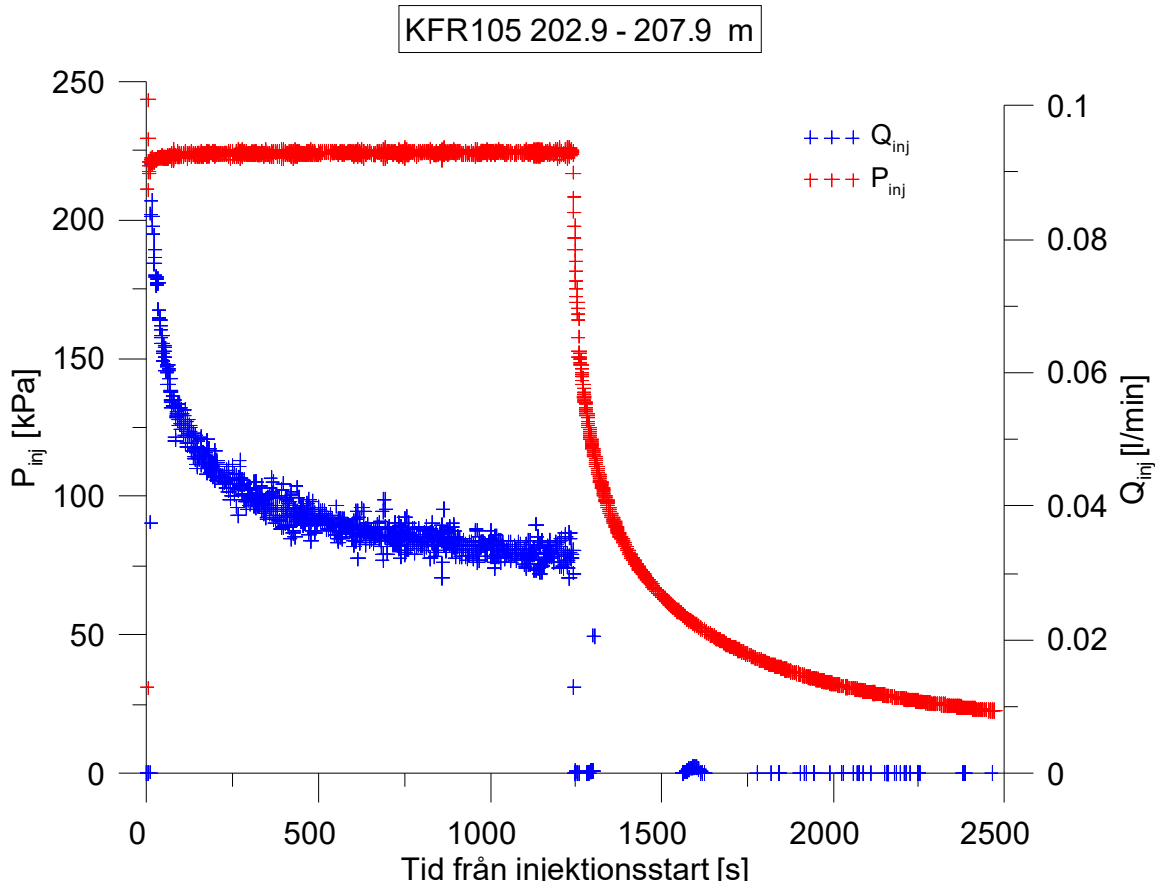


**Figure A3-93.** Linear plot of flow rate ( $Q$ ) and pressure ( $P$ ) versus time from the injection test in section 202.9-207.9 m in borehole KFR105.

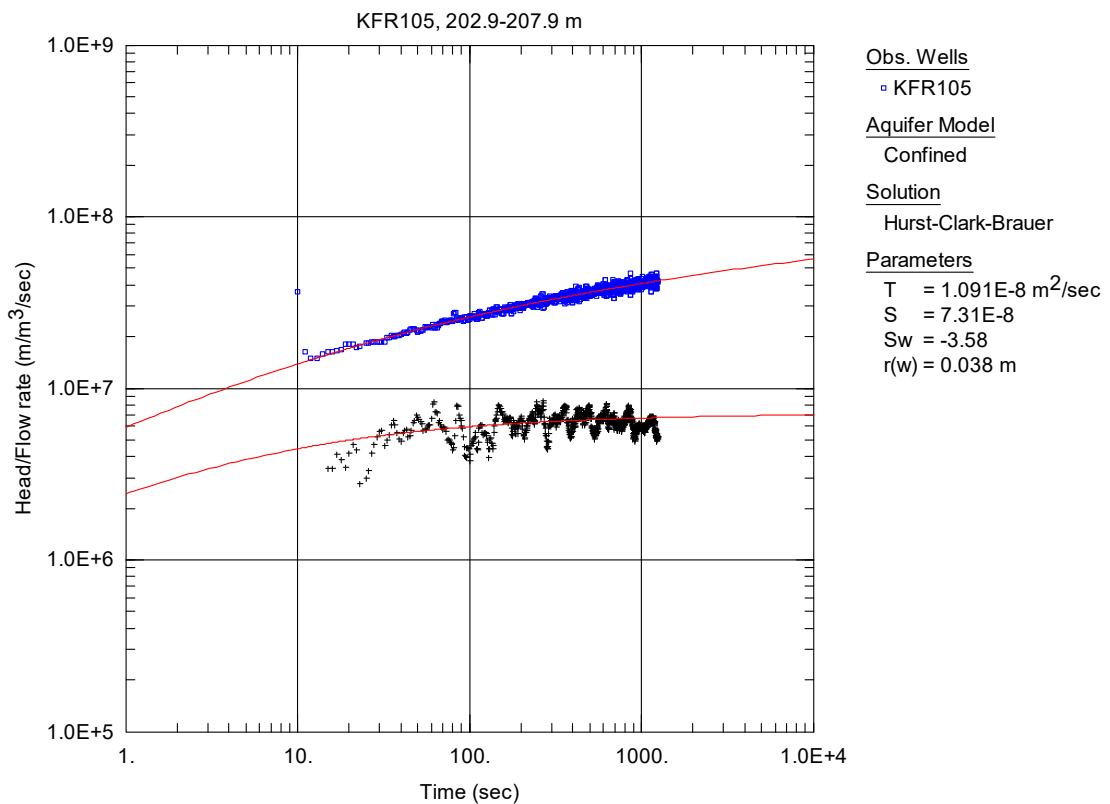


**Figure A3-94.** Log-log plot of head/flow rate (□) and derivative (+) versus time, from the injection test in section 202.9-207.9 m in KFR105.

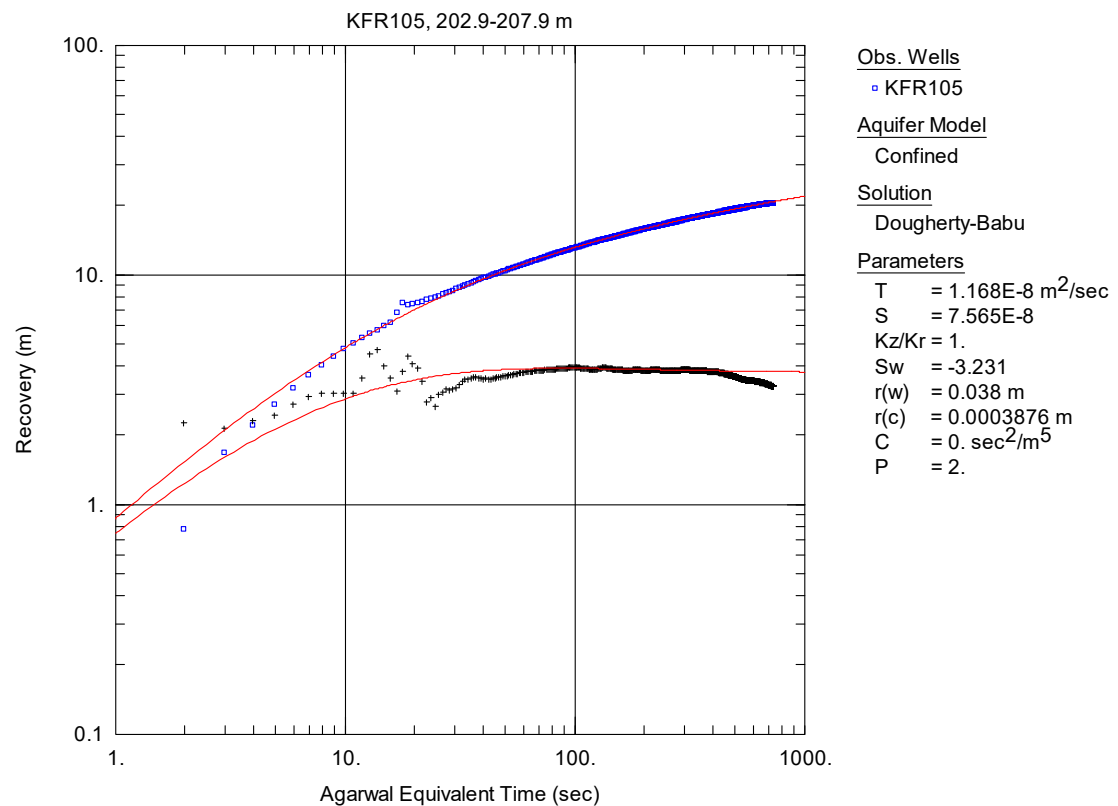


**Figure A3-95.** Log-log plot of recovery (□) and derivative (+) versus equivalent time, from the injection test in section 202.9-207.9 m in KFR105.

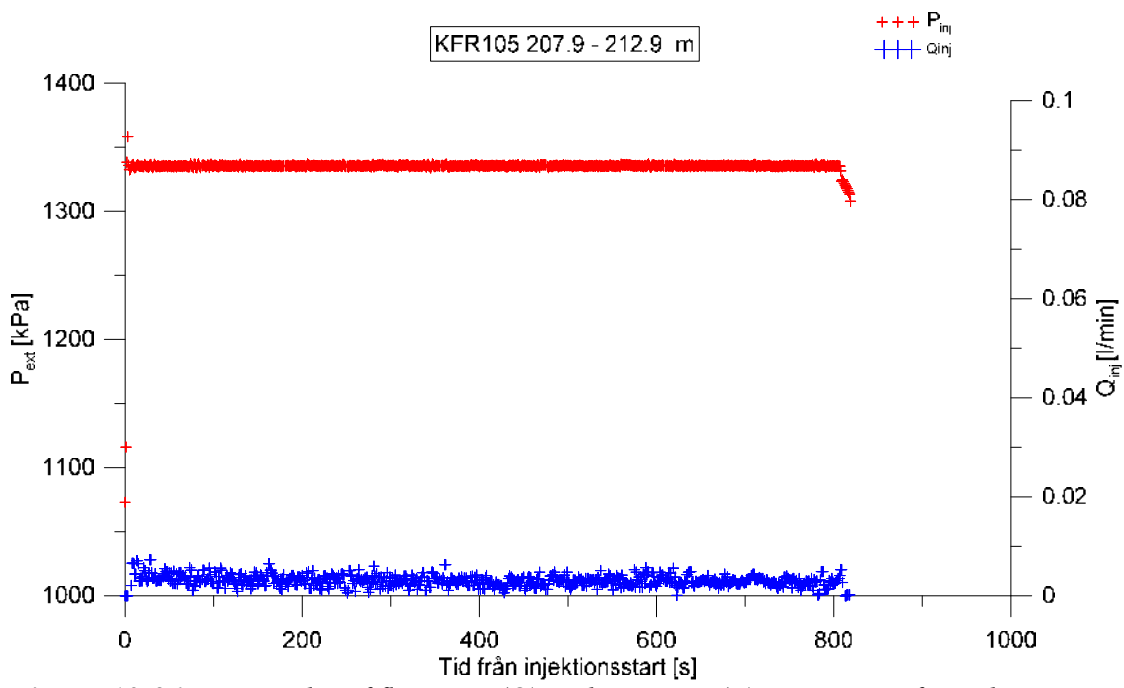


**Figure A3-96.** Linear plot of flow rate ( $Q$ ) and pressure ( $P$ ) versus time from the injection test in section 207.9-212.9 m in borehole KFR105.

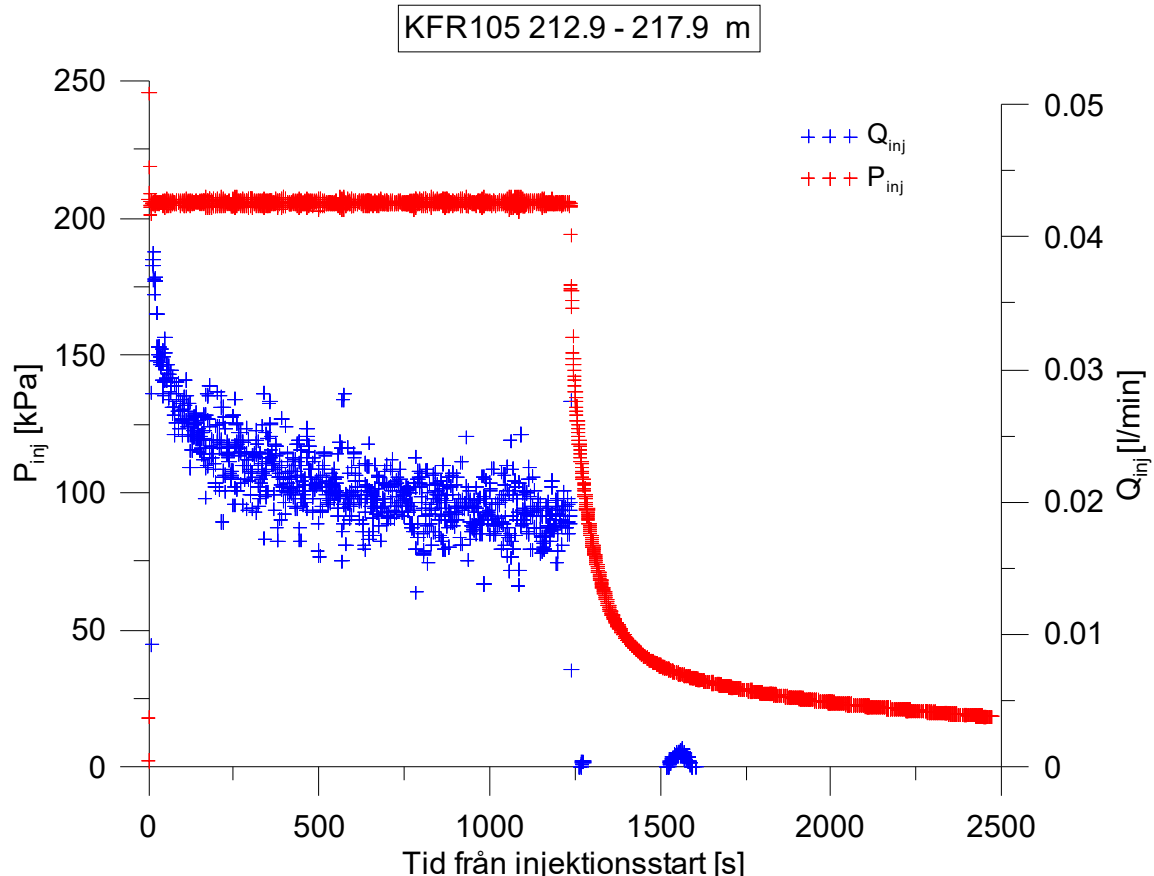


**Figure A3-97.** Linear plot of flow rate ( $Q$ ) and pressure ( $P$ ) versus time from the injection test in section 212.9-217.9 m in borehole KFR105.

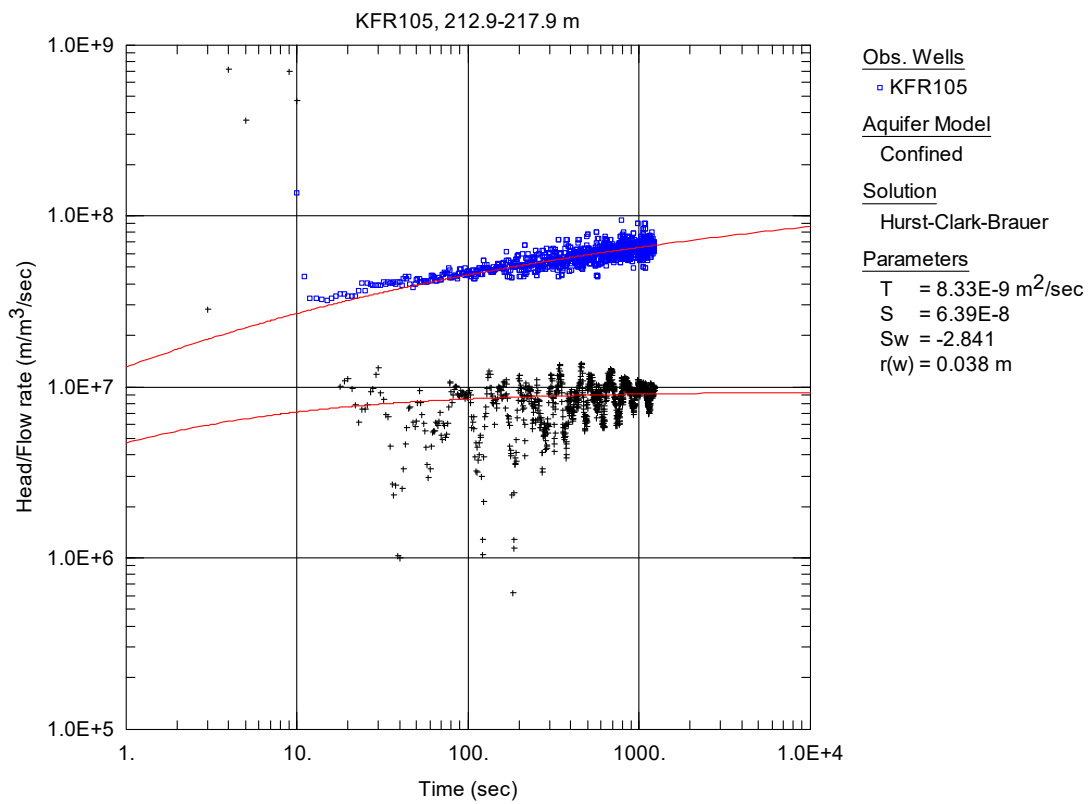


**Figure A3-98.** Log-log plot of head/flow rate (□) and derivative (+) versus time, from the injection test in section 212.9-217.9 m in KFR105.

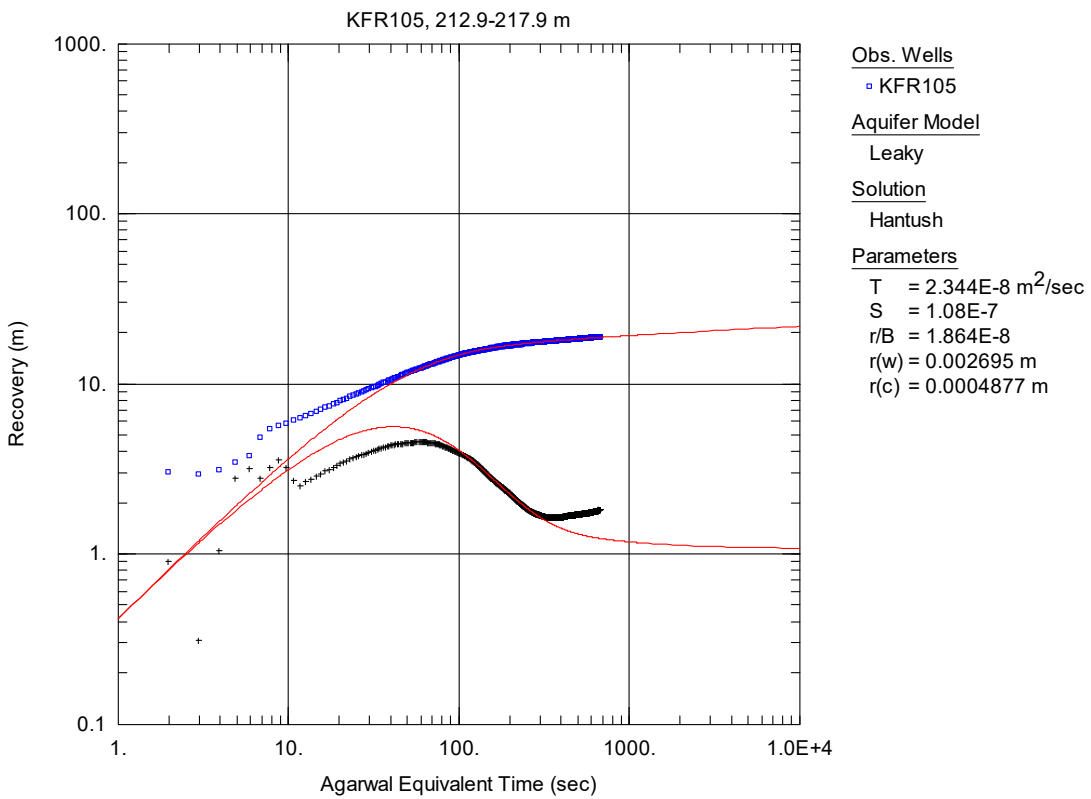


**Figure A3-99.** Log-log plot of recovery (□) and derivative (+) versus equivalent time, from the injection test in section 212.9-217.9 m in KFR105.

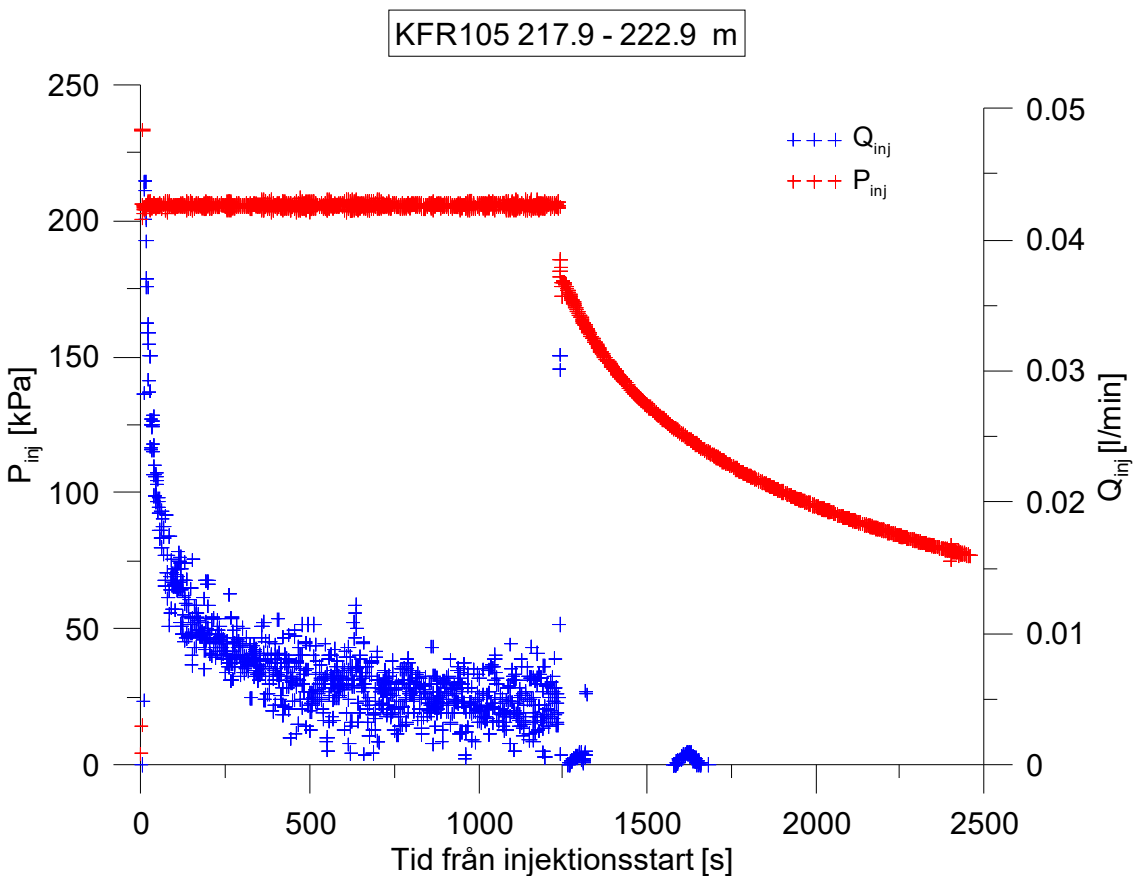


**Figure A3-100.** Linear plot of flow rate ( $Q$ ) and pressure ( $P$ ) versus time from the injection test in section 217.9-222.9 m in borehole KFR105.

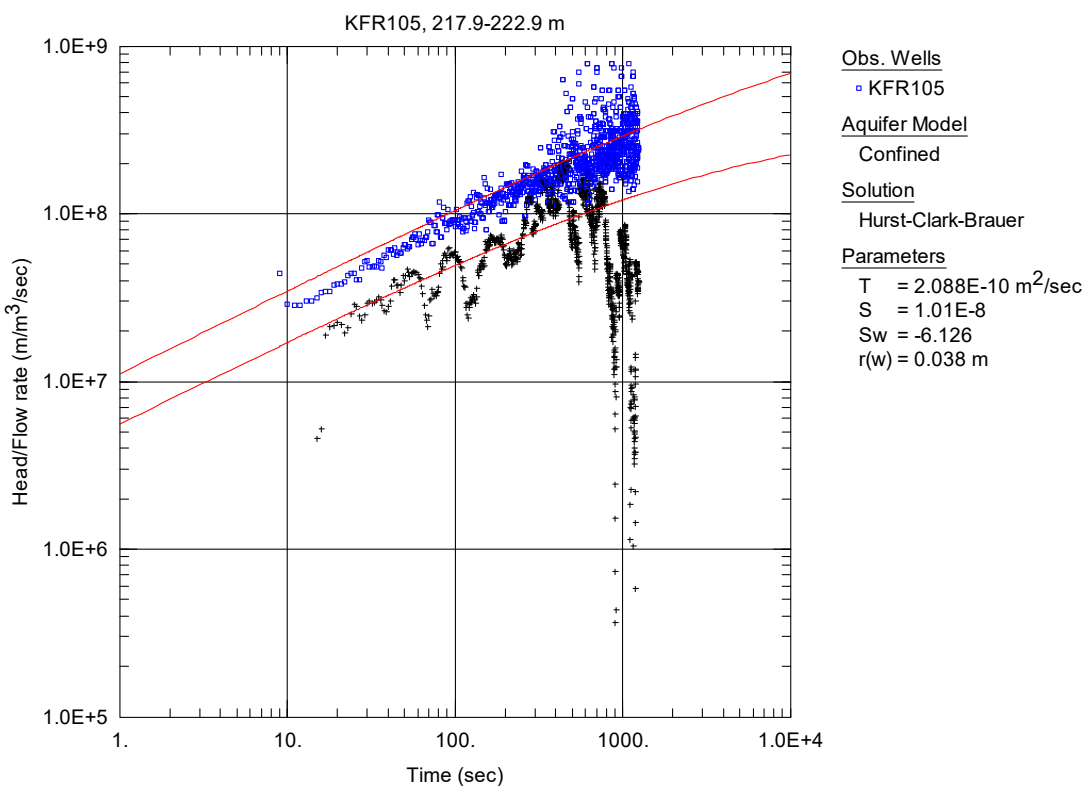


**Figure A3-101.** Log-log plot of head/flow rate (□) and derivative (+) versus time, from the injection test in section 217.9-222.9 m in KFR105.

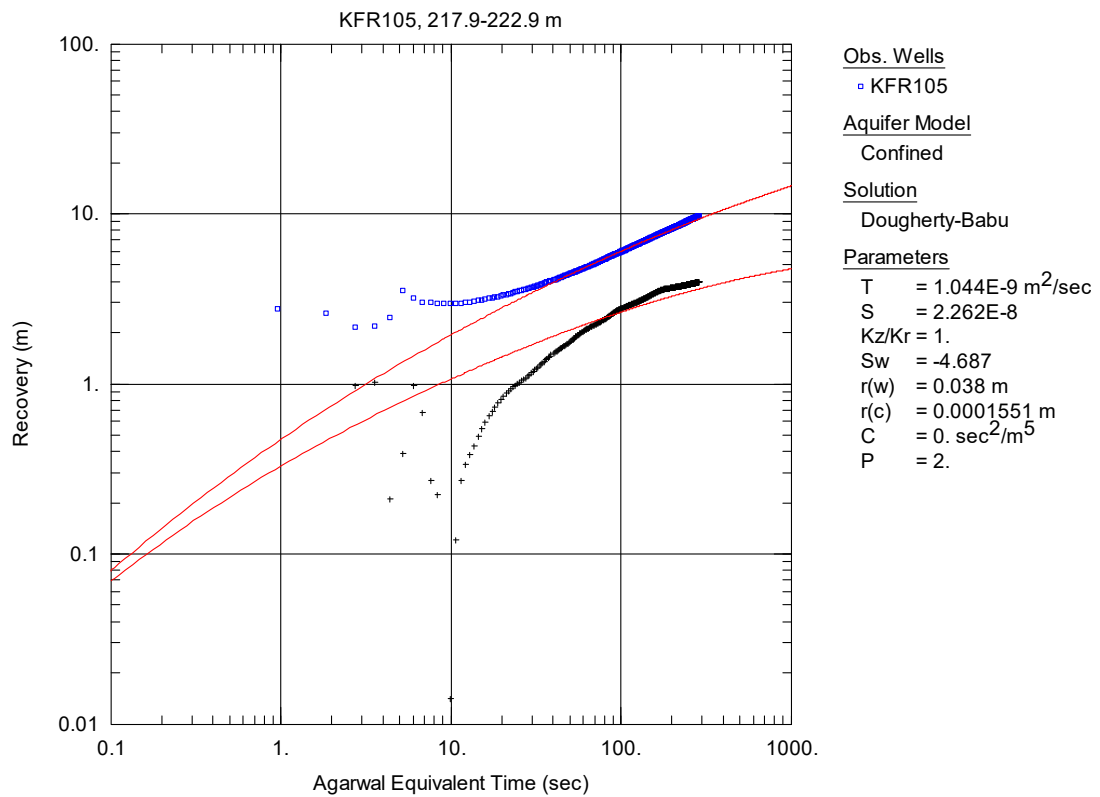


**Figure A3-102.** Log-log plot of recovery (□) and derivative (+) versus equivalent time, from the injection test in section 217.9-222.9 m in KFR105.

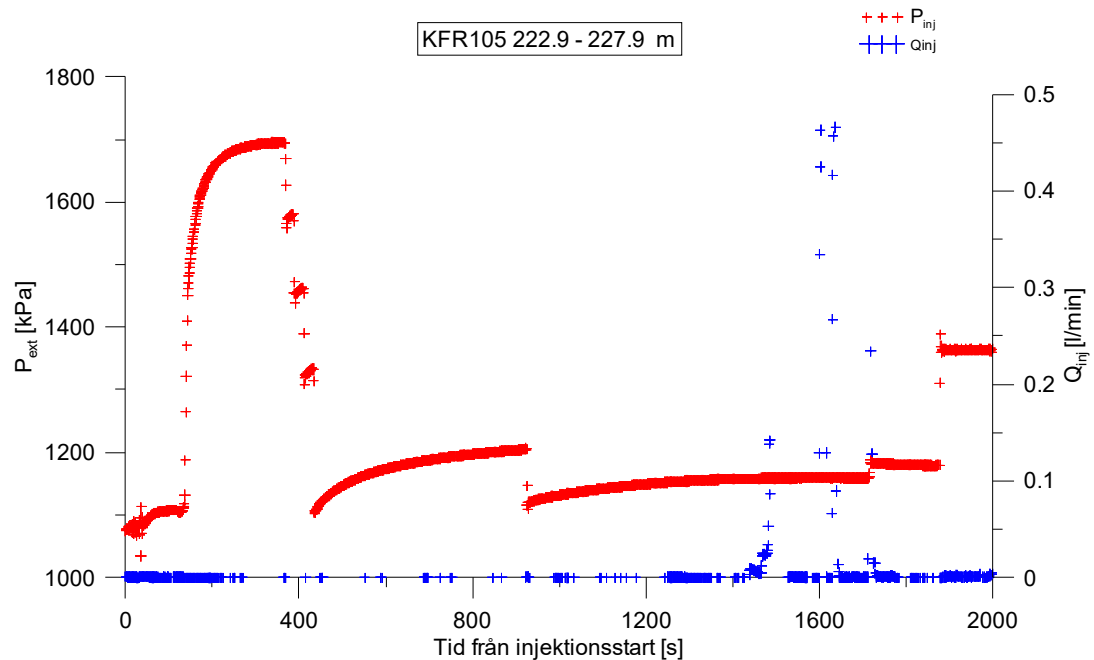


**Figure A3-103.** Linear plot of flow rate ( $Q$ ) and pressure ( $P$ ) versus time from the injection test in section 222.9-227.9 m in borehole KFR105.

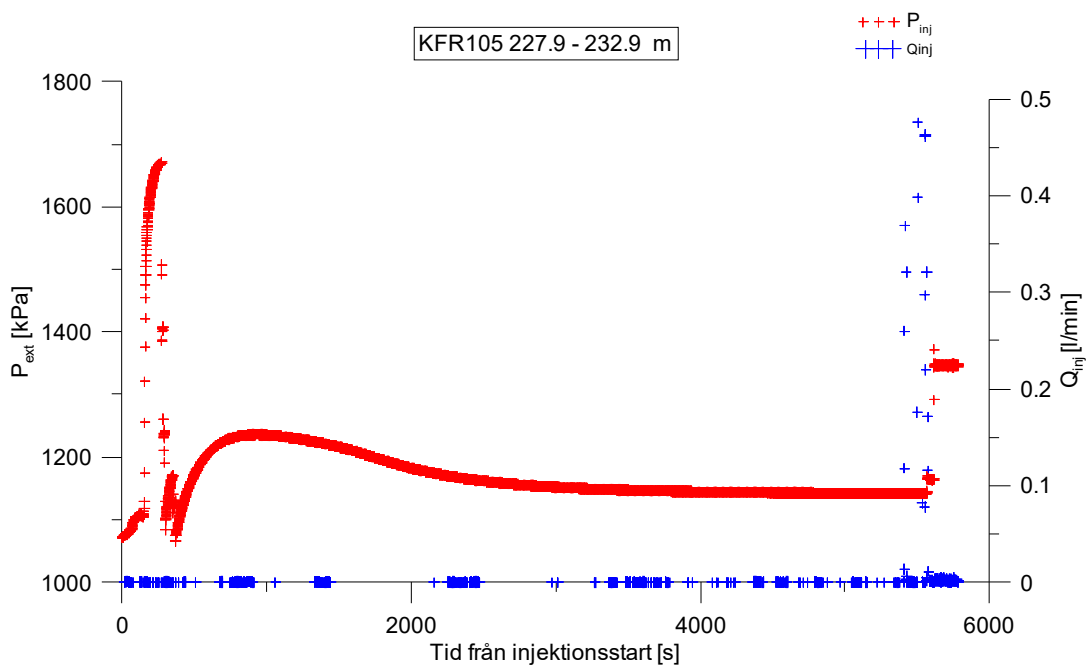


**Figure A3-104.** Linear plot of flow rate ( $Q$ ) and pressure ( $P$ ) versus time from the injection test in section 227.9-232.9 m in borehole KFR105.

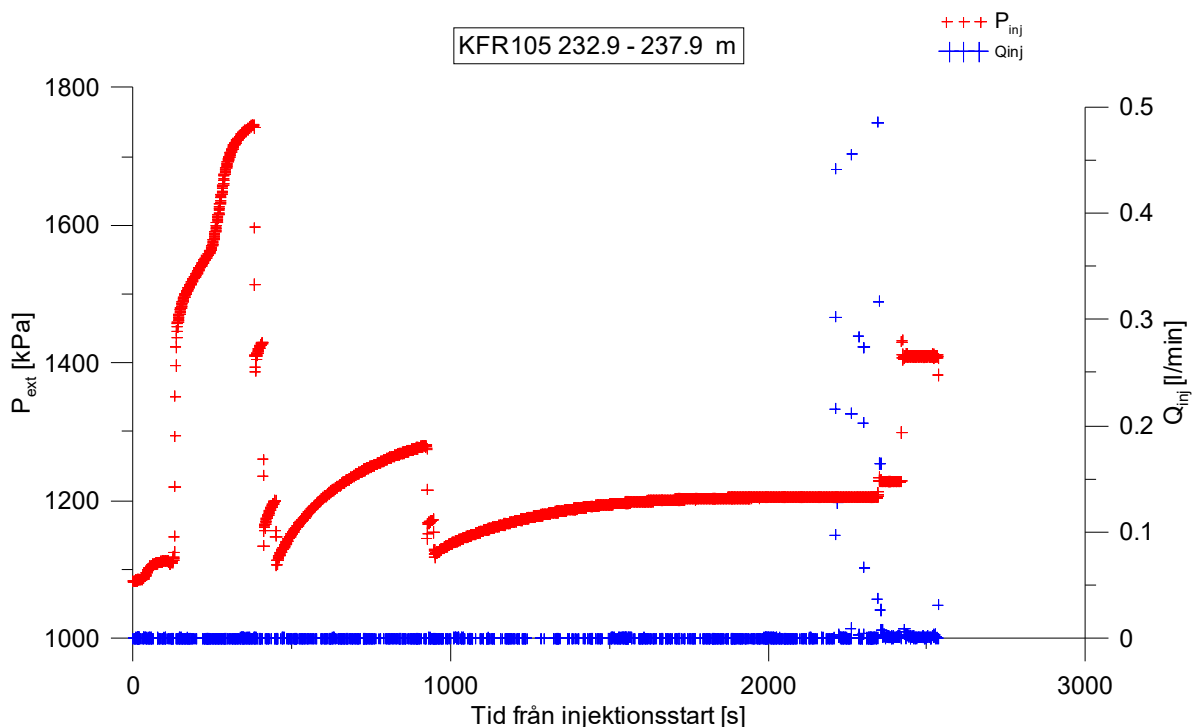


**Figure A3-105.** Linear plot of flow rate ( $Q$ ) and pressure ( $P$ ) versus time from the injection test in section 232.9-237.9 m in borehole KFR105.

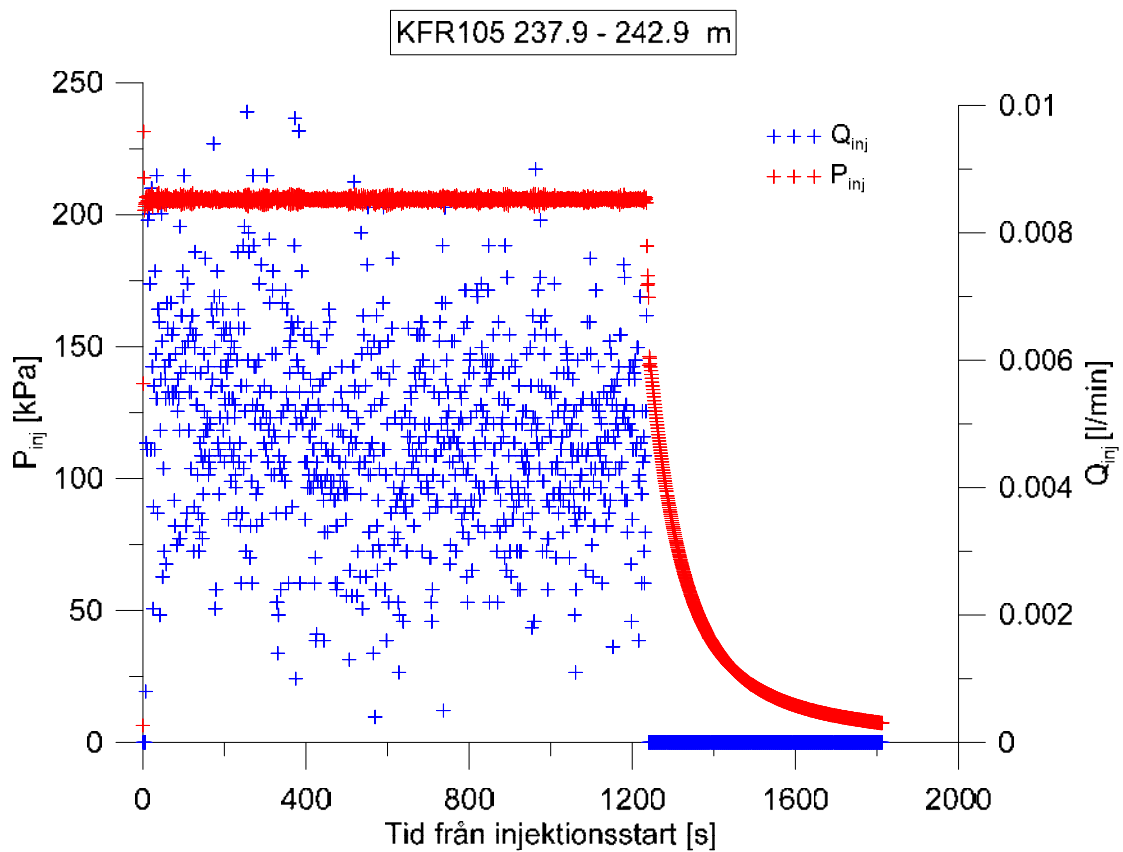


**Figure A3-106.** Linear plot of flow rate ( $Q$ ) and pressure ( $P$ ) versus time from the injection test in section 237.9-242.9 m in borehole KFR105.

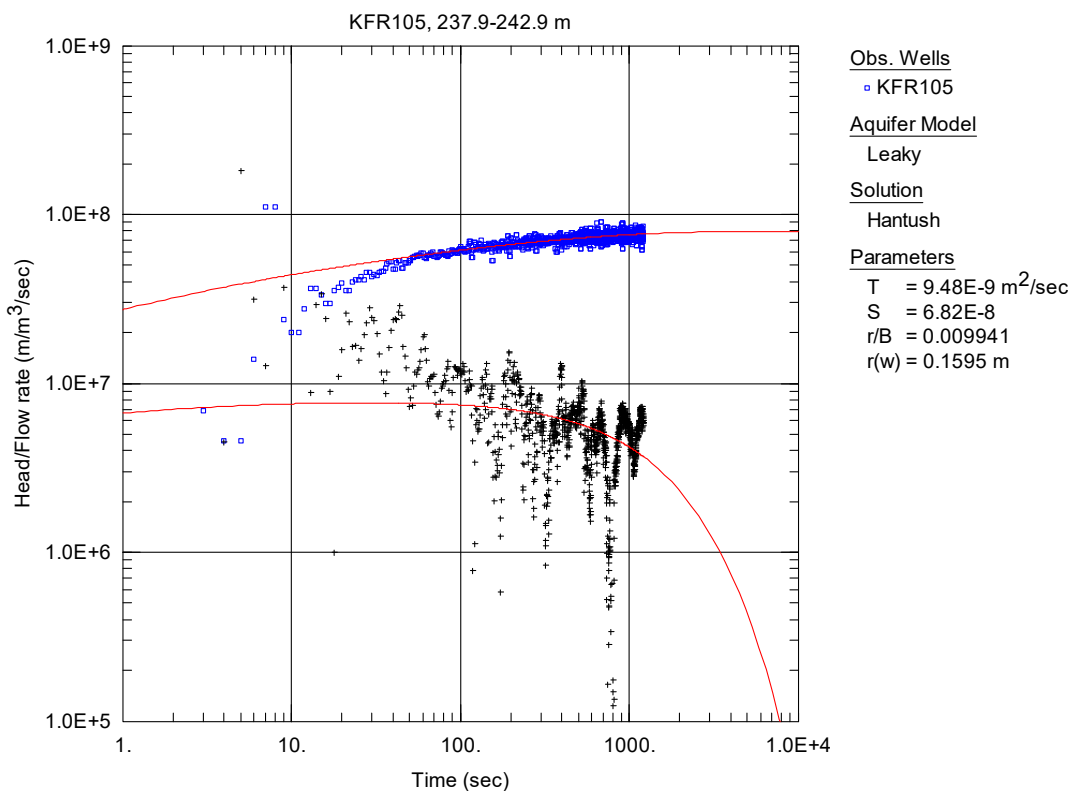


**Figure A3-107.** Log-log plot of head/flow rate (□) and derivative (+) versus time, from the injection test in section 237.9-242.9 m in KFR105.

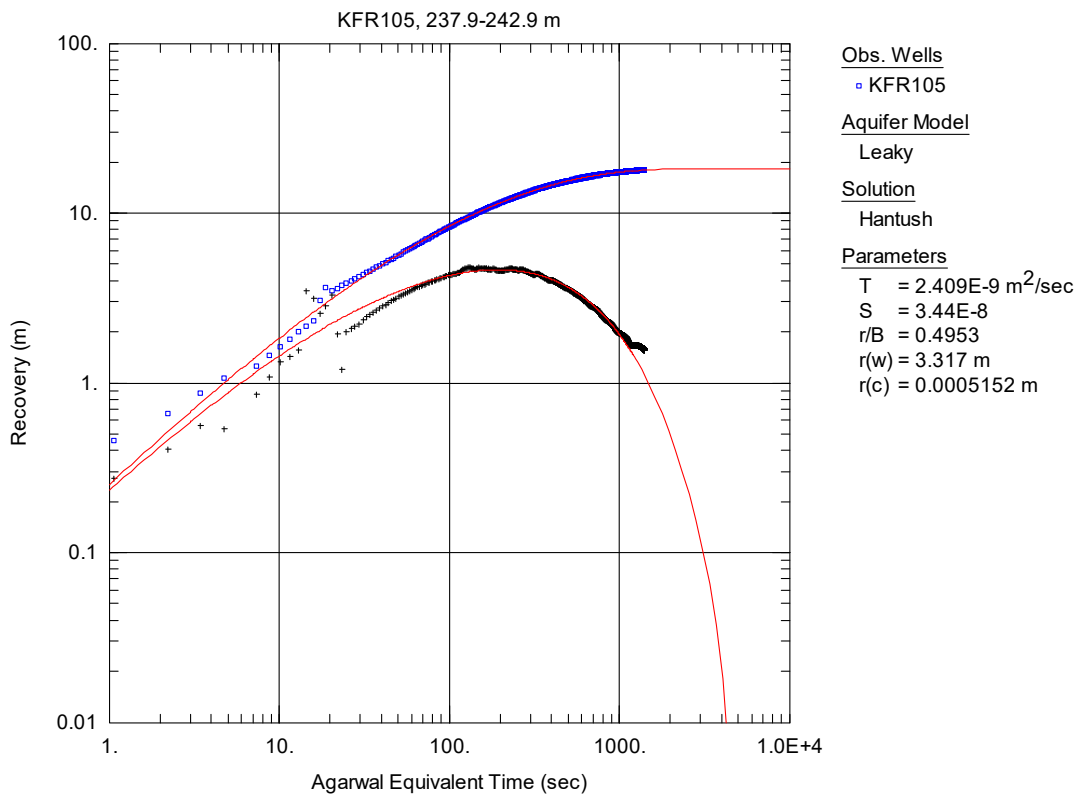


**Figure A3-108.** Log-log plot of recovery ( $\square$ ) and derivative (+) versus equivalent time, from the injection test in section 237.9-242.9 m in KFR105.

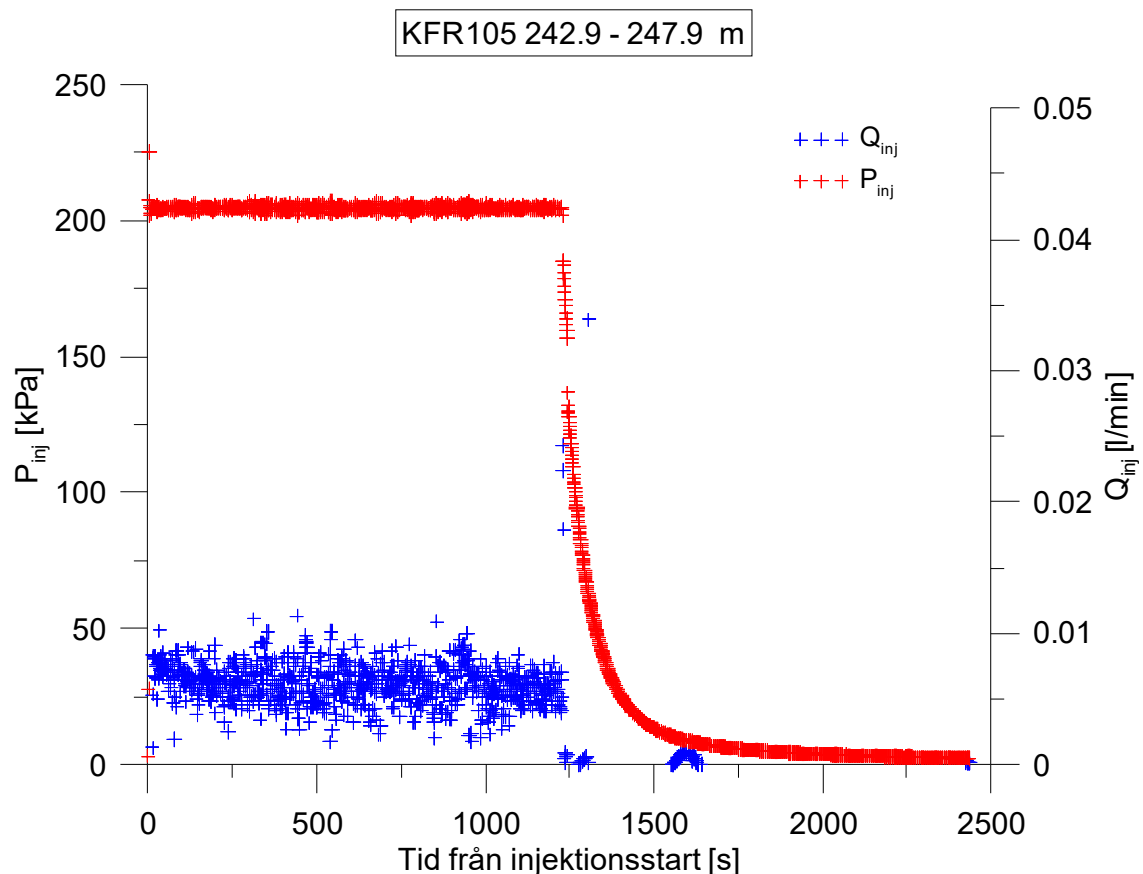


**Figure A3-109.** Linear plot of flow rate ( $Q$ ) and pressure ( $P$ ) versus time from the injection test in section 242.9-247.9 m in borehole KFR105.

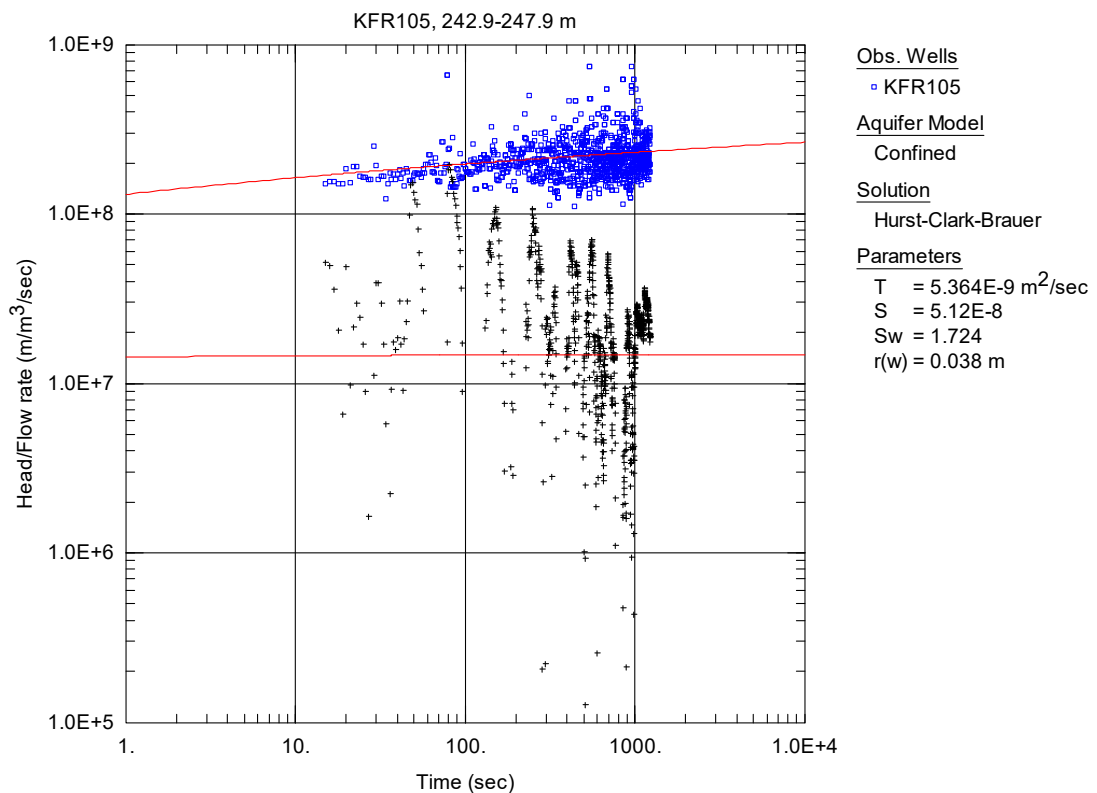


**Figure A3-110.** Log-log plot of head/flow rate (□) and derivative (+) versus time, from the injection test in section 242.9-247.9 m in KFR105.

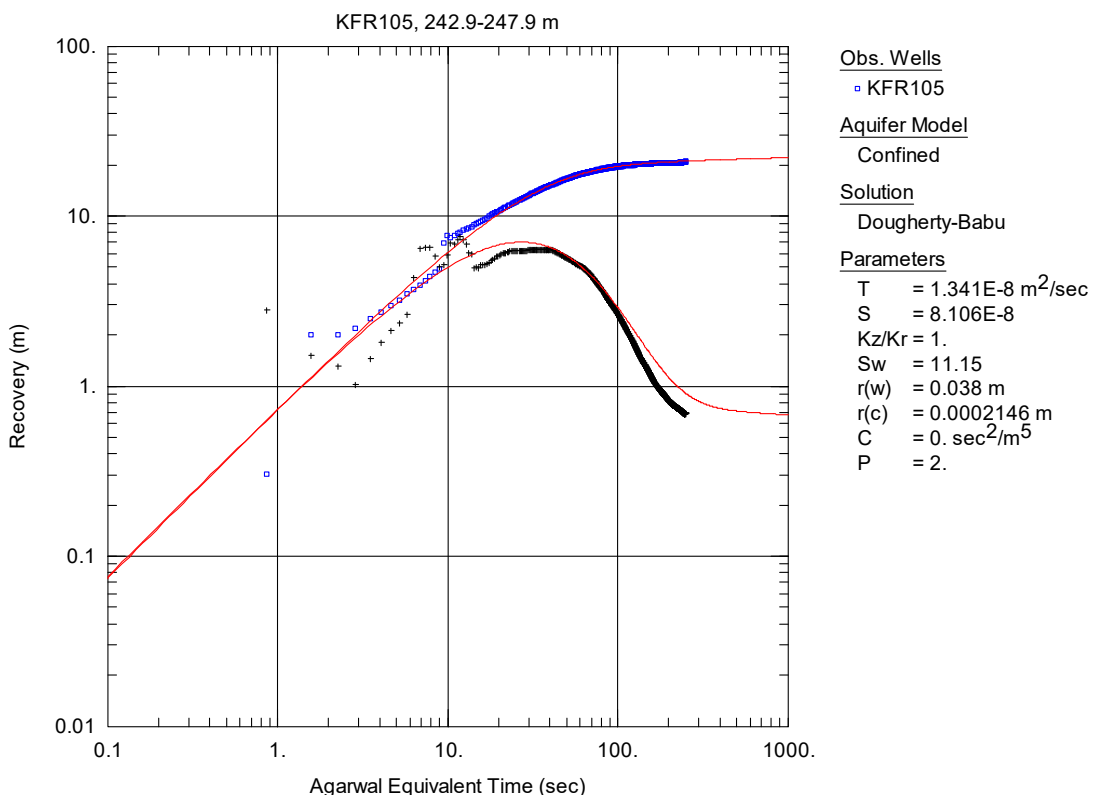


**Figure A3-111.** Log-log plot of recovery (□) and derivative (+) versus equivalent time, from the injection test in section 242.9-247.9 m in KFR105.

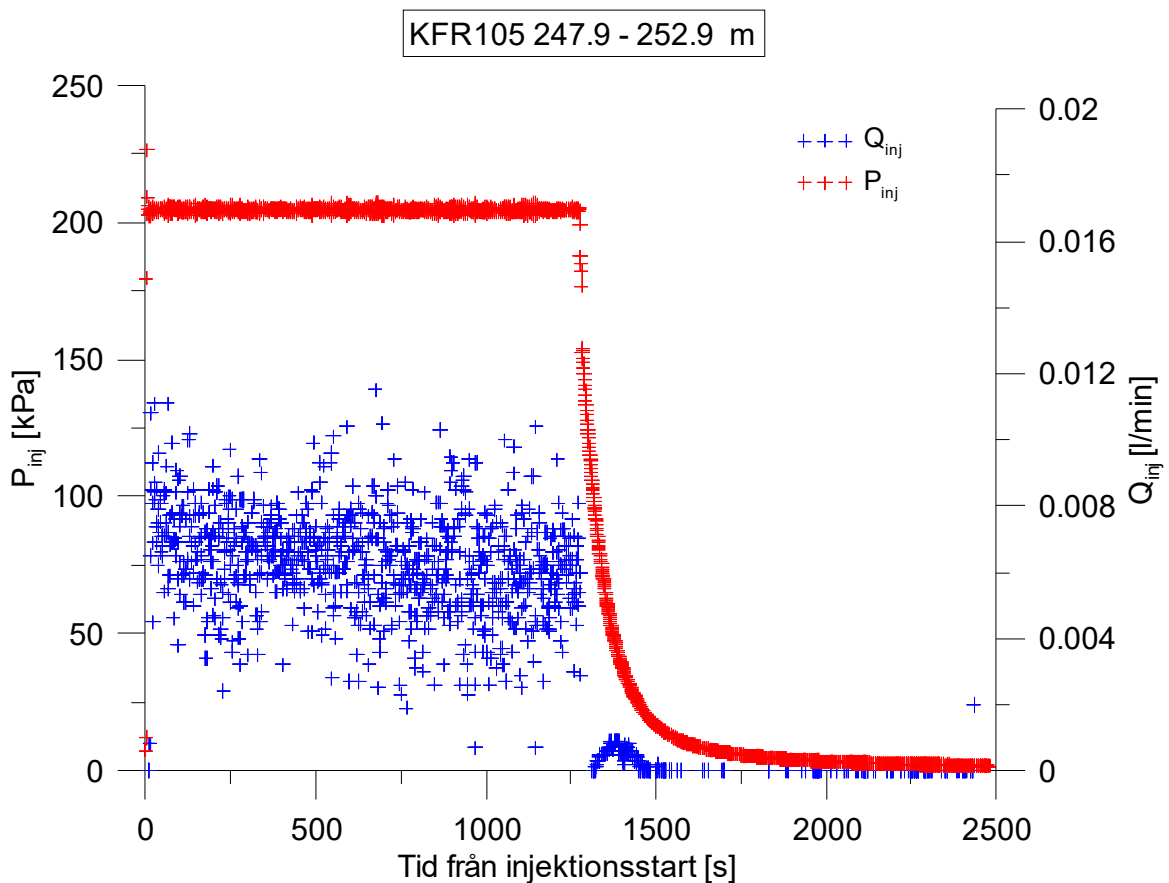


**Figure A3-112.** Linear plot of flow rate ( $Q$ ) and pressure ( $P$ ) versus time from the injection test in section 247.9-252.9 m in borehole KFR105.

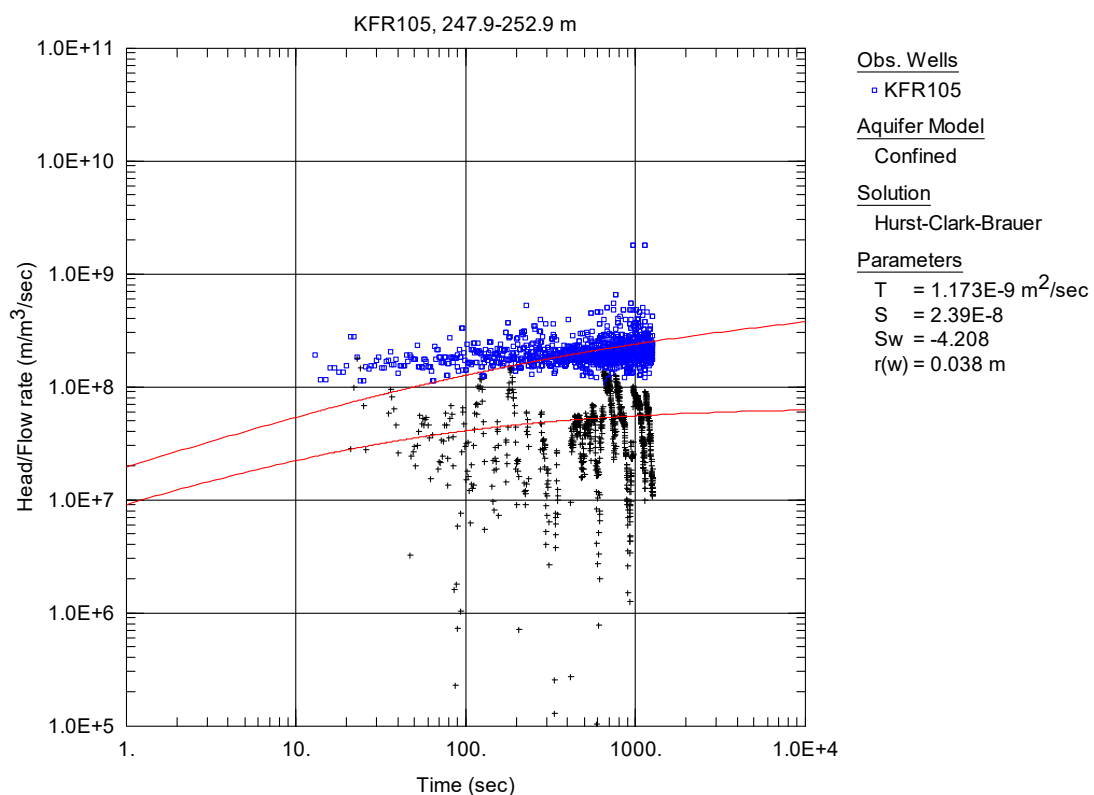


**Figure A3-113.** Log-log plot of head/flow rate (□) and derivative (+) versus time, from the injection test in section 247.9-252.9 m in KFR105.

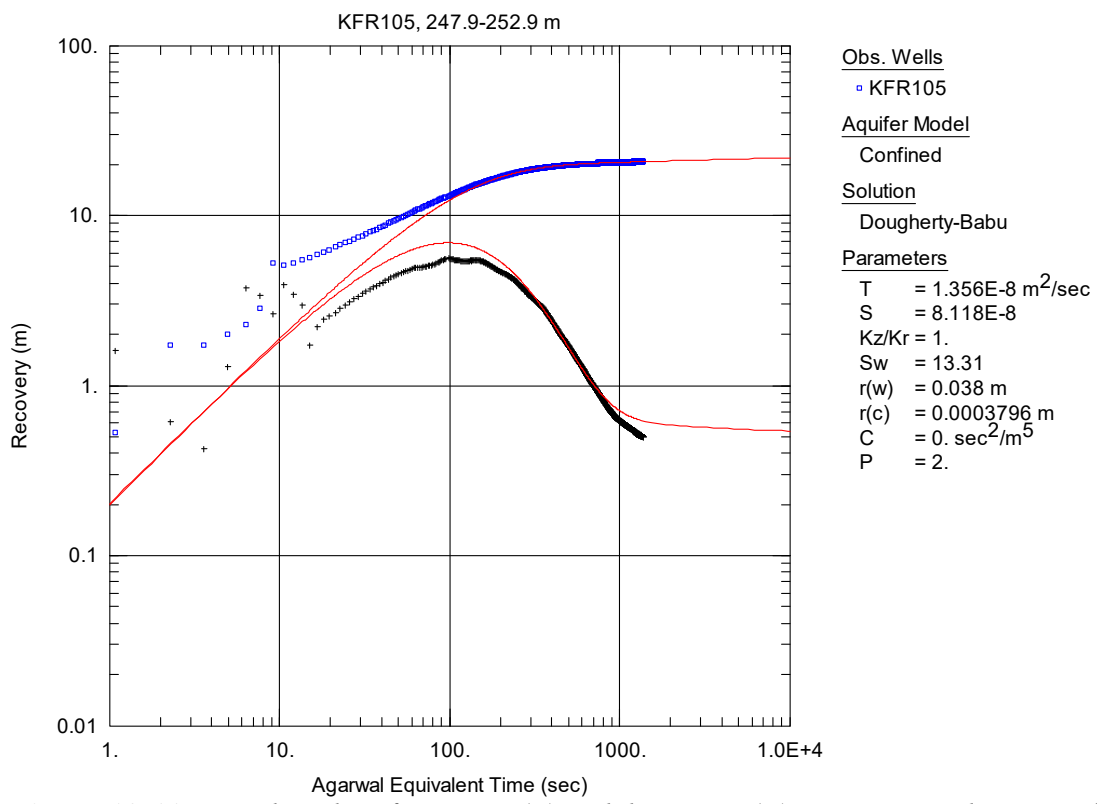


**Figure A3-114.** Log-log plot of recovery (□) and derivative (+) versus equivalent time, from the injection test in section 247.9-252.9 m in KFR105.

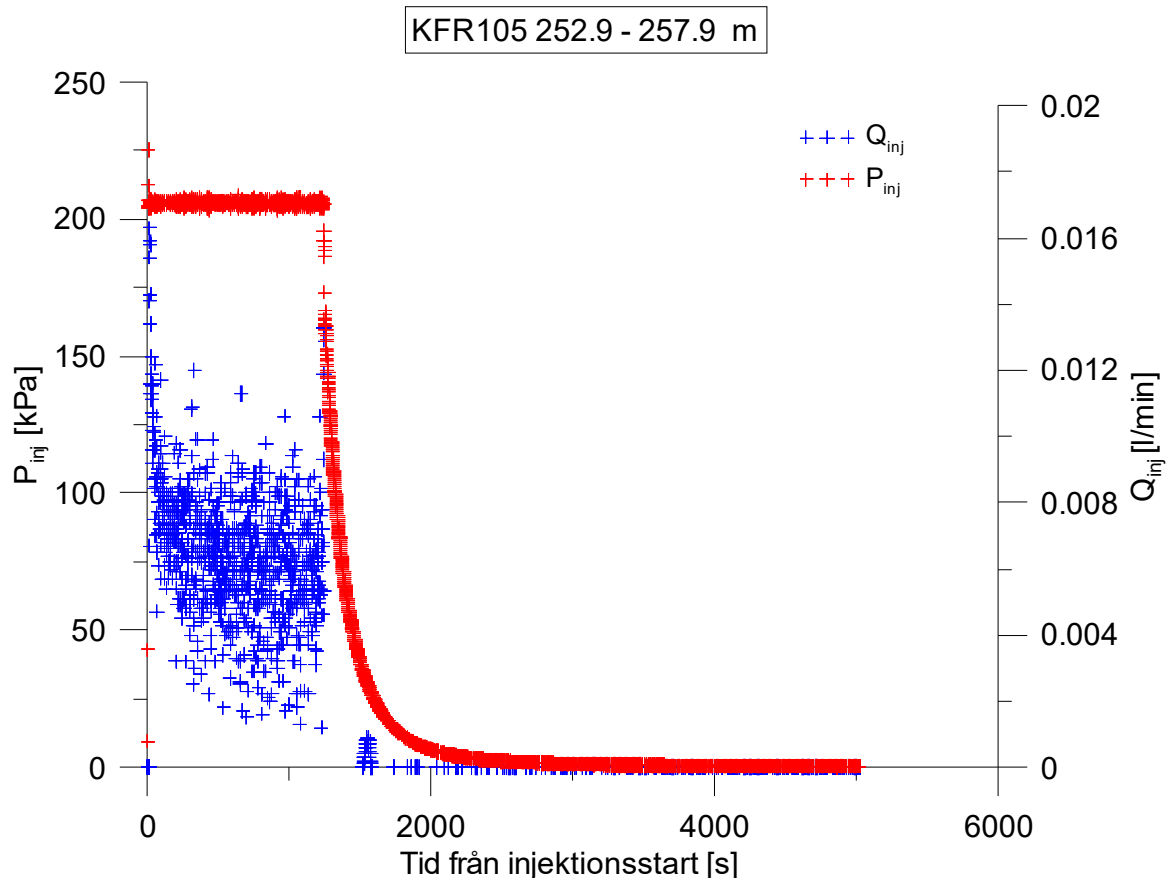


**Figure A3-115.** Linear plot of flow rate ( $Q$ ) and pressure ( $P$ ) versus time from the injection test in section 252.9-257.9 m in borehole KFR105.

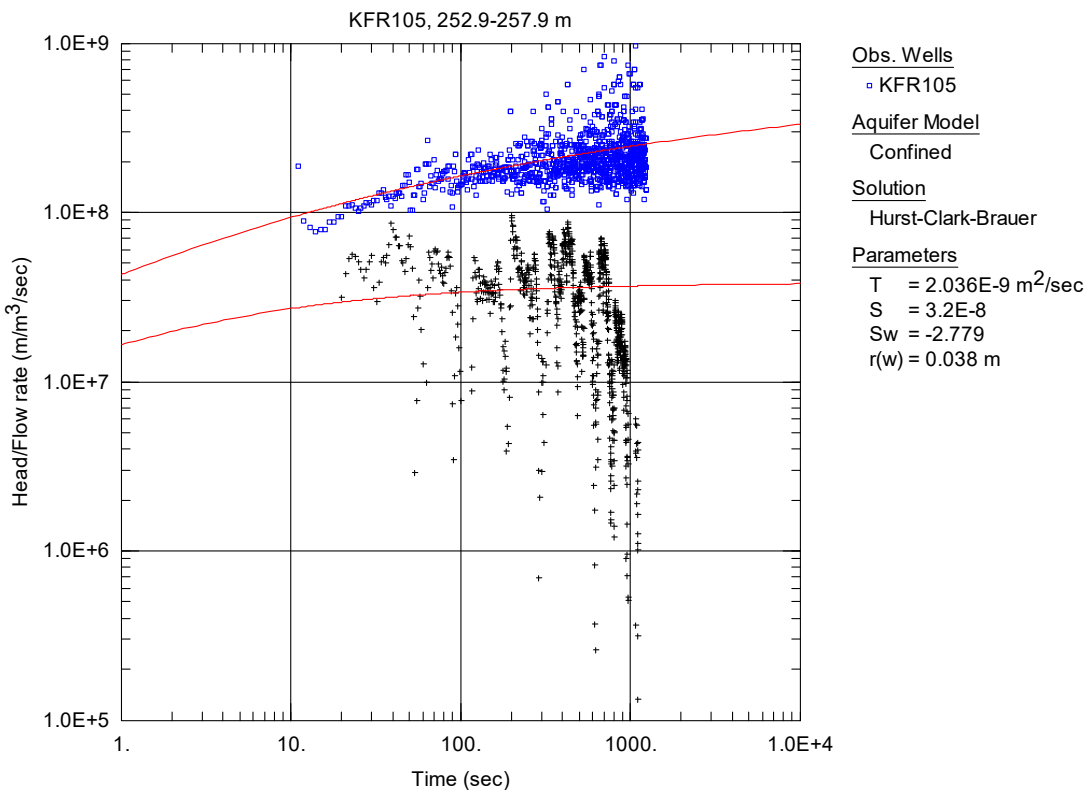


**Figure A3-116.** Log-log plot of head/flow rate (□) and derivative (+) versus time, from the injection test in section 252.9-257.9 m in KFR105.

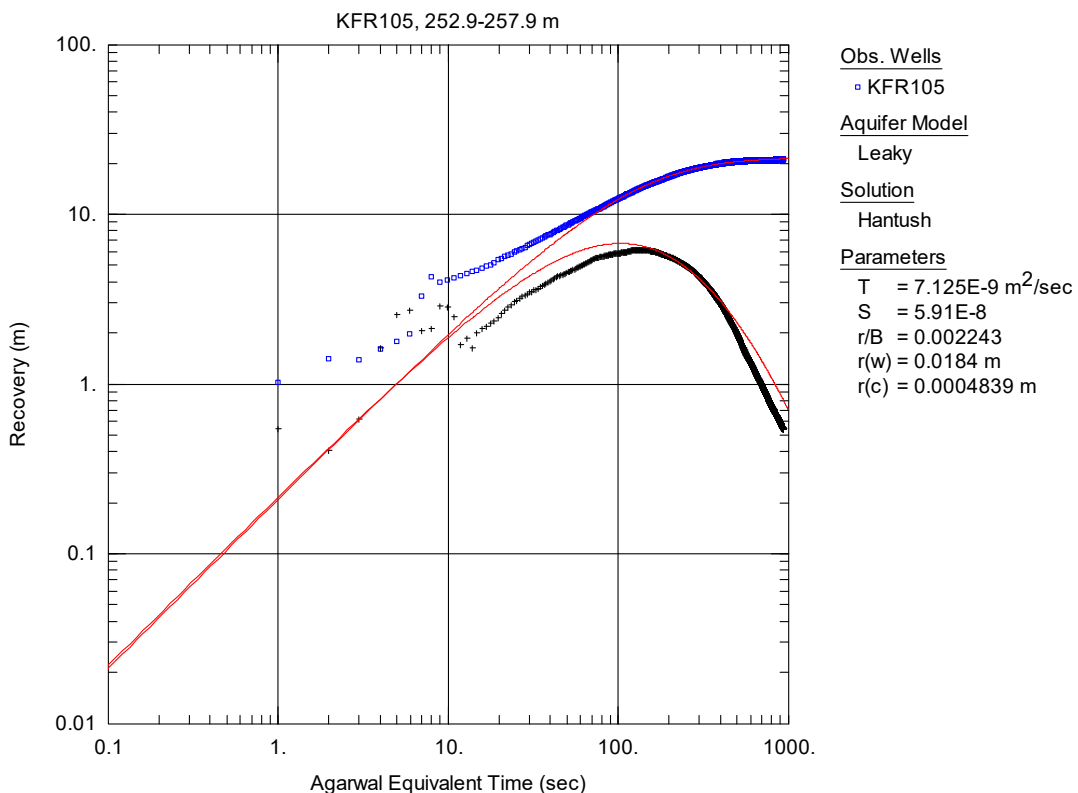


**Figure A3-117.** Log-log plot of recovery (□) and derivative (+) versus equivalent time, from the injection test in section 252.9-257.9 m in KFR105.

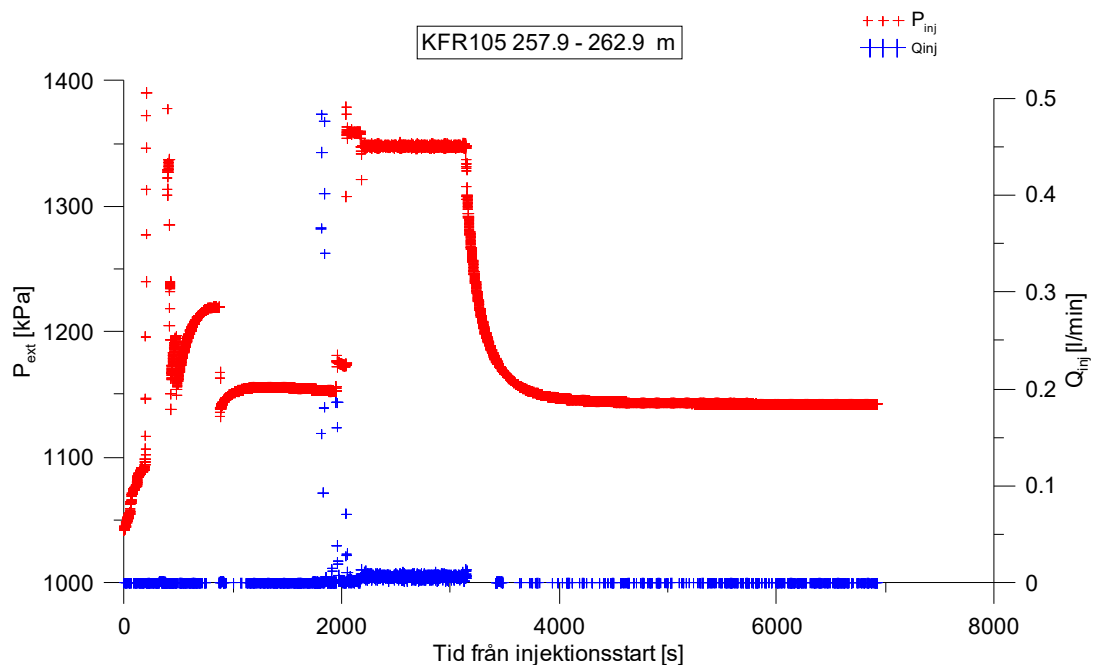


**Figure A3-118.** Linear plot of flow rate ( $Q$ ) and pressure ( $P$ ) versus time from the injection test in section 257.9-262.9 m in borehole KFR105.

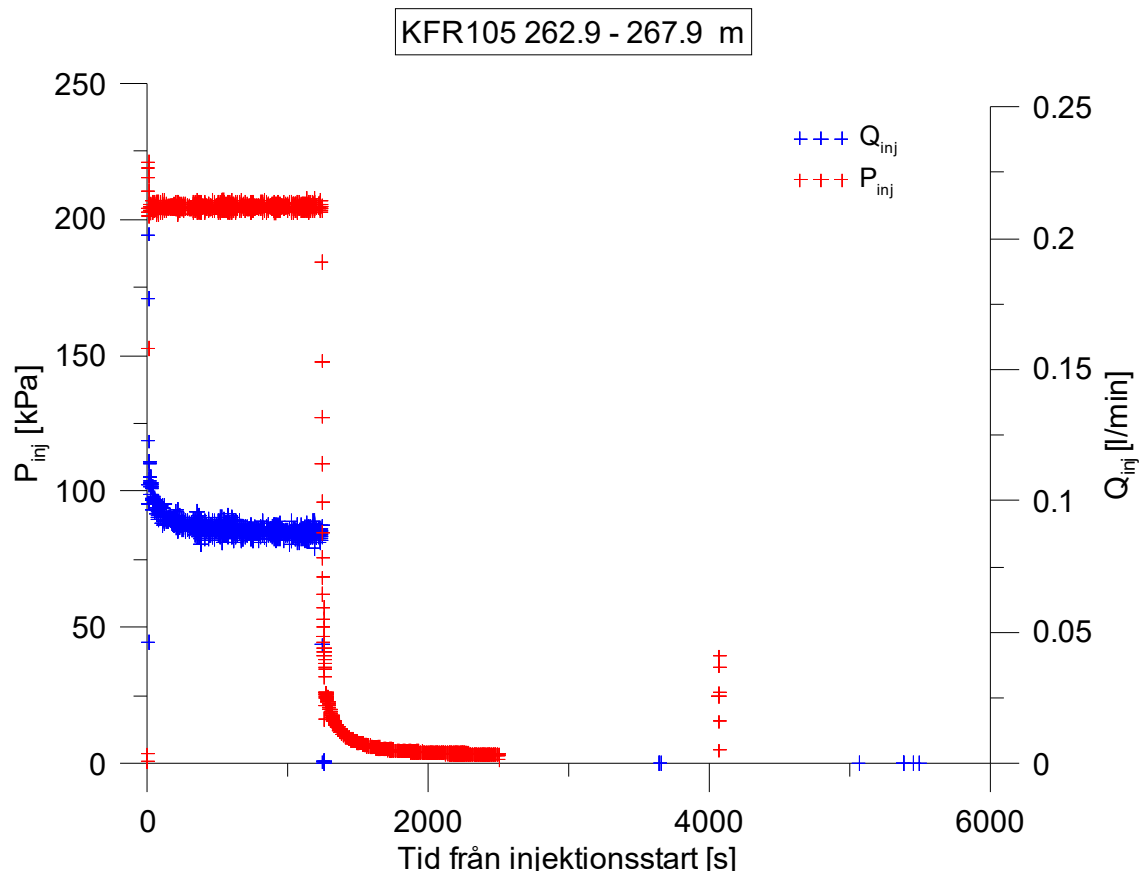


**Figure A3-119.** Linear plot of flow rate ( $Q$ ) and pressure ( $P$ ) versus time from the injection test in section 262.9-267.9 m in borehole KFR105.

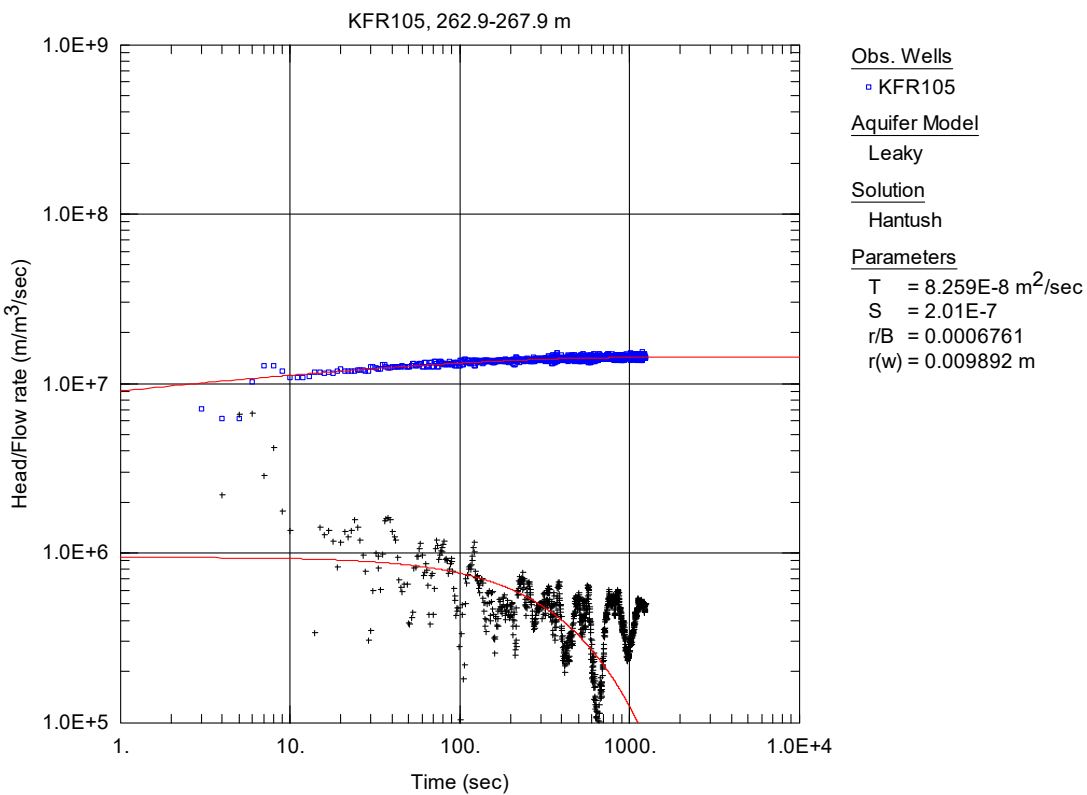


**Figure A3-120.** Log-log plot of head/flow rate (□) and derivative (+) versus time, from the injection test in section 262.9-267.9 m in KFR105.

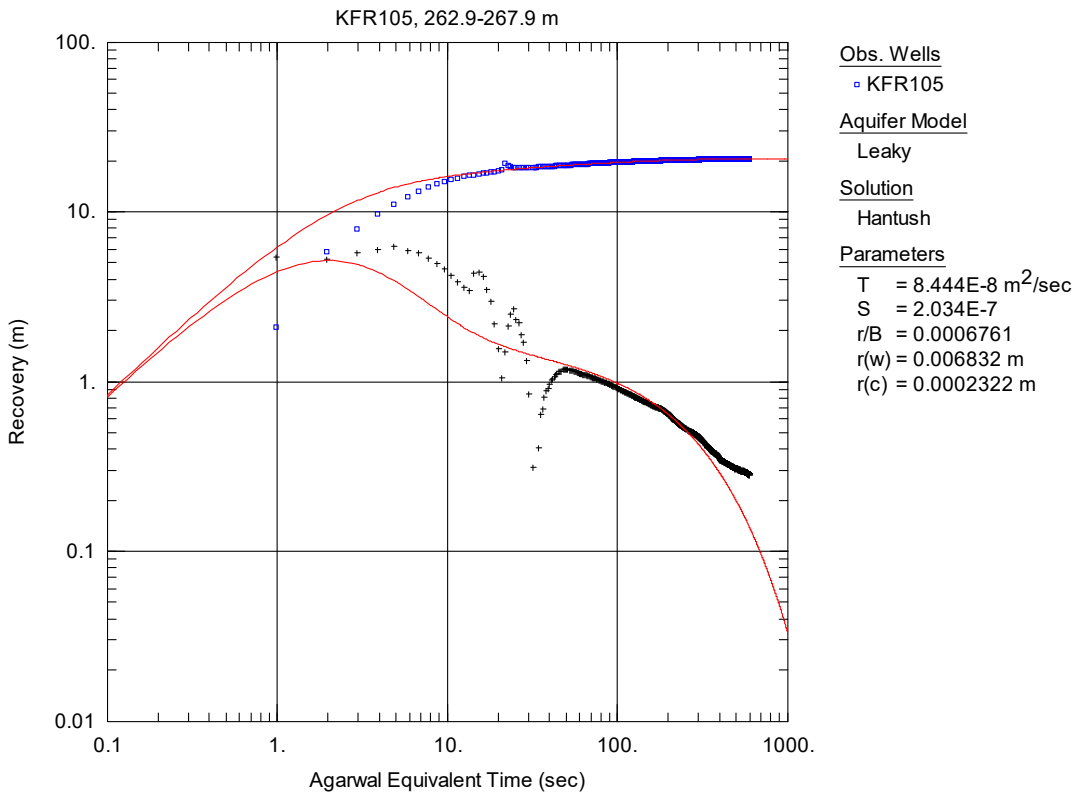


**Figure A3-121.** Log-log plot of recovery (□) and derivative (+) versus equivalent time, from the injection test in section 262.9-267.9 m in KFR105.

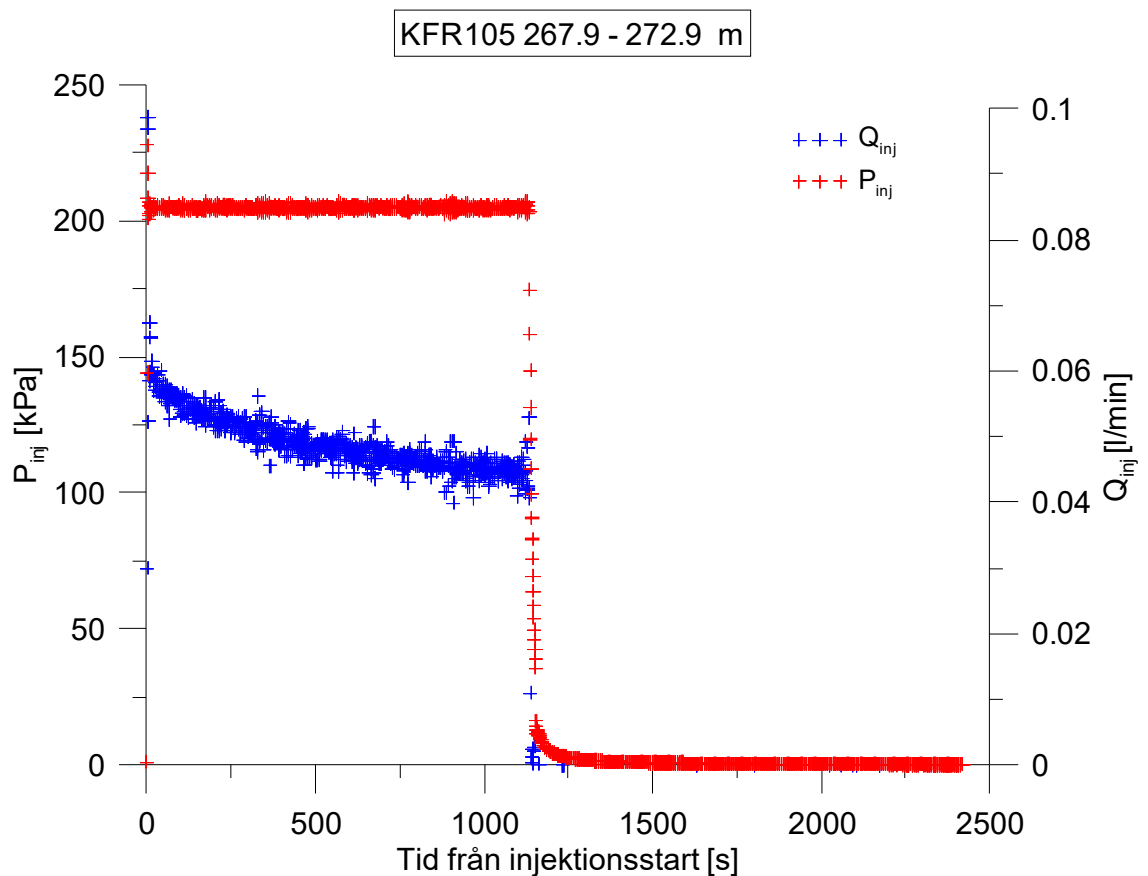


**Figure A3-122.** Linear plot of flow rate ( $Q$ ) and pressure ( $P$ ) versus time from the injection test in section 267.9-272.9 m in borehole KFR105.

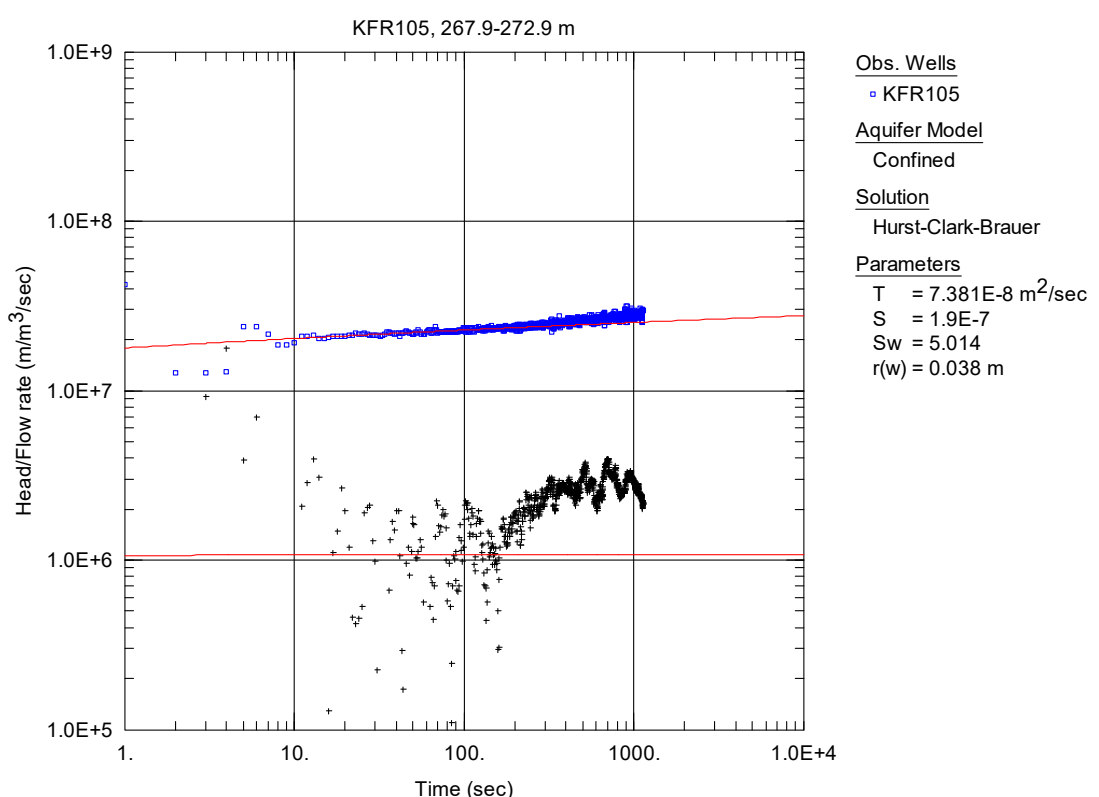


**Figure A3-123.** Log-log plot of head/flow rate ( $\square$ ) and derivative (+) versus time, from the injection test in section 267.9-272.9 m in KFR105.

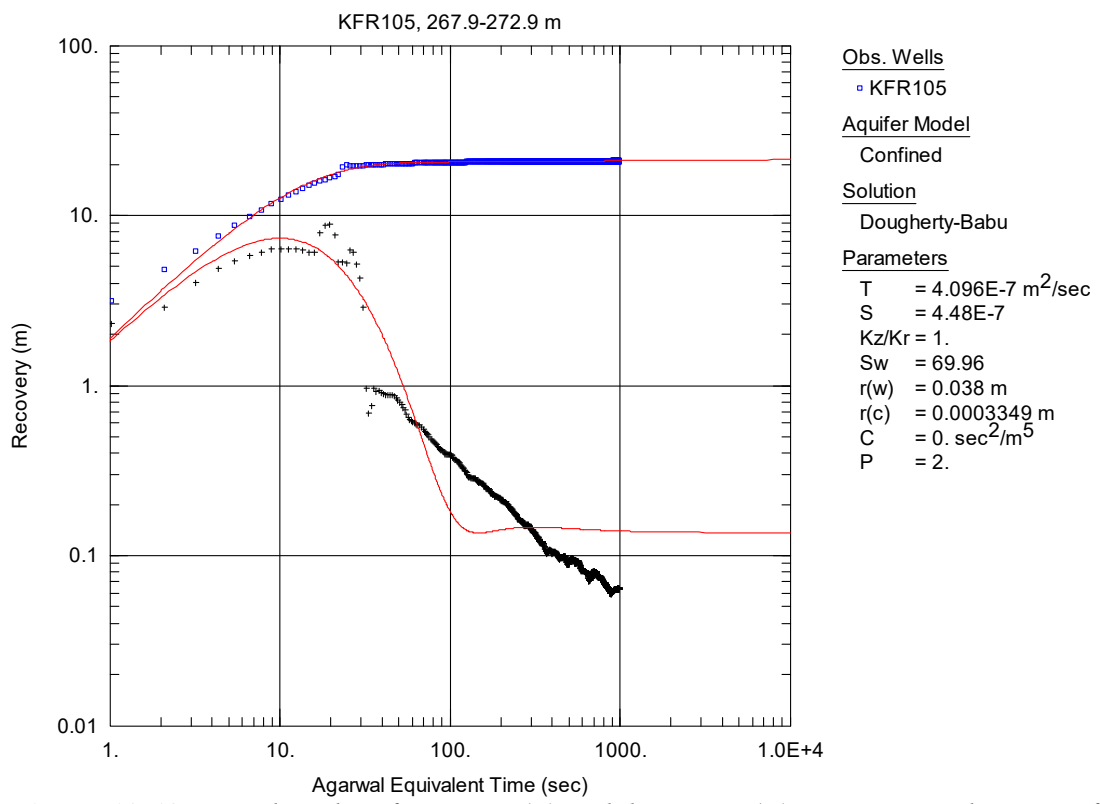


**Figure A3-124.** Log-log plot of recovery (□) and derivative (+) versus equivalent time, from the injection test in section 267.9-272.9 m in KFR105.

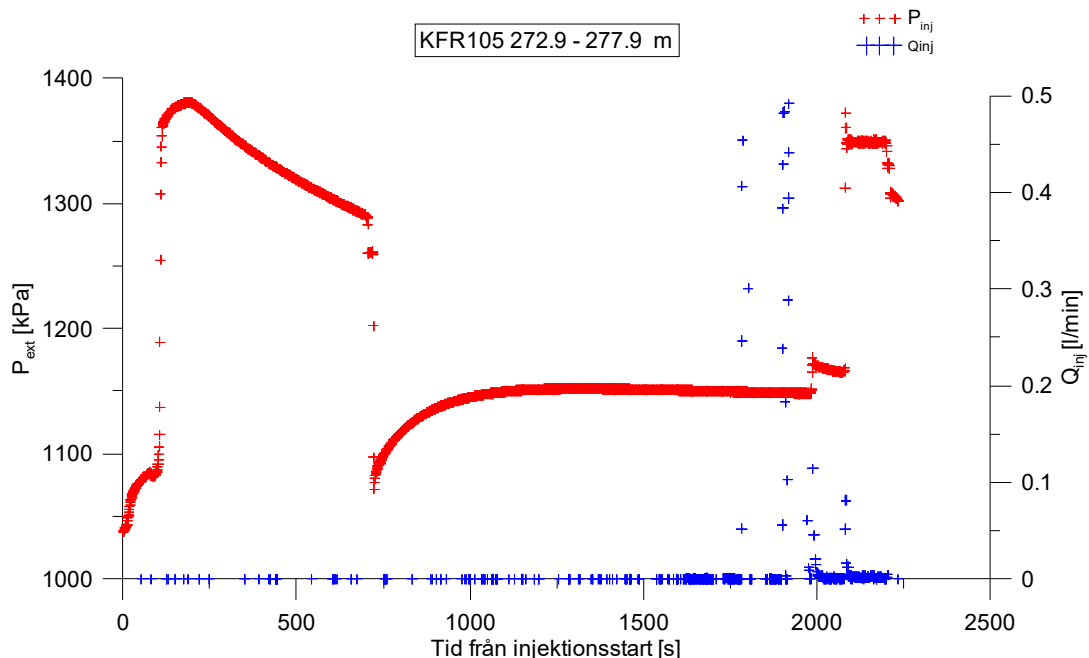


**Figure A3-125.** Linear plot of flow rate ( $Q$ ) and pressure ( $P$ ) versus time from the injection test in section 272.9-277.9 m in borehole KFR105.

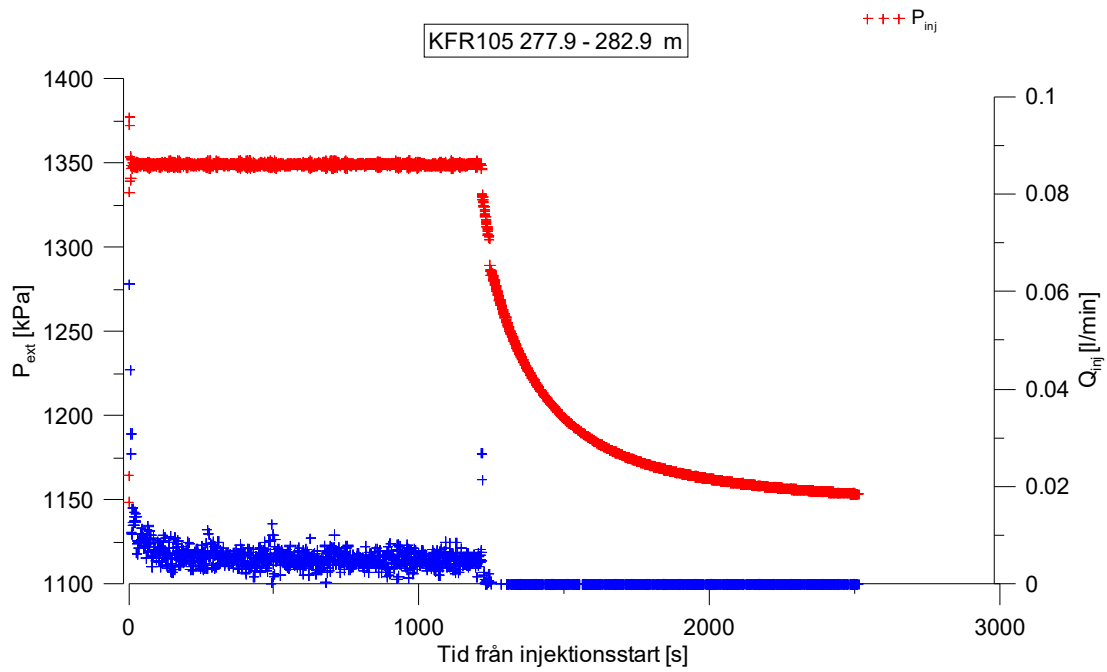


**Figure A3-126.** Linear plot of flow rate ( $Q$ ) and pressure ( $P$ ) versus time from the injection test in section 277.9-282.9 m in borehole KFR105.

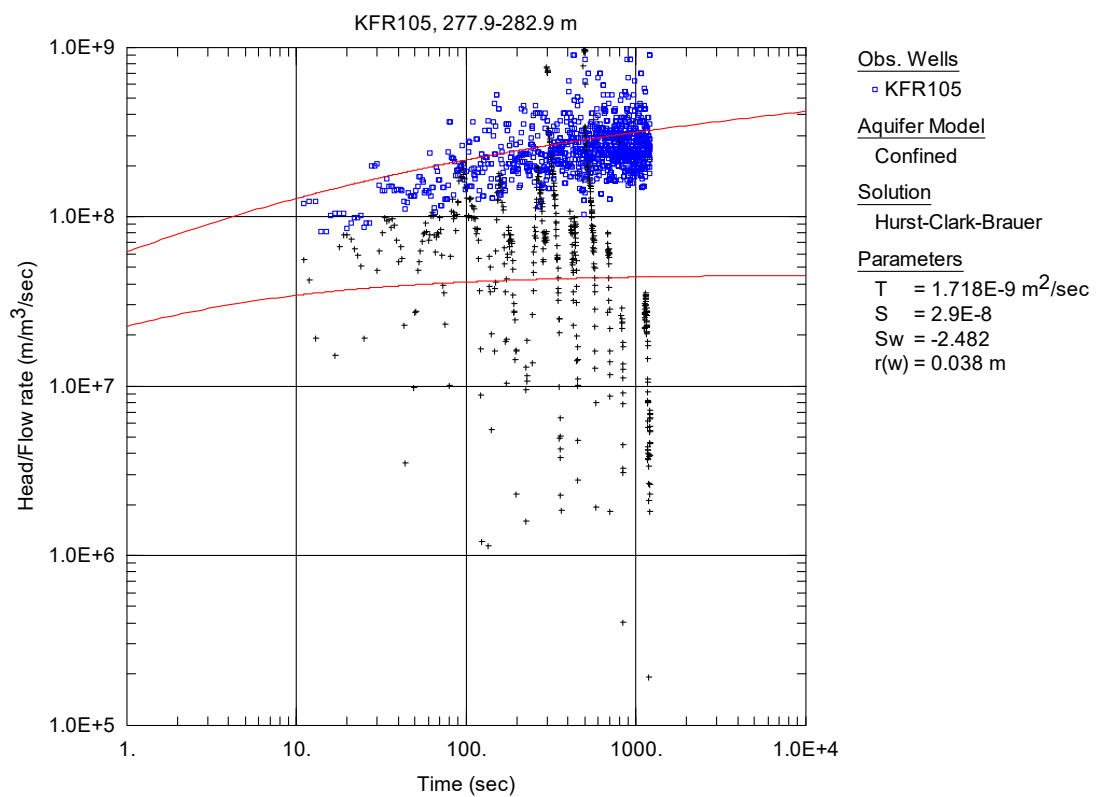


**Figure A3-127.** Log-log plot of head/flow rate ( $\square$ ) and derivative (+) versus time, from the injection test in section 277.9-282.9 m in KFR105.

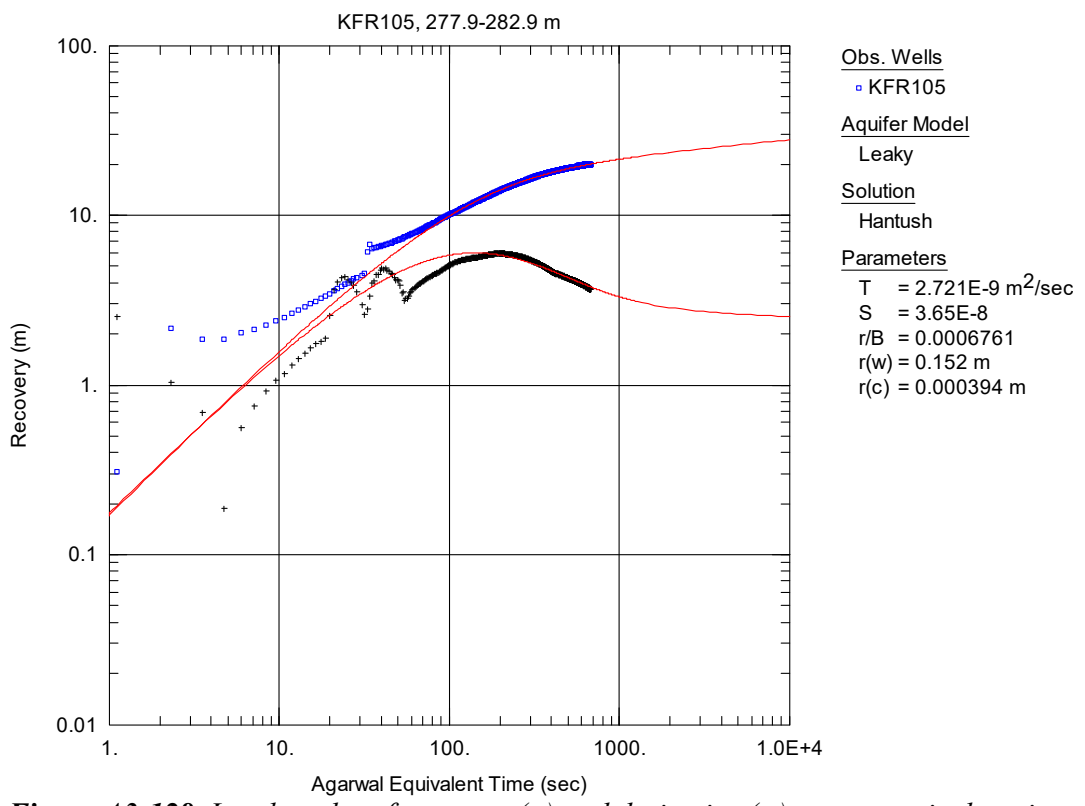


**Figure A3-128.** Log-log plot of recovery (□) and derivative (+) versus equivalent time, from the injection test in section 267.9-272.9 m in KFR105.

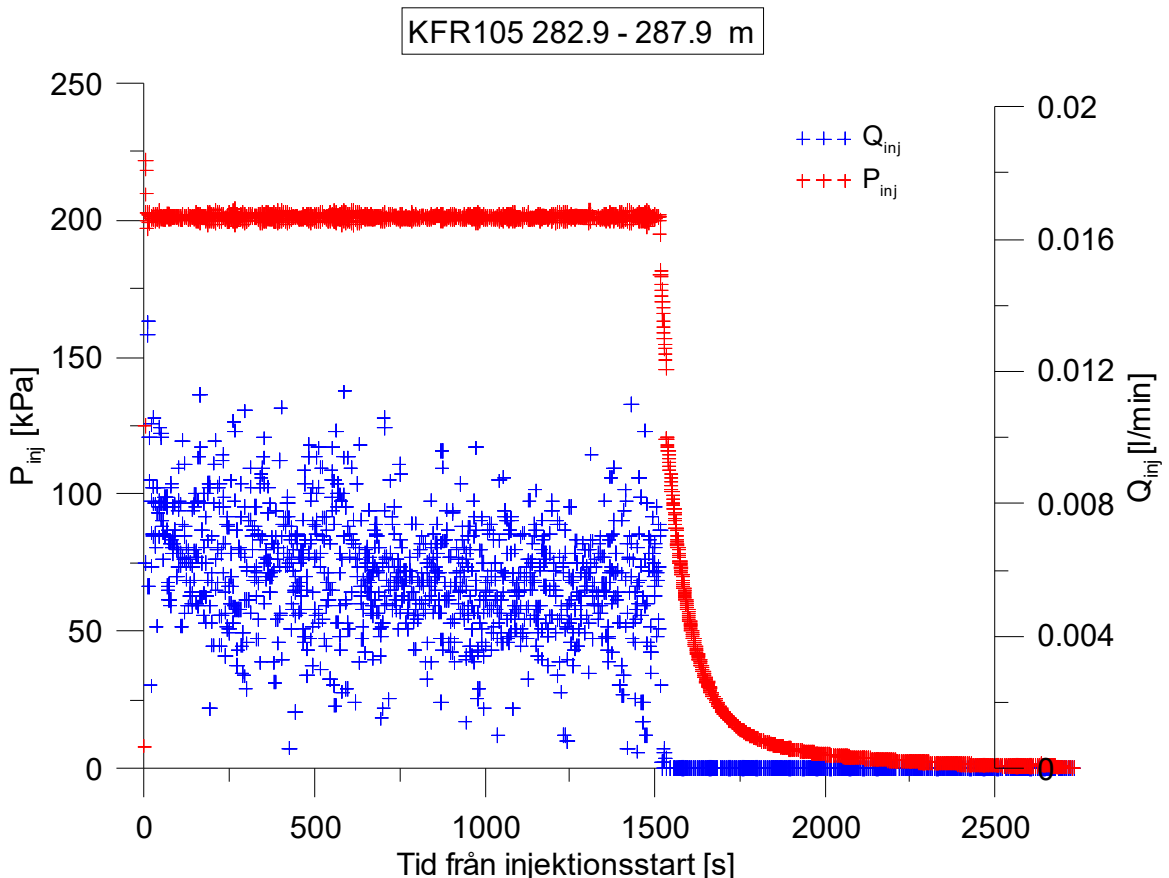


**Figure A3-129.** Linear plot of flow rate ( $Q$ ) and pressure ( $P$ ) versus time from the injection test in section 282.9-287.9 m in borehole KFR105.

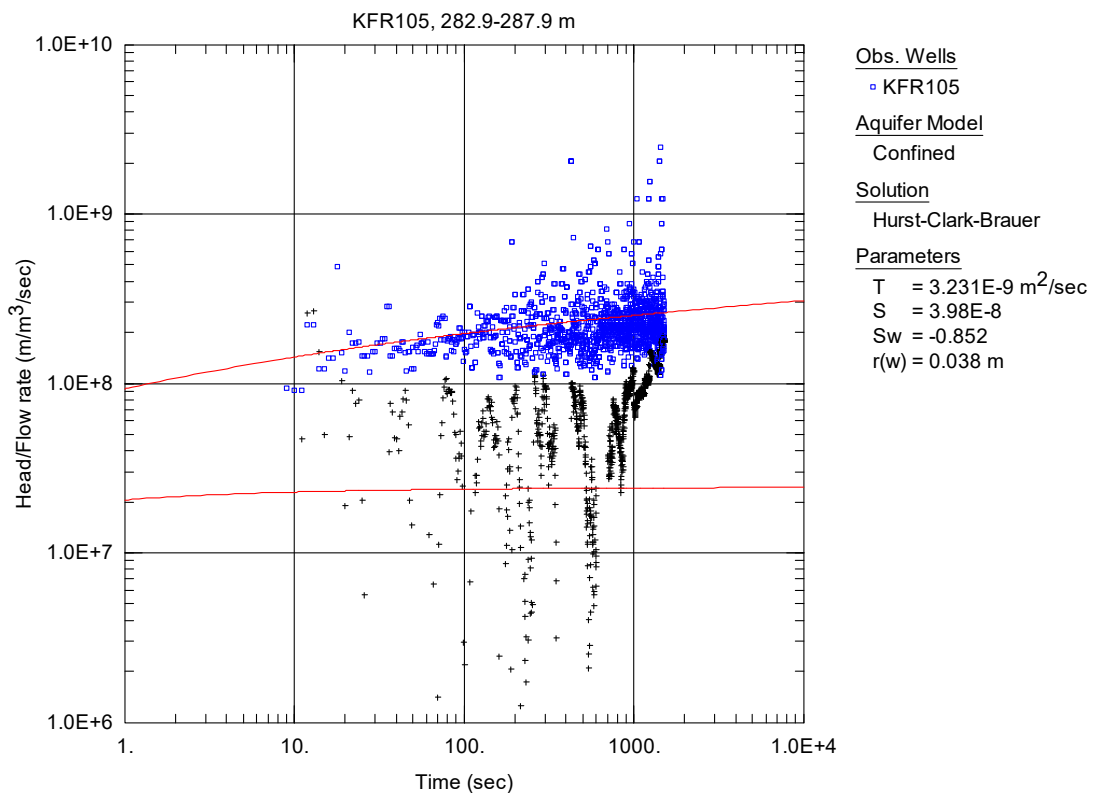


**Figure A3-130.** Log-log plot of head/flow rate (□) and derivative (+) versus time, from the injection test in section 282.9-287.9 m in KFR105.

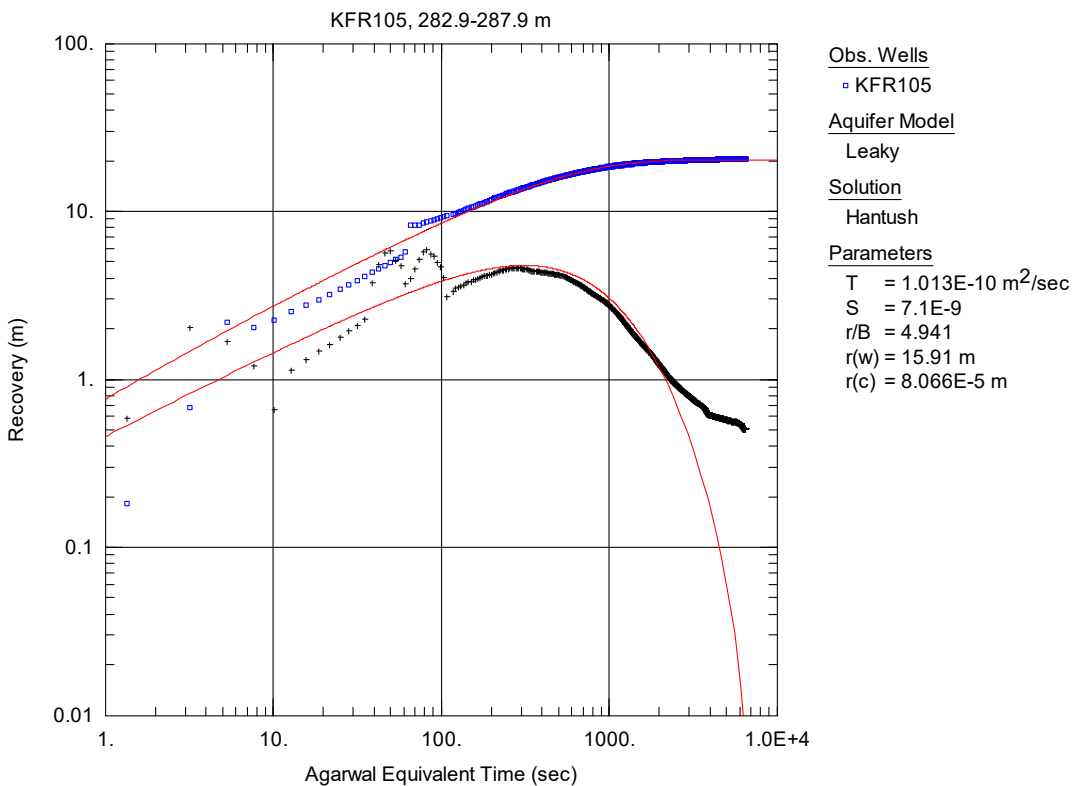


**Figure A3-131.** Log-log plot of recovery (□) and derivative (+) versus equivalent time, from the injection test in section 282.9-287.9 m in KFR105.

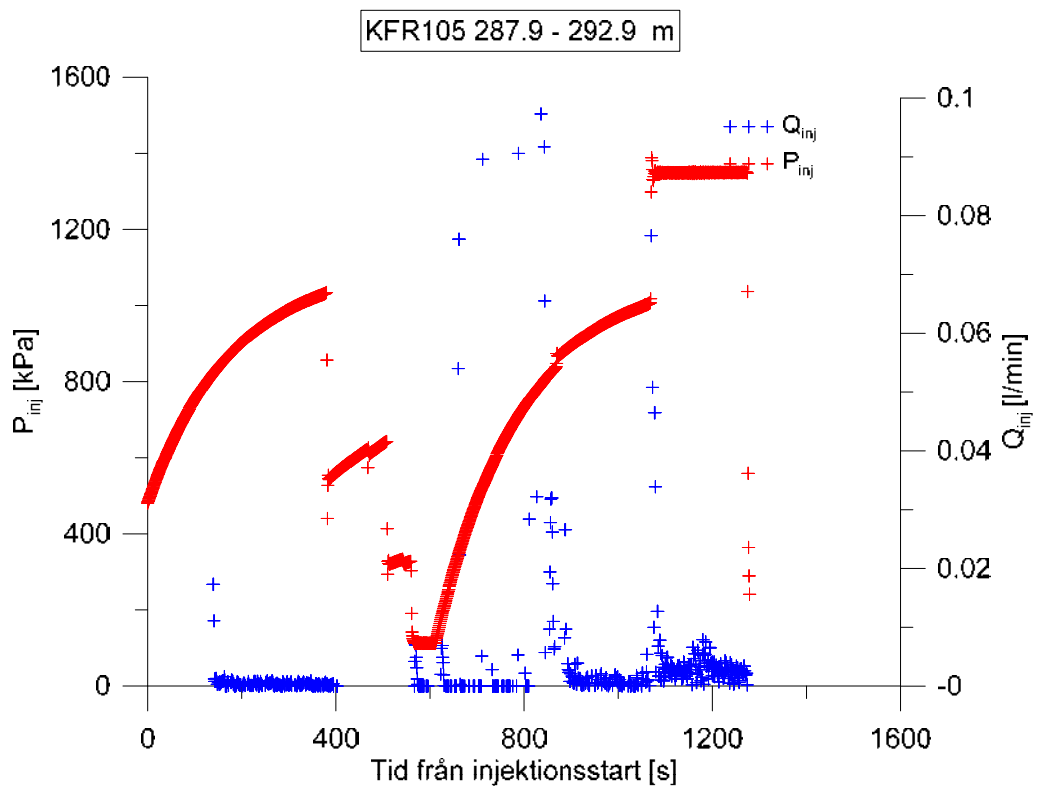


**Figure A3-132.** Linear plot of flow rate ( $Q$ ) and pressure ( $P$ ) versus time from the injection test in section 287.9-292.9 m in borehole KFR105.

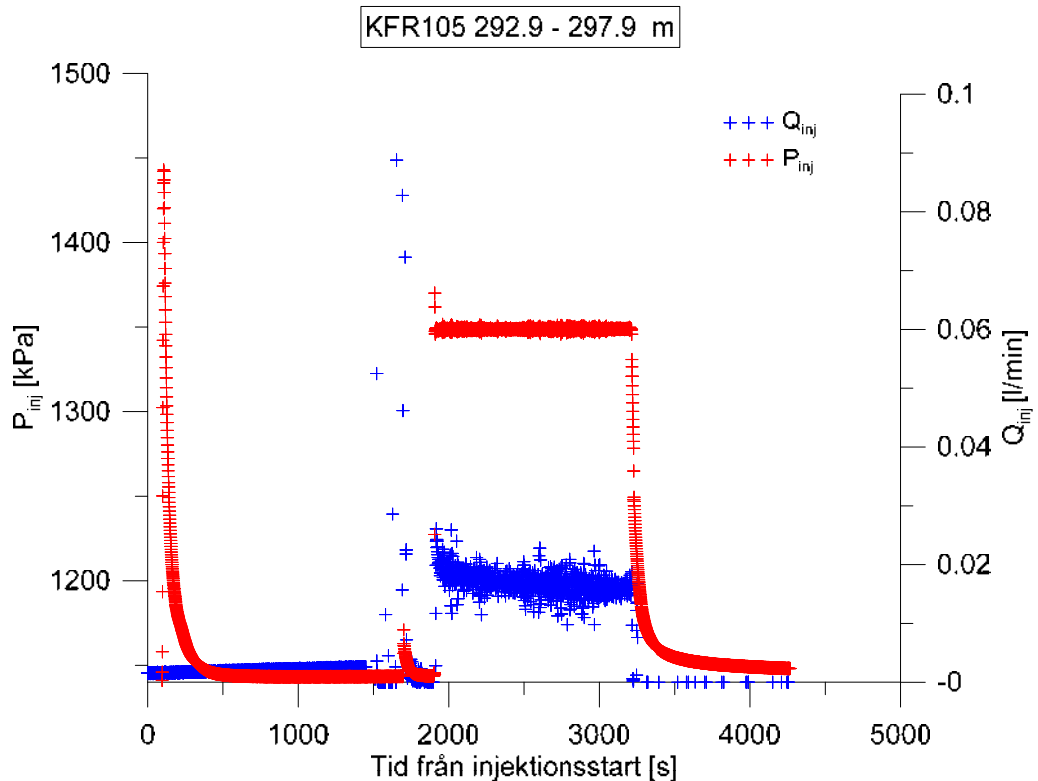


**Figure A3-133.** Linear plot of flow rate ( $Q$ ) and pressure ( $P$ ) versus time from the injection test in section 292.9-297.9 m in borehole KFR105.

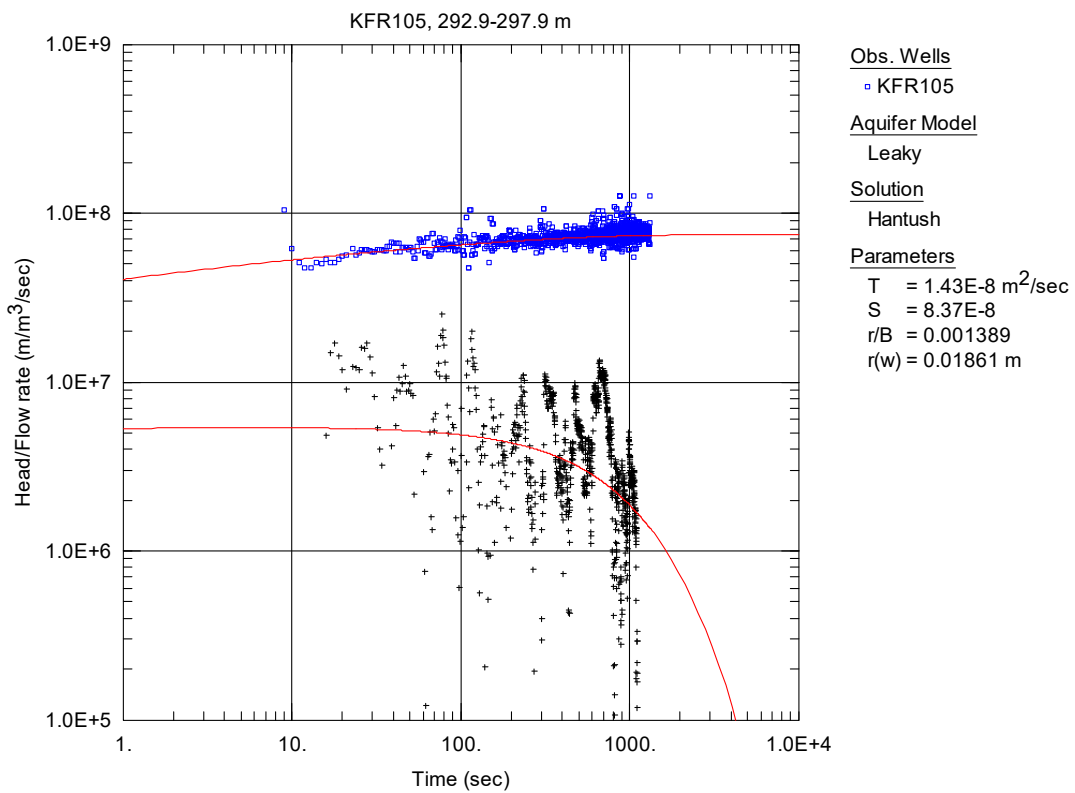


**Figure A3-134.** Log-log plot of head/flow rate (□) and derivative (+) versus time, from the injection test in section 292.9-297.9 m in KFR105.

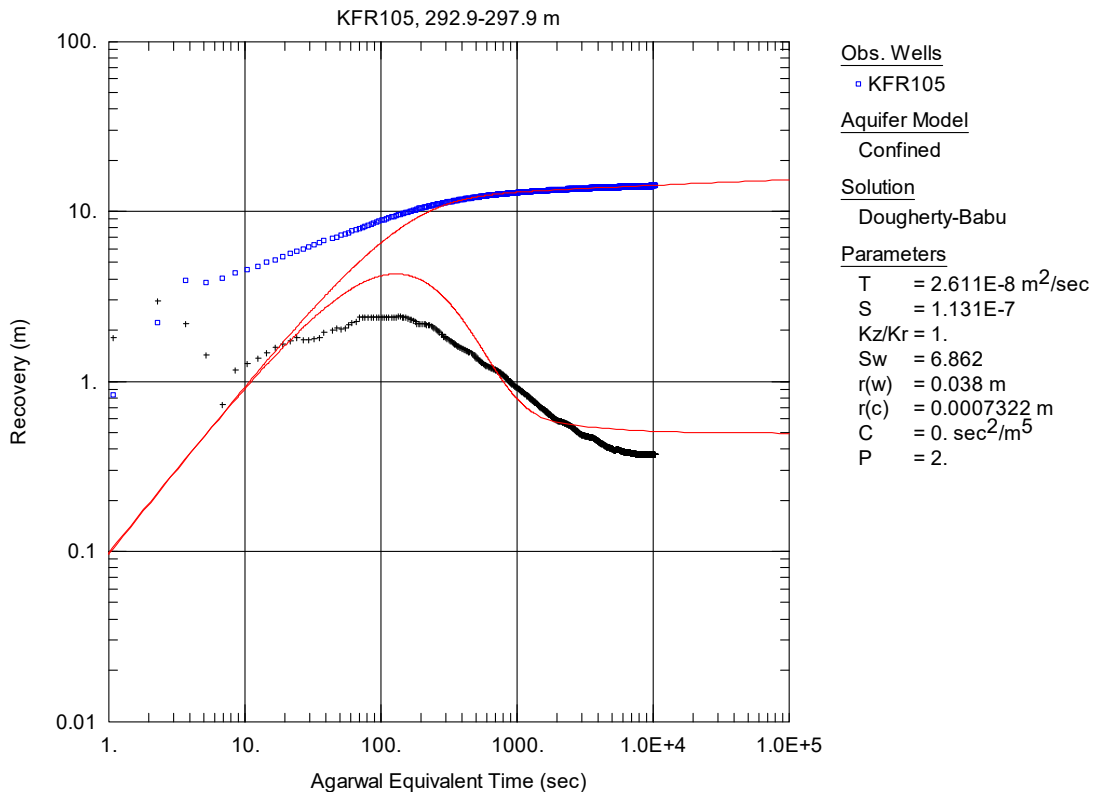


**Figure A3-135.** Log-log plot of recovery (□) and derivative (+) versus equivalent time, from the injection test in section 292.9-297.9 m in KFR105.

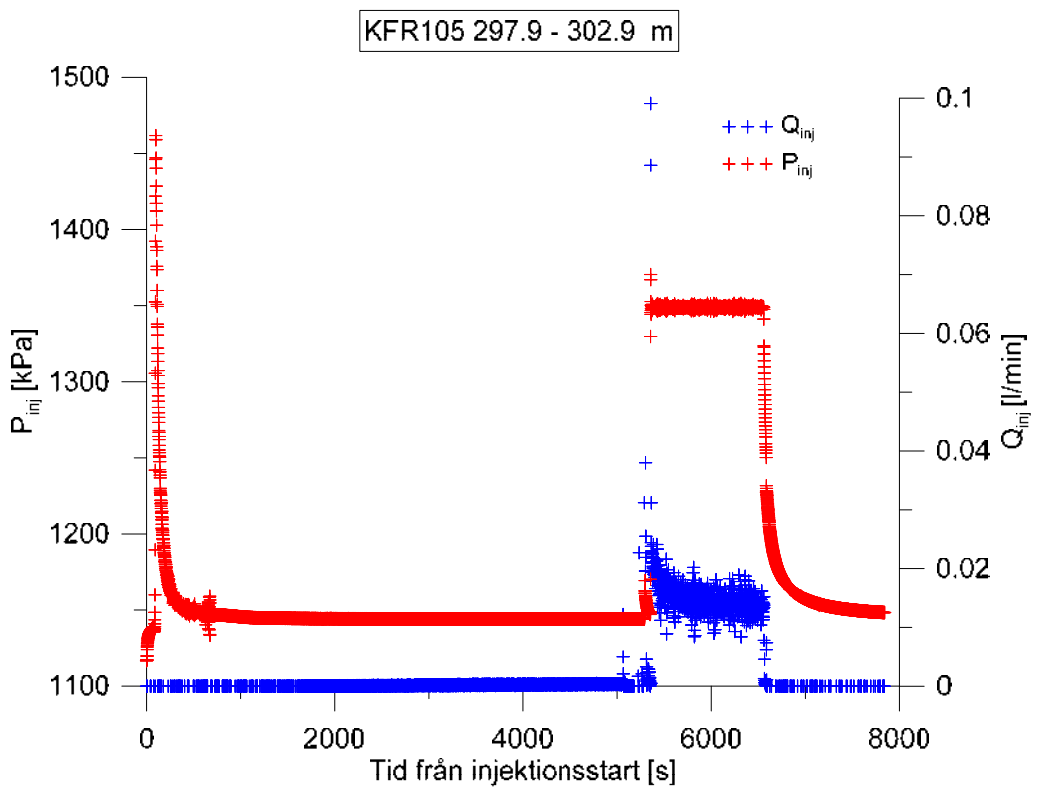


**Figure A3-136.** Linear plot of flow rate ( $Q$ ) and pressure ( $P$ ) versus time from the injection test in section 297.9-302.9 m in borehole KFR105.

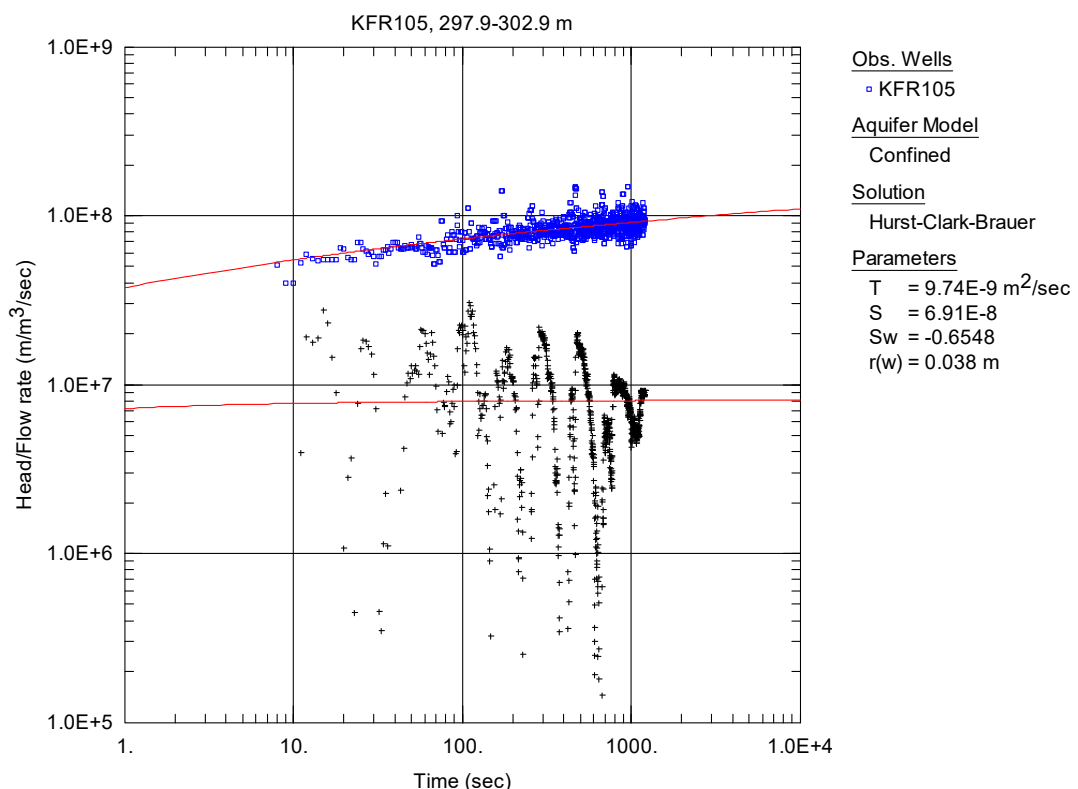


**Figure A3-137.** Log-log plot of head/flow rate (□) and derivative (+) versus time, from the injection test in section 297.9-302.9 m in KFR105.

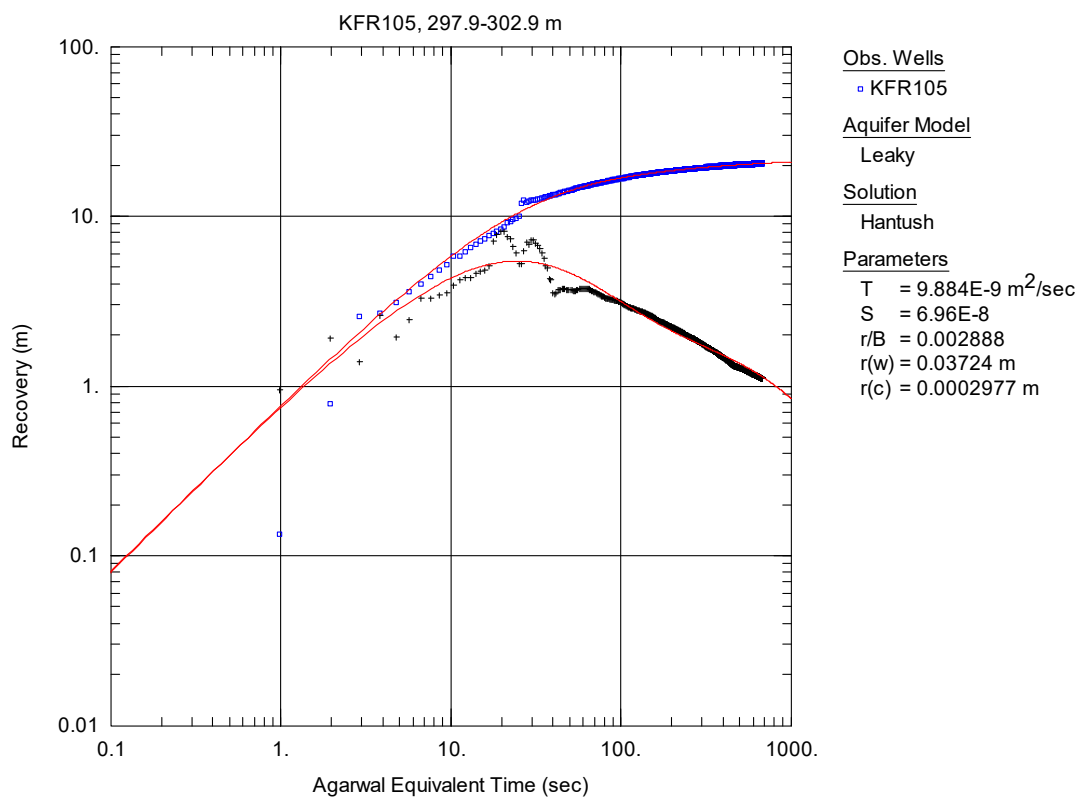


**Figure A3-138.** Log-log plot of recovery (□) and derivative (+) versus equivalent time, from the injection test in section 297.9-302.9 m in KFR105.

## Appendix 4

### Test diagrams – Injection tests – long tests in KFR105

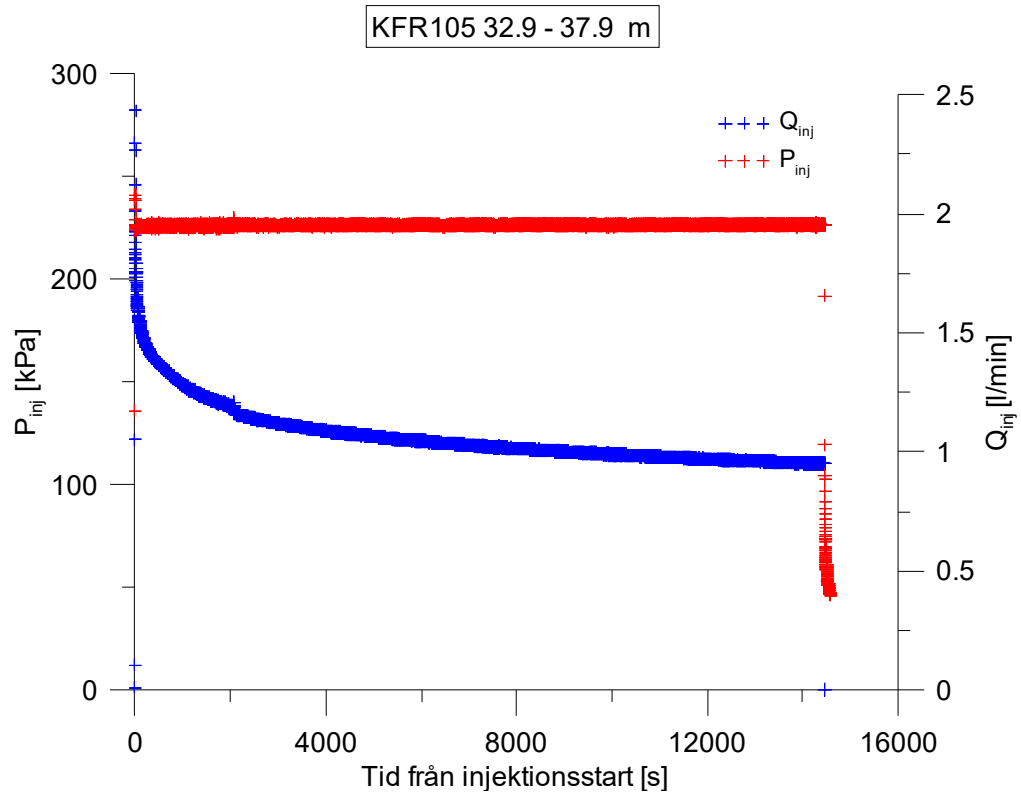


**Figure A4-1.** Linear plot of flow rate ( $Q$ ) and pressure ( $P$ ) versus time from the long injection test in section 32.9-37.9 m in borehole KFR105.

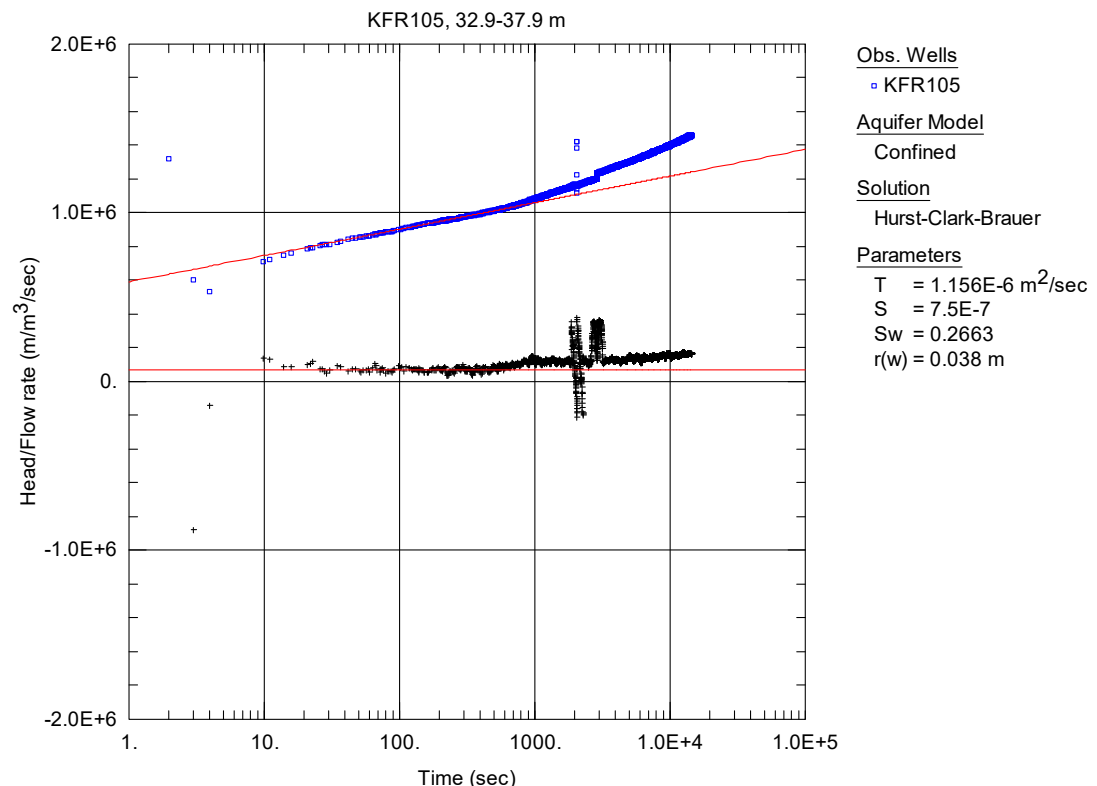


**Figure A4-2.** Log-log plot of head/flow rate (□) and derivative (+) versus time, from the long injection test in section 32.9-37.9 m in KFR105.

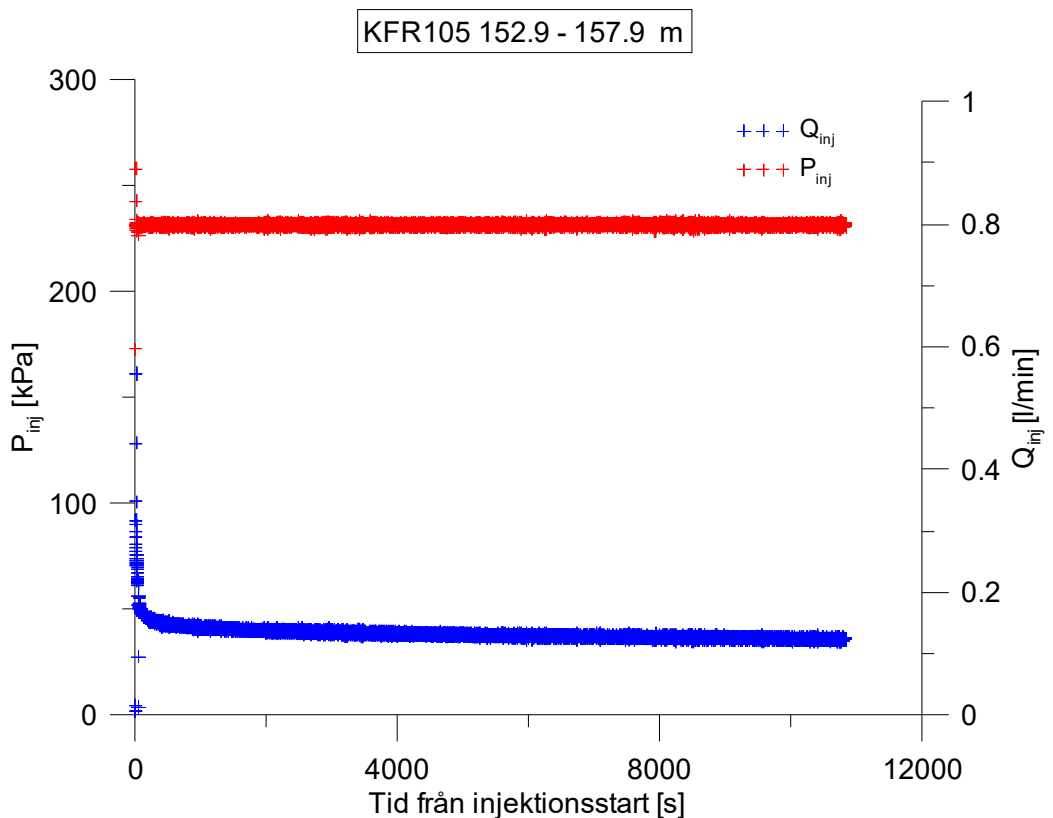


**Figure A4-3.** Linear plot of flow rate ( $Q$ ) and pressure ( $P$ ) versus time from the long injection test in section 152.9-157.9 m in borehole KFR105.

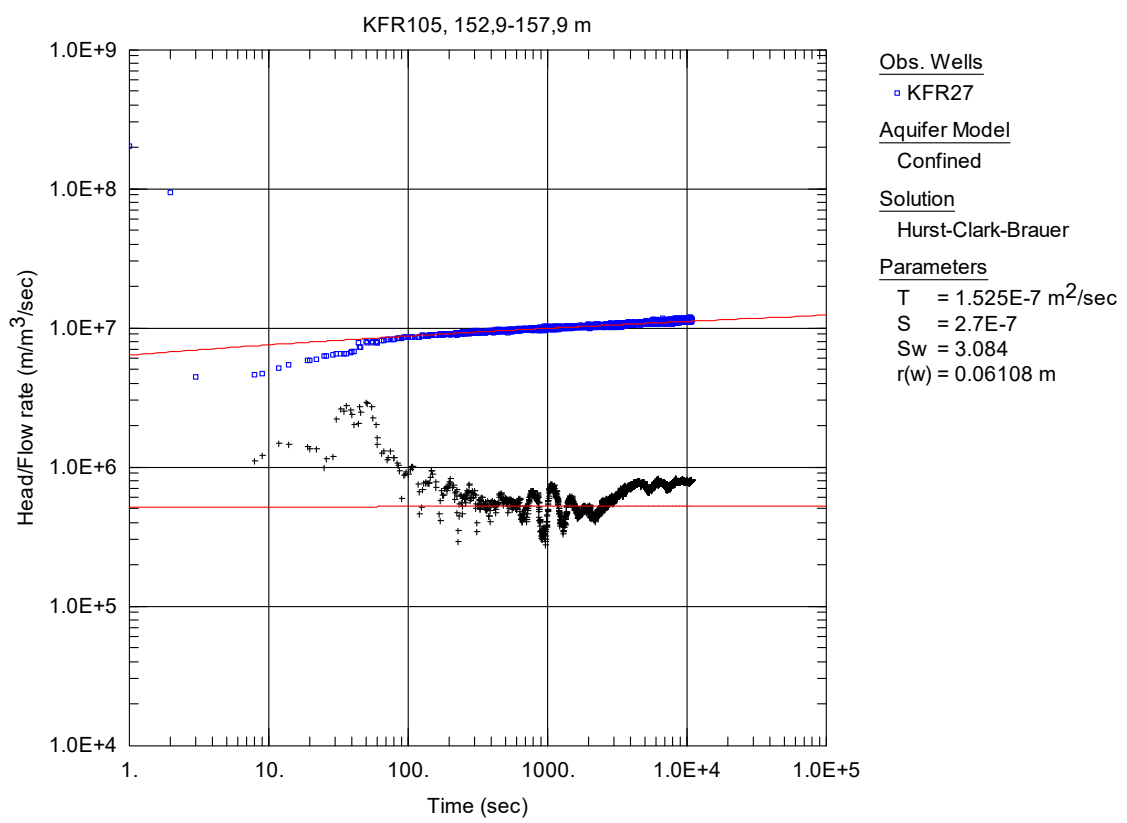


**Figure A4-4.** Log-log plot of head/flow rate (□) and derivative (+) versus time, from the long injection test in section 152.9-157.9 m in KFR105.

## Appendix 5

### Test diagrams – Injection tests – Fixed installations in KFR105

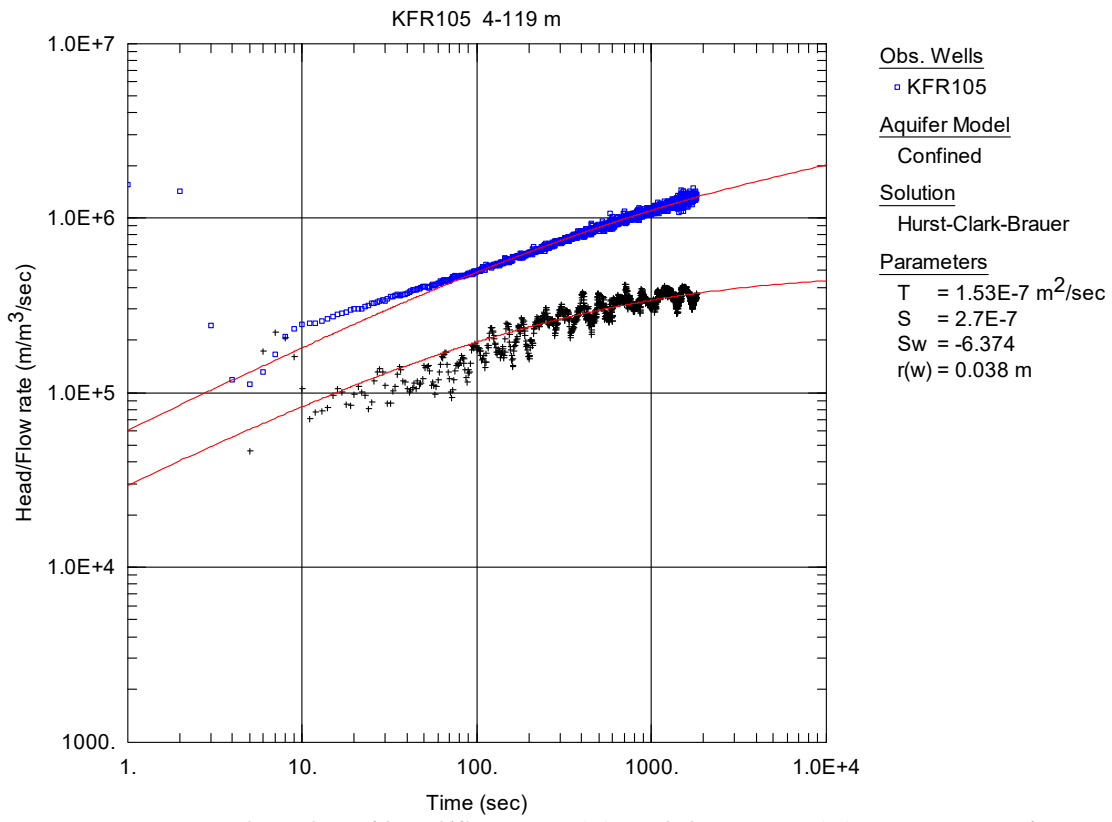


**Figure A5-1.** Log-log plot of head/flow rate (□) and derivative (+) versus time, from the injection test in section 4-119 m in KFR105.

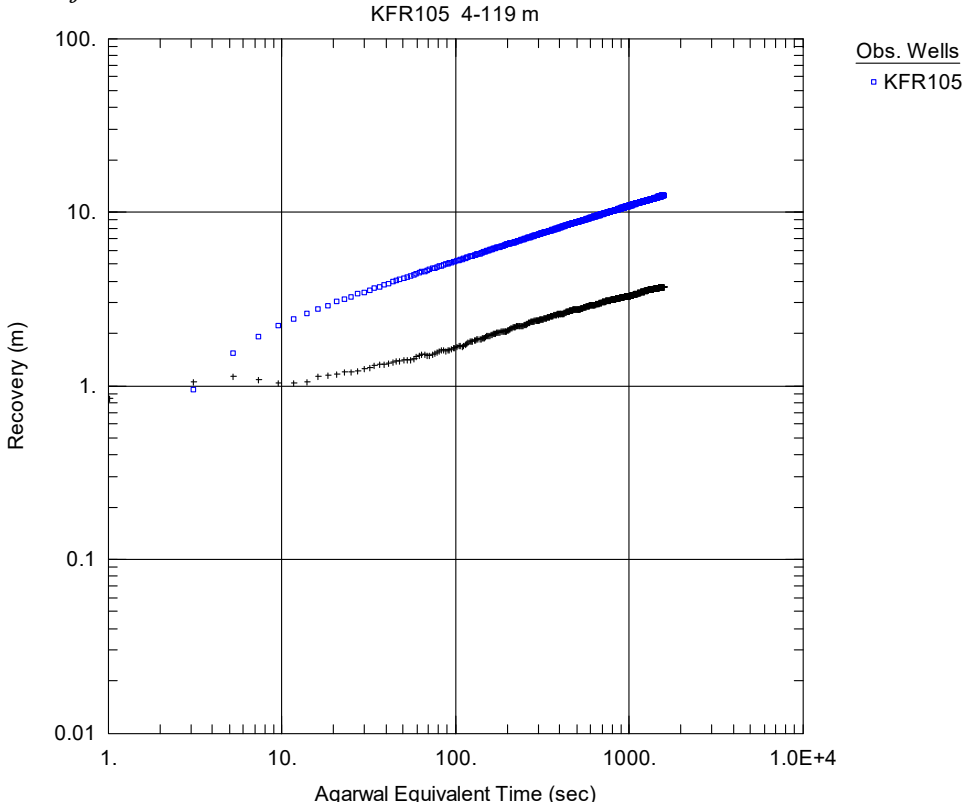


**Figure A5-2.** Log-log plot of recovery (□) and derivative (+) versus equivalent time, from the injection test in section 4-119 m in KFR105. No satisfying solution was found.

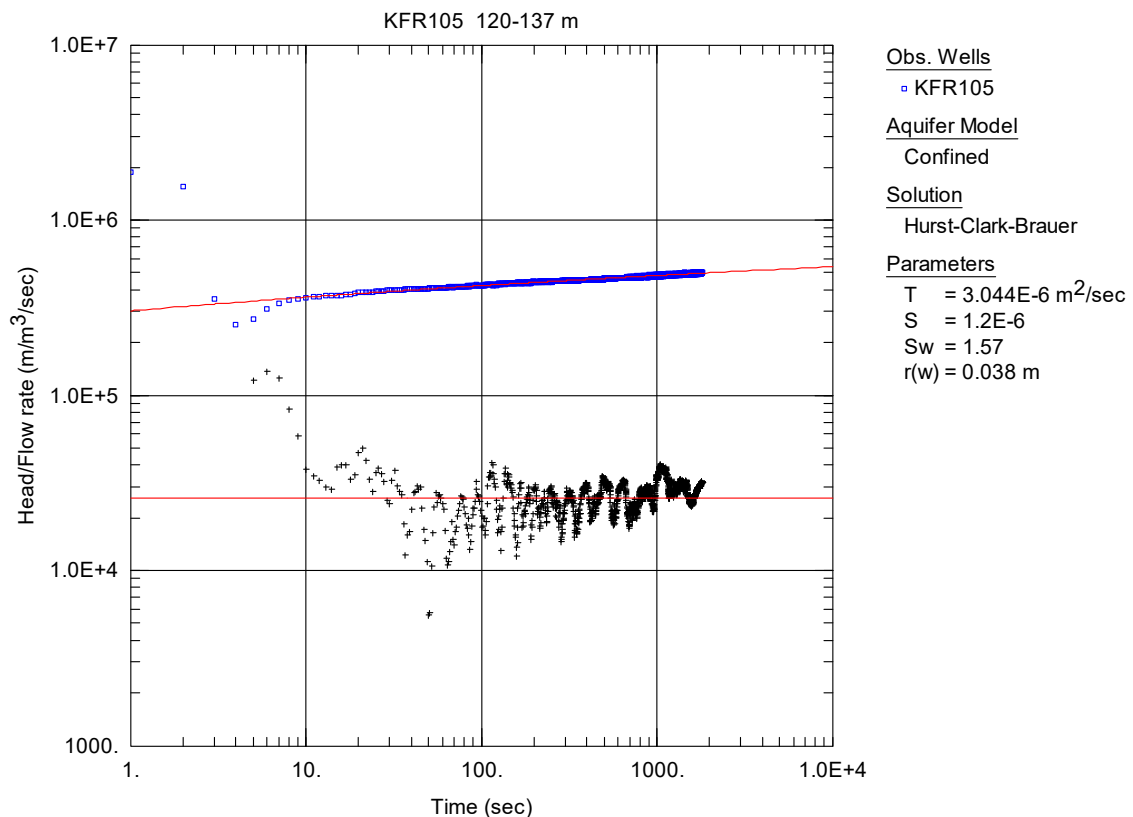


**Figure A5-3.** Log-log plot of head/flow rate (□) and derivative (+) versus time, from the injection test in section 120-137 m in KFR105.

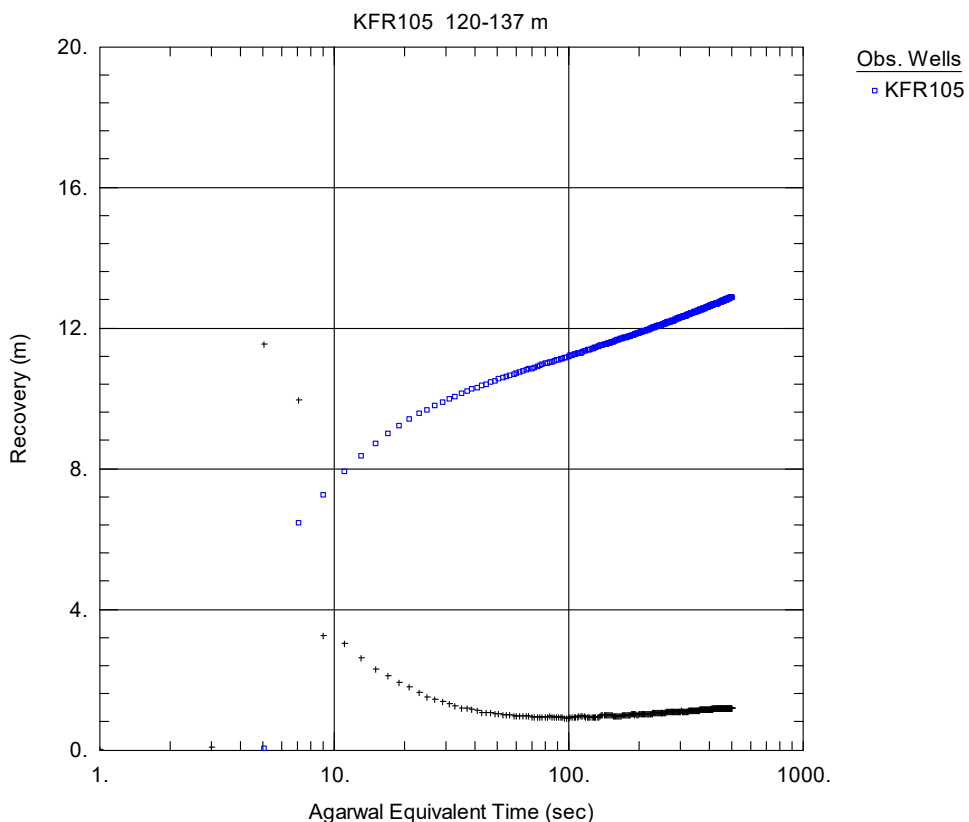


**Figure A5-4.** Log-log plot of recovery (□) and derivative (+) versus equivalent time, from the injection test in section 120-137 m in KFR105. No satisfying solution was found.

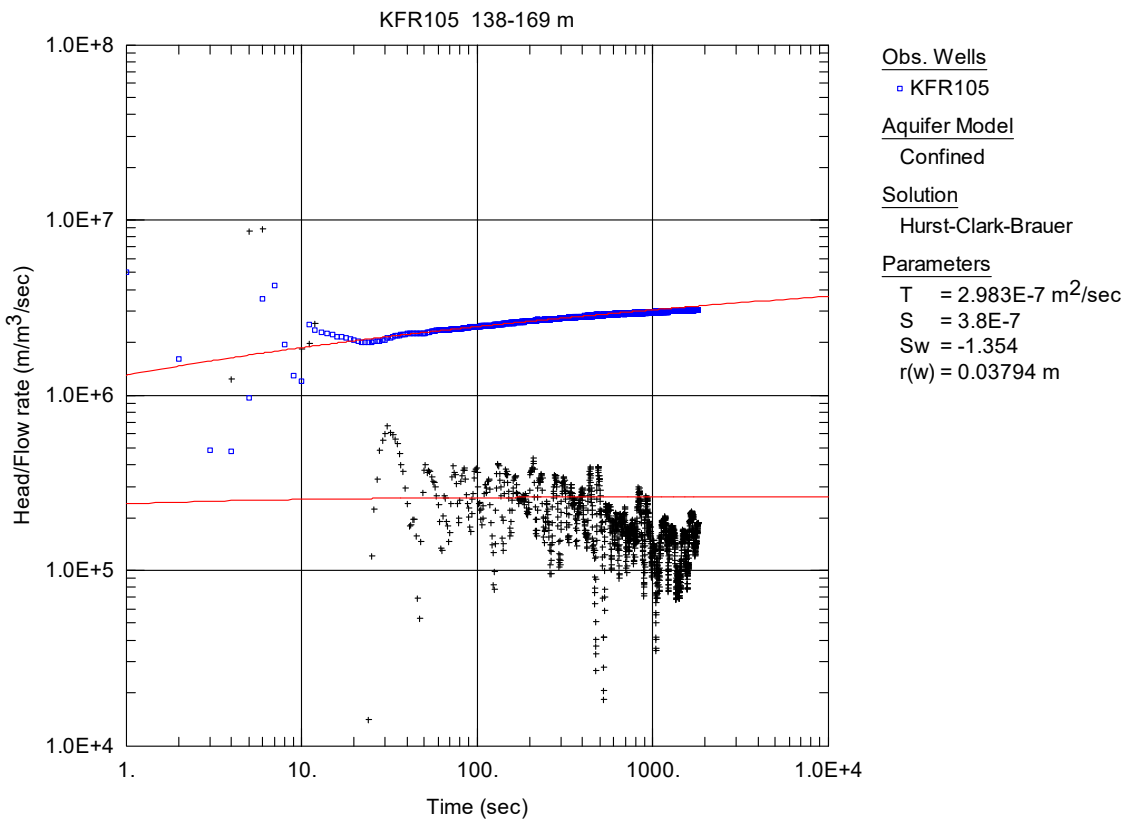


**Figure A5-5.** Log-log plot of head/flow rate (□) and derivative (+) versus time, from the injection test in section 138-169 m in KFR105.

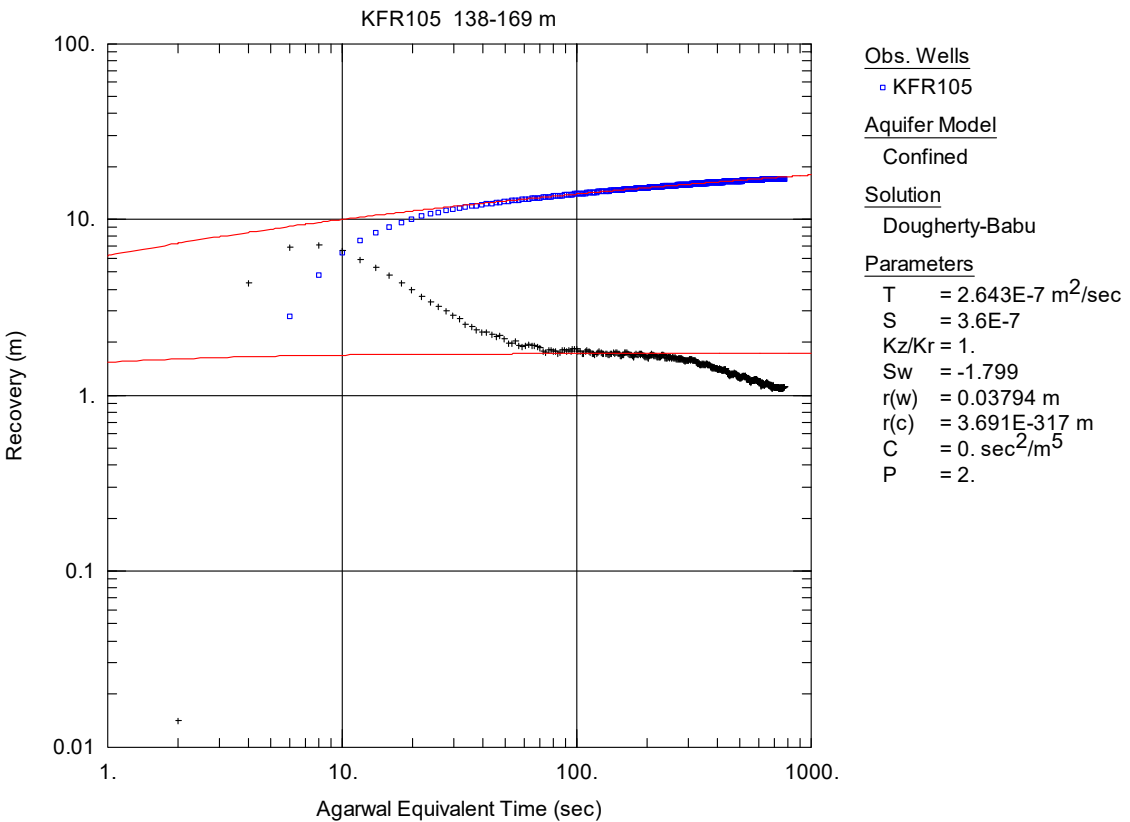


**Figure A5-6.** Log-log plot of recovery (□) and derivative (+) versus equivalent time, from the injection test in section 138-169 m in KFR105.

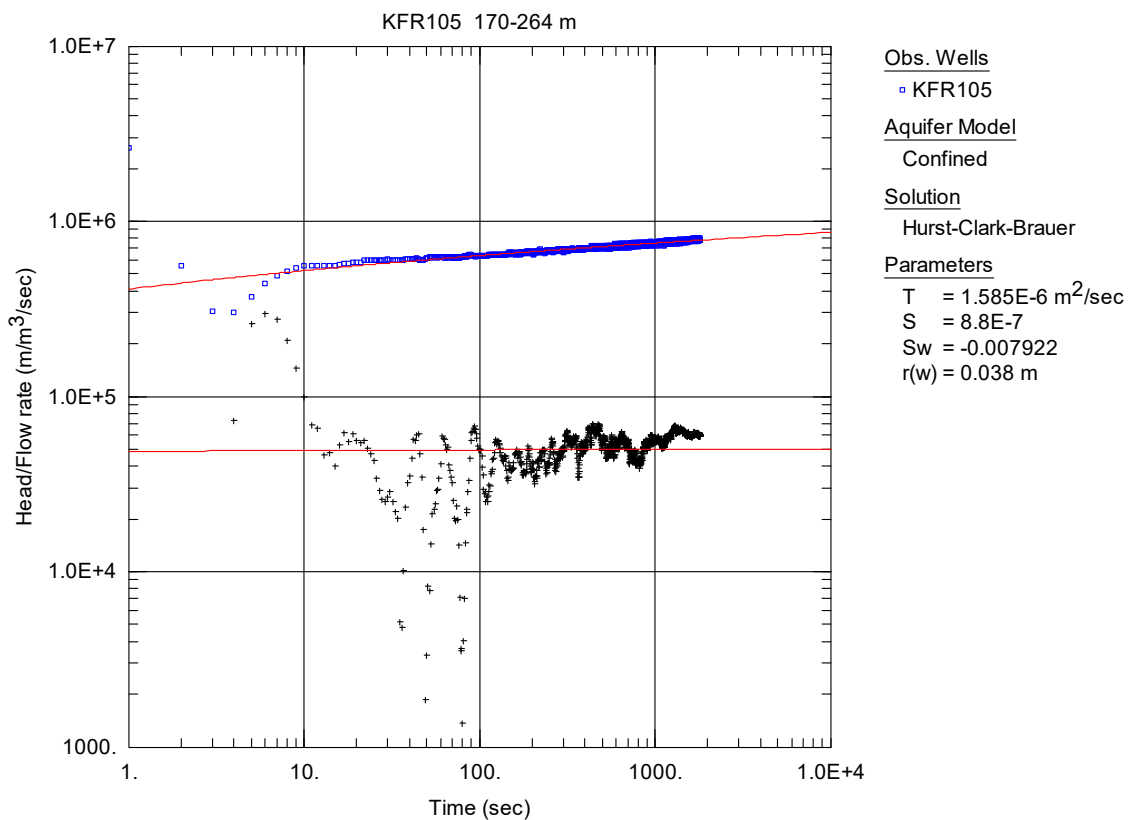


**Figure A5-7.** Log-log plot of head/flow rate (□) and derivative (+) versus time, from the injection test in section 170-264 m in KFR105.

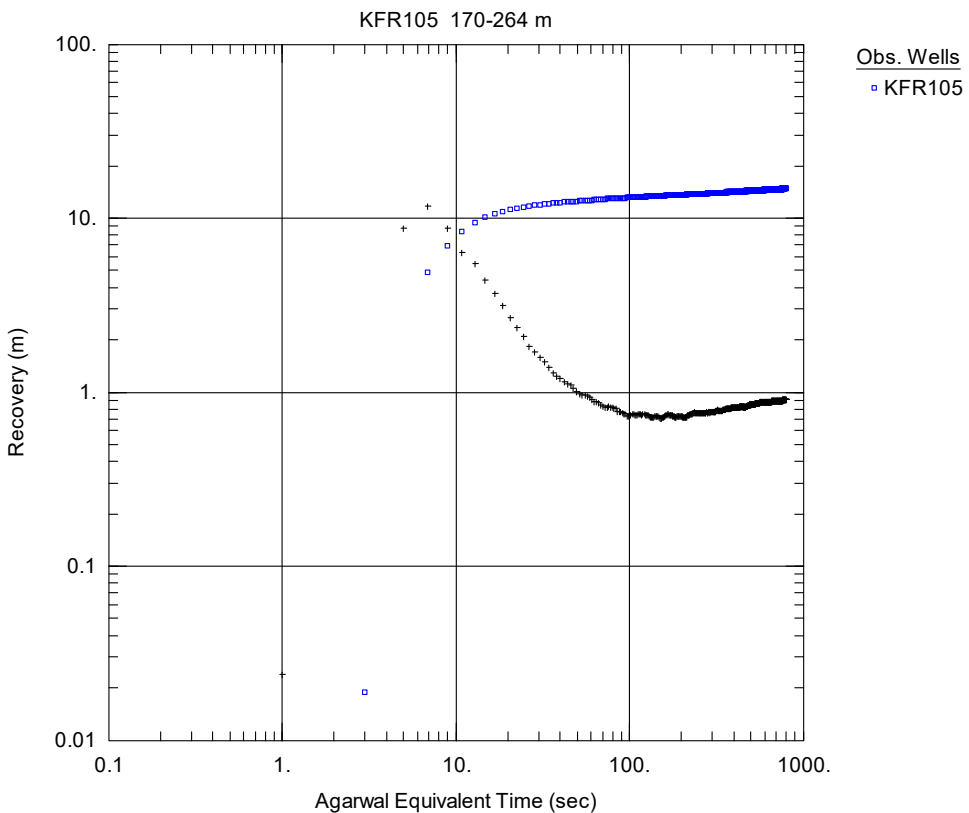


**Figure A5-8.** Log-log plot of recovery (□) and derivative (+) versus equivalent time, from the injection test in section 170-264 m in KFR105. No satisfying solution was found.

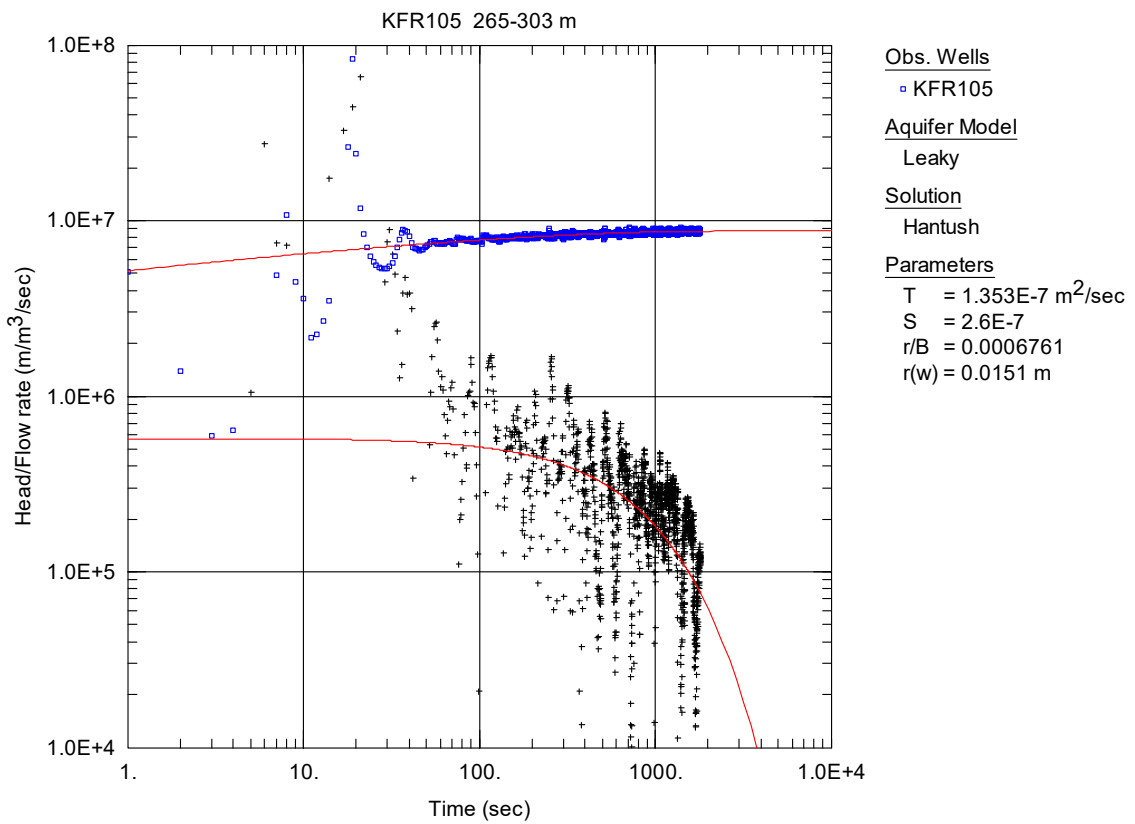


**Figure A5-9.** Log-log plot of head/flow rate (□) and derivative (+) versus time, from the injection test in section 265-303 m in KFR105.

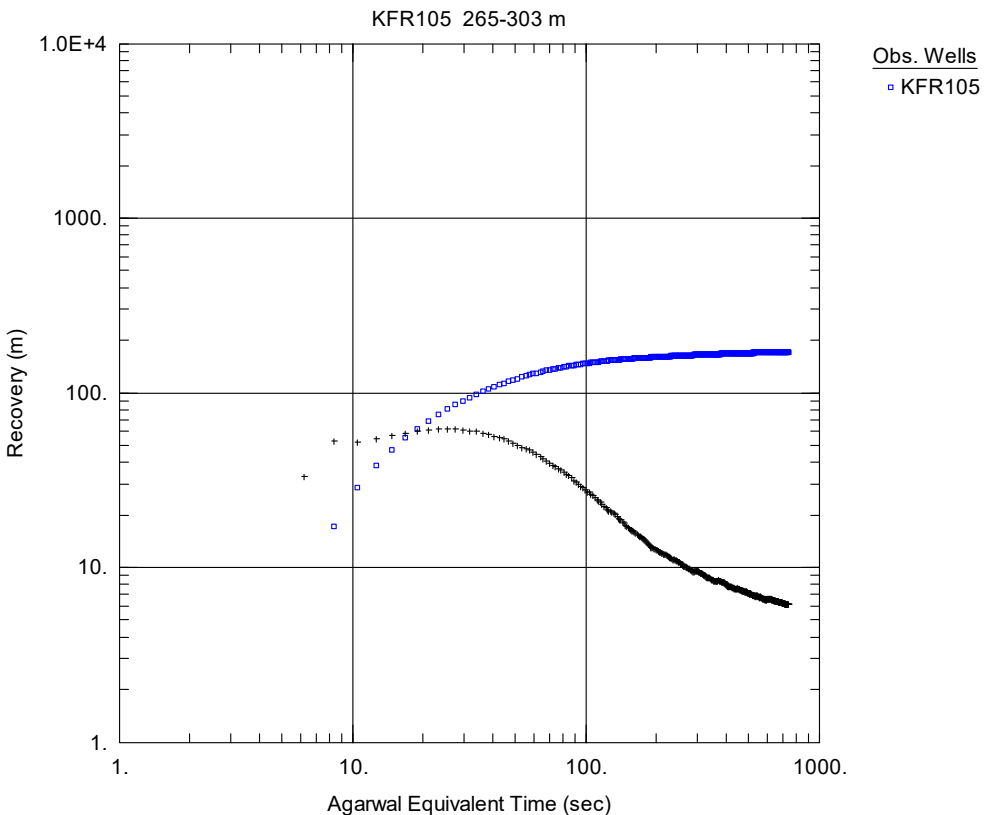


**Figure A5-10.** Log-log plot of recovery (□) and derivative (+) versus equivalent time, from the injection test in section 265-303 m in KFR105. No satisfying solution was found.



SKB is responsible for managing spent nuclear fuel and radioactive waste produced by the Swedish nuclear power plants such that man and the environment are protected in the near and distant future.

[skb.se](http://skb.se)